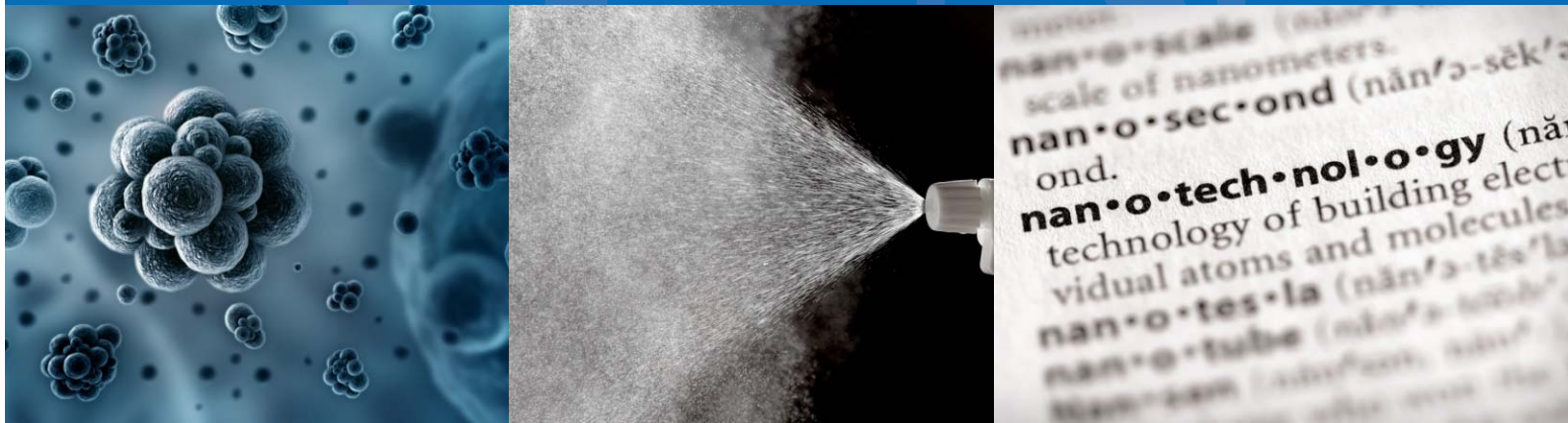




Nanomaterial Case Study: Nanoscale Silver in Disinfectant Spray



This page intentionally left blank.

Nanomaterial Case Study: Nanoscale Silver in Disinfectant Spray

August 2012

National Center for Environmental Assessment
Office of Research and Development
U.S. Environmental Protection Agency
Research Triangle Park, NC

Disclaimer

This document has been reviewed in accordance with U.S. Environmental Protection Agency policy and approved for publication. Mention of trade names or commercial products does not constitute endorsement or recommendation for use.

Table of Contents

Disclaimer	ii
List of Tables	vii
List of Figures	vii
Abbreviations	viii
Authors, Contributors, and Reviewers	xi
Preamble	xiv
Chapter 1. Introduction to this Document	1-1
1.1. Background	1-1
1.2. Purpose of this Document	1-6
1.3. How to Read this Document	1-7
1.4. Terminology	1-8
Chapter 2. Introduction to Silver and Nanoscale Silver	2-1
2.1. Conventional Silver: Uses, Occurrence in the Environment, and U.S. Standards	2-1
2.1.1. Uses of Silver and Silver Compounds	2-1
2.1.2. Occurrence of Silver in the Environment	2-2
2.1.3. U.S. Standards for Environmental Silver	2-4
2.2. Historical and Emerging Uses of Nanoscale Silver	2-6
2.3. Physicochemical Properties of Nanoscale Silver	2-10
2.3.1. Size	2-11
2.3.2. Morphology	2-12
2.3.3. Surface Area	2-13
2.3.4. Chemical Composition	2-13
2.3.5. Solubility	2-14
2.3.6. Surface Chemistry, Reactivity, and Coatings	2-16
2.3.7. Conductive, Magnetic, and Optical Properties	2-17
2.4. Analytical Methods to Characterize Nanoscale Silver	2-18
2.4.1. Methods for Laboratory Research	2-18
2.4.2. Methods to Assess Environmental Occurrence	2-20
2.4.3. Methods to Assess Workplace Occurrence	2-21
2.4.4. Methods for Quantifying Dose and Dose Metrics	2-23
2.5. Summary of Physicochemical Properties and Analytical Methods	2-25
Chapter 3. Life-Cycle Stages	3-1
3.1. Feedstocks	3-1
3.2. Manufacturing	3-2
3.2.1. Synthesis of Silver Nanoparticles	3-3
3.2.2. Manufacturing of Nano-Ag for Disinfectant Sprays	3-7
3.3. Distribution and Storage of Nano-Ag Disinfectant Sprays	3-9
3.4. Use of Nano-Ag Disinfectant Sprays	3-9
3.5. Disposal of Nano-Ag Disinfectant Sprays	3-11

3.6. Summary of Life-Cycle Stages	3-12
Chapter 4. Transport, Transformation, and Fate Processes in Environmental Media	4-1
4.1. Factors Influencing Transport, Transformation, and Fate Processes of Nano-Ag	4-2
4.1.1. Persistence	4-3
4.1.2. Particle Clustering, Deposition, and Sedimentation	4-4
4.1.3. Adsorption	4-6
4.1.4. Transport/Mobility Potential	4-7
4.2. Air	4-7
4.2.1. Diffusion	4-8
4.2.2. Particle Clustering	4-8
4.2.3. Residence Time	4-9
4.2.4. Deposition and Resuspension	4-9
4.2.5. Additional Factors	4-10
4.3. Terrestrial Systems	4-10
4.3.1. Soil	4-11
4.3.2. Plants	4-12
4.4. Aquatic Systems	4-13
4.4.1. Natural Aquatic Systems	4-13
4.4.1.1. Surface Properties	4-14
4.4.1.2. Ionic Ag and Ag Complexes in Water	4-14
4.4.1.3. Particle Clustering	4-16
4.4.1.4. Important Environmental Factors	4-16
4.4.2. Wastewaters	4-18
4.5. Transport, Transformation, and Fate Models	4-19
4.6. Summary of Nano-Ag Transport, Transformation, and Fate in Environmental Media	4-23
Chapter 5. Exposure, Uptake, and Dose	5-1
5.1. Biotic Exposure	5-4
5.2. Biotic Uptake and Dose	5-6
5.2.1. Bioavailability, Bioconcentration, and Bioaccumulation	5-7
5.2.1.1. Attributes of an Organism that Influence Bioavailability of Nano-Ag and Silver Ions	5-8
5.2.1.2. Attributes of the Environment Influencing Bioavailability of Silver Ions and Nano-Ag	5-9
5.2.1.3. Bioaccumulation Models	5-13
5.2.2. Uptake by Bacteria and Fungi	5-14
5.2.3. Uptake in Aquatic Ecosystems	5-17
5.2.3.1. Uptake by Algae	5-19
5.2.3.2. Uptake by Protozoa	5-20
5.2.3.3. Uptake by Bivalve Mollusks	5-20
5.2.3.4. Uptake by Aquatic Crustacea	5-21
5.2.3.5. Uptake by Vertebrate Eggs	5-23
5.2.3.6. Uptake by Freshwater Fish	5-25
5.2.3.7. Uptake by Saltwater Fish	5-27
5.2.3.8. Bioaccumulation in Aquatic Food Webs	5-28
5.2.4. Terrestrial Ecosystems	5-30
5.2.4.1. Uptake by Terrestrial Plants	5-30
5.2.4.2. Uptake by Soil Macrofauna	5-32
5.2.4.3. Transfer through Terrestrial Food Webs	5-33
5.3. Human Exposure	5-35
5.3.1. General Population Exposure	5-36
5.3.1.1. Respiratory Exposure	5-38
5.3.1.2. Dermal Exposure	5-39
5.3.1.3. Oral Exposure	5-39
5.3.2. Occupational Exposure	5-40
5.4. Aggregate Exposure to Nano-Ag from Multiple Sources and Pathways	5-44
5.4.1. Human Aggregate Exposure	5-45



5.4.2. Biotic Aggregate Exposure	5-47
5.5. Cumulative Exposure to Nano-Ag and Other Contaminants	5-47
5.5.1. Nano-Ag By-Products and Transformation Products	5-48
5.5.2. Examples of Nano-Ag Facilitating Absorption of Other Contaminants	5-49
5.5.3. Examples of Nanoparticles Facilitating Absorption of Other Contaminants	5-49
5.6. Models to Estimate Exposure	5-50
5.7. Human Uptake and Dose	5-51
5.7.1. Pharmacokinetics	5-51
5.7.1.1. Absorption	5-52
5.7.1.2. Distribution	5-53
5.7.1.3. Metabolism	5-56
5.7.1.4. Excretion	5-56
5.7.2. Uptake and Dose by Route	5-57
5.7.2.1. Respiratory (Inhalation and Instillation)	5-57
5.7.2.2. Dermal	5-60
5.7.2.3. Ingestion	5-61
5.7.3. Models to Estimate Dose	5-62
5.8. Summary of Exposure, Uptake, and Dose	5-62
Chapter 6. Characterization of Effects	6-1
6.1. Factors that Influence Ecological and Human Health Effects of Nano-Ag	6-3
6.1.1. Physicochemical Properties	6-4
6.1.1.1. Size	6-5
6.1.1.2. Morphology	6-7
6.1.1.3. Surface Chemistry and Reactivity	6-8
6.1.2. Test Conditions	6-11
6.1.3. Environmental Conditions	6-12
6.2. Ecological Effects	6-15
6.2.1. Microorganisms (Excluding Algae)	6-17
6.2.2. Aquatic Organisms	6-26
6.2.2.1. Algae	6-27
6.2.2.2. Aquatic Invertebrates	6-30
6.2.2.3. Aquatic Vertebrates	6-34
6.2.2.4. Model to Estimate Toxicity to Aquatic Biota	6-42
6.2.3. Terrestrial Organisms	6-44
6.2.3.1. Terrestrial Plants	6-44
6.2.3.2. Terrestrial Invertebrates	6-46
6.2.3.3. Terrestrial Vertebrates	6-50
6.3. Human Health Effects	6-52
6.3.1. In Vitro Studies	6-52
6.3.1.1. Reproduction and Development	6-54
6.3.1.2. Oxidative Stress	6-55
6.3.1.3. DNA Damage and Mutation	6-56
6.3.1.4. Pro-inflammatory Response	6-58
6.3.2. In Vivo Studies	6-60
6.3.2.1. Central Nervous System Effects	6-61
6.3.2.2. Respiratory System Effects	6-62
6.3.2.3. Liver, Kidney, and Urinary System Effects	6-63
6.3.2.4. Cardiovascular System Effects	6-64
6.3.2.5. Hematology	6-64
6.3.2.6. DNA Damage	6-65
6.3.2.7. Skin	6-65
6.3.2.8. Reproductive/Developmental Effects	6-66
6.3.3. Human and Epidemiological Studies	6-66
6.3.3.1. Medical Use Studies	6-67
6.3.3.2. Occupational Studies	6-69
6.4. Summary of Ecological and Human Health Effects	6-71

Chapter 7. Summary	7-1
7.1. Case Study Highlights	7-3
7.1.1. Terminology	7-3
7.1.2. Conventional Silver	7-4
7.1.2.1. Historic and Current Uses of Silver and Silver Compounds	7-4
7.1.2.2. Historical Environmental Silver Levels	7-4
7.1.3. Nanoscale Silver	7-5
7.2. Nanoscale Silver Case Study Summary	7-6
7.2.1. Physical-chemical Properties of Nanoscale Silver	7-6
7.2.1.1. Analytical Methods	7-6
7.2.1.2. Analytical Methods for Laboratory or Occupational Settings	7-7
7.2.1.3. Analytical Methods for Environmental Media	7-7
7.2.1.4. Analytical Methods for Quantifying Dose and Dose Metrics	7-8
7.2.1.5. CEA Workshop Findings on Analytical Methods	7-8
7.2.2. Life Cycle Characterization	7-9
7.2.2.1. Production	7-9
7.2.2.2. Distribution	7-10
7.2.2.3. Use	7-10
7.2.2.4. Disposal	7-11
7.2.2.5. CEA Workshop Findings on Life Cycle Characterization	7-11
7.2.3. Transport, Transformation, and Fate Processes	7-11
7.2.3.1. Factors Influencing Transport, Transformation, and Fate Processes in Environmental Media	7-12
7.2.3.2. Transport, Transformation, and Fate Processes in Air	7-12
7.2.3.3. Transport, Transformation, and Fate Processes in Terrestrial Systems	7-13
7.2.3.4. Transport, Transformation, and Fate Processes in Aquatic Systems	7-13
7.2.3.5. Transport, Transformation, and Fate Models	7-15
7.2.3.6. CEA Workshop Findings on Transport, Transformation, and Fate Processes	7-16
7.2.4. Exposure-Dose	7-16
7.2.4.1. Biotic Exposure and Uptake	7-16
7.2.4.2. Human Exposure and Uptake	7-18
7.2.4.3. Aggregate Exposure in Humans and Biota	7-19
7.2.4.4. Exposure and Uptake Models	7-20
7.2.4.5. CEA Workshop Findings on Exposure and Uptake	7-20
7.2.5. Characterization of Effects	7-20
7.2.5.1. Ecological Effects	7-21
7.2.5.2. Human Effects	7-22
7.2.5.3. CEA Workshop Findings on Effects	7-23
7.3. Role of Case Study in Research Planning and Assessment Efforts	7-23
7.3.1. Workshop Outcomes	7-24
7.3.2. Implications for Research Planning	7-25
7.3.3. Implications for Future Assessment Efforts	7-26
References	R-1
Appendix A. Common Analytical Methods for Characterization of Nanomaterials	A-1
Appendix B. Summary of Ecological Effects Studies of Nano-Ag	B-1
Appendix C. Summary of Human Health Effects Studies of Nano-Ag	C-1
Appendix D. Identified Research Priorities (January 2011 Workshop)	D-1

List of Tables

Table 2-1.	Selected U.S. studies of silver contamination in the environment. _____	2-3
Table 2-2.	Solubility product constants for various silver solids. _____	2-15
Table 2-3.	Types of common coatings of nano-Ag. _____	2-17
Table 2-4.	Analytical methods for nanomaterials in soil, sediment, and ground water for size fractionation and distribution, surface area, and phase and structure. _____	2-21
Table 4-1.	Formation constants for silver complexes (Ag:Ligand = 1:1) with environmentally relevant ligands. _____	4-15
Table 5-1.	Nano-Ag applications and potential routes of human exposure. _____	5-46
Table 6-1.	Experimental parameters and toxicity of nano-Ag in deionized water and natural surface waters. _____	6-15

List of Figures

Figure 1-1.	Comprehensive environmental assessment framework. _____	1-3
Figure 1-2.	Steps in the CEA process. _____	1-5
Figure 2-1.	Silver emissions to the environment by geographical region. _____	2-5
Figure 4-1.	Potential nano-Ag pathways into the environment associated with production, use, and disposal of spray disinfectants containing nano-Ag. _____	4-24
Figure 5-1.	Absorption and uptake of nanoparticles and transport to the central blood circulatory system. _____	5-52
Figure 7-1.	Comprehensive environmental assessment framework. _____	7-2
Figure 7-2.	Steps in the CEA process. _____	7-2

Abbreviations

ACGIH	American Conference of Governmental Industrial Hygienists
Ag	Silver
Ag(NH ₃) ₂ ⁺	Ionic Diamminesilver
Ag ⁺ , Ag ²⁺ , and Ag ³⁺	Ionic Silver
Ag ⁰	Zero-Valent Silver
Ag ₂ S	Silver Sulfide or Argentite
Ag ₃ AsS ₃	Proustite
Ag ₃ SbS ₃	Pyrrargyrite
Ag ₅ SbS ₄	Stephanite
AgCl	Silver Chloride or Cerargyrite
AgClO ₄	Silver Perchlorate
AgI	Silver Iodide
AgNO ₃	Silver Nitrate
AgSO ₄	Silver Sulfate
ALP	Alkaline Phosphatase
ALT	Alanine Aminotransferase
AMO	Ammonia Monooxygenase
AST	Aminotransferase
As[V]	Arsenate
ATP	Adenosine Triphosphate
ATSDR	Agency for Toxic Substances and Disease Registry
BAF	Bioaccumulation Factor
BCF	Bioconcentration Factor
BLM	Biotic Ligand Model
BMR	Basal Metabolic Rate
BSA	Bovine Serum Albumin
C ₆₀	Carbon 60, Buckminster Fullerenes, or Buckyballs
Ca ²⁺	Ionic Calcium
CaCl ₂	Calcium Chloride
CCC	Critical Coagulation Concentration
CEA	Comprehensive Environmental Assessment
Cl ⁻	Ionic Chlorine
CPB	Cetylpyridine Bromide

CPC	Condensation Particle Counter
CPF	Chlorpyrifos
DGGE	Denaturing Gradient Gel Electrophoresis
DGT	Diffusive Gradients in Thin Films
DLS	Dynamic Light Scattering
DOC	Dissolved Organic Carbon
EDS	Energy-Dispersive X-Ray Spectroscopy
EDTA	Ethylenediaminetetraacetic Acid
EPA	U.S. Environmental Protection Agency
EPS	Exopolymeric Substances
Fe ³⁺	Ferric Iron
FIFRA	Federal Insecticide, Fungicide, and Rodenticide Act
GI	Gastrointestinal
GSH	Glutathione
H ₂ O ₂	Hydrogen Peroxide
ICP	Inductively Coupled Plasma
ICP-MS	Inductively Coupled Plasma-Mass Spectroscopy
ICRP	International Commission on Radiological Protection
IL-6, IL-8, IL- β	Interleukins
K ⁺	Ionic Potassium
LOAEL	Lowest Observed Adverse Effect Level
LSPR	Localized Surface Plasmon Resonance
Mg ²⁺	Ionic Magnesium
MIC	Minimum Inhibitory Concentrations
MIP-2	Macrophage Inhibitory Protein-2
MLE	Modified Ludzack-Ettinger
MTT	3-(4,5-Dimethylthiazol-2-yl)-2,5-Diphenyltetrazolium Bromide
N ₂	Nitrogen
Na ⁺	Ionic Sodium
Na ⁺ /K ⁺ - ATPase	Sodium- and Potassium-Activated Adenosine Triphosphatase
NaAgS ₂ O ₂	Sodium-Silver Thiosulfate
NaBH ₄	Sodium Borohydride
NaCl	Sodium Chloride
NAG	N-Acetyl-B-D Glucosaminidase
nano-Ag	Nanoscale Silver
nano-Au	Nanoscale Gold

nanomaterials	Nanoscale Materials
nano-TiO ₂	Nanoscale Titanium Dioxide
NH ₂ OH.HCl	Hydroxylamine Hydrochloride
NOEC	No Observed Effect Concentration
NOM	Natural Organic Matter
OA	Oleic Acid
OECD	Organisation for Economic Co-operation and Development
PAA	Polyacrylic Acid
PBMC	Peripheral Blood Mononuclear Cell
PEC	Predicted Environmental Concentration
PEN	Project on Emerging Nanotechnologies
PHA	Phytohaemagglutinin
PMFA	Probabilistic Material Flow Analysis
PNEC	Predicted No-Effect Concentration
PO ₄ ³⁻	Phosphate
PT	Permeability Transition
PVP	Polyvinylpyrrolidone
ROS	Reactive Oxygen Species
-S	Inorganic Sulfide
S ²⁻	Sulfide
SAP	Scientific Advisory Panel
SEM	Scanning Electron Microscopy
-SH	Thiol
SMPS	Scanning Mobility Particle Sizer
SO ₄ ²⁻	Sulfate
TEM	Transmission Electron Microscopy
TNF- α	Tumor Necrosis Factor- α
U.S. EPA	U.S. Environmental Protection Agency

Authors, Contributors, and Reviewers

U.S. Environmental Protection Agency

Project Leaders: J. Michael Davis, ORD/NCEA (retired); Christina Powers, ORD/NCEA
Primary Authors: J. Michael Davis, ORD/NCEA; Patricia Gillespie, ORD/NCEA; Maureen Gwinn, ORD/NCEA; Christine Hendren, ORISE; Tom Long, ORD/NCEA; Christina Powers, ORD/NCEA
Contributors: Genya Dana, ORISE; Meredith Lassiter, ORD/NCEA; Jeff Gift, ORD/NCEA; Richard Fehir, OCSPP/OPPT; Justin Roberts, OCSPP/OPPT; Amy Wang, ORD/NCCT

ICF International*

Project Manager: Dave Burch
Primary Authors: Dave Burch, Pamela Hartman, Margaret McVey, Audrey Turley, Amalia Turner
Contributors: Rebecca Boyles, Michelle Cawley, Adeline Harris, Whitney Kihlstrom, Courtney Skuce, Kate Sullivan, Satish Vutukuru, Ronald White
Technical Editor: Penelope Kellar
Consultant Reviewer: Jo Anne Shatkin (CLF Ventures)

*This document was prepared by ICF International under EPA Contract No. EP-C-09-009 with technical direction by the U.S. EPA National Center for Environmental Assessment.

Internal EPA Reviewers

Jim Allen, ORD/NHEERL	Earl Goad, OCSPP/OPP	Scott Prothero, OCSPP/OPPT
Jim Alwood, OCSPP/OPPT	Karen Hamernik, OCSPP/OSCP	Kim Rogers, ORD/NERL
Chris Andersen, ORD/NHEERL	Kathy Hart, OCSPP/OPPT	Jessica Ryman, OCSPP/OPP
Mary Ann Curran, ORD/NRMRL	William Hazel, OCSPP/OPP	John Scalera, OEI/OIAA
Carl Blackman, ORD/NHEERL	Ed Heithmar, ORD/NERL	Prabodh Shah, OCSPP/OPPT
Will Boyes, ORD/NHEERL	Mike Hughes, ORD/NHEERL	Najm Shamim, OCSPP/OPP
Lyle Burgoon, ORD/NCEA	William Jordan, OCSPP/OPP	Jenny Tao, OCSPP/OPP
Jonathan Chen, OCSPP/OPP	Andy Kligerman, ORD/NHEERL	Patti TenBrook, Region 9
Jed Costanza, OCSPP/OPPT	David Lai, OCSPP/OPPT	Nicolle Tolve, ORD/NERL
Dave Demarini, ORD/NHEERL	Anjali Lamba, OCSPP/OPPT	John Vandenberg, ORD/NCEA
Steve Diamond, ORD/NHEERL	Jennifer McLain, OCSPP/OPP	Katrina Varner, ORD/NERL
Timothy Dole, OCSPP/OPP	Connie Meacham, ORD/NCEA	Debra Walsh, ORD/NCEA
Kevin Dreher, ORD/NHEERL	Melba Morrow, OCSPP/OPP	Barbara Wright, ORD/NCEA
Brendlyn Faison, OW/OST	Nhan Nguyen, OCSPP/OPPT	Robert Willis, ORD/NERL
Richard Fehir, OCSPP/OPPT	Matt Odegaard, ORD/NHEERL	Bob Zucker, ORD/NHEERL
Greg Fritz, OCSPP/OPPT	Marti Otto, OSWER/OSRTI	

Internal Review Coordinators

Daniel Axelrad, OA/OPEI
Ambika Bathija, OW/OST
Jane Denne, ORD/NERL
Patricia Erickson, ORD/NRMRL

Karen Hamernik, OCSPP/OSCP
Keith Houck, ORD/NCCT
Carl Mazza, OAR/IO
Ginger Moser, ORD/NHEERL

Marti Otto, OSWER/OSRTI
Nora Savage, ORD/NCER
Patti TenBrook, Region 9
Dennis Utterback, ORD/OSP

Interagency Reviewers

Department of Energy
Executive Office of the President
Occupational Safety and Health Administration

Interagency Review Coordinator

Jeff Morris*, EPA/ORD/IOAA, National Program Director for Nanotechnology

*Currently Deputy Director for Programs in EPA Office of Pollution Prevention and Toxics

Public Commenters

David Q. Andrews, Senior Scientist,
Environmental Working Group (EWG) et al.
Anonymous

Samantha Dozier, Nanotechnology Policy
Advisor, Regulatory Testing Division, People
for the Ethical Treatment of Animals (PETA)

Jaydee Hanson, Policy Director, International
Center for Technology Assessment (ICTA)

Ben Horenstein, Chair, Tri-TAC

Jeff Keane, Chief Executive Officer, Noble
Biomaterials, Inc.

Fred Klaessig, Pennsylvania Bio Nano Systems, LLC

Maria Victoria Peeler, Senior Policy Specialist,
Washington State Department of Ecology

Rosalind Volpe, Executive Director, Silver
Nanotechnology Working Group (SNWG)

Peer Reviewers

Paul M. Bertsch, Ph.D., University of Kentucky

Jaclyn Cañas, Ph.D., Texas Tech University

Robert I. MacCuspie, Ph.D., NIST

Peter R. McClure, Ph.D., DABT, SRC, Inc.

Bernd Nowack, Ph.D., Empa

Stig I. Olsen, Ph.D., Technical University of Denmark

James F. Ranville, Ph.D., Colorado School of Mines

Organizational Abbreviations

Empa Swiss Federal Laboratories for Materials
Testing and Research Technology

IO Immediate Office

IOAA Immediate Office of the Assistant
Administrator

NCEA National Center for Environmental
Assessment

NCCT National Center for Computational
Toxicology

NCER National Center for Environmental
Research

NERL National Exposure Research Laboratory
NCER National Center for Environmental
Research

NHEERL National Health and Ecological
Effects Research Laboratory

NIST National Institute of Standards and
Technology

NRMRL National Risk Management Research
Laboratory

OA Office of the Administrator

OAR Office of Air and Radiation

OCSP Office of Chemical Safety and
Pollution Prevention
OEI Office of Environmental Information
OIAA Office of Information, Analysis, and
Access
OPEI Office of Policy, Economics, and
Innovation
OPP Office of Pesticide Programs
OPPT Office of Pollution Prevention and
Toxics
ORD Office of Research and Development
ORISE Oak Ridge Institute for Science and
Education

OSCP Office of Science Coordination and
Policy
OSP Office of Science Policy
OSRTI Office of Superfund Remediation and
Technology Innovation
OST Office of Science and Technology
OSWER Office of Solid Waste and
Emergency Response
OW Office of Water

Preamble

This document is part of continuing efforts by the U.S. Environmental Protection Agency (EPA) to understand the scientific issues and information gaps associated with nanotechnology, consistent with recommendations in the EPA *Nanotechnology White Paper* ([U.S. EPA, 2007b](#)) and EPA *Nanomaterial Research Strategy* ([U.S. EPA, 2009e](#)). Engineered nanoscale materials (nanomaterials) have been described as having at least one dimension on the order of approximately 1 to 100 nanometers (nm) ([NSTC, 2011](#)). Such materials often have unique or novel properties that arise from their small size.

The specific type of nanomaterial considered in this document is nanoscale silver (nano-Ag) in a disinfectant spray application. This “case study” does not represent a completed or even preliminary assessment, nor is it intended to serve as a basis for near-term risk management decisions on possible uses of nano-Ag. Rather, the intent is to describe what is known and unknown about nano-Ag in this selected application as part of a process to identify and prioritize scientific and technical information to support long-term assessment efforts. The information used to populate this report is up to date as of March 1, 2011, when the last broad literature search to identify new information was conducted. Previous EPA case studies focused on nanoscale titanium dioxide used in drinking water treatment and in topical sunscreen ([U.S. EPA, 2010d](#)).

Like the previous case studies, this case study of nano-Ag is based on the comprehensive environmental assessment approach, which consists of both a framework and a process, the principal elements of which are illustrated in Figures 1-1 and 1-2 respectively. The organization of this document reflects the comprehensive environmental assessment framework: After a general introduction (Chapter 1) and introductory material on silver and nano-Ag (Chapter 2), Chapter 3 highlights stages of the product life cycle (research and development, feedstock processing, manufacturing, storage, distribution, use, disposal), followed by Chapter 4 on transport, transformation and fate processes, Chapter 5 on exposure-dose characterization, and Chapter 6 on ecological and health effects. Chapter 7 summarizes highlights from preceding chapters and major research issues.

Chapter 1. Introduction to this Document

1.1. Background

Nanoscale materials (nanomaterials) have been described as having at least one dimension on the order of approximately 1–100 nanometers (nm) ([NSTC, 2011](#)).¹ Although this size range is not universally accepted and continues to evolve, 100 nm is typically used as an upper bound, and this working definition is used as the size standard in this case study. Engineered nanomaterials are intentionally made, as opposed to being an incidental by-product of combustion or a natural process such as erosion, and often have unique or novel properties that arise from their small size. Like all technological developments, engineered nanomaterials offer the potential for both benefits and risks. The assessment of such benefits and risks relies on information, and, given the nascent state of nanotechnology, much remains to be learned about nanomaterials to support such assessments. This document is part of an endeavor to identify what is known and, more importantly, what is not yet known that could be of value in assessing the broad environmental implications of certain nanomaterials.

The focus of this document is a specific application of a selected nanomaterial: the use of engineered nanoscale silver (nano-Ag)² as an agent in disinfectant spray products. The U.S. Environmental Protection Agency (EPA) completed similar “case studies” of nanoscale titanium dioxide (nano-TiO₂) used for drinking water treatment and for topical sunscreen ([U.S. EPA, 2010d](#)). Such case studies do not represent completed or even preliminary assessments; rather, they are intended as a starting point in a process to identify and prioritize possible research directions to support future assessments of nanomaterials.

Part of the rationale for focusing on a series of nanomaterial case studies is that such materials and applications can have highly varied and complex properties that make considering them in the abstract or in generalities quite difficult. Different materials and different applications of a given material could raise unique questions or issues, as well as some issues that are common to various applications of a given nanomaterial or even to different nanomaterials. Focusing on only one possible example of a nano-Ag

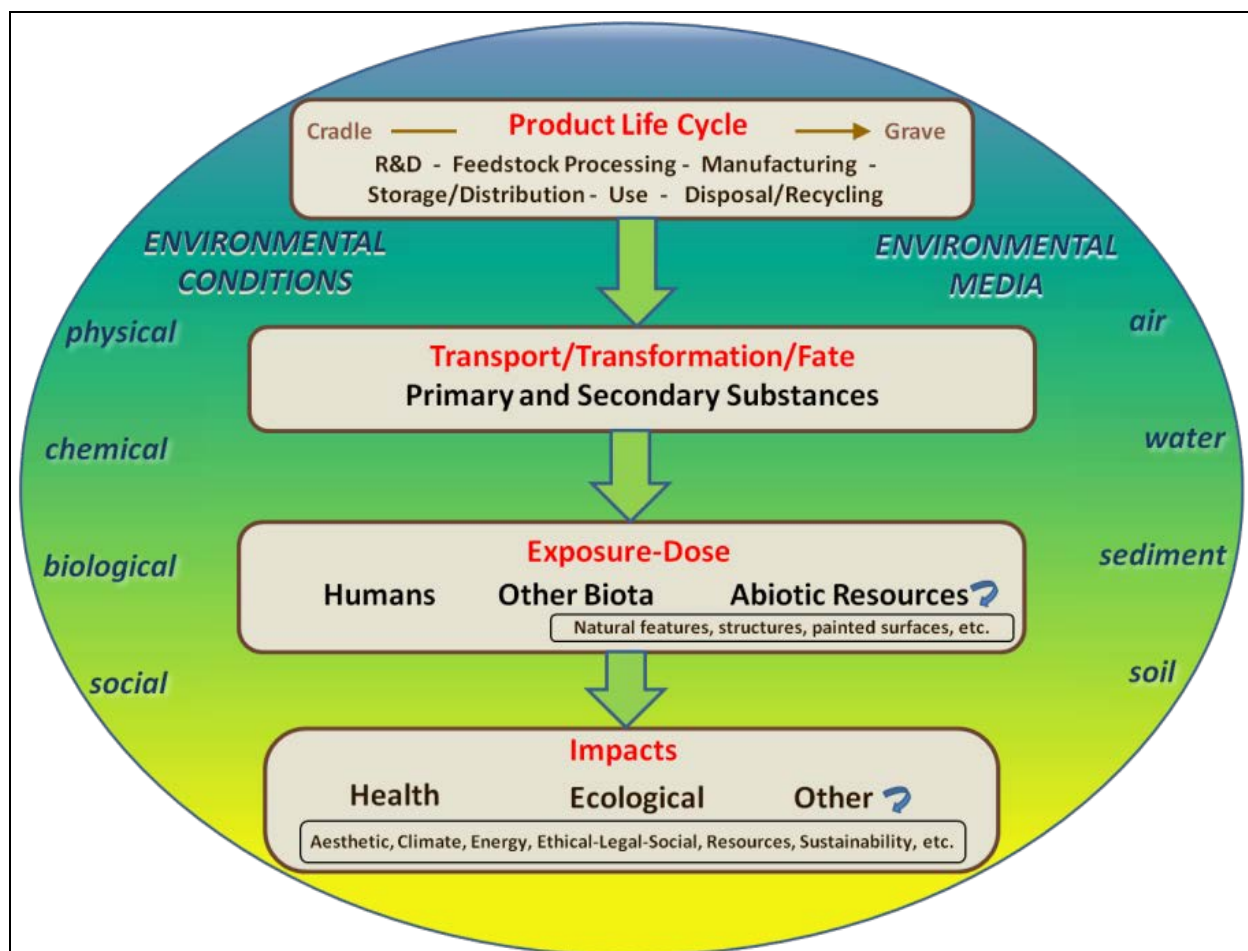
¹Key terminology (e.g., nano-Ag, conventional silver, engineered nanoparticles) used throughout this section is further defined and clarified in Section 1.4.

²Throughout this document, the term “nano-Ag” refers to silver nanoparticles that can display a range of properties and behaviors depending on specific characteristics of the particle, environmental conditions, and other factors.

application obviously does not represent all ways in which this nanomaterial could be used or all issues that different applications could raise. By considering this single application of nano-Ag, however, research directions can be identified that might pertain to nano-Ag in disinfectant spray, as well as to nano-Ag in general and even more broadly to other nanomaterials. The present case study, along with previous case studies of nano-TiO₂ used for drinking water treatment and for topical sunscreen ([U.S. EPA, 2010d](#)) and any future case studies of other nanomaterials, could assist research planning for nanomaterials at EPA and in the broader scientific community.

The process for selecting specific nanomaterials and particular applications to focus on for each case study involved individuals representing several EPA program offices, regional offices, and Office of Research and Development laboratories and centers. During an initial selection process, the individuals considered several candidate nanomaterials, including nanoscale cerium dioxide, several nanoscale carbon materials, as well as several metal and metal oxide nanomaterials. They then voted for their preferences based on, among other things, exposure potential, applicability to human and ecological risk assessment, and potential relevance of the nanomaterial to EPA programmatic interests. Nanoscale nano-TiO₂, nano-Ag, and single-walled carbon nanotubes were the top candidates based on this voting process. As discussed above, case studies were then completed on nano-TiO₂ and subsequently this document on nano-Ag was initiated. The choice of a specific application of nano-Ag, disinfectant spray in this case, was determined by a smaller team directly involved in the production of the case study document; however, similar to the selection of nanomaterial candidates, several applications were considered and disinfectant spray was then chosen based on consideration of the factors used to select candidate materials. This is not to say, however, that the selection of nano-Ag in disinfectant spray signifies a determination that it presents the greatest potential for exposure, or most relevance to risk assessment, or is clearly preferable based on any other single factor compared to all possible applications. Rather, based on information available at the time, it was deemed as the best application to focus thinking about the types of information that could inform future assessments of the potential ecological and health implications of nano-Ag.

This case study of nano-Ag, like the first case studies of nano-TiO₂ ([U.S. EPA, 2010d](#)), is built on the comprehensive environmental assessment (CEA) approach, which consists of both a framework and a process, the principal elements of which are illustrated in Figures 1-1 and 1-2 respectively. The uppermost box of Figure 1-1 lists typical stages of a product life cycle: research and development, feedstock processing, manufacturing, storage, distribution, use, and disposal (which would include reuse or recycling, if applicable). Releases to the environment associated with any stage of the product life cycle lead to what is depicted in the second box, which refers to transport, transformation, and fate



Source: <http://www.epa.gov/nanoscience/files/CEAPrecis.pdf>.

Figure 1-1. Comprehensive environmental assessment framework.

The CEA framework is used to systematically organize complex information in evaluations of the environmental implications of selected chemicals, products, or technologies (i.e., materials). The framework starts with the inception of a material and encompasses the environmental fate, exposure-dose, and impacts. Notably, the sequence of events is not always linear when, for example, transfers occur between media or via the food web. In addition, a variety of factors influence each event, including differences in environmental media and the physical, chemical, biological, and social conditions in which the material event occurs. Details on these influential factors are thus included throughout the framework when possible. The color gradient from top to bottom conveys the interactions and transfers that can occur between environmental media and conditions throughout the vertical layers of the framework.

processes that can result in secondary as well as primary contaminants spatially distributed in the environment.

The chains of events represented in the CEA framework occur within multiple environmental media (air, water, sediment, soil) and under various conditions (physical, chemical, biological, social), and any or all of these factors can be important in these events and processes. Also of note is that the single arrows connecting one facet of the CEA framework to the next actually represent numerous linkages, transfers, and feedback loops that can be far more complex than this simplified figure suggests. For example, the transfer of material from one organism to another through the food chain would represent a bidirectional exchange between transport, transformation, and fate and exposure-dose. In an

effort to convey the numerous types of complex exchanges, however, the framework does not present these interactions beyond a high-level, linear progression.

The third box in Figure 1-1, exposure-dose, goes beyond characterizing the occurrence of contaminants in the environment, as exposure refers to actual contact between a contaminant and a receptor, whether living or nonliving. Living organisms consist of humans and other biota;³ abiotic receptors can include features of the natural landscape, structures such as buildings and statues, and painted surfaces of vehicles and other objects. Exposure can involve aggregate exposure across routes (e.g., inhalation, ingestion, dermal), cumulative exposure to multiple contaminants (both primary and secondary), and various spatiotemporal dimensions (e.g., activity patterns, diurnal and seasonal changes). Dose is the amount of a substance that actually enters an organism by crossing a biological barrier or that deposits on an inanimate object.

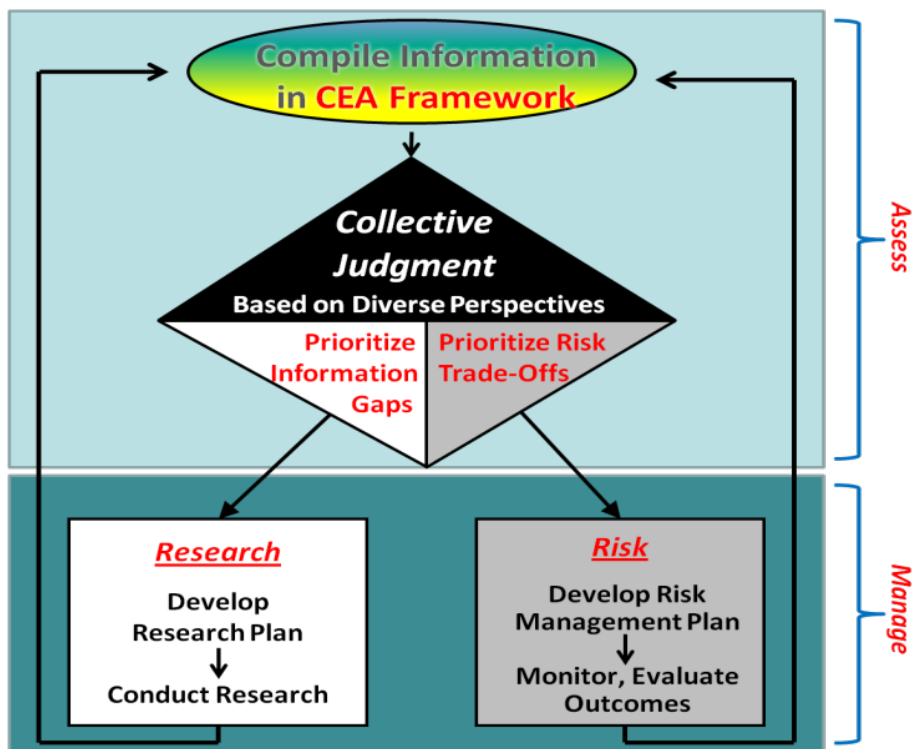
As part of a chain of cause-effect events, dose links exposure with potential impacts of various types, as indicated in the last box of Figure 1-1. Human health effects might result when a delivered dose reaches a target cell or organ; or, in an ecological context, effects might occur when a stressor is at a level sufficient to cause an adverse response in biotic or abiotic receptors (e.g., buildings, cars, other structures). Impacts encompass both qualitative hazards and quantitative exposure-response relationships and can extend to aesthetic effects (e.g., alterations in visibility, taste, and odor), climate change, energy consumption, resource depletion, and other types of effects. Although none of these effects are being excluded a priori from consideration here, their inclusion in a CEA framework would depend on having a plausible premise for expecting a discernible impact. If such a premise can be articulated for additional types of effects, the case study can be expanded to encompass their consideration within the CEA framework. Even economic and societal impacts related to sustainability could be encompassed by the CEA approach, but the focus in this case study is limited to environmental implications related to human health and ecological populations.

Not reflected in Figure 1-1 is the role of analytical methods that make possible the detection, measurement, and characterization of nanomaterials in the environment and in organisms. Characterization of the substance(s) of interest (e.g., determination of chemical identity, reactivity, purity, and other properties) is fundamental to any assessment of nanomaterials, but is not included in this high-level view of the CEA framework for the sake of simplicity.

As previously mentioned, the CEA approach consists of both a framework and a process. Compiling the information described above into the CEA framework is the first step of the CEA process (Figure 1-2). Next, a collective judgment process is used to evaluate this information and prioritize it.

³The term biota is used throughout this document to refer to all living organisms other than humans.

Collective judgment, as it has been applied in the CEA process to date, refers to a formal, structured procedure that enables a diverse group of individuals to be heard individually and represented in a transparent record of the collectively reached outcomes. In turn, it supports an essential feature of CEA: the inclusion of diverse technical and stakeholder perspectives to ensure that a holistic evaluation is achieved (ICF, 2011).



Source: <http://www.epa.gov/nanoscience/files/CEAPrecis.pdf>

Figure 1-2. Steps in the CEA process.

The CEA process involves a series of steps that result in judgments about the implications of information contained in the CEA framework. Compiling information in the CEA framework is fundamental for a given material, but is only a first step in the CEA process. Next, the information in the framework is evaluated using a collective judgment technique (i.e., a structured process that allows the participants representing a variety of technical and stakeholder viewpoints to learn from one another, yet form their own independent judgments). The result of the collective judgment step is a prioritized list of risk trade-offs and information gaps that then can be used in planning research and developing adaptive risk management plans. The knowledge gained from these research and risk management activities feeds back in an iterative process of periodic CEA updates.

Prioritization is a key objective in this holistic evaluation within the CEA process. Depending on one's objectives and the state of the science surrounding an issue, CEA can be used to prioritize (1) information gaps leading to development of a research plan that will support future assessment efforts and (2) risk trade-offs leading to development of an adaptive risk management plan. As depicted in Figure 1-2, these uses of CEA cross over from conducting assessments into management efforts after the initial identification and prioritization of information. In either instance, CEA is meant to be iterative, and thus

the results of research and risk management efforts would be used in updating the CEA framework after some period of time determined by those conducting the CEA process.

At present, the CEA framework and process are focused on helping refine research planning for nanomaterials, with particular focus on nano-Ag as it might be used in disinfectant spray products. Although CEA has been exclusively applied to planning research to date, as the knowledge base grows for nanomaterials, and it becomes feasible to identify and prioritize risk-risk and risk-benefit trade-offs with more complete information, the path leading to risk management (as shown in Figure 1-2) will be pursued. Such efforts to extend its application would strive to inform risk management decisions by providing a systematic approach for organizing and evaluating complex information from a variety of existing assessment approaches, such as life-cycle assessment, exposure assessments, ecological risk assessment, and human health assessments.

Other efforts have been made to assess the potential risks of nanomaterials by incorporating a life-cycle perspective [e.g., ([Shatkin, 2008](#); [EnvironmentalDefense - DuPontNanoPartnership, 2007](#); [Thomas and Sayre, 2005](#))] or by using collective expert judgment methods [e.g., ([Kandlikar et al., 2007](#); [Morgan, 2005](#))], primarily in a risk management context. Although the present document differs somewhat from these other efforts in its purpose—namely, this document is intended to aid in the development of research strategies that support individual assessments that subsequently could be used to evaluate nanomaterial risks—all of these endeavors complement and reinforce one another.

1.2. Purpose of this Document

This document represents the “Compile Information in CEA Framework” step of the CEA process (Figure 1-2). As such, it has supported the next step of the process, identifying and prioritizing information gaps about nano-Ag that could be relevant to conducting a CEA of nanomaterials. This document was externally reviewed prior to the collective judgment step of the CEA process and again before its final publication here to help ensure that all relevant sources were considered. This document does not, however, purport to present an exhaustive review of the literature.⁴ Instead, the document attempts to illustrate the information available from the literature within each area of the CEA framework

⁴The information used to populate this report is up to date as of March 1, 2011, when the last broad literature search to identify new information was conducted. New literature identified from the March 2011 search was incorporated into this document if the study provided added value (i.e., filled a previous data gap or elucidated a process or outcome that was previously ambiguous or unclear) to the External Review Draft released in August 2010. In some cases, information released after March 1, 2011 also was added to this document if the information was explicitly requested during peer review and provided unique insight to the implications associated with the specific application of nano-Ag in spray disinfectant.

to aid research planning that supports future assessment efforts. Thus, this case study is not an actual assessment and does not provide conclusions on potential ecological or human health impacts related to nano-Ag.

Further, it must be emphasized that this case study has been developed without a specific regulatory or policy objective in mind. EPA has the authority to regulate disinfectant spray products containing nano-Ag under the Federal Insecticide, Fungicide, and Rodenticide Act (7 U.S.C. §136), and such products might be of interest in various other policy and regulatory contexts. This document, however, is not intended to serve as a basis for near-term risk management decisions on this specific nanomaterial use.⁵ Rather, as stated above, the intent is to use this document to identify scientific and technical information that could be pertinent for future assessment efforts. The results of future assessments might, of course, provide input to policy and regulatory decision-making at that time.

When implemented for informing risk management decisions, the CEA approach is meant to be comparative, examining the relative risks and benefits of different formulation options, for example. The focus of a comparative CEA would be guided by risk management objectives. For example, nano-Ag disinfectant spray products might be compared to disinfectants containing conventional silver, or the comparison might be to a different nanomaterial formulation, such as nano-TiO₂, or to a non-spray product type or some other variable. Given that a number of different options could be of interest to risk managers, considering every potential option in the present case study is not feasible. Therefore, this document focuses solely on nano-Ag as it might be used in disinfectant spray, which is also consistent with the fact that the case study is not intended to be an assessment, but rather is meant to assist in identifying and prioritizing research related to nano-Ag that would support future assessment efforts.

1.3. How to Read this Document

As discussed above, this document presents a case study of nano-Ag in spray disinfectants with chapters corresponding to the main elements of the CEA framework (Figure 1-1). First, Chapter 2

⁵Other EPA efforts are concerned with scientific issues relevant to nanomaterials within a regulatory context. A notable example is a recent review by a Federal Insecticide, Fungicide, and Rodenticide Act Scientific Advisory Panel on hazard and exposure issues related to nano-Ag pesticide products ([U.S. EPA, 2010b](#)). As noted in the review, the Panel's purpose is to provide advice and recommendations to EPA on pesticides regarding "the impact of regulatory actions on health and the environment" (p. ii). Although this purpose fundamentally differs from that of this case study, much of the information included in the Panel's review is relevant to this case study (reflected by the fact that both publications cite many of the same literature sources). Furthermore, the potential data gaps identified in the workshop based on this case study and discussed in the last chapter of this document are generally consistent with the research needs the Federal Insecticide, Fungicide, and Rodenticide Act Scientific Advisory Panel identified.

provides an introduction to the physicochemical characteristics, historical context, and current uses of nano-Ag. Chapter 3 then describes the first level of the CEA framework, product life cycle, and the potential for release of nano-Ag and its by-products at each life-cycle stage. Chapter 4 describes the transport, transformation, and fate of nano-Ag in environmental compartments. Chapter 5 examines the potential for exposure of various receptors to nano-Ag and related contaminants, and Chapter 6 summarizes the ecological and human health effects associated with those exposures. Finally, Chapter 7 provides a high-level summary of the identified information and data gaps and describes how these findings fit into the remainder of the CEA process. Although organizing individual chapters on the current knowledge and apparent data gaps related to each main framework element facilitates a logical organization and sequential presentation of information, it also results in some compartmentalization into chapters and subsections. The document attempts to bridge such compartmentalization with cross-references between sections and the inclusion of summaries at the end of each chapter.

The information presented here was obtained from a variety of published and unpublished sources, including corporate websites and personal communications, and some information is based on inferences drawn from other materials or applications. Such information sources are used because of the limited amount of published materials on nano-Ag and its applications in the peer-reviewed literature, coupled with the limited mechanisms for making manufacturer-specific data publicly available. Given that this case study is not an assessment but, rather, a means to identify information gaps and research questions, the use of a range of information sources seems justifiable.

As discussed above and again in the summary, Chapter 7, this document is not an end in itself. The information presented in the case study served as a starting point for a workshop process during which participants from diverse technical disciplines and economic sectors identified and prioritized information gaps. This workshop process was funded by EPA and conducted independently by an EPA contractor. The focus of this workshop was to gather input on “what might we need to know to be able to conduct a CEA of nano-Ag in disinfectant spray products?” The prioritized research questions and the themes workshop participants grouped them into are listed in Appendix D, which is an excerpt of the contractor’s Workshop Summary Report ([ICF, 2011](#)). More information on the workshop, its outcomes, and the CEA process as a whole can be found in Chapter 7 and in the Workshop Summary Report ([ICF, 2011](#)).

1.4. Terminology

A number of terms used in the field of nanotechnology have specialized meanings, and definitions of certain terms could have important legal, regulatory, and policy implications. Not surprisingly, perhaps, defining such words, including the term nanomaterial itself, has often been a matter of considerable

interest and debate. For the purposes of this document, however, having a connotative definition that states the necessary and sufficient conditions that define a nanomaterial is not deemed necessary. Instead, a denotative approach is used; that is, the term “nanomaterial” denotes something that would generally be considered (or at least appears to be) an example of a material or a product that incorporates an engineered nanoscale material, regardless of whether a consensus exists regarding what properties or characteristics qualify it as such.

Although this case study focuses on “nano-Ag,” readers should note that this term encompasses a variety of materials that might possess a range of physicochemical properties. As a result, not all materials referred to as nano-Ag will necessarily behave in the same manner and exert the same biological effects. Thus, caution in extrapolating from one nano-Ag formulation to another when assessing hazards is appropriate ([U.S. EPA, 2010b](#)). Conversely, until more information is available to discern more precisely how various formulations differ in behavior and effects, pooling information from multiple sources can be useful for the purpose of this document, namely to identify potential research directions to pursue.

Some other terms used throughout this document are discussed below, primarily to explain how the terms are used here rather than to attempt to provide a formal definition of them.

- **Nano-Ag.** This document focuses primarily on engineered nanoscale silver (nano-Ag), which usually is in the form of particles in the 1- to 100-nm size range. The term “nano-Ag,” as it is used in this document, refers to a variety of formulations containing silver particles that meet this size-based definition. When reading this document, it is important to understand that the general use of this term encompasses specific formulations that can display a range of characteristics and behaviors depending on the properties of the particle, the experimental or environmental conditions, and other factors.⁶ Where information is not specific to nano-Ag, the term silver is used without the “nano” prefix.
- **Conventional silver.** To make an explicit distinction between the nanoscale material and other forms of silver not specifically engineered at the nanoscale, the term “conventional” is used in this document. Even so, materials described as conventional often contain a range of particle sizes; including some with nanoscale dimensions (see the definition of “colloid” below). In the scientific and technical literature on silver, the terms “**bulk**” and “**ionic**” also are often used to distinguish conventional from nanoscale silver. Additionally, terms such as ultrafine, particulate matter less than 0.1 micrometer (μm) diameter, and micronized grade have been used to denote nanoscale particles, but typically in a particular context or field of specialization such as aerosols and air pollution.
- **Aggregate and agglomerate.** As discussed in Chapter 4, in many circumstances primary nanoscale particles can aggregate or agglomerate into secondary particles with dimensions greater than 100 nm (a cluster that is sometimes referred to as a colloid, as described in the next paragraph). Specifically, the terms “aggregate” and “agglomerate” are used in the literature on nanomaterials and other fields to indicate the clustering of particles into a

⁶Where sources have provided documentation on size, surface coating, extent of clustering, and other salient properties or characteristics, this information is included in the case study with sources referenced appropriately.

single entity of such particles. These two terms can have specific meanings. For example, the British Standards Institution ([BSI, 2007](#)) defines aggregate as a “particle comprising strongly bonded or fused particles where the resulting external surface area may be significantly smaller than the sum of calculated surface areas of the individual components” and notes that “the forces holding an aggregate together are strong forces, for example, covalent bonds, or those resulting from sintering or complex physical entanglement.” The British Standards Institution defines agglomerate as a “collection of loosely bound particles or aggregates or mixtures of the two where the resulting external surface area is similar to the sum of the surface areas of the individual components” and notes that “the forces holding an agglomerate together are weak forces, for example van der Waals forces, as well as simple physical entanglement.” However, the meanings of aggregate and agglomerate have sometimes been interchanged, as noted by Nichols et al. ([2002](#)). This difference in meanings across, and sometimes within, the various fields that contribute to nanomaterials research highlights the emerging and multidisciplinary nature of the nanotechnology field. The nanotechnology community is an amalgam of investigators who all study nanoscale materials but whose scientific roots are in a variety of other, mature fields spanning toxicology, ecology, colloid science, materials science, and many other disciplines. The customary terminology for aggregates and agglomerates might be well established within one field, but use of these terms can elicit different interpretations within another; as a result, the definitions for these terms are not specific, nor are they consistent. Given this inconsistency in usage and, more importantly, the frequent lack of adequate information to determine which term might be more appropriately applied in a particular study or report, the term “cluster” is used in this document to subsume both aggregates and agglomerates of nanoparticles. This term has precedent within multiple disciplines and avoids confusion between potentially inconsistent connotations of the other terms. Note that, in addition to being used as a noun (as explained above), the word “aggregate” is used as an adjective (primarily in Chapter 5) to refer to exposure to a given material from multiple sources, pathways, and routes.

- **Colloid.** A “colloid” is a dynamic particle or cluster of particles often defined on the basis of size (i.e., at least one dimension between 1 and 1,000 nm) and suspended in a given medium ([Stumm and Morgan, 1995](#)); however, the term can be used rather loosely in the literature specific to nanomaterials. Wijnhoven et al. ([2009b](#)), for example, refer to colloidal silver as comprising silver particles primarily in the range of 250 to 400 nm, thereby distinguishing nano-Ag and colloidal silver. By contrast, Luoma ([2008](#)) describes a colloidal particle as containing multiple atoms of a substance measuring between 1 and 1,000 nm, and thus a colloid might or might not be a nanoparticle in that context. In this case study, although the term colloid is used at times to refer to a sub-microscale particle (especially if a cited publication uses this terminology), either the more specific term “nanoscale” or a specific size range is used when the particle size is salient to the discussion. The extent to which the properties of a cluster of primary nano-Ag particles that exceeds 100 nm are similar to the properties of conventional silver is unclear. Also unclear is the extent to which changes in conditions might initiate the formation, decomposition, or dissolution of a cluster, and there is uncertainty as well regarding what specific factors drive important changes in conditions. As will be discussed in Chapter 4, disaggregation can occur under some conditions. Given these considerations, this document does not use 100 nm as the essential and exclusive criterion for considering what might be relevant to an evaluation of nano-Ag.
- **Naturally occurring, incidental, and engineered nanoparticles.** In addition to distinctions based on size of particles, The Project on Emerging Nanotechnologies ([2009](#)) divides nanoscale materials into three classes based on the origin of the particles. Naturally




occurring nanosized particles include, for example, particles that originate from volcanic explosions, ocean spray, and soil and sediment weathering and biomineralization processes (which can result in crystals of aluminum and iron oxides with nanometer-scale dimensions). The second class is incidental nanosized particles, which are generated as by-products of processes such as combustion, cooking, or welding. The focus of this report is on the third class of nanoscale materials, engineered nanomaterials. This class comprises materials purposely generated for a specific function, such as the carbon nanotubes used in tennis rackets to make them lighter and stronger. In this case study, unless otherwise specified, references to nano-Ag indicate engineered nanoscale materials. Non-engineered types of nanosized silver (from the first or second class) are referred to as nanoscale silver, rather than nano-Ag.

This page intentionally left blank.

Chapter 2. Introduction to Silver and Nanoscale Silver

2.1. Conventional Silver: Uses, Occurrence in the Environment, and U.S. Standards

Silver (Ag) is rarely found in its pure, free form, but rather is more commonly found as an alloy with gold and other metals. Silver is also associated with minerals, the predominant form of which is argentite (Ag_2S), followed by cerargyrite (AgCl). Other minerals containing silver, in order of prevalence, are proustite (Ag_3AsS_3), pyrargyrite (Ag_3SbS_3), and stephanite (Ag_5SbS_4). Silver can exist in its metallic state (Ag^0) and in three cationic states (Ag^+ , Ag^{2+} , and Ag^{3+}), with Ag^0 and Ag^+ being most common (Lide, 2000). The most abundant silver compounds in the environment are silver sulfide (Ag_2S), silver nitrate (AgNO_3), and silver chloride (AgCl) (Wiberg et al., 2001).

 Silver is naturally released into the environment by wind and water erosion of soils and rocks containing silver. Earth's crust contains approximately 0.1 part per million (ppm) of silver, and soils  contain approximately 0.3 ppm (Boyle, 1968). Ambient water concentrations as high as 0.2 microgram per liter ($\mu\text{g/L}$) in fresh water and 0.25 $\mu\text{g/L}$ in sea water have been reported, and background silver has also been found in biota at levels of micrograms per gram ($\mu\text{g/g}$) of tissue, particularly in fish and shellfish (ATSDR, 1990). 

2.1.1. Uses of Silver and Silver Compounds

The use of silver pre-dates 2500 B.C., when the Chaldeans in present-day Iraq and Kuwait had mastered a mining technique to extract silver from lead ores. In addition to using silver as a durable metal in the production of jewelry, coins, and utensils, ancient peoples also recognized its potential to keep liquids sterile (The Silver Institute, 2009a). The Greek historian Herodotus recorded that Cyrus the Great, King of Persia from 559 B.C. to 530 B.C., had water drawn from a stream and “boiled, and very many four-wheeled wagons drawn by mules carry it in silver vessels, following the king wherever he goes at any time” (Herodotus, 1920).

The use of silver compounds for therapeutic purposes has a long history. In the 18th century, silver nitrate, often called lunar caustic, was molded into pencil-like forms and used to remove granulation tissue from wounds and to lance abscesses, while powdered silver nitrate was used to kill impurities and

to dry open wounds ([Klasen, 2000](#)). In the 19th century, physicians used silver nitrate to promote healing of burns and other wounds, and others began to research the bactericidal effects of silver. As early as 1880, physicians used a silver nitrate eye-drop solution to prevent gonococcal conjunctivitis in newborns. In the early 20th century, surgeons used silver foil, silver sutures, and other silver dressings to prevent infection in surgical wounds. Today, wound dressings containing silver and silver-based vascular and urinary catheters are used in healthcare ([Chopra, 2007](#)).

In 1839, Louis-Jacques-Mandé introduced a photographic technique that used a silver-plated sheet of copper, sensitized with iodide vapors to make the silver react with light, and a salt solution to permanently set the image on the sheet ([Metropolitan Museum of Art Department of Photography, 2004](#)). Silver is still used in photography today, but with the advent of digital photography, the percentage of its total usage continues to decline, dropping from 39% in 1979 to 13% in 2008 ([GFMS Limited, 2009](#)).

Silver has the highest thermal and electrical conductivities of any pure metal across a range of temperatures ([Lide, 2000](#)), and is therefore used in industrial applications such as household switches, switch panels in electrical appliances, batteries, and superconductors ([The Silver Institute, 2009b](#)). In 2008, industrial applications of silver accounted for 54% of the total silver used in manufacturing ([GFMS Limited, 2009](#)). Jewelry (19%), silverware (7%), and coins (8%) account for the remaining silver used in manufacturing ([GFMS Limited, 2009](#)). Other industrial uses of silver include as coatings on mirrors and compact discs, in water purification systems, as antibacterial disinfectants, and in rear window defrosters in automobiles ([The Silver Institute, 2009b](#)).

Silver iodide is used for cloud seeding. This process introduces silver iodide to clouds to induce contact freezing of supercooled liquid water (colder than 0 °C) so that the amount or type of precipitation that falls from clouds is altered ([StroyprojectLTD, 2009](#)). Supercooled liquid water is chemically unstable and thus freezes upon contact with silver iodide, an artificial ice nucleus. Freezing releases heat to the environment, thereby adding energy to the system and possibly increasing the intensity or duration of precipitation. Silver iodide can be introduced via aircraft or by ground-level dispersion devices (e.g., rockets, anti-aircraft guns, generators). The efficacy of cloud seeding is unknown, but the practice is popular in geographic locations where freshwater supplies are scarce ([U.S. NCAR, 2006](#)).

2.1.2. Occurrence of Silver in the Environment

Industrial processes such as smelting and mining, photography, and jewelry manufacture have led to elevated levels of silver being released into the environment ([U.S. EPA, 1987](#)). Typically, areas of elevated silver concentrations occur near sewage outfalls, electroplating plants, mine waste sites, and silver iodide-seeded areas ([Eisler, 1996](#)). Runoff from silver disposal sites can transport silver farther from these locations, and subsequent human activities such as dredging and construction can further

Table 2-1. Selected U.S. studies of silver contamination in the environment.

Location	Anthropogenic source	Medium	Levels measured	Source
Quinnipiac River, Connecticut	Manufacturing of silver tableware and decorative items	Water	5–500 nanograms per liter (ng/L) Max = 800 ng/L	Rozan et al. (1995)
		Sediment	15–30 micrograms per gram (µg/g) Max = 250 µg/g	
		Effluent from municipal wastewater treatment plant	120–180 ng/L	
San Francisco Bay Lower South Bay	Municipal wastewater treatment plant handling discharge from a photo processing facility	Surface sediments	0.052–1.18 µg/g, dry weight Mean = 0.388 µg/g, dry weight	Flegal et al. (2007)
		Surface water	<0.1–26.3 ng/L (total dissolved silver between 1989 and 2005)	
Michigan	None specified	Surface soil	0.5 ± 0.2 µg/g (commercial) 0.8 ± 0.5 µg/g (residential) 2.3 ± 2.2 µg/g (industrial)	Murray et al. (2004)
		Sub-surface soil	0.6 ± 0.4 µg/g (commercial) 0.5 ± 1.1 µg/g (residential) 2.2 ± 4.0 µg/g (industrial)	

transport the silver (Purcell and Peters, 1998). As presented in Table 2-1, silver contamination has been studied in several U.S. locations including the Quinnipiac River (Connecticut) (Rozan and Hunter, 2001; Rozan et al., 1995), San Francisco Bay (Flegal et al., 2007), and various sites in Michigan (Murray et al., 2004).

In the Quinnipiac River, Rozan et al. (1995) and Rozan and Hunter (2001) found that silver concentrations in the river water peaked at 800 nanograms per liter (ng/L) following rainstorms due to erosion of the silver-laden soil on the river banks and resuspension of contaminated sediments. Using cesium-137, Rozan et al. (1995) dated the highest concentrations of silver in the river bank to the 1950s, corresponding to the peak production period of the local silver industry.

Locally elevated silver concentrations have been observed in surface water near facilities that manufacture or dispose of products containing silver, including facilities that process photographs and a silver plating facility (Luoma, 2008). Ecological and toxicological effects have been linked to silver concentrations in the environment in the range of 10–100 ng/L (or lower) as demonstrated by several field and dietary toxicity studies summarized by Luoma (2008) and described here. Hornberger et al. (2000) observed biochemical signs of stress, most notably failure to reproduce, in clam species (*Corbula amurensis*) on a mudflat 2 kilometers (km) from a domestic-sewage outfall in South San Francisco Bay. Over a 30-year period, after the passage of the Clean Water Act in 1972, the amount of silver and other metals in the waste delivered to this sewage facility decreased, and the facility also improved its treatment process for wastes containing silver by adding trickle filters, clarifiers, nitrification processes, and increased retention time, and implementing other specific source controls. With these changes, the

amount of metals discharged from the sewage facility to the bay decreased. The reproductive capabilities of the clams subsequently recovered as evidenced by an increased number of months in which mature gametes were observed and an increased proportion of the population with mature reproductive tissues ([Hornberger et al., 2000](#)).

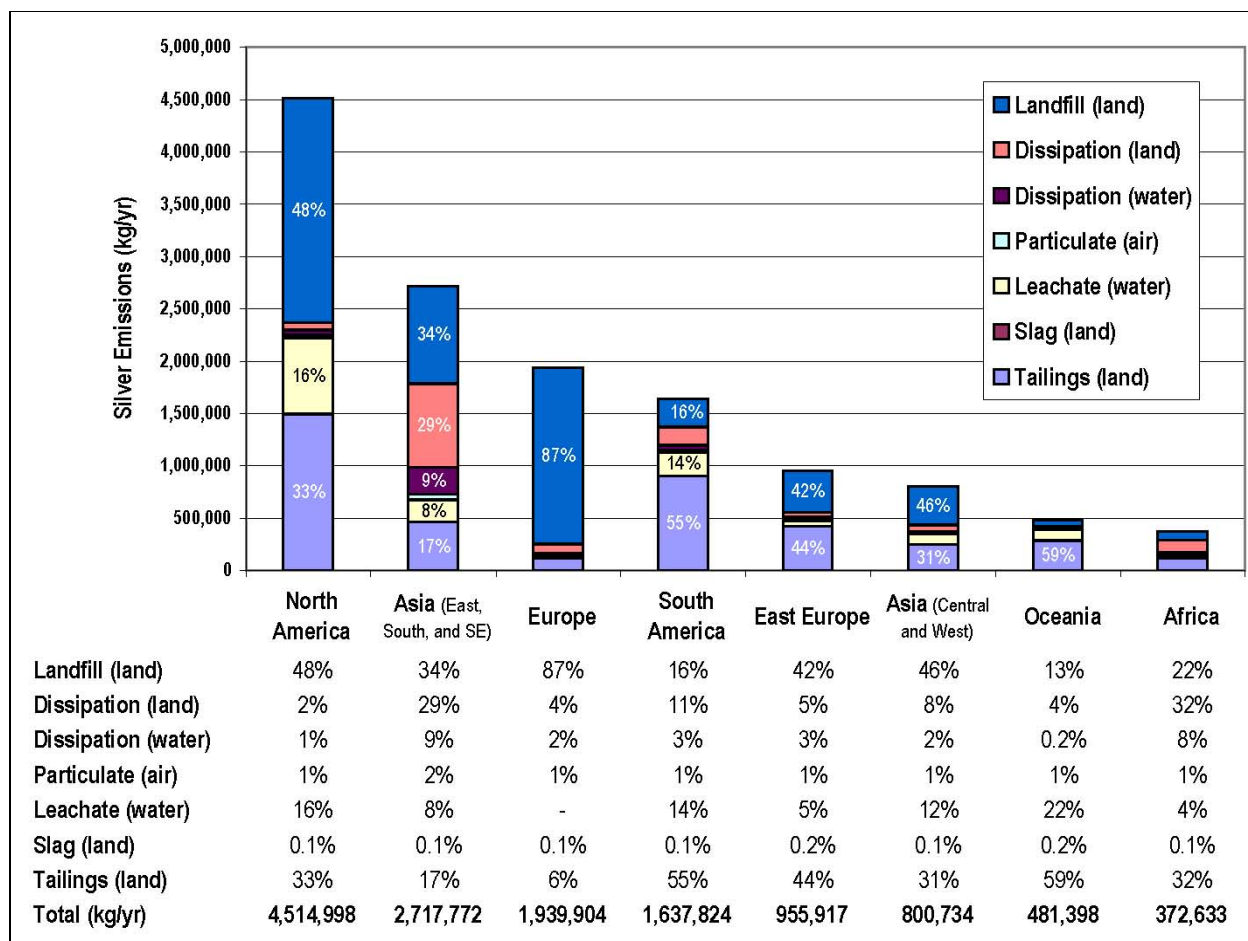
In 1978, an estimated 2.47 million kilograms (kg) of silver was emitted to the environment by the United States alone ([Smith and Carson, 1977](#)). Eighty-two percent of the annual silver loss originated from anthropogenic activities (42% from the photography industry) ([Smith and Carson, 1977](#)). In 1978, 3.7% of released silver entered the atmosphere, 28.5% ended up in the aquatic environment, and 67.8% entered the terrestrial environment ([Smith and Carson, 1977](#)).

More recently, Eckelman and Graedel ([2007](#)) characterized the emissions of silver based on data and estimations of environmental releases of silver in 1997 (Figure 2-1). Their assessment began with data on silver production, fabrication, and import/export, which were collected and estimated in a material flow analysis for 64 countries by Johnson et al. ([2005](#)). Johnson et al. concluded that their material flow analysis comprised “well over 90%” of the global silver flow, including mining and production, fabrication and manufacture, use, and waste management. Eckelman and Graedel ([2007](#)) further characterized the losses of silver by applying a series of assumptions about the percentage of silver lost in each process. For example, they assumed particulate silver emissions from incineration of municipal solid waste varied directly with the overall income level of the country, ranging from an emission factor of 0.1% for high-income countries to 0.4% for low-income countries. The variance was due to the type of furnace and pollution control technology used; the researchers assumed that high-income countries employ control technologies that are more modern and more efficient than those used in low-income countries. Thus, in high-income countries, more of the silver is captured before it is emitted to the environment resulting in a lower emission rate.

Eckelman and Graedel calculated silver emissions for 64 countries, and Figure 2-1 presents their estimates of silver emissions aggregated by geographical regions worldwide. The reported values do not account for transport of the silver from one medium (i.e., air, land, or water) to another after initial emissions. Eckelman and Graedel ([2007](#)) estimated 65% of the 2.84 million kg of silver emitted from the United States enters landfills, 18% is released to the environment via tailings and 13% is contained in leachate from the mining and productions process.

2.1.3. U.S. Standards for Environmental Silver

The U.S. Environmental Protection Agency’s (EPA’s) National Secondary Drinking Water Regulations recommend a guideline of less than 0.10 milligram per liter (mg/L) (or ppm) of total silver in



Source: Adapted with permission from Eckelman and Graedel (2007)

Figure 2-1. Silver emissions to the environment by geographical region.

The original analysis by Eckelman and Graedel (2007) examined silver emissions in 64 countries. For this report, the data have been aggregated according to the United Nations' geographical regions (U.N. Statistics Division, 2008).

North America: Canada, Mexico, United States

Asia (East, South, Southeast): China, Hong Kong, India, Indonesia, Iran, Japan, Malaysia, Philippines, Singapore, South Korea, Taiwan, Thailand

Europe: Austria, Bel-Lux, Denmark, Finland, France, Germany, Greece, Italy, Netherlands, Norway, Portugal, Spain, Sweden, United Kingdom

South America: Argentina, Bolivia, Brazil, Chile, Colombia, Peru, Venezuela

East Europe: Bulgaria, Poland, Romania, Russia, Ukraine

Asia (Central and West): Israel, Kazakhstan, Saudi Arabia, Turkey, UAE, Uzbekistan

Oceania: Australia, New Zealand

Africa: Algeria, Cameroon, Egypt, Ethiopia, Ghana, Ivory Coast, Kenya, Morocco, Namibia and South Africa, Nigeria, Sudan, Tanzania, Tunisia, Uganda, Zimbabwe

drinking water due to the potential cosmetic (not health) effects of silver ingestion, specifically argyria (i.e., an accumulation of silver in the skin that causes it to turn blue or bluish-gray) (U.S. EPA, 2009g). States may decide to enforce this standard, but enforcement is not required. Due to lack of evidence, EPA has not prescribed ambient water quality criteria for silver for human health (i.e., to protect from exposure to silver by consumption of contaminated water or organisms).

With respect to chronic water quality criteria to protect aquatic life, a few states have set or proposed threshold concentrations; for example, the North Carolina Division of Water Quality has

proposed a criterion of 0.06 µg/L ([NC DEHNR, 2007](#)). Oregon has established a 0.12-µg/L criterion in its Administrative Rules based on chronic toxicity to rainbow trout and minnows in fresh water and to mysids in salt water ([Oregon Department of Environmental Quality, 2004](#)). Texas, New York, and some regions in California have established similar chronic aquatic life criteria concentrations. Several regions in California have established maximum contaminant levels for silver between 5 and 10 µg/L. EPA proposed and then withdrew a chronic toxicity standard in the early 1990s on the grounds that additional research was needed to support the available database in the development of chronic ambient water quality criteria ([Ford, 2001](#); [U.S. EPA, 1987](#)). The Agency has, however, prescribed maximum acute concentrations of 3.2 µg/L in fresh water and 1.9 µg/L in salt water, based on acute toxicity of silver to macroinvertebrates and fish ([U.S. EPA, 2009f](#)), which is discussed in detail in Section 6.2.2. These standards are enforced through the issuance of discharge permits at the state level.

In addition to drinking water and water quality regulations, several other national and state-level regulations have been established for silver and silver compounds. An oral reference dose for silver of 0.005 milligram per kilogram per day (mg/kg-day) is included in EPA's Health Effects Summary Tables ([U.S. EPA, 2003a](#)) and in the Integrated Risk Information System database ([U.S. EPA, 2012](#)). This reference dose is based on a chronic human exposure study carried out by Gaul and Staud ([1935](#)). An occupational exposure limit of 0.01 milligram per cubic meter (mg/m³) has been derived for silver metal, compounds, and soluble silver compounds by the Occupational Safety and Health Administration ([OSHA, 2010](#)) and by the American Conference of Governmental Industrial Hygienists ([ACGIH, 2010](#)). The National Institute for Occupational Safety and Health ([NIOSH, 2010](#)) has similarly recommended an 8-hour, time-weighted average exposure limit of 0.01 mg/m³ for silver metal dust and soluble compounds. Silver is also on the list of chemicals subject to Section 313 of the Emergency Planning and Community Right-to-Know Act of 1986 ([U.S. EPA, 2010a](#)).

2.2. Historical and Emerging Uses of Nanoscale Silver

Nanoscale silver is not new. The Lycurgus Cup, a glass and bronze cup on display at the British Museum, was likely created in the 4th century A.D. ([Evanoff and Chumanov, 2005](#)). The glass in the cup appears green until light is shone through it, shifting the absorption spectrum so that the glass appears to glow red. Small gold and silver particles incorporated in the glass by the original craftsman cause the shift in the apparent color of the cup; in the 1990s, researchers at the British Museum determined the average diameter of the gold and silver particles in the glass to be 70 nanometers (nm). The Lycurgus Cup therefore represents what is likely one of the first uses of nanoscale silver. Nanoscale silver also has been

found in stained glass. The unique optical properties of nanoscale silver that prompted these early uses are discussed further in Section 2.3.7.



The literature suggests that products containing colloidal silver have been available (although not necessarily registered or supported by science) for use by humans as therapeutic agents for more than 100 years (Bottomly et al., 1909), and colloidal silver suspensions containing some particles with at least one dimension in the 1- to 100-nm range were likely employed long before their use in these applications was recorded. For example, Nowack et al. (2011) described several specific silver-based pesticides, medications, and other applications that have been in use for many decades that contain nano-sized silver particles, including some products for which particles were intentionally formulated at the nanoscale.

The specific forms of nanoscale silver used over the past 100 years in consumer products and other applications are not clear, and researchers have made the case that nanoscale particles of silver have likely been present in many (or perhaps most) of the silver products in use over time (Nowack et al., 2011). The ability to control and visualize matter at the nanoscale, however, has advanced considerably in recent years. The evolution of such techniques has allowed for stricter control over physicochemical properties of engineered nanoscale silver and greater accuracy in distinguishing single silver nanoparticles from clusters of silver nanoparticles and larger particles of silver. As a result, when precise engineering, detection, and identification of nanoscale silver became possible, the term nano-Ag was generally substituted for the term colloidal silver when referring to relatively monodisperse particles intentionally engineered at the nanoscale. The term colloidal silver is still used as defined in Section 1.4.⁷

A report by Hendren et al. (2011) is the only study to date to estimate production volumes of raw nano-Ag (i.e., nano-Ag not incorporated into products) in the United States. They estimated a range of nano-Ag production volumes using information from websites and personal communications with manufacturers explicitly producing nano-Ag (as opposed to colloidal silver), and they filled in gaps with data extrapolated from proxy parameters (e.g., number of employees, maximum possible order sizes, annual sales revenues). Hendren et al. (2011) estimated the lower bound of U.S. nano-Ag production at 2.8 tons per year and the upper bound at 20 tons per year. These estimates relied primarily on extrapolations using the number of employees at manufacturing companies as a proxy parameter from which to estimate production volumes; uncertainty in this estimated range is therefore high.

Over the past several years, the Woodrow Wilson Center's Project on Emerging Nanotechnologies (PEN) has compiled an inventory of consumer products reported by their manufacturers to contain

⁷This report generally uses the nomenclature provided by study authors in the literature. The distinction between colloidal silver and nano-Ag, as provided here, however, is not used consistently in the literature. And, as mentioned previously, the distinction in terms might be misleading due to the overlap in size ranges between colloidal silver and nano-Ag.

nanomaterials. The products in this inventory were identified through Internet searches for products reported by their manufacturers or distributors to contain silver nanoparticles. Not all manufacturers' claims that products listed in the PEN inventory contain engineered nanoparticles have been independently or scientifically validated. Based on the (unverified) data PEN has collected, however, nano-Ag is one of the most commonly used nanomaterials in manufactured consumer products,⁸ second only to carbonaceous nanomaterials ([Quadros and Marr, 2010](#)). Of the more than 1,317 consumer products included in the March 2011 PEN inventory of nanomaterial-based consumer products, nearly 25% are listed as containing nano-Ag. Consumer products based on nano-Ag represent a significant fraction of every product category examined for the PEN inventory. From March 2006 to March 2011, the number of products reported to contain nano-Ag rose from 25 to 313, a more than 10-fold increase.⁹ The inventory does not account for products that have since been removed from the market, however, so these values more accurately reflect the total amount of products that have been introduced to the market over time rather than the total amount of products currently available on the market.

The PEN Silver Nanotechnology Consumer Product Inventory contains detailed information about current consumer products reportedly containing nano-Ag and indicates that most nano-Ag products claim to eliminate bacteria and their related odors ([Project on Emerging Nanotechnologies, 2009](#); [Fauss, 2008](#)). For instance, manufacturers have introduced nano-Ag into cooking utensils to prevent bacterial contamination and to reinforce the strength of the utensils. For similar reasons, nano-Ag also has been incorporated into materials used to produce clothing, socks, fabrics, and shoe soles. Some products, such as dietary supplements, laundry detergent, body soap, toothpaste, and wall paint, appear to contain colloidal nano-Ag. One manufacturer suggests that dietary supplements containing nano-Ag promote a healthy immune system by inhibiting the growth of and possibly destroying bacteria and viruses in the digestive tract ([ConSealInternational, 2010](#)). One manufacturer claims that nano-Ag supplements can defend the body from "colds, flu, and hundreds of diseases (even anthrax)" and that silver has been used throughout history as a cure for more than 650 diseases, from AIDS to cancer ([Melchizedek, 2010](#)). Other products to which nano-Ag reportedly has been added include home furnishings, cleaning products, food storage containers, kitchen appliances, curling irons, hair dryers, make-up, burn creams, nasal sprays, soaps, dish detergents, and medical products, some of which might not be included in the PEN consumer product inventory ([Wijnhoven et al., 2009b](#)).

Spray disinfectants represent a category of the nano-Ag cleaning products that could become available for use in the home, garden, or other settings such as hospitals in the United States. Products

⁸The Project on Emerging Technologies' Consumer Products Inventory website at <http://www.nanotechproject.org/inventories/consumer>.

⁹Ibid.

intended to disinfect inanimate objects or otherwise control microorganisms, except on or within living humans or animals, are considered “pesticides,” and federal law requires that EPA register such products before they may lawfully be sold or distributed in the United States (7 U.S.C. § 136). Spray disinfectants containing nano-Ag particles might be more effective, for example, at killing bacteria than those made with larger, conventional silver particles due to the higher surface area-to-volume ratios of the smaller particles, which could result in greater reactivity (see Chapter 6). Some manufacturers have claimed that aerosol disinfectant sprays containing nano-Ag kill 99% of bacteria on various surfaces and prevent odor for long periods of time ([ConSealInternational, 2010](#); [Shanghai Huzheng Nanotechnology Co., 2009](#)). Theoretically, nano-Ag sprays could also serve as broad-spectrum fungicides, and the sprays could exhibit antiviral properties ([Sun et al., 2005](#); [Wright et al., 1999](#)). No sources were identified that compare the bactericidal or fungicidal properties of disinfectant sprays containing nano-Ag with sprays containing conventional silver. Several laboratory studies, however, have compared the effects of nano-Ag and ionic silver in a number of types of microorganisms (See Section 6.2.1).

The expanding use of nano-Ag in the consumer market suggests that, depending on the behavior of nano-Ag in the environment, background concentrations of silver, in nano and non-nano form, are anticipated to increase in some environmental media and thus could represent additional sources of long-term and incremental exposure to both humans and biota. In the home, nano-Ag spray disinfectants might be applied to walls, tables, beds, and other surfaces in order to kill harmful bacteria, particularly in the kitchen and bathroom. Outside of the home, spray disinfectants with nano-Ag might be used in hospitals, nursing homes, airports, and other public places in efforts to protect people from illness and disease.

As described in the list of key terms in Section 1.4 of this case study, materials containing colloidal silver typically contain silver particles of nanoscale dimensions. Consequently, information on conventional silver can inform the development of a comprehensive environmental assessment (CEA) for nano-Ag used in disinfectant sprays, and therefore this case study includes some information on conventional silver. At the beginning of each effects subsection, for example, is a brief summary of the conventional silver effects on the organisms of interest for that section. It is important to keep in mind though that this case study is focused on silver particles that have been specifically engineered to have nanoscale characteristics and on the fate, exposures, and effects specific to nano-Ag. Therefore, studies in which the nanoscale properties of the silver were systematically evaluated are particularly emphasized in this case study. This nuance must be considered in determining the appropriate interpretation and use of conventional silver data within the context of a nano-Ag-specific CEA.

2.3. Physicochemical Properties of Nanoscale Silver

The physicochemical properties of nanoparticles determine both their fate in the environment as well as their beneficial and harmful effects. Although the size of the nanoparticles can be the most distinguishing property when compared to conventional particles, other unique physical and chemical properties begin to emerge as particles approach the nanoscale range. For this reason, Auffan et al. suggest that “below a critical size, it is not possible to simply scale the properties of bulk materials based on the surface area to predict the properties of nanoparticles” ([Auffan et al., 2009b](#)). Other scientists agree that “although some material properties, like chemical composition and crystal structure, are the same on the nanoscale as in the bulk phase, other properties differ ... a nanoparticle retains properties of both materials in the bulk phase and molecular precursors” ([Sayes and Warheit, 2009](#)). Indeed some studies support these assertions ([Griffitt et al., 2009](#)); however, other researchers have found that despite the fact that the physicochemical properties differ, the effects of nano-silver can be similar to those produced by conventional ionic silver ([Pal et al., 2007](#)). These differing findings led the Federal Insecticide, Fungicide, and Rodenticide Act Scientific Advisory Panel ([2010b](#)) to conclude that “comparison[s] of physicochemical properties of the nano [versus] bulk materials are needed.”

Exactly which physicochemical properties of engineered nanoparticles, including nano-Ag, can be useful for predicting their behavior and interactions in the environment is unclear. Several organizations and independent researchers have published recommendations on the physicochemical characterization data that should accompany research findings on transport, transformation, and fate processes and ecological and human toxicity ([U.S. EPA, 2010b](#); [Sayes and Warheit, 2009](#); [MINCharInitiative, 2008](#); [OECD, 2008](#); [Tiede et al., 2008](#); [Oberdörster et al., 2005a](#)). These recommendations are based on a synthesis of published, peer-reviewed studies on the behavior and effects of nanoparticles, but the recommended properties vary by organization and researcher. Some of the recommendations regarding characterization before, during, and after toxicity studies are further described in Section 6.1.1. In general, the most prescribed physicochemical properties include:

- Size, including clustering tendencies;
- Morphology, including shape and crystal structure;
- Surface area;
- Chemical composition;
- Surface chemistry and reactivity;
- Solubility; and
- Conductive, magnetic, and optical properties.

Each property, as it relates to nano-Ag and to the other properties identified, is briefly discussed below. For nano-Ag spray disinfectants, Hansen et al. ([2007](#)) suggest that all of the above properties, with the exception of conductive, magnetic, and optical properties, are relevant to hazard identification. These

properties, which could affect the efficacy of the final product, also could offer clues as to which types of nano-Ag might be preferentially commercialized and thus most relevant to study as potential hazards. Additional details on the state of knowledge of physicochemical properties in relevant environmental compartments, exposure routes, and effects are provided in the chapters that follow.

2.3.1. Size

In recent years, synthesis methods have been developed to produce nanoparticles, including silver nanoparticles, of various shape and size distributions. See, for example, Bar-Ilan et al. (2009), Evanoff and Chumanov (2005), Khaydarov et al. (2009), and Tolaymat et al. (2010). Relatively monodisperse particles can be obtained within the size range of 1–100 nm (see Chapter 3 for synthesis methods).



The size distribution of nanoparticles, including silver nanoparticles, however, does not necessarily remain constant and depends on the chemical and physical environment surrounding the nanoparticles; silver nanoparticles can agglomerate or aggregate to form larger clusters of nanoparticles, as well as disperse into smaller particles or dissociate into ionic forms of silver. How rapidly the particles cluster or disperse in an aqueous medium depends on particle collision frequencies (e.g., Brownian motion and particle concentration), the energy of the particle collisions, the attractive-repulsive properties of the particles involved (e.g., repelling surface charges of two positively charged particles), and the interactions with colloidal materials such as natural organic matter present in the water. Handy et al. (2008b) summarized that “after collision, particles can remain in aqueous phase as single particles or form particle-particle, particle-cluster, and cluster-cluster aggregates.” The dispersion state describes the extent to which particles become clustered by interparticle attractive forces. Surface coatings and stabilizing agents can enhance the stability of the dispersion and maintain the original or intended size distribution.

These phenomena can affect the transport, transformation, and fate of nano-Ag particles in the environment and in humans and biota. Often, coagulation leads to the formation of larger, less mobile particle clusters (AFSSET, 2006; Wiesner et al., 2006; Aitken et al., 2004). Nano-Ag used in some products can enter the environment as individual nanoparticles, as small clusters, or potentially dissolve into ions. In other cases, the nano-Ag incorporated into consumer products as composites or mixtures could be released into the environment in an encapsulated form (Lowry and Casman, 2009). The translocation of particles depends in part on their size; hence, clusters of nano-Ag behave quite differently compared to single particles (Ma-Hock et al., 2007). The size of the nano-Ag (i.e., an individual particle versus a cluster) can determine the likelihood of release of silver ions (Ag^+) from the particle and influence the particle’s behavior in the environment (O'Brien and Cummins, 2009). Moreover, size alone might determine particle mobility in the environment and within the body (Chen and Schluesener, 2008) and enable nano-Ag to enter cells (Bar-Ilan et al., 2009; Morones et al., 2005). As emphasized by the

Federal Insecticide, Fungicide, and Rodenticide Act Scientific Advisory Panel (2010b), however, the impact of size on the biological response elicited by nano-Ag particles is less clear. Size-dependent particle mobility is discussed as it relates to potential biotic and human uptake and dose in Chapter 5, and size-dependent ecological and human health effects are discussed in Chapter 6.

2.3.2. Morphology

Nano-Ag can be synthesized into various forms, including particles, spheres, rods, cubes, truncated triangles, wires, films, and coatings (Wijnhoven et al., 2009b; Pal et al., 2007). The shape of nano-Ag particles can affect the kinetics of their deposition and transport in the environment. Depending on its surface structure and shape, a nano-Ag particle might exhibit different reactivity (Oberdörster et al., 2005a), as its shape could make it difficult for particles to approach each other. Such shape-related interactions can be controlled in some situations by adding detergents or surface coatings to the particles to change their shape or surface charge (Handy et al., 2008b).

Differences in shape and related changes in nano-Ag interactions with other particles or surrounding environmental milieu also can influence particle toxicity, as shown by Pal et al. (2007). Pal et al. (2007) studied the antibacterial activity (using *Escherichia coli*, or *E. coli*) of silver nanoparticles of various shapes. Results indicated that nano-Ag particles of various shapes could kill *E. coli*, but the inhibition results differed based on the percent of active facets in the crystal structure¹⁰. Specifically, truncated triangular silver nanoplates with a {111} lattice plane as the basal plane displayed the strongest biocidal action, compared to the spherical and rod-shaped nano-Ag particles, indicating that increasing the number of active facets on the surface of a crystalline, or highly ordered, nanoparticle increases its ability to inhibit bacterial growth.

Notably, particles with similar morphologies (e.g., spherical particles) can be synthesized with unique crystal structures, a parameter which has been shown to influence the toxicity of nanoscale titanium dioxide [Sayes et al. (2006); see Johnston et al. (2009) for a review of how crystal structure and other physicochemical characteristics influence nanoscale titanium dioxide toxicity]. No data were identified, however, on whether nano-Ag with different crystal structures, but similar shapes, could exhibit different toxicities.

¹⁰Crystal structure refers to the same repeated arrangement, or lattice, throughout the crystal of atoms, molecules, or ions that compose the crystal (Barron and Smith, 2010). Auguste Bravais, a 19th century mathematician and physicist, determined that in 3-dimensional space, 14 lattice configurations are possible such that the arrangements of the points appear identical when viewed from any other point. The crystal structures can be described in terms of the planes that join the points in the lattice. These planes are denoted using Miller Indices, which are the reciprocals of the intercepts of the crystal plane with the x, y, and z three-dimensional axes.

2.3.3. Surface Area

Because of their small size, nano-Ag particles have greater specific surface area and a greater surface area-to-volume ratio when compared to the same mass of material in larger particles ([Auffan et al., 2009b](#); [Luoma, 2008](#)). Auffan et al. estimate that a 10-nm particle has approximately 35–40% of its atoms on the surface compared to 15–20% of the atoms on a particle larger than 30 nm in diameter. This large surface area relative to mass or volume increases the reactivity and sorption behavior of nanoparticles ([U.S. EPA, 2010b](#); [Auffan et al., 2009b](#); [Tiede et al., 2008](#)). Large specific surface area enhances chemical reactivity, which means that smaller silver nanoparticles have more reaction sites (i.e., sites that can receive electrons) on their surfaces and are more sensitive to oxygen, a natural electron donor, as compared to larger particles of the same mass ([Auffan et al., 2009b](#)). Therefore, smaller particles could exhibit greater efficacy as biological agents or stressors in ecosystems or on human health, as discussed in Section 2.3.4.

Surface area also affects the ratio of silver ions on the surface of a silver particle to ions that are “buried” inside the same particle. This ratio usually increases as particle size decreases. Thus, for larger particles with smaller surface area-to-volume ratios, most of the silver ions might be unable to interact with the environment or biological surfaces. This idea is further discussed in Section 6.1.

2.3.4. Chemical Composition

As mentioned previously, silver exists in one of four oxidation states: Ag^0 , Ag^+ , Ag^{2+} , and Ag^{3+} , and the free silver ion under natural conditions is Ag^+ ([Lide, 2000](#)). Of these, Ag^0 and Ag^+ are the most commonly occurring oxidation states in the environment. Based on a review of the existing literature, Wijnhoven et al. ([2009b](#)) concluded that environmental and human health studies appear to demonstrate that forms of conventional silver that release free silver ions are more toxic than other forms of conventional silver that do not. Speciation would therefore strongly influence how much silver is available to affect living organisms. To achieve stability, positively charged silver ions will associate with negatively charged ligands¹¹ (e.g., sulfide in fresh water, sulfide and chloride in salt water) ([Luoma, 2008](#)); the reader is referred to a detailed discussion of this process in Section 4.4. The concentrations of these ligands and the bond strength between the silver ions and the ligands influence the distribution of silver as free silver ions (its more bioavailable form) and the ligand-bound forms, which exhibit varying degrees of bioavailability ([Luoma, 2008](#)).

¹¹ A ligand is a substance (e.g., atom, molecule, radical, or ion) that forms a complex around a central atom (see Section 4.4).

Chemical composition also includes the surface coating of the nanoparticle ([Sayes and Warheit, 2009](#)). Coatings can be used to stabilize the nanoparticles in solution, to prevent clustering, or to add functionality to the nanoparticle depending on its intended use. Surface coatings can influence the reactivity of the nanoparticle in various media including surface water, biological fluids, and laboratory test media ([Auffan et al., 2009b](#); [Cumberland and Lead, 2009](#)).

2.3.5. Solubility

Solubility influences the fate and behavior of nanoparticles in the environment ([Wijnhoven et al., 2009b](#)), as well as the dissolution of the nanomaterial and release of silver ions ([Auffan et al., 2009b](#)). Silver nanoparticles are composed of elemental silver (Ag^0), which is not soluble or reactive in pure water ([Wiberg et al., 2001](#)), but is soluble in acidic solutions (i.e., nitric acid); nanoscale particles have been shown to dissolve completely in less acidic conditions than conventional silver particles ([Elzey and Grassian, 2010](#)). Nano-Ag is also soluble in aqueous solutions under oxidizing conditions. The dissolution of nano-Ag in aqueous solutions involves two coupled processes: (1) oxidation with release of reactive oxygen species and (2) proton-mediated release of dissolved silver ([Liu et al., 2010a](#)). The surface oxidation of nano-Ag results in the formation of highly reactive ionic silver both adsorbed to the surface of the nanoparticle and released to the surrounding milieu. Colloidal suspensions of nano-Ag will therefore contain at least three forms of silver: nano-Ag particles, dissolved silver (both ionic silver and soluble silver complexes), and ionic silver adsorbed to the surface of nano-Ag ([Liu and Hurt, 2010](#)). Silver solids like silver sulfide and silver chloride also will form under certain environmental conditions following release of nano-Ag to the environment, and these solid precipitates exhibit varying degrees of solubility (see Table 2–2). Further, although silver chloride solids exhibit low solubility under normal conditions and silver sulfide is considered to be nearly insoluble ([Lide, 2000](#)), unlike nano-Ag, silver salts require no rate-limiting oxidation step to release silver ions to the surrounding medium ([Gammons and Yu, 1997](#)).

The rate of dissolution also can be considered proportional to particle surface area; therefore, based on surface area alone, smaller nanoparticles should dissolve faster than larger nanoparticles, and nanoparticles in general should dissolve faster than conventional-scale materials ([O'Brien and Cummins, 2009](#)). Liu et al. ([2010a](#)) examined the release rate of soluble silver from nano-Ag of different sizes (4.8 and 60 nm) and from macroscopic silver foil. As expected, the mass-based release rates were inversely proportional to particle size, with the first-order release rate constant for the 4.8-nm particle five orders of magnitude higher than that for macroscopic silver. When the data were renormalized by surface area, however, the variation in rate constants fell from five orders of magnitude to one order of magnitude, demonstrating that in this scenario, surface area drives soluble silver release rates ([Liu et al., 2010a](#)).

Table 2-2. Solubility product constants for various silver solids.

Silver compound	Formula	Solubility product constant (K_{sp})
Silver	Ag	Insoluble
Silver(I) sulfide (α -form)	Ag ₂ S	6.69×10^{-50}
Silver(I) sulfide (β -form)	Ag ₂ S	1.09×10^{-49}
Silver(I) arsenate	Ag ₃ AsO ₄	1.03×10^{-22}
Silver(I) iodide	AgI	8.51×10^{-17}
Silver(I) phosphate	Ag ₃ PO ₄	8.88×10^{-17}
Silver(I) bromide	AgBr	5.35×10^{-13}
Silver(I) chromate	Ag ₂ CrO ₄	1.12×10^{-12}
Silver(I) oxalate	Ag ₂ C ₂ O ₄	5.40×10^{-12}
Silver(I) carbonate	Ag ₂ CO ₃	8.45×10^{-12}
Silver(I) chloride	AgCl	1.77×10^{-10}
Silver(I) sulfate	Ag ₂ SO ₄	1.20×10^{-5}
Silver(I) bromate	AgBrO ₃	5.34×10^{-5}
Silver nitrate	AgNO ₃	Highly Soluble



 Increasing Solubility

Source: Lide (2000)

Particle concentration, surface morphology, surface energy, propensity for clustering, and other properties are also relevant when considering dissolution at the nanoscale. In general, the dissolution rate is higher for lower concentrations of nano-Ag; at higher concentrations, key factors that influence dissolution, like available oxygen and presence of protons (i.e., pH), might be depleted, and high concentrations of dissolved silver and ligands, which can inhibit surface reactions, might further impede dissolution (Liu and Hurt, 2010). Liu and Hurt (2010) demonstrated that a low, environmentally relevant concentration (0.05 mg/L) of citrate-stabilized nano-Ag (2–8 nm) undergoes complete oxidative dissolution at room temperature in less than 2 weeks, while the highest concentration (2 mg/L) tested took more than 4 months to completely dissolve under the same conditions.

Nanoparticle clusters might be more or less soluble, depending on how tightly they are clustered. The equilibrium solubility of the system is inversely proportional to overall particle size. Therefore, if clustering affects the surface area available to react with dissolved oxygen, the dissolution rate will decrease, but if the total reactive surface area of the nanoparticles is preserved in the cluster, the dissolution rate should differ little for the same concentration of homogeneously dispersed nano-Ag (Liu and Hurt, 2010; Borm et al., 2006a).

2.3.6. Surface Chemistry, Reactivity, and Coatings

One of the primary features of nano-Ag that distinguishes its behavior from that of ionic silver is the reactive surface of the particle that enables nano-Ag to interact (i.e., complex) or react with chemical and biological constituents in the milieu. As discussed in the previous section, oxidative dissolution of nano-Ag takes place on the surface of the particle, leading to the steady, prolonged release of soluble silver and reactive oxygen species. Nano-Ag also can undergo surface complexation with some negatively charged ligands in the environment, which can variably increase or decrease its solubility and bioavailability ([Liu et al., 2010a](#)).

The surface area of nano-Ag particles correlates with the availability of possible reactive sites and chemical reaction potential, adsorption potential, and the potential to form clusters. The same is true for surface chemistry, which dictates the important surface reactions (e.g., complexation, oxidative dissolution) that drive nano-Ag behavior in complex media. Surface charge and the thickness of the electric double layer on the surface of nanoparticles are important in determining the particle zeta potential, which is one measure of stability ([Nallathamby et al., 2008](#)). These properties, in turn, can affect the transport, behavior, interaction, distribution, bioavailability, and effects of nano-Ag particles in the environment ([O'Brien and Cummins, 2009](#); [Wiesner et al., 2009](#)). Surface charge also influences particle stability in dispersions and overall solubility ([Saves and Warheit, 2009](#); [Tiede et al., 2008](#)).

Surface charge is not the only factor that can be manipulated to control surface chemistry and reactivity. Coatings of various chemical compositions can be added to the nanoparticle surface, which in turn can influence particle behavior, including stability and overall persistence ([Handy et al., 2008b](#); [Tiede et al., 2008](#)). Some examples of coatings commonly applied to nanoparticles are provided in Table 2-3. Nano-Ag is often coated with a surfactant, polymer, or polyelectrolyte ([Lowry and Casman, 2009](#)). These coatings can impart charge to the particles (positive or negative) and stabilize them against clustering and deposition ([Nowack and Bucheli, 2007](#); [Wiesner et al., 2006](#)). For example, some nano-Ag particles are engineered to remain in water as single particles, by adding a coating to improve their water solubility and suspension characteristics, thus making them more water dispersible ([Luoma, 2008](#)). The magnitude of the effect of the coating depends on the type and repulsive forces of the coating. Small-molecular-weight coatings provide primarily electrostatic stabilization by imparting a surface charge to the particle. These repulsive forces are fairly weak and are readily blocked by cations in solution. Large-molecular-weight polymers (uncharged) can provide steric repulsions that stabilize particles against clustering and enhance transport ([Lowry and Casman, 2009](#)). In a study of nano-Ag disinfectant spray, Kvitek et al. ([2008](#)) found that nano-Ag particles with different surface coatings varied with regard to the amount of bacterial growth inhibition, based on the surface coating and the bacteria tested. Their findings imply that the surface coating characteristics can influence bactericidal effectiveness of nano-Ag sprays

Table 2-3. Types of common coatings of nano-Ag.

Type	Coatings
Emulsifiers	Bovine serum albumin (BSA) Polysorbate 80 Polyvinyl alcohol (PVA) Sodium citrate
Surfactants	Cetyltrimethylammonium bromide (CTAB) Polysorbate 80 Sodium dodecyl sulfate (SDS)
Ligands and Polymers	Polyethylene glycol (PEG) Starches/sugars Polysaccharides Polyvinylpyrrolidone (PVP)

Note: The listed coatings are examples mentioned in the literature summarized in Appendices B and C.

(see Section 6.1.1). As discussed in Section 3.2.2, however, the composition of nano-Ag surface coatings is not always reported by manufacturers.

2.3.7. Conductive, Magnetic, and Optical Properties

Silver nanoparticles have been studied and characterized by material scientists extensively over the past two decades. In addition to its biocidal effects, nano-Ag, like other noble metals such as copper and gold, interacts strongly with electromagnetic radiation, which causes nano-silver to take on unique conductive, magnetic, and optical properties. These properties facilitate the use of nano-Ag in biomolecular labeling and detection and in other electronic sensor technologies. For example, silver exhibits the highest surface plasmon resonance band among all metals, and only silver, gold, and copper display this resonance in the visible spectrum ([Wijnhoven et al., 2009b](#); [Evanoff and Chumanov, 2005](#)). (A plasmon is a quantum of a collective oscillation of charges on the surface of a solid induced by a time-varying electric field.) A high surface plasmon resonance means that the electrons on the surface of a particle are highly interactive with electromagnetic fields, and as the surface plasmons resonate, the energy can be detected, quantified, and, in the case of silver, seen in the visible spectrum. Several studies have shown that these properties strongly depend on particle size, shape, spatial ordering, composition, and surface properties ([Evanoff and Chumanov, 2005](#); [Temgire and Joshi, 2004](#); [Kamat, 2002](#); [Murphy and Jana, 2002](#); [Jin et al., 2001](#); [Henglein, 1998](#)).

2.4. Analytical Methods to Characterize Nanoscale Silver

Accurate analytical methods can help improve understanding of the behavior and properties of nano-Ag particles in various environmental media and can improve the characterization of exposure and resulting impacts. The ability to monitor nanoparticles in various media, however, relies on sufficiently sensitive instrumentation. Although measuring only the physicochemical properties that are relevant from a risk assessment or risk management perspective might be desired, the mechanistic understanding of biological effects of nanoparticles is still evolving and this list of physicochemical properties is in flux. Furthermore, because physicochemical properties of nano-Ag are dynamic and depend highly on the surrounding media, instrumentation for characterization in various environmental conditions would be useful ([Tiede et al., 2008](#)). Isolating and recovering nano-Ag particles in sample matrices ranging from animal and plant cells to soil and water could be an important step in the complete characterization of nano-Ag particles.

A few recently published review articles summarize current techniques available to characterize engineered nanomaterials ([Jiang et al., 2009](#); [Sayes and Warheit, 2009](#); [Tiede et al., 2008](#); [Maynard and Aitken, 2007](#); [Powers et al., 2007](#); [Powers et al., 2006](#)). This section highlights some of the currently available techniques used specifically in nano-Ag studies; this section, however, is not intended to present a comprehensive literature review of nanomaterial characterization techniques. The reader is referred to Appendix A and the review articles cited above for more information on such methods. Appendix A contains summary tables that present limits of detection for the techniques listed and summarize some of their advantages and disadvantages. Even so, these tables are not offered as definitive summaries of the field and should be viewed as illustrations of the complexities in nanomaterial characterization.

2.4.1. Methods for Laboratory Research

Several laboratory methods and types of instrumentation are available to characterize nano-Ag (see Appendix A). Although many of these methods are considered accurate techniques for characterization of nano-Ag and incorporate state-of-the-science instrumentation, they are usually resource intensive and require trained specialists. These methods are generally used to develop new synthesis methods, modify surface properties, and study biological interactions at the individual particle level. Despite the existence of numerous possible characterization methods, researchers face challenges in maintaining the nanoparticles as they occur in products or environmental media during characterization and also in determining the dose affecting tissues or cells.

Microscopy techniques (sometimes referred to as “single-particle imaging”) such as scanning electron microscopy (SEM) and transmission electron microscopy (TEM) can be applied to study the size,

shape, and morphology of individual particles or powder samples. These techniques are used in studies of novel synthesis methods ([Siekkinen et al., 2006](#); [Sun et al., 2002](#); [Sun and Xia, 1991](#)) where nanoparticles are embedded in a matrix. Microscopic techniques might also be used to study the biocidal properties of nanoparticles and to detect the presence and any localization of nanoparticles in biological structures. For example, SEM and TEM studies have shown the presence of nanoparticles within bacterial cells ([Shrivastava et al., 2007](#); [Baker et al., 2005](#); [Morones et al., 2005](#); [Sondi and Salopek-Sondi, 2004](#)), alveolar macrophages ([Carlson et al., 2008](#)), and HIV ([Elechiguerra et al., 2005](#)). Microscopic analyses can be conducted in conjunction with energy-dispersive X-ray spectroscopy (EDS) to determine chemical composition; for convenience, many SEM systems come equipped with EDS.

Aerosolized nanoparticulate systems are often studied using ensemble methods. Whereas single-particle imaging methods like microscopy analyze characteristics of individual particles in a sample, ensemble methods convert a signal from the entire sample of particles into size or concentration distributions. Such methods include laser diffraction ([Powers et al., 2006](#)), dynamic light scattering (DLS) ([Murdock et al., 2008](#); [McMurry, 2000](#)), centrifugal sedimentation, and impaction. Many ensemble techniques are used to characterize particulate or aerosol systems and to study ultrafine atmospheric particles, carbon nanotubes, and other nanoengineered materials.

In addition to analytical instrumentation, the development of characterization protocols also is relevant so that results are consistent, reproducible, and reliable. Sayes and Warheit ([2009](#)) suggest such protocols emphasize that characterization data for the material should be assessed in the biologically or environmentally relevant media, in the most dispersed state possible, and using more than one method. Although single-particle imaging and ensemble methods are important tools in detecting and identifying nanoparticles, each individual technique has its own advantages and limitations. For example, although DLS can detect and characterize nanoparticles at environmentally relevant concentrations, including in aerosol samples, the accuracy of DLS decreases with broader size distributions ([Powers et al., 2006](#)). Additionally, although electron microscopy methods can definitively identify small nanoparticles in simple matrices, these techniques only work with concentrations that are higher than those that are expected to occur in the environment, and they cannot be used for aerosol samples. Multiple or orthogonal methods are therefore often employed in tandem when evaluating particle characteristics to combine the respective strengths and to counterbalance the respective weaknesses of different techniques ([Powers et al., 2006](#)). The selection of which methods to use together is therefore an important step in characterizing the materials, as different methods can affect measurement results in unique ways ([MacCuspie et al., 2011](#)). MacCuspie et al. ([2011](#)) compared size range distributions for commercially available nano-Ag measured using multiple techniques and show distinct variation depending on several factors, including the methods employed, parameterization, and the length of time between dispersing materials in solution and characterizing the material. The authors recommended the use of multiple

orthogonal measurement techniques to facilitate interlaboratory comparisons and collaborations to characterize nanomaterials fully ([MacCuspie et al., 2011](#)).

2.4.2. Methods to Assess Environmental Occurrence

Detecting nanoparticles in the environment (particularly the natural environment) is challenging because available analytical methods often are not sufficiently sensitive at environmentally relevant concentrations and cannot distinguish natural materials in the nanoscale size range from manufactured nanomaterials ([Domingos et al., 2009b](#); [Simonet and Valcarcel, 2009](#)). Also, many analytical methods require sample treatment and solvent evaporation, which could cause nanoparticle clustering and precipitate formation ([Simonet and Valcarcel, 2009](#)). Detecting nanoparticles in water or soil is further complicated by the heterogeneous nature of the sample matrix and the clustering tendencies of the nanoparticles. Making such measurements in situ would help address physical and other changes in nanoparticles due to different conditions in the immediate medium, but portable equipment with sufficient sensitivity has not yet been developed ([Simonet and Valcarcel, 2009](#)). Although traditional methods to measure metals in samples (e.g., atomic absorption furnace methods) cannot differentiate between conventional silver and nano-Ag, these traditional methods can be coupled with other methods to confirm and quantify the presence of nano-Ag in a sample. Methods also can be coupled to enable detection of more than one parameter simultaneously. For example, field-flow fractionation can be coupled with inductively coupled plasma-mass spectrometry for both size and chemical analyses.

To illustrate the variety of methods available to assess nanomaterials in environmental matrices, a sample of available methods for analyzing nanomaterials in soil, sediment, and ground water is shown in Table 2-4.

In a study comparing six analytical methods for determining nanoparticle sizes (TEM, atomic force microscopy, DLS, fluorescence correlation spectroscopy, nanoparticle tracking analysis, and field-flow fractionation), Domingos et al. ([2009a](#)) concluded that the two most commonly used techniques in the literature (TEM on air-dried samples and DLS) were also the two that appear to be most prone to artifacts. Their recommendation was to use multiple analytical techniques or multiple preparation techniques, or both.

Several recent studies have employed multiple methods to characterize crystal structure, particle size, and morphology of nano-Ag particles in biological matrices. For example, Laban et al. ([2009](#)) coupled TEM with electron diffraction to verify that the particles detected within the embryos of fathead minnows were nano-Ag particles. Similarly, Asharani et al. ([2008](#)) combined TEM analysis with EDS to confirm the presence and location of nano-Ag particles in zebrafish embryos.

Table 2-4. Analytical methods for nanomaterials in soil, sediment, and ground water for size fractionation and distribution, surface area, and phase and structure.

Metric	Analytical method	Notes
Size fractionation	Centrifugation	Analyze aquatic colloids and particles extracted from soil and sediment samples. Nanoparticles must be in solution.
	Ultrafiltration—direct-flow ultrafiltration or tangential-flow ultrafiltration (TFF)	
	Field-flow fractionation (FFF)	
	Capillary electrophoresis (CE)	
	Size exclusion chromatography (SEC)	
Size distribution	Transmission electron microscopy (TEM)	In most cases, samples analyzed by electron microscopy will be destroyed and cannot be analyzed by another method (Tiede et al., 2008).
	Scanning electron microscopy (SEM)	
	Scanning probe microscopy (SPM)	
	Dynamic light scattering (DLS)	
	Laser-induced breakdown detection (LIBD)	
	Small- and wide-angle X-ray scattering (SAXS/WAXS)	
Surface area	BET (Brunauer, Emmett, Teller method of calculating specific surface area)	Only nanoparticles with a regular or pseudo-regular geometry and without significant porosity
	Calculation from TEM (length and width) and atomic force microscopy (AFM) (height) measurements, and particle nanocrystalline geometrics	
Phase and structure	Electron diffraction	XRD and XAS are nondestructive techniques (Tiede et al., 2008).
	X-ray diffraction (XRD)	
	X-ray absorption spectroscopy (XAS)	
	Raman spectroscopy	
	High-resolution transmission electron microscopy (HR-TEM)	

Source: Adapted from U.S. EPA ([2009d](#)).

2.4.3. Methods to Assess Workplace Occurrence

The potential for workplace exposure to nano-Ag exists during all manufacturing stages of nano-Ag and products containing nano-Ag, as well as during certain recycling and disposal stages. The monitoring of a specific nanomaterial poses several challenges, due to the presence of background particulate matter generated from other activities that typically occur at industrial sites. Such activities include combustion processes, metal operations where vapors can condense (e.g., soldering, welding, smelting), and mechanical processes (e.g., grinding, blending) ([Ono-Ogasawara et al., 2009](#)). Although standardized protocols exist for monitoring the suspended particulate matter at workplaces, they do not distinguish between ultrafine particles and nanoparticles.

Analysis of workplace exposure thus far has focused on measuring nanoparticles in the air. Instruments that can be used for aerosol sampling are available, but most are designed for laboratory use ([Nanosafe, 2008](#)) and lack one or more of the following attributes: portability, ease of use, capacity to distinguish nanoparticles from non-nanoparticles, different size bins in the 1- to 100-nm range, or ability to sample personal breathing zones ([Ostraat, 2009](#)). Engineered nanoparticles can be measured in the

workplace using a variety of instrumentation, including condensation particle counters, optical particle counters, fast mobility particle sizers, scanning mobility particle sizers (SMPS), electrical low pressure impactors, aerosol diffusion chargers, and tapered element oscillating microbalances.

Several studies have characterized nanoparticles at manufacturing facilities using various analytical methods. Thus far, however, only one study has been identified that characterized nanoparticles at a nano-Ag production facility. Park et al. (2009) used an SMPS to measure the size of particles in ambient air at a manufacturing facility using liquid-phase processes to produce silver nanoparticles. Also, electrostatic precipitators were used to collect particles on TEM grids to analyze surface morphology.

Because analytical instrumentation and techniques for measuring mass and number concentrations of other nanomaterials could be used directly or adapted to characterize silver nanoparticles, a few recent studies characterizing other nanomaterials at manufacturing sites are mentioned here. Fujitani et al. (2008) characterized fullerenes at a manufacturing facility using an SMPS, optical particle counter, and SEM during non-work periods, work periods, and an agitation process. Similarly, Demou et al. (2008) quantified real-time size, mass, and number concentrations using an SMPS and a condensation particle counter at a pilot plant producing metal oxide nanostructures.

Given the active research in both academic and commercial laboratories to develop new nanomaterial-based technologies, the potential exists for laboratory workers to be exposed. Tsai et al. (2009) sampled and characterized the ambient air from laboratory hoods using a fast mobility particle sizers and an SEM. These analyses were performed during the handling (i.e., pouring or transferring with a spatula) of nano-alumina and nano-Ag (Tsai et al., 2009). Inside the fume hood, the researchers observed a shift in the mean particle diameter of the originally spherical nano-Ag particles from around 60 nm to 150 nm, indicating clustering of the particles during handling. Based on testing with a 100-gram (g) sample and a 15-g sample of nano-alumina, the researchers concluded that working with smaller quantities of sample decreases the concentration of particles entering the laboratory space from the fume hood by approximately 20%.

In recent years, several governmental and environmental organizations have voiced a need for methods and protocols to monitor nanomaterials in the workplace. For example, the National Institute for Occupational Safety and Health recently published a document entitled *Approach to Safe Nanotechnology—Managing the Health and Safety Concerns Associated with Engineered Nanomaterials* (NIOSH, 2009) in which sampling and monitoring methods and equipment are discussed. The Nanoparticle Occupational Safety and Health Consortium, an industry-led consortium of participants from academia and governmental and nongovernmental organizations, is helping to define best practices for working safely with engineered nanoparticles (NOSH Consortium, 2008). The Nanoparticle Occupational Safety and Health Consortium has developed portable air monitoring methods suitable for daily monitoring in nanoparticle research and development and in manufacturing settings. In 2008, the

NanoSafe2 project, a European Community-sponsored project for safe production and use of nanomaterials, released a report that highlighted findings in measurement methodologies for nanoparticle detection and measurement with various types of online and offline monitoring instruments ([Nanosafe, 2008](#)). The report provides examples of new nano-aerosol measurement equipment that is easy to transport and use. No commercially available equipment, however, is currently available for long-term monitoring. The report also recommends that monitoring at workplaces include not only personal sampling and measurements inside the facility, but also measurements of nanomaterials in drains and in the exhausted air to help ensure protection of the environment. Finally, several companies are developing or have developed air monitoring devices for nanoparticle detection; the parameters that each device measures vary ([TRS Environmental, 2009](#); [vandenBrink, 2008](#); [Bennett, 2005](#)).

2.4.4. Methods for Quantifying Dose and Dose Metrics

Researchers and risk assessors often quantify dose¹² in terms of mass (e.g., in micrograms per cubic meter [$\mu\text{g}/\text{m}^3$] for inhalation exposures, or in mg/kg-day for ingestion exposures), but, for some substances, mass might not be the physical parameter most closely correlated with biological response. For example, dose of asbestos fibers is typically characterized by number concentration (i.e., number of particles in a specific quantity of exposure medium) of fibers of specific shape and composition ([Maynard and Aitken, 2007](#)). For nanoparticles, dose can be measured in terms of number concentration (e.g., the number of particles inhaled per volume of air) and surface area concentration (e.g., the surface area of the particles inhaled per volume of air, square meters per cubic meter [m^2/m^3]) in addition to mass concentration.

In some respects, using mass as the primary metric for characterizing dose is an attractive option for nanoparticles; for example, measuring mass for a pollutant is standard procedure, and instrumentation for conducting such measurements is widely available ([Maynard and Aitken, 2007](#)). Oberdörster et al. ([2005a](#)) suggested that measuring mass concentrations for inhalation or intratracheal instillation studies of nanomaterials and conducting gravimetric and chemical analyses of filter samples can provide relatively accurate dose characterization when compared to surface area or particle number metrics. In some cases, estimating particle surface area or number concentration from measures of mass concentration also might be possible based on the estimated diameter of the particles; however, when the distribution of particle sizes is wide or the number of very large particles is great, using mass concentration to calculate number

¹²The term dose is used in several ways across the risk assessment community. Here, dose refers to “potential dose,” as defined by the EPA Integrated Risk Information System (IRIS): “The POTENTIAL DOSE is the amount ingested, inhaled, or applied to the skin.” (http://www.epa.gov/ncea/iris/help_gloss.htm).

concentration could be unreliable. Other potential drawbacks to using mass as the primary metric for characterizing dose are also apparent. Nanoparticles have been shown in many cases to be more toxic than larger particles with the same chemistry; specifically, researchers have shown that the toxicity of insoluble materials increases with decreasing particle size on a mass-to-mass basis ([Mark, 2007](#)). This might occur because the increased specific surface area of nanoparticles compared to larger particles elevates the potential for biological reactions more than mass alone would predict ([Oberdörster et al., 2005a](#)).

Evidence suggests that particle number might be highly correlated with health effects and might be a relevant dose metric. Wittmaack ([2007](#)) found for titanium dioxide that particle number is the dose metric that correlates best with pulmonary inflammation response. Although devices to count particles are available, even the most complex and powerful detection units are limited to the detection of particles with diameter of about 10 nm or greater ([Maynard and Aitken, 2007](#)). These instruments also tend to be very expensive, which could preclude the use of this technology to obtain information about particle size or size distribution. Tsuji et al. ([2006](#)) also questioned the value of measuring only particle number and using this as a dose metric because particle number does not necessarily correlate with health effects as well as other dose metrics.

Surface area might be another appropriate metric for characterizing dose ([Oberdorster et al., 2007](#); [Tsuji et al., 2006](#); [Oberdörster et al., 2005b](#)). In general, the increased surface area of nano-sized particles can change their chemical reactivity, bioavailability, and the biological responses they can induce ([Luoma, 2008](#); [Mark, 2007](#)); thus, surface area concentration might be highly correlated with response. Direct, real-time measurement of particle surface area has become possible in recent years. One device, the Nanoparticle Surface Area Monitor (TSI Model 3550), filters only particles that deposit in the alveolar or thoracic region of the respiratory system ([Maynard and Aitken, 2007](#)). Such measurement systems, however, are not yet cost-effective.

Although identifying a single dose metric that best reflects risk might be desirable, the toxicity and reactivity of nanoparticles appear to be functions of multiple factors, including surface area, number, shape and size, and composition. For this reason, Maynard and Aitken ([2007](#)) suggested that different metrics (e.g., particle number concentration, surface area concentration, mass concentration, or length concentration) might be selected for different aerosol sprays depending on factors such as these. Similarly, Oberdörster et al. ([2005a](#)) suggested that mass, surface area, and particle number are essential dose metrics for nanoparticles and that, when possible, dose should be characterized by all three measures.

2.5. Summary of Physicochemical Properties and Analytical Methods

The size, morphology, surface area, chemical composition, surface chemistry and reactivity, and solubility of nano-Ag particles are all thought to play a role in determining their use and effectiveness in commercially available spray disinfectant solutions, behavior in the environment, and human and ecological exposure potential and toxicity. These properties are interdependent, however, and can change as nano-Ag particles are dispersed in different solutions, move between environmental compartments, and are transported within living organisms. Adequate characterization of nano-Ag could help when evaluating potential risks associated with its use in disinfectant sprays, and the chapters that follow highlight the physicochemical properties of nano-Ag that might be pertinent at each stage of a CEA.

Sensitive analytical methods underpin characterizing the presence and physicochemical properties of nano-Ag in the laboratory, natural environment, workplace, and living organisms. Laboratory methods such as spectroscopy, chromatography, electron microscopy, and spectrometry help researchers characterize nano-Ag and its interaction in environmental media (e.g., in water, air, sediment, or soil), within organisms, and in cells. These same methods cannot necessarily be used to detect and characterize nano-Ag outside of the laboratory for several reasons. Instruments are not easily portable and are expensive; environmentally relevant nano-Ag concentrations can occur below current method and instrument detection limits; and the methods cannot yet consistently distinguish between naturally occurring nanoparticles and engineered nanoparticles such as those used in nano-Ag spray disinfectants. Additional information on analytical methods is presented in Chapters 4, 5, and 6 regarding specific methods used to study the transport, transformation, and fate processes of nano-Ag, the potential exposure of humans and biota to nano-Ag, and the effects of such exposure.

This page intentionally left blank.

Chapter 3. Life-Cycle Stages

The first step in a comprehensive environmental assessment is to examine the life-cycle stages of the nanoscale product. This chapter provides a description of information available about the life cycle of nano-Ag spray disinfectant products to support the discussions in the chapters that follow about environmental transport, transformation, and fate processes; potential exposure pathways for humans and biota; and possible effects resulting from exposure to nano-Ag. As noted in a recent Federal Insecticide, Fungicide, and Rodenticide Act Scientific Advisory Panel review of issues related to nano-Ag in pesticides ([2010b](#)), any use of nano-Ag as a pesticide (including as a disinfectant) could cause nano-Ag or a related by-product derived from such use to enter the environment. In the environment, the potential exists for human and biotic exposure. For this case study, by-products comprise material waste from feedstock processing and manufacturing, secondary pollutants formed through chemical or other transformations of primary pollutants, and, within organisms, metabolic products derived from primary toxicants ([Davis, 2007](#)).

3.1. Feedstocks

Anthropogenic sources of silver emissions into the environment include:

- mining, smelting, and coal combustion operations;
- manufacturing, use, and disposal or recycling of products containing silver; and
- waste discharges from mining operations, industrial processes, and wastewater treatment facilities ([Purcell and Peters, 1998](#)).

A report commissioned by The Silver Institute ([2009b](#)) estimates that 76.6% of the world's 2008 silver supply of 27,631,905 kilograms (kg) came from mining, with North America and Latin America leading the world's mining ([GFMS Limited, 2009](#)). Approximately 28% of this amount was mined in operations where the main revenue source is silver. Of the remaining mined supply, 37% was recovered from lead and zinc mining operations, and the rest from gold (11%), copper (23%), and other metal (2%) mining operations. These ores are typically mined using open-pit or underground methods and are enriched using flotation and smelting processes. Silver metal is extracted electrochemically using the Parkes, Moebium, or Balbach-Thum process. In a silver mass flow analysis conducted by Johnson et al. ([2005](#)), the authors estimated that 20% of the ore mined for silver enters the environment through mine tailings, although the authors suggest that further research could refine this estimate.

The remaining silver in the world's 2008 supply came from other net government sales (3.5% in 2008) and the recycling of silver scrap (19.9% in 2008), including silver recovered from jewelry, photographic chemicals, discarded computers, and other manufactured products that originally contained silver components ([GFMS Limited, 2009](#)). The annual survey of The Silver Institute ([2009a](#)) states that 95% of annual silver consumption is for industrial, photographic, and jewelry applications.

What percentage of the total silver feedstock supply is used to produce nano-Ag is not clear. Mueller and Nowack ([2008](#)) state that worldwide nano-Ag production could be as high as 5% of total silver production, and a “best guess” for the worldwide production of nano-Ag based on this assumption is 500,000 kg per year (approximately 550 tons per year). To form their estimate, Mueller and Nowack reviewed data collected by survey and personal communications about the quantity of nano-Ag manufactured in Switzerland and extrapolated from this estimate to apply to the entire world. As discussed in Section 2.2, only one study to date—Hendren et al. ([2011](#))—has employed a systematic approach to estimating a range of current nano-Ag production volumes in the United States, and that range spans an order of magnitude (2.8–20 tons per year).

3.2. Manufacturing

Manufacturing procedures for nano-Ag are generally proprietary. For example, the Top Nano Technology company website advertises that the company has “kilogram-scale manufacturing” capability for nano-Ag, but information about their manufacturing process is not accessible through the U.S. Patent Office database, the company website, or written inquiries to the company ([Chou, 2010](#)). A search of the U.S. Patent Office database did reveal some patented, company-specific manufacturing processes, so those processes, and others described in the peer-reviewed literature, are incorporated into the section that follows. In general, limited data were identified on specific points of release or the quantity of nano-Ag released as a result of the manufacturing process. This lack of data is consistent with statements included in the report on nano-Ag from the Federal Insecticide, Fungicide, and Rodenticide Act Scientific Advisory Panel ([2010b](#)).

The Project on Emerging Nanotechnologies ([2009](#)) reports that, as of 2009, the companies producing spray disinfectant solutions that purportedly incorporate nano-Ag include American Biotech Labs, ConSeal International, Inc., Daido Corporation, GNS Nanogist Co., Lion Corporation, Shanghai Huzheng Nanotechnology Co. Ltd., Skybright Natural Health, and Top Nano Technology. This list, however, is not comprehensive, as manufacturing of products potentially containing nano-Ag continues to expand. Furthermore, the Project on Emerging Nanotechnologies notes that selection of products for inclusion on the list and the information presented on specific products is based on data that are publicly available on company websites, and none of the information has been independently verified ([2009](#)).

3.2.1. Synthesis of Silver Nanoparticles



Silver nanoparticles can be synthesized using wet-chemistry methods (chemical reduction), laser ablation, radiolysis, and vacuum evaporation methods. Krutyakov et al. (2008) and others have published comprehensive reviews discussing the strengths, drawbacks, and challenges of available nanoparticle synthesis methods. Tolaymat et al. (2010) searched the scientific literature to collect information about how nano-Ag is synthesized. Relying on the synthesis methods described in nearly 200 papers, they concluded that the synthesis of nano-Ag particles almost exclusively produces spherical elemental silver particles with a diameter of less than 20 nanometers (nm). In the synthesis of nanoparticles, controlling more than a single factor is difficult without altering other variables. For example, as particle size is manipulated, other characteristics, such as crystal structure and shape, could be altered unintentionally as a result.

Chemical reduction of silver ions is the primary method for rapidly producing large quantities of silver nanoparticles (Zhang et al., 2007a), and indeed Tolaymat et al. (2010) reached this same conclusion based on their review of the literature on the synthesis of nano-Ag. The chemical reduction of transition metal salts to generate zero-valent particles (not necessarily nanoparticles) was first described by Faraday in 1857 (Bonnemann and Richards, 2001). Following this early discovery, Carey Lea described the reduction of silver nitrate (AgNO_3) in the presence of trisodium citrate (1889), which was subsequently extended to gold nanoparticles by Turkevich et al. (1951) by reducing chloroauric acid with sodium citrate.

With the use of a reducing agent, silver ions (Ag^+) in solution are reduced from a positive valence to a zero-valent state (Ag^0) (Zhang et al., 2007a). Because zero-valent silver tends to cluster, a primary challenge is to maintain the nanoparticles in the desired size range. Controlling size range is generally accomplished by using surface coatings such as surfactants, polymers, or stabilizing ligands (Zhang et al., 2007a). The choice of reducing agent and the order and rate of mixing can alter the rates of nucleation and particle growth (Bonnemann and Richards, 2001). Thus, particle size and dispersion can be controlled by altering the synthesis process. Manipulation of laboratory conditions also enables the shape of the nanoparticles (e.g., rods, wires, disks, spheres) to be controlled (Yu and Yam, 2004; Sun and Xia, 2002).

There are many variations on the basic theme of chemical reduction. The common elements, however, are AgNO_3 as a feedstock, an aqueous solvent or a nonpolar solvent, a reducing agent, and a stabilizing agent, most often a surfactant (Goia and Matijevi, 1998). When AgNO_3 is used as a feedstock, nitrate (NO_3) will likely result from the reaction and can then be a by-product of concern (Tolaymat et al., 2010). In their review of nano-Ag synthesis methods reported in the literature, Tolaymat et al. (2010) found that AgNO_3 is the most commonly reported silver salt precursor used in synthesis. Reduced metal atoms are insoluble and thus tend to cluster, eventually forming solid particles. The driving force behind the reduction is the difference between the reduction and oxidation (redox) potentials of the two half-cell

reactions ([Goia and Matijevi, 1998](#)). The system achieves greater oversaturation as the redox potential increases. For instance, sodium borohydride (NaBH_4) is a relatively strong reducing agent compared to ascorbic acid, and as such, a larger redox potential is attained with NaBH_4 . The larger redox potential results in a more rapid reaction with more nuclei forming, thus resulting in smaller particles, as the available silver is distributed among many nuclei. If a weaker reducing agent is used, such as ascorbic acid, the reaction rate can be increased by elevating the temperature. If larger particles are desired, a weaker reducing agent is used because it will cause a slower reaction and lead to the formation of fewer nuclei. The available silver will be consumed by the smaller number of particles, resulting in a larger final particle size. Further growth can occur by continued addition of metal atoms, leading to crystals with a regular shape and few internal grain boundaries. If aggregation takes place, the resulting particles will be spherical and polycrystalline, with internal grain boundaries. Both mechanisms can occur in the same system.

Examples of other mild reducing agents are sodium citrate ([Lee and Meisel, 1982](#)) and sugars ([Panáček et al., 2006](#); [Kvitek et al., 2005](#)). An advantage of using sodium citrate is that it has low toxicity compared to stronger reducing agents such as sodium borohydride. A disadvantage of sodium citrate is its lower reduction activity, which necessitates higher temperatures and results in longer reaction times ([Zhang et al., 2007a](#)). Kvitek et al. (2005) and Panáček et al. (2006) used sugar as the reducing agent and ammonia as the complexing agent to form diamminesilver cation $[\text{Ag}(\text{NH}_3)_2]^+$. By controlling ammonia concentration and varying the type of sugar, the researchers could control particle size. The redox potential for $\text{Ag}(\text{NH}_3)_2^+$ is lower than that for silver ions, and the ensuing slower reaction leads to fewer nuclei and larger particles. Kvitek et al. (2005) obtained particles ranging from 45 to 380 nm. Panáček et al. (2006) obtained particles in the 25- to 450-nm range.

Leopold and Lendl (2003) used a stronger reducing agent, hydroxylamine hydrochloride ($\text{NH}_2\text{OH}\cdot\text{HCl}$), combined with a solution of AgNO_3 . According to the researchers, the advantages of this method are a rapid reaction rate, a narrow particle size distribution, reliably reproducible results, and the ability to carry out the process at room temperature. The size distribution of the particles can be controlled by changing the order and rate of mixing of the reactants. The adjustments of these variables that Leopold and Lendl (2003) used yielded spherical particles with an average diameter that varied from 23 to 67 nm.

The choice of stabilizing agent also influences the final product. A method by Sun et al. (2005) using 4-(2-hydroxyethyl)-1-piperazineethanesulfonic acid (i.e., HEPES buffer) at pH 7.4 produced “face-center-cubic phase” particles between 5 and 20 nm, with a mean diameter of 10 nm. In this study, human serum albumin was used to stabilize the particles, rendering them suitable for study of their ability to inhibit HIV growth. Niskanen et al. (2010) developed a method to stabilize silver nanoparticles through the use of amorphous copolymers of acrylic acid and butyl acrylate-methyl methacrylate. This specific polymer produced 4-nm particles that were then aged to obtain relatively monodisperse particles of approximately 12 nm. The acrylic acid was shown to form a hydrophilic layer on the silver nanoparticles,

thereby promoting dissolution of silver ions while individual nanoparticles remained attached to the coating via thiol-silver bonds. Hu et al. (2008) developed a method to produce very small nano-Ag particles by using polyacrylic acid (PAA) as a surfactant. The authors noted that the carboxylic groups in the PAA bonded well to the silver nanoparticles, effectively limiting their growth. Their method uses polyols as both the solvent and the reductant, and the synthesis is performed at the boiling temperature of the solvent. Through careful selection of the PAA chain length and the specific polyol (ethylene glycol, diethylene glycol, or triethylene glycol), the authors could produce particles <10 nm with good dispersion.

Repeatability and reproducibility of nano-Ag synthesis can be augmented by other techniques, such as microwaving or sonication. Yin et al. (2002), for example, developed a method to synthesize nano-Ag based on the Tollens method for electroless plating. The researchers mixed a solution of AgNO₃ with an activator (sodium hydroxide) and a reducing agent (formaldehyde and sorbitol). This procedure was carried out in a sonicator (ultrasound bath), which the researchers believe promoted a more uniform concentration profile, leading to a narrow size distribution in the samples.

Zhang et al. (2007a) presented a detailed discussion of the micro-emulsion method. This type of synthesis involves either a mixture of water, surfactant, and oil, or a mixture of water, surfactant, co-surfactant, and oil. The system can involve oil micelles in water, or water micelles in oil. The discussion by Zhang et al. (2007a) focused on water-in-oil micro-emulsion, also referred to as “reverse micelles.” The basic principle is that the reduction reaction takes place in water droplets, which are covered by surfactant molecules. As the particles enlarge, the surfactant molecules then become adsorbed to the particle surfaces, halting further growth and preventing them from forming clusters. The diameter and shape of the particles can be controlled by the size and shape of the droplets. This technique can produce relatively stable, small particles (2–5 nm average diameter), with a narrow size distribution. To initiate the reaction, two micro-emulsions are mixed—one carrying the silver salt and the other carrying the reducing agent. The micelles coalesce, and the reactants mix.

In addition to serving as reactors, the reverse micelles act as templates for the shapes of the nanoparticles (Zhang et al., 2007a). A low surfactant concentration gives rise to spherical particles. Higher concentrations can produce rods or columns. In a mixed cationic-anionic surfactant solution, “worm-like” micelles form, producing nanowires. The reducing agent, water content, AgNO₃ concentration, and chain length of the alkane used as the solvent also influence particle morphology. Despite achieving tight control of particle size and flexibility in shape, this method has several disadvantages, including potentially high expense because it requires large amounts of surfactants and solvent. Also challenging is the removal of the surfactants and solvent from the nanoparticles and nanoparticle products. As mentioned previously, manufacturers of nano-Ag and the spray products to which they are added often do not report—and in some cases do not characterize—the composition of the surface-active agents in their products. As a result, products as-manufactured might contain multiple uncharacterized substances, which

presents a challenge to evaluating as-manufactured materials systematically. Furthermore, stable dispersions are obtained only at low concentrations. Because of these disadvantages, the authors noted that the method is not currently suitable for large-scale manufacturing ([Zhang et al., 2007a](#)).

Wet-chemical methods often leave trace amounts of reducing agents or surfactants on silver nanoparticle surfaces ([Amendola et al., 2007](#)). Some unconventional methods have therefore been developed for applications requiring pure nanoparticles. For example, laser ablation of pure silver immersed in a solvent generated nanoparticles with a logarithmically normal particle size distribution ([Amendola et al., 2007](#)). In an earlier study, laser ablation of conventional silver in aqueous sodium dodecyl sulfate solution generated silver nanoparticles for which the size could be increased by using more radiation power or decreased by adding more surfactant ([Mafune et al., 2000](#)).

Researchers are also investigating the possibility of using plants or other biota to synthesize metallic nanoparticles, including nano-Ag ([Harris and Bali, 2008](#)). Other nontraditional "green" chemistry techniques for nano-Ag synthesis also have emerged recently, including the use of purified rhamnolipids from bacteria ([Kumar et al., 2010](#)), incubation of proteobacteria with silver nitrate ([Suresh et al., 2010](#)), modification of the Tollens process by UV-irradiation, glucose reduction, and use of nontoxic chemicals ([Le et al., 2010](#)). Organic waste (specifically banana peels) rich in lignin ([Bankar et al., 2010](#)) has been used, as have flavonoid-rich tea extracts to synthesize nano-Ag particles while protecting cells from reactive oxygen species ([Moulton et al., 2010](#)).

Several relatively recent patents have been granted for silver nanoparticle synthesis. Although the information obtained from the patents does not generally indicate which, if any, have been adopted for use in large-scale manufacturing, the patents do provide perspective on potential developments. Available descriptions, however, are brief. For example, Oh et al. ([2003](#)) proposed a method to produce silver and silver-alloyed nanoparticles in a surfactant solution. As with other similar methods, the technique involves using a reducing agent to produce silver nanoparticles from a silver salt solution; the use of the surfactant in this method presumably controls nanoparticle size. Holladay et al. ([2004](#)), who are associated with American BioTech, a nano-Ag spray disinfectant manufacturer, hold a patent that describes a method for generating nano-Ag particles between 5 and 20 nm by immersing electrodes (including silver-coated wires) in a 15-gallon plastic container filled with water. The patent claims that the silver particles are dispersed evenly through the water by the rotation of an impeller in the container.

Despite the lack of details associated with nano-Ag patents, assuming that the bulk of nano-Ag is produced using wet-chemistry methods involving liquid-phase materials and processes is reasonable because of the inherent disadvantages of other synthesis methods. A recently published study characterized airborne silver nanoparticles inside a manufacturing facility located in Korea ([Park et al., 2009](#)). The authors of this study assume that wet-chemistry methods result in less inhalation exposure to nanoparticles than gas-phase reactions but that inhalation of aerosolized particles from liquid-phase processing is not negligible. This large manufacturing facility, producing 3,000 kg of silver nanoparticles

per month, uses AgNO₃ as feedstock and employs a chemical reduction method. The manufacturing of nano-Ag occurs in four stages: The chemical reduction step is followed by filtering, drying, and grinding stages. Real-time monitoring and sampling of silver nanoparticles using scanning mobility particle sizer and long differential mobility analyzer techniques at the facility indicated that the highest concentration of airborne nanoparticles occurred after the reaction stage, when some aerosolized nano-Ag particles were released into the air. The researchers also noted that particles deposited on the floor and other surfaces following the release of particles to the air at the end of each stage. The study authors did not attempt to quantify emissions data on a mass-released-per-mass-produced basis. More details on the potential occupational exposure scenarios implied by this study are included in Section 5.3.2.

3.2.2. Manufacturing of Nano-Ag for Disinfectant Sprays

The production, characterization, and handling of nano-Ag for use in disinfectant sprays require specialized technical expertise, and the available data suggest that this expertise might be developed in-house at companies that manufacture nano-Ag disinfectant sprays ([Sawafta et al., 2008](#); [Holladay et al., 2004](#)). Sawafta et al. (2008) described a “nanocomposite” of at least two metals, including silver, in solution where the metal nanoparticles are created either by “mechanical/physical size reduction processes” or “co-precipitation processes.” Size reduction is further described with steps including grinding, pulse laser evaporation, sonication, and sorting by centrifugation or magnetic separation. Alternatively, production of nano-Ag might occur at facilities that exclusively produce nano-Ag and other engineered nanomaterials in large volumes, which are then sold to manufacturers of spray disinfectants. When contacted, ConSeal International, Inc. reported that they produce and sell more than 2,500 gallons annually of their nano-Ag disinfectant spray, NanoSil, which they claim contains nano-Ag ([Gilmore, 2010](#)); they did not specify, however, whether the nano-Ag in their disinfectant spray was manufactured on site or purchased from another source.

Based on available patent data and data presented on company websites (unverified), some major operations that manufacture spray bottle products containing nano-Ag involve mixing various ingredients, mechanical or chemical processes to achieve uniform product consistency, filtration processes to remove impurities, intermediate storage of the prepared bulk spray product in tanks, and finally automated dispensing into bottles ([ConSealInternational, 2010](#); [Park et al., 2009](#); [Shanghai Huzheng Nanotechnology Co., 2009](#); [Sawafta et al., 2008](#); [Holladay et al., 2004](#)). Thermal heating or cooling steps also can be involved, depending on the ingredients, spray formulation, and desired properties. Although bulk spray liquid can be produced in batches in mixing vessels and transferred to intermediate storage, dispensing and packaging can be accomplished using continuous, automated processes.

Individual bottles, sealed after completion of quality control, might be packaged into cardboard cartons for distribution and retail sales.

A 2008 U.S. patent application ([Sawafta et al., 2008](#)) describes a metallic nanocomposite synthesized for its biocidal properties. As explained in the application, to create a spray disinfectant, the nanocomposite can be combined with hypochlorite or another chlorine-releasing compound; chlorhexidine or another biguanide molecule with the chemical formula $C_2H_7N_5$; quaternary ammonium salts commonly used as germicides, disinfectants, and sanitizers; or other ionic liquids, surfactants, soaps, or detergents. The information included in the patent application supports the likelihood described above that nano-Ag manufacturing processes will require mixing a variety of ingredients in a potentially wide range of ways. The composition of coatings, residual impurities from the synthesis process, and proprietary ingredients in the spray disinfectant product might not be disclosed—or even identified—by manufacturers. As a result, the degree to which the different nano-Ag powders and suspensions and spray disinfectant products differ among manufacturers and between batches is unknown.

No data are currently available on nano-Ag releases from the manufacturing of the spray disinfectant product or on air concentrations in facilities that manufacture these products. During the manufacture of nano-Ag sprays, releases of nano-Ag, other spray ingredients, or by-products of the spray could occur. Preliminary handling of large quantities of nano-Ag prior to creating the spray disinfectants, such as unpacking, sampling for quality control, measuring, and transporting nanoparticles, could lead to release of nano-Ag to the air or surfaces in the facility. Depending on the quality of packaging and storage conditions at facilities where manufacturers acquire nano-Ag in large volumes and stockpile the raw material for extended periods, nano-Ag and associated substances might be released to ambient air. Similarly, mechanical processes such as mixing, grinding, or agitation of liquids can cause nano-Ag to escape to the ambient air. As Park et al. ([2009](#)) demonstrated, wet-chemistry handling processes also can emit nano-Ag to the air. Once bulk spray is produced, other activities such as storage, addition of other ingredients, and dispensing into bottles could result in particle releases to the environment, resulting in the potential for worker exposure. Available data on exposures are described in Section 5.3.2. In addition to the potential for exposure during routine manufacturing operations, accidental short-term exposure at high doses might occur at spray production facilities. These exposures could occur as a result of incidents ranging from major accidents to medium-scale adverse events, such as a leak or break in process vessels or pipes, to minor events such as small chemical spills.

Finally, nano-Ag, other spray ingredients, or by-products from disinfectant spray-manufacturing facilities could enter waste streams including landfill waste and wastewater streams by way of fluids released from flushing and cleaning of processing equipment, improperly treated processing waste, and cleaning of contaminated surfaces.

3.3. Distribution and Storage of Nano-Ag Disinfectant Sprays

Disinfectant sprays are most likely distributed in sealed plastic bottles. The principal method of retail distribution likely is through the transport of cardboard cartons, each containing several dozen spray bottles. Although the boxes with spray bottles might be stored at intermediate distribution facilities, they are apt to be opened only at the retail location where the individual units are ultimately sold to customers. The possible scenarios for releases during transport include damage to the cartons or leakage from the bottles as a result of mishandling of cartons, faulty packaging, or improper stacking of cartons in transport vehicles, or spills that result from accidents involving transport vehicles. If the bottles are sealed properly and not damaged during transport, releases of product prior to use might be limited to breakage of bottles or large-volume spills of the liquid spray at retail locations where silver sprays are sold. Product shelf lives are currently unknown, and potential for release exists during removal of products from shelves and subsequent disposal.

3.4. Use of Nano-Ag Disinfectant Sprays

Disinfectant sprays can be used on a wide variety of surfaces, including walls, floors, sinks, door knobs, light-switch covers, telephones, appliances, tables, and chairs (See Section 2.2). Sprays are likely to be used in both residential and institutional settings, such as hospitals, restaurants, and schools. Nano-Ag from the use of sprays likely will be found in the air, on the intended surfaces, and on unintended surfaces contaminated by overspray, including humans, pets, and food, particularly when used in confined spaces. Spraying of kitchen surfaces with nano-Ag products could result in the transfer of the particles to food items and to light switches, door knobs, telephones, and other surfaces that are often touched. Additional activities involving the sprayed surfaces could release more nano-Ag or spray by-products. For example, subsequent cleaning of the surface with products containing oxidizing agents, such as hydrogen peroxide (H_2O_2), could oxidize the nano-Ag and release ionic silver. Concomitant release of other spray ingredients also would occur and could affect the behavior of nano-Ag. Surfaces sprayed with nano-Ag products could be wiped down with paper towels, disposable dust cloths, or other single-use products; these disposable products then are likely to enter municipal waste collection systems and landfills (e.g., see Benn and Cavanagh ([2010](#)) below).

Nano-Ag disinfectants sprayed on sinks, bathtubs, and toilets could enter wastewater streams or septic tanks. Similarly, fabric or clothing that is sprayed and then laundered also could release nano-Ag and by-products into wastewater. As described by Benn and Westerhoff ([2008](#)), several clothing manufacturers have advertised clothing products containing nano-Ag. The processes by which the

nano-Ag is added to the textile products are generally not available in the literature, but the likelihood that at least some of these products have been treated with nano-Ag coatings is high, and such applications are expected to result in similar releases of nano-Ag to the environment as for textiles sprayed with nano-Ag disinfectant. As a result, the discussion of nano-Ag releases from products that have been coated with a nano-Ag solution could provide insight to this discussion.

Benn and Westerhoff (2008) found that three of six brands of socks containing nano-Ag leached the particles, at different rates, during wash simulations using tap water or distilled water with no soap. Geriano et al. (2009) conducted a follow-up study in which the quantity and form of nano-Ag released during washing simulations were determined using nine different fabrics with different methods of silver incorporation into the fibers. They found that, under typical washing conditions (pH 10) the dissolved concentrations were 10 times lower than in a cycle with pH 7, but that the addition of bleaching products accelerated the dissolution of Ag. During other washing simulations in which the fabrics were placed in steel washing containers agitated with steel balls, Geriano et al. found that most of the silver particles that were released were in the size fraction >450 nm; the authors attributed this to the dominant role of mechanical stress caused by the agitation and the presence of the steel balls. Authors also noted that a conventional silver textile did not show any significant difference in the released silver particle size distribution compared to the nano-Ag products. In a similar experiment, Kulthong et al. (2010) investigated the release of nano-Ag from antibacterial fabrics into artificial sweat. Using both commercially produced and laboratory-prepared fabrics containing nano-Ag and four formulations of artificial sweat, the authors found that silver was released from the various fabrics at rates ranging from 0 to 322 milligrams per kilogram (mg/kg) of fabric weight. Release rates depended on the amount of silver coating, fabric quality, method of fabric preparation, and components of the artificial sweat. These results suggest that aspects of the textile manufacturing process, such as incorporation of nanoparticles into fabrics versus spraying onto fabrics, and specific washing parameters, such as use of bleaching agents and water pH, can influence the amount of nano-Ag that could enter wastewater streams when products are laundered or that could come into contact with human skin via leaching into perspiration (Kulthong et al., 2010; Geranio et al., 2009; Benn and Westerhoff, 2008). Benn and Cavanagh (2010) also analyzed the amount of silver that could be released by use in the home of several consumer products containing nano-Ag. The analysis included washing clothing articles containing nano-Ag, release of silver into tap water from toothpaste and shampoo that include nano-Ag, and release while cleaning with nano-Ag detergents. The authors calculated that the amount of silver released by the use of these household products could be as high as 470 micrograms (μg) of silver per day for a single consumer (conservative assumptions were made regarding the amount of silver released from individual products).

Commercial establishments such as restaurants and hospitals might purchase bulk quantities of spray solutions containing nano-Ag for use with spray-gun applicators. For example, the usage instructions for NanoSil from ConSeal International, Inc. (2010) suggest using a spray gun or mop for

application. Excess product remaining after spraying is likely to be disposed of into municipal wastewater streams, as would the water used to rinse spray guns or mops after use.

Nano-Ag disinfectant sprays might also be used outdoors; for example, sprays might be used to disinfect outdoor trash cans, outdoor furniture and children's toys, or boats or other recreational equipment. From these applications, nano-Ag and by-products might directly enter natural waters or soil, rather than being processed at wastewater treatment facilities. Kaegi et al. (2010) have reported that about 30% of the silver originally incorporated in outdoor paint as nano-Ag was released to the environment over the course of one year (primarily during rain events); similar processes could transport silver from outdoor objects treated with nano-Ag disinfectant sprays.

Shanghai Huzheng Nanotechnology Co. Ltd. (2009) reports on their website that their products will continue to protect against bacteria for up to 24 hours after application. This claim suggests that particles will continue adhering to the surfaces to which they are applied for up to a day. Research by Brady et al. (2003) suggests that a silver disinfectant continues to effectively inhibit bacterial growth on a solid glass surface despite repeated rinsing under tap water; other non-silver disinfectants did not show the same effectiveness. A subsequently published letter to the editor of the journal, however, questions the applicability of the results because the film created by the disinfectant, rather than the silver, could have prevented bacterial growth (Schuster et al., 2004). Additionally, the authors of the letter suggested that incubating the glass tiles under humid conditions between tests rather than at room temperature artificially increased bacteria growth over normal conditions and overstated the effectiveness of the disinfectant spray. They also questioned whether the surface disinfectant would be as effective on porous surfaces such as wood as it purportedly was on glass.

The size of droplets from spray disinfectant products likely will vary based on the formulation of the liquid used as a delivery medium and the delivery system (Hagendorfer et al., 2009; Pandis and Davidson, 1999). By using a propellant gas spray, Hagendorfer et al. (2009) produced nanoscale water droplets that contained a homogenous nanoparticle distribution. Following application, the liquid evaporated, leaving a nano-Ag-containing residue. The physical and chemical properties of the droplet residue after evaporation are likely influenced by the composition of the formulation, including the physical properties of the solvents used (Hagendorfer et al., 2009; Pandis and Davidson, 1999)

3.5. Disposal of Nano-Ag Disinfectant Sprays

The most likely scenario for disposal of spray bottles is through household wastes, whether those containers are taken to a landfill or recycled. Regardless of the pathway, any nano-Ag and associated substances remaining in the bottles ultimately would enter municipal solid waste streams. If the waste is incinerated, nano-Ag might be released to the air. If the waste is deposited in landfills, nano-Ag could

leach into the soil and eventually enter the ground water. Alternatively, if containers are recycled, both workers and consumers could come in contact with nano-Ag in the manufacturing and use of products made from recycled materials that previously contained nano-Ag spray. The disposal of bottles that are unopened or contain unused portions of spray would be an additional source of nano-Ag and other spray ingredients in municipal solid waste streams. That disinfectant sprays or materials that have come in contact with them might be disposed of improperly is also possible, for example, in wooded areas, rivers, or other illegal dumping grounds. In such cases, nano-Ag could directly enter the environment.

3.6. Summary of Life-Cycle Stages

The life cycle of nano-Ag used in spray disinfectants begins with the extraction or recovery of conventional silver from mining operations. As much as 5% of silver production could be nano-Ag, but substantial uncertainty is associated with this figure ([Mueller and Nowack, 2008](#)). Various methods of nano-Ag production are reported in the literature and in patent filings, but how many of these are used on an industrial scale or which are used most frequently in general or in the production of spray disinfectants is unknown. Results of bench-scale syntheses of nano-Ag suggest that wet chemical processing is more efficient than other production processes; wet chemical processing is likely to result in lower inhalation exposures during the manufacturing stage than solid- or vapor-phase processes ([Park et al., 2009](#)). No information specific to releases of nano-Ag and associated substances to the environment during distribution, use, or disposal of spray disinfectants was identified. At any of these life-cycle stages, nano-Ag could be released to the air (especially to indoor air during use) or to surfaces within homes and public spaces. Disposal could result in the release of nano-Ag, other spray ingredients, or nano-Ag by-products to the environment by way of landfills or wastewater streams.

Chapter 4. Transport, Transformation, and Fate Processes in Environmental Media

The production, use, and disposal of engineered nano-Ag eventually will lead to its occurrence in air, soil, and water ([Wiesner et al., 2006](#)). Chapter 4 examines what might happen to nano-Ag after its release to the environment at various stages of the product life cycle for spray disinfectants. Nano-Ag released to air, water, or soil then could be transported or transformed through chemical, physical, and biological processes. Although the transport, transformation, and fate processes of nano-Ag-associated contaminants, such as waste by-products related to feedstocks and manufacturing, is also of relevance to a comprehensive environmental assessment, the current insufficiency of information on these associated contaminants precludes their coverage in this chapter.

Current literature suggests that the fundamental properties governing the environmental fate of engineered nanoparticles in general are not thoroughly understood,¹³ and studies on transport, transformation, and fate processes of nano-Ag, although beginning to emerge, are still relatively few. The lack of data on the transport, transformation, and fate processes of nano-Ag by-products and waste produced after disposal precludes a comprehensive discussion in this chapter and represents a potential data gap for a comprehensive environmental assessment of nano-Ag. This chapter does, however, summarize what is known about the environmental behavior as well as transport and transformation processes of engineered nanoparticles (and specifically nano-Ag, when available), the physical-chemical properties of these particles, and the characteristics of the environmental media that can affect the behavior of these particles.

Section 4.1 provides a brief discussion of the chemical and physical characteristics and processes that influence transport, transformation, and fate processes of nano-Ag in environmental media. The sections that follow provide the available information regarding nano-Ag behavior in indoor and ambient air (Section 4.2), terrestrial systems (Section 4.3), and aquatic systems (Section 4.4). A discussion of models that might be used for evaluating the transport, transformation, and fate processes of nano-Ag, or silver ions released from nano-Ag, in environmental media is provided in Section 4.5.

¹³The recent Federal Insecticide, Fungicide, and Rodenticide Act Scientific Advisory Panel review ([U.S. EPA, 2010b](#)) came to a similar conclusion.

4.1. Factors Influencing Transport, Transformation, and Fate Processes of Nano-Ag

The literature indicates that aerosols of atmospheric nanoscale particles formed by combustion processes (e.g., from cars, incinerators) have been studied at length; relatively little, however, is known about aerosols from *engineered* nanomaterials ([Ma-Hock et al., 2007](#)). Aerosols of engineered nanoparticles are synthesized in the laboratory to have unique physicochemical properties and certain functional properties for use in commercial products ([Jiang et al., 2009](#); [Ma-Hock et al., 2007](#)). These “intentional” nanoparticles are controlled for size and shape and designed for functionality, and might have a surface coating or other surface modifications to help increase the product’s stability and persistence after its release (see Section 4.1.1) ([Oberdörster et al., 2005b](#)).

For decades, health-related aerosol exposures have been represented in terms of mass concentration measurements alone. For assessing exposure to airborne nanoparticles, other factors such as particle number, particle shape and surface area, surface chemistry (including coatings), and the degree to which particles agglomerate or aggregate to form clusters¹⁴ play a critical role in determining nanoparticle distribution and fate within the environment and in evaluating their potential health impacts ([Jiang et al., 2009](#); [Ma-Hock et al., 2007](#); [Maynard and Aitken, 2007](#)).

Once released into the environment, nanoparticles would be expected to behave generally in one or more of the following ways: (1) stay in suspension as individual particles; (2) form clusters with other particles (and potentially deposit or undergo facilitated transport); (3) dissolve in a liquid; or (4) chemically transform based on reactions with natural organic matter (NOM) or other environmental constituents ([Luoma, 2008](#)). Transformation can affect size, shape, and surface chemistry of the particles and their coatings, and this process will affect their ultimate distribution, persistence, and toxicity in the environment ([Lowry and Casman, 2009](#)). Transformation can lead to substances that present a very different hazard than the untransformed material that was originally released ([Maynard, 2006](#)).

As described in the following sections, the **distribution and fate of nano-Ag within the environment depends on the physical and chemical processes that occur in the environment and the characteristics of the environmental system** ([Boxall et al., 2007](#)), as well as characteristics of the particles, as described in **detail in Section 2.3**. The presence of spray ingredients or materials used in the manufacturing process



¹⁴As summarized by Nichols et al. ([2002](#)) and discussed in more detail in Chapter 1, the meanings of the terms “aggregate” and “agglomerate” as they refer to the formation of particle “clusters” are sometimes interchanged in the literature; thus, the definitions of these terms are neither specific nor consistent. To simplify the discussion for this case study, the term “cluster” is used throughout this document to indicate an aggregate or agglomerate of nanoparticles, regardless of the nature or strength of particle cohesion or the mechanisms by which the particles assemble.

also can potentially affect the environmental behavior of nano-Ag, although no specific information regarding this phenomenon was identified during development of this case study.

For the remainder of this chapter, much of the information presented is applicable to engineered nanoparticles in general, as few fate and transport studies specific to nano-Ag were identified.

4.1.1. Persistence

Although silver, in general, can accumulate in water, sediments, soils, and biological organisms, the behavior and persistence of silver ions and silver nanoparticles are fundamentally different. Free silver ions can associate with other ions, but the ion itself is intrinsically persistent, although it can be converted to other species (i.e., speciate). In contrast, a nano-Ag particle is not necessarily persistent. For example, particles can dissolve or disassemble (i.e., not persist in the particulate form); sorb (as single particles or clusters) to soil or sediment, where they can persist long term; undergo direct oxysulfidation to form nanoscale silver sulfide precipitates that can persist for a long period of time; form complexes with ligands and organic matter that can variably increase or decrease persistence of the nanoparticle; and silver nanoparticles also can form (or re-form) from ionic silver in the presence of humic and fulvic acids ([Akaijge et al., 2011](#); [Maccuspie, 2011](#); [Liu et al., 2010a](#); [Liu and Hurt, 2010](#); [Salnikov et al., 2009](#)). Because these reactions depend on the interplay of multiple environmental factors, the equilibrium species are expected to change as nano-Ag, dissolved silver, and silver solids are transported through various conditions.

As introduced in Section 2.3.5, Liu and Hurt ([2010](#)) demonstrated that citrate-stabilized nano-Ag particles (Ag^0 ; 2–8 nanometers [nm]) at low, environmentally relevant concentrations are not expected to be persistent in complex, aquatic systems containing dissolved oxygen. Complete oxidative dissolution of nano-Ag particles, however, can take up to several months, during which nano-Ag particles might interact with and impact receptors. Complex conditions in environmental systems including changes in pH, temperature, presence of ligands and organic matter, among other factors, also can influence the persistence of nano-Ag. For example, decreasing temperature, increasing pH, increasing nano-Ag concentrations, or increasing concentrations of NOM, all within ranges of environmentally relevant values, have generally been shown to increase nano-Ag stability ([Liu and Hurt, 2010](#)).

In complex systems, the equilibrium distribution of nano-Ag and ionic silver will vary with the environmental conditions (e.g., dissolved oxygen concentrations, presence of organic matter), making possible a cycle of oxidation/dissolution (decreasing presence of particles) and reduction/formation (increasing presence of particles), thereby increasing overall persistence of nano-Ag in the colloidal

system. This dynamic equilibrium can be illustrated by the multiple ways in which organic matter can stabilize nano-Ag:

- the organic matter could bind to nano-Ag surfaces and block its reaction sites, thus preventing oxidative dissolution, complexation with other constituents, and silver salt formation;
- humic and fulvic acids that make up organic matter could act as reductants that convert Ag^+ to Ag^0 , thus forming silver nanoparticles from dissolved ionic silver; or
- organic matter could compete with Ag^0 for oxidants such as hydrogen peroxide (H_2O_2), which would also limit reactive dissolution ([Akaighe et al., 2011](#); [Liu and Hurt, 2010](#); [Salnikov et al., 2009](#)).



Some types of silver nanoparticles in commercial products are engineered to have charged functional groups or surface coatings to increase stability, and these surface treatments can variably affect long-term persistence of nano-Ag in environmental media. MacCuspie ([2011](#)) examined the effect of three different capping agents—bovine serum albumin, citrate, and starch—on nano-Ag (10–20 nm) persistence under a variety of environmentally relevant conditions. In general, the bovine serum albumin-capped nano-Ag exhibited greater stability in the presence of high electrolyte (i.e., sodium chloride [NaCl] and calcium chloride [CaCl_2]) concentration and a range of pH values (stable at pH 2, 3, 7, and 9) than citrate-capped nano-Ag (relatively stable only at pH 7 and 9). The starch-capped nano-Ag, however, exhibited the greatest stability at the widest range of pH values (relatively stable at pH 2–9) ([2011](#)). It is reasonable to expect, however, that surface coatings could be degraded by chemical or biological reactions, which will further affect the persistence of the nano-Ag over time in ways dependent on both the presence of a coating and the type of coating used.



4.1.2. Particle Clustering, Deposition, and Sedimentation



The formation of particle clusters, deposition to surfaces from air, and sedimentation from water are closely related phenomena. As described by Navarro et al. ([2008a](#)) and Wiesner et al. ([2006](#)), clustering¹⁵ describes the interaction between two mobile objects (transport). Deposition refers to the settling of a mobile particle or cluster from the air onto a water surface or land, and sedimentation—another form of deposition—is the process of settling from the water column or aqueous phase of soils onto aquatic sediments or the particulate phase of soils.

The extent of nanoparticle clustering depends on the properties of the particle (e.g., shape, size, surface area, surface charge, surface coating) and the characteristics of the environmental system ([Tiede et](#)

¹⁵See footnote 14.

[al., 2009](#); [Handy et al., 2008b](#)). Silver nanoparticles are often coated to reduce the formation of clusters, thereby maintaining the high surface area-to-volume ratio (and corresponding increase in surface reactivity) of the dispersed single silver nanoparticles ([Kandlikar et al., 2007](#)). Other spray ingredients and environmental conditions might also affect nano-Ag clustering by altering the surface coating and physicochemical characteristics of the original particles (as discussed in more detail in Sections 4.2–4.4) ([Lowry and Casman, 2009](#); [Handy et al., 2008b](#)).

The rate and extent of particle clustering depend also in part on ionic strength and ionic composition. In general, increasing ionic strength (e.g., additions of salt) and the presence of divalent cations such as Ca^{2+} (ionic calcium) and Mg^{2+} (ionic magnesium) increase the rate and extent of clustering and can affect the stable size of the clusters formed ([Cumberland and Lead, 2009](#); [Lowry and Casman, 2009](#); [Handy et al., 2008b](#)). According to Lee et al. ([2007](#)), the presence of a sufficiently high concentration of salt (NaCl at 100 millimoles per liter [mM]) appears to reduce the thickness of the electric double layer on the surface of nanoparticles and decrease the zeta potential (a measure of stability behavior of a colloid) below its critical point, leading to the formation of nanoparticle clusters. As discussed by Mukherjee and Weaver ([2010](#)), competing, similarly charged ions can promote clustering of nano-Ag to different extents. These authors found that Ca^{2+} stimulated clustering (i.e., increased the average cluster size) of nano-Ag to a greater extent than K^+ (ionic potassium) and Na^+ (ionic sodium).

Li et al. ([2010c](#)) tested the early-stage aggregation kinetics of nano-Ag (spherical, monodisperse particles, outer oxidized layer) in the presence of competing cations in a sodium bicarbonate buffer by using electrolyte solutions of NaCl, NaNO_3 , and CaCl_2 at neutral pH with and without fulvic acid coating. For each electrolyte solution, they found that in the early stage of aggregation kinetics, an initial particle-size decrease (dissolution) preceded an increase in the clustering rate of nano-Ag—a process they called “dissolution-accompanied aggregation.” The adsorption of anions imparts a negative surface charge that varies with both pH and electrolyte concentration; the electrostatic force stabilizes particles and prevents clustering while electrolyte addition balances and screens the surface charge-inducing destabilization and clustering. The critical coagulation concentration (CCC) for nano-Ag—defined as the concentration at which the maximum clustering rate is achieved—for the three electrolyte solutions were determined to be 40, 30, and 2 mM for NaCl, NaNO_3 , and CaCl_2 , respectively. The CCC highly depends on the characteristics of the surface coating of the nanomaterial; as a result, the CCC values provided here are relevant only to this specific context.

The pH of a medium will change the surface charge of particles, thereby affecting the size of clusters that form ([DunphyGuzman et al., 2006](#)). As pH of the system increases, the number of negatively charged sites in the system increases, elevating the potential for adsorption of the nanoparticles to positively charged species ([O'Brien and Cummins, 2009](#)). Elzey and Grassian ([2010](#)) investigated the size distribution and fractionation of manufactured nano-Ag in aquatic systems at pH ranges of 0.5–6.5 and determined that clustering of nano-Ag occurred between pH 6.5 and 3; independent (unclustered)

nano-Ag particles existed at pH values between 2.5 and 1. A pH of 0.5 resulted in nearly complete (93%) dissociation of nano-Ag particles into ionic silver.

Mukherjee and Weaver (2010) studied the clustering behavior of metallic nanoparticles including nano-Ag (prepared using Ag nanopowder <100 nm, 99.5% purity, surfaces organically coated, specific surface area 5 square meters per gram [m^2/g]; Sigma-Aldrich) and claimed that clustering of nanoparticles increases as the pH approaches the isoelectric point pH (pH_{iep}) for that specific type of nanoparticle. This pH_{iep} represents the pH at which the surface of the particle carries no net electrical charge and is the point of a particle's minimum solubility, where it will precipitate from solution. By contrast, the farther away from the pH_{iep} , the greater the stability of the individual particle (and the increased likelihood that the particles would stay suspended and become transported). Mukherjee and Weaver (2010) suggested that the pH_{iep} for nano-Ag is 2.0.

The transport of nanoparticles in general depends largely on their size; for this reason, among others, clusters of engineered nanoparticles will behave quite differently compared to single engineered nanoparticles (Ma-Hock et al., 2007). Generally, nanoparticle clusters are less mobile than individual nanoparticles in environmental media because they deposit faster and to a greater extent than individual nanoparticles when suspended in air, in water, or in aqueous phases of soil (Nowack and Bucheli, 2007). As summarized by Luoma (2008), most nanoparticles that associate with dissolved materials or particles in water likely will deposit in soils or in aquatic sediments (Luoma, 2008). Changes in aquatic or soil chemistry and physical disturbance, however, can lead to dissociation of nanoparticles from materials to which they were attached and resuspension in air or water. The formation of clusters and therefore of larger particles that are trapped or eliminated through deposition or sedimentation reduces concentrations of bioavailable engineered nanoparticles in the water column, but uptake by soil- or sediment-dwelling organisms or filter feeders can still occur (Nowack and Bucheli, 2007).

4.1.3. Adsorption

Adsorption, conceptually similar to both deposition and the formation of clusters as introduced above, is the binding of molecules or particles to an abiotic or a biotic surface. The potential of the nanoparticle to adsorb to a surface is influenced by its surface area, surface charge, and degree of clustering, as well as the presence of surface coatings (O'Brien and Cummins, 2009). Because of their high surface area-to-volume ratio and surface reactivity, nanoparticles can adsorb pollutants or other spray ingredients, which might change the transport, solubility, and bioavailability of both the nanoparticles and the pollutants in the environmental systems and modify their toxic effects (Navarro et al., 2008a).

4.1.4. Transport/Mobility Potential

Once nanoparticles are released into the environment, their transport is a critical factor in assessing their impact and ultimate fate in the environment. Generally, nanoparticle transport on the molecular or particle scale is dominated by Brownian motion (random motion of small particles suspended in a gas or liquid). Weaker forces such as London or van der Waals are responsible for attachment behaviors that ultimately determine particle mobility ([Biswas and Wu, 2005](#)). Transport or mobility potential of nano-Ag is affected by the characteristics of the nanomaterial (including those of the material matrix and surface coatings), associated substances from manufacturing or product formulation, and the environmental medium ([O'Brien and Cummins, 2009](#)).

The greater potential mobility of nanoparticles in the environment relative to the mobility of larger particles implies a greater potential for exposure because they are dispersed over greater distances and their effective persistence in the environment increases. The physical movement of a nanoparticle, however, is restricted by its small size and propensity to adsorb to surfaces ([Borm et al., 2006b](#)). The propensity of nanoparticles to adsorb to abiotic and biotic surfaces or to form clusters can particularly decrease their mobility in porous media such as soil ([Borm et al., 2006b](#); [Wiesner et al., 2006](#)).

4.2. Air

Nano-Ag in spray disinfectants could be released into air in several ways:

- During manufacturing of nano-Ag spray products, nano-Ag might be released to indoor air during standard mechanical operations, including mixing, grinding, or agitation of liquids. Nano-Ag released in indoor air might subsequently be transported to outdoor air ([Quadros and Marr, 2010](#); [Grassian, 2009](#); [Mueller and Nowack, 2008](#))
- During manufacturing, storage, and disposal, nano-Ag might be released to indoor or outdoor air via fugitive emissions, spills, cleaning operations, and other accidental or unintentional releases.
- The consumer use of spray disinfectants containing nano-Ag will result in direct emissions of nano-Ag and other substances to indoor air and possibly to outdoor air if used outdoors or transported from the indoor environment to outdoor air.
- Disposal of spray products or contaminated containers via incineration might release nano-Ag to ambient air ([Blaser et al., 2008](#)).
- Some nano-Ag particles that deposit to soil might experience secondary transport via wind and become resuspended into ambient air. Once deposited, however, nanoparticles would be unlikely to resuspend in the air or re-aerosolize given their propensity to cluster or attach to surfaces ([Aitken et al., 2004](#); [Colvin, 2003](#)).

Overall, few studies are available on the transport, transformation, and fate processes of nanoparticles in indoor and outdoor air. Information obtained from the literature provides a general

description of the behavior of particles in general and some nanoparticles in air, although information specific to nano-Ag is limited. As discussed below, available information suggests that particle behavior will vary based on particle size, the extent of particle clustering, and other parameters such as surface coatings. Notably, the magnitude of nano-Ag release into air is unknown.

4.2.1. Diffusion

Several processes and factors influence the fate of airborne particles in indoor and outdoor environments, including size, chemical characteristics, the nature of interactions with other airborne particles, residence time in the air, and distance traveled prior to deposition ([U.S. EPA, 2007b](#)). The fate of airborne particles outdoors could also be influenced by meteorological factors, including wind, temperature, and relative humidity ([Navarro et al., 2008a](#)). Nanoparticles might be in the form of single particles or in clusters that are larger than the primary particle ([Grassian, 2009](#)) (see Section 2.3). Individual nano-sized particles likely will follow the laws of gaseous diffusion when released to air, with their diffusion rate inversely related to their diameter (i.e., smaller particles will diffuse more quickly) ([U.S. EPA, 2007b](#)). Due to their high diffusion coefficients, nanoparticles (based on size alone) should diffuse more readily than micrometer-sized particles ([Aitken et al., 2004](#)). The dynamics of airborne nano-sized particles suggest that they generally will follow airflows and not be influenced by mechanisms such as gravitational settling and inertial deposition ([Maynard, 2006](#)). They are, however, more likely than larger particles to deposit to surfaces via diffusion.

Once they are emitted to the indoor atmosphere, nanoparticles will diffuse according to a concentration gradient, from high-concentration zones to low-concentration zones. Nanoparticles will mix rapidly through indoor air and quickly disperse, and can be carried by various air movements caused by differences in temperature, ventilation, or the movement of people or objects. For nanoparticle aerosols released during discreet uses of a disinfectant spray product, concentrations at the emission source can therefore drop fairly quickly over time. These aerosols can diffuse over greater distances (e.g., throughout the interior of a home) and persist for a relatively long time in the indoor environment ([AFSSET, 2006](#); [Aitken et al., 2004](#)), although diffusive deposition will decrease their airborne concentration (see Section 4.2).

4.2.2. Particle Clustering

Nanoparticles in aerosol sprays are typically in the form of clusters ([Biswas and Wu, 2005](#)), although some commercial products are engineered to have surface coatings to help stabilize the liquid suspensions against clustering so that they remain dispersed within the gas. Particle clusters have a much

larger aerodynamic diameter than single nanoparticles and thus disperse and deposit differently. Single nanoparticles are generally not observed in dispersed nanomaterials in the atmosphere, even when using relatively high-energy dispersion methods (e.g., through spraying) ([Ma-Hock et al., 2007](#)).

4.2.3. Residence Time

Nanoparticles as single particles have short residence times in air because of their rapid diffusion, diffusive deposition to surfaces, and association with larger particles. In attaching to larger particles (0.1–1 micrometer [μm]), however, they are likely to persist longer in the atmosphere ([AFSSET, 2006](#); [Biswas and Wu, 2005](#); [Aitken et al., 2004](#)) and thus can diffuse over greater distances (e.g., on a regional scale). In general, particles in the 0.1- to 10- μm range have the longest residence time in the atmosphere ([Biswas and Wu, 2005](#)). Longer residence time in the atmosphere allows more time for the particles to be mobilized by wind and other forces; therefore, long-range atmospheric transport of nanoparticles is possible (including transport up to the global scale) if the nanoparticles attach to a larger particle ([Wiesner et al., 2006](#)).

4.2.4. Deposition and Resuspension

Particles suspended in the indoor air could be removed from the atmosphere and deposited onto floors, walls, and other surfaces. Single nanoparticles might remain suspended in the air until they are randomly deposited on a surface due to Brownian motion. Once on a surface, the nano-Ag could sorb to dust particles and either remain on a particular surface or become resuspended after the surface is disturbed (e.g., by individuals who touch or clean the surface). Nano-Ag also could form larger clusters or sorb to dust particles in air; larger, non-nanoscale particles are more susceptible to gravitational settling, which might remove larger particles from the atmosphere more quickly than nanoscale particles and deposit them closer to the emission source ([AFSSET, 2006](#); [Aitken et al., 2004](#)).

Eventually, all particles in the ambient air are deposited (dry deposition) or washed out (wet deposition) to aquatic or terrestrial systems (e.g., soil and plants) ([Mueller and Nowack, 2008](#)). Some nano-Ag particles that have become deposited could experience secondary transport via wind and become resuspended into ambient air and deposited elsewhere. Once deposited, however, nanoparticles likely would not be resuspended in the air or re-aerosolized ([Aitken et al., 2004](#); [Colvin, 2003](#)). Aerosol particles that contact one another generally stick together because of attractive London or van der Waals forces and form clusters ([Aitken et al., 2004](#)). London or van der Waals forces also act to keep a particle attached to a surface. Once clustered (or attached), small particles would be much more difficult to resuspend.

4.2.5. Additional Factors

As discussed in Section 4.1, nanoparticles for use in commercial spray products are synthesized to have unique physicochemical properties and certain functional properties ([Jiang et al., 2009](#); [Ma-Hock et al., 2007](#)). They might be engineered to have a surface coating or other surface modifications to help stabilize them against cluster formation and deposition and to increase the product's persistence after its release ([Wiesner et al., 2006](#); [Oberdörster et al., 2005b](#)). Spray ingredients also might affect the transport and persistence of nano-Ag in air. In addition to its physical properties, the transport and ultimate fate of a sprayed product are affected by the environmental or meteorological factors that it encounters (e.g., magnitude of air currents, temperature, relative humidity) ([Navarro et al., 2008a](#)).

4.3. Terrestrial Systems

Nano-Ag in spray disinfectants can enter terrestrial ecosystems in several ways:

- During manufacturing, distribution, use, or disposal of nano-Ag spray products, nano-Ag might be transported into ambient air and subsequently deposited or washed out to aquatic or terrestrial systems ([Mueller and Nowack, 2008](#)).
- Disposal of spray products containing nano-Ag might result in nano-Ag release to soil ([Navarro et al., 2008a](#)). Plastic/polymer containers with bound nano-Ag could be disposed of in landfills, and nano-Ag could subsequently be released to the surrounding soil at a rate dependent on environmental conditions at the landfill (e.g., amount of organic matter, pH) ([Reinhart et al., 2010](#)). Disposal products are either incinerated (whereby nano-Ag could be released into the air and deposited on soil and plants) or deposited in solid waste landfills. Land-filled sewage sludge could result in leaching of the nano-Ag into subsoils and ground water ([Blaser et al., 2008](#)).
- Products containing nano-Ag might wash down a sink or bathtub drain or be discharged from a washing machine into a wastewater treatment plant. Sewage sludge (separated during the wastewater treatment process) is sometimes applied as a fertilizer to agricultural soils ([Blaser et al., 2008](#)). Therefore, nano-Ag might be released into soil via sewage sludge. Runoff flows along the ground surface could transfer nanoparticles in the sewage sludge to nearby terrestrial systems or aquatic systems ([O'Brien and Cummins, 2009](#); [Blaser et al., 2008](#)).
- Some nano-Ag particles that deposit on soil might experience secondary transport via wind and become resuspended into ambient air and re-deposited into aquatic or terrestrial systems. As stated previously, however, once deposited, nanoparticles would be unlikely to resuspend in the air or re-aerosolize given their propensity to cluster or attach to surfaces ([Aitken et al., 2004](#); [Colvin, 2003](#)).

Overall, information on the transport, transformation, and fate processes of nanoparticles in terrestrial systems is limited. Information obtained from the literature provides a general description of the behavior of nanoparticles in soil and plants; limited information specific to nano-Ag was identified.

4.3.1. Soil

The fate of nanoparticles released to soil is likely to vary depending on the physical and chemical properties of the nanoparticles, the presence of other spray ingredients, and the complex characteristics of the soil environment (e.g., redistribution of nanoparticles by biota). Climatic conditions (e.g., precipitation, temperature) also can determine how the nanoparticles are physically transferred (e.g., by runoff, drainage, leaching) ([AFSSET, 2006](#)).

Due to their size, nanoparticles are potentially mobile in soils ([AFSSET, 2006](#)). Nanoparticles are small enough to fit into the spaces between soil particles, and therefore might travel farther than larger particles before becoming trapped in the soil matrix. Alternatively, nanoparticles released to soil can be strongly sorbed to soil due to their high surface areas, and therefore become immobile. The strength of the sorption of any nanoparticle to soil will depend on its size, chemistry, applied particle surface treatment, the presence of other substances, and the conditions under which it is applied ([O'Brien and Cummins, 2009](#); [U.S. EPA, 2007b](#)). The propensity of a nanoparticle to adsorb to soil surfaces can make it less mobile ([Borm et al., 2006b](#); [Wiesner et al., 2006](#)). Changes in a subsurface soil's solution chemistry (e.g., by introducing a rainfall event), however, can result in nanoparticles becoming detached from soil surfaces and leaching to ground water. The risks associated with nano-Ag contamination of ground water are not currently understood ([Torkzaban et al., 2010](#)).

Properties of the soil environment (e.g., soil type, soil organic matter, pH, ionic strength, presence of other pollutants) also could affect nanoparticle transport ([O'Brien and Cummins, 2009](#); [U.S. EPA, 2007b](#)). Interactions between nanoparticles and soil organic matter alter the degree of nanoparticle clustering in soils (see Section 4.1.2). Soil porewater is generally rich in dissolved organic molecules (e.g., soluble organic matter and humic and fulvic acids) that can enhance colloidal stability of nanomaterials and increase their mobility ([Jaisi and Elimelech, 2009](#)). Changes in pH can affect the size of the cluster, adsorption potential, and mobility in environmental media, as discussed in Section 4.1.3. Soils are not static, and changes to their constituents (e.g., the addition of fertilizers or rain) can decrease soil pH and hence can increase the mobility of contaminants ([ATSDR, 1990](#)). As discussed in Section 4.1.4, the presence of salt ions in soil can promote the association of nanoparticles, thus reducing their bioavailability or physically restraining nanoparticle-organism interactions. Nanoparticles might adsorb other pollutants and become transport vectors for these pollutants. This resulting complex could change

the transport, bioavailability, and toxicity of both the nanoparticles and the other pollutants in the soil ([Navarro et al., 2008a](#)).

4.3.2. Plants

Exposure and uptake of silver and nano-Ag in terrestrial plants are discussed further in Section 5.2.4.1, however, the potential for subsequent transport and transformation in terrestrial plants is briefly discussed here. Evidence indicates that conventional silver is taken up by some terrestrial plants from highly contaminated soils and remains largely in the root system after exposure via contaminated soil, although some distribution to leaves and other plant tissues is possible ([Hirsch, 1998a](#)) (See Section 5.2.4.1). As discussed further in Section 5.2.4.1, Harris and Bali ([2008](#)) examined transport and fate of aqueous AgNO₃ in two metal-tolerant plants, *Medicago sativa* (alfalfa) and *Brassica juncea* (a type of mustard plant). TEM with energy dispersive X-ray spectroscopy revealed clusters of large numbers of spherical-shaped silver nanoparticles with a size distribution reportedly centered around 50 nm. The authors did not report which plant tissues were examined (e.g., root, stem, leaves). The sequestration of nano-Ag led the authors to recommend using these plant species to synthesize large quantities of nano-Ag particles.

Plants could be exposed to nano-Ag in air, water, and soil. Airborne nanoparticles could attach to leaves and other aerial parts of plants ([Navarro et al., 2008a](#)). Once on the leaf surface, nanoparticles could be translocated to different tissues of the plant. If nano-Ag is present in soils, plant roots could interact with nano-Ag associated with soil material and in soil pore water. The mobility of nanoparticles in pore water is an essential condition for interactions with plant roots or fungal hyphae. In the presence of certain organic compounds, nanoparticles will have improved mobility in soils, and could thus interact more efficiently with plant roots ([Navarro et al., 2008a](#)).

Nowack and Bucheli ([2007](#)) and Ma et al. ([2010](#)) hypothesize that nanoparticles in general could interact with plant roots through several mechanisms, including adsorption onto the surface of roots, assimilation into root cell walls, and uptake into root cells. Nowack and Bucheli ([2007](#)) suggest that nanoparticles might diffuse into the apoplast (i.e., intercellular space); from this location, they could be taken up by apoplastic membranes or could enter the xylem at sites of damage. Both groups suggest possible translocation to shoots and leaves from there. As noted by Nowack and Bucheli ([2007](#)), uptake into roots is likely to depend on the shape, size, and composition of nanoparticles and on plant species anatomy. Based on observations of the behavior of other metal complexes in plants, nanoparticles might be transported to plant shoots once they are present in the xylem ([Nowack and Bucheli, 2007](#)). Data specific to nano-Ag is limited but suggests that it can be taken up by terrestrial plants ([Yin et al., 2011](#); [Ma et al., 2010](#)) (See Section 5.2.4.1). Evaluations of nano-Ag transport and transformation within

terrestrial plants are also extremely limited but indicate that translocation of silver after nano-Ag exposure is possible (See Section 5.2.4.1). The extent to which silver and nano-Ag might transfer through terrestrial plants to other portions of the terrestrial food web is discussed in Section 5.2.4.3.

4.4. Aquatic Systems

Nano-Ag in spray disinfectants could be released into aquatic systems in several ways:

- During manufacturing, nano-Ag might be transported into ambient air and subsequently deposited or washed out to aquatic or terrestrial systems ([Mueller and Nowack, 2008](#)). Washing of manufacturing equipment or disposing of water used during production could potentially also result in direct releases to waste water streams.
- During its use, a product containing nano-Ag could be washed down the sink or bathtub drain, or be discharged from a washing machine and material could be released into the sewage system, wastewater collection and treatment facilities ([U.S. EPA, 2010b](#)), and eventually to water bodies. Sewage sludge (separated during the wastewater treatment process) is sometimes applied as a fertilizer to agricultural soils ([Blaser et al., 2008](#)). Therefore, nano-Ag might be released into soil via sewage sludge. Runoff flowing along the ground surface (which causes erosion) could transfer nanoparticles in the sewage sludge to nearby waterways ([O'Brien and Cummins, 2009](#); [Blaser et al., 2008](#)).
- After its use, a spray containing nano-Ag might be transported into ambient air and subsequently deposited in water bodies.
- Disposal of spray products containing nano-Ag might result in release of nano-Ag to soil ([Navarro et al., 2008a](#)). Disposal of by-products released during the manufacturing process might result in a similar type of discharge to soil. Land-filled sewage sludge could cause the silver to leach into subsoil and ground water and to migrate to surface water ([U.S. EPA, 2010b](#); [Blaser et al., 2008](#)).

Overall, few studies are available on the transport, transformation, and fate processes of nanoparticles in natural aquatic systems. Information obtained from the literature provides a general description of the behavior of nanoparticles in water and sediments, although information specific to nano-Ag is limited.

4.4.1. Natural Aquatic Systems

As discussed in Section 6.2.2, aquatic organisms are highly susceptible to silver ion toxicity in natural waters. Therefore, the behavior of nano-Ag in water will strongly influence whether significant incidences of exposure and toxicity to aquatic organisms can be expected. The key chemical, physical, and environmental factors in natural waters that could affect fate and transport behavior of nano-Ag in aquatic systems are discussed below.

4.4.1.1. Surface Properties

As described in Section 2.3, the surface properties of nano-Ag are among the most critical determinants governing its mobility and fate in aquatic systems. Particles in suspension settle at rates that depend on particle size, density, and shape. Waterborne nanoparticles generally settle more slowly than larger particles of the same substance. Due to their high surface area-to-mass ratios, however, nano-sized particles can sorb to sediment particles and become removed from the water column ([U.S. EPA, 2007b](#); [Oberdörster et al., 2005b](#)). The surface properties of nano-Ag govern its stability and mobility as colloidal suspensions or their clustering into larger particles and deposition in aquatic systems ([Navarro et al., 2008a](#)). Nano-Ag particles can be engineered with surface coatings to improve water solubility and suspension characteristics (see Section 4.4.1.4).

4.4.1.2. Ionic Ag and Ag Complexes in Water

The mechanisms of action that govern toxicity of nano-Ag particles and ionic silver are the subject of ongoing research, as investigators seek to determine whether nanoscale silver toxicity is due to the particles themselves and their intrinsic properties, the particles releasing silver ions, or some synergistic combination of the two ([Lubick, 2008](#)). For this reason, the behavior of ionic silver in the environment is relevant to understanding potential impacts of disinfectant sprays that include nano-Ag.

The form of silver in the water is governed in part by water chemistry. In studies over the past few years, a very small proportion of the total dissolved silver in water has been observed to remain as free silver ions, meaning that other forms predominate in the aquatic environment ([Blaser et al., 2008](#); [Luoma, 2008](#)). The free silver ion has a strong tendency to associate with negatively charged ions (ligands) in natural waters to achieve stability. Ligands can occur in solution, on particle surfaces, on dissolved organic matter, or in biological tissues ([Luoma, 2008](#)). Spray ingredients and other substances involved in the manufacturing process also could act as ligands. The distribution of free silver ions and silver complexes depends on the concentration of silver, concentrations of the different negatively charged ligands (such as chloride, sulfide, thiosulfate, and dissolved organic carbon), and the strength of the bond between each ligand and the silver ion ([Choi et al., 2009](#); [Blaser et al., 2008](#); [Luoma, 2008](#)). Table 4-1 presents the ligands with which most silver is expected to complex in the aquatic environment and the log-normalized formation constants that quantify the relative affinities of each group of ligands for silver (see Table 2-2 for solubility constants of solid silver compounds). Although complexation of silver with some ligands under certain environmental conditions leads to the formation of silver precipitates (Ag_2S , AgCl) that will generally deposit to sediments, other complexes (AgCl^{2-} , silver thiolates) will be present in the dissolved phase under certain conditions.

Ligands that strongly hold silver are abundant in most sediments; therefore, silver ions tend to bind readily to particulate matter ([Blaser et al., 2008](#); [Luoma, 2008](#)). The availability of oxygen in sediments, which is a function of both the depth of the water above the sediment and the depth of a particular sediment sample, tends to dictate the form of silver bound to the particles. Strong complexes with organic material predominate at the sediment surface and in sediments in shallow water, where oxygen is usually present and sulfides typically are not. In deeper sediments and in deeper water sediments, where oxygen is absent, silver forms stable precipitates with sulfide ([Luoma, 2008](#)).

Silver ions form especially strong complexes with free thiol (-SH) ligands and with the sulfide ligands that are present in NOM dissolved in water. Silver ions also can interact strongly with the chloride anion (Cl⁻), although the nature of that reaction differs depending on whether the medium is fresh water or sea water. In general, concentrations of chloride ions are low in fresh water,

Table 4-1. Formation constants for silver complexes (Ag:Ligand = 1:1) with environmentally relevant ligands.

Ligand	Formation constant with silver (log K)
Inorganic sulfides	14–21
Organic sulfides (thiols)	12–15
Thiosulfate	8.2
Iodide	6.6
Nitrogen(ammonia and amino)	3–6
Chloride	3
Oxygen (carboxylates)	<2

Source: Adapted from Andren and Bober ([2002](#))

Note from source: Constants are conditional, usually because of differences in ionic strength. Corrections to actual constants generally should result in less than one order of magnitude change. Complexes with reduced sulfur compounds are many orders of magnitude more stable than with other ligands, and no realistic background chemistry (pH and competing cations) would make silver-reduced sulfur complexes unimportant.

but silver ions could react with any chloride ions present to produce silver chloride, most of which precipitates out of solution under normal conditions. Dissolved sulfides, organic materials, and chloride ions likely will complex with essentially all the free silver ions in fresh waters (making it unavailable for uptake by organisms) and drive the free silver ions to very low levels ([Luoma, 2008](#)).

In sea water, chloride occurs in very high concentrations. Multiple chloride ions can react with each silver ion to form soluble silver-chloro complexes that keep silver in solution. Although this silver-chloro complex dominates in solution in sea water, sulfide complexes also could be present ([Luoma, 2008](#)).

4.4.1.3. Particle Clustering

In water, the physical structure of nanoparticles can be modified, and hence the properties of the particles can change ([AFSSET, 2006](#)). Interactions with some environmental compounds can increase the stability and thus the bioavailability of nanoparticles, while interactions with others can promote clustering ([Navarro et al., 2008a](#)). The formation of clusters can significantly affect the transport of particles in aquatic systems. Clusters of nanoparticles that settle can be expected to accumulate in sediments (unless disruption of sediments [e.g., through dredging] causes re-mobilization of the sediment particles). Those that do not settle can travel in the water column from the point of release ([Lowry and Casman, 2009](#)). Nanoparticle clusters are assumed to be less bioavailable than single nanoparticles ([Navarro et al., 2008a](#)). The formation of clusters through sedimentation affects the concentrations of nanoparticles that are bioavailable to organisms. Although clustered or adsorbed nanoparticles are less mobile, they still can be taken up by sediment-dwelling animals or filter feeders (see Chapter 5) ([Nowack and Bucheli, 2007](#)).

4.4.1.4. Important Environmental Factors

As is true for nanoparticles in general, environmental factors that influence the dispersion and deposition behavior of nano-Ag include salinity (ionic strength), the presence of surface coatings (i.e., engineered surface coating or NOM), pH, and water hardness (the concentration of competing cations, such as Ca^{2+} and Mg^{2+}). Results of a recent study by Gao et al. ([2009](#)) on the behavior of nano-sized silver in complex natural waters suggested that dissolved organic carbon, pH, and the concentrations of electrolytes (e.g., Ca^{2+} and Mg^{2+}) help control the formation of clusters (see Section 4.1.2).

Typical aquatic environments, including rivers, lakes, and estuaries, contain monovalent and divalent salts, as well as NOM ([Saleh et al., 2008](#)). Particles of all dimensions are more likely to associate as salinity increases ([Luoma, 2008](#)). Thus, nanoparticles will tend to form clusters to a greater degree in salt water (which has a high ionic strength and higher pH [seawater has a pH of about 7.9]) than in fresh water ([Lowry and Casman, 2009](#); [Klaine et al., 2008](#)). Even small increases in salinity above that of fresh water (~2.5 parts per trillion [ppt]) can cause a rapid loss of colloids through clustering and precipitation processes ([Stolpe and Hasselov, 2007](#)). When the concentration of the chloride anion increases to a certain point, however, the dominant equilibrium species shift to soluble silver-chloro complexes including AgCl^0 (the neutral and most bioavailable complex), AgCl^{2-} , AgCl_3^{2-} , and AgCl_4^{3-} , which act to keep silver in suspension, thus increasing mobility. Moreover, a high percentage of silver adsorbed to suspended sediments in lower salinities (i.e., in brackish or estuarine water) will desorb from these suspended particles at high salinities ([WHO, 2002](#)).

Another factor affecting the transport and distribution of nanoparticles in the aquatic environment is surface coating, either that which is acquired upon release to the environment (e.g., coating by NOM) or a coating that is engineered onto the nanoparticles ([Nowack and Bucheli, 2007](#)). The interactions between nanoparticles and NOM can influence nanoparticle transport, transformation, and fate processes in aquatic systems. The formation of larger nanoparticle clusters by high-molecular-weight NOM compounds might favor deposition of the particles into sediments, likely decreasing their bioavailability. Solubilization by natural surfactants such as lower molecular-weight NOM compounds, however, might increase their mobility and their bioavailability to organisms ([Navarro et al., 2008a](#)).

The behavior of conventional silver in aquatic systems, which has been well studied, also could be relevant to understanding the behavior of nano-Ag in these systems. Silver, with a distribution coefficient of $10^{4.5}$ – 10^6 (based on filtrate and particulate silver concentrations in various aquatic systems), is known to be an extremely particle-reactive metal ([Andren and Bober, 2002](#)). Silver thus has a comparatively short residence time in aquatic systems; it is quickly scavenged from the water column and ends up in sediments.

As a ubiquitous component of aquatic systems, NOM can influence the surface speciation and charge of nanoparticles, thereby affecting their mobility and their propensity to cluster or deposit ([Navarro et al., 2008a](#)). NOM (containing negatively charged humic and fulvic acids) could coat the surface of nanoparticles, resulting in particles that tend to stay dispersed rather than form clusters ([Handy et al., 2008b](#)). As mentioned in Section 4.1.2, however, in the presence of certain electrolyte solutions containing high CaCl_2 , adsorbed humic acid on nanoparticles leads to enhanced particle clustering ([Chen and Elimelech, 2007](#)). NOM can stabilize particles against forming clusters in water, which can enhance transport in aqueous environments and ground water ([Lowry and Casman, 2009](#)).

In addition to NOM, artificially produced organic compounds might be used to stabilize nanoparticle suspensions ([Navarro et al., 2008a](#)). Some nano-Ag particles are engineered to disperse and remain as single particles (i.e., not form clusters), increasing the possibility of the persistence and accumulation of non-associated forms in natural waters. Surface coatings can be added to improve water solubility and suspension characteristics ([Luoma, 2008](#)). Metallic nanoparticles often are coated with inorganic or organic compounds to maintain their stability and mobility as colloidal suspensions ([Navarro et al., 2008a](#)). The potential effect of spray ingredients co-occurring with nano-Ag on the stability and mobility of suspensions is unclear.

The pH of water could influence the rate of nanoparticle clustering, depending on the surface charge of the particles involved ([Handy et al., 2008b](#)). In general, the mobility of silver increases under conditions of increased acidification (lowering of pH) ([Luoma, 2008](#)). Water hardness will alter the chemistry that controls particle clustering (and ultimately ecotoxicity; see Section 6.1) ([Handy et al., 2008b](#)). Hard water (in contrast to soft water) has a high mineral content. Nanoparticle surface charge effects could be influenced by the concentrations of competing cations like Ca^{2+} and Mg^{2+} that might

screen off a negatively charged surface. Nanoparticle dispersion in aquatic systems likely will be influenced by the free cation concentration ([Handy et al., 2008b](#)).

4.4.2. Wastewaters

The formation of particle clusters, surface charge, and surface area of nano-Ag, as well as the presence of other spray ingredients and the treatment method in use, will affect removal efficiency and fate of nano-Ag in wastewater ([O'Brien and Cummins, 2009](#)). At a treatment facility, sorption processes and chemical reactions likely would affect nanoparticles. Those nanomaterials that do not sorb during the primary treatment phase could be removed via settling in the secondary clarifier, after which they might become entrapped in larger sludge flocs. Although wastewater treatment plants can remove much of the nano-Ag and associated free silver ions from the wastewater, some silver might survive treatment, remain in the treated water, and ultimately be discharged into water bodies. Additionally, nanomaterials that are removed in the wastewater treatment process could be released into soil via sewage sludge, which is sometimes applied as a fertilizer to agricultural soils ([Benn and Westerhoff, 2008](#); [Blaser et al., 2008](#)). Runoff along the surface of the ground then could transfer nanoparticles in the sewage sludge to nearby terrestrial systems or waterways ([O'Brien and Cummins, 2009](#); [Blaser et al., 2008](#)). Land-filled sewage sludge could cause the nano-Ag to leach into subsurface soil and ground water ([Blaser et al., 2008](#)).

Tiede et al. ([2010](#)) investigated the fate of nano-Ag in activated sludge and found that a significant fraction of nano-Ag (>90%) in wastewater treatment systems was removed with the sludge solids; that still would leave some fraction of nano-Ag in wastewater, however, that could be released to aquatic environments.

Kiser et al. ([2010](#)) identified two types of nano-Ag that are found in the greatest quantities in commercial products that contain nano-Ag—non-functionalized nano-Ag (not associated with a functional group) and functionalized nano-Ag containing a carboxyl functional group. Both types of nanoparticles were sorbed to activated sludge and removed during wastewater treatment but to different extents. Approximately 97% of the non-functionalized nano-Ag was biosorbed and removed from the wastewater; only 39% of the functionalized nano-Ag was sorbed and removed. The authors believe that the functionalization of the nano-Ag impeded its interaction with the biomass (i.e., the activated sludge) and resulted in less removal. These functionalized nanoparticles could persist to a greater extent in wastewater effluent.

Kim et al. ([2010a](#)) examined sewage sludge products from a large-scale wastewater treatment plant and characterized the nature of the nano-Ag that had accumulated. They discovered that nano-Ag was transformed into silver sulfide (Ag₂S) nanocrystals, with excess sulfur attached to the surface of the Ag₂S. This transformation likely occurred during the sedimentation process in which the surrounding

environment is anaerobic, reduced, and sulfur rich. These observations are consistent with those reported by Kaegi et al. ([In Press](#)), where enhanced sulfide in nonaerated mixed liquor resulted in the near complete transformation of nano-Ag into Ag₂S. Such discoveries makes considering the properties of Ag₂S essential in understanding the complete life cycle of nano-Ag.

In some rural areas of the United States, formal wastewater or solid-waste collection methods might not be available as they are in municipal settings. Households in these areas might rely on septic systems that could be compromised or be otherwise ineffective or might dispose of wastewater through pipes into a pond or the woods. Additionally, rural environments could be exposed to illegal or unmonitored disposal of manufacturing waste products (e.g., into informal landfills, onto roadsides, and into aquatic systems). To the extent that such sources might exist, these exposure pathways should be considered.

4.5. Transport, Transformation, and Fate Models

Most current models are not appropriate for use in predicting nano-Ag fate and transport through environmental compartments ([U.S. EPA, 2010b](#)). Linking adapted models of the dispersive and convective movement of airborne particles and gases with models of transport, transformation, and fate of chemicals and particles in surface waters and soils, however, could help predict the environmental transport, transformation, and fate of nano-Ag and silver ions released from those particles. The potential influence of other spray ingredients or other substances used in manufacturing on the fate and transport of nano-Ag also could be incorporated into the model. Such a comprehensive model, however, has yet to be developed for nano-Ag.

The U.S. Environmental Protection Agency (EPA) and others have used environmental models widely to simulate diffusive and convective movement of aqueous-phase chemicals through environmental compartments (e.g., soils, sediments, water) and partitioning of the chemicals between media (e.g., between solid and aqueous phases). Examples of such models are included in the Models Knowledge Base compiled by EPA's Council for Regulatory Environmental Modeling.¹⁶ Transport of nano-Ag clusters or nano-Ag sorbed to organic particles could be simulated with particulate matter transport models for surface waters. Although adapting models designed to predict transport, transformation, and fate of suspended solids or organic matter of small sizes (e.g., the Particle Tracking Model, developed by the Army Corps of Engineers) to nanoparticle transport is possible, these models might need to be adapted to include additional processes, including particle clustering, sorption to

¹⁶<http://www.epa.gov/crem/knownbase/index.htm>

suspended particles, and possibly colloidal behavior. Evaluation of such models by comparing model outputs with measured values also could be challenging, given the questionable reliability of analytical methods to detect nanoparticles at environmentally relevant concentrations (i.e., in the nanogram/liter [ng/L] range) (Luoma, 2008; Demirbilek et al., 2005). Models that can be used specifically to estimate the transport, transformation, and fate of nano-Ag in air and soils have not been developed, but some fate and transport models have been proposed for evaluating the transport, transformation, and fate of nano-Ag, or silver ions released from nano-Ag, in water and sediments. These models are described below. In addition, Gottschalk et al. (2010) recently described a probabilistic material flow model used for assessing the environmental exposure to engineered nanoscale titanium dioxide particles. A brief discussion of this modeling approach is also provided below.

Although empirical data on nano-Ag concentrations in the environment are lacking, a recent study by Mueller and Nowack (2008) used computer modeling to predict nano-Ag concentrations in air, water, and soil in Switzerland based on simplifying assumptions and a substance flow analysis. The authors acknowledged that transformation, degradation, and bioaccumulation of nano-Ag are likely important factors in characterizing substance flow through environmental compartments, but that these factors were not considered in the analysis. In addition, flows through secondary compartments (e.g., ground water, sediment) were not modeled due to inadequate data available for these compartments.

The volumes of different environmental compartments for the entire country were calculated as the surface area multiplied by depth for soil, surface water, and air:

- soil volume = agricultural and nonagricultural surface areas multiplied by 0.2- and 0.05-meter (m) mixing depths, respectively;
- surface water volume = surface area multiplied by 3-m mixing depth; and
- air volume estimated as volume of air within 1 kilometer (km) of ground level across the country.

Homogeneous and complete mixing within each medium was assumed. Predicted environmental concentrations (PECs) were calculated for “realistic exposure scenarios” (based on nano-Ag use worldwide, estimated as 500 tons per year) and for “high exposure scenarios” (based on 1,230 tons nano-Ag per year, or 5% of the world-wide extraction of 25,620 tons of silver that is not used in jewelry, photography, or industry) and were compared to calculated predicted no-effect concentrations. Allocation of worldwide nano-Ag use to Switzerland was based on the country’s share of the total population of industrialized countries (i.e., 0.0068). The investigators estimated that more than 15% of nano-Ag is used in sprays and cleaning agents, and that most (85%) of that nano-Ag is discharged into wastewater from wastewater treatment plants. Of the remaining 15%, approximately 5% is discharged to air, 5% is discharged to soils, and 5% is disposed of in waste incineration plants. For nano-Ag discharged in wastewaters, the investigators further assumed that 97% of nanoparticles are removed in packed-bed filters and that, on average, 97–99% of suspended particles are removed during treatment. Finally,

overflow wastewater discharge during storm events was assumed to be 5–10% of total wastewaters. In the realistic scenario, the PECs for nano-Ag were 0.0017 microgram per cubic meter ($\mu\text{g}/\text{m}^3$), 0.03 microgram per liter ($\mu\text{g}/\text{L}$), and 0.02 microgram per kilogram ($\mu\text{g}/\text{kg}$) for air, water, and soil, respectively. In the high emission scenario, PECs were 0.0044 $\mu\text{g}/\text{m}^3$, 0.08 $\mu\text{g}/\text{L}$, and 0.1 $\mu\text{g}/\text{kg}$ for air, water, and soil, respectively. Authors stated that the risk quotients (calculated as PEC/predicted no-effect concentration) were notably less than 1.

Blaser et al. (2008) modeled fate and transport of silver ions, instead of nano-Ag particles, in the Rhine River to assess potential risks from use and disposal of plastic and textile consumer products containing nano-Ag. They assessed the likely fate of silver ions released to municipal wastewaters from washing and wearing textiles spun with nano-Ag and contact with water of plastics coated or impregnated with nano-Ag. Their model estimated silver ion concentrations in the water column and in the top layer of sediments for three different scenarios (“minimum,” “intermediate,” and “maximum” emission scenarios). Silver ion releases were estimated from silver content in biocidal plastics and textiles. The fraction of wastewater treated was assumed to be 80–90% and the fraction of silver removed by filtration and treatment was assumed to be 85–99%. Data on release rates of silver ions from different types of plastics embedded with nano-Ag and from products with surface applications of nano-Ag are sparse, and measured rates vary substantially among different formulations.

The model, which simulates silver ion fate and transport processes in river waters and sediments, estimated PEC ranges of 4–40, 10–140, and 30–320 ng/L in river water for the “minimum,” “intermediate,” and “maximum” emission scenarios, respectively. Predicted silver ion concentrations increase in both the water column and sediments downstream as the river flows through populated areas with wastewater treatment facilities (Blaser et al., 2008). In the top layer of the sediment, the PEC ranges for the scenarios were 0.04–2, 0.1–6, and 0.3–14 milligrams per kilogram (mg/kg), respectively. In the interstitial waters of the sediments, calculated PECs for the scenarios were 9, 30, and 70 ng/L, respectively. The investigators reported that the PECs calculated for the river water were generally consistent with the range of empirical data available for silver concentrations in river waters (>0.01–148 ng/L). The sediment PECs, however, were generally higher than the range of measured data for river sediments (0.2–2 mg/kg), but they were well below the value of 150 mg/kg reported for heavily affected river beds. The proportion of the silver ions that is likely to be bioavailable, however, depends on the availability of organic and inorganic sulfides and other materials in the river to bind silver ions, as discussed in Section 4.4.1.4 and in Chapter 5.

Musee (2011) applied a mathematical model to compute quantities of several nanomaterial (including nano-Ag) flows from nanoenabled cosmetic products into terrestrial and aquatic ecosystems in the Johannesburg Metropolitan City of South Africa through four potential release pathways. These included wastewater from a treatment plant, direct runoff into the environment (i.e., untreated streams), solid waste (i.e., directly disposed materials after product use), and use of sewage sludge for agricultural

applications. PECs were reported to depend primarily on wastewater treatment plant efficiency, as well as product matrix, dilution factor, and other factors. Musee reported PECs for nano-Ag ranging from 2.7×10^{-3} $\mu\text{g/L}$ to 2.7×10^{-1} $\mu\text{g/L}$ in the aquatic environment under a realistic dilution factor of 1 and an assumed high removal efficiency. Although these values resulted in risk quotients (hazard quotients) <1 for the terrestrial environment, hazard quotients >1 were reported for the aquatic environment, indicating potential risk to the aquatic environment ([Musee, 2011](#)).

Gottschalk et al. ([2010](#)) developed a probabilistic material flow analysis (PMFA) framework to derive PECs for a range of nanomaterials in environmental media. The PMFA uses a whole life-cycle perspective and takes into account uncertainty and variability in model inputs to calculate concentrations of nano-Ag in all “natural” environmental compartments (atmosphere, soil, surface water, sediment, and ground water) and “technical” environmental compartments (production, manufacturing, use, recycling, and disposal in waste incineration and sewage treatment plants). Using the PMFA, PECs (reported as range of lower quantiles [Q(0.15)] to upper quantiles [Q(0.85)]) were derived for nano-Ag and other nanomaterials from all anticipated sources in the United States, European Union, and Switzerland either for 2008 or as the annual increase in concentration ([Gottschalk et al., 2009](#)). Because production volumes for the nanomaterials evaluated in this study were scaled based on number of inhabitants in each of the three geographic regions, the PEC ranges for each environmental compartment differed little among these three areas. As a result, only the data for the United States are presented here.

In general, U.S. PECs were lowest for nano-Ag in air (0.0020–0.0097 nanogram per cubic meter [ng/m^3]), surface water (0.088–0.428 ng/L), and sewage treatment plant effluent (16.4–74.7 ng/L) and highest in sediments (increase between 153 and 1,638 nanograms per kilogram per year [ng/kg-yr]), sewage treatment plant sludge (1.29–5.86 mg/kg), and sludge-treated soil (increase between 526 and 2,380 ng/kg-yr). Despite high PECs for sludge-treated soil, the expected contribution of nano-Ag to PECs in the soil compartment as a whole was quite low (increase between 6.6 and 29.8 ng/kg-yr) because sludge-treated soils account for only 1% of agricultural soils ([Gottschalk et al., 2009](#)).

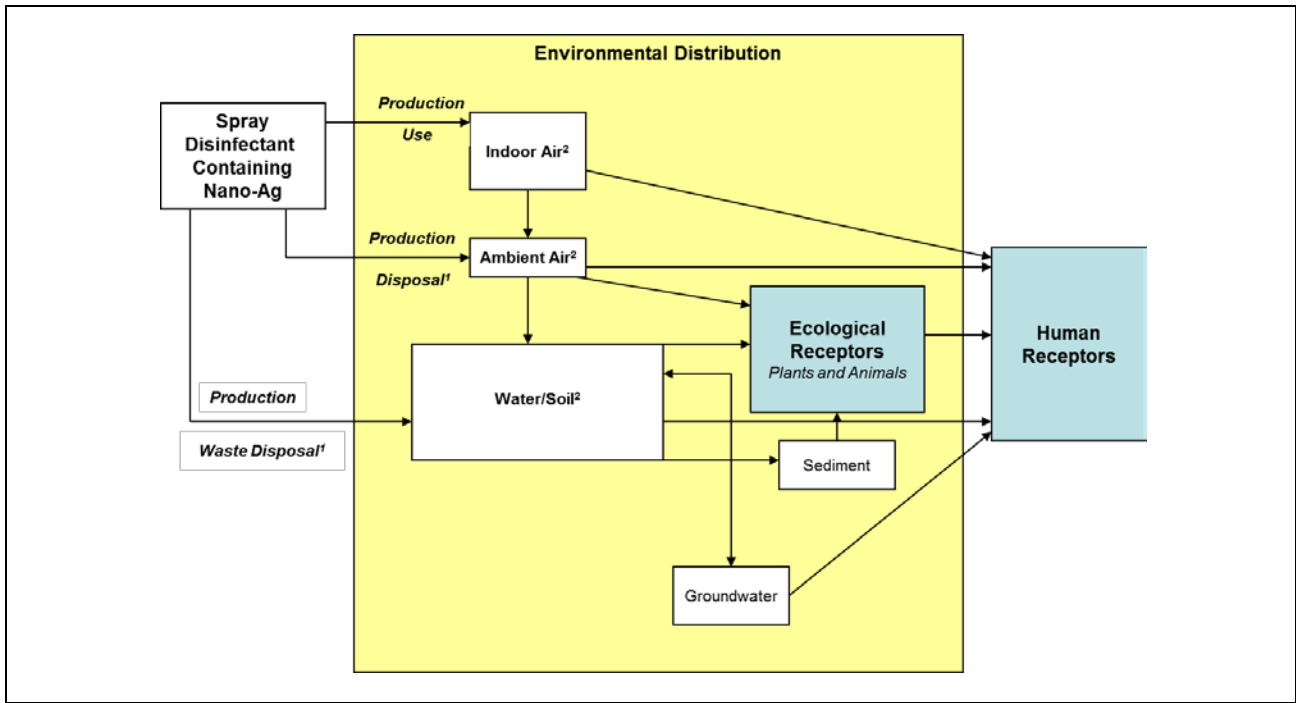
Although Gottschalk et al. ([2010](#)) believe that the PMFA is applicable to predict concentrations of compounds in the environment when little information is available concerning environmental fate and exposure characteristics, the added value of their approach over that of Mueller and Nowack ([2008](#)) has yet to be evaluated by other researchers. Some of the principal assumptions included in the PMFA (e.g., homogeneous mixing of material in environmental compartments on a country- or continent-wide scale) were not actually built into the Monte Carlo simulation and sensitivity analyses. Some results (e.g., total mass, mass flux) estimated by the PMFA are in the form of ranges extending more than two orders of magnitude for several environmental compartments and pathways. As also noted by the authors, additional empirical data are still required to generate useful model input distributions.

4.6. Summary of Nano-Ag Transport, Transformation, and Fate in Environmental Media

The important potential pathways of nano-Ag and by-products into the environment associated with the production (including manufacturing, distribution, and storage), use, and disposal of spray disinfectants containing nano-Ag are summarized in Figure 4-1. Nano-Ag can be released into air, water, and soil at various stages of the life cycle. Within these media, nano-Ag can be transported, transformed, and spatially distributed in the environment. Ultimately, ecological or human receptors could be exposed to nano-Ag and associated contaminants.

One of the primary pathways for release of nano-Ag in spray disinfectants could occur through indoor use, where it might be sprayed into the air and onto a surface. Transport of nano-Ag from the indoor environment to the outdoor environment, where it could partition into the ambient air, water, and soil, is then possible. Release of nano-Ag in spray disinfectants also might occur during production or as a result of waste disposal. For example, a product containing nano-Ag that is wiped up with a paper towel and then discarded in the trash could end up in a landfill, with subsequent leaching into subsoil and ground water and possible migration to surface water. A product containing nano-Ag that is washed down a sink or bathtub drain might enter wastewater treatment plants, and treated water containing nano-Ag subsequently could be released into water bodies. Other spray ingredients and substances involved in the manufacture of nano-Ag sprays could co-occur with nano-Ag in the environment and potentially modify its fate and transport behavior, although information regarding this possibility was not identified during development of this case study.

Either a model focused on the movement of airborne particles and gases or one designed to predict the fate and transport of chemicals and particles in surface waters and soils (or a combination of these two model types) could serve as a basis for developing a comprehensive model for predicting environmental fate and transport of nano-Ag and the associated release of silver ions. Such a comprehensive model, however, has yet to be developed for nano-Ag.



Source: Adapted with permission of Elsevier; Nowack and Bucheli (2007).

Figure 4-1. Potential nano-Ag pathways into the environment associated with production, use, and disposal of spray disinfectants containing nano-Ag.

¹Waste disposal includes products containing nano-Ag that might be incinerated, washed down a sink or bathtub drain, or discharged from the washing machine into wastewater treatment plants, land-filled sewage sludge, or sewage sludge used as a fertilizer on agricultural fields. This nano-Ag then could migrate into water or soil media and be distributed throughout various environmental compartments.

²Dynamic relationships between single nano-Ag particles and clusters exist in indoor air, ambient air, and water and soil compartments.

Chapter 5. Exposure, Uptake, and Dose

This chapter examines the potential for biota and humans to be exposed to primary and secondary contaminants associated with nano-Ag in disinfectant spray products. As described in preceding chapters, nano-Ag and associated materials (e.g., feedstock and manufacturing waste by-products, co-product ingredients) constitute primary contaminants that might be released to different environmental media at one or more stages during the life cycle of the material. Once released, nano-Ag and associated materials might undergo physicochemical and biological transformation processes that result in exposing biota and humans to various secondary contaminants. From a comprehensive environmental assessment standpoint, all of these primary and secondary contaminants are of potential relevance. At present, however, attention is directed first to nano-Ag as the primary contaminant of interest.

As previously discussed, throughout this chapter, the term nano-Ag is used to refer in general to any type or formulation of engineered silver nanomaterials and might encompass a variety of physical and chemical properties. As noted in Chapter 1, no clear demarcation between exposure-dose and effects exists, and thus, some overlap of information in Chapter 5 on exposure and uptake with information in Chapter 6 on effects is unavoidable. To the extent possible, reference to studies cited in both chapters is limited in Chapter 5 to discussion of exposure-dose and in Chapter 6 to discussion of effects.

Exposure to a substance requires contact between the substance and the surface of an organism via one or more environmental media (i.e., water, air, soil). For internal exposure to occur, the substance must penetrate the organism's cell walls, cell membranes, or other barriers between the organism and its environment; that is, the substance must be bioavailable to the organism. Transfer of a substance from any of these environmental media and across exchange boundaries results in an internal dose that is distributed by the circulatory system to organs.

Several terms are used throughout this chapter in describing the characterization of exposure-dose ([U.S. EPA, 2005, 1992](#)). *Exposure* is contact of an agent with the outer boundary of an organism. *Exposure concentration* is the concentration of a substance in its transport or carrier medium at the point of contact. *Dose* is the amount of a substance available for interaction with biological receptors or in metabolic processes after crossing the outer boundary of an organism. *Applied dose* is the amount of substance presented to an absorption barrier and available for absorption (although not necessarily having yet crossed the outer boundary of the organism). In non-experimental settings, *potential dose*, a more general term, is the amount ingested, inhaled, in contact with the skin, flowing past gills, or in contact with other exchange boundaries (e.g., surface of plant roots). *Absorbed dose* is the amount crossing a specific absorption barrier (e.g., gills, digestive tract) through one or more uptake processes. *Internal dose*

is a more general term, representing all of the substance that has been absorbed by one or more exchange boundaries. Finally, *delivered dose* is the amount of a substance available for interaction with a particular organ, tissue, or cell. The portal of entry determines the extent to which the substance might be transformed (e.g., by the liver following ingestion) prior to reaching the general circulation. Where the exchange boundary (e.g., gills) is the site of toxic action, potential dose might equal delivered dose for that boundary.

Metrics describing exposure for nano-Ag can either be units of total Ag per unit mass or volume of exposure medium (e.g., nanogram of silver per liter of water [ng(Ag)/L(water)]) or number of particles per unit volume of exposure medium. In either case, the mean and distribution of sizes and shapes, among other physicochemical characteristics, of nano-Ag particles need to be reported to adequately describe exposure. The amount of total silver per unit mass or volume of exposure medium is the measure most often used and the measure that is most precise. The same concentration of total silver, however, can result from a few large nanoparticles per unit volume or many smaller nanoparticles per unit volume. For that reason, the size distribution of particles should be reported along with total silver concentration in an exposure medium.

Particle size is best described by a distribution (e.g., percentiles), but the common practice in literature is to specify only a mean and range of particle sizes. In addition, the metric for size is usually the diameter of spherical particles. If nano-Ag particles are not spherical in shape, the investigators should report the shape. Because the characteristics of nano-Ag in a starting material in the laboratory can change after its addition to air, water, or soil (e.g., clustering of particles, dissolution of particles), characterizing the nano-Ag particles once in an exposure medium also is important. In the discussion below, the units of exposure are total silver per unit volume, with particle-size distributions characterized as reported (e.g., mean, range).

Chemicals and substances that cannot be biodegraded beyond inorganic compounds ultimately can persist and in some cases accumulate in both environmental media and biota. *Bioavailability* is defined as the availability of a substance in an environmental medium for absorption by an organism in contact with that medium (e.g., absorption of a substance inhaled with air or ingested with food). *Bioconcentration* refers to the direct uptake and accumulation of a substance from an external medium (e.g., from water through gills for aquatic organisms), while *bioaccumulation* occurs from both direct uptake from an external medium *and* ingestion of a substance. Both bioconcentration and bioaccumulation require that some fraction of the substance is bioavailable in environmental media. Bioconcentration of an agent can occur across cell walls (e.g., plants) or across specialized exchange surfaces (e.g., gills of aquatic invertebrates or fish), whereas bioaccumulation applies to animals only ([U.S. EPA, 2003b](#)). In natural environments, the ratio of the chemical concentration in an animal to the chemical concentration in its

environment generally is referred to as a bioaccumulation factor (BAF). Bioavailability is a prerequisite for toxicity ([Luoma, 2008](#)), and therefore, often is assessed indirectly by evaluating the toxicity of an agent to organisms under specified conditions ([Berthet et al., 1992](#)).

Chemicals that sorb to the external surface of organisms, but cannot penetrate the outer layer (e.g., epidermis, cell wall) because of large size, surface charge, or other properties are generally not considered to be bioavailable. Nanoparticles sorbed to an external surface of organisms, however, can in some cases damage cell walls or cell membranes or provide a steady release of ions that affect the organisms' performance (e.g., survivorship, growth, reproduction; see Chapter 6). Different coatings and surface properties of nano-Ag products might enhance or inhibit sorption to gill surfaces or uptake by the gastrointestinal (GI) tract. A nano-Ag particle that associates with and disrupts essential cell processes at the external membrane, or delivers silver ions that do so, therefore, is considered bioavailable for purposes of this document. This approach is consistent with the convention used by Luoma ([2008](#)).

Toxic effects following exposure depend not only on delivered dose, but also on the timing and patterns of exposure to the substance in environmental media, bioavailability of the substance from a specific medium to particular organisms through their uptake processes, fate of the substance in the organism, and the sensitivity of the organism to the substance. The disposition of the substances within the organism includes its metabolism (possibly to more toxic entities), distribution, storage, and excretion. The behavior of organisms in their environment can play a key role in their exposure profiles. For example, exposure scenarios for children can differ drastically from those for adults because they spend more time in contact with floor surfaces and they mouth a variety of objects that adults would not. Other characteristics of an organism (e.g., age, reproductive status, size, health status, individual exposure to other agents) can modify its sensitivity to a toxic substance, that is, its response to a given exposure, as discussed in Chapter 6.

Because limited information is available on the releases of nano-Ag during manufacturing, storage, use, and disposal of products such as spray disinfectants, quantitative, data-driven estimates of the potential geographic extent of releases and media concentrations of nano-Ag and associated contaminants are not yet possible. Thus, conceptual models are currently necessary to identify the most likely significant exposure pathways and routes of intake. Shatkin ([2008](#)) suggests that a risk assessor can “step through” the life cycle of a specific product to identify points in the manufacturing, storage, distribution, and application of a new product that might result in releases to the environment and exposures of biota or humans. Thus, a risk assessor can deduce, from limited information on the product, as well as general manufacturing and distribution practices for similar products, some likely release points in the life cycle of a new product and the context in which releases might occur.

Nano-Ag can be released to the environment at various points in the life cycle of a disinfectant spray, as described in Chapter 3, and many of these release scenarios could be similar to those for nano-Ag contained in other end-use products such as fabrics. Human occupational exposures and silver releases into the environment are possible during the synthesis of nano-Ag particles from feedstocks and the manufacture of disinfectant spray products that incorporate nano-Ag. Some of the most likely and significant exposure scenarios can be identified from the potential release scenarios described in Chapter 3 and existing knowledge of the characteristics and behavior of nano-Ag and associated substances (e.g., silver ions, transformation products, waste products, by-products) in the environment.

This chapter characterizes current knowledge of measured nano-Ag exposure and uptake and internal dose (i.e., absorption of nano-Ag by organisms). Exposure and dose data are presented first for biota in Sections 5.1 and 5.2, respectively. Exposure data then are presented for humans in Section 5.3. General discussions of the potential for aggregate and cumulative exposures involving nano-Ag are presented in Sections 5.4 and 5.5, respectively. As will be discussed in Section 5.4, aggregate exposure to nano-Ag from disinfectant sprays and other products or sources determines the total potential and internal doses of nano-Ag. Cumulative exposures to nano-Ag from multiple substances and other types of nanoparticles are examined in Section 5.5. Because limited product formulation data are available, the evidence for co-exposure to other spray constituents is not evaluated in detail, although such an evaluation could be relevant in a comprehensive environmental assessment. Section 5.6 includes a brief discussion of exposure models. Human uptake and dose from exposure to nano-Ag are discussed in Section 5.7.

Improved methods to measure, monitor, and predict environmental concentrations of nano-Ag likely will be necessary to assess current and future nano-Ag exposures in human and ecological populations. Also, information on how exposure to nano-Ag particles translates into internal dose of either nano-Ag, silver ions, or both, is needed to evaluate possible modes of action¹⁷ of nano-Ag in different groups of organisms.

5.1. Biotic Exposure



As discussed in Chapter 3, uses of nano-Ag in spray disinfectant products could lead to two potential types of environmental releases: (1) down the drain to wastewater treatment plants, with subsequent release of treated water to surface waters and (2) land application of sewage sludge in

¹⁷“Mode of action” is defined and discussed in greater detail in Section 6.2, footnote 22.

agricultural areas. These releases are similar to those from nanofunctionalized textiles, as described by Blaser et al. (2008). Wastewater containing nano-Ag from manufacturing facilities also could reach wastewater treatment plants, and nano-Ag not removed during the wastewater treatment process could enter surface waters through effluent. Thus, exposure of aquatic organisms via the water column and sediments in riverine through coastal environments is possible. Additional exposure of aquatic animals to silver accumulated in their food also could occur. Luoma (2008) argues that if mass discharges of silver from nano-Ag applications reach levels equivalent to those during historically high levels of discharge in the 1980s, silver concentrations in aquatic systems will also mirror those during historical periods of elevated releases. For environmental concentrations of this magnitude to occur, however, concentrations entering wastewater treatment plants would have to be much higher than those during the 1980s to account for improvement in wastewater treatment technologies. But assuming that such elevated silver mass discharges to environmental compartments are possible, Luoma hypothesized that nano-Ag levels in the waters of South San Francisco Bay, for example, could reach concentrations of 26–189 ng/L, which is similar to those previously observed during the 1980s when discharges of conventional silver to the environment were occurring at a rate of approximately 550 kilograms (kg) per year (Smith and Flegal, 1993). Given this scenario, Luoma further argues that nano-Ag discharges at that rate might increase concentrations in the sediment of San Francisco Bay by more than an order of magnitude from a 2007 baseline of approximately 0.2 parts per million (ppm) (or 200 micrograms per kilogram [$\mu\text{g}/\text{kg}$] sediment) to concentrations of approximately 3 ppm (3,000 $\mu\text{g}/\text{kg}$ sediment). Blaser et al. (2008) estimated similar concentrations for the Rhine River following anticipated increases in nano-Ag releases. Note, however, that these estimated concentrations represent releases of nano-Ag from all sources, not from spray disinfectants alone. Such theoretical projections are the only estimates of potential environmental exposures of nano-Ag currently available because monitoring technology for measuring nanoparticle concentrations in the ng/L range is still under development. Estimating the relative contribution of nano-Ag from spray disinfectants to total nano-Ag exposures from all sources also is not yet possible.

As discussed in Chapter 4, the anticipated life-cycle stages and behavior of nano-Ag in environmental compartments suggest that accumulation of nano-Ag in the terrestrial environment generally will not be as great as in the aquatic environment (particularly in sediments); however, as discussed above, soil biota and agricultural crops could be exposed to high concentrations of nano-Ag where sewage sludge is used to amend soils. In addition, sewage sludge or solid waste containing nano-Ag might be disposed of in landfills, which could result in exposure of terrestrial organisms or leaching of nano-Ag into ground water. Exposures of reptiles, birds, and mammals could occur through incidental soil ingestion in agricultural areas, and the sensitivity to ingested silver in these organisms is expected to be low (as for humans). Herbivores might encounter nano-Ag accumulated in plants, while insectivores might be exposed to nano-Ag accumulated in their prey. Airborne nano-Ag in outdoor

environments based on indoor uses is expected to be insignificant; outdoor uses, however, might result in inhalation exposure of animals and exposure of plants through their foliage.

Localized accidental releases or spills could create “hot spots” of nano-Ag contamination. Accidental releases to terrestrial or aquatic environments might occur at bulk material storage facilities or during transport of nano-Ag from one facility to another during the production, manufacture, distribution, and disposal of products containing nano-Ag (see Chapter 3). Empirical data or modeling results appear to be lacking regarding accidental releases of nano-Ag throughout the life cycle of nano-Ag sprays and other products. Risk assessments could require special consideration of accidental release scenarios.

5.2. Biotic Uptake and Dose

Investigations of the absorption, distribution, metabolism, and excretion, as well as pharmacokinetics, of nanoparticles in general and of nano-Ag in particular have not yet been conducted on species from many of the major groups of organisms (e.g., algae, macrophytes, higher plants, annelids, echinoderms, arthropods, mollusks, amphibians, reptiles, birds), although some data exist on aquatic species, primarily fish ([Handy et al., 2008a](#)). In the context of the current case study, the uptake of nano-Ag in the environment by different groups of organisms would depend on the likelihood of exposure via different pathways leading from the production, storage, use, and disposal of consumer products containing nano-Ag.

Few techniques have been developed that can accurately quantify dosimetry for nano-Ag, and therefore differentiating between exposure and uptake in biota is difficult. The primary dose metric used for ecological effects studies is an exposure concentration expressed in terms of mass. Depending on the study, the term “mass” could correspond to the mass of silver in the nanoparticles added, mass of total silver in solution, mass of silver ions, or mass of free silver in solution, although the form is not always specified. Some studies have attempted to normalize the dose across various types of nanoparticles by expressing concentration in terms of moles. **Dose-dependent effects have been observed in multiple organisms at various time scales as detailed in Appendix B,** but the mechanisms that allow the penetration of nano-Ag into and across membranes and into the cells of tissues in biota are not yet well understood. The rate of uptake, tissue or whole-body concentrations, and the fate of nano-Ag at the cell, tissue, and organism level are not currently known ([Luoma, 2008](#)).

As described in the introduction, metrics describing exposure for nano-Ag can either be units of total Ag per unit mass or volume of exposure medium (e.g., ng[Ag]/L[water]) or number of particles per unit volume of exposure medium. In either case, the mean and distribution of sizes and shapes of nano-Ag particles also need to be reported to adequately describe exposure. In the discussion below, the units of

exposure are total silver per unit volume, with particle-size distributions characterized as reported (e.g., mean, range).

The discussion of biotic uptake and dose of nano-Ag is divided into four major sections. The first section provides general descriptions of bioavailability, bioconcentration, and bioaccumulation of nano-Ag and conventional silver in biota (Section 5.2.1) as the terms apply to the remainder of Section 5.2. The subsequent three sections focus on specific aspects of the uptake of nano-Ag, silver ions, and conventional silver by: bacteria and fungi (Section 5.2.2), aquatic ecosystems (Section 5.2.3), and terrestrial biota in agricultural settings (Section 5.2.4). Throughout, nano-Ag is distinguished from silver ions and from other forms of silver to the extent possible. In addition, dose is addressed, wherever possible, by reporting absorption of nano-Ag or silver ions through the surface of an organism to its interior, rather than the adsorption of either onto exterior surfaces (e.g., gills, GI tract).

5.2.1. Bioavailability, Bioconcentration, and Bioaccumulation



Chemicals and substances that cannot be biodegraded beyond inorganic compounds ultimately can persist and in some cases accumulate in both environmental media and biota. The relationship between external exposure and internal dose is influenced by bioavailability, bioconcentration, and bioaccumulation, and thus these concepts are described briefly here. Within the organism, the potential for systemic effects depends on the bioavailability of the nano-Ag at the organism's exchange boundary, the release of silver ions from the particles, and either or both being absorbed and delivered to target organs or tissues ([Lowry and Casman, 2009](#)). Chronic effects depend, moreover, on the ability of organisms to detoxify or excrete nano-Ag or silver ions derived from the particles. Silver, conventional or nano-sized, that is not excreted can accumulate in an organism ([Berthet et al., 1992](#)) and could be passed up the food chain ([Bianchini and Wood, 2008](#)). Bioavailability of nano-Ag is likely to be a function of its form, the characteristics of the environmental exposure medium, and characteristics of the organism for several reasons:

- Properties of the nano-Ag such as size, potential to form clusters, or surface properties and coatings can influence its uptake. Alternatively, each of these considerations can facilitate or preclude the binding of nano-Ag to other particles that might or might not be available for uptake.
- Characteristics of the environmental medium (e.g., surface water pH, temperature, presence of calcium carbonate, sulfates, other salts, dissolved and particulate natural organic matter [NOM] and other organic materials) can modify the bioavailability of nano-Ag through the binding of nano-Ag or silver ions in a nonbioavailable form.
- Characteristics of the organism and its route(s) of intake (e.g., acidic environment of the GI tract, fish gill active transport of silver ions through ionic sodium [Na⁺] uptake channels) can affect bioavailability and biocompatibility of nano-Ag and silver ions.

Processes that readily transport nanoparticles from one environmental medium to another reduce bioavailability in the first medium. For example, when nano-Ag is released to aquatic systems, many agents in natural waters can bind to nano-Ag and silver ions, which results in precipitation or sedimentation of the silver (see Section 4.4.1). Silver that has precipitated out of solution is no longer directly bioavailable to organisms in the water column; depending on its form, however, it might be more available to organisms in the sediment.

Attributes of organisms that help to determine bioavailability of silver ions and nano-Ag to them are discussed in Section 5.2.1.1. Environmental factors that can modify bioavailability of silver ions and nano-Ag are discussed in Section 5.2.1.2. Use of bioaccumulation models is discussed briefly in Section 5.2.1.3. The potential for bioaccumulation of nano-Ag or silver ions from nano-Ag is examined for aquatic and terrestrial food webs as part of the broader discussion about uptake in aquatic and terrestrial organisms in Sections 5.2.3 and 5.2.4, respectively.

5.2.1.1. Attributes of an Organism that Influence Bioavailability of Nano-Ag and Silver Ions

The type of organism, its structure, and its physiology are key determinants of the mechanisms by which it might be able to absorb nano-Ag and silver ions from the environment. Uptake of silver ions and nano-Ag from the environment can depend on whether the organism is a prokaryote or eukaryote, its cell size, cell wall or membrane construction, type of circulatory system, respiratory physiology, and other major aspects of its body plan and physiology. At this time, however, data concerning the influence of basic phylogenetic attributes on absorption or adsorption of nano-Ag are lacking for most groups of organisms ([Choi et al., 2009](#); [Handy et al., 2008b](#)). Sections 5.2.2 through 5.2.4 examine potential uptake routes for silver ions and nano-Ag for different groups of organisms and describe evidence for the degree of penetration into epithelial and systemic cells and extracellular matrices.

Within a group of organisms, the degree to which an individual absorbs silver ions from its environment is likely to depend on many aspects of its condition, such as its life stage, reproductive status, existing body burden of silver, osmotic status, and nutritional and overall health condition. These conditions as well as an animal's behavior (e.g., filter feeding) also might affect potential exposure to nano-Ag. Note that if nano-Ag particles adhere to an organism's external surfaces, and if the particles release silver ions, the concentration of silver ions in the immediate vicinity of the organism would be expected to be higher than concentrations of silver ions in the surrounding medium. Measuring the silver ion concentrations in a micro-thin, "unstirred" layer of water or viscous medium (e.g., mucus) immediately surrounding the organism without mixing, and thereby contaminating, that layer with the surrounding medium, however, would be technically challenging.

5.2.1.2. Attributes of the Environment Influencing Bioavailability of Silver Ions and Nano-Ag

As described in Section 4.1.2, several characteristics of the environment can affect the fate and transport of nanoparticles in water and in soil. These characteristics are likely to influence the amount of nano-Ag and silver ions that organisms come in contact with in different exposure media. Characteristics of the environment that influence the bioavailability of nanoparticles in general and nano-Ag specifically differ for aquatic and terrestrial systems.

For aquatic systems and metallic nanoparticles, several characteristics of surface waters can affect particle fate, including salinity (e.g., freshwater, estuarine, marine), hardness, organic matter content, and pH (see Section 4.4.1.4). Processes that can remove nano-Ag from suspension and silver ions from solution are noted below ([Gao et al., 2009](#); [Wijnhoven et al., 2009b](#); [Luoma, 2008](#)):

- Aggregation (referred to in this case study as the formation of clusters) of nano-Ag particles with each other into larger particles that settle out of suspension;
- Complexing of nano-Ag with NOM, which might create larger particles that settle out of the water column; and
- Complexing of nano-Ag or silver ions with inorganic materials, forming insoluble precipitates.

These processes deposit the silver to the sediments where, depending on the particles and sediment chemistry, nano-Ag and silver ions might be more or less bioavailable to benthic organisms.

To date, essentially no data have been published that indicate the fate of nano-Ag particles released to surface waters ([Wijnhoven et al., 2009b](#)). Data are available, however, concerning the bioavailability of silver ions introduced to surface water in the form of the highly soluble silver nitrate (AgNO_3). Therefore, factors that affect the bioavailability of silver ions from AgNO_3 released to surface waters are discussed first. Factors that might influence the bioavailability of nano-Ag particles are considered second.

Environmental Factors that Affect Bioavailability of Silver Ions

Many ligands exist for silver ions in natural surface waters (see Section 4.4.1.2). As discussed in Chapter 4, silver-complexing agents include inorganic ligands (e.g., chloride $[\text{Cl}^-]$, bicarbonate, thiosulfate), simple organic ligands (e.g., amino acids, ethylenediaminetetraacetic acid [EDTA]), and complex polydispersed organic ligands such as humic and fulvic acids ([Bianchini and Wood, 2008](#)).

In natural fresh waters, concentrations of free silver ions are likely to be very low ([Luoma, 2008](#)) (see Table 4.1 in Chapter 4, which lists the solubility products of common silver compounds in water). Silver ions bind very strongly to reduced sulfur in natural waters, and sulfide (S^{2-}) concentrations typically exceed free silver concentrations in the environment by several orders of magnitude ([Blaser et al., 2008](#)). The general assumption has been that ligands present in the water will reduce bioavailability

(and toxicity) of metals to aquatic biota by reducing the free metal ion concentrations ([Bianchini and Wood, 2008](#)). Blaser et al. (2008) concluded that in freshwater systems, silver is expected to be bound to S^{2-} either in the form of colloidal silver sulfide (Ag_2S) solid-phase clusters or as an Ag_2S surface complex on organic matter. As discussed in Section 2.3.5, Ag_2S solids are relatively stable and insoluble in water ([Blaser et al., 2008](#)).

In wastewater treatment plants, silver ions are easily removed because of their strong sorption to suspended particles. Most silver ions that might reach surface waters should rapidly bind to ligands, settle out of the water column, and become incorporated into the sediments, although repeated resuspension back into the water column during scouring by storm events and by bioturbation (animal-sediment interactions) is possible ([Blaser et al., 2008](#)).

Toxicity tests with aquatic organisms confirm that bioavailability of silver ions is reduced in the presence of excess sulfides. Reactive S^{2-} , as found in zinc sulfide clusters for example, reduces the acute toxicity of silver ions to both daphnia ([Bianchini et al., 2002](#)) and rainbow trout (*Oncorhynchus mykiss*) ([Mann et al., 2004](#)). With a ratio of sulfide to total silver of 250 to 20, Bianchini et al. (2002) observed no toxicity in *Daphnia magna* neonates after 48 hours at a silver concentration as high as 2.1 micrograms per liter ($\mu g/L$) (or 19 nanomoles per liter [nM] \times 108 grams per mole [g/mol] of silver), while in the absence of sulfide (less than 5 nM), the 48-hour LC_{50}^{18} for neonate *D. magna* was estimated to be 0.18–0.26 $\mu g/L$. The daphnia accumulated more total silver in the presence of sulfide than in its absence ([Bianchini et al., 2002](#)) owing to accumulation of unabsorbed sulfide-bound conventional silver on the gills (on thoracic appendages) and in the digestive tract, but the sulfide ligand appeared to shield the organism from toxicity ([Bianchini et al., 2005b](#)).

In fresh waters, Cl^- also can react with silver ions to form relatively insoluble silver chloride ($AgCl$) precipitates, thereby reducing the concentration of silver ions, as demonstrated in several studies reported by Bielmyer et al. (2008). In seawater, however, the abundance of chloride anions favors the creation of soluble silver-chloro complexes, of which the circumneutral $AgCl^0$ (i.e., at a pH favoring the neutral complex instead of ionic disassociation) has been shown to passively enter and accumulate in rainbow trout ([Wood et al., 2002](#); [Hogstrand and Wood, 1996](#)).

Environmental Factors that Affect Bioavailability of Nano-Ag Particles

Many environmental factors could affect bioavailability of nano-Ag particles in aquatic ecosystems (see Section 4.4.1.4), including surface water chemistry (e.g., ionic strength, pH, dissolved materials) and suspended solids. Together with physicochemical properties of particles (e.g., size, shape, surface area),

¹⁸Lethal concentration is the chemical concentration at which 50% of the exposed organisms die; this effect level is commonly used to estimate the toxicity of a substance to a specific group of organisms.

environmental factors influence dissolution potential, clustering potential, resulting particle surface properties, and interactions with dissolved and particulate organic matter in surface water ([Boxall et al., 2007](#)). Also, the capacity of wastewater treatment plants to remove nano-Ag from sewage (and to “dispose” of it in sewage sludge) influences the overall amount of nano-Ag likely to reach surface waters.

Metallic nanoparticles released to surface waters tend to become coated with NOM quickly ([Gao et al., 2009](#); [Navarro et al., 2008a](#); [Boxall et al., 2007](#)). In aquatic ecosystems, the organic matter usually originates from one or more of the following sources ([Navarro et al., 2008a](#)):

- Fulvic compounds from humic substances, primarily from decomposition of plant materials from terrestrial sources;
- Rigid biopolymers including polysaccharides and peptidoglycans produced by phytoplankton or bacteria; and
- Flexible biopolymer recombination of decomposed organic materials.

Sorption to large clusters of organic matter or high-molecular-weight materials tends to remove nanoparticles from solution, depositing them to the sediments ([Handy et al., 2008b](#); [Klaine et al., 2008](#)). On the other hand, complexation with low-molecular-weight organic materials might enhance the particles’ ability to stay in suspension ([Hyung et al., 2007](#)). Also relevant to the bioavailability of nano-Ag are any processes that might sequester free metal ions after their release to water from suspended nanoparticles, such as complexation with available sulfides. No studies regarding the specific fate and bioavailability of nano-Ag in the environment were identified for this case study. See Section 6.1 for additional discussion of factors that might affect the bioavailability of nano-Ag as indicated by toxicity tests with specified modifications to either the nano-Ag (e.g., coatings) or the test water (e.g., pH, Cl^- , ionic strength).

The rate of release or dissolution of silver ions from nano-Ag particles, and hence the bioavailability of silver ions, generally decreases with increasing particle size owing to surface-volume relationships. For example, Ho et al. ([2010](#)) examined dissolution of nano-Ag particles due to oxidation in vitro with bacterial and mammalian cells. Using spherical nano-Ag particles of 5–20 nanometers (nm) in diameter, they found that the rate of dissolution of nano-Ag particles decreased with increasing particle size.

Toxicity tests have confirmed that sulfides can reduce the bioavailability of nano-Ag or silver ions released from the nanoparticles. Choi et al. ([2009](#)) compared the toxicity, and by inference the bioavailability, of nano-Ag (average size 15 ± 9 nm) to an enriched concentration of nitrifying bacteria in the absence and presence of several possible ligands, including S^{2-} , sulfate (SO_4^{2-}), Cl^- , phosphate (PO_4^{3-}), and EDTA. The source of the bacteria was a local nitrifying activated sludge plant in Missouri ([Choi et al., 2008](#)). The biomass suspensions were aerated with pure oxygen to maintain a dissolved oxygen concentration of approximately 20 milligrams per liter (mg/L) before the nano-Ag or silver ions were added. Sulfide was the most effective ligand in reducing nano-Ag toxicity to the bacteria (80%

reduction inferred from increased oxygen uptake rates). A back-scattered electron detector coupled with a secondary electron detector was used to locate nano-Ag particles and Ag₂S complexes attached to the surface of the bacteria. Scanning electron microscopy (SEM) in conjunction with energy dispersive x-ray analysis identified elemental composition. These techniques revealed that the nano-Ag particles reacted with the S²⁻ to form new Ag_xS_y complexes and precipitates that did not oxidize during 18 hours of aeration. The toxicity of the test medium was enhanced, however, at S²⁻ concentrations higher than 1 mg/L, presumably from inhibition of bacterial metabolism by the free available S²⁻ ([Choi et al., 2009](#)).

Release of silver ions from nano-Ag also is enhanced in oxidative conditions. In *in vitro* testing of bacterial and mammalian cells under quasi-physiological conditions, Ho et al. ([2010](#)) found increasing silver ion release rates, increasing toxicities, and therefore increasing bioavailability of silver ions from nano-Ag particles with increasing concentrations of hydrogen peroxide (H₂O₂), a reactive oxygen species (ROS), in the exposure medium.

In saltwater systems, the high ionic strength of seawater and high concentration of Cl⁻ can lead to both the formation of nano-Ag clusters, which could precipitate out of the water column, and the formation of soluble silver-chloro complexes; which of the two processes dominates will depend on the water chemistry, presence of NOM, and nano-Ag surface treatments ([Maccuspie, 2011](#)). Also in saltwater systems, exopolymeric substances, rich in polysaccharides and anionic colloidal biopolymers, are secreted by phytoplankton and bacteria. Such substances could either protect the organisms from interactions with nanoparticles (e.g., by initiating extracellular clustering of nanoparticles or by binding metal ions), or enhance interactions (e.g., by adsorbing and holding nanoparticles in the immediate vicinity of cell surfaces) ([Miao et al., 2009](#)).

Using seawater, Miao et al. ([2009](#)) demonstrated rapid and complete clustering of polyvinylpyrrolidone (PVP)-coated nano-Ag (60–80 nm), leaving no detectable particles smaller than 220 nm in solution. The addition of natural organic compounds or thiols greatly enhanced the presence of nano-Ag in solution. Miao et al. ([2009](#)) found further that diatoms exposed to nano-Ag in the seawater accumulated silver linearly with the estimated free silver ions in solution at higher nano-Ag concentrations. It was not clear whether the higher accumulation of silver in the diatoms (measured as microgram Ag per mg diatom carbon [$\mu\text{g}/\text{mg}$]) resulted solely from influx of silver ions into or beyond the cell wall, or included accumulation of the neutral complex AgCl⁰, which was a few orders of magnitude more prevalent in the solution ([Miao et al., 2009](#)).

Although Tiede et al. ([2010](#)) reported that approximately 90% of nano-Ag added to sewage will transfer to the sludge, the form of silver adsorbed to the sludge solids was not characterized in this study. Two studies investigated the presence of nano-Ag in municipal wastewater treatment plants and reported only nano-sized Ag₂S ([Kim et al., 2010a](#)) and the near complete transformation of nano-Ag to Ag₂S ([Kaegi et al., In Press](#)) (see Section 4.4.2). Their findings suggest that insoluble Ag₂S might be formed in

situ under anaerobic, sulfur-rich conditions during wastewater treatment ([Kim et al., 2010a](#); [Kaegi et al., In Press](#)).

The bioavailability of nano-Ag (and ionic silver released from nano-Ag) in sewage sludge applied to terrestrial environments has not been investigated. Soils contain numerous ligands that can complex nano-Ag and silver ions, and sewage sludge has substantial particulate organic matter to which nano-Ag could bind depending on its size and surface coating (see Sections 4.1.2 and 4.3.1). The degree to which nano-Ag might be available in sewage sludge applied to agricultural fields depends on properties of the particles, properties of the sludge, and the soil medium.

5.2.1.3. Bioaccumulation Models

Models to estimate bioaccumulation of nano-Ag or silver ions released from nano-Ag in aquatic and possibly terrestrial food webs are relevant because the nano-Ag in spray disinfectants is expected to be released into wastewaters (see Chapter 3). An existing model that could be adapted for aquatic food webs for at least the silver ions released from nano-Ag is the U.S. Environmental Protection Agency's (EPA's) Bioaccumulation and Aquatic System Simulator model. Bioaccumulation and Aquatic System Simulator is a ligand-binding model for positive ionic inorganic substances that includes toxicokinetic, physiological, and ecological processes affecting chemical uptake directly from water in fish ([Barber, 2008](#)). Models for nano-Ag uptake from food via the GI tract, however, are not yet available.

For terrestrial ecosystems, a first step would be to examine the availability of measured conventional silver accumulation factors for terrestrial plants and soil invertebrates. Baes et al. ([1984](#)) cite a plant-soil bioconcentration factor (BCF) value of 0.138 for "above-ground" and 0.10 for "below-ground" terrestrial plant parts consumed by humans, where the plant BCF value is based on total dry-weight silver concentrations in the plants and soils. Values less than 1.0 generally indicate a very low concern for bioconcentration (e.g., BCF values <100 are considered of low concern by programmatic EPA offices), which might explain the paucity of data on conventional silver uptake by plants. If the behavior of nano-Ag in the soil is similar to the behavior observed for ionic silver in other plant-soil studies, nano-Ag could accumulate at low levels in metal-tolerant plant root systems (Sections 5.2.4.1 and 5.2.4.3). If such accumulation occurs, small mammals or other biota that consume roots and tubers might be able to hyper-accumulate nano-Ag. No models were identified that investigate this food pathway in terrestrial ecosystems. Bioaccumulation of inorganic chemicals from soils by earthworms (a commonly studied soil organism) has been investigated for conventional silver compounds. The results of these bioaccumulation studies vary: Some studies suggest that conventional silver does not bioaccumulate in earthworms ([Ratte, 1999](#)) while other studies demonstrate that bioaccumulation from soil or pore water does occur, but the kinetics of bioaccumulation are not well characterized ([Nahmani et al., 2009](#); [2007](#)). A recent study, however, did demonstrate bioaccumulation of both nano-Ag and silver ions in earthworms,

with BAFs statistically significantly higher for ionic silver than for nano-Ag coated with either PVP or oleic acid ([Shoults-Wilson et al., 2011a](#)).

5.2.2. Uptake by Bacteria and Fungi

Many bacteria and fungi readily take up conventional silver and nano-Ag, as summarized in this section by type of organism.

Bacteria. Only oxidized nano-Ag particles, that is, particles with chemisorbed silver ions on the surface, exert antimicrobial effects ([Lok et al., 2007](#)). Such effects might be due to the combination of the nano-Ag and the silver ions that are tightly adsorbed (via physical or chemical forces) on the particle surface ([Lok et al., 2007](#)). Reduced nano-Ag appears to be unstable and easily oxidized.



Prokaryotes such as bacteria have a cell wall that separates them from their environment. Unlike the more advanced eukaryotes, bacterial cells cannot perform phagocytosis or endocytosis, the two processes by which nanoparticles might be absorbed into eukaryotic cells or organisms. Most bacteria excrete siderophores, which chelate the relatively insoluble Fe^{3+} (ferric iron) ions in the environment, forming a soluble complex that the bacteria absorb by active transport ([Raymond, 2003](#)). Although other metal ions (e.g., aluminum) have been reported to complex with siderophores ([del Olmo et al., 2003](#)), no reports of silver ion chelation were found. In the environment, the ion for which siderophores have the highest affinity is Fe^{3+} ([Raymond, 2003](#)).

The membrane structures of bacteria are classified into two groups: gram-positive and gram-negative. The structural differences occur in the key component of the cell wall, peptidoglycan, located immediately outside the cytoplasmic membrane. The cell wall of gram-positive bacteria (e.g., *Bacillus*, *Clostridium*, *Listeria*, *Staphylococcus*, *Streptococcus*) includes an ~30-nm-thick peptidoglycan layer, while the cell wall of gram-negative bacteria (e.g., *Escherichia*, *Salmonella*, *Pseudomonas*) includes only a thin, ~2- to 3-nm layer of peptidoglycan. The gram-negative cell wall also contains an additional outer membrane composed of phospholipids and lipopolysaccharides facing the external environment. The largest pores in the outer membrane of gram-negative bacteria secrete bacterial proteins out of the cell and can measure almost 10 nm in diameter ([Bitter et al., 1998](#)). These pores are likely to “open” only as needed for protein transport across the membrane ([Filloux, 2004](#)). Fixed porins, which allow diffusion of smaller molecules in both directions across the outer cell membrane, are smaller, with effective diameters for solutes of 1–2 nm. Yet despite the small pore sizes of both membranes, Xu et al. ([2004](#)) demonstrated that nanoparticles up to 80 nm can enter *Pseudomonas aeruginosa* cells. Furthermore, bacteria can then extrude these nanoparticles through the living cell membranes via an extrusion pump consisting of two outer membrane proteins (MexA and MexB) and one inner membrane protein (OperM), even though the pores associated with this extrusion pump are more than 50 times

smaller than the nanoparticles they extrude. Cellular invasion and extrusion mechanisms of these larger nanoparticles are not well understood.

Studies investigating uptake of nano-Ag by gram-positive bacteria are few ([Panáček et al., 2006](#)), with most studies focusing on gram-negative bacteria. Sondi and Salopek-Sondi ([2004](#)), Morones et al. ([2005](#)), and Hwang et al. ([2008](#)) have shown that nano-Ag anchors to and penetrates the cell wall of gram-negative bacteria. Wijnhoven et al. ([2009b](#)) and others have proposed that the physical penetration changes the structure of the cell membrane (presumably the outer membrane first), which could increase its permeability and result in uncontrolled transport of materials into and out of the cytoplasm. Others have suggested the antibacterial mechanism of nano-Ag is the formation of free radicals that damage the membrane ([Kim et al., 2007](#); [Danilczuk et al., 2006](#)). Hwang et al. ([2008](#)) proposed a synergistic toxic effect of nano-Ag and silver ions from the nano-Ag in producing ROS in two strains of bioluminescent bacteria (DS1 and DK1) sensitive to oxidative-stress damage. With nano-Ag sorbed to the bacterial cell wall surface, silver ions can move into the cells and produce ROS inside. Hwang et al. ([2008](#)) hypothesized that the membrane damage caused by the nano-Ag attachment and insertion demonstrated by Morones et al. ([2005](#)) also might disrupt the ion efflux system, thereby preventing expulsion of the silver ions from the bacterium.

Pal et al. ([2007](#)) assessed the influence of nano-Ag shape on toxicity to the gram-negative *Escherichia coli* bacterium. They found that truncated, triangular, silver nanoplates exhibited the strongest antibacterial activity and reported the top “basal plane of truncated triangular silver nanoplates [i.e., a {111} facet] is a high-atom-density surface” ([Pal et al., 2007](#)). Images obtained with energy-filtering transmission electron microscopy (TEM) revealed that many of the nano-Ag particles adhered to the cell surfaces were coincident with pits (depressions) in the cell wall. Using high-angle annular dark-field scanning transmission electron microscopy, Morones et al. ([2005](#)) demonstrated that individual, roughly spherical, nano-Ag with {111} facets attached directly to the outer cell membrane. In addition, nano-Ag was found throughout the interior of cells. That physical disruption of cell membrane integrity by nano-Ag might be the primary cause of antibacterial effects has been proposed, however, with accumulation of nano-Ag in the cytoplasm occurring as a secondary effect ([Neal, 2008](#)).

One difficulty with interpreting literature on the interaction of nano-Ag with gram-negative bacteria is that investigators do not distinguish the cytoplasmic membrane of the cell wall from the external membrane ([Hwang et al., 2008](#); [Pal et al., 2007](#); [Morones et al., 2005](#)), which together are only 2–3 nm thick. These distinctions are important for gaining a better understanding of the specific site and mechanism of entry for nano-Ag into gram-negative bacteria.

Nitrifying bacteria. Nitrifying bacteria oxidize inorganic nitrogen compounds for energy (chemoautotrophic). They can also oxidize ammonium ions to nitrites and nitrates, and are common in municipal wastewaters. Key enzymes for these processes, including ammonia monooxygenase and nitrite oxidoreductase, are organized along internal membrane systems. Choi et al. ([2008](#)) examined the effects

of exposing nitrifying bacteria to nano-Ag (average size 14 ± 6 nm), silver ions (from AgNO_3), and AgCl colloids (average size 250 nm). Interactions between microbes and nano-Ag were examined using environmental SEM, which can image hydrous samples. The images revealed that nominally 10-nm nano-Ag from a commercial source, when mixed with nitrifying bacteria in suspension, formed clusters in extracellular polymeric substances (from the bacteria), which resulted in larger particles ranging from 200 nm to a few micrometers. Electron micrographs demonstrated nano-Ag attached to bacterial cells. Choi and Hu (2008) found that metabolic inhibition of nitrifying bacteria (as inferred from oxygen uptake measurements) corresponded to the fraction of nano-Ag less than 5 nm in diameter, suggesting that only small nano-Ag particles penetrate the cell wall and membrane.

Fungi. Fungi are eukaryotic organisms with a cell nucleus and distinct organelles. Nano-Ag is fungicidal against many common fungi, including the genera *Aspergillus*, *Candida*, and *Saccharomyces* (Wijnhoven et al., 2009b). Yeast is a unicellular fungus. The cell wall, plasma membrane, and periplasmic space between the wall and membrane together account for approximately 15% of the total cell volume (Feldmann, 2005). The membrane is selectively permeable, and the cells are capable of both endo- and exocytosis. Both the cell wall and membrane are involved in budding (reproduction). To investigate uptake and mode of action of nano-Ag on microfungi, Kim et al. (2009) used a budding yeast *Candida albicans* exposed to spherical nano-Ag with an average diameter of 3 nm. TEM revealed that treated fungal cells exhibited pits and holes in their cell walls and transmembrane pores through which cellular constituents could leak. Comparisons, such as exposing yeast to surface-coated nano-Ag or to silver ions from AgNO_3 , were not provided.

Ionic silver in solution can form nano-Ag in the presence of some fungi. For example, extracellular nano-Ag particles between 5 and 25 nm in diameter have been produced by exposing the filamentous fungi *Fusarium oxysporum* (Ahmad et al., 2003) and *Aspergillus fumigatus* (Bhainsa and D'Souza, 2006) to aqueous silver ions. Nano-Ag 5–15 nm in size is stabilized by proteins secreted by the fungus (Ahmad et al., 2003). Given the relatively low concentrations of ionic silver in surface waters, this particular mechanism of nano-Ag formation is probably without consequence except for green synthesis methods.

Mukherjee et al. (2001) found “intracellular” nano-Ag of 25 ± 12 nm in *Verticillium* exposed to aqueous silver ions. Electron microscopy revealed that the nano-Ag particles formed adjacent to the cell wall surface but external to the plasma membrane, possibly as a result of reduction of the ions reaching the periplasmic space by plasma membrane enzymes. No toxicity to the fungus was observed; the cells continued to multiply after exposure and synthesis of nano-Ag. In this case, the fungi were essentially removing free silver ions from the environment. Sauluo et al. (2010) also found intracellular nano-Ag in addition to nano-Ag on cell surfaces of yeast (*Saccharomyces cerevisiae*) exposed for 24 hours to a nanocomposite film (thin layer of nano-Ag particles, 5–10 nm in diameter, embedded in an organo-silicon matrix) coating stainless steel. Damage to the cell wall structure and protein configurations inside the cells was observed, but nucleic acids appeared normal.

Viruses. Viruses are obligate intracellular parasites that replicate only within a living host. Viruses themselves are not living cells having independent metabolic processes; they consist of a core of DNA or RNA encapsulated in a glycoprotein coat. Speshock et al. (2010) found that Tacaribe virus exposed to nano-Ag particles 10–25 nm in diameter prior to the virus' introduction to and infection of host cells facilitated virus entry into the cells along with virus-attached nano-Ag. Once inside the cells, the virus pre-treated with nano-Ag exhibited a significant reduction in viral RNA production and progeny virus release compared with unexposed virus controls. The investigators concluded that nano-Ag likely was binding to the virus surface membrane (e.g., to the thiol groups found in cysteine) and entering host cells via endocytosis. The mechanism by which the nano-Ag deactivates viral replication in the host cells has not yet been demonstrated. Other investigators have found that nano-Ag particles in the range of 1–10 nm can bind to the HIV-1 virus, which inhibits the virus from binding to host cells (Elechiguerra et al., 2005).

5.2.3. Uptake in Aquatic Ecosystems

In general, conventional silver contamination of aquatic ecosystems is thought to be of more concern than contamination of terrestrial systems because of the high toxicity of silver ions to many groups of aquatic organisms (Kramer et al., 2009). Historically, most notable impacts of conventional silver in the environment have been in the immediate vicinity of silver mines (Ratte, 1999) and in some estuaries receiving wastewaters containing silver from photographic facilities (Flegal et al., 2007). As a notable example, evaluations in San Francisco Bay suggest that waste silver originating at a photographic processing plant was discharged from a regional water quality control plant through the late 1970s and subsequently accumulated in estuarine sediments to high levels, leading to the Bay's characterization as the "Silver Estuary" (Flegal et al., 2007). Even after active discharging of silver wastes ceased, silver concentrations remained elevated. For example, in intertidal mudflats of the southern reach of the estuary, or South Bay, concentrations measured during that time were approximately 0.2–0.6 microgram per gram ($\mu\text{g/g}$) (i.e., two to six times higher than regional background levels of less than 0.1 $\mu\text{g/g}$). Concentrations of silver in the clam *Macoma petalum* dropped from approximately 100 $\mu\text{g/g}$ in the late 1970s to 2–4 $\mu\text{g/g}$ by the late 1990s. Silver concentrations in the Asian clam *Corbula amurensis* dropped from approximately 4 $\mu\text{g/g}$ to 0.5 $\mu\text{g/g}$ over the same time period. In both species, the drop in body tissue silver corresponded with improved maturation of gonadal tissues and readiness to spawn. To date, however, those scenarios appear to be the only real-world, documented situations in which silver contamination has caused a high accumulation and adverse effects in aquatic biota (in benthic bivalves).

Once nano-Ag reaches an aquatic ecosystem from wastewater treatment facilities, or other sources, its fate and the likelihood that it will contact aquatic biota depend on many factors. First, properties of the particles (e.g., size, shape, coatings) and water chemistry (e.g., dissolved organic carbon, ionic strength,

pH) will influence the extent to which the particles remain in suspension, partition to dissolved organic carbon in the water column, form clusters with each other, and adsorb to suspended particles and plankton. As noted in Chapter 4 and Section 5.2.1, the chemistry and content of natural fresh water, estuarine water, and salt water generally favor formation of silver complexes and clusters that settle out of the water column to the surface of the sediment bed. In freshwater systems, the formation of Ag_2S and S^{2-} complexes removes silver ions from solution, while in saltwater systems the formation of AgCl or AgCl^{2-} predominates depending on the water chemistry, leading to both removal (AgCl precipitates) and retention of silver ions in solution (soluble AgCl^{2-}). Silver nanoparticles, on the other hand, might remain in suspension if coated to prevent the formation of clusters or complexation with, or adsorption to, other particles. Laboratory tests of the toxicity of nano-Ag to freshwater aquatic organisms generally use one or more methods to ensure suspension of the nano-Ag in the water column. The methods generally do not reflect conditions in natural surface waters. The current consensus is that nano-Ag rarely remains in suspension in natural ecosystems, although opinions differ as to whether advances in technologies to keep particles in suspension will alter this particle behavior ([Luoma, 2008](#)).

For animals, uptake of nano-Ag from water or pore water in sediments might occur at the gill surface during respiration, following ingestion with food (e.g., detritus, algae, smaller animals), or dermal absorption, depending on the form and bioavailability of nano-Ag and silver ions in food, water, and sediments. Uptake into an organism versus adsorption to its surface depends on the nanoparticulate chemistry at exterior surfaces, which could cause the particles to form clusters, and the behavior of the particles inside cells and circulatory fluids (e.g., blood plasma) ([Handy et al., 2008a](#)). Assuming that nano-Ag particles remain in suspension in the water column, as the particles come in contact with the surfaces of organisms, the following three scenarios are possible:

- No interaction; nano-Ag drifts away from the organism and continues movement in the water according to Brownian motion. This option seems most likely for nano-Ag with some type of surface coating, either a natural one acquired post-release (e.g., dissolved organic matter) or manufactured (e.g., to keep nano-Ag in suspension until a spray disinfectant is used).
- Nano-Ag particles adhere (adsorb) to the surface(s) of the organism; for example, to the cell wall surface of phytoplankton and macrophytes, the carapace and appendages of crustacean zooplankton, the epidermis of larval forms of invertebrates, the outer surface of aquatic eggs, and, for larger animals (e.g., mussels, crabs, fish), to the exchange surface of gills, olfactory receptors, and the lining of the GI tract for ingested particles. Uptake of silver ions released from the nano-Ag in the vicinity of organisms is expected to the same degree as uptake of silver ions released from dissolved silver salts, conventional silver powders, or other sources of silver ions.
- Nano-Ag particles penetrate the surface of an organism. Whether a silver nanoparticle can penetrate the outer cell wall or membrane of an organism depends on properties of the particle and characteristics of the organism. Depending on the organism, various uptake mechanisms are possible for nano-sized particles. Sorption to natural low-molecular-weight organic materials in the surface water or some manufactured surface coatings might

facilitate uptake of nano-Ag at the cell wall or cell membrane by increasing the particles' lipophilicity.

Where nano-Ag particles do penetrate cell walls, cell membranes, circulatory systems, or interstitial spaces of organisms, they might interfere with cellular structure and function by physical (mechanical) forces, by providing a continuing source of free silver ions, or by both types of action. How the route of uptake of nano-Ag (and silver ions from the particles) is influenced by surface modifications of the particles is currently unknown ([Behra and Krug, 2008](#)). Presumably, smaller particles are more likely to be taken up by endocytosis than larger particles. Routes of uptake for silver ions and nano-Ag are discussed below by type of aquatic organism and environment: (1) freshwater algae, (2) freshwater protozoa, (3) mollusks, (4) aquatic crustacea, (5) fish eggs, (6) freshwater fish, and (7) saltwater fish.

5.2.3.1. Uptake by Algae

Freshwater algae appear to take up silver ions rapidly, presumably through a copper ion transporter in the cell membrane ([Lee et al., 2005](#)), resulting in high BCFs (e.g., 10,000 liters per kilogram [L/kg] wet weight) ([Ratte, 1999](#)). To evaluate the toxicity to and uptake of nano-Ag in green algal cells, Navarro et al. ([2008b](#)) exposed *Chlamydomonas reinhardtii* for 1 hour to nano-Ag and silver ions with and without cysteine as a ligand to decrease free silver ions in solution. The nano-Ag particles were evaluated for size and zeta (ζ) potential using dynamic light scattering and were visually inspected using TEM. Particle size ranged from 10 to 200 nm with a median of 40 nm; the diameter of 98% of particles was within 25 ± 13 nm. According to measurements with diffusive gradients in thin films, the maximum concentration of silver ions (most of the labile silver measured) comprised approximately 0.9–1% of the total silver in solution, while measurements with a Ag-ion-selective electrode indicated that the silver ion concentrations were 0.7–1.2% of the total silver. With the addition of algae, silver ions dropped to 0.1% after 1 hour. The inhibition of algal photosynthesis in the presence of AgNO_3 was completely eliminated by the addition of equimolar concentrations of cysteine. Several indirect lines of evidence led the authors to conclude that the toxicity of nano-Ag to the algae required interaction between the algae and nanoparticle, but was mediated by silver ions released from the nanoparticles either at the algal interface or near the algal interface where products of algal metabolism, notably H_2O_2 , might be secreted.

In saltwater systems, the high ionic strength of sea water and high concentration of Cl^- can favor either the formation of nano-Ag particle clusters or soluble silver-chloro complexes. Available natural organic compounds (e.g., humic substances and thiols) can behave as surfactants, binding with nano-Ag and stabilizing some of the particles in suspension ([Hyung et al., 2007](#)). Exopolymeric substances secreted by phytoplankton and bacteria ([Verdugo et al., 2004](#)) could either protect the organisms from nanoparticle toxicity or enhance toxicity, as discussed in Section 5.2.1.2 ([Wilkinson and Reinhardt, 2005](#)).

Algal uptake of nano-Ag in sea water was examined using the diatom *Thalassiosira weissflogii* ([Miao et al., 2009](#)). Diatoms are eukaryotic single-celled algae encased in a silica-based rigid “frustule”

(essentially two glass half shells, or valves, fused together). Nutrients were limited to enhance excretion of carbohydrates by the cells. Initial solutions of 60- to 80-nm nano-Ag in deionized water were well dispersed, but when added to sea water, nano-Ag rapidly formed clusters, with no particles detectable in a less-than-200-nm filtrate. The addition of natural organic compounds (fulvic acid from the Suwannee River) stabilized some of the nano-Ag in suspension, and the addition of thiols increased nano-Ag particle concentrations in the less-than-220-nm filtrate by a factor of 100. Because toxicity was not enhanced by the addition of thiols, Miao et al. (2009) concluded that one or more protective mechanisms occurred: Such protective mechanisms might be the carbohydrate coating of the silica shell repelled the particles, the nano-Ag particles were too large to penetrate pores in the shells, or the coating of nano-Ag with organic material prevented interaction with the diatoms. The exopolymeric coatings excreted by the cells contain covalently bound proteins that might bind silver ions. The authors concluded further that the observed toxicity of the nano-Ag was due to the release of free silver ions in the vicinity of the cell; nano-Ag did not penetrate the cells.

Whether inside the algal cell or sorbed to the surface, nano-Ag can act as a continual, slow-release source of silver ions (Lubick, 2008). To date, the data are consistent with nano-Ag adsorption to the outer cell wall and release of silver ions in the immediate vicinity of the cell wall.

5.2.3.2. Uptake by Protozoa

Using the single-celled flagellate protozoan *Paramecium caudatum*, Kvitek et al. (2009) demonstrated that nano-Ag particles approximately 30 nm in diameter were not toxic at concentrations as high as 25 mg/L (paramecia survived for 7 days; the 1-hour LC₅₀ was 39 mg/L), whereas silver ions caused immediate death of all of the paramecia at concentrations as low as 0.4 mg/L (see Section 6.2.2). The size and ζ potential of the nano-Ag particles were measured by dynamic light scattering, and size was confirmed with TEM. Modifying the nano-Ag with Tween 80 (1% w/w), a nonionic surfactant, increased the bioavailability (as reflected in measures of toxicity) of the nano-Ag to the paramecia somewhat, with a measured 1-hour LC₅₀ of 16 mg Ag/L.

5.2.3.3. Uptake by Bivalve Mollusks

Investigators have noted that surface sediment-dwelling and filter-feeding mollusks are likely to ingest engineered nanoparticles released to the environment, particularly if the nanoparticles associate with natural particles (Moore, 2006). Mollusks accumulate conventional pollutants sorbed to suspended particles and sediment (Galloway et al., 2002; Livingstone, 2001). Lamellibranch bivalves (e.g., mussels, scallops, cockles, most clams) filter food from the water passing over their gills, with cilia moving the food particles to the mouth. Nanoparticles might be trapped and ingested with the phytoplankton and

suspended detritus that comprise the food ([Wijnhoven et al., 2009b](#)). Moore ([2006](#)) postulated that benthic marine bivalves such as the blue mussel (*Mytilus edulis*) might absorb ingested nanoparticles by endocytosis.

Moore et al. ([1997](#)) and Owen ([1970](#)) demonstrated uptake of nano-sized particles and their deposition in the digestive glands of marine mussels (*Mytilus edulis*) and cockles (*Cardium edule*), respectively. In the case of mussels, the nanoparticles were composed of sucrose polyester oil (particle diameters not reported). In vitro experiments demonstrated that isolated hepatopancreatic digestive cells from the mussel took up the particles by endocytosis, and the internalized vesicles containing nanoparticles subsequently attached to and released their contents in the lysosomal degradative compartment of the cells ([Moore et al., 1997](#)). In the case of cockles, animals were fed nanoparticles comprising colloidal graphite and iron oxide in vivo, and animals were sacrificed and tissues removed and fixed at several time intervals. The electron micrographs of digestive cells showed that some phagosomes in the cells engulfed single particles (phagocytosis) of 50 to 300 nm in diameter. Smaller nanoparticles appear to have been ingested by pinocytosis (i.e., through pinocytic vesicles with a characteristic granular outer coat). Both types of vesicles transferred their contents to primary phagosomes in subapical regions of the digestive cells, which ultimately connected to the lysosomal degradative compartment ([Owen, 1970](#)).

Although uptake of nano-Ag by bivalve mollusks has not yet been evaluated, the rate of uptake likely would depend on the rate at which the animal moves water over its gills and the proportion of nano-Ag particles large enough to be trapped by the gill lamellae, but small enough not to be ejected from the food ingestion stream. Water filtration rates would depend on temperature and the size of the mollusk, as well as reproductive status and other factors.

5.2.3.4. Uptake by Aquatic Crustacea

Uptake of silver ions from water has been examined for several species of crustacea, with BCFs as high as 1,100 and >2,200 for *Gammarus pulex* ([Terhaar et al., 1977](#)) and the freshwater cladoceran *D. magna* ([Garnier-Laplace et al., 1992](#)), respectively. Uptake of silver ions is associated with branchial sodium- and potassium-activated adenosine triphosphatase (Na⁺/K⁺-ATPase) in both crayfish ([Grosell et al., 2002](#)), which are tolerant of conventional silver, and in daphnia ([Bianchini and Wood, 2003](#)), which are sensitive to conventional silver. Uptake of nano-Ag or silver ions from the nanoparticles could occur in crustacea through the adhesion of nano-Ag or nano-Ag clusters to the external carapace (e.g., planktonic crustacean) or gills (macrocrustacea). In addition, transport of ingested nano-Ag across the gut epithelium by endocytosis might be possible.

Zooplankton feed by filtering large volumes of water through setae (i.e., structures similar to tiny combs) on their appendages. The setae collect larger bacteria, algal cells, and possibly nanoparticle

clusters (Baun et al., 2008a). Ingestion of nanoscale titanium dioxide (nano-TiO₂) clusters has been verified by their presence in the gut of *D. magna* (Baun et al., 2008a). Adhesion of clusters of nano-TiO₂ to the exoskeleton and antennae of *D. magna* and carbon-60 (C₆₀) to antennae of the marine copepod *Acartia tonsa* also have been demonstrated (Baun et al., 2008a). Nano-Ag particles also could sorb to the exoskeleton and antennae of planktonic invertebrates.

Zhao and Wang (2010) used a radiotracer method with ^{110m}Ag to estimate uptake and efflux of nano-Ag particles (carbonate coated, hydrodynamic diameter 40–50 nm, predominant particle size 20 nm) in water and in food by *D. magna*. At low concentrations, the investigators found slower uptake of nano-Ag than free silver ions (from AgNO₃). At higher nano-Ag concentrations in water, uptake increased disproportionately, possibly due to direct ingestion of the particles by the organism. To estimate dietary assimilation efficiency, algal cells were pretreated with nano-Ag (with free silver ions removed by addition of cysteine) for 12 hours and the *Daphnia* then were allowed to ingest the nano-Ag-treated algal cells for 15 minutes. The assimilation efficiencies measured for algal associated nano-Ag ranged from approximately 22% to 45%, with the lower assimilation efficiency associated with a higher nano-Ag concentration in the algae.

Zhao and Wang (2010) also assessed *Daphnia* depuration rates after uptake of nano-Ag or free silver ions (AgNO₃) from water only. The percent radioactivity remaining in the cladocerans after transfer to clean water declined rapidly in the first 2 days, followed by a slower elimination rate. After 4 days depuration in clean water, retained ^{110m}Ag was similar for both the high (500 µg/L) and low (5 µg/L) nano-Ag exposures (4.6–6.7%), whereas the 4-day retention after exposure to free silver ions was significantly lower (2%). The investigators did not attempt to determine the distribution of retained ^{110m}Ag in the animals (e.g., along gut lining, in internal tissues, on exoskeleton) or whether the retained ^{110m}Ag from nano-Ag was associated with nano-Ag particles.

For the silver depurated over the 4-day period, most was released to water (approximately 45–73%), with the remainder released with molts of the exoskeleton (approximately 12–15%) and in feces (10 to almost 40%) and a small fraction (2–4%) in neonates. Elimination in feces was highest for the high nano-Ag exposure (500 µg/L), presumably because a larger proportion of the nano-Ag moved straight through the gut without assimilation. The investigators did not discuss possible mechanisms of elimination to water, nor did they determine whether the amount remaining after 4 days was associated with nanoparticles.

After developing a model of nano-Ag uptake from both water and food using biokinetic parameter values for the low-concentration exposures, Zhao and Wang (2010) estimated that approximately 70% of the uptake of silver from nano-Ag by *Daphnia* in the environment would be via ingestion with food. Thus, zooplankton exposure to silver can occur from nano-Ag associated with algae.

Although studies specific to the uptake of nano-Ag by other crustaceans are lacking, multiple studies have demonstrated the toxicity of nano-Ag to these organisms (see Section 6.2.2.2 and Appendix

B). Those studies indicate that uptake, or at least sorption to gill and possibly GI epithelia, with subsequent release of silver ions, does occur.

5.2.3.5. Uptake by Vertebrate Eggs

Several university laboratories are assessing uptake of chemicals and nanoparticles by eggs and embryos of the freshwater zebrafish *Danio rerio*. Three have published recently on uptake of nano-Ag in aqueous suspension ([Bar-Ilan et al., 2009](#); [Asharani et al., 2008](#); [Nallathamby et al., 2008](#)) and all have reported that nano-Ag can be incorporated in the body of developing embryos. Asharani et al. (2008) prepared nano-Ag “capped” with either soluble potato starch or bovine serum albumin (BSA) to prevent cluster formation (both capping agents are considered nontoxic). TEM and surface plasmon resonance analyses of stock solutions indicated an average size range of 5–20 nm, with a broader distribution of sizes for the BSA-capped particles. Embryos of an unspecified age (likely less than 6 hours post-fertilization) were exposed for 72 hours to one of five concentrations of capped nano-Ag or only to the capping agent or to control water. Concentration-dependent toxicity was observed as described in Section 6.2.2.3 and Appendix B. Tissue analysis revealed significantly higher concentrations of residual total silver in test organisms than in the controls, although no concentration data were provided in the study report ([Asharani et al., 2008](#)). TEM examination of older zebrafish embryos showed nano-Ag deposits throughout the body, including the trunk, tail, skin, heart, and brain, and clusters of nano-Ag throughout the epidermis. Closer examination of the trunk and tail showed most nano-Ag particles deposited inside cell nuclei, with fewer in the cytoplasm. In the nuclei, nano-Ag particles were found as distinct clusters. The investigators noted that nano-Ag appeared as clusters in most organs except the brain, where they remained dispersed.

Laban et al. (2009) also observed “clumps” of nano-Ag distributed throughout fathead minnow (*Pimephales promelas*) embryos after nano-Ag had attached in large quantities to the chorion surface. Asharani et al. (2008) reported that nanoparticles that enter early embryonic cells (e.g., 4-cell stage) have a high chance of being distributed throughout the embryo, although they did not state whether any of their embryo exposures started at that stage (e.g., less than 1.5 hours after fertilization). Nano-Ag particles also could be transported across the epidermis of later stage embryos.

Smaller nano-Ag particles can be absorbed more readily than larger nano-Ag particles. While investigating the toxic mode of action of nano-Ag, Bar-Ilan et al. (2009) exposed 4- to 6-hour-old (post fertilization) sphere-stage embryos to four size groups (3, 10, 50, and 100 nm) and concentrations of either nano-Ag or nanoscale gold (nano-Au), which is relatively inert. Exposure water was renewed daily for up to 10 days. The smaller size groups (3 and 10 nm) of nano-Ag produced a higher incidence of sublethal effects than the larger sizes (50 and 100 nm), although mortality was similar across sizes. Exposure to nano-Au in the same size categories and series of concentrations produced no measurable

toxicity. Instrumental neutron activation analysis demonstrated that both nano-Ag and nano-Au adsorbed to or were taken up by the embryos. The investigators provided no information on whether the size of the nano-Au influenced the quantity of gold associated with the embryo, although they cited other studies indicating better “translocation” of smaller sizes. Fent et al. (2010) studied the uptake and distribution of fluorescent core-shell silica nanoparticles (FSNP) in the early life stages of zebrafish using 60- and 200-nm particles. They found localization of both sizes of particles mainly in the egg chorion; the embryos did not exhibit overt embryotoxicity.

The method by which nano-Ag enters the outer egg chorion was elucidated using real-time visualization of nano-Ag particles traversing the zebrafish chorion (Nallathamby et al., 2008; Lee et al., 2007). Nano-Ag has the highest quantum yield of Rayleigh scattering of the “noble” metal nanoparticles, and scattering intensity is proportional to the volume of the particles. The bright particles can be observed directly using dark-field single-nanoparticle optical microscopy and spectroscopy. Also, the localized surface plasmon resonance spectra (wavelength/color) show size dependence, which allows a size category to be estimated for nanoparticles of different visible colors. Using these techniques, Lee et al. (2007) and Nallathamby et al. (2008) estimated the proportion of nano-Ag used in their initial experiments to be ~75% particles of 5–15 nm diameter, ~23% particles of 16–30 nm, and only ~1% particles as large as 31–46 nm. They prepared the particles by reducing silver perchlorate (AgClO_4) and then washing and centrifuging the resulting nano-Ag to obtain highly purified particles without surface coating. By adjusting the concentration of sodium chloride (NaCl) in the medium to maintain a low ionic-strength solution, they could keep the ζ potential of the particles high, and the particles were stable in solution (i.e., did not form clusters) for months (Nallathamby et al., 2008).

Lee et al. (2007) also demonstrated that the single nanoparticles in the test water did not form clusters and could pass through zebrafish chorionic pores (500–700 nm in diameter) by diffusion (Brownian motion). Some single particles remained in the pores, but most passed through into the chorionic fluid where they continued to move by Brownian motion, as demonstrated by real-time video. Some particles also diffused back out of the egg through the chorionic pores. The Brownian motion in the chorionic fluid inside the egg was 26 times slower, however, than in the water in which the eggs were placed, owing to the higher viscosity of the chorionic fluid than water. Few clusters of nano-Ag were observed in the fluid. Estimated diffusion coefficients for the nano-Ag in the chorionic fluid revealed a viscosity gradient across the embryo, yolk, and chorion. The nano-Ag that stayed (possibly adsorbed) in the chorionic pores appeared to serve as nucleation sites for nano-Ag cluster formation, physically clogging some chorionic pores, which would limit oxygen and waste exchange between the embryo in the egg and its environment. This laboratory also demonstrated a counterclockwise movement of fluid within the chorion with a range of viscosity gradients, with slower movement of nano-Ag in the more viscous portions of the chorionic fluid (Nallathamby et al., 2008).

Most zebrafish embryos treated with nano-Ag concentrations less than 0.08 nM at or before the cleavage stage (8-cell) completed development at 120 hours post-fertilization ([Lee et al., 2007](#)). Examining these fish using single-nanoparticle optical microscopy and spectroscopy, researchers identified nano-Ag embedded in multiple organs, notably in the retina, brain, heart, gill arches, and tail. Thus, some of the nano-Ag particles that entered the egg by diffusion reached the embryo the same way and were taken up into the body of the developing embryo, possibly by endocytosis. Higher exposure concentrations resulted in higher incidence of deformed and dead embryos, as discussed in Section 6.2.2.3.

5.2.3.6. Uptake by Freshwater Fish

Fish are exposed to chemicals in solution or in suspension in water at both their gills and GI epithelia. Between the aquatic milieu and the external surface of the fish is an “unstirred layer,” usually with polyanionic mucus secretions ([Handy et al., 2008a](#)). The unstirred layer tends to be more viscous and move more slowly than bulk water, thereby holding nanoparticles at the external surface of the organism ([Handy et al., 2008b](#)). The various ligands present on the cell surface also are predominantly anionic. Nanoparticles should generally diffuse across the mucous layer more slowly than single molecules such as electrolytes and metal ions, and cationic nanoparticles might bind to strands of mucoproteins hindering their uptake ([Handy et al., 2008a](#); [Handy and Shaw, 2007](#)). Cell surfaces also might present ligands for nano-Ag (e.g., gill epithelium is predominantly anionic) ([Handy and Eddy, 2004](#)).

At the gills, metal cations can move through the epithelial membrane using specialized cation transporter channels. Most nano-Ag particles, however, are too large to traverse the cation channels, which have a pore diameter less than 1nm. In the gut, where endocytosis is one method by which the epithelial cells absorb nutrients, nanoparticle uptake through vesicular transport is possible ([Handy et al., 2008a](#)).

Nano-Ag, however, need not cross epithelial membranes to affect fish; adsorption to the gill membranes is sufficient for nano-Ag to deliver silver ions, which are toxic to fish. Investigators have hypothesized and provided evidence that exposure to silver ions blocks the Na^+/K^+ -ATPase active transport of Na^+ from fresh water across the gills into fish ([Bury et al., 1999](#); [Morgan et al., 1997](#)). Recent studies suggest that the mechanism of action of silver ions on the gill might be more complex and that silver ions are absorbed by the basolateral gill membrane into the bloodstream, where they then travel to and concentrate in the kidneys. Bury ([2005](#)) found increased sodium ion efflux rather than decreased sodium ion uptake in juvenile rainbow trout (*O. mykiss*) exposed to sublethal concentrations of silver ions (added as AgNO_3). The Na^+ ionic balance of the fish was restored by day 21 of the exposure, although kidney K^+ -dependent *p*-nitrophenol phosphatase activity was reduced and the total silver concentration in

both gills and kidneys was elevated 20-fold. Indirect in vitro evidence suggested that the gill basolateral membrane could sequester silver in membrane vesicles. The fish then could absorb the silver or expel it back into the surrounding water ([Bury, 2005](#)).

Many studies measure total silver tissue burden following exposure to nano-Ag, although some traditional methods used for tissue analysis (such as mass spectrometry) cannot distinguish silver nanoparticles from silver ion concentrations ([Griffitt et al., 2009](#)). A chronic study (10–38 days) investigating the effect of nano-Ag on caudal fin regeneration in *D. rerio* reported that nano-Ag had penetrated fish organelles, including mitochondria, nuclei, and blood vessels ([Yeo and Pak, 2008](#)). The investigators measured the residual silver concentrations in fish muscle, intestine, and testes following exposure to nano-Ag, but did not report the specific particle size or the age of the test organism. They did report, however, that the total silver concentration was highest in the muscle 2 hours post exposure, but that total silver concentrations in the muscle and testes decreased to nearly zero by about 100 hours post exposure. Conversely, total silver concentrations in intestinal tissues of zebrafish, both with and without amputated fins, continued to increase through 140 hours post exposure ([Yeo and Pak, 2008](#)).

Farkas et al. ([2011](#)) demonstrated that at least some types and small sizes of nano-Ag particles can penetrate through the fish gill multicellular epithelial layer and enter gill cells by using in vitro cultured primary gill cells of rainbow trout. Nanoparticle coating was an important factor for whether nano-Ag entered cells. Citrate-coated nano-Ag particles, 3–40 nm in diameter, with an average of 12 nm, were readily taken up into gill cells cultured in monolayers, whereas PVP-coated nano-Ag particles, from 1–60 nm with an average size of 7 nm, entered gill cells to a much lesser extent over the 48-hr exposure period. As seen through light microscopy, the citrate-coated nano-Ag particles appeared to accumulate in light-dense clusters around, but not in, the nuclei of the gill cells. Using TEM, the particles also could be seen in as yet unidentified lamellar structures inside the cells. The slightly smaller PVP-coated nano-Ag particles could not be seen in cells by using light microscopy, but were seen via TEM inside cells as single particles or in small clusters of particles. No loss of silver was observed over a 48-hour depuration period, and the authors speculated that elimination of nano-Ag particles from cells was unlikely or inefficient. Using a multilayer gill epithelium in culture, Farkas et al. ([2011](#)) demonstrated that PVP-coated nano-Ag primarily passes over and between the cells to penetrate the multiple layers comprising the epithelium, whereas the citrate-coated nano-Ag tended to be absorbed into individual cells. These results emphasize that the type of coating on nano-Ag particles can influence their behavior and transport at biological interfaces such as fish gill epithelia. The results also demonstrate uptake of nano-Ag by gill epithelial cells.

5.2.3.7. Uptake by Saltwater Fish

Many investigators believe the uptake and effects of nano-Ag in saltwater fish occur by different mechanisms than in freshwater fish. Freshwater and anadromous fish must be able to maintain body fluids that are hyperosmotic compared with surrounding fresh waters, and they do so with active ionic transport. Silver ions released by nano-Ag near or sorbed to the gill membranes are actively absorbed by the Na^+/K^+ -ATPase ion channels in the gills. Saltwater fish, on the other hand, are somewhat hypo-osmotic with respect to surrounding sea water, and free silver ions in the water column readily bond with abundantly available Cl^- to form AgCl , which precipitates from solution. For example, investigations of the gulf toadfish (*Opsanus beta*), which can survive in a wide range of salinities if acclimated, have indicated silver uptake. Above the isosmotic point of approximately 32% sea water, toadfish drink the water and absorb Na^+ , Cl^- , and water across the GI tract and actively excrete Na^+ and Cl^- across the gills and secrete ionic magnesium (Mg^{2+}) into urine (Wood et al., 2004). At lower salinities, the toadfish actively takes up Na^+ and Cl^- across the gills and retains the ions in the kidneys. Wood et al. (2004) acclimated toadfish to salinities ranging from 2.5 to 100% sea water, followed by 24-hour exposure to $2.18 \mu\text{g Ag/L}$ as $^{110\text{m}}\text{Ag}$ -labelled AgNO_3 . Speciation of silver varied with salinity: The silver chloride anion AgCl_3^{2-} dominated at 100% salinity and declined with decreasing salinity, while another silver chloride anion, AgCl_2^- , dominated at intermediate salinities (10–60% sea water). Neutral dissolved AgCl^0 was negligible at higher salinities but gradually increased with decreasing salinity to a concentration approximately equal to AgCl_2^- at the lowest salinity (2.5%). At all salinities, total silver ion concentrations in solution decreased over the 24-hour exposure period due to adsorption and precipitation. Only 5% of the total silver initially present in the test solutions was accounted for by the amount found in the toadfish. Maximum total silver accumulation in the toadfish occurred at the lowest salinity tested, 2.5% sea water; minimum uptake occurred at 40% sea water.

Wood et al. (2004) also found that silver concentrations in bile were higher at lower sea-water concentrations. Of the toadfish tissues, the liver showed the highest internal accumulation of silver, while muscle concentrations were lowest. The authors concluded that silver ions entering the gills were efficiently absorbed by the blood and distributed to other organs. They attributed the variation in patterns of total silver accumulation in different tissues and at different salinities to at least two factors: (1) salinity-dependent changes in the silver speciation and (2) salinity-dependent changes in the ionoregulatory physiology of the fish (Wood et al., 2004). The relative importance of ingestion and GI tract absorption became greater with increasing salinity after the isosmotic point.

Nichols et al. (2006) examined total silver accumulation in gills and plasma of toadfish exposed for a longer duration, 6 days. The investigators found the same pattern of decreasing silver accumulation with increasing salinity, which was expected given the lower bioavailability of AgCl complexes formed at higher salinities. The group also compared total silver uptake in water with and without NOM obtained

from the Suwannee River. The addition of NOM appeared to reduce gill accumulation of silver in toadfish only at salinities less than 40‰ sea water. At higher salinities, the organic matter did not appear to influence silver accumulation in gills. In contrast, the addition of organic matter appeared to increase silver concentrations in blood plasma at salinities less than 40‰ sea water. The investigators hypothesized that the organic matter helped to keep more silver in solution, facilitating gill uptake of silver ([Nichols et al., 2006](#)).

Information presented in this section regarding the uptake of conventional silver might be relevant for this case study; however, no data specific to the uptake of nano-Ag by saltwater fish were identified. Additional information would be useful to fully assess the potential for exposures for saltwater fish.

5.2.3.8. Bioaccumulation in Aquatic Food Webs

As discussed previously, nano-Ag that sorbs to or is absorbed by organisms is defined as bioavailable for the purposes of this document. A consumer organism (e.g., herbivore, carnivore) that feeds on smaller organisms (e.g., phytoplankton, zooplankton, eggs, small fish) will ingest the nano-Ag and other conventional silver compounds that are on or in their food. The question then becomes to what extent the nano-Ag on or in the food is bioavailable to the consumer, either via interaction with the gut epithelial cells or absorption by those cells followed by the particles passing through to the circulatory system. This question is examined below for water-column and sediment communities. What remains unknown for all groups is how the route of uptake of nano-Ag (and silver ions from the particles) is influenced by surface modification of the particles ([Behra and Krug, 2008](#)).

Water-Column Organisms

Algae, the primary producers in the water column, show high bioconcentration of silver inside cells when exposed to free silver ions, with BCF values as high as 10,000 to 100,000 in some studies ([Ratte, 1999](#)). Studies of algae exposed to nano-Ag focus on toxicity endpoints (e.g., growth inhibition) and the contribution of silver ions to toxicity, rather than on calculating BCF values ([Navarro et al., 2008a](#)). Concentrations of total silver versus nano-Ag on or in the cell walls or in the cell cytoplasm have not been explored. At a minimum, however, algal cells might concentrate nano-Ag particles relative to particulate concentrations in the water column by adhesion of nano-Ag to the external cell wall, as has been demonstrated for bacteria ([Morones et al., 2005](#)).

Bioconcentration or bioaccumulation of free silver ions in filter-feeding zooplankton, the next step up pelagic food webs, is on the order of a factor of 1000–5000, somewhat lower than for algae ([Ratte, 1999](#)). Zooplankton might sorb nano-Ag to setae, cilia, antennae, other appendages, gills, and the GI tract epithelium ([Zhao and Wang, 2010](#); [Baun et al., 2008a](#)). This sorption would not be considered bioaccumulation for those organisms, but could lead to bioaccumulation in their consumers.

Bioaccumulation of nano-Ag would require uptake of the particles after ingestion, possibly by endocytosis along the consumer's GI tract. Bioconcentration of silver ions could occur if nano-Ag particles sorbed to gills, and then the water's chemistry promoted the release of silver ions from the particles. On the other hand, crustacean zooplankton, which shed their carapace at regular intervals, might facilitate sedimentation of nano-Ag particles sorbed to their exoskeletons ([Ratte, 1999](#)).

Some forms of complexed silver are bioaccumulated in aquatic crustaceans without evidence of toxicity or internal absorption. Several studies have demonstrated bioaccumulation of silver atoms bound with inorganic (-S) or thiol (-SH) sulfides without evidence of toxicity, presumably owing to a lack of free silver ions ([Kramer et al., 2009](#); [Bianchini et al., 2002](#)). In the presence of S^{2-} , complexed silver can be ingested and accumulated in the digestive tract of *D. magna*, enhancing the apparent "whole-body" silver burden even though none is absorbed into the body of the animal ([Bianchini et al., 2005b](#)). Although not associated with internal accumulation or toxicity of silver ions to the *D. magna* themselves, the silver is passed along the food chain to consumers of *D. magna* ([Bianchini and Wood, 2008](#)). For the consumers, the ingested silver might or might not be adsorbed or absorbed by the GI tract.

Fish exhibit low BCF values for silver ions relative to BCFs reported for algae and zooplankton, and the potential for bioconcentration or bioaccumulation of nano-Ag, either in solution or in food, has not been examined. BCF values for free silver ions of approximately 1–350 have been measured for the body and viscera of fish on a wet-weight basis compared with surrounding water (i.e., for *Cyprinus carpio*, *P. promelas*, and *O. mykiss*) ([Ratte, 1999](#)). Measures of bioaccumulation of total silver from the diet were not found. For ingested nano-Ag that is adsorbed to or in food, the low pH in the gut might favor formation of AgCl from silver ions released from silver nanoparticles ([Panyala et al., 2008](#)), thereby favoring dissolution of the nano-Ag in the gut. Larger nano-Ag particles with smaller surface-to-volume ratios might take longer to dissolve, however, and they could be excreted in feces if not absorbed or adsorbed by the gut. For mammals, small nano-Ag particles can be absorbed into the blood stream, accumulated in the liver, and excreted back into the gut lumen in bile through exocytosis ([Sadauskas et al., 2007](#)). The silver then might be reabsorbed by the gut or excreted in feces ([Sadauskas et al., 2007](#)).

The evidence cited above indicates that in general, bioaccumulation of silver atoms or compounds appears to decrease with increasing trophic level in water-column food webs. The highest BCF values are reported for algae (i.e., 10,000 to 100,000), with lower values reported for zooplankton (e.g., 5000) and fish (i.e., 1 to 350). Fish show limited absorption of silver from their diet or from water in the first place, and hence limited accumulation ([Ratte, 1999](#)). No data are available on potential bioaccumulation of nano-Ag specifically.

The extent to which water-column biota might alter nano-Ag after coming in contact with nanoparticles in the environment is another consideration for food chain accumulation ([Behra and Krug, 2008](#)); no studies were identified, however, that examined the bioavailability of nano-Ag in various water-column biota to consumer organisms up the food chain.

Sediment Organisms

Sediment is likely to be an important sink for nano-Ag clusters, nano-Ag, silver ions sorbed to particles, and silver ions precipitated in insoluble compounds. Detritus (i.e., decaying plant and animal materials) and microorganisms form the base of food webs originating in the benthos. Benthic detritivores and filter-feeders contact and ingest relatively large quantities of detritus, associated microorganisms, and plankton near the sediment surface. Thus, silver in sediments could enter aquatic food webs through benthic organisms.

In general, BCF values for small crustaceans exposed to soluble silver salts added to sediment/water systems are close to or less than 1 ([Ratte, 1999](#)). BCF values measured for the same organisms (e.g., freshwater *G. pulex*, aquatic *Chironomus luridus*) in water only, however, can be three orders of magnitude higher (e.g., 1100) ([Ratte, 1999](#); [Garnier-Laplace et al., 1992](#)). These findings suggest that much of the silver in sediments is not bioavailable, presumably due to the high availability of ligands for silver ions in sediments.

One category of benthic organism that can bioaccumulate total silver by a factor of 1,000 or more is bivalve mollusks ([Ratte, 1999](#)). As filter feeders, bivalves can accumulate silver ions directly from water and from any silver on or in their food near the sediment/water interface. Terhaar et al. ([1977](#)) determined wet-weight BCF values of up to 1,400 for the freshwater bivalve *Ligumia* spp. In San Francisco Bay, the *Macoma petalum* clam accumulated total silver at concentrations five to seven times higher than in the phytoplankton ([Reinfelder et al., 1998](#)) and acquired between 40 and 95% of the silver through their diet ([Griscom et al., 2002](#)).

The extent to which silver transfer from the benthos into aquatic food chains might occur depends on many factors, including bioavailability and the consumer organisms. No studies of nano-Ag bioaccumulation in benthic invertebrates or their predators were identified.

5.2.4. Terrestrial Ecosystems

The uptake of dissolved silver ions and complexes from soils by terrestrial plants and soil micro- and macrofauna has been investigated in a few laboratory and field experiments. Uptake of nano-Ag by soil invertebrates has been investigated in the laboratory.

5.2.4.1. Uptake by Terrestrial Plants

Available evidence indicates that terrestrial plants can take up and accumulate silver ions when conventional silver is present at high concentrations in the surrounding medium. For instance, sweet corn (*Zea mays* cv. Sundance), lettuce (*Lactuca sativa* cv. Ithaca), oats (*Avena sativa* cv. Hercules), turnips



(*Brassica rapa* cv. Just Right), and soybeans (*Glycine max* cv. HT1779) grown on soils amended with sewage sludge spiked with Ag₂S showed below-ground accumulation of silver after exposure for 76, 56, 64, 54, and 93 days, respectively. Total silver concentrations in the roots of these plants after exposure to soil with 12 or 106 mg/kg silver ranged from 2.0 to 33.8 milligrams per kilogram (mg/kg) dry weight, which was significantly greater than concentrations in corresponding controls (Hirsch, 1998a). Silver concentrations in the aboveground parts of the same plants were consistently lower than in the roots of the same plants and only portions of the stalks of corn and oats had concentrations that were significantly higher than in corresponding controls (Hirsch, 1998a). In a similar study by the same author with higher concentrations of silver (68 mg/kg or 155 mg/kg) in the soil, a significantly higher concentration (0.69 mg/kg dry weight) of silver was observed in lettuce leaves compared to corresponding controls, but no significant difference from control was detected in the leaves of chinese cabbage (*Brassica campestris* cv. China Doll), or spinach (*Spinacia oleracea* cv. Melody) (roots were not examined) (Hirsch, 1998a). The ability of plants to take up and accumulate silver ions in plant tissues, however, remains inconclusive as Ag₂S is less soluble than other forms of silver. Concentrations of silver in trees grown in areas subject to silver iodide (AgI) cloud seeding exhibited total silver concentrations between 1 and 13 mg/kg in aboveground leaves, twigs, bark, and wood (Klein, 1978). In this case, exposure through deposition on leaves would have been possible in addition to root exposures.

Harris and Bali (2008) demonstrated “hyper” accumulation of silver ions by *Brassica juncea* (a mustard plant) and *Medicago sativa* (alfalfa), two species known to be metal tolerant. The plants were grown hydroponically from seeds for 4 weeks in demineralized water, and then moved to Petri dishes containing aqueous solutions of AgNO₃ at concentrations up to 1% silver by weight. The ratios of silver in the plant tissues (entire plant assays) to the silver concentration in the aqueous growth medium ranged from 6 to 67 for alfalfa and from 10 to 124 for mustard.

Limited evidence is available comparing uptake and translocation of conventional silver in terrestrial plants to nano-Ag, however, available data suggest that nano-Ag is taken up by some plants. Yin et al. (2011) reported that nano-Ag coated with gum arabic were internalized by common grass (*Lolium multiflorum*) by either direct uptake in the roots followed by the release of ionic silver species within the root tissues, or by dissolution of the nano-Ag particles on the root surface followed by internalization of the ionic species by the roots. The investigators noted that most available evidence suggests that nano-Ag adsorbs to plant roots and crosses the cell membrane by oxidative dissolution, at which point internalized silver can be translocated to other plant tissues (Yin et al., 2011).

Stampoulis et al. (2009) reported total silver concentrations in zucchini shoots exposed by roots to nano-Ag in hydroponic solution that were almost five times higher than in zucchini shoots exposed to equivalent concentrations of conventional (powdered) silver. Conversely, Hawthorne et al. (2012) reported that uptake of Ag was not particle-size dependent (i.e., similar concentrations reported for nano-Ag and bulk Ag). Ma et al. (2010) reported unpublished findings in their laboratory that show

nano-Ag particles as large as 40 nm could be taken up at the roots and transported to shoots of the dicot thale cress (*Arabidopsis thaliana*), although most of the nano-Ag adhered to the root cap. These studies suggest that formulations of nano-Ag and conventional silver are taken up by plants and that transport of at least silver ions to shoots occurs. In support of this hypothesis, Judy et al. (2011) demonstrated that tobacco plants (*Nicotiana tabacum* L. cv Xanthi) accumulate gold (Au) following exposure to 100 mg Au/L nano-Au (5, 10, or 15 nm; coated with tannic acid) in deionized water. Inductively coupled plasma-mass spectrometry (ICP-MS) analysis detected mean gold concentrations of 40.3, 95.8, and 61.7 mg Au/kg dry tobacco weight for the 5-, 10-, and 15-nm nano-Au treatments, respectively. Gold was verified to be present not only on the leaf surface but throughout the plant tissue cross section.

5.2.4.2. Uptake by Soil Macrofauna

The limited available studies suggest that invertebrates might take up nano-Ag and silver ions from soil. Nematodes, which are multicellular, usually microscopic, organisms in soil communities that feed on bacteria and detritus, have been shown to take up nano-Ag (Meyer et al., 2010; Roh et al., 2009), as have earthworms (*Eisenia fetida*) (Shoults-Wilson et al., 2011b) (see Section 5.2.4.3).

Using genomic, proteomic, and cellular-level endpoints, Roh et al. (2009) demonstrated uptake of nano-Ag particles in the nematode *Caenorhabditis elegans*. 3-day-old nematodes cultured on agar growth medium with *E. coli* for food were exposed to nano-Ag in water for 24 or 72 hours. The nano-Ag particles (smaller than 100 nm) were dispersed in deionized water by sonication for 13 hours, stirring for 7 days, and filtering through a cellulose membrane with pore size of 100 nm to remove nano-Ag clusters in solution. Measures of light scattering using dark-field microscopy indicated uptake of nano-Ag into the body of the nematodes and clustering of nano-Ag predominantly around the uterine area. The investigators used physical rather than chemical means to disperse the nano-Ag in aqueous solution to provide relevance to environmental exposures, and they demonstrated that nano-Ag was absorbed into the body of the nematode by some unidentified mechanism(s).

Using darkfield microscopy in combination with a CytoViva visible and near-infrared hyperspectral imaging system, Meyer et al. (2010) also demonstrated ingestion and absorption of nano-Ag by *C. elegans*. All three types of roughly spherical particles used (citrate-coated particles with a mean diameter of 7 nm and PVP-coated particles with mean diameters of 21 and 75 nm) were internalized by the nematodes. The citrate-coated 7-nm particles caused the nematode to retain developing eggs, which allowed the investigators to visualize transfer of nano-Ag into the fertilized eggs. In a soil environment with organic matter capable of sorbing nano-Ag, however, nano-Ag and silver ions might be largely immobilized and not available for uptake by nematodes.

The study by Judy et al. (2011) using nano-Au offers some insight into whether silver nanoparticles might be taken up by another soil macroinvertebrate. Judy et al. (2011) reported accumulation of Au in

the tissue surrounding the gut lumen of tobacco hornworms (*Manduca sexta*) after consumption of nano-Au-treated tobacco. These concentrations were detectable by synchrotron μ XRF scans of hornworm cross sections from each treatment (0 or 100 mg Au/L deionized water; treatment particle diameter size classes of 5, 10, and 15 nm). ICP-MS also verified that the gold detected in the hornworms was attributable to nano-Au from the plant material.

5.2.4.3. Transfer through Terrestrial Food Webs

As discussed in Section 4.3, the major pathway by which nano-Ag from indoor uses of spray disinfectants could reach terrestrial ecosystems is expected to be application of sewage sludge to soils (e.g., for agriculture). Terrestrial organisms also might be exposed to nano-Ag in contaminated water from flooding or crop irrigation, or possibly through deposition of nano-Ag suspended in air following outdoor use of nano-Ag products. With the possible exception of areas near silver mining operations ([Kramer et al., 1994](#)), bioaccumulation of silver in macroflora and macrofauna of terrestrial ecosystems, even in areas with silver-spiked sludge applications ([Hirsch, 1998a](#)), does not appear to have been observed. This section discusses uptake of silver ions in solution or in soils by plants, and whether nano-Ag applied to soils could reach herbivorous species. The potential for nano-Ag applied to soils in sewage sludge to reach insectivorous wildlife through soil invertebrates in direct contact with soils is considered. Finally, this section considers the potential for indirect ecological effects of nano-Ag as a result of inhibition of soil microorganisms (e.g., decomposing bacteria, nitrifying bacteria, nitrogen-fixing bacteria, fungi), which could disrupt soil nutrient cycling to support food webs. To date, however, no data on the presence of nano-Ag in soils have been published ([Wijnhoven et al., 2009b](#)).

Transfer through Terrestrial Plants

A single published study of plants exposed to nano-Ag in soils or solution was found. Investigators exposed zucchini to nano-Ag in hydroponic solutions and found that some form of silver, possibly silver ions, was transported to shoots ([Stampoulis et al., 2009](#)). Translocation of gold from roots to other plant parts was also demonstrated by Judy et al. ([2011](#)) following exposure of tobacco plants to nano-Au.

Some studies have demonstrated that most silver ions and complexes dissolved in solution and taken up by metal-tolerant plants accumulate in the roots, possibly in intercellular spaces (e.g., apoplast) ([Nowack and Bucheli, 2007](#)), and are not transported to other parts of the plant ([Ratte, 1999](#)). As noted previously, some metal-tolerant terrestrial plants have been demonstrated to hyper-accumulate silver ions from water ([Harris and Bali, 2008](#)). Young *B. juncea* (a mustard plant) and *M. sativa* (alfalfa) plants exposed to high concentrations of AgNO_3 exhibited BCF values greater than 10 (concentration in fresh, hydrated plants:concentration in water), with silver sequestration occurring in the form of large numbers of silver nanoparticle clusters.

As yet, no evidence indicates that nano-Ag in soils with sewage sludge amendments is likely to accumulate in the foliage, fruits, or vegetables of plants above ground; however, higher concentrations of nano-Ag in soils, might lead to different conclusions. If nano-Ag or silver ions in soil pore water are taken up by plant roots, they might be sequestered in the roots, possibly as nanoparticles in extracellular spaces such as the apoplast. Some silver, probably in the form of silver ions, however, might be transported to plant shoots and beyond. Whether nano-Ag, and excess silver in any form, in sewage sludge applied to agricultural fields might accumulate in root and tuber vegetables has not yet been investigated.

Among herbivorous wildlife, only two groups might be highly exposed to total silver in plants due to their ecology; however, these exposures might still be below the thresholds for toxic effects. Small burrowing mammals that consume plant roots might ingest quantities of nano-Ag stored in the roots of metal-tolerant plants, and grazing animals might ingest silver that accumulates in stems of a variety of herbaceous plants. Herbivorous insects feeding on plant roots and stems also might be exposed to accumulated silver. The potential for silver exposure via these pathways to affect grazing animals and insects has not been investigated. The potential bioavailability of nano-Ag particles sequestered in plant roots of the hyper-accumulating species also has not been examined.

Transfer through Soil Macrofauna

Shoults-Wilson et al. ([2011b](#)) reported the bioaccumulation of nano-Ag in earthworms (*Eisenia fetida*) exposed to nominal concentrations of 10 or 100 mg AgNO₃/kg dry soil or nano-Ag at concentrations of 10, 100, or 1,000 mg Ag/kg dry soil (30–50 nm nominal size range; coated with either oleic acid [OA] or PVP) for 28 days. Authors noted that measured tissue concentrations of silver were concentration-dependent and that organisms exposed to similar doses accumulated significantly lower concentrations when exposed to nano-Ag compared to AgNO₃ (up to 5.5-fold less accumulation from nano-Ag-treated soils than from AgNO₃-treated soils). Accumulation was noted to be comparable between the two nano-Ag treatments, OA and PVP, even though the former displayed hydrophobic behavior while the latter displayed hydrophilic properties (hydrophobicity is often inversely correlated with bioavailability). Similarly, no significant differences in tissue concentration or BAF between the two treatments were observed.

Judy et al. ([2011](#)) reported measured nano-Au in greater concentrations in the tobacco hornworm (*Manduca sexta*) after it fed on treated tobacco (*Nicotiana tabacum* L. cv *Xanthi*) for 1 week than was measured in the treated tobacco alone (experimental set-up was designed to disallow access to plant roots). Authors reported that concentrations in the hornworm tissue exceeded that of the dried tobacco tissue by mean factors of 6.2, 11.6, and 9.6 for the 5-, 10-, and 15-nm treatments, respectively, suggesting that some nanometals might accumulate in soil invertebrate tissues following ingestion of lesser contaminated plants.

Disruption of Ecological Functions of Soil Microorganisms

Nano-Ag toxicity in soil microorganisms could adversely affect an ecosystem at large. Of particular concern are the possibilities that silver might inhibit bacteria that fix atmospheric nitrogen (in symbiosis with legumes and other plant species), disrupt denitrifying bacteria (which convert nitrates to nitrogen gas), and impair decomposing and lithotrophic bacteria and other microbes that release essential nutrients from inorganic and organic matter in soils ([Panyala et al., 2008](#)).

Senjen ([2007](#)) reported that few studies have been conducted that directly evaluate the community-level effects of nano-Ag exposure for soil microbial communities. Many laboratory studies, however, have evaluated the toxicity of nano-Ag to microorganisms that might be found in soils, particularly bacteria (see Section 6.2.1). In theory, disruption of the nutrient cycling roles of soil microorganisms could result in a cascade of adverse impacts on the structure and composition of terrestrial plant communities, and then on the animal communities as well. A risk assessment based on projections for nano-Ag discharge to the Rhine River in 2010 concluded that most silver released into wastewater would be collected in sewage sludge, which often is spread on agricultural fields ([Blaser et al., 2008](#)). Environmental concentrations were predicted for the river water, river sediment, interstitial water of the sediments, and the wastewater entering sewage treatment plants. Although Blaser et al. ([2008](#)) could not exclude possible risks to benthic organisms in the river, they concluded that the nitrifying bacteria in the sewage treatment plants were at negligible risk of impairment.

5.3. Human Exposure



One obstacle to measuring or estimating exposure of humans to nanoparticles is the lack of consensus regarding the particle properties that require characterization and on which metric to use to express exposure concentrations or dose. Further complicating human exposure assessments is the lack of broadly applied methods for distinguishing background and incidental exposures from source-specific contributions to total nanoparticle exposures. For example, atmospheric particle collection methods that collect ultrafine inorganic particles cannot, without further chemical analyses, separate the fraction comprising manufactured nanoparticles ([SCHER, 2009](#)). Data on nanomaterial use in consumer products rely on information provided by the manufacturers and do not account for uses that might be “off-label,” or products that incorporate nanomaterials but are not labeled as such. In addition, independent investigations of some nano-enabled products have revealed that actual particle size range, concentration, composition, and purity often differ from what is reported by the manufacturer, and different products with different formulations would result in exposure to a variety of substances in conjunction with the nanomaterials added intentionally to the products. This section describes the current methods and data

available for evaluating human exposure to nano-Ag from spray disinfectant use in homes and institutions (Section 5.3.1) and during manufacture (Section 5.3.2).

5.3.1. General Population Exposure

Chemical form, shape, concentration, zeta potential, exposure route(s), and media concentration(s) have been highlighted as important parameters when evaluating human exposures to nanoparticles (SCHER, 2009; Wijnhoven et al., 2009a). The application scenario (including how much, how long, how often, and how many people use the product) of a chemical also should be considered. Despite the rapid penetration of nanomaterials into the consumer market, little information on their content or the content of other ingredients in consumer products is publicly available. The absence of that information precludes a complete exposure assessment. At the time of the last literature search for this document, no studies were identified that empirically examined exposure to nano-Ag from spray products, and only one study (Hagendorfer et al., 2009) was found that examined the form of nano-Ag released from spray products that contain nanomaterials (see Section 3.4)¹⁹. The results of this study suggest that single silver nanoparticles and clusters with diameters less than 100 nm can remain as aerosols for at least several minutes following use of a gas-propellant sprayer delivering a water-based nano-Ag suspension to the air.



Although the nano-Ag released from the spray nozzle is homogeneously dispersed in nanoscale water droplets, the nano-Ag particles and the clusters formed after release can remain suspended in air after the water evaporates. Conversely, no silver particles of any size were detected in the air following use of a pump spray mechanism, suggesting that any single silver nanoparticles or clusters were more likely to settle onto surfaces close to the spray nozzle (the size range of these particles was not investigated in this study) (Hagendorfer et al., 2009). These findings suggest that consumers might be exposed to nano-Ag aerosols or to nano-Ag particles that have settled on surfaces during or after use, depending on the spray delivery mechanism. The degree to which the use of solvents other than water affect dispersion of nano-Ag in aerosolized liquid droplets, how quickly the liquid solvent evaporates in air and on surfaces, and the form of the nano-Ag to which consumers are exposed, however, are unclear.



Hansen et al. (2008) recently developed a framework for conducting general population exposure assessments from products containing nanomaterials. As part of this framework, they categorized the 580 products listed in the 2007 Woodrow Wilson Center consumer product inventory based on whether the nanoparticles were bound to the surface of the product, suspended in liquid, suspended in solids, or available as free, airborne particles. Using these characteristics, exposures were categorized as “expected”

¹⁹Two additional studies (Nazarenko et al., 2011) and (Quadros and Marr, 2011) that examine nano-Ag released from spray products containing nanomaterials became available after the completion of the last literature search and were not identified during peer-review.

(e.g., due to direct exposure to liquids containing nanoparticles or free, airborne nanoparticles), “possible” (e.g., due to release of surface-bound nanoparticles owing to wear and tear), or “not expected” (e.g., particles are encapsulated in solids and are not released). Based on the types of products claiming to use nanomaterials and the likely exposure scenarios for those products, the authors concluded that nano-Ag has the highest possible consumer exposure of all nanomaterials considered, with roughly 25% of the products categorized as “possible” exposures and 50% categorized as “expected” exposures ([Hansen et al., 2008](#)). Most of the exposure scenarios (53) for nano-Ag were for surface-bound products, but a large proportion of scenarios was for exposure to nano-Ag suspended in liquids (33) or suspended in solids (28) ([Hansen et al., 2008](#)). For spray disinfectants, inhalation, oral, and dermal exposures could be either to the wet formulation or to dry nano-Ag particles after the carrier vehicle evaporates.


Expert elicitation has been used to assess potential for exposure to approximately 50 nanomaterials used frequently in consumer products ([Wijnhoven et al., 2009a](#)). A panel of seven experts from the Netherlands National Institute for Public Health and the Environment was assembled to independently identify the most significant exposure characteristics and to rank consumer products according to potential exposure. Characteristics of each product and the nanomaterial in the product were used to generate rankings of potential exposure (high, medium, or low). Six product categories in which nanomaterials are purportedly used were assigned the rank of “high” potential for exposure: sunblock cosmetics, oral hygiene products, health products, fuel, coatings and adhesives, and cleaning products. Cleaning products (the category under which nano-Ag spray disinfectants would fall) were generally labeled by Wijnhoven et al. (2009a) as “do-it-yourself,” suggesting that products requiring application by the user might lead to higher exposures. For cleaning products containing nanomaterials, the expert panel determined that the characteristics of primary concern are the form of the product (e.g., spray, powder, liquid, suspension, solid, coating), the form of the nanomaterial (e.g., free particles, particles fixed inside a matrix), the potential for direct versus indirect exposure from application (e.g., direct exposure to nanoparticles in the product, indirect exposure from particles released from the product), and potential exposure route (e.g., inhalation, dermal, oral). The characteristics of nano-Ag sprays led them to be categorized as “high-potential-exposure” products. These characteristics include: the spray form of the product, in which particles are free and not fixed; the potential for direct exposure through application; and the potential for exposure through multiple indirect routes.

In one of the few studies that have modeled exposure to nanoparticles, Mueller and Nowack (2008) analyzed nano-Ag, nano-TiO₂, and carbon nanotube use and release into the environment in Switzerland, albeit using substantially simplified assumptions as discussed in Sections 3.1 and 4.5. They estimated release rates for products containing nano-Ag and concluded that, although sprays and cleaners account for only 15% of the nano-Ag in consumer products, the bulk of release (95%) from this use occurs during application when the consumer is likely to be exposed ([Mueller and Nowack, 2008](#)).

Wardak et al. (2008) created a hypothetical exposure scenario for the use of an air-freshener spray containing nano-Ag that would also act as a disinfectant. Based on expert elicitation, Wardak et al. (2008) concluded that the most significant human exposures would occur via inhalation and dermal pathways and that the most significant environmental exposures would result from water entrainment (i.e., suspension of nano-Ag in water) after disposal. This approach, which is similar to that used by Wijnhoven et al. (2009a), was reported by the authors to be useful for estimating risk when few or no data on environmental concentrations exist. The authors assumed that the nano-Ag would be contained in a liquid matrix (Wardak et al., 2008). Exposures during and after application were considered possible. Inhalation was estimated to be the primary exposure route, followed by dermal, and to a lesser degree ingestion. Exposure to workers who manufacture or use nano-Ag spray disinfectant in occupational settings is discussed in Section 5.3.2.

The potential for secondary human exposures, after nano-Ag particles have been released into the environment outside of homes and facilities where used or released, has not been investigated. Environmental nano-Ag can change form in the environment due to processes such as dissolution, cluster formation, complexation, and other processes that can significantly affect its transport, transformation, and fate processes and potential biological activity, as described in Section 4.1.1. The silver itself cannot be degraded and persists indefinitely.


5.3.1.1. Respiratory Exposure

Consumers could be exposed to nano-Ag particles as a result of inhaling spray disinfectants during application or disposal, particularly in confined spaces (e.g., laundry room or kitchen). Data on spray use and disposal, and on the concentrations of ingredients other than nano-Ag, such as capping agents and stabilizers involved in the manufacturing process and disposal of waste by-products, were not identified in the literature. The concentrations of nano-Ag in end-use products, the application rates, and the use profiles for these products are not yet known (refer to discussion in Section 2.2), but some hypotheses have been proposed. Wardak et al. (2008) independently surveyed eight experts from five areas of expertise (environmental sciences, toxicology, chemistry, material sciences, and technology policy) and asked them to score (from 1 = low to 5 = high) the exposure and hazard potential of nano-Ag disinfectant air-freshener sprays.  The authors concluded that inhalation by users represented the highest potential human exposures. The experts believed that nano-Ag spray uses also might result in elimination of useful bacteria in susceptible populations (Wardak et al., 2008).

Children in the home might inhale aerosols containing nano-Ag formed when others are spraying the material; no data were found, however, on the proximity of children to adult disinfectant spraying activities or how long nano-Ag from the air-freshener sprays would remain airborne. Children might be

exposed to higher concentrations of airborne nano-Ag near the floor level from original spraying activities and from resuspension of dust and nanoparticles containing nano-Ag as they crawl or play on the floor. Again, no information was found to quantify this possibility. Children also have higher metabolic rates than adults, and therefore must consume more oxygen. With higher inhalation rates relative to body weight than adults, children will experience higher exposures to air pollutants than adults at the same ambient air concentrations ([Bearer, 1995](#)).


5.3.1.2. Dermal Exposure

Dermal exposure to nano-Ag could result from spray deposition on the skin or by contact with a surface that has been sprayed or a cleaning accessory used during application (e.g., cleaning rag, paper towel, sponge). The expert elicitation described by Wardak et al. ([2008](#)) for an air freshener scenario indicated that the potential for exposure via skin contact was medium-high, which was greater than the potential for ingestion exposure but less than the potential for inhalation exposure. Individuals with cuts or abrasions of the skin might be more likely to absorb nano-Ag following dermal contact. 

Children might be a susceptible population for dermal exposure because the skin of infants and young children and young adults has been shown to be more permeable to some substances than that of older adults ([Hostynek, 2003](#)), although no data for nano-Ag were found. Furthermore, children often have cuts and scratches from play activities.

5.3.1.3. Oral Exposure

The potential exists for inadvertent ingestion of nano-Ag through hand-to-mouth contact following dermal exposure in the home ([Drake and Hazelwood, 2005](#)). Wardak et al. ([2008](#)) concluded that the potential for exposure via ingestion was medium-low, below the potential for inhalation and dermal exposure, and therefore not of primary concern. Inhalation of nano-Ag also could result in exposure via the GI tract following mucociliary clearance of the lung ([SCHER, 2009](#)).

For children (e.g., toddlers), oral exposures could occur from mouthing objects that have been sprayed with nano-Ag, and touching or handling sprayed objects and then mouthing their hands. Although no studies were identified that examined children's exposure to nano-Ag sprayed in the home, the exposure pathways could be pertinent for children in homes where such sprays are used intensively or for cleaning toys. Children could be more highly exposed than adults to nano-Ag that reaches food and water in the home because they consume more food and water per unit body weight than adults ([Bearer, 1995](#)). 

5.3.2. Occupational Exposure

As the number of products containing nanomaterials in commercial distribution increases, the number of workers involved in the manufacturing of nanomaterials is also likely to increase. Lack of knowledge regarding nanomaterial manufacturing processes requires that precautionary assumptions be made about potential exposure routes and likelihood of exposure during manufacturing and by-product disposal; therefore, all possible exposure routes (i.e., respiratory, dermal, oral) are currently considered for occupational settings. The Occupational Safety and Health Administration and the National Institute for Occupational Safety and Health recommend and set limits on conventional silver concentrations in the workplace environment at 0.01 milligram per cubic meter (mg/m^3) (equivalent to 10 micrograms per cubic meter [$\mu\text{g}/\text{m}^3$]) for an 8-hour workday and 40-hour workweek ([U.S. EPA, 2009g](#)). The American Conference of Governmental Industrial Hygienists (ACGIH) recommends threshold limit values of 0.01 and 0.1 $\mu\text{g}/\text{m}^3$ for soluble silver and metallic silver, respectively ([U.S. EPA, 2009g](#)).

The differences, sometimes spanning an order of magnitude, between occupational exposure limits set by different agencies led Drake and Hazelwood ([2005](#)) to review the toxicity literature on chronic exposure to conventional silver. They concluded that the potential effects of chronic exposure to conventional silver depend on its chemical form. Soluble forms of silver are more readily absorbed by the body and therefore can more readily cause adverse health outcomes. For example, in an occupational exposure study of workers employed in silver manufacturing ([Armitage et al., 1996](#)), silver reclamation workers exposed to soluble silver compounds showed the highest blood levels, with an average of 6.8 $\mu\text{g}/\text{L}$ (range = 1.3–20 $\mu\text{g}/\text{L}$, $n = 19$), while jewelry makers exposed to metallic silver had the lowest, ranging from 0.2 to 2.8 $\mu\text{g}/\text{L}$ ($n = 9$). Blood silver levels ranged from 0.1 to 23 $\mu\text{g}/\text{L}$ among workers in all of the factories (no exposure levels were measured), while 11 of 15 agricultural workers with no occupational exposure had blood silver concentrations below the detection limit of 0.1 $\mu\text{g}/\text{L}$, and no blood silver concentrations were higher than 0.2 $\mu\text{g}/\text{L}$.

Workers exposed to conventional silver and to silver fumes and dusts, which might contain nanoparticles, have displayed clinical symptoms due to dermal, ocular, and inhalation exposures ([Panyala et al., 2008](#); [Drake and Hazelwood, 2005](#); [Rosenman et al., 1987](#)). The literature commonly reports the effects of these exposures, but few specifics are reported on measured exposure levels. In one study where ambient exposure levels were reported, Pifer et al. ([1989](#)) evaluated workers exposed to silver via inhalation. Air sampling indicated an 8-hour time-weighted-average airborne silver concentration of 1–100 $\mu\text{g}/\text{m}^3$, with most silver present in insoluble forms. Elevated blood silver concentrations (mean of 0.010 microgram per milliliter [$\mu\text{g}/\text{mL}$] among 80% with detectable blood silver levels) and body burdens were reported in these workers relative to controls; however, no instances of argyria were reported.

Tsai et al. ([2009](#)) measured exposure from the transfer of nano-Ag and nano-alumina powder from inside fume hoods to the worker breathing zones for three common hood designs. This study is one of the

few reporting personal levels of exposure associated with the occupational handling of nanomaterials. Despite the use of common laboratory precautions, the release of airborne nanoparticles into the laboratory environment and the researchers' breathing zone was substantial. Results indicate that researchers should not transfer powders in a fume hood because the highest breathing-zone concentrations resulted from the constant-flow hood. Tsai et al. (2010) then compared the efficacy of a recent hood design, the air-curtain hood, to the other hood designs using the same procedures, but with aluminum oxide nanoparticles only 27–56 nm in size. Because the nanoparticles could cluster in the bulk powder, the concentrations of airborne particles with diameters measuring from 5 nm up to 20,000 nm were measured in the breathing zone. Release of particles from the hood was negligible for particle clusters greater than 500 nm in size; but releases of clusters in this size range were again highest for the constant-flow hood. Furthermore, pouring the nanomaterial manually from one beaker to another in the constant-flow hood resulted in particle concentrations ranging between approximately 500 and 1,500 particles/cubic centimeter (cm³) in the breathing zone (particle size was primarily 100- to 200-nm clusters; peak particle concentration was 7,000 particles/cm³). Releases were lower for the air-curtain hood, and ranged from non-detectable to approximately 500 particles/cm³. These studies suggest that procedures generally considered adequate to protect workers during handling of harmful substances might not be sufficient while handling nanomaterials.

Once released in an occupational setting, nanoparticles can be inhaled and might deposit in the lungs (Kreyling et al., 2002; Oberdorster et al., 1995). Only two occupational exposure studies to date (Lee et al., 2011; Park et al., 2009) have examined workplace exposure specifically to nano-Ag during the manufacturing process. Park et al. (2009) assessed exposure to nano-Ag in the liquid phase during a wet chemical process at a commercial production facility in Korea. Although most field studies that have analyzed nanomaterial exposure in the workplace have concentrated on the gas-phase production process because of the clear potential for inhalation of powders and aerosol particles, the investigators argue that the potential remains for exposure to nanomaterials during liquid-phase processes, which are frequently used to manufacture nano-Ag. In this study, Park et al. (2009) report that the production of nano-Ag at the facility involves a four-stage process: (1) batch reaction based on wet chemical methods, (2) filtering, (3) drying, and (4) grinding. Of these stages, the investigators demonstrated that at least three had the potential for worker exposure (filtering was not explicitly described). During the batch reaction process, the nano-Ag reaction mixture is allowed to age before the filtration stage. The real-time air-particle monitor in the reaction room was located 1 meter from the hatch of the main reactor, which was under a ventilation hood. Nanoparticle concentrations in the room were about 6×10^4 , 5×10^4 , and 2×10^4 particles/cm³ for particles with average diameters of 100 ± 5 nm, 200 ± 5 nm, and 20 ± 5 nm, respectively, after about 13 hours. At that point, the reactor hatch was opened for 1 hour to allow sampling of particles to characterize nano-Ag. During that time, the concentrations of the 20- and 200-nm nanoparticles in the room air remained relatively stable, but the concentration of 100-nm nanoparticles

increased to about 9×10^4 particles/cm³. TEM images indicated that the particles collected in the reaction room were nano-Ag. According to Park et al. (2009), nano-Ag 50–60 nm in diameter formed clusters in the room air. Concentrations of nano-Ag were estimated by subtracting the background particle concentrations before operations started from the particle concentrations during the silver processing. Similar results were observed during the grinding and drying processes. When the dryer door was opened at the end of the drying period, the number of 60- to 100-nm particles in the air doubled. During the grinding process (1 hour), irregular increases in nanoparticles in the air were observed as workers disturbed particles that had settled on the floor. After the ventilation system was turned on, these irregular increases were reduced. When the grinder hatch was opened, however, the concentration of 30- to 40-nm particles in the air spiked. These results indicate that nano-Ag in a solution can be aerosolized in the workplace air, where workers can inhale the nano-Ag particles (Park et al., 2009) and that the particles might deposit on exposed skin. Nano-Ag in the air also might settle on clothing or on floors, eventually resulting in a secondary exposure when the nano-Ag is disturbed during clothing removal, sweeping, or walking in a room without an adequate ventilation system.

Lee et al. (2011) used a combination of personal air samples, area monitors, and real-time monitors to examine potential workplace exposures at two different nano-Ag manufacturing facilities in Korea. Filters were used to collect nano-Ag in worker breathing zones and in work areas; silver mass concentrations on the filters were analyzed using an inductively coupled plasma (ICP) method, and nano-Ag particles were identified and characterized using TEM and energy dispersive X-ray analysis. Real-time aerosol monitoring also was conducted using scanning mobility particle sizers and dust monitors to capture the particle number concentrations for particles with diameters ranging from 15 to 710.5 nm and 0.3 to 20 micrometers (μm), respectively.

The first facility examined by Lee et al. (2011) synthesized nano-Ag in a pilot ICP reactor with an electric atomizer and utilized no control technologies outside of natural ventilation. Workers fed silver powder, the precursor material, into the reactor and collected the nano-Ag particles from the collector. All processes between precursor feeding and nano-Ag collection took place in a closed, negative pressure system, indicating that under normal circumstances, releases of nano-Ag and precursors should occur only during feeding and extraction of materials. The highest silver mass concentration (0.00102 mg/m^3) was measured in the personal air sample of one of the two operators of the feeding process. Although no personal air samples were taken for workers collecting nano-Ag from the reactor, the silver mass concentration in the area nearest the collector was 0.00034 mg/m^3 , which was about three times higher than in the other area air samples. The authors noted that all silver mass concentrations measured in personal air and area samples were below occupational exposure levels for silver dust (0.1 mg/m^3) and soluble silver compounds (0.01 mg/m^3) established by ACGIH. Nano-Ag particle number concentrations for the 15–710.5 nm size fraction were measured both in the ICP reactor and in workplace air. Although concentrations in the reactor ranged from about 60,000 to 2.3 million particles/cm³, with a fairly

consistent average particle size of 20–30 nm, concentrations in workplace air were relatively low (less than 7,000 particles/cm³) despite the lack of control technologies, and the average particle size was around 400 nm, suggesting that nano-Ag clustering occurred once the nano-Ag particles escaped from the reactor into the workplace air ([Lee et al., 2011](#)).

The second nano-Ag manufacturing facility examined by Lee et al. ([2011](#)) used an attrition milling system with ventilation and a fume hood to manufacture nano-Ag solutions from sodium citrate and silver nitrate. Both chemicals were weighed, milled (i.e., pulverized), added to a wet tank, stirred, and sonicated before they were mixed together in a reactor. No personal air samples were collected at this facility, but several area monitors were placed in two laboratories in the facility. Throughout the manufacturing process, silver mass concentrations in workplace air ranged from 0.00003 to 0.00043 mg/m³, with the exception of one very short-duration measurement (9.6 minutes compared to 162- to 223-minute sampling durations for the other areas), which was 0.00118 mg/m³. The conditions that led to this higher concentration were not described in the study, but the authors reported that all of the measured concentrations were again below the ACGIH occupational exposure levels for silver dusts and soluble silver compounds. The scanning mobility particle sizers and dust monitors revealed that concentrations in the smaller 15- to 710.5-nm size fraction ranged from about 400 to 3,500 particles/cm³, and particle number concentration in the larger 0.3- to 20- μ m fraction ranged from about 1,000 to 2,200 particle/cm³. Peaks in particle number concentrations in both size fractions occurred when sodium citrate was weighed and mixed with water, when the sodium citrate and silver nitrate were mixed, and when the equipment was cleaned ([Lee et al., 2011](#)).

Unlike traditional occupational exposure studies like that of Park et al. ([2009](#)) and Lee et al. ([2011](#)), which focus on workers involved in extracting or refining the material, exposure to a nano-Ag disinfectant spray could involve occupational use by janitorial service workers who might be chronically exposed. No studies measuring or modeling this type of exposure to a nanomaterial were found in the literature. In addition, the possibility of transport of nano-Ag from workers to their homes warrants consideration. The risk of secondary exposures could be lowered by using protective uniforms that remain at the facility where they would be cleaned and by establishing decontamination protocols before workers return home.

Seipenbusch et al. ([2008](#)) studied the release of spherical platinum (Pt) nanoparticle aerosols into a simulated workplace environment under particle-free conditions and with pre-existing background aerosol concentrations (simulated by spherical submicron oil droplets or micron-sized silica spheres). The nano-Pt aerosol had a median particle diameter of 7–8 nm, whereas the background aerosols had particle sizes in the range of 100–1,000 nm. The study monitored particle-size distributions and total number concentrations over several hours of release of nano-Pt and found that collision between nanoparticles within their own size class and with the background aerosol, if present, was the primary mechanism driving changes in particle size and number concentration. The authors concluded that nanoparticles are

unlikely to reach receptors in the form of the original, released aerosol. The nanoparticles are likely to increase in size by homogeneous clustering within their size class or heterogeneous clustering with background aerosols. Methner et al. (2010) demonstrated the same phenomenon, but across many different sizes, shapes, and compositions of nanoparticles, many of which are not possible for nano-Ag (e.g., fibers, tubules, oxides).

Additional information on exposure to nano-Ag and associated substances during the manufacturing process of nano-Ag and disinfectant sprays and on occupational use of end products would aid in understanding chronic workplace exposures more fully. Traditionally, such information also has proved relevant to the study of subchronic exposure because mechanisms and health effects can be extrapolated to lower exposures in the general population before a complete body of research is available. Occupational exposures historically have been the first indication of toxic effects that ultimately might be occurring more broadly or more subtly within the population (e.g., exposure to mercury by hat makers, exposure to asbestos by shipyard workers, exposure to radium by watch dial painters).

5.4. Aggregate Exposure to Nano-Ag from Multiple Sources and Pathways

Nano-Ag has been advertised as a constituent in at least 313²⁰ consumer products currently on the market, although the content of nano-Ag in these products has not been verified. And as described in Section 1.4, silver nanoparticles can occur naturally in the environment or can be produced unintentionally. Humans and biota are therefore likely to be exposed to nano-Ag from multiple sources and through multiple pathways.

The simplified exposure scenarios mentioned below consider only engineered nano-Ag and assume that the nano-Ag entering the environment would remain in its current form; however, the surface chemistry of nano-Ag might be significantly altered as a result of “aging” and transformation processes in complex environmental systems (as discussed in Chapter 4). Chemical and biological transformations of nano-Ag might occur as a result of reduction and oxidation (redox) reactions, particle dissolution, or interactions with pollutants or organic matter, which, in turn, might result in changes in particle form, clustering, transport, and pathways of exposure (Wiesner et al., 2009). The susceptibility of nano-Ag to transformation and complexation might limit exposure to nano-Ag itself, while increasing exposure to

²⁰The Project on Emerging Technologies’ Consumer Products Inventory website at <http://www.nanotechproject.org/inventories/consumer>.

nano-Ag complexes, silver ions released from nanoparticles, and other transformation products (see Section 5.2).

5.4.1. Human Aggregate Exposure

Potential routes of human exposure for some possible nano-Ag applications are provided in Table 5-1.

Because nano-Ag might be used in various applications, numerous pathways exist for human and ecological exposures, some of which could overlap, resulting in aggregate exposures to nano-Ag from many sources. Many of the nano-Ag applications listed in Table 5-1 could be used by the same individuals at approximately the same time. For example, an individual might inhale aerosol particles from a nano-Ag spray used to clean and disinfect surfaces in the home, wear a bandage containing nano-Ag on the skin, and consume an oral nano-Ag dietary supplement. Also, a single product could lead to exposure through multiple routes ([Wijnhoven et al., 2009b](#)). While using a spray disinfectant, the nano-Ag solution might be sprayed unintentionally on the skin, the aerosol particles inhaled (and possibly coughed up and subsequently swallowed), and ingested from foods in contact with the disinfected surfaces.

As one or more nano-Ag products are used in the home, particularly disinfectant sprays, nano-Ag could accumulate on surfaces and in airborne dust. Removal mechanisms for airborne nano-Ag are limited to normal leakage and, perhaps less commonly, slow transfer to outdoor air when windows are open, transfer through a central vacuum system, or capture of particles on heating and cooling system filters, which generally have not been designed for this purpose. High efficiency particulate air filters can remove some proportion of nanoparticles in the air, but are designed to remove only 99.7% of particles 300 nm or larger. Buildup of nano-Ag in carpets, furniture, and floors might lead to higher exposure of children and pets in particular.

The aggregate exposure of children might be higher than that of adults. Children are more likely to crawl and play on surfaces sprayed with disinfectants than adults and their inhalation rates are higher than adults ([Bearer, 1995](#)). They also might be exposed through toys to which manufacturers have added nano-Ag to keep the toys bacteria free. Finally, the skin of young children can be more permeable to some substances than that of adults, and cuts and scratches from play activities break the dermal barrier to absorption of most substances.

Table 5-1. Nano-Ag applications and potential routes of human exposure.



Product category	Product subcategory	Product examples	Expected exposure route
Food and beverage	Cleaning	Food product sterilizing sprays	Inhalation, dermal
	Cooking utensils, coatings	Cutting and chopping boards, kitchenware and tableware, baby-bottle brushes	Dermal, oral
	Storage	Refrigerator fresh boxes, storage bags and containers, baby bottles, mugs	Dermal, oral
	Supplements	Colloidal metal in water	Oral
Personal care and cosmetics	Skin care	Body creams, hand sanitizers, beauty soaps, face masks	Dermal
	Oral hygiene	Tooth brushes, tooth cleaners, toothpastes	Oral
	Cleaning	Elimination wipes and sprays	Inhalation, dermal
	Hair care	Hair brushes, hair masks	Dermal
	Baby care	Pacifiers, tooth developers	Dermal
	Over-the-counter products	Foams, condoms	Dermal
Textiles and shoes	Clothing	Fabrics and fibers, socks, shirts, caps, jackets, gloves, underwear	Dermal, oral
	Other textiles	Sheets, towels, shoe care, sleeves and braces	Dermal, oral
	Toys	Plush toys	Dermal, oral
Electronics	Personal care	Hair dryers, wavers, shavers	Dermal
	Household appliances	Refrigerators, washing machines	Dermal
	Computer hardware	Notebooks, (laser) mouse, keyboards	Dermal
	Mobile devices	Mobile phones, game systems	Dermal
Household products/home improvement	Cleaning	Cleaning products for bathroom, kitchen, toilets: detergents, fabric softeners	Inhalation, dermal, oral
	Coating	Sprays, paint supplements	Inhalation, dermal
	Furnishing	Pillows	Dermal
	Furnishing/coating	Showerheads, locks, water taps	Inhalation, dermal
Filtration, purification, neutralization, sanitization	Filtration	Air filters, ionic sticks	Inhalation
	Cleaning	Disinfectant sprays	Inhalation, dermal
Medical products	Anesthesiology	Breathing masks, endotracheal tubes	Inhalation
	Neurosurgery, Cardiology	Catheters	Intravascular, intrathecal, intravesical, urethral
	Eye care	Contact lenses	Ophthalmic
	Patient care	Incontinence materials	Dermal
	Orthopedics	Implants, stockings	Intramedullary, dermal
	Pharmaceuticals	Dermatitis, acne, ulcerative colitis treatments; HIV-I replication inhibition	Oral, dermal
	Surgery	Gowns, face masks, slings for reconstructive surgery	Inhalation/dermal/ intraperitoneal
	Wound care	Hydrogel for wound dressing	Dermal

Adapted with permission of Informa Healthcare; Wijnhoven et al. (2009b).

5.4.2. Biotic Aggregate Exposure

Biota also could be exposed to nano-Ag through multiple sources and routes, but exposure might be significantly affected by environmental parameters ([Luoma, 2008](#)). Although initially released as nanoparticles, the subsequent transport, transformation, and fate of the particles depend on many environmental characteristics in the receiving media. Nanoparticles in surface waters might associate to form microparticles or sorb to other materials and fall out of suspension into sediments. Water conditions and chemistry might make the nanoparticles either more or less available for uptake by biota ([Navarro et al., 2008a](#)). Transport, transformation, and fate processes of nano-Ag in the environment are discussed in Chapter 4 of this document, and bioavailability of nano-Ag in different environmental media is discussed in Section 5.2.1.

Although exposure of biota to nano-Ag can be mitigated through various environmental processes, some exposure is likely given that many nanoparticles are engineered to maximize their dispersion in water ([Lee et al., 2007](#); [Balogh et al., 2001](#)). Development of biocidal nano-Ag products for potential use in the home (e.g., clothes washers, surface sprays, cosmetics) or in occupational settings (e.g., industrial misters and foggers, architectural coatings, water filters) could lead to the release of nano-Ag during manufacturing, use, and disposal. Once released into sewer systems, very small nano-Ag particles that escape filtration-capture during wastewater treatment can be released back into aquatic ecosystems, where they could impact biota that are particularly susceptible to aggregate exposure via direct uptake from the water and ingestion of contaminated prey ([Navarro et al., 2008a](#)). In cases where sewage sludge from wastewater treatment is applied to land for soil amendments or for disposal, nano-Ag might be absorbed by plants, leached to ground water, or contained in runoff to surface waters ([Blaser et al., 2008](#)). Terrestrial biota then might be exposed to nano-Ag through ingestion of contaminated soil and prey, as well as through contact with contaminated media.

5.5. Cumulative Exposure to Nano-Ag and Other Contaminants

Given their high surface area-to-volume ratio and enhanced chemical reactivity, nanoparticles can modify the bioavailability of other toxic agents, such as manufacturing by-products, transformation products, waste products, and other contaminants present in the environment. Moreover, given the possible processes by which nanoparticles sorb to or are absorbed into cell walls and cells (see Section 5.7), they also might act as carriers of other chemicals or nanomaterials onto or into cells. Thus, nano-Ag particles serving as carriers could increase exposure of organisms to additional toxic agents.

Nano-Ag might be coated with agents that exhibit toxicity during manufacturing or adhere to toxic agents after release into the environment. Navarro et al. (2008a) observed that metallic engineered nanoparticles often are coated with inorganic or organic compounds or surfactants (e.g., sodium dodecyl sulfate) to maintain a colloidal suspension of the nanoparticles in the end product. In the future, nano-Ag might be combined with other materials to enhance certain properties for specific end uses. Cumulative exposure to other substances released during the manufacturing process and other ingredients of disinfectant sprays also might be a relevant consideration.

The potential for nano-Ag releases to result in increased exposure to manufacturing by-products or transformation products in the environment is discussed in Section 5.5.1. Whether nano-Ag might specifically facilitate absorption of other toxic agents or nanomaterials is discussed in Section 5.5.2. Evidence that some other types of nanoparticles facilitate absorption of other contaminants by living organisms is presented in Section 5.5.3.

5.5.1. Nano-Ag By-Products and Transformation Products

At this time, no information suggests that nano-Ag manufacturing processes result in the formation of hazardous by-products; however, relatively few data on large-scale manufacturing of nano-Ag are currently available. Information is similarly lacking regarding other materials used in manufacturing other ingredients of disinfectant sprays. Manufacturing of nano-Ag might therefore result in increased exposure to hazardous by-products, and nano-Ag might facilitate the absorption of toxic by-products in living organisms. This consideration is relevant in toxicity testing as well. For example, Samberg et al. (2010) found that “unwashed” nano-Ag received from a commercial producer of nanomaterials was toxic to human epidermal keratinocytes in vitro, with significant dose-dependent decreases in viability, whereas the same nano-Ag product washed five times did not diminish cell survival. The investigators concluded that the residual formaldehyde solvent and methanol by-product from the production of the silver nanomaterial were probably responsible for the observed toxicity.

As stated in Chapter 4, transformation of nano-Ag to other silver forms and complexation with other materials will occur in environmental media following release of nano-Ag from the spray disinfectant life cycle (see Section 4.1). Although exposures of humans and other biota to these nano-Ag transformation products are expected to occur, such exposures have yet to be characterized.

Nano-Ag also can sorb to other materials in water or soils, and Navarro et al. (2008a) suggested that sorption of nanoparticles to low-molecular-weight NOM might increase bioavailability of the nanoparticles and increase the chances of other contaminants to “hitch a ride” with the nanoparticles into aquatic organisms, in particular.

5.5.2. Examples of Nano-Ag Facilitating Absorption of Other Contaminants

Silver nanoparticles act as carriers of silver ions, possibly delivering them directly to a biological surface or into cells, where they might interact directly with the cell machinery ([Asharani et al., 2009](#); [Miura and Shinohara, 2009](#); [Lee et al., 2007](#); [Hussain et al., 2005](#)). If nano-Ag particles adhere to cell surfaces, they can serve as a continuous delivery system for silver ions to the cell. If so, greater human health and ecological risks can be expected from nano-Ag than from comparable quantities of ionic silver because not all silver ions that are free in solution will necessarily come in contact with a biological surface. No reports that nano-Ag facilitates the delivery or entry of other toxic chemicals to or into living organisms were found in the readily available literature; other nanomaterials, however, have been shown to facilitate the absorption of other substances (see Section 5.5.3).

5.5.3. Examples of Nanoparticles Facilitating Absorption of Other Contaminants

Nano-Ag spray disinfectant formulations could contain other chemicals with which nano-Ag might react, resulting in a synergistic effect that facilitates the uptake of the other contaminants. Although not yet demonstrated with nano-Ag, studies have shown synergistic uptake of contaminants occurring with polymer fumes ([Johnston et al., 2000](#)), diesel particulate matter ([Wallace et al., 2007](#)), and some nanoparticles, which are described further in this section. Furthermore, medical applications are being developed using nanoparticles as carriers for targeted drug delivery ([McNeil, 2009](#)). In general, however, the capacity of nanoparticles to sorb and facilitate uptake of other contaminants depends on the structure and composition of the nanoparticle.

Zhang et al. ([2007b](#)) found an increase in the accumulation of cadmium in the gills and viscera of carp in the presence of nano-TiO₂. Similarly, Sun et al. ([2007](#)) found an increased accumulation of arsenic in carp exposed to arsenate (As[V]) in the presence of titanium dioxide. The As[V] sorbed quickly to nano-TiO₂ in the water. Both nano-TiO₂ and arsenic concentrations were highest in the intestines, stomach, and gills, and somewhat lower in the liver, muscles, and skin. Much of the internally accumulated arsenic might have been released from nano-TiO₂ at the epithelium of the gills and GI tract. Some nano-TiO₂ reached the liver as well, presumably with sorbed arsenic.

Baun et al. ([2008b](#)) evaluated the potential effects of C₆₀ nanoparticles (Buckminster fullerenes, or buckyballs) on the bioavailability of 13 organic toxicants, as measured by their toxicity to the green alga *Pseudokirchneriella subcapitata* and the freshwater invertebrate *D. magna*. They observed no change in the toxicity of methyl parathion to the algae or daphnia in the presence of C₆₀, while the toxicity, and by

inference the bioavailability and uptake (see Section 5.2.3), of pentachlorophenol was reduced 1.9-fold in the presence of C₆₀. On the other hand, the presence of C₆₀ enhanced phenanthrene toxicity to daphnia by 60%. Analysis showed 85% sorption of phenanthrene to C₆₀ clusters ([Baun et al., 2008b](#)). In contrast to nano-Ag, however, C₆₀ nanoparticles form spherical molecular cages that can carry molecules trapped to some degree in their interior. This mechanism is not expected for nano-Ag particles.

Moore ([1997](#)) reported uptake of sucrose polyester nanoparticles in seawater by the hepatopancreas of whole mussels. The uptake of sucrose polyester nano-“droplets” increased the uptake (160%) and cellular toxicity (122%) of anthracene, a polycyclic aromatic hydrocarbon. Anthracene damaged the lysosomal system (measured as lysosomal membrane stability) in the hepatopancreatic cells, indicating that although the sucrose polyester was not biodegradable (even in lysosomes), the polycyclic aromatic hydrocarbon must have been released into the cell ([Moore, 2006](#)).

Despite these examples, however, there are no indications that the structure of nano-Ag particles is likely to facilitate uptake of other contaminants into biota. Clusters of nano-Ag might house other chemical contaminants in the inter-particle spaces; however, clusters of nano-Ag also might be less likely to be absorbed because of their larger size than nano-Ag particles.

5.6. Models to Estimate Exposure

Models can be used to provide initial estimates of potential release scenarios, behavior in the environment, exposure pathways, dosimetry, and toxicity, provided that the attributes of nano-Ag particles that influence fate, transport, and dosimetry are adequately considered. Modeling focused on tracking environmental transport, transformation, and fate after release can assist in estimating the potential for human and biotic exposures, linking release estimates with models of uptake and dose ([Shatkin, 2008](#)). EPA uses various models to estimate exposures for chemical assessments, some of which are described on the websites for the Council for Regulatory Environmental Modeling ([U.S. EPA, 2009c](#)) and the Center for Exposure Assessment Modeling ([U.S. EPA, 2009a](#)). For example, the Exposure and Fate Assessment Screening Tool Version 2.0 is a publicly available program that EPA uses for screening-level assessments of conventional industrial chemicals. The tool provides estimates of aquatic, general population, and consumer exposure based on chemical release data ([U.S. EPA, 2007a](#)).

Quantifying exposure or dose using measured environmental or occupational concentrations is not yet possible because nano-Ag concentrations have not been widely measured in relevant media. Instead, exposure concentrations can be estimated using a fate and transport model (Section 4.5) with inputs based on measured or assumed release scenarios (not covered in detail in this case study). Potential and internal doses can be predicted by models of dosimetry or pulmonary deposition (Section 5.7.3), pharmacokinetics (Section 5.7.1), and bioaccumulation (Section 5.2.1.3). Mode-of-action models can be used to estimate

doses delivered to target organs. All models described in these sections use chemical concentrations on a mass basis (e.g., mg/L, mg/kg) to predict chemical behavior (e.g., diffusion along concentration gradients). The applicability of this approach for nanomaterials, which exhibit some properties and behaviors that cannot be attributed strictly to changes in mass concentration, has not yet been determined.

5.7. Human Uptake and Dose

As described previously in this chapter, internal dose is the amount of a substance that enters an organism by crossing a biological barrier. Quantifying internal dose, or at least administered (i.e., potential) dose (e.g., quantity inhaled or ingested whether absorbed or not), enables estimation of individual or population-level risk, or both ([U.S. EPA, 1992](#)). Measuring and understanding the dose-response relationship is integral to predicting the human health impacts resulting from an exposure. Because nanoparticles possess unique, size-dependent properties that are not necessarily related to mass, however, their uptake and dose are not understood as well as that of traditional substances, which typically use mass as a dose metric ([Borm et al., 2006a](#)). A summary of the various metrics that can be used to best characterize nano-Ag dose is presented in Chapter 2. This current section builds on that summary by presenting information on uptake of nano-Ag and dose levels in laboratory mammals. Current knowledge on uptake and dose of nano-Ag in humans is also presented when available, but most information on this topic is inferred from studies involving laboratory mammals.

This section begins by summarizing what is known regarding the internal behavior (i.e., pharmacokinetics) of nano-Ag. A discussion of uptake and dose in laboratory mammals then follows. Uptake of nano-Ag through different routes has been investigated predominantly in laboratory rats. For all terrestrial organisms, including laboratory animals used for toxicological studies and as models for human health effects, the route of exposure is critical in determining the dose that ultimately enters the body. Information relevant to nano-Ag uptake and dose to humans is therefore presented here according to the inhalation, ingestion, and dermal routes of uptake. This section concludes with a brief discussion of models to estimate nano-Ag dose.

5.7.1. Pharmacokinetics

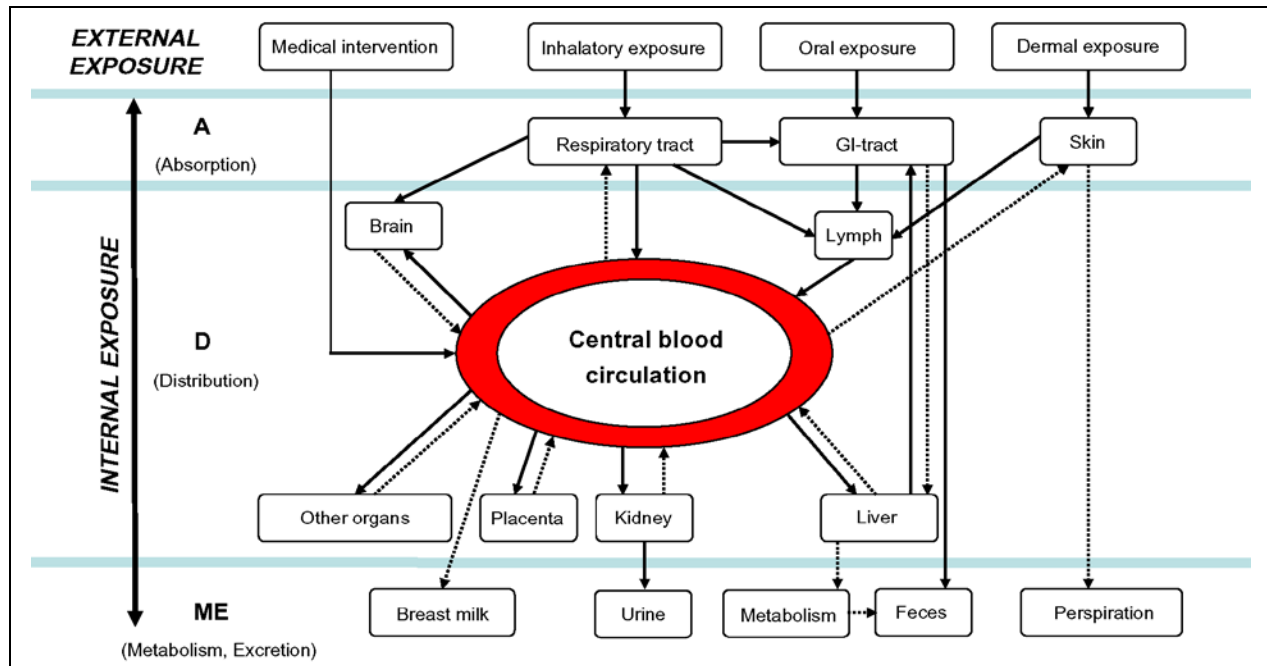


Pharmacokinetics, the study of the fate of a substance after it has entered a body, encompasses the absorption, distribution, metabolism, and excretion of a substance. By extension, toxicokinetics focuses on the fate of a toxic substance once present within the body. Understanding toxicokinetics is essential to understanding the mechanism of action and resulting toxicity of a toxic substance. Figure 5-1 illustrates an overview developed by Hagens et al. (2007) of physiological paths by which nanoparticles have been

confirmed to travel, and other paths that are hypothesized to be relevant. Although this figure was developed for nanoparticles in general, and thus does not indicate which pathways are more relevant for nano-Ag, it could serve as a framework within which the pharmacokinetics of nano-Ag could be represented once adequate data are available.

5.7.1.1. Absorption

Absorption encompasses the events that lead from external exposure of a substance to its uptake and transport to the central blood circulatory system. The concept of dose involves the absorption or uptake of a substance, and in vivo studies of dose often focus on the amount of a substance absorbed by an organism (i.e., how much of the substance moves from the external environment to the internal space of an organism). Penetration into the body depends on the specific properties of the nanoparticle, including charge, hydrophobicity, and surface coating, and the physiology of the particular organ. Studies identified for this case study that examine the absorption of a substance are discussed later in this section according to exposure route. An evolving concept relevant to the discussion of absorption of a



Source: Reprinted with permission of Elsevier; Hagens et al. (2007).

Figure 5-1. Absorption and uptake of nanoparticles and transport to the central blood circulatory system.

This figure, developed by Hagens (2007), depicts the organs and other parts of the body involved in the absorption, distribution, metabolism, and excretion (i.e., the pharmacokinetics) of a nanoparticle that enters the body. Solid lines show paths that have been confirmed to pertain to nanoparticles; dotted lines represent hypothetical routes. Although not all-inclusive, this figure illustrates how nanoparticles might enter and be transported to various parts of the body.

nanoparticle into the body is its “corona” ([Cedervall et al., 2007](#)). A corona is a layer of biomolecules that forms on the surface of a substance once it is absorbed into a physiological system. This layer can have important implications regarding how the substance interacts with the surrounding tissue. The concept of a corona is not particularly new or unique to colloid science or the study of nanoparticles; for example, Lynch and Elder ([2009](#)) note that researchers using medical devices have been aware of the same phenomenon. When a nanoparticle contacts extracellular bodily fluids, proteins and other molecules compete to attach to the particle surface, thereby coating the nanoparticle. Because of the extremely high surface area-to-volume ratio of a nanoparticle, the absorption potential is significantly greater than for larger particles. Once the particle is encapsulated by these biomolecules, it is this corona that encounters the cell surfaces and might determine a cell’s initial reaction to the particle ([Lynch and Elder, 2009](#)). One complicating factor in studying this phenomenon is that the composition of the corona is not static. Instead, its composition is determined largely by competitive binding, with a constant tendency toward equilibrium between the corona and its surroundings ([Cedervall et al., 2007](#)). In a recent review, a European Commission scientific committee noted that the composition of the corona is thought to determine, in part, a particle’s ability to cross membranes and enter cells or organelles ([SCHER, 2009](#)). For example, a particle coated with polyethylene glycol polymer was not available for cellular uptake, thereby increasing the particle’s lifetime in the blood, whereas serum albumin (a plasma protein) coatings increased nanoparticle uptake by macrophages. For the current case study, no information specific to the effect of protein coatings on nano-Ag particles was identified.

5.7.1.2. Distribution

Nanoparticles apparently can be distributed via blood circulation following absorption into the body. Anecdotal case reports of medicinal exposures and occupational studies suggest that humans exposed to conventional silver and nano-Ag through various routes in occupational or medicinal settings showed elevated levels of silver in their blood and urine (see Section 6.3.3). Few controlled studies examining the systemic distribution of nano-Ag were identified. Because distribution appears to differ in accordance with the route of exposure, general observations on distribution are presented briefly here and are further described in Section 5.7.2 on human uptake and dose by route.

As demonstrated by the studies described in the next section, distribution of silver throughout the body via blood circulation might be widespread following exposure to nano-Ag and subsequent absorption. This pattern would be consistent with the general behavior of nanoparticles following absorption, where they appear to have the potential to distribute to most, if not all, organs throughout the body ([Hagens et al., 2007](#)). Information presented by these authors suggests, however, that the relative extent of distribution to various organs is not well understood for nanoparticles in general, and patterns

among substances might vary. For example, the authors note that how readily nanoparticles in circulation can cross the blood-brain barrier or how nanoparticles are eliminated from the body is not clear.

Two studies that demonstrated general distribution of silver in the body following exposure to nano-Ag are summarized here. In a 28-day study of the toxicity and distribution of silver following oral administration of nano-Ag particles approximately 53–71 nm (60 nm average) in diameter to rats, Kim et al. (2008) observed that silver distributed to the stomach, liver, kidneys, lungs, testes, brain, and blood, with dose-dependent accumulation rates reported for all of these tissues (organs are listed in decreasing order of observed silver concentration). In the kidney, authors observed gender-specific accumulation of silver, with females accumulating about twice the mass of silver as males. In a similar study conducted by Sung et al. (2009), systemic distribution of silver in rats was reported for animals exposed via inhalation to nano-Ag aerosols averaging approximately 18–19 nm in diameter. Statistically significant ($p < 0.01$) increases in silver concentrations were reported in the lungs, liver, kidneys, brain (excluding the olfactory bulb), and whole blood (organs are listed in order of decreasing silver concentration). That the nano-Ag used in this case was generated by the thermal-condensation method (see International Organization for Standardization 10801:2010; International Organization for Standardization 10808:2010) should be noted. Although these studies have been reported in some secondary sources as having demonstrated distribution of nano-Ag to internal organs (Hussain and Schlager, 2009; Kaluza et al., 2009), neither of them actually examined tissues for nano-Ag particles following necropsy. Total silver concentrations in the various tissues were determined after wet digestion using an atomic absorption spectrophotometer with a Zeeman graphite furnace in both studies. Light microscopy was used to identify histopathological changes in various tissues. In their review, Wijnhoven et al. (2009b) noted that no studies have determined whether silver distributed to various rat tissues following oral, inhalation, or dermal exposure to nano-Ag remains in nanoparticulate form; all studies measured only total silver concentrations. For substances that are absorbed by the body into the blood, transfer to the brain is generally restricted by the blood-brain barrier. Examples of conventional silver crossing the blood-brain barrier have been identified in the literature and summarized in at least one review (Lansdown, 2007). Consensus on this phenomenon has not been reached, however, and reports of functional consequences are inconsistent, suggesting that penetration of this barrier by conventional silver is low (Lansdown, 2007). With respect to silver present as nano-Ag, one study used SEM to demonstrate nano-Ag particles in brain tissues of rats following subcutaneous injection of nano-Ag (Tang et al., 2008). The authors suggested that nano-Ag could penetrate the blood-brain barrier by transcytosis (i.e., the transport of substances into the interior of a cell by way of vesicles or intracellular sacs); only brain tissues, however, were examined for nano-Ag particles. A separate possible route to the central nervous system specific to inhaled substances, however, is via the olfactory nerve, which connects the nasal cavity with the olfactory bulb in the brain. This potential method for distribution of nano-Ag is discussed below in the section describing dose of inhalation exposures.

Lankveld et al. (2010) investigated tissue distribution of silver in rats over time, up to 16 days following intravenous injection of 20-, 80-, or 110-nm-diameter nano-Ag particles. Regardless of particle size and injection frequency (one time or once daily for 5 days), the investigators found that silver was rapidly distributed out of the blood to the liver, spleen, and lungs and to a lesser extent to the brain, heart, kidneys, and testes. During repeated injections, silver concentrations in the brain, heart, and testes never exceeded an average of 40 nanograms per gram (ng/g organ), whereas silver concentrations by day 5 in the spleen, for example, exceeded 5,000 ng/g organ for the 80-nm-Ag injection. By day 17 of the experiment (12 days after the 5-day repeated injections stopped), silver could not be detected in the blood, but relatively high levels remained in the lungs (600 ng/g organ for 80-ng-Ag injections, 200 ng/g for 110-nm-Ag injections), liver (1,100 ng/g organ for 80- and 110-nm-Ag injections), and spleen (several thousand ng/g organ). Remaining silver in all organs was much less for the 20 nm-Ag injection group. In the brain, by day 17, approximately 20 ng/g of Ag remained from the 110-nm Ag injections, 10 ng/g for the 80-nm-Ag injections, and 3 ng/g for the 20-nm-Ag injections. The 20-nm particles distributed mainly to the liver, followed by kidneys and spleen, whereas the larger particles distributed mainly to the spleen, followed by liver and lung. Tissues were not examined for the presence or distribution of silver in nano-Ag particles; rather, only total silver content (and concentration) was quantified. Garza-Ocanas et al. (2010) administered nano-Ag less than 3 nm in diameter coated with BSA via intraperitoneal injection in rats to study the fate of the particles in organs including the liver, heart, and brain. They reported significant accumulation of nano-Ag particles (1–2 nm in diameter), as verified by ICP-MS and TEM techniques, in the liver and heart. Brain tissues showed no evidence of nano-Ag particle content, although both tissue pathology and ICP-MS indicated that silver permeated the blood-brain barrier, presumably silver ions released from the nano-Ag elsewhere in the body.

No animal studies identified in the literature describe the distribution of nano-Ag following controlled dermal application of nano-Ag, but the use of nano-Ag in topical burn treatment might provide useful information. In one case study, a teenage burn patient was treated with a nano-Ag-coated mesh applied over the burned skin. After 1 week, liver and kidney effects and skin discoloration from silver absorption were observed (Trop et al., 2006). Silver concentrations in plasma (107 µg/kg) and urine (28 µg/kg) also were elevated. Once the mesh was removed, silver and liver enzyme levels returned to normal, and clinical symptoms disappeared. In another case, a burn patient developed neurological problems following a 2-week exposure to a cream containing silver. Upon autopsy 4 months later, elevated silver concentrations were detected in the brain, indicating that silver must have crossed the blood-brain barrier, but a complicating factor in this case was a pre-existing kidney condition (Iwasaki et al., 1997). As described in Section 5.7.2.2, absorption of nano-Ag through damaged dermal tissues (as was present for the burn patients in the aforementioned cases) is greater than for healthy tissue (Larese et al., 2009).

5.7.1.3. Metabolism



The liver typically serves a detoxifying function in the body by removing harmful substances from the blood and metabolizing them to forms that can be excreted more easily from the body. Once nano-Ag particles enter the GI tract, either as a result of absorption or distribution, the particles would presumably enter the portal vein for transport to the liver. No evidence of metabolism of nano-Ag by liver enzymes has been reported ([Wijnhoven et al., 2009b](#)). This observation is not unexpected, given that inert metals typically are not transformed by the body into different chemical forms. Wijnhoven et al. ([2009b](#)) suggested that nano-Ag might bind to metallothioneins, which are proteins that bind to metals and are involved in metal regulation and transport out of cells; the authors, however, present no specific evidence for this activity.

5.7.1.4. Excretion

The European Commission's Scientific Committee on Emerging and Newly Identified Health Risks ([2009](#)) suggested that two physiological methods of excretion can occur for nanoparticles that have been absorbed in the body and are present in the circulatory system. Clearance of nanoparticles by urination requires that nanoparticles be absorbed by the gut epithelium and undergo glomerular filtration in the kidneys; the nanoparticles then would be shunted to the bladder and excreted in the urine. Alternatively, nanoparticles could travel in bile from the liver to the intestine and be excreted in feces ([SCHER, 2009](#)). Other pathways of excretion also might exist, including transport out of the body through sweat or saliva, but no information was identified regarding these methods. Wijnhoven et al. ([2009b](#)) have suggested that these other routes might be less important but provided no firm evidence as to why.

Human studies of occupational exposures have shown that exposure to conventional silver results in elevated silver levels in feces and urine ([Pifer et al., 1989](#); [Rosenman et al., 1987](#)). Pifer et al. ([1989](#)) compared fecal silver concentrations in workers exposed for at least five years in positions with high exposure potential in an Eastman Kodak plant to a control set of employees at the plant in positions with low exposure. Measured concentrations in indoor air at the facility were reported as 1–100 $\mu\text{g}/\text{m}^3$, with the majority present in insoluble forms. Although no cases of argyria were reported, 80% of silver workers had detectible blood silver concentrations (mean of 0.010 $\mu\text{g}/\text{mL}$ among those with detectible blood silver levels), and none of the individuals in the low-exposure group had detectible blood silver levels. Fecal concentration among workers was higher than in the control group (i.e., 15 $\mu\text{g}/\text{g}$, compared to 1.5 $\mu\text{g}/\text{g}$ in controls). Body burdens also were calculated and reported to be 14 $\mu\text{g}/\text{kg}$ in workers, which was seven times the level observed in control samples. In one case study, Trop et al. ([2006](#)) reported that the body can clear silver from the blood once the exposure has been terminated. Cases of argyria and

argyrosis (accumulation of silver in the eye), which are generally believed to be irreversible conditions, demonstrate that the body cannot completely clear silver from all organs. How much of an absorbed dose remains as a residual burden, however, is not well understood ([Wijnhoven et al., 2009b](#)). Wijnhoven et al. ([2009b](#)) also did not identify information in their review regarding whether the silver excreted following exposure to nano-Ag would be released as nano-Ag or as other forms of silver.

5.7.2. Uptake and Dose by Route

5.7.2.1. Respiratory (Inhalation and Instillation)

In contrast to fine particles with diameters in the 1- to 2.5- μm range, which are deposited mainly in the peripheral lung, inhaled nanoparticles can be deposited throughout the respiratory tract: in the oral and nasal cavities, the tracheobronchial region of the respiratory tract, and the alveolar region of the lung ([Oberdörster et al., 2005b](#)). Deposition of particles within the respiratory system depends largely on particle size and chemistry and on breathing force ([Wijnhoven et al., 2009b](#)).

The International Commission on Radiological Protection (ICRP) developed and continues to update the Human Respiratory Tract Model for Radiological Protection, which can be used to predict the fractional deposition of single particles (not clusters) in the human respiratory tract. Oberdörster et al. ([2005b](#)) and Mark ([2007](#)) used the ICRP model to estimate size-dependent deposition patterns of nanoparticles; these studies produced similar results. In general, the ICRP model estimates that very small nanoparticles (i.e., 1-nm diameter) primarily deposit in the nasopharyngeal region, slightly larger nanoparticles (i.e., 5–10 nm) deposit about equally in all three regions of the respiratory tract, and larger nanoparticles (i.e., 20–100 nm) deposit primarily in the alveolar region. Mark ([2007](#)) found that the projected probability of nanoparticles reaching the alveoli peaked at a size of approximately 20 nm, with lower probabilities of deposition in the alveoli for both smaller and larger nanoparticles. Nanoparticle deposition, especially for particle sizes of 20 nm and smaller, is governed by Brownian motion and diffusion, which allows movement of particles into the alveolar region of the lung, where larger particles (which are transported via bulk air flow) generally are not deposited ([Elder et al., 2009](#)). For nanoparticles between 20 and 100 nm in size, deposition probability dropped for all three regions of the respiratory tract ([Mark, 2007](#)). Nonetheless, the ICRP model indicated that for nanoparticles measuring between 10 and 100 nm, the highest *fractional* deposition would occur in the alveolar region ([Lynch and Elder, 2009](#)).

Each region of the respiratory tract employs different mechanisms for clearing inhaled particles from the mucosal surface ([Oberdörster et al., 2005b](#)). Nanoparticles that deposit in any region of the respiratory tract can, however, undergo chemical clearance through dissolution. Solutes then can bind to proteins or be absorbed into the blood or lymphatic system and translocated to other parts of the body via

the circulation system. As discussed previously, an important feature of nano-Ag particles is their ability to adsorb biomolecules (e.g., lipids, proteins), which alter the particle's surface properties. Biomolecules adsorbed along the way to the circulatory system could influence the ability of the nanoparticles to interact with cells and systems they encounter ([Lynch and Elder, 2009](#)). Because translocation of the nanoparticles depends on their physical and chemical properties, nano-Ag deposited in the lung and translocated to other parts of the body might carry a biological marker of its deposition site until other biomolecules displace those that are initially adsorbed. The surface corona of proteins and other biomolecules surrounding a nanoparticle can affect its solubility, clustering, uptake, and distribution in the body ([Lynch and Elder, 2009](#)).

Unlike chemical clearance mechanisms, physical clearance (i.e., translocation) mechanisms differ somewhat for the three regions of the respiratory tract, and many of these clearance processes appear to be more effective for some sizes of nanoparticles than for others. Nanoparticles deposited in the alveolar region of the respiratory tract might be physically cleared from the alveolar region by: (1) macrophage phagocytosis followed by mucociliary transport along the tracheobronchial tree to the GI tract (i.e., particles are internalized by cells, gradually moved in a mucus flow by cilia to the trachea, eventually reaching the esophagus, where they are swallowed); (2) translocation across the alveolar epithelium; (3) translocation into interstitial sites; and (4) blood circulation ([Elder et al., 2009](#); [Chen and Schluesener, 2008](#); [Geiser et al., 2008](#); [Kreyling et al., 2002](#); [Oberdörster, 1988](#)). Nanoparticles deposited in the tracheobronchial region are generally cleared through similar mechanisms as for the alveolar region but also through lymphatic drainage and neuronal uptake, and nanoparticles deposited in the nasopharyngeal region are typically cleared through epithelial translocation and neuronal transport ([Elder et al., 2009](#); [Chen and Schluesener, 2008](#); [Geiser et al., 2008](#); [Kreyling et al., 2002](#); [Oberdörster, 1988](#)). These mechanisms, and their removal efficiencies for different-sized particles, are described in more detail below (neuronal transport is discussed in the Olfactory Nervous System subtopic at the end of this section).

From a few studies conducted by others, Elder et al. ([2009](#)) concluded that larger particles and clusters of nanoparticles (especially those greater than 100 nm in size) are more likely to be taken up by alveolar macrophages than single nanoparticles. Takenaka et al. ([2000](#)) examined the fate of 20-nm diameter nano-Ag in rats at 1, 4, and 7 days after intratracheal instillation. They found the nano-Ag particles in larger clusters taken up by alveolar macrophages and inside the alveolar walls at all three time intervals. A small proportion of single particles also was observed. The appearance of clusters of nano-Ag particles in the macrophages seemed unchanged up to 7 days after instillation, and no substantial changes in silver concentrations were observed in the lung, liver, and lung-associated lymph nodes over time.

Liver silver concentrations remained approximately 3% of that in the lungs. Based on these observations, the investigators suggested that such clusters do not rapidly translocate to other organs.

Because alveolar macrophage phagocytosis appears to be an inefficient clearance mechanism for nanoscale particles, most physical clearance of nanoparticles from the different regions of the respiratory tract occurs through epithelial endocytosis, and—in the alveolar and tracheobronchial regions—further translocation across the epithelial cells to the interstitium ([Oberdörster et al., 2005b](#)). Although subsequent translocation from epithelial cells and interstitial sites to the circulatory system is not well understood, such clearance processes appear to be size-dependent, favoring nanoscale particles ([Oberdörster et al., 2005b](#)).

Nano-Ag is thought to reach the bloodstream after inhalation dosing via three pathways: (1) ingestion after movement up the mucociliary escalator, (2) passage into the lymph nodes, and (3) direct entry via alveolar epithelial cells ([Ji et al., 2007](#)). Inhalation studies of rats exposed to nano-Ag have demonstrated absorption of silver through the lungs into the circulatory system and distribution to other organs as well ([Sung et al., 2009](#); [Takenaka et al., 2001](#)). Takenaka et al. ([2001](#)) exposed rats via inhalation using whole-body exposure chambers and reported a cumulative dose to each rat of approximately 7.2 micrograms (μg) of nano-Ag particles approximately 15 nm in size. Total silver concentrations in various organs and biological systems were monitored, and the distribution of silver was observed. The highest silver concentration and total content were observed in lung tissue. Elevated concentrations also were reported for the liver and blood, with measurable amounts reported in these components 7 days after exposure. Lower levels were measured in other organs, including lymph nodes, kidneys, blood, heart, and brain (listed in order of decreasing concentration).

Researchers in Korea administered differing doses of aerosolized nano-Ag to rats and monitored total silver concentrations in organs over 28 days. These researchers found that lung concentrations of silver showed a dose-dependent relationship following exposure ([Hyun et al., 2008](#); [Ji et al., 2007](#)).

Whether nano-Ag particles are distributed in the bloodstream to other organs or only the silver ions reach the circulatory system is not yet known. The eventual fate of the inhaled nano-Ag also is unclear at this time.

Olfactory Nervous System

For inhaled substances, the olfactory nerve represents another pathway to the brain. This pathway is treated here as a subtopic of inhalation exposure; it is given special attention because it represents a potential exposure and distribution route to the central nervous system that does not require passage through the blood-brain barrier.

The olfactory nerve facilitates the sense of smell by extending from the nasal cavity to the olfactory bulb of the brain, where the sensation of smell is processed. As described in detail in a review by Illum

(2000), substances that deposit on the nasal olfactory mucosa and enter into the olfactory nerve can be transmitted directly to the brain without encountering the blood-brain barrier. Entry of drugs and other substances to the olfactory bulb of the brain through the olfactory nerve has been demonstrated, and evidence indicates that this pathway might have an upper size limit of 200 nm (Elder et al., 2009; Elder et al., 2006; Oberdörster et al., 2004). Oberdörster et al. (2004) noted that results from several studies (including their own research using radiolabeled carbon nanoparticles) suggest that this nerve serves as a pathway to the central nervous system for soluble metals and nanomaterials. In that study, approximately 20% of the carbon nanoparticles deposited on the olfactory mucosa of the rats was translocated to the olfactory bulb in the brain (Oberdörster et al., 2004). Oberdörster et al. noted that once deposited in the olfactory bulb, nano-Ag might be able to travel to other areas of the brain, a possibility also noted by Lynch and Elder (2009). Transfer from the olfactory bulb to other parts of the brain, however, was not confirmed by these researchers, and no studies confirming this possibility were identified for this case study. No studies focusing specifically on the transport of nano-Ag to the olfactory bulb via this pathway were identified for this case study.

5.7.2.2. Dermal

In their review, Elder et al. (2009) summarized evidence regarding the interaction of various nanoparticles with skin. The results varied, with different degrees of penetration into and through skin observed in both in vitro and in vivo studies involving human skin and that of other organisms (e.g., rats, pigs). They noted that nanoparticles of varying composition have been absorbed into the blood in scenarios involving mechanical flexing of the skin and damaged skin patches as well as passage through hair follicles (for particles smaller than ~5 nm).

Elder et al. (2009) noted that nanoparticle penetration of the skin is influenced by surface coatings and geometry of the particles. For example, Monteiro-Riviere and Riviere (2009) reported that skin is “surprisingly permeable” to some nanoparticles, and in particular quantum dot nanoparticles, which are readily absorbed. In addition, the formulation of the nanoparticles that contact the skin might also influence the skin’s permeability by altering its barrier properties. For example, dimethyl sulfoxide facilitates absorption of substances through the skin by removing much of the lipid matrix of the stratum corneum, leaving holes and shunts (Lehman-McKeeman, 2008). The vehicle in which the nanoparticles are dissolved or suspended also might influence partitioning between the stratum corneum and the vehicle. Elder et al. (2009) concluded that dermal absorption of nanoparticles does not appear to occur readily but can take place under certain conditions, and the factors dictating the extent to which absorption occurs are varied and complex.

Only a few experiments on dermal penetration of nano-Ag were identified for this case study. Larese et al. (2009) reported that nano-Ag can pass through normal human skin (i.e., full-thickness

abdominal skin) in vitro at a rate of 0.46 nanogram per square centimeter (ng/cm²) and through damaged skin at a rate five times higher. The silver nanoparticles used in this experiment were coated with PVP to prevent clustering in an aqueous suspension. TEM of skin samples following exposure were reported to show silver nanoparticles in the stratum corneum and the upper layers of the epidermis “in some slices.” Based on observations from studies using other nanoparticles, Larese et al. (2009) inferred that nanoparticles between 7 and 20 nm can penetrate into the hair follicle, and particles less than 30 nm can passively penetrate the deepest skin layers, probably through the intercellular route (Larese et al., 2009). Samberg et al. (2010) applied nano-Ag particles 20 and 50 nm in size in solutions ranging from 0.34 to 34.0 µg/mL to the backs of pigs for 14 days. TEM demonstrated the presence of nano-Ag within the superficial layers of the stratum corneum for the 50-nm particles and on the top layer of the stratum corneum for the 20-nm particles. Although some of the lower tissue layers exhibited symptoms of chronic irritation such as focal inflammation (epidermis and dermis) and edema (epidermis), no evidence of nanoparticle penetration into these lower layers of the skin was found. Samberg et al. (2010) therefore hypothesized that silver ions released from the nanoparticles in the stratum corneum might translocate to lower tissue layers and cause the observed lesions.

Receptor characteristics also might affect internal dose following dermal exposure. Certainly the presence of cuts or scratches would enhance dermal absorption of nano-Ag and other substances. Recent data indicate possible sexual differences in retention of nanoparticles after dermal absorption. Using tracer techniques, Gulson et al. (2010) demonstrated that outdoor application of a sunscreen containing nano-⁶⁸ZnO (zinc oxide) resulted in absorption of small amounts of Zn, measured as ⁶⁸Zn in the blood. Retention of the ⁶⁸Zn tracer in blood was higher in women than in men, although the sample sizes were small (*n* = 17 subjects total).

5.7.2.3. Ingestion

Absorption of conventional silver following ingestion has been reported; for example, Boosalis et al. (1987) observed that 10–20% of ingested silver metal was absorbed in the GI tract, mainly by the duodenum and small intestines. Nanoparticles, however, do not appear to be readily absorbed. In separate review discussions, Mark (2007) and Elder et al. (2009) noted that the few studies investigating the uptake and deposition of various nanoparticles to the GI tract have typically demonstrated that ingested particles pass through without absorption and are eliminated quickly. Specific to nano-Ag, Kim et al. (2008) reported that ingestion of nano-Ag by rats resulted in distribution of silver in a range of tissues, with dose-dependent accumulation of silver observed in all tissues evaluated. Specifically, in a 28-day oral administration study of nano-Ag particles approximately 53–73 nm in diameter, silver was detected in the blood, stomach, brain, liver, kidneys, lungs, and testes, indicating that silver was distributed systemically (Kim et al., 2008). Silver uptake in kidneys was observed to be sex-specific, with silver

accumulation in females twice as high as in males ([Kim et al., 2008](#)). The investigators did not demonstrate, however, that nano-Ag particles were absorbed by the GI tract. In another recent evaluation of the ability of nano-Ag to cross the human intestinal wall using an in vitro model, Bouwmeester et al. ([2010](#)) reported limited (0.5%) translocation of nano-Ag across the membrane, with no dependency on size in the range of 20–112 nm in diameter (results not yet published; year indicates date of release of preliminary data). As is the case with other routes of exposure, surface properties of nano-Ag present in the GI system are likely to influence uptake across this biological barrier, especially given the changes in acidity and the negatively charged mucous layer in the small intestine ([Elder et al., 2009](#)).

5.7.3. Models to Estimate Dose

No models for estimating the pharmacokinetics of nano-Ag were identified for this case study. Some models for nanoparticle deposition within the body have been developed that, by extension, could be useful in evaluating dose for nano-Ag. One such model that ICRP developed estimates human and rat airway particle dosimetry by modeling deposition of nanoparticles based on their size ([Price et al., 2002](#); [ICRP, 1994](#)). Researchers including Mark ([2007](#)), Maynard and Kuempel ([2005](#)), and others have used to this model to predict where in the respiratory tract particles of different sizes are likely to deposit, as described in more detail above (see Section 5.7.2.1).

5.8. Summary of Exposure, Uptake, and Dose



Currently available data indicate that over 300 consumer products on the market could contain nano-Ag, suggesting that an understanding of aggregate exposure from numerous sources might be useful for accurately determining exposure pathways and estimating dose levels. Nano-Ag disinfectant spray use alone can result in inhalation, ingestion, and dermal exposure to nano-Ag. Through environmental pathways, nano-Ag might bind to other molecules, which can affect bioavailability to both biota and humans.

Biotic Exposure and Uptake

Few data exist to determine the extent to which nano-Ag is present in the environment and whether it is bioavailable to organisms. Most current models for estimating exposure and fate are not suitable for simulating nanoparticles in general or nano-Ag in particular, and therefore require modification and additional research. For biota, the aquatic environment is expected to be a greater source of potential exposure than the terrestrial environment, and sediment also appears to be more a more likely exposure

pathway given that nano-Ag preferentially accumulates in sediment. Exposure and bioavailability are strongly affected by environmental factors, such as pH, the presence of other ligands (including sulfides), other particles, and the nature of the environmental medium in which the nano-Ag is present. Ingredients of spray formulations might also alter the behavior of nano-Ag or exhibit increased uptake in the presence of nano-Ag. Some of these factors affect silver in general (e.g., presence of excess sulfides, ligands), and evaluations in the laboratory have confirmed that they also affect the bioavailability of silver present in nanoparticle form. Some environmental factors might particularly affect nano-Ag because of specific properties of this form of silver.

Bacteria and fungi readily take up nano-Ag, which is consistent with the well-known antibacterial properties of silver. Bioaccumulation by aquatic organisms has been studied to a limited extent and some organisms (e.g., algae, eggs of vertebrates) readily take up nano-Ag. Other biota, including bivalve mollusks and aquatic crustaceans, bioaccumulate conventional silver and some nanoparticles, but nano-Ag bioaccumulation has not been specifically studied in these organisms. Some microorganisms appear to have the ability to synthesize nano-Ag. Bioaccumulation in fish appears to occur to a limited extent and is more likely in freshwater than saltwater species. Nano-Ag particles appear to adsorb to fish gills, which then could serve as a pathway for delivering silver ions to the animal. In embryonic zebrafish, nano-Ag particles were absorbed and accumulated in tissues, including the brain, and silver entered the nuclei of cells in diverse organs. Nano-Ag particles can enter via chorion pores. Overall, bioaccumulation of nano-Ag appears to decrease with increasing trophic level in water-column food webs.

Some terrestrial plants bioaccumulate silver to a limited extent, although conventional silver is rarely absorbed beyond plant roots. Due to the smaller size and increased surface area of nano-Ag, the potential exists for greater release, and therefore uptake, of silver ions from nano-Ag compared with ions released from conventional silver; however, few data on the uptake of silver of any type are available for terrestrial plants. Limited evidence suggests that invertebrates might absorb nano-Ag that is bioavailable in soil. Bioaccumulation of nano-Ag in larger terrestrial organisms has not been studied. The possibility remains, however, that terrestrial ecosystems could be impacted if microorganisms in soil and elsewhere in terrestrial ecosystems are affected by nano-Ag.

Human Exposure and Dose

With the growing use of nano-Ag (especially in consumer products), elevated human exposures to nano-Ag through a range of scenarios is increasingly possible. Several expert elicitation and modeling exercises have concluded that use of nano-Ag in a spray solution is likely to result in consumer exposure (including potential exposures to sensitive subpopulations) via inhalation and dermal pathways ([Wijnhoven et al., 2009a](#); [Wardak et al., 2008](#)); however, no data focusing on nano-Ag were identified for

this case study. Persons in consumer households, particularly children, can be exposed orally by hand-to-mouth behaviors after touching or handling treated surfaces. Occupational exposures to nano-Ag in powders or solutions used in manufacturing might also result in inhalation and dermal exposures, with the potential for subsequent ingestion exposures (e.g., from hand-to-mouth or contact with treated surfaces). These exposures appear to differ from those known for conventional silver, because smaller particles have a greater potential to become aerosolized or to penetrate the skin. Occupational studies of conventional silver have not shown clear associations of effects with particular exposures due to small sample sizes and confounding factors. Perhaps because many of the human studies are retrospective (as described in the following chapter), few data on exposure characterization are available. Only two occupational exposure studies specific to nano-Ag were identified for this case study.

With respect to the human uptake of nano-Ag, considerations relevant to understanding uptake and dose include the properties of particles and the route of exposure. Surface properties, such as charge, and surface characteristics, such as the coating and presence of biomolecules that sorb to the surface of the nanoparticle, can affect absorption. Other spray ingredients or materials used in the manufacturing process might associate with nano-Ag and thereby exhibit increased uptake. Current data suggest that silver from nano-Ag crosses biological membranes following oral and inhalation exposure, with resulting accumulation in the lungs, liver, kidneys, stomach, brain, and blood. Whether soluble silver, silver ions, or nano-Ag particles are entering various tissues after exposure to nano-Ag is unclear. Whether conventional silver can cross the blood-brain barrier in humans is controversial; no evidence to date indicates that nano-Ag particles, even particles as small as 1–2 nm, can penetrate the blood-brain barrier in mammals. No evidence exists regarding the metabolism or transformation of nano-Ag in tissues, nor regarding urinary or fecal excretion pathways and whether they differ from conventional silver excretion.

Deposition of nano-Ag in the human respiratory tract is expected to differ from that of conventional silver, but the degree to which this difference in lung deposition quantitatively influences distribution to other tissues is unclear ([Elder et al., 2009](#); [Lynch and Elder, 2009](#)). In animal studies ([Sung et al., 2009](#); [Ji et al., 2007](#); [Takenaka et al., 2001](#)), the finding of elevated silver concentrations in extrapulmonary tissues and blood following inhalation exposure to nano-Ag aerosols provides qualitative evidence of absorption of silver by the respiratory tract, followed by distribution to other tissues. The finding of very high silver concentrations in the lungs following exposure, compared with other organs, however, suggests that, at the tested concentrations, translocation to other tissues is not extensive. Possible routes of translocation to other tissues following deposition of silver nanoparticles in the respiratory tract include direct translocation to the brain olfactory bulb from the nasal olfactory epithelium via the olfactory nerve, translocation (of particles and silver ions) to lymph nodes and blood following

alveolar deposition, and translocation via mucociliary clearance to the digestive tract following macrophage engulfment of alveolar-deposited particles ([Ji et al., 2007](#)).

Treatment of burn wounds in humans has resulted in kidney, liver, and skin accumulation of silver, and in one case neurological effects were observed, suggesting silver might have entered the brain. Silver absorption has been demonstrated across healthy human skin samples exposed to suspensions of nano-Ag, but the degree to which this observation was due to transport of the silver nanoparticles or silver ions released from those particles in the stratum corneum is unknown. Rates of silver absorption were five-fold higher in skin samples damaged by abrasion.

Ingestion exposures to nano-Ag appear to result in lower relative absorption and subsequent dose compared to other exposure pathways. Conventional silver has been demonstrated to cross the intestinal barrier following ingestion exposure. The limited data for nano-Ag suggest particle characteristics, including surface modification, affect whether nano-Ag is absorbed or excreted following ingestion. Models do not currently exist for estimating nano-Ag distribution in the body. Models developed for other particle types could be applied for nano-Ag if such models adequately consider chemistry and surface properties.

As expressed by the Federal Insecticide, Fungicide, and Rodenticide Act Scientific Advisory Panel, broad data gaps about potential exposures (and toxicity) related to nano-Ag exist ([U.S. EPA, 2010b](#)). Attempting to follow the risk assessment paradigm for nano-Ag exposures, Christensen et al. ([2010](#)) concluded that available data relevant to exposures and toxicity are inadequate at this time for use in regulatory decision-making. When examining nano-Ag as a hypothetical registration under the Registration, Evaluation, Authorisation and Restriction of Chemicals program in Europe, the Netherlands National Institute for Public Health and the Environment ([Pronk et al., 2009](#)) also identified key data gaps in particle characterization, exposure, uptake, and toxicity. These gaps were large enough at that time to prevent implementation of the Registration, Evaluation, Authorisation and Restriction of Chemicals process for this widely used material.

This page intentionally left blank.

Chapter 6. Characterization of Effects

This chapter summarizes the effects of nano-Ag on humans and biota associated with the use of nano-Ag in spray disinfectants. The preceding chapters in this case study have laid a foundation for this chapter by providing an exposure context for characterizing such effects. In this chapter, Section 6.1 provides information on the factors that influence the effects of nano-Ag on ecological receptors and human health. The ecological effects resulting from exposure to nano-Ag are discussed in Section 6.2, and relevant results from ecotoxicological studies are summarized for microorganisms (Section 6.2.1), aquatic organisms (Section 6.2.2), and terrestrial organisms (Section 6.2.3). Human health effects resulting from exposure to nano-Ag are discussed in Section 6.3, and relevant information is presented for in vitro studies (Section 6.3.1), in vivo studies (Section 6.3.2), and human health and epidemiological studies (Section 6.3.3). Because nano-Ag releases are likely to result in the formation of silver compounds and discharges of silver ions, the ecological and human health effects of other silver species also are discussed, when appropriate. The technology to differentiate the effects of silver nanoparticles from those of the silver ions released from the nanoparticles is still developing. As a result, determining whether the observed effect is due to the nanoparticle per se, the silver ions alone, or the silver ions modulated by the nanoparticle is not always possible. Few ecological and human health effects studies distinguish between the effects the silver nanoparticle and the silver ions released by the nanoparticle; where this distinction has been made by investigators, it is presented here.

A few reviews are available on the ecological and human health effects of exposure to silver compounds and silver ions ([Lansdown, 2007](#); [Ratte, 1999](#)); comparatively few studies, however, are available on the effects of silver nanoparticles. The Scientific Advisory Panel (SAP) for the Federal Insecticide, Fungicide, and Rodenticide Act (FIFRA) concluded in its 2009 meeting on the evaluation of hazards and exposure of nano-Ag that data gaps about potential hazards of nano-Ag are broad, and that the hazard profile for nano-Ag can differ significantly from that for conventional silver and other silver species ([U.S. EPA, 2010b](#)). As noted in Chapter 1, the findings presented in this case study generally support the FIFRA SAP conclusions. Consistent with studies of other nanomaterials ([Ostrowski et al., 2009](#)), most studies of nano-Ag have investigated the ecological or human health effects of various formulations of silver nanoparticles and silver ions, and relatively few have investigated the effects of end-use products containing nano-Ag or their life-cycle by-products. Moreover, the term “nano-Ag” encompasses a variety of materials with a diverse range of physicochemical properties. As a result, not all materials referred to as nano-Ag will necessarily behave the same or cause the same ecological or human

health effects. Various members of the scientific community and the FIFRA SAP have cautioned against extrapolating from one nano-Ag formulation to another when assessing hazards. The current dearth of information, however, necessitates compiling results from studies using various nano-Ag formulations to detail the current state of knowledge about the potential toxicological properties of nano-Ag. Therefore, for the purposes of this case study, available information from all nano-Ag materials is described together, but individual particle characteristics are noted in parallel.

This chapter focuses on characteristics of the nanoparticle, exposure media, and biological receptors that might influence the degree to which nano-Ag is toxic to humans and biota. In general, Section 6.1 focuses on nanoparticle properties and factors of the exposure environment that can influence nano-Ag toxicity, because these data are relevant to both ecological and human health effects. As noted in Chapters 1 and 5, there is no sharp demarcation between exposure-dose and effects, so some overlap is unavoidable between the information on exposure and dose, presented in Chapter 5, and the information on effects, presented here. To the extent possible, discussion of studies cited in both chapters is limited in Chapter 5 to discussion of exposure-dose and in this chapter to discussion of effects.

Evidence is growing that nano-Ag in particular forms and under certain testing conditions can be toxic to bacteria, fungi, algae, aquatic invertebrates, terrestrial invertebrates, and fish, and to mammalian brain, liver, skin, and stem cells ([Kahru and Dubourguier, 2010](#); [Panyala et al., 2008](#)). The breadth of representative species for which nano-Ag toxicity has been studied and the scope of these studies, however, are too narrow to draw definitive conclusions regarding the degree to which nano-Ag might present a threat to environmental and human health ([Wijnhoven et al., 2009b](#)). Until recently, the consensus was that the toxicity of silver in the environment depended mainly on the concentration of free silver ions to which an organism is exposed ([Khaydarov et al., 2009](#)). Results from recent studies, however, suggest that some adverse effects on biota can be attributed to properties of the silver nanoparticle itself; furthermore, these effects might be exacerbated by the release of silver ions at the biological interface ([Choi et al., 2009](#); [Laban et al., 2009](#); [Roh et al., 2009](#); [Navarro et al., 2008b](#); [Lee et al., 2007](#)). These properties are described in more detail in Section 6.1.

The following sections are not meant to be an exhaustive review of the ecological and human health effects literature for nano-Ag, silver compounds, or silver ions. Instead, this chapter is intended to highlight recent work on the effects of nano-Ag particles and to identify the information status and gaps for assessing potential risks of nano-Ag in spray disinfectants.

6.1. Factors that Influence Ecological and Human Health Effects of Nano-Ag

Because many variables are associated with synthesis, characterization, and behavior of nano-Ag in experimental and environmental conditions, identifying the primary property(ies) of nano-Ag that contribute to an effect is extremely difficult. The complexity of the factors influencing ecological and human health effects of nano-Ag also makes comparing the respective influence and importance of the different properties extremely difficult. That many of the novel properties exhibited by nanoparticles result from their small size is widely accepted, but other factors have been noted as variably contributing to the effects of nanoparticles on biota and humans ([Luoma, 2008](#)).

For example, in a study comparing nano-gold and nano-Ag toxicity to zebrafish embryos, nano-gold induced minimal sublethal toxic effects at the end of a 120-hour exposure period at the highest concentration tested, while nano-Ag particles of the same size and at the same concentration resulted in nearly 100% mortality ([Bar-Ilan et al., 2009](#)). **This study demonstrated that nanoparticle size alone does not dictate toxic effects, and it highlights the potential importance of nanoparticle chemical composition in eliciting a toxic response.** In a study comparing the toxicity of nanoparticles of different metals to fish, aquatic invertebrates, and algae, Griffitt et al. ([2008a](#)) concluded by process of elimination that particle chemistry appears to be the most influential characteristic of the nanoparticle because the investigators did not identify a relationship between size, surface area, or zeta (ζ) potential and toxicity. Other physicochemical properties, such as morphology, surface treatments, and solubility of particles, however, also might significantly influence the toxicity of nano-Ag ([Choi et al., 2008](#)). Furthermore, any particle properties that influence bioavailability in general also will influence the effects of nano-Ag on an organism, as interaction between the nanoparticle and the organism (or at least silver ions released from the particles) is necessary to induce an effect. Factors that influence all substances in the environment might also affect the toxicity of nano-Ag to humans and biota, including exposure medium, type of organism, environmental bioavailability, route(s) of exposure, and the physicochemical properties and size distribution of the nano-Ag particles. Furthermore, although processes in the environment and within the body can detoxify harmful substances to a certain degree, the health of some receptors might be sufficiently compromised such that small concentrations can trigger an adverse effect. This particular factor, which undoubtedly contributes to the toxicity of nano-Ag in some susceptible or vulnerable populations, however, has not yet been explored in the literature.

Although nanoparticle synthesis, characterization, and detection techniques have advanced considerably in recent years, the influence of various physicochemical properties of nano-Ag has not been fully elucidated using well-characterized nano-Ag under controlled conditions ([U.S. EPA, 2010b](#)). Nor

have experimental or environmental characteristics been the focus of most toxicity studies to date. As a result, the factors and conditions that drive nano-Ag toxicity in specific exposure scenarios have not yet been determined, and data on the influence of physicochemical properties and experimental and environmental conditions are still somewhat limited. This section focuses on factors that have been demonstrated in the supporting literature to be pertinent to nano-Ag; however, findings related to other types of nanomaterials are noted when relevant.

6.1.1. Physicochemical Properties

Size, chemical composition, and surface treatment appear to be three of the most critical nanotoxicity metrics ([Bar-Ilan et al., 2009](#)). Other physicochemical properties such as shape, doping, and purity (or impurities) also could influence the outcomes of nano-Ag toxicity tests, but that information is usually not reported in ecological and human health effects studies. Databases describing detailed nanoparticle properties and health effects are being developed ([Miller et al., 2007](#)); these include the National Institute for Occupational Safety and Health/Centers for Disease Control and Prevention Nanoparticle Information Library,²¹ Rice University/International Council on Nanotechnology Nanotechnology Environment, Health and Safety Database,²² the Organisation for Economic Co-operation and Development (OECD)-maintained Database on Research into the Safety of Manufactured Nanomaterials²³ and Oregon State University's Nanomaterial-Biological Interactions Knowledgebase.²⁴

The need to characterize basic physical and chemical attributes of the nanomaterials used in toxicity studies has been noted in numerous reports and journal articles ([Auffan et al., 2009a](#); [DEFRA, 2007](#); [Powers et al., 2007](#); [Warheit et al., 2007b](#); [Powers et al., 2006](#)). The Minimum Information for Nanomaterial Characterization Initiative ([2008](#)) has provided recommendations for the minimum required physical and chemical parameters that should be reported for nanomaterials used in toxicological studies. These parameters would establish generally what the material looks like, what the material is made of, and what factors affect how the material interacts with its surroundings. The specific attributes for minimal characterization recommended by the Minimum Information for Nanomaterial Characterization include particle size or size distribution, agglomeration state or aggregation (i.e., clustering), shape, overall composition (including chemical composition and crystal structure), surface composition, purity (including levels of impurities), surface area, surface chemistry (including reactivity and hydrophobicity),

²¹<http://www.cdc.gov/niosh/topics/nanotech/NIL.html>

²²<http://icon.rice.edu/virtualjournal.cfm>

²³<http://webnet.oecd.org/NanoMaterials/Pagelet/Front/Default.aspx>

²⁴<http://oregonstate.edu/nbi/nanomaterial.php>

and surface charge ([MINCharInitiative, 2008](#)). For more information on nanomaterial physicochemical properties that could influence ecological and toxicological effects, readers are referred to detailed reports listing information recommended to include in nanomaterial studies, including publications by OECD ([2008](#)), Taylor ([2008](#)), and Warheit et al. ([2007a](#)).

Furthermore, methods for establishing the toxic potential of chemicals, in general, have not been fully standardized internationally. Multiple organizations (e.g., OECD, the U.S. Environmental Protection Agency [EPA], the European Union) have proposed different sets of standard testing protocols, and efforts are currently underway to develop a set of harmonized testing guidelines for establishing chemical toxicity. Because consistent protocols have not yet been developed, not all results from the toxicological studies described in this chapter (and in greater detail in Appendices B and C) can be compared directly. Questions also exist about the suitability of current EPA and other standard testing guidelines for assessing nanomaterials. A general overview of the issues associated with the various guidelines for assessing physicochemical properties, human health effects, and ecological effects, as they pertain to nanomaterials, is available in a nano-Ag case study released by the Netherlands National Institute for Public Health and the Environment ([Pronk et al., 2009](#)).

In the following subparts of this section, key properties affecting toxicity of nano-Ag are discussed, including size, particle shape and crystal structure, and surface chemical composition and reactivity.

6.1.1.1. Size

Although nanoparticles are defined as particles having at least one dimension in the 1- to 100-nanometer (nm) range, not all nanoparticles within this range exhibit the same novel properties that distinguish them from their conventional counterparts. It has been argued that the unique size-dependent properties that necessitate a classification separate from conventional materials occur primarily in particles 1–30 nm in size, and that larger particles (31–100 nm) generally do not exhibit properties distinct from particles larger than 100 nm ([Auffan et al., 2009a](#)). The smaller size of nano-Ag might allow it to enter an organism more easily than its conventional counterpart. For example, for nanoparticles to penetrate the membrane of zebrafish embryos, they must be small enough to diffuse easily through transmembrane porins, which are proteins that facilitate passage of small molecules across the membrane, without attaching to the walls of the chorion²⁵ pore canal. These porins are approximately 0.5–0.7 micrometer (µm) in diameter. Once in the chorionic space, nanoparticles have been shown to penetrate the amnion and enter the inner mass of the embryo where they can interact directly with cellular

²⁵The chorion is the outermost of two membranes surrounding the embryo; the inner membrane is the amnion.

organelles and potentially disrupt cellular processes (Lee et al., 2007). As discussed in Chapter 5, Lee et al. (2007) used optical microscopy to observe the uptake of single silver nanoparticles by zebrafish embryos in real time. They reported that nanoparticles can enter cells by passive transport (i.e., Brownian diffusion) through the chorion pore canals and that the diffusion coefficients are inversely proportional to the radius of the nanoparticles. Although most nanoparticles were observed to penetrate the embryo, some that entered the chorion pore canals docked at the chorionic surface and formed clusters with other nanoparticles. Lee et al. (2007) speculated that larger silver nanoparticles (>31 nm) embed in the chorion pore canals and act as sites where clustering could occur. These clusters might eventually block the canals, thus inhibiting normal chemical transport between the egg and its environment.

The intrinsic properties of materials in the nanoscale size range, such as enhanced reactivity and unique surface structures, can result in higher dissolution rates, reduction and oxidation (redox) reactions, or increased generation of reactive oxygen species (ROS), all of which can in turn affect toxicity in a size-dependent manner (Auffan et al., 2009a). As a result, toxicity studies using the same protocol and test species likely are not directly comparable if the studies do not use nano-Ag within a similar size range or with the same surface coating (see Section 6.1.1.3). Furthermore, if studies use nano-Ag with average sizes greater than 30 nm (or if the nano-Ag material is not characterized in experimental conditions), the studies might not capture the toxic effects related to unique nanoscale properties if the hypothesis regarding particle size proposed by Auffan et al. (2009a) holds true. For example, Choi et al. (2008) observed that growth inhibition in nitrifying bacteria correlated strongly with the availability of particles less than 5 nm in diameter and not with silver nanoparticles that were 10 nm or larger. Morones et al. (2005) also observed that, although bacteria were exposed to silver nanoparticles with an average size of 21 nm, the average size of nano-Ag penetrating the membranes of *Escherichia coli* was about 5 nm.

Nano-Ag particle size, however, might be correlated with other properties that affect toxicity, such as the surface area-to-volume ratio, which in turn affects the ratio of reactive silver ions to unavailable silver atoms. The ratio of silver ions on the exterior of the particle available to react with a biological surface to the silver atoms that are “buried” within the interior of the particle and blocked from interaction might influence nano-Ag toxicity levels. For example, equivalent total silver concentrations (by mass) of nano-Ag and conventional silver (or even different sizes of nano-Ag) do not contain equivalent amounts of silver ions available to react with a biological surface and induce toxicity. Most of the silver in the larger particles is blocked from interacting with the environment or biological surfaces, whereas relatively more of the silver in nano-Ag will be on the surface and readily available as the size of the nano-Ag decreases. As a result, the methods used now to assess chemical toxicity might not account for variation in biological responses related to particle size. Furthermore, several studies have proposed that the combination of silver nanoparticles and silver ions is more toxic to some receptors than either form of

silver alone ([Bae et al., 2010](#); [Sotiriou and Pratsinis, 2010](#)). Sotiriou and Pratsinis ([2010](#)) proposed that multiple modes of action exist for nano-Ag, and which mode of action dominates under specific conditions is influenced by whether silver nanoparticles are smaller or larger than 10 nm in diameter. They posited that silver nanoparticles smaller than 10 nm dissociate into silver ions more readily than those larger than 10 nm because of higher specific surface area and greater surface curvature. As a result, the chance that a nanoparticle of less than 10 nm will interact directly with the receptor before that nanoparticle completely dissociates is small. Silver ions therefore appear to drive the toxicity of nano-Ag in this size fraction. For silver nanoparticles with diameters greater than 10 nm, however, the release rate of silver ions relative to silver content is reduced, allowing more time for the nanoparticle to attach to the receptor surface and disrupt or damage that surface while shedding silver ions in a concentrated area. This suggests that the particle effect is driving the toxicity of nano-Ag in the nano-Ag size fraction larger than 10 nm. As discussed in Chapter 2, individual nano-Ag particles can form clusters under various conditions; in turn, particle clustering might influence the particle toxicity. For example, Zook et al. ([2011](#)) report that the size of nano-Ag clusters correlates with hemolytic toxicity where larger clusters resulted in less toxicity than smaller clusters at the same doses between 13.8 and 55.0 micrograms per milliliter ($\mu\text{g}/\text{mL}$) (the highest dose, 110 $\mu\text{g}/\text{mL}$, resulted in almost complete hemolysis regardless of cluster size).

Note that many of the studies investigating nano-Ag effects in humans and biota do not report the average sizes or the size ranges of the nano-Ag materials used. Where size is reported, some investigators report only the size distribution provided by the manufacturer, especially in the case of commercial nano-Ag materials. This size distribution might not be representative of actual particle sizes, given the potential for nano-Ag to form clusters (see Chapter 4). One example was reported by Miao et al. ([2009](#)), where the manufacturer's information identified the average size of silver nanoparticles in a commercial powder form as 10 nm, but the investigators experimentally determined the size of the nano-Ag primary particles to be between 60 and 70 nm.

6.1.1.2. Morphology

Shape and crystal structure also can influence toxicity. A recent review by Auffan et al. ([2009a](#)) examined unique properties at the nanoscale and observed that particles with diameters less than 30 nm exhibit increased reactivity (e.g., changes in surface reaction rates, redox state, adsorption capacity) on crystal facets due to size-dependent changes in crystalline structure. It has been shown that {111} facets, which are high-atom-density surfaces, are more reactive than {100} facets in silver crystals (see Section 2.3.2) ([Hatchett and White, 1996](#)). Pal et al. ([2007](#)) reported the first comparative study on the bactericidal properties of silver nanoparticles of different shapes. The study demonstrated that interactions

with gram-negative *E. coli* bacteria were shape-dependent, with truncated triangular silver nanoparticles that have the {111} basal plane exhibiting higher bactericidal activity than spherical and rod-shaped silver nanoparticles, which are dominated by {100} facets. A dose of 10 micrograms (μg) of truncated triangular silver nanoparticles added to 100 milliliters (mL) of nutrient broth with a bacterial concentration of 10^7 colony forming units per milliliter (CFU/mL) completely inhibited growth for at least 24 hours, while 100 μg of silver ions (added as silver nitrate $[\text{AgNO}_3]$)²⁶ or spherical silver nanoparticles resulted in growth inhibition only for up to 10 hours post-exposure, after which bacterial colonies appeared to grow at a normal rate (Pal et al., 2007). Morones et al. (2005) observed that the silver nanoparticles most likely to be found on the surface of the bacterial membrane are those having more {111} facets. The nanoparticles that interact with the cell membrane, such as those with {111} facets, are those that are most likely to penetrate the cell; interacting with the cell membrane can result in the disruption of membrane processes, damage to the membrane, and the release of silver ions directly to the membrane surface in high concentrations. Therefore, morphology can play a key role in conferring toxicity (Morones et al., 2005).

6.1.1.3. Surface Chemistry and Reactivity

Lok et al. (2007) found that partially oxidized silver nanoparticles were more toxic to *E. coli* than freshly prepared zero-valent (reduced) nano-Ag. Oxidation of zero-valent nano-Ag produces ionic silver, which is likely bound to the surface of the nanoparticle but could become available through desorption or dissolution. The investigators reported that partially oxidized (i.e., oxidized surface) nano-Ag decreased adenosine triphosphate (ATP) levels in *E. coli* cells by 90%, while exposing *E. coli* to reduced nano-Ag did not elicit a response different from that of the controls. Additionally, silver nanoparticles synthesized under an atmosphere of molecular nitrogen (N_2), which precludes surface oxidation, exhibited no antibacterial activity. The investigators also observed that oxidized silver nanoparticles do not appear to elicit a toxic response in silver ion-resistant *E. coli* strains, indicating that under these conditions nano-Ag does not produce a toxic response that is completely independent of silver ion effects (Lok et al., 2007).

The surface chemistry of nanoparticles can be changed by coatings that in turn can influence the particle's toxicity. Nanoparticle surface coatings have been demonstrated to influence cellular uptake, binding of serum proteins in vivo, ROS generation, and immunosuppression or stimulation response to a high degree in vertebrates (Bar-Ilan et al., 2009). Surface coatings are frequently applied to nanoparticles to functionalize them for a specific purpose or to stabilize them in suspensions. These coatings can

²⁶Where investigators draw comparisons between the effects of nano-Ag and silver ions added as AgNO_3 , they generally have concluded that the nitrate concentrations in these solutions are too low to elicit a toxic effect and that any observed effects are attributable to the silver ions.

influence the bioavailability or biocompatibility (i.e., the capability of the nanoparticle to coexist with biological tissue without causing adverse effects) of the nanoparticle, which in turn can affect toxicity ([Limbach et al., 2005](#)). Surface coatings that are used to ensure stability can facilitate an interaction between the nanoparticle and the organism. Consequently, such treatments can have a profound effect on the behavior of nano-Ag in the environment and its bioavailability to humans and biota. Metallic nanoparticles can be coated with organic or inorganic compounds that prevent the formation of clusters in solution ([Navarro et al., 2008a](#)) or control the size of clusters ([Zook et al., 2011](#)), both of which can influence the transport properties of the nanoparticles and maximize the number of individual nanoparticles in suspension. Stability of nano-Ag in suspension in spray disinfectants, for example, is important for product efficacy. When used as a bactericide in water, silver nanoparticles must remain suspended to be effective; therefore, in aquatic environments, coatings that keep nano-Ag in suspension can result in higher concentrations of nano-Ag in the water column and increased exposure of fish and other aquatic biota. Furthermore, the chemicals used to coat nanoparticles could inherently be toxic to certain organisms. For example, Stampoulis et al. ([2009](#)) reported that in the absence of nano-Ag, the surfactant sodium dodecyl sulfate significantly inhibited zucchini (*Curcubita pepo*) seed germination and root growth when added to reverse osmosis water. In turn, when added to the nano-Ag solution, the surfactant appeared to amplify the toxic effect of nano-Ag.

Several examples of the effect of surface-coated nano-Ag on toxicity were identified in the literature. For example, Ahamed et al. ([2008](#)) compared the uptake by mouse embryonic fibroblasts of nonfunctionalized silver nanoparticles with a nonuniform hydrocarbon surface layer and functionalized silver nanoparticles coated with the polysaccharide gum arabic. After 24 hours at a nano-Ag concentration of 50 µg/mL, most of the nonfunctionalized nano-Ag had formed clusters and had not penetrated cell organelles, while the functionalized (i.e., coated) nano-Ag was distributed throughout the cells. The investigators also reported higher levels of genotoxicity, as determined by measuring levels of the p53 protein (a molecular marker for DNA damage) and two DNA repair proteins, Rad51 and phospho-H2AX. They observed that exposure to functionalized nano-Ag resulted in more upregulation of these proteins than nonfunctionalized nano-Ag, suggesting that the functionalized nano-Ag causes greater genotoxicity ([Ahamed et al., 2008](#)). Kvittek et al. ([2009](#)) investigated the effects of surfactant- and polymer-modified nano-Ag on the protozoan *Paramecium caudatum* and found that surface modification using a nonionic surfactant, Tween 80, increased the materials' toxicity. In contrast, modification with the polymers PVP 360 (polyvinylpyrrolidone with an average molecular weight of 360 kilo-Daltons [kDa]) and PEG 35,000 (polyethylene glycol with an average molecular weight of 35 kDa) did not significantly affect the toxicity of nano-Ag in those organisms.

Nano-Ag also can be coated by biological substances released by or contained within organisms. Kahn et al. (2011) used a nano-Ag-resistant strain of *Bacillus pumilis* to investigate a mechanism of bacterial resistance to nano-Ag toxicity and discovered that exopolysaccharides secreted by this resistant strain of bacteria coated the silver nanoparticles, thus preventing direct contact of the silver nanoparticle with the bacterial cell. When nano-Ag was coated with these exopolysaccharides and exposed to strains of *E. coli*, *Staphylococcus aureus*, and *Micrococcus luteus* that were not resistant to nano-Ag, growth rates were still comparable to those of controls, whereas when these strains were exposed to nano-Ag not coated with exopolysaccharides, growth rates were reduced substantially (statistical significance not reported). The exopolysaccharide-secretion mechanism of tolerance might be selected for in bacteria exposed continuously to nano-Ag in an environmental milieu.

Surface coatings also can influence the ζ -potential of the silver nanoparticle, which affects the particle's electrostatic attraction to biological surfaces. Some investigators have claimed that direct contact between the nanoparticle and a bacterial membrane is required for bactericidal activity (El Badawy et al., 2011; Neal, 2008) (refer to Section 6.2.1). El Badawy et al. (2011) examined the toxicity to *Bacillus* of four types of nano-Ag representing four different surface-charging scenarios, ranging from very negative to very positive. The investigators demonstrated that toxicity was correlated with surface charge (as measured by ζ -potential) of nano-Ag, with the most negative surface charges resulting in the least toxicity. The most negatively charged (-38 millivolt [mV]) citrate-coated nano-Ag was the least toxic to *Bacillus* species, which are similarly charged themselves (-37 mV). As the surface charge changed from negative to positive, the electrostatic repulsion between the bacterial cell and the nano-Ag decreased, eventually allowing the nano-Ag to overcome the electrostatic barrier surrounding the cell. As a result, nano-Ag formulations with a smaller negative charge were more toxic. Specifically, PVP-coated nano-Ag (ζ -potential of -10 mV) was more toxic than uncoated²⁷ H₂-nano-Ag (-22 mV), which was more toxic than the citrate-coated nano-Ag (-38 mV). Finally, when the nano-Ag was coated with positively charged ($+40$ mV) branched polyethyleneimine, attraction between the positively charged nano-Ag and the negatively charged bacterial cell resulted in the highest degree of toxicity. Furthermore, toxicity following exposure to the branched-polyethyleneimine nano-Ag was greater than that of ionic

²⁷Elemental silver nanoparticles are inherently unstable in solution; without the aid of stabilizers or specific types of preparation, they will immediately form clusters. As a result, the term “uncoated,” as used by some investigators and manufacturers to describe nano-Ag, as supplied or produced, is often misleading. Silver nanoparticles are likely coated with a by-product of the synthesis process (e.g., OH⁻) or a mild stabilizer (e.g., citrate, hydrocarbon) before a coating intended to functionalize the nanoparticles (e.g., PVP, polysaccharide) is applied. Although this document provides information on surface treatments of nano-Ag, as provided by investigators and manufacturers, determining whether nanoparticles reported as “uncoated” in the literature were actually pre-treated to preserve the presence of stable nanoscale particles was not possible.

silver alone, indicating that the physical interaction of the silver nanoparticle with the cell was a key component of the nano-Ag mode of action, at least in *Bacillus*. Also in this study, El Badawy et al. (2011) determined that under these conditions surface charge was more highly correlated with nano-Ag toxicity to *Bacillus* than shape and size.

6.1.2. Test Conditions



Experimental study design can significantly influence results obtained in toxicity testing. For example, because the toxicity of nano-Ag is related in part to the solubility of the nanoparticle (i.e., the rate at which the nanoparticle releases silver ions), the time allowed for nano-Ag to dissociate can drastically affect toxicity. One striking example was provided by Ivask et al. (2010) in a study of toxicity of nano-Ag to several *sod*-deficient strains of *E. coli* (i.e., luminescent bacteria that lack a particular enzyme in oxidative stress response) and wild-type strains of *E. coli*. The investigators reported that the ranges of EC_{50}^{28} for the different strains of *E. coli* exposed to nano-Ag were much higher in 30-minute exposures (5.8–571 milligrams/liter [mg/L]) than in 2-hour exposures (3.11–45.9 mg/L), suggesting that results from experimental designs in which exposure duration differs by a matter of hours might not be comparable.

Methods of mixing such as sonication and ultrasound can be used in the preparation of nanoparticle suspensions to increase stability and the contact of the nanoparticles with the test organism or cells. The importance of standardizing sonication procedures and reporting them along with experimental results for reproducibility is described in Taurozzi et al. (2011). Other reports note that when these mixing methods are a part of aquatic toxicity testing procedures, they can result in an overestimate of toxicity of nanoparticles compared to results under realistic (natural) conditions (Gao et al., 2009). For example, Laban et al. (2009) exposed fathead minnow (*Pimephales promelas*) embryos to nano-Ag solutions that had been either sonicated or stirred. Stirring mimics fin movement by males in natural conditions, while sonication is not expected to represent any process in the natural environment. The investigators found that sonicating the nano-Ag solutions from two commercially produced nano-Ag products for 5 minutes before adding the embryos resulted in LC_{50}^{29} that were statistically significantly lower than when nano-Ag solutions were stirred (Laban et al., 2009).

²⁸Effective concentration is the chemical concentration at which 50% of the exposed organisms experience a specific effect; this effect level is commonly used to estimate the toxicity of a substance to a specific group of organisms.

²⁹Lethal concentration is the chemical concentration at which 50% of the exposed organisms die; this effect level is commonly used to estimate the toxicity of a substance to a specific group of organisms.

The medium used in experimental studies also can affect the apparent toxicity of nano-Ag. For example, nano-Ag in a liquid medium might only delay bacterial growth, while equivalent mass concentrations of nano-Ag added to plated agar appears to inhibit bacterial growth completely, although results are not always consistent from study to study ([Pal et al., 2007](#); [Sondi and Salopek-Sondi, 2004](#)). In water, damaged microbial cells can release intracellular substances that cause nanoparticles to cluster and fall out of suspension, ultimately resulting in decreased numbers of silver nanoparticles in the water ([Sondi and Salopek-Sondi, 2004](#)). No such microbial-induced clustering of nanoparticles seems to occur on agar plates.

The antibacterial effect of nano-Ag also seems to depend in part on initial bacterial density used in experiments (measured in terms of bacterial CFUs) ([Sondi and Salopek-Sondi, 2004](#)). Antibacterial activity is generally higher at lower bacterial cell concentrations. Because the high CFUs used in many experiments are rarely found in the environment, the bactericidal effect of nano-Ag in “real-life” systems might be underestimated using current experimental techniques ([Sondi and Salopek-Sondi, 2004](#)).

6.1.3. Environmental Conditions

The characteristics of the environmental medium in which nano-Ag exposure occurs can affect the properties of nano-Ag that ultimately influence toxicity. For example, changes in the pH, ionic strength, dissolved oxygen content, temperature, quantity of natural organic macromolecules, light availability, and quantity of ligands in the environment can significantly affect nano-Ag dissolution, bioavailability, and reactivity, all of which can affect toxicity ([Dasari and Hwang, 2010](#); [Liu and Hurt, 2010](#); [Cumberland and Lead, 2009](#); [Gao et al., 2009](#); [Choi and Hu, 2008](#)).

The type of liquid medium and the characteristics of that medium also can affect the behavior of nano-Ag. For example, nano-Ag released in wastewater can disperse silver ions, form complexes with ligands, cluster to form larger silver particles, or remain as nanoparticles to varying degrees depending on the characteristics of the wastewater (see Section 4.4.2). Few studies, however, have examined nano-Ag effects in complex natural media. For example, one recent study compared the effects of nano-Ag on bacteria and aquatic invertebrates in natural waters obtained from different locations in a river-estuarine system ([Gao et al., 2009](#)) (see below; see also Sections 6.2.1 and 6.2.2.2), and another study investigated the effect of nano-Ag on bacterial diversity in natural estuarine sediments ([Bradford et al., 2009](#)) (see Section 6.2.1). Most toxicity studies, however, have added nano-Ag to deionized water and other experimental media purely to establish the maximum toxic potential of the test material outside of natural systems.

Kvitek et al. (2008) demonstrated that unmodified nano-Ag in deionized water can remain well-dispersed, exhibiting “long-term³⁰ stability” in solution. As the pH of the system was lowered and the solution became acidic, however, Kvitek et al. (2008) observed that the nano-Ag particles slowly formed clusters, a condition that can influence particle uptake by aquatic organisms. Liu and Hurt (2010) also demonstrated that citrate-stabilized nano-Ag phase partitioning was highly dependent on pH, and that silver ion release rates increased at lower pH. They noted, however, that changes in pH affected ion release kinetics only in the presence of dissolved oxygen. Yet, because Kvitek et al. (2008) did not report the dissolved oxygen content of the solution in which the unmodified nano-Ag was reportedly stable, their data are of limited value in determining the effect of pH on nano-Ag properties that influence toxicity.

Nano-Ag forms clusters in media with high salt content, thereby diminishing its antibacterial activity (Gan et al., 2004). Because of the high ionic strength of sea water, particle association can occur rapidly when nano-Ag solutions are released to estuaries and coastal environments, thus preventing the large-scale dispersion of nano-Ag in the water column. Liu and Hurt (2010) offered a different perspective, however, arguing that the inhibition of oxidation (i.e., formation of silver ions on the surface of nanoparticles) is less dependent on salt content (i.e., ionic strength) and more dependent on the higher pH of sea water when compared to deionized water. They suggested that the clustering due to increases in ionic strength results in the formation of larger particle associations, but that the amount of available surface area with which oxygen can react is preserved. This implies that ionic strength has little effect on oxidation of nano-Ag in solution, and could have a correspondingly small effect on nano-Ag environmental effects if the formation of silver ions on the surface of the nanoparticle and subsequent release are the principal actions conferring nano-Ag toxicity.

Natural organic compounds in sea water can have surfactant and binding qualities that stabilize nano-Ag suspensions, thus making the particles more available for sorption to or uptake by specific aquatic organisms (Miao et al., 2009). Gao et al. (2009) found that increasing dissolved organic carbon (DOC) content generally decreased nano-Ag toxicity to both bacteria and *Ceriodaphnia dubia*. Other natural organic compounds, such as humic substances and carboxylic acids, also adsorb quickly onto nanoparticle surfaces and stabilize them in suspension by providing an electrostatically charged coating (Cumberland and Lead, 2009; Fabrega et al., 2009). The molecular composition of natural substances can influence toxicity. For example, Dasari et al. (2010) compared the relative toxicity of nano-Ag to natural aquatic bacterial assemblages in the presence of two types of humic acid (commercially available terrestrial humic acid vs. Suwannee River water). The study authors discovered that the type of humic

³⁰“Long-term” was not defined.

acid present in the nano-Ag exposures statistically significantly affected bacterial viability count. Also, whether samples were exposed to light influenced bacterial viability in the presence and absence of nano-Ag and both humic acid substances. These results suggest that overall, the presence of light increases the inhibition of bacterial growth and amplifies the toxicity of nano-Ag and humic acids, but that the degree of toxicity observed might differ by geographic location due to variability in the molecular composition of humic substances.

Gao et al. (2009) also experimentally examined the effects of natural surface-water characteristics on the dispersion, bioavailability, and toxicity of manufactured nanoparticles, including nano-Ag. Toxicity was examined in the freshwater invertebrate, *C. dubia*, and in bacteria using a 48-hour bioassay and METPLATE analysis, respectively. Characteristics of the materials used and toxicity test results are provided in Table 6-1.

The manufacturer reported the nominal diameter of the nano-Ag to be in the 20- to 30-nm range, although transmission electron microscopy revealed the average size of the nano-Ag in suspension to be approximately 80 nm in deionized water, as well as in one river-water sample, and more than 100 nm in two other river-water samples (Table 6-1) (Gao et al., 2009). The average size of nano-Ag suspended in the water sample taken from the river SR3 delta was in the μm range. Note that differences in total silver measured in solution indicate differences in sorption of some of the silver to inorganic ligands and DOC.

The bacterial bioassay, known to be sensitive to dissolved metal ions, indicated no toxicity at the two highest DOC concentrations (45.71 and 10.18 mg C/L). The nano-Ag solution prepared in deionized water was the most toxic to both the bacteria and *C. dubia*. Gleaning specific conclusions from these experiments, however, is challenging due to the co-variation among some water chemistry parameters.

Nano-Ag from spray disinfectants might end up in treated and untreated wastewaters; consequently, other constituents of wastewater might influence nano-Ag toxicity (see Sections 4.4.2. and 5.2.1.2). For example, wastewater often contains an abundance of organic and inorganic ligands with which nano-Ag and silver ions form strong complexes (Choi et al., 2009; Blaser et al., 2008). Information on how ligands might influence the bioavailability of nano-Ag, which in turn influences the effect of nano-Ag on organisms, is presented in Section 5.2.1.2. Choi et al. (2009) investigated the influence of ligands on the toxicity of nano-Ag to nitrifying bacteria and found that a range of ligands, including chloride, phosphate, $\text{H}_2\text{EDTA}^{2-}$, and sulfide, reduced toxicity to varying degrees, although

Table 6-1. Experimental parameters and toxicity of nano-Ag in deionized water and natural surface waters.

Water characteristics	Deionized water	River-water samples		
		Headwater (SR1)	Midsection (SR2)	Delta (SR3)
pH	Not reported	4.7	7.15	7.56
Alkalinity (mg CaCO ₃ /L)	~0 ^a	6	88	132
Ionic strength (mM)	~0 ^a	0.94	3.34	475
Dissolved organic carbon (mg C/L)	~0 ^a	45.71	10.18	2.3
Na ⁺ (mM)	~0 ^a	<1	<1	31.38
Ca ²⁺ (mM)	~0 ^a	<1	<1	6.61
Mg ²⁺ (mM)	~0 ^a	<1	<1	30.94
Ag _{Total} (µg/L)	~0 ^a	<10 ^b	<10 ^b	<10 ^b
Silver characteristics and toxicity assays				
Diameter nano-Ag (nm)	~80	~80	~300	>1000
Nominal Ag (mg/L)	1000	1000	1000	1000
Measured total Ag (mg/L) ^c	1.67	0.54	0.043	0.66
MetPLATE bacterial LC ₅₀ (µg/L)	47.79	No toxicity	No toxicity	112
<i>Ceriodaphnia dubia</i> 48-hr LC ₅₀ (µg/L)	0.46	6.18	0.77	0.70
95% Confidence limits (µg/L) probit analysis (for <i>C. dubia</i>)	0.45–0.47	5.5–6.7	0.75–0.80	0.66–0.73

^a Not measured, but assumed to be approximately 0

^b The detection limit for Ag is 10 µg/L

^c After mixing and filtering to remove particles larger than 1.6 µm

Source: Data extracted from Gao et al. (2009).

sulfide was the only ligand to reduce nano-Ag toxicity by more than 40%. At a 1-mg Ag/L concentration in deionized water, nano-Ag inhibited nitrification by 100%. After sulfide was added to achieve a final sulfide concentration of 10 micromoles per liter (µM), toxicity decreased by about 80%. Miao (2009) reported that adding thiols (–SH) to aqueous suspensions of nano-Ag increased the dispersion of nano-Ag several orders of magnitude beyond levels predicted for the natural environment. No toxicity was observed in the marine diatom *Thalassiosira weissflogii*, however, when it was exposed to nano-Ag in the presence of thiols. The investigators believed this lack of toxicity might have been due to the large size of the nano-Ag (60–70 nm), the protective layer of natural organic matter around the nano-Ag that prevented a direct interaction between nano-Ag and the algal cell, the concentrations of nano-Ag used, or a combination of these factors (Miao et al., 2009).

6.2. Ecological Effects

In its conventional form, silver can be toxic to fish, aquatic invertebrates, algae, some terrestrial plants, fungi, and bacteria (U.S. EPA, 1993). The ecological effects of conventional silver have been

studied extensively; although some data gaps remain, tests and environmental case studies have revealed that conventional silver can be toxic to biota at aqueous concentrations at or below 50 nanograms per liter (ng/L) ([Wijnhoven et al., 2009b](#)). Some of the organisms most sensitive to conventional silver are freshwater and marine phytoplankton, freshwater salmonids, and marine invertebrates in early life stages ([Luoma et al., 1995](#)). Although conventional silver can be extremely toxic to biota, concentrations of free silver ions are not expected to be high enough in most natural systems to adversely affect these organisms ([Luoma, 2008](#)). Nano-Ag, however, might present a higher risk to ecosystems because it could become more bioavailable under certain conditions and provide a reservoir of silver ions that could be delivered directly onto the surface of an organism or to cell constituents. Despite this possibility, relatively few studies have investigated the effects of nano-Ag on organisms other than bacteria and laboratory rodents. Moreover, such single-species tests likely do not capture the influence of nano-Ag on structural and functional complexities at the ecosystem level. In addition, studies have not explored the ecological effects from actual nano-Ag technologies at the product level, although manufacturers report that these products are available on the market.

Although in vitro studies dominate the literature investigating nano-Ag ecological toxicity, the prevalence of in vivo studies has increased in recent publications. Ecological effects studies predominantly investigate nano-Ag effects associated with acute exposure (generally 96 hours or less), and only a few studies examine nano-Ag effects over subchronic and chronic exposure periods. Studies of ecological effects indicate that exposure to nano-Ag could lead to adverse effects on higher level endpoints such as survival, growth, and reproduction, and on sublethal endpoints such as phenotypic changes, gene expression, and oxidative stress. Reported indirect effects of nano-Ag include pore clogging, solubilization of toxic compounds, and production of ROS ([Navarro et al., 2008a](#)).

Because the dose in all studies discussed in this section was given as either mass concentration or nanoparticle number in exposure media, these are the dose metrics provided here. Converting all concentration data to the same units was not possible due to a lack of information provided by many study authors on the factors used to define their units of measurement (e.g., for parts per million [ppm], whether this unit is based on ppm by mass, number, or another metric is not always stated). Nominal nano-Ag concentrations in the studies were based on total silver, silver ions, free silver, or added nano-Ag content. This information is provided in the tables in Appendix B that summarize the ecological effects studies; measured concentrations are also presented when provided in the studies. The studies are presented in Appendix B in alphabetical order by author for each of the ecological effects sections; the reader is referred to this appendix for study details not presented in this chapter. The following sections present the available data on the effects of nano-Ag on non-algal microorganisms (Section 6.2.1), aquatic organisms (algae in Section 6.2.2.1, invertebrates in 6.2.2.2, and vertebrates in 6.2.2.3), and

nonmammalian terrestrial organisms (plants in 6.2.3.1, invertebrates in 6.2.3.2, and vertebrates in 6.2.3.3). For each group of organisms, the discussion is organized into three parts: known effects of conventional silver exposure, effects of nano-Ag exposure, and nano-Ag mode of action.³¹ This organization is intended to capture the potential effects of nano-Ag, silver ions released from the silver nanoparticles, and common silver complexes.

6.2.1. Microorganisms (Excluding Algae)

The effects of silver ions on microbial communities are well-documented, and nano-Ag could have similar effects. That the proposed use of nano-Ag in this case study is for disinfectant sprays implies that a certain level of antimicrobial efficacy is expected and desired at the application site. Once the spray is used, however, nano-Ag is expected to enter the environment, as discussed in Chapter 2, where effects might occur in natural microbial communities. Such communities are key to nutrient decay and recycling processes that support overall ecosystem functioning ([Navarro et al., 2008b](#)); nano-Ag spray use therefore could result in unintended antimicrobial effects potentially leading to ecosystem cascade effects. In addition, nano-Ag might disrupt beneficial gut microflora found within the digestive systems of higher level organisms ([Sawosz et al., 2007](#)). The antimicrobial activity of nano-Ag has been demonstrated in laboratory tests with isolated prokaryotic species, including *E. coli* ([Hwang et al., 2008](#); [Pal et al., 2007](#); [Morones et al., 2005](#); [Sondi and Salopek-Sondi, 2004](#)), *Pseudomonas aeruginosa* ([Morones et al., 2005](#)), *Vibrio cholerae* ([Morones et al., 2005](#)), *Bacillus subtilis* ([Yoon et al., 2007](#)), and nitrifying cultures ([Choi et al., 2009](#); [Choi et al., 2008](#); [Choi and Hu, 2008](#)) and in eukaryotic species, including *Saccharomyces cerevisiae* ([Saulou et al., 2010](#)). The results from these studies demonstrate that the range of microorganisms potentially susceptible to nano-Ag toxicity spans gram-positive, gram-negative, prokaryotic, eukaryotic, autotrophic, heterotrophic, mesophilic, and halophilic species. Studies specific to nano-Ag effects on microbes, however, remain limited in number and scope compared to those investigating effects of exposure to other forms of silver. Furthermore, only a handful of studies to date have attempted to determine nano-Ag bacterial toxicity in more complex natural media ([Liang et al.,](#)

³¹Mode of action is defined in the U.S. EPA Cancer Guidelines as “a sequence of key events and processes, starting with interaction of an agent with a cell, proceeding through operational and anatomical changes and resulting in cancer formation” ([U.S. EPA, 2005](#)). Multiple definitions for mode of action exist within the regulatory context. For the purposes of this document, mode of action refers to the key steps in the toxic response at the target site that are responsible for the physiological outcome or pathology of the chemical. Because mode of action is inherently linked to effects, completely separating the discussion of mode of action from the discussion of adverse effects (e.g., physical disruption of cell membrane is both an effect and mode of action for lethality) is sometimes not possible. Where possible in this chapter, mode of action is discussed in a section following effects to highlight the processes that might be responsible for the observed adverse effects (e.g., reduced reproductive success, increased mortality).

[2010](#); [Park et al., 2010b](#); [Bradford et al., 2009](#); [Gao et al., 2009](#)), and even these studies were limited in scope and not necessarily representative of nano-Ag behavior in highly complex ecosystems. As a result, the available studies provide limited insight into potential impacts from intentional and unintentional releases of nano-Ag into the environment.

Known Effects of Conventional Silver Exposure on Microorganisms

Silver is a relatively toxic substance for microbes; for example, when compared to 12 other metals, silver was identified as the most toxic to microbial soil communities ([Cornfield, 1977](#)). Silver can inhibit microbial growth, affecting sensitive communities such as ammonifying, nitrogen-fixing, and chemolithotrophic³² bacteria ([Albright and Wilson, 1974](#)). The bacterial plasma and cytoplasmic membrane are important target sites because silver ions cause the release of ionic potassium (K⁺) from bacteria ([Jung et al., 2008](#)). Silver exposure also reduces DNA transcription in bacteria, which results in a delay or complete inhibition of microbial growth. Other evidence suggests that silver exposure to bacteria and fungi leads to changes in membrane structure and deposition of silver throughout the cell via formation of electron-dense granules (by combination of silver with cell constituents) ([Saulou et al., 2010](#); [Feng et al., 2000](#)). The antimicrobial mode of action of conventional silver is only partially understood, but is believed to be the result of contact of the silver compounds with microbial cell walls, followed by release of silver ions that combine with –SH groups of enzymes, ultimately leading to the deactivation of microbial proteins ([Yoon et al., 2007](#); [Morones et al., 2005](#)).

Effects Specific to Nano-Ag Exposure on Microorganisms

Examples of recent studies investigating the effects of nano-Ag on microorganisms are presented in detail in Section B.2 of Appendix B. These studies illustrate that exposure of microorganisms to nano-Ag frequently results in growth inhibition, inhibition of nitrifying enzymatic processes, arrest in fungal cell cycles, cell membrane damage (e.g., pitting, perforation), cell membrane process disruption, and ROS generation.

In experimental conditions, the bacterial cell density and nano-Ag concentrations are generally high, and contact between nanoparticles and bacteria is generally ensured. In natural systems, significantly more reactive surfaces are available with which both the nanoparticle and bacteria can interact, and concentrations of both might be much lower than in experimental settings, which might result in relatively rare contact between nanoparticles and bacteria ([Neal, 2008](#)).

³²Chemolithotrophic bacteria are those that derive energy from the oxidation of inorganic materials.

Sensitivity to nano-Ag varies among phyla, among species, and even among studies using the same species. Shrivastava et al. (2007) reported that gram-negative bacteria were more sensitive to nano-Ag than gram-positive bacteria. For the gram-negative species *E. coli* and *Salmonella typhi* (drug-resistant strains), 100% inhibition of growth was observed at a nano-Ag concentration of 25 µg/mL, while no growth inhibition was noted in the gram-positive species *Staphylococcus aureus* at the same concentration. Even at 100 µg/mL, the growth of *S. aureus* was only partially inhibited (Shrivastava et al., 2007). Kvittek et al. (2008) also reported that *E. coli* was more sensitive to exposure to unmodified silver nanoparticles than *S. aureus*, but further comparisons of six gram-positive bacterial strains to four gram-negative strains indicated that other factors beyond gram-status influence sensitivity. The difference in minimum inhibitory concentrations (MICs) appeared to be species-specific, rather than gram-status-specific, as both the gram-positive and gram-negative bacteria displayed the same range of MICs (1.69–6.75 µg/mL). In a comparison between mesophilic (i.e., thriving in moderate temperatures) and halophilic (i.e., thriving in high-salinity environments) bacteria, Sinha et al. (2011) reported that 2 millimoles per liter (mM) nano-Ag was more toxic to the marine, gram-negative, halophilic *Marinobacter* species than to all other bacteria species tested. Nano-Ag had no effect on the growth of the other halophile EMB4, which is a gram-positive strain. *Marinobacter* has a thinner protective peptidoglycan layer around the cell and contains a higher percentage of negatively charged cardiolipins than gram-positive halophiles and gram-positive and gram-negative mesophiles. These results indicate that some bacteria in marine ecosystems could be particularly susceptible to nano-Ag exposures, while others might remain unaffected.

Another area of concern resulting from increases in nano-Ag released to the environment is the potential effect of nano-Ag and associated compounds on bacteria used in wastewater treatment processes or located in areas where wastewater effluent is discharged (Bradford et al., 2009; Choi et al., 2008). Although many different types of bacteria can be used at different stages of the wastewater treatment process, nitrifying bacterial communities³³ are considered especially vulnerable due to their slow growth rate and history of sensitivity to other environmental pollutants (Choi et al., 2009; Choi et al., 2008; Choi and Hu, 2008). Furthermore, nitrifying bacteria are critical to processes involving nutrient removal in wastewater treatment (Neal, 2008). If nitrifying bacterial concentrations were significantly reduced or eliminated in wastewater treatment bioreactors, chemical nutrients (e.g., ammonia) in the wastewater would not be removed, which might ultimately result in eutrophication in areas where the wastewater is

³³Nitrifying bacterial communities can include a mixture of species responsible for oxidizing ammonia to nitrite or from nitrite to nitrate, including bacteria in the *Nitrospira*, *Nitrosococcus*, *Nitrobacter*, *Nitrospina*, and *Nitrosomonas* genera. The exact composition of nitrifying communities is often not characterized in experimental studies.

discharged ([Grady et al., 1999](#)). Eutrophication can cause anoxia and other reductions in water quality, leading to adverse effects on aquatic biota.

Nitrifying bacteria are sensitive to nano-Ag exposure, but seemingly less so than *E. coli*. Nitrification occurs in nitrifying bacterial communities by a two-step process involving three specific enzymes. Of these three critical enzymes, the enzyme partially responsible for the oxidation of ammonia, ammonia monooxygenase (AMO), appears to be the most sensitive to nano-Ag exposure. A concentration of 1 mg/L nano-Ag inhibited nitrification (measured as change in AMO-related oxygen uptake rates) by 100% in a respirometric assay, while silver ions inhibited growth by 83% at this concentration ([Choi et al., 2009](#)). Choi and Hu ([2008](#)) determined that nano-Ag inhibited the growth of nitrifying cultures ($EC_{50} = 0.14$ mg/L) more than silver chloride (AgCl) colloids and silver ions (as AgNO₃). They also found that intracellular ROS concentrations increased significantly compared to the controls when bacteria were exposed to nano-Ag, and that this increase correlated strongly with growth inhibition ($R^2 = 0.86$). Choi et al. ([2008](#)) demonstrated that at 1 mg Ag/L in nitrifying suspension, nano-Ag, silver ions, and AgCl colloids inhibited respiration by approximately 86%, 42%, and 46%, respectively.

Bradford et al. ([2009](#)) examined the effects of nano-Ag concentrations of up to 1 mg/L on bacterial abundance and diversity in an estuarine microcosm study. The investigators reported that the lowest concentration used in this study (0.25 mg/L) was an order of magnitude higher than the concentration expected from the highest estimated release of engineered nanoparticles from nano-enabled products, as estimated by Boxall et al. ([2007](#)). After applying 1/20th of the total nano-Ag dose to 20 liters (L) of estuarine water over ~3.8 kilograms (kg) of estuarine sediment for 20 days (followed by a 10-day period with no dosing), Bradford et al. determined that nano-Ag exposure at a total concentration of 1 mg/L did not affect bacterial abundance and had a small statistically significant effect on bacterial diversity on the sediment surface at the highest concentration tested (1 mg/L) when compared to controls. The authors argued, however, that this difference was likely due to chance (based on a similarity profile permutation procedure) arising from the presence of other sediment-dwelling organisms in these samples with their own associated bacterial communities that differ from those at the sediment surface. To assess bacterial diversity, the investigators used a nested polymerase chain reaction-denaturing gradient gel electrophoresis method to amplify the 16S ribosomal RNA fragment in the bacteria species. They reported that the DNA primers they used were specific to “*Bacteria*,” but which species they included in this classification is unclear. Nevertheless, multiple studies have used similar methods to establish nitrifying community structures in wastewater treatment processes and to establish bacterial diversity in communities not associated with the nitrification process ([Mills et al., 2008](#); [Muhling et al., 2008](#)), so nitrifying species among others likely were included in this analysis. Because nitrifying bacteria generally will be found in areas where wastewater is discharged into the environment due to higher concentrations

of ammonia in these locations, and because the samples were taken from an area that received discharges of wastewater effluent, such bacteria likely also were present in the sediment cores. Without reporting which species comprised the clusters in the estuarine sediment, Bradford et al. (2009) argued that impacts on bacteria in estuarine sediment likely will be negligible at nano-Ag concentrations expected from estimated future releases (<1 mg/L). The investigators also reported, however, that the transformation of nano-Ag into other forms of silver (e.g., Ag^+ , AgCl , AgCl_2^- , AgCl_3^{2-}) within the experimental tanks was not studied, but such transformations would be expected to influence the potential impacts of nano-Ag in estuarine waters (Bradford et al., 2009).

As discussed in Chapter 5, Kim et al. (2010a) determined that activated sewage sludge from wastewater treatment plants not located near major industrial sources of silver or photochemical processors could contain high concentrations of silver in the form of nano-sized silver sulfides. Although silver sulfide is relatively insoluble in water, some evidence from studies with other nanomaterials indicates that nano-sized sulfide complexes might dissolve more readily than their conventional counterparts (Liu et al., 2009). As a result, some studies have begun to examine the effects of nano-Ag on bacteria in sewage, activated sewage sludge, and in sediments (Gao et al., 2011; Khan et al., 2011; Liang et al., 2010). In a study using a Modified Ludzack-Ettinger (MLE) activated sludge treatment system, Liang et al. (2010) determined that most of the nano-Ag in the reactor strongly adsorbed to activated sludge. The investigators first compared the effect of nano-Ag to that of silver ions on activated sludge and then investigated the effects of a shock load of nano-Ag on bacterial activities and community structure in the MLE reactor. In the first part of the experiment, sludge was spiked with 1 mg Ag/L of either PVA-capped nano-Ag (average size 21 nm) or ionic silver, and nitrification inhibition was assessed (measured as specific oxygen uptake rates) using short-term batch extant respirometry. They found that nano-Ag and ionic silver inhibited nitrification in the sludge samples by about 41.4% and 13.5%, respectively. In a study examining the effects of 0.5 mg/L nano-Ag (average size 66 nm) on denitrification (i.e., reduction of nitrate) in river sediments, Gao et al. (2011) reported no significant inhibition of nitrate-reducing processes, but they did report that acetate degradation, another indicator of nitrogen-cycling bacterial response, was reduced two-fold when compared to the controls. The authors suggested that because of the lack of statistically significant inhibition of nitrate reduction at 0.5 mg/L nano-Ag (the IC_{50} ³⁴ for *Pseudokirchneriella subcapitata*, a sensitive model aquatic organism), denitrifying bacteria are less sensitive to nano-Ag than some other aquatic organisms; the effect on acetate degradation, however,

³⁴Inhibitory concentration is the chemical concentration at which a given percentage (in this case, 50%) of the exposed organisms demonstrate a response in a chosen endpoint; this effect level is commonly used to estimate the toxicity of a substance to a specific group of organisms.

implies that exposure to nano-Ag at higher concentrations could result in an adverse effect on the broader nitrogen-cycling process ([Gao et al., 2011](#)).

In the second part of the experiment conducted by Liang et al. ([2010](#)), the PVA-capped nano-Ag was fed into the MLE reactor at a continuous rate for 12 hours, achieving a peak silver concentration of 0.75 mg/L. Autotrophic growth was significantly inhibited, with maximum inhibition (46.5%) occurring 14 days after completion of the shock-load administration. A shift in the community structure of the bacteria also was observed after the shock loading. The dominant ammonia-oxidizing genus *Nitrosomonas* and one of the dominant nitrite-oxidizing genera *Nitrospira* were significantly reduced while another dominant nitrite oxidizing genus, *Nitrobacter*, was completely eliminated from the system following the nano-Ag shock load. These results suggest that short-term respirometric assays (like the first part of the experiment) might underestimate the toxicity of nano-Ag to nitrifying bacteria in continuous flow systems because short-term assays do not account for longer term kinetics of metal internalization and effects due to continuous exposures. The authors note, however, that inhibition observed in this study was nearly half that observed in the study by Choi et al. ([2008](#)), which used the same experimental method, but on enriched nitrifying cultures instead of on activated sludge. Liang et al. ([2010](#)) hypothesized that the reduction in toxicity in the activated sludge could be due to the presence of exopolymeric substances (EPS) secreted by the bacteria that act as biological barriers between bacterial cells and silver nanoparticles.

Little information is available on the effects of nano-Ag on fungi compared with bacteria. In a study comparing the antimicrobial efficacy of different nanomaterials in combination with their effect on mammalian cell viability, Martinez-Gutierrez et al. ([2010](#)) reported that nano-Ag MICs for three species of fungi ranged from 3 to 25 µg/mL. The range of MICs for the 10 species of bacteria exposed to nano-Ag in the same experiment was 0.4–1.7 µg/mL, suggesting that, overall, fungi might be less sensitive to nano-Ag than bacteria.

Based on a study of the model fungus *Candida albicans*, Kim et al. ([2009](#)) observed that exposure to nano-Ag resulted in a loss of membrane potential and an increase of pitting on the cell surface, which was tentatively linked to the formation of large pores through the cell walls and membranes and subsequent cell death. The MIC of nano-Ag for this species was 2 µg/mL. Exposure to 40 µg/mL nano-Ag also resulted in the arrest of the fungal cell cycle, most likely by inhibiting some of the cellular processes necessary for bud growth. This fungus, however, is commensal with humans and not commonly found in the “external” environment. Saulou et al. ([2010](#)) examined nano-Ag effects on cell composition and ultrastructure of *S. cerevisiae*, a yeast that can be found outside of humans. The investigators reported damage to the cell membrane similar to that reported for *C. albicans* by Kim et al. ([2009](#)) and further reported changes to intracellular proteins. Adhesion of fungal cells to silver nanoparticles embedded in an

organosilicon matrix for 24 hours resulted in a 1.4-log reduction of viable cell counts compared to the control. Saulou et al. ([2010](#)) attributed this antifungal activity to a multifactorial nano-Ag mode of action whereby the nanoparticle both disrupts the cell membrane processes and causes changes in the intracellular structures.

Hypothesized Nano-Ag Mode(s) of Action in Microorganisms

Silver ions released from silver nanoparticles are often purported to be the primary source of toxicity from exposure to nano-Ag, particularly for higher level organisms. Several studies have investigated whether the nanoparticles inherently exacerbate the toxic effects or cause them outright. The full sequence of events that causes silver nanoparticles to be toxic to bacteria and fungi is still largely unknown or unconfirmed, although several recent studies have attempted to elucidate such mode(s) of action ([Kim et al., 2009](#); [Choi and Hu, 2008](#); [Hwang et al., 2008](#); [Lok et al., 2006](#); [Morones et al., 2005](#)).

Several possible modes of action are discussed in the literature concerning nano-Ag effects on microorganisms. These are (1) membrane disruption through direct attachment of the nanoparticle to the bacterial membrane, (2) cellular invasion and enzyme disruption by nanoparticles, (3) changes in cell membrane permeability, (4) interference with cellular S-containing compounds, and (5) intracellular ROS accumulation ([Kim et al., 2009](#); [Hwang et al., 2008](#); [Pal et al., 2007](#); [Lok et al., 2006](#); [Panáček et al., 2006](#); [Morones et al., 2005](#); [Sondi and Salopek-Sondi, 2004](#)). That several of these events might act together to result in cell death is probable, but the specific processes and interactions required for toxicity have not been fully confirmed.

Choi and Hu ([2008](#)) present one example of how potential modes of action can work in tandem in a study assessing the effects of nano-Ag on autotrophic bacteria. Although apoptosis occurred and silver nanoparticles adsorbed to the surface of the microbial cell walls, cell membrane leakage was not evident. The investigators believed that cell death occurred partially as a result of intracellular ROS generation by the silver ions released at the membrane surface, although this was not proven directly. Silver ions delivered at the membrane surface have been shown to damage DNA and to induce apoptosis without causing visible damage to the outer bacterial wall or cytoplasmic membrane ([Inoue et al., 2002](#)). The toxic effects cannot be explained completely by ROS generation, however, because silver ions did not induce the same level of toxicity at similar intracellular ROS concentrations and total silver mass concentrations ([Choi and Hu, 2008](#)). Thus, the higher degree of toxicity exhibited by nano-Ag might also have resulted from the presence of particles smaller than 5 nm that were able to cross the cell membrane and interact directly with cell constituents, releasing silver ions directly to sensitive areas. Choi and Hu ([2008](#)) also postulated that nano-Ag in the cell likely disrupted enzyme function, ultimately causing cell death.

As discussed in Section 6.1.1.1, the driving factor in the nano-Ag mode of action might be either silver ions or nano-Ag particle interactions with the cell wall, depending on the size fraction of the nano-Ag material in the suspension. But overall, several studies have now suggested that nano-Ag and silver ions together are more toxic than either silver species alone ([Bae et al., 2010](#); [Sotiriou and Pratsinis, 2010](#)), and inconsistencies in the literature on this point are likely the result of uncharacterized clustering states, the presence of residual silver ions left over from particle synthesis, and unquantified characteristics of the exposure medium ([El Badawy et al., 2011](#); [Bae et al., 2010](#); [Sotiriou and Pratsinis, 2010](#)).

Many studies suggest that heightened antibacterial activity of nano-Ag (compared to conventional silver or silver ions alone) is related to a physical disruption of membrane function and cellular processes, most likely due to the direct contact of the nanoparticle with the cell membrane. El Badawy et al. ([2011](#)) reported this physical interaction as the “limiting step” in the nano-Ag mode of action; until the silver nanoparticle can overcome the electrostatic barrier surrounding the bacterial outer membrane or peptidoglycan layer, the nanoparticle is not free to interact with, disrupt, and damage the cellular membrane, and therefore cannot release ionic silver directly to the biological surface or within the cell itself. Because surface charge of nano-Ag largely depends on the coating (both chemical or biological), nano-Ag can be negatively or positively charged, as demonstrated by El Badawy et al. ([2011](#)) and discussed in Section 6.1.1.3. When nano-Ag is negatively charged, it naturally repels negatively charged bacteria, thus establishing an electrostatic barrier. Jin et al. ([2010](#)) proposed that this barrier can be overcome, however, by ion bridges formed by cations present in environmental media. In their study, Jin et al. ([2010](#)) reported that toxicity to gram-negative bacteria increased in the presence of divalent cations such as Mg^{2+} (ionic magnesium) and Ca^{2+} (ionic calcium), which are thought to form a bridge between negatively charged silver nanoparticles and the lipid polysaccharide layer surrounding the bacterial cell wall. Such bridges can change cell permeability and facilitate transport of silver nanoparticles across the outer cell membrane and the peptidoglycan layer of gram-negative species, ultimately leading to membrane disruption or damage.

Several studies have reported the presence of pits or perforations on microbial surfaces, and Sondi and Salopek-Sondi ([2004](#)) confirmed by energy dispersive X-ray analysis that nano-Ag was incorporated into *E. coli* cell membranes. This effect also has been reported in the fungus *C. albicans*, where exposure to nano-Ag resulted in pitting of the cell wall and a breakdown of the cell membrane permeability barrier. The authors postulated that the membrane effects occurred through physical perturbation of the lipid bilayers on the outer membrane, which causes ion leakage, pore formation, and dissipation in the electrical membrane potential. The destruction of the membrane integrity also could have inhibited normal fungal budding processes ([Kim et al., 2009](#)). Saulou et al. ([2010](#)) took the analysis one step farther

in their investigation of structural changes to both the cell wall and the intracellular proteins of *S. cerevisiae*. They observed electron-dense granules that were considered likely to be silver based on transmission electron microscopy images; these granules were distributed along the cell wall and inside the cell. They also observed disordered secondary structures of proteins, which could lead to deactivation of enzymes critical to fungal metabolic processes (e.g., cell antioxidant defense mechanisms).

In a proteomic³⁵ analysis, Lok et al. (2006) demonstrated that certain envelope protein expressions in *E. coli* were significantly altered after exposure to 0.4- and 0.8-nanomole per liter (nM) bovine serum albumin-stabilized nano-Ag. This observation suggests that the ATP-dependent preprotein translocase, which is associated with the inner membrane, had ceased to function. In a typical cell, mature proteins are translocated to the outer membrane, but if that process is inhibited, protein precursors simply build up in the cytoplasm. This study also indicated that *E. coli* exposed to nano-Ag experience a decrease in proton motive force, which was observed in the near complete loss of intracellular K⁺. Nano-Ag also decreased cellular ATP levels, which might also have contributed to cell death (Lok et al., 2006).

To demonstrate the effect of membrane disruption on cell invasion, certain antibiotics have been used to increase permeability and porosity in bacterial membranes, which allows the ingress of silver nanoparticles as large as 80 nm (Kyriacou et al., 2004; Xu et al., 2004). Although many investigators have observed through optical microscopy that nanoparticles can accumulate in the cytoplasm of bacterial cells, very little information is available to explain the process by which cell invasion occurs. For example, Pal et al. (2007) noted that the cell walls of bacteria treated with nano-Ag were significantly damaged (the type of damage was not specified). They also determined that nanoparticles had accumulated in the cell walls and membrane and inside the cells, but did not report the mode by which the nanoparticles were transported into these areas. Lok et al. (2006) observed silver nanoparticles attached to the surface of *E. coli* cells and within the cells, but again the mode of transport was not reported. They did, however, observe perforation of the cell walls. Neal (2008) hypothesized that nano-Ag, like other metals, might lead to the release of lipopolysaccharide proteins from gram-negative bacteria, causing the formation of pits in the outer membrane. This morphology change increases permeability and leads to uncontrolled transport through the plasma membrane, finally resulting in overall cell malfunction and death.

Bacterial membranes exposed to nano-Ag might be compromised as a result of lipid peroxidation by ROS, which form as natural by-products of aerobic metabolism but can increase considerably under conditions of stress (Choi and Hu, 2008). Some support for ROS-mediated adverse cellular effects comes from a study using stress-specific bioluminescent *E. coli* (Hwang et al., 2008). The bioluminescent

³⁵A proteomic analysis evaluates the structure, function, interactions, and control of proteins.

response of the bacteria indicated that superoxide radicals, which are a type of ROS, were generated in response to nano-Ag exposure, and that protein and membrane damage also occurred, most markedly at a concentration of 0.4 mg Ag/L. At a concentration of 0.5 mg/L, the reduction in the growth rate of the *E. coli* strains was statistically significant. Silver nanoparticles also have been observed to embed in nitrifying cell flocs when added to nitrifying cultures, resulting in toxicity to the membrane-bound AMO enzyme (Choi et al., 2009). Choi et al. (2009) speculated that toxicity occurred as the result of small (<5 nm) silver nanoparticles entering the cell, where they generated ROS or interfered with cellular S-containing compounds in the respiratory path. Section 5.2.2 discusses the findings of various studies on membrane disruption and permeability in gram-negative bacteria, suggesting various ways that nano-Ag could enter bacterial cells.

6.2.2. Aquatic Organisms

Due to the range of products into which nano-Ag is thought to be incorporated and the fact that wastewater could be one of the most significant release pathways (see Chapter 3), the aquatic environment might act as a substantial reservoir for nano-Ag and ionic silver discharged from silver nanotechnologies or silver complexes formed as a result of those discharges.

Ionic silver is the only form of silver that has been broadly tested on aquatic organisms. From these tests, ionic silver was deemed the second most toxic metal to aquatic organisms, after mercury (Luoma, 2008). Silver ions in the aquatic environment occur only at very low doses, however, suggesting that under natural conditions, contact between silver ions and aquatic organisms might be relatively rare (Blaser et al., 2008). On the other hand, several studies report that nano-Ag functionalized to remain stable in suspension might pose a significant risk to aquatic species if the nanoparticles are in this state in the aquatic environment (Kvitek et al., 2009; Asharani et al., 2008; Lee et al., 2007).

Of the available data on nano-Ag effects, most concentrate on effects in either aquatic organisms or bacteria. Kahru and Dubourguier (2010) compared nano-Ag with six other types of engineered nanomaterials in a toxicity-grid exercise and determined that nano-Ag was one of the two most toxic to aquatic organisms. This assessment was based on an LC₅₀ of less than 1 mg/L for *D. magna* that was deemed “extremely toxic” relative to all but one of the other nanomaterials tested. Despite evidence suggesting that lower order aquatic organisms like *Daphnia* can be highly sensitive to nano-Ag exposure, most of the research conducted on nano-Ag effects on aquatic organisms has focused on fish, with very little attention paid to nano-Ag effects on aquatic plants and invertebrates (Griffitt et al., 2008; Luoma, 2008). At this point, the comparative toxicity of silver nanoparticles and conventional silver to aquatic organisms is unclear, with studies reporting both enhanced toxicity of nano-Ag to aquatic organisms

([Chae et al., 2009](#)) and lower toxicity relative to silver ions ([Miao et al., 2009](#); [Griffitt et al., 2008](#)).

Because nano-Ag sheds silver ions, the distinction between nano-Ag toxicity and silver ion toxicity is not always clear, so some studies have focused explicitly on investigating the effects due to exposure to silver ions from AgNO₃ in comparison to silver ion effects as mediated by the silver nanoparticle ([Navarro et al., 2008a](#); [Navarro et al., 2008b](#)).

The silver nanoparticles and silver ions released from nano-Ag are also likely to form complexes with ligands and other materials in the aquatic environment, as discussed in Chapter 4. Silver complexes will be most common in the particulate form, both suspended in the water column and deposited to the sediment; however, no studies have been conducted investigating the effects of silver in the particulate fraction or for silver thiolates in benthic organisms ([Blaser et al., 2008](#)).

6.2.2.1. Algae

Most studies examining the effects of nano-Ag on biota have focused on bacteria and higher level organisms, with only a few focused on plants. Even fewer studies are available for marine plants, with the focus for most aquatic plants centering on freshwater species. At present, algae are the only aquatic plants for which nano-Ag effects have been investigated.

Algae are primary producers, acting as the food base in aquatic ecosystems, and algae in the oceans provide much of Earth's oxygen. In addition to being an ecologically important group of organisms, algae can sometimes act as indicators of aquatic ecosystem change. As such, algal toxicity tests are integral to the investigation of potential effects on the aquatic environment resulting from the release of nano-Ag.

Known Effects of Conventional Silver Exposure on Algae

Silver ions are highly algicidal, and various silver compounds (e.g., AgNO₃, sodium-silver thiosulfate [NaAgS₂O₂], silver sulfate [AgSO₄]) can cause toxic effects in both freshwater and marine algae ([Ratte, 1999](#)). Exposure to silver has been shown to reduce freshwater growth rates in *Chlamydomonas eugametos*, *Chlorella vulgaris*, *Haematococcus capensis*, and *Scenedesmus accuminata* at concentrations of 0.01 mg/L or less ([Hutchinson and Stokes, 1975](#)). Conversely, chronic exposure to silver (up to 0.05 mg/L) promoted algal growth in *Selenastrum capricornutum*, but higher silver concentrations (up to 0.1 mg/L) inhibited growth ([Schmittschmitt et al., 1996](#)).

Effects Specific to Nano-Ag Exposure on Algae

Examples of recent studies investigating the effects of nano-Ag on algae are presented in detail in Section B.3 of Appendix B. Effects on algae are measured at the population level, for example, in terms

of population growth. Effects on both freshwater and marine algal species have been investigated, as described below.

In a comparative study by Griffitt et al. (2008), the freshwater green alga *Pseudokirchneriella subcapitata* was reported to be more sensitive to nano-Ag (96-hour $EC_{50} = 0.19$ mg/L) than fish (48-hour $EC_{50} = 7.07$ and 7.2 mg/L for adult and juvenile zebrafish [*Danio rerio*], respectively). *P. subcapitata* was slightly less sensitive than the aquatic invertebrates that were tested (48-hour $EC_{50} = 0.040$ and 0.067 mg/L for *Daphnia pulex* adults and *C. dubia* neonates, respectively).

Exposure to nano-Ag resulted in significant inhibition of growth, chlorophyll *a* production, and photosystem II quantum yield in the marine diatom *Thalassiosira weissflogii* (Miao et al., 2009). The investigators used photosynthetic yield as a toxicity endpoint because of the importance of this process to aquatic ecosystems. To eliminate the possibility that the direct effect of nano-Ag was being masked by indirect effects from much higher concentrations of free silver ions in the immediate vicinity of the nanoparticles, Miao et al. (2009) removed the silver ions from solution either by filtration or complexation with thiols. No significant toxicity to the diatom was observed following silver ion removal. The authors tentatively concluded that toxicity was mainly due to the release of silver ions, rather than from the direct interaction of nanoparticles with the diatom. The authors then challenged this conclusion, however, by pointing out that the silver nanoparticles used might not have been appropriate for eliciting toxic effects because of their large size (60–70 nm), the wide range of concentrations used, or the presence of organic compounds in the sea water that complexed with the nanoparticles and made them less bioavailable. These caveats suggest that further research using different-sized particles and experimental conditions could be useful to understanding toxic effects of nano-Ag on *T. weissflogii* and other diatoms.

In a separate study, photosynthetic yield of the freshwater green alga *Chlamydomonas reinhardtii* also was reduced after exposure to nano-Ag (5-hour $EC_{50} = 829$ nM [based on total Ag] or 8 nM [based on free silver ions at the beginning of the experiment]) (Navarro et al., 2008b). The EC_{50} values for silver ions determined in this study were 2–13 times higher than those shown in other studies to inhibit growth in several algal species, including *C. reinhardtii*. The exposure duration for this study was only 5 hours, however, while most algal toxicity studies evaluate effects after exposure durations of 1 or more days. Navarro et al. (2008b) argued, however, that algal toxicity cannot necessarily be attributed to the concentration of silver ions in original suspensions. They observed that nano-Ag was more toxic than $AgNO_3$ to *C. reinhardtii* based on free silver ion content at the beginning of the experiment. In other words, the lower free silver ion concentrations measured in the nano-Ag test waters compared with the free silver ion concentrations measured in $AgNO_3$ solutions could not account for the higher toxicity observed in the nano-Ag test vessels. Silver nanoparticles appear to continue to release silver ions over

time, whereas silver ions from AgNO₃, which is highly soluble, are released quickly. Thus, the investigators speculated that the heightened toxicity of silver nanoparticles to algae compared with soluble silver compounds was due in part to the nanoparticles' ability to act as prolonged sources of silver ion delivery. Because the release and uptake of silver ions could depend on interaction between the nanoparticle and the algal cell, assimilation of silver ions into the cell from nano-Ag might be more efficient ([Navarro et al., 2008b](#)). Whether silver ions form at the algal surface or in the water following interaction of the nanoparticle with secreted algal products, however, is unclear.

The sensitivity of blue-green algae (i.e., cyanobacteria) in comparison to freshwater green algae has also been investigated in both a laboratory microcosm experiment and a field enclosure experiment in the same study ([Park et al., 2010b](#)). The microcosm experiment was conducted in a lab under controlled conditions using eutrophic lake water. In this experiment, the blue-green alga *Microcystis aeruginosa* UTEX 2388 and the green algal species *Ankistrodesmus convolutes* and *Scenedesmus quadricauda* were exposed to 1 mg/L of two different types of nano-Ag formulations. The first formulation (nano-Ag F1) was prepared using reduction of AgNO₃ by tannic acid to create nano-Ag ranging in size from 10 to 50 nm, and the other formulation (nano-Ag F2) was prepared by adding AgNO₃ to sodium persulfate and Tween 20, which resulted in a suspension containing silver oxide (Ag₂O) nanoparticles ranging in size from 20 to 50 nm. The field enclosure experiment was conducted with the same materials, but in a portion of a eutrophic lake, where the enclosures were left open at the top, resulting in temporal changes in sunlight and precipitation. Exposure of *M. aeruginosa* to nano-Ag F1 and F2 after 10 days resulted in growth inhibition of 93 and 95%, respectively, in the microcosm experiment and 55 and 64%, respectively, in the field enclosure experiments. Comparatively little or no inhibitory effect was exhibited by the freshwater green algal species at this concentration in either experiment.

In addition to the effects observed in the toxicity studies, due to the propensity of nano-Ag to form clusters and complexes, some speculate that high nano-Ag exposures might lead to increased cell density, shading, and clogging that produce adverse effects that cannot be attributed to the toxicity of the silver nanoparticles ([Navarro et al., 2008a](#)). Although this result has not been confirmed for nano-Ag, nanoscale titanium dioxide was shown to adsorb to algal cell surfaces and increase cellular weight by more than two-fold (exposure concentration not specified) ([Huang et al., 2005](#)).

Hypothesized Nano-Ag Mode(s) of Action in Algae

Only one study has specifically explored the nano-Ag mode of action in algae. Depending on whether observed effects are the result of direct nanoparticle effects or indirect effects resulting from the release of silver ions from the nanoparticle on the surface of the algae, the mode of action might differ.

In the study by Miao et al. (2009) investigating the effect of nano-Ag on growth and photosynthetic yield in the marine diatom *T. weissflogii* under different nutrient conditions, investigators distinguished between the direct effects of the silver nanoparticle and the indirect effects of released silver ions, and proposed a potential mode of action. They reported that the silver ions released from the nanoparticles appeared to be driving the toxic responses, and that the growth endpoint was more sensitive than photosynthetic yield to silver ion exposure, indicating that the photosynthetic system was not the primary target of the silver ions. Under nutrient-limited conditions, this diatom seemed to be less susceptible to adverse effects of nano-Ag and produced significantly higher levels of carbohydrates, which indicates the generation of polysaccharide-rich EPS. EPS could be involved in processes that regulate the uptake and subcellular distribution of silver ions, and higher EPS levels might protect algae from oxidative damage associated with exposure to certain metals. As a result, under nutrient-rich conditions, a potential mode of action for nano-Ag toxicity in this species might be ROS accumulation leading to oxidative damage.

6.2.2.2. Aquatic Invertebrates

Known Effects of Conventional Silver Exposure on Aquatic Invertebrates

Data for the effects of conventional silver on benthic organisms are highly varied due to the complex processes occurring in the sediment and differences in experimental designs and species characteristics. In general, the amphipod *Hyaella azteca* is believed to be among the most sensitive benthic invertebrates in the limnic environment, exhibiting a 10-day LC₅₀ as low as 1.6 milligrams Ag per kilogram (mg/kg) dry weight when exposed to AgNO₃. Like most aquatic organisms, *H. azteca* is markedly less sensitive to other silver species like silver thiosulfate and silver sulfide; toxicity of these silver complexes is limited, however, primarily due to significantly lower bioavailability in the benthic environment (Hirsch, 1998b).

More data are available for silver toxicity to freshwater planktonic invertebrates, such as the water flea, *Daphnia magna*, which is also among the most sensitive planktonic invertebrates identified in laboratory toxicity studies. Acute LC₅₀s for *D. magna* are as low as 5 micrograms total silver per liter (µg/L) when unfed organisms are exposed to silver added as AgNO₃ (Erickson et al., 1998). Increased mortality and decreased growth and reproduction in *D. magna* also have been reported following chronic exposure to dissolved silver (IC₂₀³⁶ = 2.56 µg/L) (Naddya et al., 2007).

³⁶Inhibitory concentration is the chemical concentration at which a given percentage (in this case, 20%) of the exposed organisms demonstrate a response in a chosen endpoint; this effect level is commonly used to estimate the toxicity of a substance to a specific group of organisms.

A toxic mode of action similar to that in freshwater fish is believed to lead to the toxic effect on freshwater invertebrates from exposure to conventional silver. That sequence of events, discussed further in Section 6.2.2.3, involves silver inhibition of branchial ionic sodium/potassium-ATPase (Na^+/K^+ -ATPase), which ultimately leads to failure in the organism's ability to regulate ionic transport ([Bianchini and Wood, 2003](#)).

Studies on silver toxicity to marine invertebrates are not abundant and often are not comparable to one another due to differences in experimental procedures. The existing data suggest that juvenile bivalves are among the most sensitive marine organisms, with toxicity to silver ions occurring in the <1- to 14- $\mu\text{g}/\text{L}$ range. Toxicity endpoints observed in marine invertebrates include increased mortality and delayed or abnormal development ([Ratte, 1999](#)). The primary mode of action dictating silver toxicity to marine invertebrates is suspected to be different from that in freshwater invertebrates and fish. Silver toxicity to marine invertebrates is not associated with osmotic or ionoregulatory disruption at the hemolymph level, but silver still could act on the Na^+/K^+ -ATPase enzymes at the gill level, only producing different effects (e.g., increased changes in univalent and divalent cations in tissues, change in intracellular ion concentrations) ([Bianchini et al., 2005a](#)).

Effects Specific to Nano-Ag Exposure on Aquatic Invertebrates

Examples of recent studies investigating the effects of nano-Ag exposure on aquatic invertebrates are presented in detail in Section B.4 of Appendix B. Currently, the toxic endpoints that have been examined for nano-Ag exposure to aquatic invertebrates include mortality, immobility, and embryonic development. Mortality and immobility endpoints have been examined for the unicellular eukaryote, *P. caudatum* and two species of water flea, *D. pulex* and *C. dubia*. Reproductive toxicity and genotoxicity have been examined in the aquatic midge *Chironomus riparius*, and embryonic development and adult reproductive toxicity have been examined in the estuarine oyster *Crassostrea virginica*.

Exposure of *P. caudatum* to nano-Ag without surface modification resulted in significantly lower toxicity ($\text{LC}_{50} = 39 \text{ mg}/\text{L}$) than that observed for many bacteria (LC_{50} values from 1.69 to 13.5 mg/L) ([Kvitek et al., 2009](#)). No toxic effects were observed in *P. caudatum* at nano-Ag concentrations lower than 25 mg/L , but mortality occurred at silver ion concentrations of 0.4 mg/L , indicating that silver ions are more toxic to *P. caudatum* in terms of total silver added.

Interspecies differences and environmental or experimental conditions could affect toxicity to aquatic invertebrates, as evidenced by the much higher sensitivity of *C. dubia* to nano-Ag added to natural waters than that of paramecia exposed to nano-Ag in deionized water. Under different experimental conditions not using natural water samples, adult *D. pulex* and *C. dubia* neonates exhibited significantly higher sensitivity ([Navarro et al., 2008a](#)) than that noted by Kvitek et al. (2009) in *P. caudatum*, although

this observation might be due in part to differences in experimental conditions. A recent study reported an LD₅₀³⁷ range of 3 to 4 µg/L for *D. magna* exposed to nano-Ag synthesized using different ratios of silver nitrate to sodium citrate, resulting in three different sizes (36, 52, and 62 nm) of silver nanoparticles. A lack of statistically significant differences in toxicity among the three size fractions indicated that toxicity was not a function of size, at least in sizes above 36 nm ([Li et al., 2010b](#)). As discussed in Section 6.1, however, several factors can influence the toxicity of nano-Ag to biota. Allen et al. ([2010](#)) demonstrated the range of LC₅₀s that can result from small changes to the experimental design of the study. Their study examined the relative toxicity to *D. magna* of silver ions (added as AgNO₃), commercially available nano-Ag (“uncoated” and “organically coated” Sigma Aldrich Ag-nanoparticles³⁸ [SA nano-Ag]), and laboratory-synthesized nano-Ag (coated with coffee or citrate). The investigators also examined differences in nano-Ag toxicity when *D. magna* were unfed versus fed and exposed to unfiltered versus filtered (100 nm) suspensions. The LC₅₀ values for unfed *D. magna* exposed to unfiltered silver ions and both the unfiltered coffee- and citrate-coated nano-Ag were comparable (around 1 µg/L), while the LC₅₀ for the uncoated SA nano-Ag was an order of magnitude higher (16.7 µg/L) and the LC₅₀ for the coated SA nano-Ag was higher still (31.5 µg/L). When organisms were fed, the LC₅₀ for coated SA nano-Ag jumped to about 176.4 µg/L. In unfed organisms, if the suspensions were filtered, the LC₅₀s for the SA nano-Ag dropped an order of magnitude, making the results comparable to those for the laboratory-synthesized nano-Ag and the silver ions, which changed very little when filtered.

Griffitt et al. ([2008](#)) proposed that the large difference in nano-Ag toxicities exhibited by various aquatic organisms could largely depend on feeding strategies. Exposure of the filter-feeding water flea *C. dubia* to unspecified concentrations of nano-Ag resulted in significant mortality when added to samples of headwaters, midsection, and delta waters of the Suwannee River, with lower toxicity observed for headwaters ([Gao et al., 2009](#)). *Daphnia* also appear to be more sensitive to nano-Ag than adult and juvenile zebrafish and algae ([Griffitt et al., 2008](#)). Because *daphnia* are particulate filter feeders, they might encounter relatively large numbers of nanoparticles over the course of an acute exposure period. Nanoparticles also might adhere to invertebrate exoskeletons, interfering with swimming and appendage movement. Significant changes in mobility and behavior have been observed in *D. magna* on which carbon-60 clusters have formed, although these changes were not explicitly linked to particle adhesion ([Lovern et al., 2007](#)).

³⁷Lethal dose is the chemical dose at which 50% of the exposed organisms die; this effect level is commonly used to estimate the toxicity of a substance to a specific group of organisms.

³⁸Synthesis and treatment (i.e., stabilizing agents) of “uncoated” nano-Ag were not reported, and “organic coating” for coated nano-Ag was considered proprietary by the manufacturer.

One chronic ecotoxicity experiment evaluating the effects of nano-Ag exposure to aquatic invertebrates was identified in the literature. In this study, Nair et al. (2011) observed effects on pupation and adult emergence in *C. riparius* after exposure to nano-Ag (40–70 nm) concentrations ≥ 0.2 mg/L for 25 days. The authors also observed a statistically significant change in the sex ratio of exposed midges relative to controls, showing a greater average number of females in treated groups. A comet assay further revealed a dose-dependent increase in DNA damage in treated larvae, with effects statistically significant at the 1-mg/L exposure concentration. Nair et al. (2011) concluded that exposure to nano-Ag could result in developmental and reproductive failure along with genotoxicity in *C. riparius*.

One published study on the effects of nano-Ag in benthic marine invertebrates also was identified in the literature. This study evaluated the effects of nano-Ag on the estuarine oyster *C. virginica* (Ringwood et al., 2010). The investigators examined the toxicity of nano-Ag on reproductive and embryonic development endpoints because oysters release their gametes into the surrounding water, where they might be exposed to nano-Ag. Newly fertilized oyster embryos were administered a single dose of nano-Ag (in seawater, average size 25 nm), with doses ranging from 0.0016 to 1.60 $\mu\text{g Ag/L}$ nano-Ag, and development was assessed 48 hours after treatment. Adult oysters were subjected to the same treatment regime at doses ranging from 0.0016 to 16 $\mu\text{g Ag/L}$, and lysosomal destabilization (an indicator of gamete viability) was assessed after 48 hours. Statistically significant effects when compared to controls were observed on embryonic development at a nano-Ag concentration of 1.6 $\mu\text{g Ag/L}$, and lysosomal integrity of adult hepatopancreas tissues was statistically significantly affected at 0.16, 1.6, and 16.0 $\mu\text{g Ag/L}$. The authors were unsure, however, whether the statistically significant response of the adult *C. virginica* at 0.16 $\mu\text{g Ag/L}$ also was biologically significant; previous studies by these investigators have demonstrated that lysosomal destabilization rates that exceed 30–40% result in high levels of impaired gamete viability (and thus reproductive failure). As such, the 1.6 $\mu\text{g Ag/L}$ -concentration would be the first level for which both statistically and biologically significant effects have been confirmed.

Hypothesized Nano-Ag Mode(s) of Action in Aquatic Invertebrates

Very little information specific to nano-Ag on the mode of action causing toxicity to aquatic invertebrates was located. One study examined differential gene expression in *C. riparius* exposed to 1 mg/L nano-Ag (Nair et al., 2011). Results suggested possible mechanisms involving the down-regulation of ribosomal protein L15, affecting ribosomal assembly (and protein synthesis as a result), and the up-regulation of GnRH1, a gonadotropin-releasing hormone gene that could lead to reproductive failure. The authors did not investigate the effects of silver ions on *C. riparius*, and thus whether these observed effects were nanoparticle specific is unclear.

Nano-sized particles have been reported to enter the digestive gland cells of blue mussels and cockles by endocytosis ([Moore, 2006](#)). Once in the cell, nanoparticles could become embedded in cell constituents and contribute to oxidative damage by preventing the cell from extruding the particles, although no direct evidence supports this hypothesis. Nano-Ag also might adhere to the surfaces of sperm cells spawned freely into the water by organisms using this reproductive strategy (e.g., seaweed, mussels, clams). Adhesion to the sperm cell surfaces might affect fertilization success in aquatic invertebrates, as was demonstrated in the marine seaweed, *Fucus serratus*, when exposed to carbon black. But whether nano-Ag would be available in suspension in sufficient quantities for adhesion to occur is unclear ([Nielsen et al., 2008](#)). Furthermore, as observed in *D. magna* exposed to carbon-60, direct particle adhesion to zooplankton exoskeletons might result in adverse effects on behavior and mobility ([Lovern et al., 2007](#)).

6.2.2.3. Aquatic Vertebrates

Of the data available on nano-Ag toxicity to aquatic organisms, fish studies are the most abundant. In addition to fish, only one other group of aquatic vertebrates was examined in the supporting literature for nano-Ag effects: A single study was available in the published literature for nano-Ag effects on amphibians. Ongoing research is investigating the effects of nano-Ag on two species of whale ([Wise et al., 2009](#)), but overall, published research on the toxicity of nano-Ag to aquatic mammals, amphibians, and other aquatic vertebrates is very limited or nonexistent at this time.

Known Effects of Conventional Silver Exposure on Aquatic Vertebrates

Acute silver LC₅₀s for the most sensitive fish species are between 2.5 and 10 µg/L. Chronic no observed effect concentrations³⁹ (NOECs) and maximum acceptable toxic concentrations were between 0.4 and 0.7 µg/L for sensitive fathead minnows exposed to AgNO₃ ([Ewell et al., 1993](#)). Concentrations of AgNO₃ at or above 17 µg/L resulted in premature hatching and 15% reduced growth in rainbow trout (*Salmo gairdneri*) fry ([Davies et al., 1978](#)). Other silver compounds that are less soluble, such as Ag-thiosulfate and AgCl, exhibited very little toxicity to developing *S. gairdneri* ([Hogstrand et al., 1996](#)).

Silver toxicity to freshwater fish is believed to result from silver ion interaction at the negatively charged gill surface, where nano-Ag inhibits the basolateral Na⁺/K⁺-ATPase-dependent transport across the gills. Due to the inhibition of the ionic transport system, normal electrochemical gradients are

³⁹The highest tested concentration at which no adverse effects are observed on the aquatic test organisms at a specific time of observation.

disrupted, and fish lose the ability to actively control the transport of ions across the gills, which can result in a net loss of ions from the blood plasma, osmoregulatory failure, and ultimately in circulatory collapse causing death ([Bar-Ilan et al., 2009](#)). Although fish bioaccumulate silver, the toxic mode of action in freshwater fish does not appear to be the result of internal silver accumulation, but rather the accumulation of silver at the gill surface ([Ratte, 1999](#)).

One study examined the effects of silver ions on survival and morphology of zebrafish (*D. rerio*) embryos and on behavior and development of larval zebrafish ([Powers et al., 2010a](#)). At concentrations as low as 1 μM silver ions, delayed hatching was observed. Survival decreased at concentrations of 3 μM and observed dysmorphology increased. Swimming performance was impaired at concentrations below the thresholds for survival and dysmorphology indicating that long-term survival could be affected (due to persistent behavioral effects), even at concentrations that appear otherwise nontoxic in studies examining only physiological endpoints.

The mode of action of silver toxicity to marine fish is not well understood, but appears to be very different from that of freshwater species. Toxicity is speculated to be equally attributable to processes taking place at the gill surface and those occurring in the gut of the fish ([Grosell and Wood, 2001](#)). Silver induces ionoregulatory failure in marine fish, although typically at concentrations that are one to two orders of magnitude higher than in freshwater fish ([Pedroso et al., 2007](#)). Preliminary (unpublished) research underway at Duke University's Center for Environmental Implications of Nanotechnology suggests that silver toxicity to Atlantic killifish (*Fundulus heteroclitus*) embryos and larvae is not due entirely to exposure to silver ions, as previously thought ([Matson, 2010](#)). The investigators reported that conventional silver toxicity did not follow a linear response curve along an increasing salinity gradient. Instead, toxicity decreased up to a certain chloride concentration and then increased again at salinities similar to those in estuarine environments. The reason underlying the U-shaped salinity-toxicity relationship is unknown (this response is not observed in adult *F. heteroclitus* under the same conditions), but the investigators proposed that the observed toxicity might be due to the concentration of total dissolved silver in solution.

Effects Specific to Nano-Ag Exposure on Aquatic Vertebrates

Examples of recent studies investigating the effects of nano-Ag on fish are presented in detail in Section B.5 of Appendix B. The only species of fish for which nano-Ag toxicity tests have been published are freshwater zebrafish (*D. rerio*) and fathead minnow (*P. promelas*), and the anadromous rainbow trout (*Oncorhynchus mykiss*), Japanese medaka (*Oryzias latipes*), and European perch (*Perca fluviatilis*). One study also examined the effects of nano-Ag on the American bullfrog (*Rana catesbeiana*). *D. rerio*, the most widely used test organism for investigating the effects of nano-Ag in fish, are gaining popularity as

model organisms in toxicological studies due to the high degree of homology to the genome of other vertebrates (including humans) and similarities in physiologic responses to various stressors across vertebrate species ([Postlethwait et al., 2000](#)). They also display rapid ex utero and post-fertilization development and high fecundity. The transparent embryos, with tissues turning opaque upon cell death, allow for real-time analysis of developmental effects in addition to real-time monitoring of nanoparticle transport ([Bar-Ilan et al., 2009](#); [Lee et al., 2007](#)). Fish study endpoints can include tissue and whole-body concentrations of chemicals (e.g., bioaccumulation, as discussed in Section 5.2.3.8), mortality, behavioral markers (e.g., coughing and abnormal swimming), and morphological malformations (e.g., pericardial edema, bent spine, small head).

A recent study using *O. latipes* reported that this species is susceptible to nano-Ag with observed effects at concentrations at or above 25 µg/L, but that changes in gene expression possibly indicative of nano-Ag toxicity occurred at concentrations as low as 1 µg/L ([Chae et al., 2009](#)). Moreover, the gene expression patterns observed in *O. latipes* exposed to nano-Ag were distinguishable from those observed following exposure to silver ions (added as AgNO₃), indicating a distinct nanoparticle effect. The genes analyzed were hepatic biomarkers associated with metals detoxification, antioxidant defense, cellular responses to stressors, toxin binding and transport, catalysis, cell-cycle arrest, apoptosis, DNA repair, biotransformation and detoxification of endogenous and exogenous compounds, iron metabolism, and immune system response. Chae et al. (2009) found that nano-Ag at concentrations of 1 and 25 µg/L significantly affected gene expression in the six genes examined at various time points during the 10-day exposure period. Although all tested genes responded differently to nano-Ag and silver ions, the largest statistically significant differences were observed in the heat shock protein HSP70, a stress protein; p53, a DNA repair and apoptosis-inducing protein; and transferrin, an iron transport protein. As more ecological toxicity tests attempt to elucidate a mode of action by investigating the induction of such “stress-response genes,” however, keeping in mind that gene induction in response to stressors does not necessarily indicate an adverse effect at the organism level is important. Genes responding to stress are expected to provide some resistance to adverse effects up to a certain threshold exposure level ([Crawford and Davies, 1994](#)). Furthermore, the impact of changes at the molecular level due to exposure to toxicants has not been investigated fully or correlated to changes that might occur in dynamic populations of these same organisms. This caveat is applicable to all toxicogenomic studies discussed hereafter.

In a conference presentation, Wise et al. (2009) reported that nano-Ag is highly cytotoxic (in a concentration-dependent manner) and genotoxic to *O. latipes*. Additionally, nano-Ag appears to be more toxic to this species than silver ions (added as AgNO₃). Although the 96-hour LC₅₀ for nano-Ag and silver ion exposures to *O. latipes* were comparable (34.6 vs. 36.5 µg/L), significantly more mortality occurred at higher nano-Ag concentrations than at equivalent concentrations of silver ions from AgNO₃, and

statistically significant gene induction was less common following exposure to AgNO₃ ([Chae et al., 2009](#)). Laban et al. ([2009](#)) reported that dissolved silver from AgNO₃ was more toxic to *P. promelas* embryos than dissolved silver released from nano-Ag.⁴⁰ They reported a AgNO₃ LC₅₀ of 15 µg/L, which is below the level of dissolved silver released by the silver nanoparticles in any treatment group (18–95 µg/L). The investigators compared the toxicity of nano-Ag solutions that had been briefly sonicated to those that had only been stirred, and measured the concentrations of dissolved silver in each type of solution. Although the dissolved silver concentrations were not significantly different between the stirred and sonicated samples, the sonicated samples were 10 times more toxic than the stirred samples, suggesting that nano-Ag toxicity cannot be attributed purely to the concentration of dissolved silver released from the nanoparticle. This result, however, is not always corroborated in other studies. Kennedy et al. ([2010](#)) reported that silver ions were more acutely toxic (LC₅₀ = 5.7 µg/L) to *P. promelas* than nano-Ag of various sizes and coatings (LC₅₀s = 6.6–125.6 µg/L) at equivalent total silver concentrations. But when exposed to equivalent amounts of silver ions and “fractionated” nano-Ag (defined as the dissolved fraction of the silver nanoparticles), the resulting LC₅₀s for nano-Ag (LC₅₀s = 1.5–5.6 µg/L) were about the same or statistically significantly lower than that of AgNO₃, depending on the nano-Ag material used. These results suggest that the dissolved fraction (i.e., silver ions) of nano-Ag in suspension was driving toxicity. The investigators caveat, however, that the filtration method used did not remove silver nanoparticles with diameters less than 4 nm from the fractionated samples.

Lower sensitivity than described for *O. latipes* was also observed in *O. mykiss* exposed to nano-Ag in the form of Nanocid[®], a water-based colloidal suspension designed by Nano Nasb Pars Co. (Tehran, Iran) for use as a disinfectant in aquaculture. In addition to lethality, reported effects included hypoxia, lethargy, unusual swimming behavior, elevated gill ventilation, and darkening of the body, although the concentrations at which these effects occurred were not reported. The 96-hour LC₅₀ was 2.3 mg/L, which is almost two orders of magnitude higher than that reported for other fish species. Characterization of the test material was not reported, however, and particle clusters could have formed, reducing the number of nanoparticles in suspension ([Shahbazzadeh et al., 2009](#)). A more recent study examined the cytotoxic effects of nano-Ag (PVP- and citrate-coated) on the tissues of *O. mykiss* in vitro ([Farkas et al., 2011](#)). The citrate-coated nanoparticles were more readily taken up by the tissues than the PVP-coated nanoparticles, but cell viability was reduced in all exposures to all nanoparticle types and sizes (starting at nano-Ag concentrations of 0.1 mg/L). Higher levels of reduced glutathione (GSH) were reported at exposure levels ≥0.1 mg/L citrate-coated particles and ≥1 mg/L PVP-coated particles. Uptake was also observed by Scown et al. ([2010](#)) of “uncoated” nano-Ag (10 and 35 nm; surface treatment not reported by

⁴⁰Defined as ionic silver released from silver nanoparticles and dissolved silver nanoparticles.

manufacturer) in the tissues of *O. mykiss* after exposures to 10 µg/L nano-Ag. These exposures resulted in increased expression of the *cyp1a2* gene in the gill tissue of exposed fish, suggesting a possible increase in oxidative metabolism, although no effects on lipid peroxidation were observed.

Zebrafish (*D. rerio*) have been examined in the embryonic, juvenile, and adult life stages for lethal and sublethal toxic effects, including the influence of nano-Ag on caudal fin regeneration. Bar-Ilan et al. (2009) investigated the size-dependent toxicity of nano-Ag on *D. rerio* embryonic development using 3-, 10-, 50-, and 100-nm silver nanoparticles. The embryos exhibited almost 100% mortality at nano-Ag concentrations of 250 µM, regardless of the size of the nanoparticle. LC₅₀ values (93.31 µM for 3-nm particles to 137.26 µM for 100-nm particles) indicated that toxicity is loosely size dependent, although only at certain concentrations and time points. In a study by Asharani et al. (2008), mortality was higher in *D. rerio* embryos exposed during the cleavage period of development (2- to 8-cell stages, up to approximately 1 hour post-fertilization) than in those exposed after the cleavage period when embryos are entering epiboly (4 to 6 hours post-fertilization). Embryos exposed earlier were more sensitive, exhibiting an LC₅₀ of 25 µg/mL, compared to embryos exposed later in development that exhibited an LC₅₀ of 50 µg/mL (Asharani et al., 2008). Developmental effects of nano-Ag were also examined in *O. latipes* embryos by Wu et al. (2010). Morphological defects including heart malformations, edema, spinal abnormalities, and finfold abnormalities were reported at concentrations of nano-Ag (25 nm) at and above 100 µg/L. These effects were observed as a U-shaped dose-response curve, with delayed hatching and abnormalities in embryos exposed to the lower and higher concentrations of the dose distribution. These results suggest the need for a greater understanding of the mechanism of developmental toxicity of nano-Ag.

Bar-Ilan et al. (2009) reported that 3-nm and 10-nm silver nanoparticles seemed to produce the greatest amount of statistically significant sublethal toxic effects (based on seven quantified effects) in *D. rerio* embryos at a concentration of 100 µM nano-Ag when compared to a range of other nano-Ag concentrations. Overall, 100 µM nano-Ag exposure resulted in embryos having 31–46% smaller heads, 87–119% larger yolk sacs, 31–68% smaller caudal fins, and 38–55% smaller eyes than the controls. In addition, embryos were 14–25 mm shorter, and had 5π–14π more axial curvature and 16–64% larger pericardial sacs, but these were not statistically significantly different from the controls (Bar-Ilan et al., 2009). At 120 hours post-fertilization, the embryos had not depleted their yolk sacs, which were their only source of food throughout the exposure period. The underdeveloped bodies of the exposed embryos suggest that nano-Ag exposure inhibited the uptake of nutrients from the yolk sac, although how nutrient uptake was impaired was not investigated. Lee et al. (2007) reported a threshold for *D. rerio* of 0.19 nM nano-Ag, above which no embryos exposed at the eight-cell stage developed normally. At concentrations higher than 0.19 nM, all embryos were either dead or deformed, and the incidence of deformities

decreased as the number of dead embryos increased. Mortality ranged from 20% to 90% at nano-Ag concentrations of 0.05 to 0.72 nM, respectively, and deformities ranged from approximately 2% at 0.05 nM nano-Ag to 42% at 0.19 nM (Lee et al., 2007). Some sublethal toxic effects, such as yolk sac and pericardial edema, also were observed in *P. promelas* exposed to nano-Ag concentrations up to 20 mg/L (Laban et al., 2009). Several studies have demonstrated that nano-Ag exposure contributes to mortality and sublethal developmental effects on *D. rerio* embryos in a concentration-dependent manner; the results from these studies, however, cannot be compared directly due to different experimental designs and dosing methods (Bar-Ilan et al., 2009; Asharani et al., 2008; Lee et al., 2007).

Additional phenotypic and physiological endpoints shown to be affected by *D. rerio* exposure to nano-Ag at concentrations greater than 50 µg/mL are decreased heart rate, hatching delay, accumulation of blood in the blood vessels near the tail, apoptosis, slimy external skin coating, finfold abnormalities, tail and spinal cord flexure and truncation, cardiac malformation, head edema, eye malformation, hemorrhaging, blood clots, and distortion of the yolk sac (Bar-Ilan et al., 2009; Asharani et al., 2008; Yeo and Kang, 2008; Lee et al., 2007). Laban et al. (2009) observed similar abnormalities in developing *P. promelas* embryos exposed to nano-Ag. One concern in the testing of nano-Ag for toxic effects is that residual silver ions from the nano-Ag feedstock might be present in nano-Ag stock solutions and therefore be responsible for the observed effects. Asharani et al. (2008) investigated whether exposure to silver ions alone could result in the effects observed in developing zebrafish embryos following exposure to the nano-Ag test material. They reported that exposure of *D. rerio* embryos to concentrations of silver ions equivalent to the range of nano-Ag concentrations shown to result in gross malformations did not affect any of the phenotypic endpoints examined. The highest silver ion concentration tested (20 nM) resulted in 10% mortality and hatching delay in 4% of the embryos, but did not significantly affect overall development of the embryos. The results indicate that the observed sublethal toxic effects were not the result of residual silver ions in the exposure medium left over from the synthesizing process.

Phenotypic changes such as those described above have been observed in *D. rerio* embryos exposed to toxic chemicals other than nano-Ag. For example, Lee et al. (2007) noted that finfold abnormalities, tail and spinal cord flexure and truncation, cardiac malformation, and yolk sac edema have all been observed in embryos exposed to dichloroacetic acid and cadmium. The specific eye malformation (no formation of retina or lens), however, resulting from exposure to nano-Ag has not been reported in literature describing exposure of *D. rerio* to any other toxic chemical (Lee et al., 2007).

Danio rerio can regenerate many body structures, including the spinal cord, optic nerve, heart, and fins (Yeo and Pak, 2008). The effect of nano-Ag on caudal fin regeneration was investigated by Yeo and Pak (2008). At a concentration of 4 ppm, nano-Ag significantly inhibited regeneration, and exposure to

0.4 ppm delayed, but did not completely inhibit, caudal fin regeneration. Exposure to 0.4 and 4 ppm nano-Ag resulted in defects in regeneration observed within 10 days following amputation.

Griffitt et al. (2009) investigated the effects of the NOEC of nano-Ag on adult *D. rerio* gill histology and gene expression, and compared these responses to those elicited by soluble silver concentrations (through addition of AgNO₃) equivalent to those released by the nano-Ag after 48 hours. Although the dissolved silver concentrations were comparable between the nano-Ag and AgNO₃ solutions, gill filament widths were significantly larger in those zebrafish exposed only to the dissolved silver from the AgNO₃ solutions. The gill tissues and whole carcasses of zebrafish exposed to nano-Ag, however, contained significantly higher concentrations of total silver than those of the zebrafish exposed only to soluble silver. Another study examining oxygen consumption of *P. fluviatilis* exposed to nano-Ag reported evidence supporting that nano-Ag might act on the gills externally, thereby reducing gas exchange at the gill surface (Bilberg et al., 2010). The investigators measured the basal metabolic rate (BMR) and critical oxygen tension (P_{crit}) of *P. fluviatilis* by automated intermittent closed respirometry. Results showed no effect on the BMR of exposed fish, but did show an increase in P_{crit} by 50% after exposure to 300 µg/L nano-Ag for 24 hours. Exposure to AgNO₃ caused an increase in both BMR and P_{crit} at exposure concentrations lower than those of nano-Ag. These results indicate that *P. fluviatilis* could be vulnerable to hypoxia following exposures to nano-Ag, albeit at very high exposure levels.

The single study that assessed the effects of nano-Ag on the amphibian *Rana catesbeiana* conducted an in vitro cultured tail fin biopsy assay using tadpole tissue (Hinther et al., 2010). *R. catesbeiana* tissues show extreme sensitivity to thyroid hormone action, making them good model species for assessing potential effects to human health, for which thyroid hormone is essential. The investigators reported LC₅₀ values of 0.25 mg/L for AgNO₃ and 0.95 mg/L for nano-Ag. They also observed disruption of non-thyroid-hormone-mediated cellular stress response pathways at higher concentrations of nano-Ag (≥2.75 mg/L) and altered thyroid-hormone action at lower concentrations of nano-Ag (0.6–550 µg/L). Similar responses were not observed after exposure to equivalent concentrations of silver ions alone. How these stress responses at the subcellular level translate to effects at the organism level is unclear, but they could represent a sensitive endpoint that has not yet been evaluated in amphibians (Hinther et al., 2010).

Because the research presented in this section suggests that aquatic organisms are susceptible to nano-Ag toxicity, the effects on fish and other aquatic species at the organism level suggest that impacts from nano-Ag at the population and ecosystem level are possible. Research investigating nano-Ag effects on sperm whales (*Physeter macrocephalus*) and North Atlantic right whales (*Eubalaena glacialis*) (Wise et al., 2009); Atlantic tomcod (*Microgadus tomcod*) (Nichols et al., 2009); and Atlantic killifish (*F. heteroclitus*) (Matson, 2010) is currently underway. Preliminary results indicate that nano-Ag is toxic

to both cells and genetic constituents of cells in both whale species in a concentration-dependent manner, although whale cells appear to be less sensitive than those of medaka (*O. latipes*) (Wise et al., 2009). These data can be used as an indication of the body of information that might become available in the next several years.

Hypothesized Nano-Ag Mode(s) of Action in Aquatic Vertebrates

The toxic mode of action of nano-Ag in fish has not been fully elucidated. Although silver nanoparticles have been observed inside fish embryos and toxic effects have been quantified, these results serve only to allow speculation concerning the mode of action. Griffitt et al. (2009) examined the transcriptional profiles of *D. rerio* adults exposed to nano-Ag and soluble silver (from AgNO₃). Despite having similar concentrations of soluble silver in both exposure groups, the zebrafish exposed to nano-Ag exhibited a significantly different gene expression profile than those fish exposed to only the soluble silver, indicating that the nano-Ag mode of action differs significantly from that of silver ions. As examined by Chae et al. (2009), the independent expression of genes in the *O. latipes* liver that act as indicators for carcinogenesis, mutagenesis, DNA repair, and oxidative damage indicates that rapid biotransformation and detoxification was occurring in the liver. If biotransformation and detoxification were indeed occurring, this suggests that nano-Ag might induce apoptosis, which is assumed to result from nano-Ag-generated ROS. No direct evidence, however, is available to link ROS to toxicity in this case; cytotoxicity from ROS was inferred only from the response of the indicator genes. Furthermore, Griffitt et al. (2009) did not measure induction of any *D. rerio* genes currently mapped to oxidative stress regulation when the fish were exposed to nano-Ag NOEC concentrations, indicating that ROS generation alone might not completely explain toxic effects from nano-Ag exposure.

Several studies (Laban et al., 2009; Asharani et al., 2008; Lee et al., 2007) have demonstrated the ability of fish embryos to take up silver nanoparticles (see Section 5.2.3). Lee et al. (2007) demonstrated that silver nanoparticles can penetrate the egg chorion through the chorionic pore canals by passive transport. From there, some nanoparticles penetrated the embryo itself and embedded in several zebrafish organs (Lee et al., 2007). Another study showed that nano-Ag deposits on the skin and uniformly within the body, showing a particular affinity for the cell nucleus (Asharani et al., 2008). One study also reported penetration and accumulation in all organelles—including the nucleus—of the gill, muscle, and regenerated fin tissue of zebrafish (age not specified) (Yeo and Pak, 2008). Because accumulation in the nucleus can lead to genomic damage, this observation supports other results indicating a genomic response to nano-Ag exposure in *O. latipes*. Yeo and Pak (2008) reported upregulation of five genes involved in apoptosis 50 hours post-fertilization in *D. rerio* embryos exposed to nano-Ag. Increased apoptosis in response to nano-Ag might result from increased production of free radicals. Additional

evidence that nano-Ag exposure increases free radicals that could cause DNA damage comes from observations in a study by Yeo and Kang (2008), in which levels of the enzyme catalase, which is responsible for removing free radicals, increased in *D. rerio* exposed to 10 and 20 parts per trillion (ppt) nano-Ag. Although Rojo et al. (2007) did not observe any developmental effects or mortality in *D. rerio* at nano-Ag concentrations up to 5 ppm, they did measure increased expression of genes involved in detoxification and regulation of the oxidative stress response. The role of oxidative stress, DNA damage, and apoptosis in the toxicity pathway also has been examined in adult *D. rerio* (Choi et al., 2010). Histological analysis of the liver revealed hepatic cell cords and TUNEL-positive apoptotic changes, and p53-related genes were upregulated in treated fish, suggesting that oxidative stress and apoptosis are associated with toxic effects in the livers of adult zebrafish. Hinthner et al. (2010) also demonstrated disruption of cellular stress-response pathways in amphibians at relatively high concentrations of nano-Ag, as shown through alterations in *hsp30* and *CAT* transcripts. An alternative mode of action for nano-Ag at low concentrations also was proposed by Hinthner et al. (2010) for toxicity to amphibians. At low doses, nano-Ag seemed to affect thyroid-hormone signaling pathways that are crucial to embryonic development, as shown through alteration of the thyroid-hormone-induced thyroid hormone receptor beta (TR β) and thyroid-hormone-repressed *Rana* larval keratin type I (RLKI).

Nano-Ag has been observed to interfere with cardiac muscle function, preventing the flow of blood through the body of the embryo (Asharani et al., 2008). Nano-Ag might inhibit cardiac function directly by interacting with cardiac cells, disrupting normal cell functioning, and weakening the pumping of the heart. The weakened pumping of the heart results in restricted blood flow, which might indirectly affect the ability of the embryo to access vital energy sources contained in the blood. Following a loss of blood flow, nano-Ag deposits in the brain, which could interfere with signal transduction and other nervous system processes, leading to a loss in neurological function. A loss of neurological function is supported by observed insensitivity of the larvae to touch. The silver nanoparticle, by simply attaching to a biological surface (e.g., a developing zebrafish organ), might act as a foreign body, thereby limiting functionality of the cell or organ to which it has attached (Asharani et al., 2008). For example, Handy et al. (2008a) noted that although engineered nanoparticles are typically too large to exploit direct uptake channels to nerve cells, they are probably capable of attaching to the epithelium and interacting with receptors. Such interactions might interfere with olfactory function, such as chemical signaling, leading to changes in behavior that affect survival.

6.2.2.4. Model to Estimate Toxicity to Aquatic Biota

The computational models that are currently being recommended for use in predicting the toxicity of nano-Ag and related silver species are limited in number and scope. At this time, no models appear to

be available for assessing toxicity from nano-Ag particles, but two models can be used to estimate the toxicity of silver ions released from the particles. The models apply only to the aquatic environment, however, and no terrestrial toxicity models appear to be available at this time. The models discussed here are used to estimate predicted no-effect concentrations (PNECs) for aquatic biota in the water column ([Mueller and Nowack, 2008](#)) and to predict metal toxicity to fish ([DiToro et al., 2001](#)).

Predicted Water Column No-Effect Concentration Model

Mueller and Nowack's ([2008](#)) fate and transport model (described in Section 4.5) estimated a PNEC for aquatic biota based on a published study by Yoon et al. ([2007](#)) of acute nano-Ag toxicity with two bacteria, *B. subtilis* and *E. coli*. The threshold concentrations (equivalent to a NOEC) for these species in water (20 and 40 mg/L, respectively) were divided by an assessment factor of 1000, in accordance with the Technical Guidance Document on Risk Assessment published by the European Chemicals Bureau ([Mueller and Nowack, 2008](#); [ECB, 2003](#)). The ratios of the predicted environmental concentrations (PEC) of nano-Ag in water of 0.03 µg/L for the "realistic scenario" and 0.08 µg/L for the "high scenario," to the PNEC of 20 µg/L (for bacteria) were orders of magnitude less than 1.0 (i.e., less than a hazard quotient of 1.0). The investigators did not, however, consider silver ions potentially released from the nanoparticles. Mueller and Nowack ([2008](#)) noted that release of nano-Ag particles is of secondary importance to the release of silver ions from the nanoparticles given the higher toxicity of ionic silver, for which the authors cite Blaser et al. ([2008](#)). Gottschalk et al. ([2009](#)) report a modal PEC for nano-Ag in surface water of 0.116 ng/L and a Q(0.85) of 0.428 ng/L in the United States.

Biotic Ligand Model

A biotic ligand model (BLM) has been developed as a predictive tool to enable estimation of acute metal toxicity in an aqueous environment when several aspects of the water chemistry are known ([DiToro et al., 2001](#)). The BLM accounts for several water chemistry parameters, including ionic chlorine (Cl⁻) concentration and the amount of dissolved organic matter, to predict the amount of free metal ion available to bind to the fish gill. For acute toxic effects on fish, the gill is considered a proximate site of toxic action. The biotic ligand binding site is thought to be one or more sensitive enzyme systems (carbonic anhydrase or Na⁺/K⁺-ATPase) ([Bielmyer et al., 2008](#)). Accumulation at the surface of gills is relevant to a possible mode of action of nano-Ag because gill transport of silver and other ions also varies with water chemistry. Notably, however, the BLM was specifically developed to model binding and toxicity of metal cations, and consequently that this model would adequately predict the behavior and toxicity of nano-Ag and other metals when present in nanoparticle form is unlikely.

6.2.3. Terrestrial Organisms

Very few studies have investigated the effects of nano-Ag on terrestrial organisms, with no investigations of nano-Ag toxicity in soils ([Wijnhoven et al., 2009b](#)). This section summarizes knowledge regarding conventional silver and nano-Ag effects on several types of terrestrial organisms, including plants, invertebrates, and vertebrates.

6.2.3.1. Terrestrial Plants

Only recently have some studies emerged that investigate the effects of plant exposure to nano-Ag. At this point, literature on the effects from environmental exposure to nano-Ag are still lacking, with most studies relying on experimental procedures that do not mimic natural conditions and endpoints that might not be relevant to environmental assessment. Nonetheless, these studies provide some insight into the potential responses of higher order plants to nano-Ag exposure.

Known Effects of Conventional Silver Exposure on Terrestrial Plants

Although data on the effects of silver in higher plants are limited and highly varied, a review by Ratte ([1999](#)) suggests that plants are most sensitive to silver during germination and growth. Lettuce (*Lactuca sativa*), radish (*Rhaphanus sativas*), and maize (*Zea mays*) seeds exposed to AgNO₃ exhibited reduced germination and growth at or below 7.5 mg/L AgNO₃ ([Ewell et al., 1993](#)). Spiking sewage sludge with 5.2 and 120 mg Ag/kg dry weight, however, did not have a statistically significant effect on growth or emergence of lettuce, turnips, oats, and soybeans. In fact, the mean fresh weight of the lettuce leaves increased significantly in the groups exposed to silver, although a change in dry weight was not observed ([Hirsch, 1998a](#)).

Effects Specific to Nano-Ag Exposure on Terrestrial Plants

Summaries of three recent relevant studies investigating the effects of nano-Ag on terrestrial plants are provided in Section B.6 of Appendix B. These studies suggest that nano-Ag might be toxic to higher order plants at concentrations above 10 ppm, although statistical significance was not always reported ([Kumari et al., 2009](#); [Rostami and Shahsavar, 2009](#); [Babu et al., 2008](#)). In a review article, Ma et al. ([2010](#)) described phytotoxicity of nano-Ag to plant seedlings and to plant cells. In their own research, Ma et al. ([2010](#)) found that very low concentrations of nano-Ag (<1 ppm) sized 20–80 nm could be toxic to seedlings of thale cress (*Arabidopsis thaliana*) by stunting growth in a concentration- and particle size-dependent manner. Similarly, Hawthorne et al. ([2012](#)) reported that nano-Ag reduced zucchini (*Cucurbita*

pepo) plant biomass and transpiration by 49–91% compared to equivalent concentrations of conventional silver, while shoot silver content did not differ based on particle size or concentration. Nano-Ag also was found to inhibit seed growth and produce cell damage in grass (*Lolium multiflorum*) (Yin et al., 2011). For a given mass, smaller nano-Ag particles had a greater impact on plant growth than similar concentrations of larger particles; however, when doses were expressed in units of specific surface area, the effects were comparable. Authors suggested that such alterations could be directly attributed either to the nanoparticles themselves or to the ability of nano-Ag to deliver dissolved silver to critical biotic receptors (Yin et al., 2011).

Rostami and Shahsavari (2009) demonstrated that submerging olive (*Olea europaea* L.) explants, or the part of the plants used to initiate a culture, in nano-Ag solutions with concentrations ranging from 100 to 400 ppm effectively eliminated bacterial contamination in the explants, but also resulted in a high percentage of plant mortality. When the investigators added nano-Ag to a prepared medium in lower concentrations (2–6 ppm) and allowed the explants to grow in the contaminated medium for 30 days, the nano-Ag exposure seemed to result in more than a 50% decrease in plant mortality up to 4 ppm when compared to controls (statistical significance not reported); mortality then again increased slightly (~20%), although this increase was reported as not statistically significant.

In a toxicity assay, Babu et al. (2008) reported that nano-Ag exposure induced a dose- and duration-dependent mitodepressive and cytotoxic effect on onion (*Allium cepa*) meristems (root tips). Exposure of *A. cepa* meristems to nano-Ag resulted in a reduced frequency of mitotic index, which is a measure of cell proliferation, and increased frequency of chromosomal aberrations. These results occurred at all nano-Ag concentrations tested and at every exposure duration, although results were not always statistically significant for shorter exposure durations (Babu et al., 2008). Kumari et al. (2009) also reported a nano-Ag concentration-dependent effect on *A. cepa* mitotic index, but the decrease was significantly different from the control group only at concentrations at or above 50 ppm. Babu et al. (2008) reported a significant reduction in frequency of cell division even in the groups exposed to the lowest concentration of nano-Ag (10 ppm) for 2 hours, and at higher concentrations (20–50 ppm) within 1 hour. A significant increase in chromosomal aberrations was observed by Babu et al. (2008) in all treatment groups after a 0.5-hour exposure and by Kumari et al. (2009) at all treatment groups except the lowest concentration group (25 ppm) at the end of a 4-hour exposure period. Chromosomal aberrations described in both studies include chromatin bridge, stickiness, disturbed metaphase, and breaks and fragments (Kumari et al., 2009; Babu et al., 2008).

In unpublished research by Cho et al. (2008b) presented at the first meeting of the Asian Horticultural Congress in 2008, the investigators reported that nano-Ag inhibits the growth and elongation of lettuce and pak-choi roots in a concentration-dependent manner. Nano-Ag exposure also

reduced lettuce and pak-choi fresh and dry weights with an increase in concentration above the 0.04-ppm treatment level. At 0.04 ppm, however, nano-Ag appeared to optimize growth, resulting in 10% and 20% increases in the weight of lettuce and pak-choi, respectively. This U-shaped concentration-response curve is similar to that reported by Rostami and Shahsavari (2009) in olive explants, indicating the presence of a narrow nano-Ag threshold at which plant performance is optimized, but above and below which plant performance is inhibited.

Hypothesized Nano-Ag Mode(s) of Action in Terrestrial Plants

Although few data exist on the specific mode of action for nano-Ag in terrestrial plants, comparisons to conventional silver and silver ions suggest that its mode of action differs from its conventional counterparts. Stampoulis et al. (2009) compared the toxicity of nano-Ag, “bulk” silver, and ionic silver in zucchini (*Curcubita pepo*) and determined that 1,000 mg/L nano-Ag resulted in a 69% greater reduction in biomass when compared to 1,000 mg/L conventional silver. The authors also found that exposure to 10 mg silver ions/L (from AgNO₃) produced an effect similar to that of nano-Ag, but that exposure to the supernatant containing silver ions released from the 1000-mg/L nano-Ag solution resulted in significantly more growth when compared to the nano-Ag solution, indicating that toxicity of nano-Ag is not due entirely to dissolution of the silver ion (Stampoulis et al., 2009).

Some authors have proposed that the reduction of the mitotic index in *A. cepa* meristems results from DNA transcription inhibition at S-phase, and that the observed mitotic abnormalities are indications that mitotic spindle function is impaired, likely due to nano-Ag interactions with tubulin-SH groups (Kumari et al., 2009; Babu et al., 2008). Babu et al. (2008) posit that the observed chromosome stickiness might be the result of “intermingling” chromatin fibers leading to connections between chromosomes at the sub-chromatic level. They also argue that nano-Ag has a clastogenic effect, as observed in the induction of the chromosomal breaks and micronuclei, which might result in a loss of genetic material.

6.2.3.2. Terrestrial Invertebrates

Terrestrial invertebrates include those living in soils and aboveground. Few studies have been conducted on nanomaterial toxicity to terrestrial invertebrates, and even fewer have specifically focused on nano-Ag. Because the terrestrial environment has not been thoroughly investigated for pathways of concern, very little information is available on suspected routes of exposure. Nano-Ag in soils is likely to form complexes with organic matter and thiols, which might render it largely unavailable for uptake, as discussed in Section 5.2.4.2. If nano-Ag were applied in sprays directly to the surface of plants, plant-dwelling invertebrates might ingest particles unbound to organic matter. This type of application,

however, is considered “off-label,” or not in accordance with product instructions for indoor spray disinfectants.

Known Effects of Conventional Silver Exposure on Terrestrial Invertebrates

Silver toxicity has not been studied extensively in terrestrial invertebrates. Some data presented by Ewell et al. (1993) at the 1st Argentum International Conference on the Transport, Fate, and Effects of Silver in the Environment indicate that silver is toxic to the earthworm *Lumbricus terrestris* at concentrations above 62 mg Ag/kg when chronically exposed to artificial soil contaminated with AgS. Because the worms did not bioaccumulate silver after the 28-day exposure period, the investigators determined that direct contact of the dermal tissues with silver in the soil particles resulted in the observed reduction in growth, although the mode of action has not been elucidated.

Effects Specific to Nano-Ag Exposure on Terrestrial Invertebrates

Few studies were found that explicitly examined nano-Ag toxicity to soil invertebrates; study details are provided in Section B.7 of Appendix B. Roh et al. (2009) examined the effect of nano-Ag on DNA transcription, survival, growth, and reproduction in wild type and mutant strains of the soil nematode *Caenorhabditis elegans*. Using microarray analysis, the investigators observed that exposure to nano-Ag resulted in the significant upregulation of 415 gene probes⁴¹ and significant downregulation of 1,217 gene probes. The investigators found that survival and growth were not affected by exposure to nano-Ag in any of the treatment groups for the wild type and mutant *C. elegans* strains tested. Reproduction, however, decreased significantly in all strains at all concentrations, with only one exception: Reproduction was not statistically significantly affected in one *C. elegans* type evaluated at the lowest concentration. Exposure to silver ions from AgNO₃ did not result in any significant effect on survival or growth, but did significantly reduce reproduction potential. The degree to which reproduction potential decreased, however, was greater in *C. elegans* exposed to nano-Ag than to silver ions. Exposure to silver ions resulted in a different gene expression pattern than that of nano-Ag. Silver ion concentrations of 0.1 and 0.5 mg/L resulted in the statistically significant induction of four *hsp* gene groups, which are heat shock proteins, but did not result in the upregulation of the gene probes significantly affected by exposure to nano-Ag (Roh et al., 2009).

Another study of nano-Ag toxicity to *C. elegans* did observe growth inhibition after exposure to PVP-coated and citrate-coated nano-Ag (Meyer et al., 2010). Statistically significant growth inhibition

⁴¹A probe is a specific sequence of single-stranded DNA or RNA, usually labeled with a radioactive atom, that is designed to bind to, and therefore single out, a particular segment of DNA to which it is complementary.

was observed after exposure to 5 mg/L of citrate-coated nano-Ag, and 50 mg/L of PVP- and citrate-coated nano-Ag. The investigators performed a separate assay in which they fed DNA-damaged bacteria to *C. elegans* as a negative control to account for the possibility that the observed growth deficiency was confounded by nano-Ag toxicity to the bacterial food supply. Their results showed that growth inhibition was not mediated by toxicity to the bacteria and was indeed due to exposure to nano-Ag. Meyer et al. (2010) also accounted for possible confounding due to toxic effects of the PVP and citrate coatings and found that exposure to these chemicals alone seemed to stimulate growth above the levels of control. Measurements of dissolved silver in the exposure media revealed that citrate-coated nano-Ag released less dissolved silver than PVP-coated nano-Ag. This, coupled with evidence that exposure to PVP supernatant induced much higher toxicity than exposure to pure citrate supernatant, indicated that the toxicity observed is due mainly to the release of silver ions (Meyer et al., 2010).

Reproductive toxicity of the earthworm *Eisenia fetida* was assessed by Heckmann et al. (2011) in a limit-test toxicity screening conducted according to the OECD guidelines for assessing earthworm reproductive toxicity. After exposure to 1,000 mg/kg soil PVP-coated nano-Ag for 28 days, complete reproductive failure (0% cocoon production) was observed in the earthworms. Survival was statistically significantly decreased in *E. fetida* exposed to AgNO₃ when compared to controls, but was not affected in groups treated with nano-Ag. Although the nanoparticles were very thoroughly characterized, authors were unable to identify any clear correlation between toxicity and specific particle characteristics (Heckmann et al., 2011). Similarly, in another reproductive toxicity test, *E. fetida* exposed to 727.6 or 773.3 mg/kg nano-Ag (with oleic acid and PVP coatings, respectively) showed a significant decrease in reproduction (Shoults-Wilson et al., 2011a); the effect of AgNO₃ was more pronounced with decreased reproduction reported at 94.21 mg/kg. Another study involving *E. fetida* examined avoidance of soils contaminated with nano-Ag as a behavioral endpoint and found it to be a more sensitive indicator of toxicity than growth and mortality (Shoults-Wilson et al., 2011b). Earthworms were exposed to untreated soil and soil treated with nano-Ag coated with PVP, oleic acid, or citrate. The investigators observed avoidance behavior in *E. fetida* after 48 hours of exposure to nano-Ag-treated sandy loam soils at concentrations of 6.92–7.42 mg/kg-soil, which are comparable to PECs of nano-Ag in sewage sludge (see Section 4.5). *E. fetida* avoided soils treated with nano-Ag and AgNO₃ at equivalent total silver concentrations, indicating that under these circumstances and based on silver mass alone, both substances were equally toxic. The avoidance response to AgNO₃ was immediate, however, whereas avoidance of nano-Ag was observed only after the 48-hour exposure. The investigators estimate that a maximum of 10–15 % of the total silver added as nano-Ag would have dissociated from the nanoparticles after 48 hours. As a result, they argue that these results preclude an association between avoidance of nano-Ag and concentrations of silver ions released from the nano-Ag. Furthermore, avoidance of soils treated with

smaller (15–25 nm) citrate-coated particles was statistically significantly higher than in soils treated with larger (30–50 nm) PVP-coated particles in the same type of soil. The investigators could not, however, distinguish between effects of coating and effects of size in this case and could not explain why avoidance of nano-Ag-treated soils was delayed compared to that of AgNO₃-treated soils.

Another species of earthworm, *Lumbricus terrestris*, was examined for mortality and levels of apoptosis (a more sensitive sublethal endpoint than survival or reproductive capability) in various tissues after exposure to two types of nano-Ag (average size 20.2 nm and 8.8 nm, respectively) via water, food, and soil ([Lapied et al., 2010](#)). *L. terrestris* experienced 40% mortality after exposure to 100 mg/L of 20-nm nano-Ag and 10 mg/L of 8.8-nm nano-Ag in water. No mortality was observed at lower exposure concentrations in water or in the experiments in which earthworms were exposed to nano-Ag in soil and food. Apoptotic response (measured as apoptotic cells/square millimeter [mm²]) was statistically significantly increased when *L. terrestris* was exposed to 100 mg nano-Ag (20 nm) in 1 L water or 1 kg soil or food. When *L. terrestris* was exposed to the 8.8-nm nano-Ag in water, food, and soil, statistically significant increases in apoptotic response were observed at and above 5 mg/L water, 20 mg/kg food, and 4 mg/kg soil.

Survival, hatchability, and growth of insect larvae exposed to nano-Ag were examined by Sap-Iam et al. ([2010](#)) following exposure of the larvae of the mosquito *Aedes aegypti* to nano-Ag concentrations ranging from 0.01 to 5 ppm. The investigators reported that mortality increased in a dose-related manner, increasing from 0 to 12% in larvae exposed to 1 ppm nano-Ag, followed by an increase to 90% mortality in the 5-ppm exposure group after 3 hours. This effect was even more pronounced in larvae treated with silver ions; mortality increased to 90% after 17 hours of exposure to 1-ppm silver ions.

Hypothesized Nano-Ag Mode(s) of Action in Terrestrial Invertebrates

The mode of action for nano-Ag on terrestrial invertebrates is not yet known. Roh et al. ([2009](#)) attempted to elucidate part of the mode of action for nano-Ag toxicity by analyzing expression in genes mapped to specific metabolic processes in the wild type and mutant *C. elegans* strains. The investigators reported that the significant induction of the *sod-3* gene, which is a superoxide dismutase protein, in *C. elegans* exposed to nano-Ag confirms that oxidative stress contributes to nano-Ag toxicity. These gene expressions are correlated with reproduction; this does not, however, necessarily support a causal relationship. The investigators also propose that the loss in function of certain genes might improve the reproductive potential of *C. elegans* when exposed to nano-Ag, possibly related to antioxidant response. The significant upregulation of these genes could have occurred as a compensatory mechanism in the absence of this primary antioxidant enzyme gene. The sequence of processes or events by which the *sod-3* gene contributes to a decrease in reproductive potential, however, was not explored ([Roh et al., 2009](#)).

The role of oxidative stress in the nano-Ag toxicity pathway is challenged by the results of Meyer et al. (2010). Exposure to nano-Ag resulted in comparable growth inhibition of the wild-type N2 *C. elegans* and the mutant strains *sod-2* and *mev-1*, which are known to be sensitive to oxidative stress.

Ahamed et al. (2010), however, produced similar results to those of Roh et al. (2009) in a proteomic analysis of the exposure of *Drosophila melanogaster* to 50 and 100 µg/mL of polysaccharide-coated nano-Ag. The investigators observed statistically significantly higher levels of malondialdehyde (an end product of lipid peroxidation), and *sod* and *cat* (antioxidant enzymes) in exposed larvae than in controls, showing statistically significant levels of oxidative stress. The investigators speculate that this generation of free radicals leads to DNA damage (inferred from observations of upregulated p53 and p38 levels in exposed larvae). These results were dose- and time-related, showing increases in effect from 24 to 48 hours. This evidence suggests, but does not confirm, a causal relationship between these toxic endpoints, and suggests a mode of action involving the induction of free radicals by nano-Ag exposure resulting in DNA damage and ultimate apoptosis of the cell.

6.2.3.3. Terrestrial Vertebrates

Because silver is not considered a significant risk to higher order organisms, ecotoxicological studies have traditionally focused on more sensitive and more susceptible (i.e., having greater potential for exposure) lower order organisms. Many studies investigating human health toxicity rely on mammalian bioassays from which a human response to nano-Ag is inferred; these studies are covered in detail in Section 6.3 on human health effects. Non-mammalian terrestrial vertebrates are discussed in this section, although the available data are limited to avian species.

Known Effects of Conventional Silver Exposure on Terrestrial Vertebrates

No studies were identified that have investigated conventional silver toxicity to non-mammalian terrestrial vertebrates. The 1992 data call-in for EPA's Silver Reregistration Eligibility Decision for silver and silver compounds in pesticides, however, required that one avian study be conducted using the formulated product under consideration for reregistration (U.S. EPA, 1993). As a result, proprietary studies might exist that have investigated effects on avian species.

Effects Specific to Nano-Ag Exposure on Terrestrial Vertebrates

Only two studies examining nano-Ag toxicity to terrestrial vertebrates were identified, and only one of these examined the direct effects of nano-Ag. These studies are presented in detail in Section B.8

of Appendix B. In a study by Grodzik and Sawosz (2006), chicken eggs were injected with nano-Ag to investigate its effect on the development of chicken embryos. Special attention was paid to the bursae of Fabricius (lymphoid glands contributing to immune system development) in the embryos. Although nano-Ag exposure did not affect the weight of the embryos or the weights of the hearts, livers, and eyes of the chicks, some effects were observed in the bursae of Fabricius. The investigators reported that embryos exposed to nano-Ag developed fewer and smaller lymph follicles in the bursae of Fabricius than in the control groups; statistical significance was not reported. They also observed that the surfaces of the primary and secondary canals extending between the lymphoid follicles in the bursae were larger and more wrinkled than in the controls (Grodzik and Sawosz, 2006). What effect, if any, the abnormalities observed in the bursae of Fabricius might have on normal development of the chicks is unclear. Furthermore, the nano-Ag material used in the study was not well-characterized, so the size, shape, stability, and other properties that might affect toxicity are not known.

The other study examining nano-Ag effects on terrestrial organisms is primarily a study of the caecum microflora⁴² and secondarily an examination of the histological effects of nano-Ag in tissues in the duodena of 10-day-old quail (*Coturnix coturnix japonica*) free-fed nano-Ag in drinking water (Sawosz et al., 2007). Gut flora are sometimes likened to a virtual organ within an organ because of the high level of metabolic activity associated with these organisms (O'Hara and Shanahan, 2006). Bacterial colonization in the gut has been shown to heighten immunological function in animals, and the bacterial composition in the gut might influence variations in immunological response.

The only significant effect reported in the study by Sawosz et al. (2007) was on the content of the gut microflora in the quail exposed at the highest nano-Ag concentration. Of the nine bacterial species included in the microbial caecum profile, four significantly increased in density at the 25-mg/kg nano-Ag level. Why the concentrations were reported in terms of mg/kg, when the nano-Ag was dispersed in water, is not clear from the report. The four affected bacterial species were the gram-positive lactic acid bacteria *Lactobacillus salivarius*, *Lactobacillus fermentum*, *Leuconostoc lactis*, and *Actinomyces naeslundii*. Sawosz et al. (2007) could not explain why the densities of these bacteria increased while the other species remained unchanged when exposed to nano-Ag, a known antimicrobial agent. Furthermore, the investigators note no currently available data suggest that nano-Ag interacts with constituents of the digestive tract or that it can be absorbed from the digestive tract. In this experiment, they hypothesized that nano-Ag successfully penetrated the gastric acid barrier to the stomach and passed through to the duodenum (Sawosz et al., 2007).

⁴²The caecum microflora is the natural bacterial population in the gut organs of animals and humans.

Hypothesized Nano-Ag Mode(s) of Action in Terrestrial Vertebrates

Because significant toxicity to non-mammalian terrestrial vertebrates exposed to nano-Ag has not been reported, modes of action for toxicity have not been explored.

6.3. Human Health Effects

The bactericidal effects of conventional silver have led to the incorporation of conventional silver into a range of consumer products, and as described in Chapter 2, the use of nano-Ag in antiseptic products has increased markedly in recent years. As described in Chapters 2, 4, and 5, and Section 6.1, differences in the behavior of conventional silver and nano-Ag appear to be attributable to differences in key properties, including surface area, reactivity, and quantum behavior ([ACHS, 2009](#)). This section examines and summarizes the evidence for nano-Ag-induced health effects from in vitro studies (Section 6.3.1), in vivo studies (Section 6.3.2), and human health and epidemiological studies (Section 6.3.3) as they pertain to the use of nano-Ag in spray disinfectants. In each section, the effects of conventional silver are described first, followed by information on the effects relevant to the nano-Ag life cycle specific to this use scenario. For more comprehensive information regarding the health effects of nano-Ag in general, the reader is referred to reviews by Wijnhoven et al. ([2009b](#)) and Panyala et al. ([2008](#)).

6.3.1. In Vitro Studies



Separating the physical properties affecting nano-Ag toxicity from experimental factors has proven to be an ongoing challenge in the field of nanoparticle exposure. In vitro studies can provide a useful evaluation of controlled dose and exposure scenarios and material characteristics to help identify the processes and factors potentially contributing to nano-Ag toxicity. Because testing environments for in vitro studies, however, are not identical to those for in vivo systems, in vitro studies cannot be compared directly to real-world exposures. Despite such limitations, in vitro studies can be a useful approach for exploring possible mechanisms of action at the cellular and molecular levels, as well as a tool in deciding whether or what further testing is appropriate to pursue.

Nano-Ag properties and relevant effects of nano-Ag exposure on different cell types and endpoints observed in key in vitro studies are presented in detail in Section C.2 of Appendix C, with studies presented in alphabetical order by author. Many studies have demonstrated the ability of nanoparticles to penetrate cells, although the mechanism appears to depend on the cell type, particular particle type, and exposure method. Additionally, many researchers have reported that exposures can be cytotoxic. Other

endpoints observed in association with exposure to nano-Ag include oxidative stress, induction of cytokines and chemokines as markers of inflammation, DNA and molecular damage, growth inhibition, mitochondrial perturbation, and changes in cellular morphology (see Section C.2 of Appendix C for citations and study details).

Known Effects of Conventional Silver Exposure In Vitro

The potential destabilizing effect of metal ions, including silver ions, on the mitochondrial electron transport chain has been well understood for some time. Chappell et al. (1954) demonstrated that using conventional silver electrodes to pass electricity through rabbit cerebral cortex cells increased ATPase activity, which could not be replicated with the same currents using different electrodes. Application of AgNO₃ to the cells similarly increased activity, and experiments using pigeon breast muscle mitochondria resulted in the same effects following exposure to AgNO₃. This study indicated that silver ions could increase mitochondrial respiration.

Almost four decades after the work of Chappell et al. (1954), Almofti et al. (2003) showed that, when isolated mitochondria from rat liver cells were similarly treated with silver ions, the mitochondria immediately swelled and metabolism accelerated. These mitochondrial reactions have been shown to be a preliminary step along the mitochondrial permeability transition (PT) path, a cascade of events resulting from increased permeability of proteinaceous pores in the inner mitochondrial membrane. Certain conditions including the presence of calcium and inorganic phosphate increase the likelihood of PT, which is characterized by the subsequent release of apoptogenic proteins into the cytoplasm. Silver ions induced proteinaceous pores opening, resulting in the release of the apoptogenic protein cytochrome c and apoptosis-inducing factor from the mitochondrial intermembrane space, thereby leading to programmed cell death. Notably, increased respiration and mitochondrial swelling occurred in a dose-dependent pattern correlated with silver ion concentration, and the effects were more profound in the presence of inorganic phosphate. The kinetics of silver ion effects on the mitochondria was markedly different from the classical calcium and inorganic phosphate PT. Mitochondrial respiration and swelling were immediate and independent of inorganic phosphate concentration, and known inhibitors of classical PT could not block the effect of conventional silver. The diameter of the pore opened by silver ion-PT was also larger, although whether this pore was distinct or one associated with classical PT is unclear; the pore, however, did not remain open as it does in classical PT. Additionally, the conventional silver effect was blocked by (but could be reversed following) treatment with GSH or dithiothreitol. These substances keep the sulfhydryl groups from being reduced during oxidative stress, suggesting that silver ions were causing PT by binding to the sulfhydryl groups on mitochondrial membrane proteins. Taken together, these results

suggest that silver ions induce nonclassical PT, characterized by increased mitochondrial respiration and cytochrome c signaling due to binding of silver ions to mitochondrial membrane proteins.

More recent in vitro work has examined the effect of exposure to silver on neurotoxicity endpoints and reproductive and developmental effects. With regard to neurotoxicity, Powers et al. (2010b) examined effects of silver ions on the viability, division, and differentiation of neuronotypic PC12 cells in vitro, using chlorpyrifos (CPF), a known developmental neurotoxicant, as a positive control. After 1 hour of exposure, DNA synthesis was inhibited more by exposure to 10 μM silver ions than by exposure to 50 μM CPF. Longer exposures to 10 μM silver ions reduced cell viability. With onset of cell differentiation, DNA synthesis was inhibited even further, and the acetylcholine phenotype was preferentially expressed over the dopamine phenotype.⁴³ Exposing the PC12 cells to 1 μM silver ions, on the other hand, enhanced cell numbers by suppressing ongoing cell death and impaired differentiation for both neurotransmitter phenotypes. In a similar study, Hahn et al. (2010) examined the effects of silver ions on the viability of PC12 cells, L929 fibroblasts, and spiral ganglion cells. Results showed that exposure to 10 mmol/L silver ions resulted in suppression of tissue growth without inhibiting neuronal cell growth.



Effects Specific to Nano-Ag Exposure In Vitro

Information on health effects specific to nano-Ag that have been observed in vitro is also available. Information is presented in the following sections according to notable toxicity endpoints, including reproduction and development endpoints (Section 6.3.1.1), oxidative stress (Section 6.3.1.2), damage to DNA and mutagenic effects (Section 6.3.1.3), and pro-inflammatory response (cytokine induction) (Section 6.3.1.4).

6.3.1.1. Reproduction and Development

Li et al. (2010a) evaluated the cytotoxic effects of nano-Ag on embryonic attachment and outgrowth of mouse embryos at the blastocyst stage. Blastocysts were pre-treated with 25 or 50 μM nano-Ag (~13 nm) to determine apoptosis, cell proliferation, and developmental potential and results compared to controls. Cells treated with 50 μM nano-Ag showed clear evidence of apoptosis and statistically significant inhibition of cell proliferation. Cytotoxic effects observed at this dose level led to the impaired development of blastocysts. At 50 μM nano-Ag, embryo attachment to fibronectin-coated



⁴³“Phenotype” in this case refers to a distinct behavior profile resulting from interacting neuronal networks modulated by different nerve centers in the brain.

culture dishes was higher, and a lower incidence of post-implantation developmental stages was observed. According to the study authors, these results indicate that nano-Ag affects implantation and the potential of blastocysts to develop into postimplantation embryos *in vitro*.

6.3.1.2. Oxidative Stress

Oxidative stress is a state of imbalance between radical-generating and radical-scavenging activities within a cell's mitochondrial metabolism. During the metabolism of oxygen by the electron transport chain, the production of ROS occurs. Studies have demonstrated that the ability of nanoparticles to generate ROS plays a key role in inducing toxicity. Elevated ROS production overpowers the cellular antioxidant defenses and decreases mitochondrial function. These events enhance oxidative stress, resulting in cellular damage including mitochondrial apoptosis and necrosis ([Xia et al., 2006](#)). Nano-Ag appears to generate ROS by disrupting ion and electron flux across the mitochondrial membrane, thereby interfering with the electrochemical gradient ([Almofiti et al., 2003](#)). ROS can react with critical cellular molecules (lipids, proteins, nucleic acids, and carbohydrates) and generate additional radicals. Cellular defense mechanisms such as the production of GSH peroxidase, which scavenges radicals, can counteract ROS generation, at least to some extent.

Many studies have focused on the effect of nano-Ag on skin cells due to its use in treating wounds. These studies might be useful in estimating the potential effects of dermal exposure to nano-Ag in disinfectant spray, despite the differences in the exposure scenarios. Arora et al. ([2009](#)) studied dermal fibroblasts and primary liver cells to examine possible cellular responses following dermal exposure to an antimicrobial gel for wound treatment. They showed that exposure to spherical nano-Ag particles with diameters 7–20 nm did not cause cell death despite intracellular incorporation of the particles, and that cellular antioxidant defenses were upregulated in both primary fibroblasts and primary liver cells. In a similar model of therapeutic treatment conducted by Asharani et al. ([2009](#)), starch-coated nano-Ag caused mitochondrial damage and dose-dependent ROS damage in lung fibroblast and glioblastoma cell lines. Separately, Asharani et al. ([2009](#)) measured DNA damage, presumably from ROS, and observed G2/M cell-cycle arrest possibly due to DNA damage repair following exposure to starch-capped globular particles of nano-Ag 6–20 nm in size. Although cell death was observed by Asharani et al. ([2009](#)) but not by Arora et al. ([2009](#)), both studies concluded that nano-Ag resulted in increased ROS production. Possible explanations for differing toxicities include differences in doses, properties of particles, and cellular sensitivity.

Three additional *in vitro* studies involving oxidative stress might be relevant when evaluating effects from exposure to spray disinfectants containing nano-Ag. First, a study conducted by Liu et al. ([2010b](#)), involving exposure of four human cell models (A549, SGC-7901, HepG2 and MCF-7) to

nano-Ag particles led to damage to the cellular membrane. Particles with diameters of 5, 20, and 50 nm were tested at the same mass dose (1 milligram per milliliter [mg/mL]). Elevated ROS levels in cells were measured in affected cells, which were arrested at S phase, and the ROS-generating capability was observed to be inversely proportional to the particle size.

Additionally, Carlson et al. (2008) and Hussain et al. (2005) observed decreased mitochondrial function in alveolar macrophages and liver cells, respectively, in response to nano-Ag exposure. Alveolar macrophages might be vulnerable upon exposure to sprays because their generation is the primary response in the deep lung following insult (macrophages act to phagocytose or endocytose foreign matter). The liver is one organ known to be affected in people exposed to conventional silver (Venugopal and Luckey, 1978). Carlson et al. (2008) used many of the same protocols in their study as Hussain et al. (2005), making comparisons between these two studies feasible and appropriate.

Carlson et al. (2008) observed that a loss of mitochondrial function was associated with exposure to a range of sizes of spherical nano-Ag particles (15 nm, 30 nm, and 55 nm in diameter; reported by the manufacturer), with the greatest effect observed for the 15-nm size. The toxic effect on mitochondrial function was measured by the degree of mitochondrial reduction of the tetrazolium salt 3-(4,5-dimethylthiazol-2-yl)-2,5-diphenyltetrazolium bromide (MTT) assay. For smaller particle sizes, lower doses of nano-Ag were sufficient to achieve a significant decrease compared to controls. In the same assay, no significant MTT reduction was observed when the cells were exposed to nanoscale titanium dioxide.

In liver cells, Hussain et al. (2005) observed that nano-Ag 15 nm and 100 nm in diameter showed a similar ability to impede mitochondrial function, as measured by MTT reduction, and to increase ROS production. Unlike Carlson et al. (2008), however, no significant difference was observed between the effects at different particle sizes. These studies also measured levels of the potent antioxidant GSH because it plays a key role in maintaining oxidation-reduction equilibrium within cells. Both studies found that GSH was dramatically reduced following increased exposure to nano-Ag, with a size-dependent trend, in macrophages and independently in the liver cells. Both studies also noted a dose-dependent loss of cell viability that the authors assumed was due to oxidative stress (Carlson et al., 2008; Hussain et al., 2005).

6.3.1.3. DNA Damage and Mutation



As described in Section 6.2 for biota, the antiseptic properties of nano-Ag are in part due to its ability to bind to and alter the cell membrane and for silver ions to alter the cell's DNA, which in turn interrupts cell proliferation. Nano-Ag might cause DNA damage within mammalian cells by several modes of action. By affecting the mitochondria, nano-Ag can cause an increase in ROS (as described in

the previous section), which can interact with and damage proteins or DNA ([Asharani et al., 2009](#)). Additionally, silver ions have been observed in vitro to bind directly with DNA and RNA ([Chi et al., 2009](#)). Furthermore, DNA repair mechanisms, which operate in normal functioning of the cell, depend on ATP. Reduction in cellular ATP levels through interference with mitochondrial respiration could hamper the essential enzymes for DNA repair, leading to damage ([Asharani et al., 2009](#)). DNA damage or a reduction in ATP can interfere with the cell cycle, and thus cellular proliferation ([Asharani et al., 2009](#); [Sweet and Singh, 1995](#)).

Surface coating is one property of nanoparticles that can influence toxicity (see Section 6.1.1.3); the genotoxicity of nano-Ag coated with a detergent (such as might occur in an environmental exposure) was examined by Chi et al. ([2009](#)). In this study, the investigators exposed calf thymus DNA to nano-Ag (20–50 nm, spherical) and demonstrated genotoxicity, but only in combination with a detergent. No effect was observed when the DNA was exposed to detergent alone or to nano-Ag alone. The researchers concluded that the detergent cetylpyridine bromide (CPB) formed a complex, reducing the distance between the nano-Ag particles and the calf thymus DNA. This effect was maintained until the concentration exceeded 3.3 µg/mL, when the electrostatic repulsive forces between the DNA and the particle apparently overcame the attraction from the CPB and the genotoxicity decreased.

In an exposure system using mouse embryonic and fibroblast cells, Ahamed et al. ([2008](#)) showed the DNA damage-repair proteins to be upregulated upon exposure to nano-Ag. Exposures were conducted with both nonfunctionalized and polysaccharide-functionalized nano-Ag. Similar effects on the expression of DNA damage proteins Rad51 and phosphorylated H2AX were observed for functionalized and nonfunctionalized particles, including upregulation of the cell-cycle checkpoint protein p53. The result of p53 activation is cell-cycle arrest, senescence, or apoptosis. Both nonfunctionalized and functionalized particles induced cell death in mouse embryonic and fibroblast cells, as measured by annexin V and MTT assays. Annexin V expression was lower in mouse fibroblast cells treated with functionalized nano-Ag than in those treated with nonfunctionalized nano-Ag. Mouse embryonic cells, however, did not display much difference when treated with functionalized or nonfunctionalized nano-Ag, suggesting mouse embryonic cells are more sensitive than fibroblast cells to both types of nano-Ag used in this study. Despite initiating these common responses, nano-Ag functionalized with the polysaccharide gum arabic appeared to be more genotoxic than nonfunctionalized nano-Ag (statistical significance was not reported). The coating (i.e., functionalization) of the particles was believed to prevent the formation of particle clusters, allowing functionalized nano-Ag to disperse throughout the cell. Nonfunctionalized nano-Ag tended to form clusters, resulting in exclusion from some organelles such as the nucleus and mitochondria.

Activation of p53 has been linked to ROS production; the mechanism by which p53 is upregulated following nano-Ag exposure, however, is unclear. Some evidence indicates that nano-Ag can directly interact with DNA and the DNA replication machinery. Yang et al. (2009) demonstrated in a cell-free assay that nano-Ag (30–50 nm in size) in various forms can influence DNA replication as measured by polymerase chain reaction fidelity. The authors observed similar results in *E. coli* in which the particles became bound to the genomic DNA and influenced replication. Cha et al. (2008) measured a decrease in DNA content of cells exposed to nano-Ag. Microscale silver also resulted in a decrease, but neither exposure was observed to affect mitochondria or GSH. ROS production can also lead to genotoxicity, as described in the previous section. Research investigating whether either DNA damage or p53 activation is caused directly by nano-Ag or indirectly through ROS generation is lacking.

Potential genotoxicity of nano-Ag also has been evaluated in vitro using the single cell gel electrophoresis assay (or comet assay) and the chromosome damage assay, with results suggesting that exposure to nano-Ag can result in DNA damage. Kim et al. (2010b) examined genotoxicity in L5178Y cells and BEAS-2B cells exposed to nano-Ag particles via the comet assay, with and without metabolic activation. The comet assay indicated that exposure to nano-Ag resulted in genotoxicity, with statistically significant differences in tail movement values in both cell lines and at all dose levels when compared to the respective control groups. The genotoxicity of nano-Ag also was evaluated using the comet assay and chromosomal aberration test in human mesenchymal cells in a study conducted by Hackenberg et al. (2011). In both tests, DNA damage was observed after 1, 3, and 24 hours at 0.1 µg/mL. In contrast, Lu et al. (2010) conducted a comet assay, in which human skin HaCaT keratinocytes were exposed to 100 µg/mL of citrate-coated nano-Ag (30 nm). The authors found that the coated particles were not genotoxic.

The Kim et al. (2010b) study also examined the mutagenic potential of nano-Ag particles through the mouse lymphoma thymidine (tk^{+/−}) assay, with and without metabolic activation in L5178Y cells. Results showed that although small colonies were slightly more mutagenic than large colonies in plates with and without metabolic activation, nano-Ag did not cause a statistically significant increase in the mutation frequency at any concentration. Therefore, exposure to nano-Ag was not considered mutagenic.

6.3.1.4. Pro-inflammatory Response

Several in vitro studies have investigated the effects of nano-Ag on pro-inflammatory cytokine induction within the cell. Cytokines are considered to be classic indicators of toxic effects and have been implicated in effects from exposure to other nanoparticles, particularly in the vascular system (Kreyling et al., 2006). Lung cell models have shown upregulation of pro-inflammatory cytokines following exposure to ultrafine (nano-sized) particulate matter (Brown et al., 2007). Brown et al. (2007) suggested that this

induction is caused by intracellular ROS generation. On the other hand, chromium and manganese exposures both cause induction of the pro-inflammatory cytokines Interleukin-8 (IL-8) and Interleukin-6 (IL-6) in airway epithelial cells, effects that are thought to be mediated through the epidermal growth factor receptor pathway (Pascal and Tessier, 2004). Although several signals could trigger cytokine production, including ROS, the specific signal resulting from nano-Ag exposure remains unclear.

Carlson et al. (2008) evaluated the production of several cytokines in alveolar macrophages and found that, at all doses evaluated (5, 10, and 25 $\mu\text{g}/\text{mL}$) for a range of sizes of nano-Ag (15, 30, and 55 nm), the cells produced significantly increased amounts of tumor necrosis factor- α (TNF- α), a central mediator of immune response; macrophage inhibitory protein-2 (MIP-2), a signal that recruits neutrophils to sites of inflammation; and Interleukin 1 β (IL-1 β), a mediator in the inflammatory response. IL-6, another pro-inflammatory signal, was not induced. Similarly, Greulich et al. (2009) observed that human mesenchymal stem cells exposed to nano-Ag concentrations ranging from 5 to 50 $\mu\text{g}/\text{mL}$ decreased production of IL-8, a neutrophil attractant, and IL-6. At concentrations less than 5 $\mu\text{g}/\text{mL}$, however, statistically significant increases in IL-8 production were observed when compared with controls. Samberg et al. (2010) reported a statistically significant dose-dependent decrease in viability of human epidermal keratinocytes (HEKs) and statistically significant increases in IL-1 β , IL-8, TNF- α , and IL-6 production following exposure to 0.34 $\mu\text{g}/\text{mL}$ unwashed nano-Ag of various sizes. Nano-Ag from the same source that was washed several times, however, had no effect on cell viability. The investigators believe that the toxicity of the unwashed nano-Ag preparation could be attributed to residual contamination of the nano-Ag with formaldehyde and methanol by-products of the nanomaterial production.

In a study by Trickler et al. (2010), the interactions between nano-Ag particles (25, 40, and 80 nm in diameter) and primary rat brain microvascular endothelial cells (rBMEC) were evaluated using an in vitro blood-brain barrier model to estimate pro-inflammatory mediators, including IL-1 β , IL-2, TNF- α , and prostaglandin E2 (PGE2). Pro-inflammatory responses were correlated with increased permeability of rBMEC and size of nano-Ag particles. The concentration of TNF- α and IL-1 β over time diminished at 40 and 80 nm when compared to the time-release profile at 25 nm. Larger particles (i.e., 80 nm) had less effect on rBMEC than smaller particles, which induced greater effects on all endpoints at lower concentrations or shorter times. Study authors noted that nano-Ag particles might interact with the cerebral microvasculature producing a pro-inflammatory cascade, which, if left unchecked, could further induce brain inflammation and neurotoxicity.

In a study conducted by Hackenberg et al. (2011), human mesenchymal stem cells were exposed to 0.01, 0.1, 1, or 10 $\mu\text{g}/\text{mL}$ of nano-Ag (< 50 nm), and cytokine release of IL-6, IL-8, and vascular endothelial growth factor (VEGF) was evaluated using the ELISA technique. Statically significant

increases of IL-6, IL-8, and VEGF release were observed at 1 µg/L, indicating human mesenchymal stem cell activation.

Shin et al. (2007) obtained peripheral blood mononuclear cells (PBMCs), including lymphocyte and monocyte cells, from blood drawn from healthy human volunteers. The cells were incubated in the presence of 1, 5, 10, 15, 20, or 30 ppm nano-Ag for 72 hours. The PBMCs then were resuspended in a complete medium supplemented with phytohaemagglutinin (PHA, 5 µg/L) in the absence or presence of 1, 3, 5, 10, or 20 ppm nano-Ag. PHA was used to stimulate the PBMCs to divide and produce cytokine. Nano-Ag levels greater than 15 ppm were observed to be cytotoxic and inhibited the PHA-induced cytokine production in a dose-dependent manner. The PHA effect on cell division was not affected.

6.3.2. In Vivo Studies



In vitro studies, discussed above, can improve the understanding of factors potentially contributing to the effects of nano-Ag. In vivo studies elucidate the whole-animal exposure response. Both in vitro and in vivo studies can provide insight on possible modes of action that can be used in interspecies extrapolation, with the goal of better understanding the effect of nano-Ag in a human exposure scenario (Sutter, 1995). As previously mentioned, however, the recent review conducted by the FIFRA SAP cautions that differences in the formulation of nano-Ag (e.g., generated in a laboratory vs. commercially available) reduce the reliability of extrapolating effects from experimental studies to effects of exposures to commercial products (U.S. EPA, 2010b). This section summarizes the effects of in vivo exposures of nano-Ag in animal studies. The subsections that follow describe noteworthy points, followed by a summary of the key studies. Nano-Ag properties and relevant effects of nano-Ag exposure on different cell types and a range of endpoints observed in key in vivo studies are presented in detail in Section C.3 of Appendix C, with studies presented in alphabetical order by author.



Known Effects of Conventional Silver Exposure In Vivo

The Agency for Toxic Substances and Disease Registry (ATSDR) provided a comprehensive overview of the known effects of exposure to conventional silver in their 1990 publication, *Toxicological Profile for Silver*, citing numerous scientific publications reporting health effects in animals exposed to conventional silver by inhalation, ingestion, or dermal exposure (ATSDR, 1990). ATSDR determined a no observed adverse effect level of 181.2 milligrams Ag per kilogram per day (mg/kg-day) based on animal mortality from a study by Walker et al. (1971) of rats ingesting AgNO₃ in drinking water over a 2-week exposure period. The lowest observed adverse effect level (LOAEL) for this study was 362.4 mg Ag/kg-day. In a chronic 37-week study of rats also ingesting AgNO₃ in drinking water, the LOAEL



associated with decreased weight gain was 222.2 mg Ag/kg-day ([Matuk et al., 1981](#)). ATSDR did not report specific immunological, developmental, reproductive, carcinogenic, or systemic (e.g., respiratory or GI) effects in animals resulting from ingestion of conventional silver. Oral exposure studies also demonstrated that conventional silver was deposited in the liver, spleen, bone marrow, lymph nodes, skin, and kidneys of rats ([ATSDR, 1990](#)). Dermal exposure of guinea pigs to conventional silver resulted in a LOAEL of 137.13 mg Ag/kg-day associated with decreased weight gain compared to unexposed animals; the treated animals were given 2 mL of 0.239 M AgNO₃ solution on an area of skin measuring 3.1 square centimeters (cm²) for 8 weeks ([Wahlberg, 1965](#)).

Effects Specific to Nano-Ag Exposure In Vivo

Health effects specific to nano-Ag exposure and possibly relevant to exposures associated with the use of spray disinfectants are discussed in this section. The following sections present information on effects on the central nervous and respiratory systems (Sections 6.3.2.1–6.3.2.2); effects on the liver, kidney, and urinary system (Section 6.3.2.3); effects on the cardiovascular system (Section 6.3.2.4); effects on hematology (Section 6.3.2.5); DNA damage (Section 6.3.2.6); effects on skin (Section 6.3.2.7); and effects on reproduction/development (Section 6.3.2.8).

6.3.2.1. Central Nervous System Effects



Several studies have examined the translocation of nano-Ag particles into the brain and the potential for effects. In rats, Takenaka et al. ([2001](#)) observed accumulation of nano-Ag in the brain 7 days after an acute (6-hour) inhalation exposure to nano-Ag; however, no adverse pulmonary effects were reported (see Section 5.7.2.1 for study details). Tang et al. ([2008](#)) subcutaneously injected nanoscale and microscale silver at 62.8 mg/kg into rats and observed that nano-Ag crossed the blood-brain barrier and accumulated in the brain, while silver microparticles did not. Unlike other studies such as the one conducted by Takenaka et al. ([2001](#)), which simply measured accumulation, neuronal degeneration and necrosis endpoints were measured as indicated by pyknotic, necrotic neurons. Incidences of electron-dense globular substances in both normal and pyknotic neurons were observed in vascular endothelial cells of the rats treated with nano-Ag, but not in those treated with microscale silver. Tang et al. ([2008](#)) concluded that nano-Ag accumulation in neurons over time increased the incidence of necrosis in these cells.

Two additional studies were identified that suggest exposure to nano-Ag could result in central nervous system effects through altered gene expression. Rahman et al. ([2009](#)) evaluated the effects of nano-Ag (25 nm) on gene expression in different regions of the mouse brain following exposure by

intraperitoneal injection in adult male C57BL/6N mice. After 24 hours of exposure, the caudate nucleus, frontal cortex, and hippocampus were analyzed using the Mouse Oxidative Stress and Antioxidant Defense Arrays; positive results were observed, with gene expression varying by brain region. Lee et al. (2010) also investigated the effects of nano-Ag on gene expression by exposing mice to nano-Ag of similar size over 2 weeks using a nose-only exposure system. Alterations in gene expression were observed for genes in the cerebrum and in the cerebellum, including genes associated with motor neuron disorders, neurodegenerative disease, and immune cell function, indicating potential neurotoxicity and immunotoxicity.

6.3.2.2. Respiratory System Effects

The most complete analysis of effects of nano-Ag on the respiratory system appears to have been conducted by Sung et al. (2009; 2008), who observed changes in rat lung function and inflammation parameters following exposure to nano-Ag (average size 18–19 nm) concentrations ranging from 0.7×10^6 to 2.9×10^6 particles/cubic centimeter (cm^3), although statistically significant ($p < 0.01$ – 0.05) changes were observed only at the highest dose. Statistically significant increases in inflammatory markers (albumin, lactate dehydrogenase, and total protein levels) in the bronchoalveolar lavage fluid were observed in females at the highest dose. Decreases in tidal volume, minute volume, and peak inspiration flow in males and increases in incidences of alveolar macrophage inflammation, chronic alveolar inflammation, and mixed cell perivascular infiltrate in males and females were statistically significant in the high-dose group, compared with the control group (Sung et al., 2009; 2008).

Although Ji et al. (2007) and Takenaka et al. (2001) contributed to the knowledge of potential health effects from inhalation of nano-Ag, they did not specifically examine respiratory endpoints. The 28-day inhalation exposure paradigm and analysis from Ji et al. quantified silver concentration in tissues but did not report any significant respiratory effects of exposure. In an acute exposure paradigm, Takenaka et al. (2001) measured silver in the lungs and found that only 4% of the initial silver burden remained 7 days after exposure; however, the functional effects of this accumulation were not examined. Takenaka et al. (2001) suggested that the rapid clearance of silver from the lungs could be due to phagocytosis of fine particles by macrophages or direct access of ultrafine particles in the alveolar wall to blood capillaries.

Hyun et al. (2008) evaluated the “real-life effects” of repeated exposure to nano-Ag (13–15 nm) on the nasal respiratory mucosa of rats. In the study, rats were exposed to nano-Ag via an inhalation chamber to low, mid, and high nano-Ag exposure levels, each quantified using three different metrics: particles/ cm^3 , square nanometers per cubic centimeter (nm^2/cm^3), and $\mu\text{g}/\text{m}^3$. Mid- and high-dose animals showed a significant increase in the size and number of goblet cells containing neutral mucins following

exposure to nano-Ag for 28 days (6 hours per day, 5 days per week). No histopathological changes in the nasal cavities and lungs in treated animals were observed relative to the control group. A slight increase in some mucins, including sulfomucins, was observed at the mid- and high-dose levels, but the level of increase was not associated with a toxicological outcome. Increased mucin production has been shown to be associated with a variety of respiratory diseases, however, so this endpoint might warrant further investigation (Jeong et al., 2006; Rogers, 2003; Jeffery and Li, 1997).

The study of respiratory-related health effects from exposure to nanoparticles has grown out of the study of ambient ultrafine particulate matter exposure studies. Exposure to ultrafine particles has been shown to have greater health consequences for susceptible populations, such as those with pre-existing respiratory disorders (U.S. EPA, 2009b; Pietropaoli et al., 2004). No studies were identified in the current literature examining nano-Ag health effects in models of susceptible populations.

6.3.2.3. Liver, Kidney, and Urinary System Effects

Consistent with its role in detoxification, the liver has been shown to accumulate a disproportionate amount of silver following exposure to nano-Ag (Sung et al., 2009; Kim et al., 2008; Sung et al., 2008). An oral 28-day toxicology study (Kim et al., 2008) dosed rats with a 0.5% aqueous carboxymethyl-cellulose vehicle and low (30 mg/kg), middle (300 mg/kg), and high (1,000 mg/kg) levels of 60-nm diameter nano-Ag powder suspended in the vehicle. The study was said to have been performed according to OECD test guideline 407, but the exact method of oral administration was not reported. Tissue damage was primarily observed in the liver, as indicated by incidences of bile-duct hyperplasia and inflammatory cell infiltration. Incidences of bile-duct hyperplasia, dilation of the central vein, and increased foci also were recorded for the kidneys.

In an acute oral dose study by Cha et al. (2008), the livers of mice fed either microscale or nanoscale silver were examined for RNA upregulation and for pathology. As observed using RNA analysis, seven genes in the apoptotic pathway and five in the inflammatory pathway were induced in the livers of nanoparticle-exposed mice. Histopathology of livers exposed to both micro- and nano-Ag showed infiltration of lymphocyte immune cells, suggesting inflammation. Mice treated with nano-Ag exhibited additional pathologies that were not observed in those exposed to microscale silver, including hemorrhages in the heart, lymphocyte infiltration in the intestine, and congestion in the spleen.

Elevated levels, reaching statistical significance, of alanine aminotransferase (ALT), aspartate aminotransferase (AST), and alkaline phosphatase (ALP) were also reported by Park et al. (2010a) following administration of 1 mg/kg nano-Ag. Similarly, Twari et al. (2011) observed a statistically significant increase in these and other liver function enzymes in Wistar rats injected with a solution of

nano-Ag for 32 weeks. These results suggest that repeated exposures to 1 mg/kg nano-Ag or higher might result in hepatotoxicity.

Ji et al. (2007) conducted a 28-day inhalation study in which concentrations of spherical aerosolized nano-Ag were delivered at multiples of 100 micrograms per cubic meter ($\mu\text{g}/\text{m}^3$) (the American Conference of Governmental Industrial Hygienists occupational exposure limit) for dust generated from conventional silver. The doses represented one-half, one, and five times the limit. The geometric mean diameters of nano-Ag particles in the low-, mid-, and high-concentration chambers were reported to be 12.61, 12.60, and 15.38 nm, respectively. Significant effects (vacuolization and hepatic focal necrosis) in this study were found not to be dose-related. These findings support the conclusions of the subchronic oral study conducted by Kim et al. (2008) described above and the subchronic inhalation study conducted by Sung et al. (2009) described in Section 6.3.2.2, in which the authors demonstrated bile duct hyperplasia in high-dose male and female rats. Christensen et al. (2010) investigated the feasibility of conducting a human health risk assessment for nano-Ag by conducting a literature review and similarly concluded that “the liver is expected to be a (or the) major target organ of systemic toxicity of nano-silver.”

6.3.2.4. Cardiovascular System Effects



Only one known study has evaluated effects of nano-Ag on the cardiovascular system. In this 24-hour study, Rosas-Hernández et al. (2009) exposed rat coronary endothelial cells to 0, 0.1, 0.5, 1, 5, 10, 50, or 100 $\mu\text{g}/\text{mL}$ of nano-Ag in aqueous solution. Mitochondrial function decreased at concentrations at 10 $\mu\text{g}/\text{mL}$ or less and was associated with an increase of LDH activity, an indicator of membrane disruption. At higher concentrations, the investigators observed an increase in cell proliferation that was dependent on increased production of nitric oxide. At a low concentration (5 $\mu\text{g}/\text{mL}$), nano-Ag had a vasoconstrictive effect on isolated rat aortic rings, while a vasodilative effect was observed at a high concentration (100 $\mu\text{g}/\text{mL}$). No effects were observed when the endothelium was removed from the aortic ring. These findings suggest that cardiovascular effects of nano-Ag target the vascular endothelium and could have opposite effects depending on particle size.

6.3.2.5. Hematology



Studies suggest that silver is transported to the blood of rats exposed orally (Kim et al., 2008) and via inhalation (Sung et al., 2009) to nano-Ag, but whether nano-Ag particles or just silver ions are responsible is not known. If nano-Ag is absorbed by the blood, functional consequences to the circulatory system might result. To evaluate potential medical uses in the treatment of thrombotic disorders, nano-Ag

was injected into mice to evaluate the behavior of platelets. Shrivastava et al. (2009) found that nano-Ag inhibited platelet aggregation in a dose-dependent manner in the whole blood. Results from cellular assays suggested that the particles might have affected the signaling necessary for aggregation. Many modes of action are possible. Twari et al. (2011) also has reported changes in hematology parameters, including increased white blood count, decreased platelet count, decreased hemoglobin, and decreased red blood count, in rats injected intravenously with nano-Ag at dose levels ranging from 4 to 40 mg/kg for 32 weeks.

6.3.2.6. DNA Damage

Although genotoxicity of nano-Ag has been observed in vitro, two studies were identified that evaluated DNA damage in vivo. In a study conducted by Kim et al. (2008), rats were orally exposed for 1 month to 30, 300, or 1,000 mg/kg-day of nano-Ag at 10 milliliters per kilogram (mL/kg) dosing volumes. The bone marrow of exposed rats was evaluated for chromosomal damage using a micronucleus test, and the investigators reported no significant difference compared to controls. An incomplete description of the statistical procedures was provided in this study, however, and no positive controls were used to evaluate the production of micronuclei. The data presented by Kim et al. (2008) for the treated male animals showed a modest trend toward increased micronuclei as a function of dose, using 10 animals per dose and 3 doses plus the control, but no statistical analysis was described to demonstrate either a statistically significant or nonsignificant trend. The investigators indicated that nano-Ag was found in the blood, but no information was provided to demonstrate that the nano-Ag was actually detected in the bone marrow. In summary, the investigators indicate no genetic toxicity in bone marrow in vivo caused by nano-Ag, but the data might actually show a weak effect.

Another in vivo genotoxicity study was conducted by Twari et al. (2011), in which a comet assay was conducted on blood cells after Wistar rats were injected intravenously with nano-Ag. Results showed a statistically significant increase in comet tail length from high to low dose; these results indicate damage to the DNA strand in the high-dose group.

6.3.2.7. Skin

As part of the study discussed in Section 6.3.1.3 that examined the effects of nano-Ag in primary human epidermal keratinocytes in vitro, Samberg et al. (2010) examined whether nano-Ag particles (~20–50 nm in diameter) could penetrate porcine skin in vivo and cause morphological alterations of the skin cells. Because of its comparable thickness and absorption rates, porcine skin is considered to be a good model for human skin (Monteiro-Riviere and Riviere, 1996). Pigs were topically dosed daily for

14 days with nano-Ag concentration ranging from 0.34 to 34 $\mu\text{g/mL}$, after which skin samples were examined both macroscopically and microscopically. Although macroscopic observations revealed no gross edema or erythema at any tested dose, microscopic observations showed dose-dependent increases in morphological changes at tissue layers below the stratum corneum. These changes included intracellular and intercellular epidermal edema at 0.34 $\mu\text{g/mL}$; moderate epidermal edema and focal epidermal and dermal inflammation at 3.4 $\mu\text{g/mL}$; and severe epidermal edema with severe dermal inflammation, epidermal hyperplasia, and parakeratosis at 34 $\mu\text{g/mL}$. The observed responses were not affected by particle size or washing and were reported to be typical of irritation following exposure to jet fuels ([Monteiro-Riviere et al., 2001](#)). As discussed in Section 5.7.2.2, however, no nano-Ag has been detected in tissue layers below the stratum corneum, prompting Samberg et al. ([2010](#)) to hypothesize that the observed effects resulted from translocation of silver ions to deeper tissues following their release from nano-Ag in the stratum corneum. Similar effects in pigs exposed dermally also were reported by Nadwory et al. ([2008](#)), with some increased inflammatory cell apoptosis, decreased expression of pro-inflammatory cytokines, and decreased gelatinase activity observed.

6.3.2.8. Reproductive/Developmental Effects

In a study by Li et al. ([2010a](#)), the cytotoxic effects of nano-Ag on implantation of mouse embryos at the blastocyst stage were evaluated in vivo by embryo transfer. Blastocysts were pre-treated with 25 or 50 μM nano-Ag (~ 13 nm) and transferred, and the uterine content examined at 13 days post-transfer. At 50 μM nano-Ag, increased resorption of post-implantation embryos and decreased fetal weight were observed.

6.3.3. Human and Epidemiological Studies

Nano-Ag has long been present as a fraction in colloidal silver, which is considered to be a form of “conventional silver” for the purposes of this document largely because the broad range of particle sizes that can fall under the definition of colloid does not allow for the study of the isolated effect of nanoscale particles, and because many colloidal suspensions have not been well characterized (see Section 2.2 for more detail). Recent interest in mining the colloidal silver database has yielded some information, however, suggesting that certain historical colloidal silver products have been relatively well-characterized and were found to contain relatively monodisperse nanoscale particles ([Silver Nanotechnology Working Group, 2009](#)). For example, Muller ([1926](#)) investigated exposure effects from a colloidal silver medical product, Collargol, and reported that the average particle size was 10–20 nm. Most historical studies, however, do not characterize the particles in the exposure thoroughly, and the



specific presence of nano-Ag is often difficult to determine. The following sections are intended as an overview of the state of the science of health effects from conventional silver (including the conservative assumption that colloidal silver is a form of conventional silver) exposure only. Particle properties of the exposures are reported, as available.

Chronic exposure to conventional silver has been shown commonly to result in argyria (discoloration of the skin) and argyrosis (discoloration of the eyes), due to tissue incorporation of soluble forms of conventional silver ([Wijnhoven et al., 2009b](#)). AgNO₃ is associated with lowered blood pressure, diarrhea, stomach irritation, and respiratory irritation. Inhalation or ingestion of conventional silver salts can result in fatty degeneration of the liver and kidneys, as well as blood cell abnormalities ([Venugopal and Luckey, 1978](#)). Studies have shown that soluble silver compounds can accumulate in organs, muscle tissue, and the brain, while elemental silver appears to have no known severe health effects ([Drake and Hazelwood, 2005](#)). This difference in absorption is thought to be due to differences in solubility, which is the reasoning supporting the differing threshold limits for soluble silver (0.01 milligram per cubic meter [mg/m³]) and metallic silver (0.1 mg/m³) proposed by the American Conference of Governmental Industrial Hygienists. The following sections summarize several key human studies on the health effects of exposure to different silver forms (given the limited data available for these studies, and that no relevant studies specific to nano-Ag were available, a study table appendix was not developed for this section). No studies were identified that addressed the topic of susceptible populations. Taken together, they function to provide a context for considering the human health consequences of nano-Ag.

6.3.3.1. Medical Use Studies

Known Effects of Conventional Silver Exposure

Conventional silver has long been used for medicinal purposes. Colloidal silver has been used as a dietary supplement to treat illness and, in combination with sulfadiazine, as a treatment for burns ([Drake and Hazelwood, 2005](#)). The Nanotechnology Project inventory of commercially available products reported to contain nanomaterials includes examples of these types of nano-Ag products, although the presence of nano-Ag in these products has not been verified ([Project on Emerging Nanotechnologies, 2009](#)). Germ Slayer by Aluwe, LLC, for example, is a colloidal silver, liquid dietary supplement that is reported to contain 20 ppm nano-Ag. This product is intended to kill viruses and bacteria while not harming the body, and the manufacturer recommends that it be taken upon sign of infection.

Ingestion of dietary supplements can lead to extremely high exposures, such as an estimated 70–90 µg/day ([Wijnhoven et al., 2009b](#)). In vitro studies of burn creams, such as Acticoat, show cytotoxicity upon exposure ([Paddle-Ledinek et al., 2006](#); [Fraser et al., 2004](#); [Lam et al., 2004](#)) and raise

concerns that these products might cause health effects. Acticoat is described as a nano-Ag-coated, high-density polyethylene mesh developed by Smith & Nephew, Inc., with approximately 0.2–0.3 milligram (mg) of silver per mg of mesh ([Trop et al., 2006](#)). Although the magnitude of these exposures is unlikely to occur in the case of a spray disinfectant, the health effects associated with exposure via dietary supplements and burn creams might illustrate worst-case scenarios for ingestion and dermal contact, respectively.

Mirsattari et al. ([2004](#)) described the case of a 71-year-old man who, upon taking a homemade colloidal silver dietary supplement for 4 months, developed seizures, followed by coma, and death. His blood-plasma-silver level was 41.7 nM, as compared to the normal range of 1.0–2.3 nM, and his urinary level for a 24-hour period was 47.28 nM, as compared to the normal range of 0.0–0.46 nmol/L. Additionally, silver levels in erythrocytes and in cerebral spinal fluid were extremely high. No other significant contaminants were found in the body. Blood purification attempts successfully removed silver from the blood, reducing the plasma-silver level from 41.7 to 1.9 nmol/L over 6 days. The silver concentration in the brain measured at autopsy, however, was elevated, with 0.068 microgram per gram ($\mu\text{g/g}$) reported in the cerebrum (compared to 0.029 $\mu\text{g/g}$ in a control sample). The cellular mechanism of conventional silver neurotoxicity in this case is not clear ([Györi et al., 1991](#); [Rungby et al., 1987](#); [Rungby and Danscher, 1983](#)).

Two other clinical cases documenting neurological effects following conventional silver exposure have been reported by Ohbo et al. ([1996](#)) and Iwasaki et al. ([1997](#)). The exposure scenario described by Ohbo et al. ([1996](#)) involved a schizophrenic patient who had been addicted to antismoking pills containing conventional silver and displayed convulsive seizures and argyria. The patient reportedly ingested more than 20 mg of silver per day for 40 years. Blood-serum -silver levels were elevated at 1.2 micrograms per deciliter ($\mu\text{g/dL}$) (normal levels are less than 0.05 $\mu\text{g/dL}$). Levels of silver in blood plasma observed by Mirsattari et al. ([2004](#)) were more than three times those found in this study. Sixty-three days following treatment, serum -silver levels had been reduced to 0.2 $\mu\text{g/dL}$ and seizure activity ceased. Iwasaki ([1997](#)) studied a case involving a burn patient treated with a silver sulfadiazine cream; the male patient developed severe neurotoxicity that reduced brain tissue weight (determined post mortem), decreased mental ability, and increased blood-silver levels. Although the patient eventually died, his renal function had previously been compromised, which is thought to have contributed to the dramatic toxicity observed in this case.

Other investigations of asymptomatic general argyria from medical applications are reported by Kakurai et al. ([2003](#)) and Van de Voorde et al. ([2005](#)). Exposures in these cases were associated with silver acupuncture needles and argyrophedrine nose drops, respectively. Argyria is the most common health effect from exposure to conventional silver in general; as the cases above illustrate, confounding

and small sample sizes impair the ability to demonstrate statistically significant associations between the exposures and outcomes ([Drake and Hazelwood, 2005](#)).

Effects Specific to Nano-Ag Exposure

Nano-Ag toxicity has not been extensively studied with regard to medical use; several studies of nano-Ag wound dressings, however, provide insight on the potential effects resulting from dermal exposure. For example, Trop et al. ([2006](#)) documented the case of a previously healthy, 17-year-old patient who suffered burns over 30% of his body as the result of an accident. After cleaning and debriding the patient's wounds under anesthesia, the burns were covered with Acticoat and moistened with sterile water and the areas were wrapped with sterile gauze. The Project on Emerging Technologies' nanomaterial database reports that the concentration of nano-Ag in Acticoat is 70–100 ppm and the particle size ranges from 1 to 100 nm ([2009](#)).

The patient's Acticoat dressings were changed on days 4 and 6 following surgery. On day 6, the patient presented with argyria-like skin discoloration, lack of energy, loss of appetite, elevated liver enzymes, a slightly enlarged liver and spleen, and normal renal function. On day 7, laboratory tests revealed concentrations of 107 micrograms silver per kilogram ($\mu\text{g}/\text{kg}$) in the blood and 28 $\mu\text{g}/\text{kg}$ silver in the urine. The patient reportedly was not exposed to any other form of silver. The Acticoat dressings were immediately removed, and the patient's facial discoloration reversed. At 7 weeks, however, the levels of silver in the blood and urine, although four-fold lower, remained elevated; 10 months following treatment, silver concentration had returned to within normal levels (0.9 $\mu\text{g}/\text{kg}$ in the blood and 0.4 $\mu\text{g}/\text{kg}$ in the urine) ([Trop et al., 2006](#)).

6.3.3.2. Occupational Studies

Known Effects of Conventional Silver Exposure

Although case studies of human exposure to conventional silver are common, no studies were identified that specifically report effects from exposure during the manufacture or use of nano-Ag spray disinfectants. A few studies evaluated the effects of exposure to nano-Ag or substances containing nano-Ag, where the exposure route could be similar to possible exposures to commercial spray disinfectants. These studies are described below and are also mentioned in Section 5.7.1.4.

Rosenman et al. ([1987](#)) conducted a cross-sectional study of workers in a plant producing AgNO_3 , silver oxide, AgCl , and silver cadmium oxide powders, as well as silver ingots. Air sampling in the factory by the Occupational Safety and Health Administration resulted in calculated time-weighted averages, assuming an 8-hour exposure period, of 0.04–0.35 mg/m^3 . Particle size and other dosimetric

factors were not measured. Of the 27 workers in the study, 6 had general argyria and 20 had argyrosis. Most study participants had high levels of silver in the blood (mean of 1.0 $\mu\text{g}/100\text{ mL}$, with range 0.05–6.2 $\mu\text{g}/100\text{ mL}$) and in the urine (mean 11.3 $\mu\text{g}/\text{L}$, with range 0.5–52.0 $\mu\text{g}/\text{L}$), and 30% of the workers complained of nose bleeds and respiratory irritation. Kidney dysfunction, indicated by levels of the urinary enzyme N-acetyl-B-D glucosaminidase (NAG), was significantly correlated with blood-silver levels ($p < 0.05$); yet blood-silver levels were not a significant predictor of NAG levels when normalized by age. Cadmium was also found in significant levels in the urine of the workers, and this additional exposure, and exposure to solvents, makes definitive associations difficult.

Pifer et al. (1989) compared workers exposed for at least five years in positions with high exposure potential in an Eastman Kodak plant to employees at the plant in positions with low potential for exposure. Air sampling provided 8-hour time-weighted average air-borne silver concentrations of 1–100 $\mu\text{g}/\text{m}^3$, with most silver in insoluble forms. Although no cases of argyria were noted in the study, 80% of silver workers had detectible blood-silver levels, while none of the study controls had detectible levels. No organ function tests were performed as part of the study.

Case reports of individuals occupationally exposed to conventional silver complement the epidemiology studies by providing a more in-depth view of the response at the individual level. Williams et al. (1999) described the case of a 51-year-old man who displayed corneal and conjunctival argyrosis following seven years of employment in a silver refinery. Concentrations of silver in air were between 0.11 and 0.17 mg/m^3 . No other functional abnormalities were observed. Similarly, Cho et al. (2008a) described the case of a 27-year-old employee of the mobile telephone industry whose job was to apply plating to mobile telephone subunits with aerosolized silver. After four years of occupational exposure, the employee developed general argyria. The employee's blood-silver concentration was 15.44 $\mu\text{g}/\text{dL}$, as compared to normal values between 1.1 and 2.5 $\mu\text{g}/\text{dL}$, and the urinary silver concentration was 243.2 $\mu\text{g}/\text{L}$, as compared to normal values between 0.4 and 1.4 $\mu\text{g}/\text{L}$. Despite these high internal silver levels, a complete blood count, chemistry panel, liver function test, and routine urinary analysis did not demonstrate any adverse functional effects.

Similarly, clinical examinations, both general and neurological, reported by Williams and Gardner (1995) demonstrated no negative health outcomes in the cases of two conventional silver reclamation workers with blood-silver levels of 49 and 74 $\mu\text{g}/\text{L}$. One of these workers, a 42-year-old process engineer exposed for two years, mostly through shoveling insoluble silver halide and silver oxide-containing ash, showed no argyria or other negative signs of exposure. Personal air samples in different areas of the plant measured air-silver compound concentrations of 0.0085, 1.03, and 1.36 mg/m^3 . The other reclamation worker, a 51-year-old engineer working in a refinery dominated by soluble AgNO_3 and metallic silver species for seven years, presented argyrosis and fingernail discoloration, but no other effects of exposure

were noted following clinical examination. Personal air sampling in the refinery area measured the highest concentrations ranging from 0.10 to 0.17 mg/m³ atmospheric silver. Following improved safety measures to reduce exposure, both men's blood-silver levels decreased as measured at 6, 12, and 18 months.

Effects Specific to Nano-Ag Exposure

No studies investigating nano-Ag toxicity resulting from occupational exposure were identified for this case study.

6.4. Summary of Ecological and Human Health Effects


As described in earlier chapters, the behavior of engineered nanoparticles is greatly influenced by the properties of the particles and the composition and chemistry of the surrounding environment. This influence also extends to the toxicity of nanoparticles, and some evidence suggests that particle size and surface properties affect nano-Ag toxicity. No conclusive determinations have been made concerning the degree to which specific particle or environmental properties influence nano-Ag toxicity. Particular emphasis, however, has been placed on surface coatings, which can affect the degree to which particles form clusters thereby influencing the level of uptake into the organism and cells, and subsequently organelles, including the cell nucleus.



Most information available on the effects of conventional silver and nano-Ag on biota is from bacterial studies. A robust database exists regarding the toxicity of colloidal silver and silver salts in aquatic organisms, but information on the toxicity of nano-Ag in the aquatic environment is relatively scarce. Even fewer data are available for terrestrial organisms on the effects of exposure to conventional silver or nano-Ag.

Although the effects of silver ions from nano-Ag particles are presumed to be similar to effects of silver ions from conventional silver, the rate of ion release and the proximity of that release to the receptor surface appear to affect toxicity, as demonstrated in bacterial assays. These studies also have demonstrated that nano-Ag can result in adverse effects on gram-negative, gram-positive, autotrophic, heterotrophic, and nitrifying species of bacteria. Microbial assays suggest that nano-Ag also can result in greater toxicity to bacteria than silver ions alone. Studies on embryonic zebrafish, a freshwater vertebrate, indicate that nano-Ag can be taken up and can affect development. Studies in which nano-Ag was sonicated demonstrate higher toxicity, suggesting that the form of the silver (i.e., as particles or ions) plays a role in inducing a toxic response.

Silver ions and complexes interfere with ion transport pathways in freshwater invertebrates, and appear to affect marine organisms by altering ionic tissue concentrations. Differences in the toxic responses from exposure to ionic silver, silver complexes, and nano-Ag have been observed, and these responses tend to vary with water quality conditions. Overall, many model aquatic organisms (e.g., *C. reinhardtii*, *D. magna*, *D. rerio*) are sensitive to nano-Ag exposure, but they appear to be less sensitive than bacteria. Some evidence from studies on fish indicates that exposure to nano-Ag activates certain “stress-response” genes and that the particles can enter key organs and organelles, resulting in physical and toxic effects. Additional evidence, although limited, indicates that nano-Ag is cytotoxic, inhibits growth, and alters the genome in some plants and soil macroinvertebrates.

Conventional silver affects mitochondrial and cytochrome c signaling in mammalian cells, which can cause cell death. Exposure to conventional silver also causes argyria and argyrosis, which are cosmetic effects associated with the distribution of silver in the body following circulation in the blood.  Gastrointestinal distress, seizures, and neurotoxicity have been reported in humans ingesting very high levels of colloidal silver. At the cellular level, nano-Ag has been shown to bind to and enter cells, generate ROS, affect mitochondrial function, and result in genotoxicity.

In vivo mammalian studies with conventional silver suggest systemic toxicity, reported as decreased weight gain following ingestion and dermal exposure, and cell death following inhalation exposure. Nano-Ag has been demonstrated to cause upregulation of gene expression pathways for cell death, inflammation in the liver and kidney following ingestion exposure, and adverse effects in the heart, intestine, and spleen. Inhalation exposure to nano-Ag also was demonstrated to affect liver, kidney, and lung function. Nano-Ag has been shown to accumulate in the olfactory bulb and brain following inhalation exposure, although the toxic effects have not been elucidated fully. Genotoxicity has not been demonstrated in whole-animal studies.

For spray disinfectants, the potential for human and biotic nano-Ag toxicity depends on the level of exposure to nano-Ag and related silver compounds from these products, and also aggregate exposure to nano-Ag from other products containing nano-Ag. Toxicity of nano-Ag is dictated by the abundance and bioavailability of nano-Ag in environmental compartments, suggesting that factors influencing release scenarios, transport, transformation, and fate processes, and exposure potential of nano-Ag all influence toxicity.

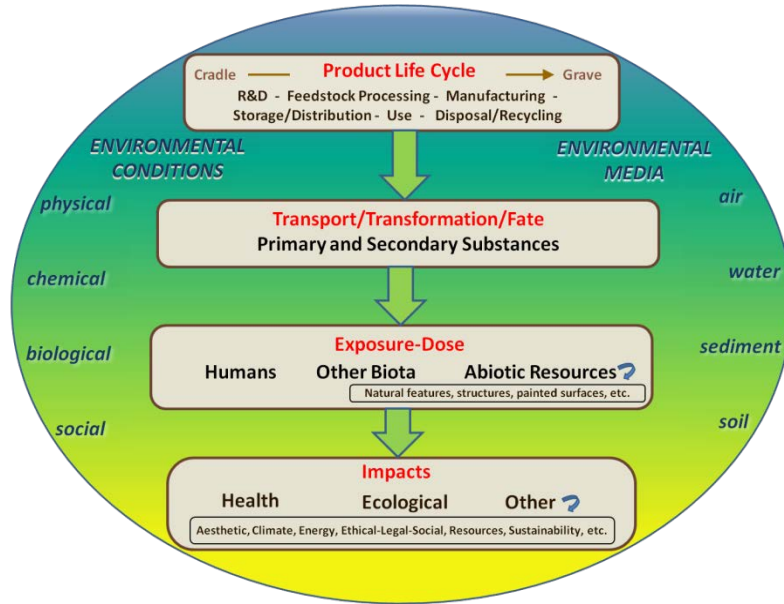
Chapter 7. Summary

This chapter summarizes the information presented in the preceding chapters on nanoscale silver (nano-Ag) in disinfectant spray and highlights several information gaps identified in this document, particularly issues that were prioritized through a collective judgment process at a workshop held in January 2011 ([ICF, 2011](#)). The outcomes of that workshop and their relevance to future research and risk assessment efforts also are described.

As discussed in the Preamble and Chapter 1, this case study makes use of the Comprehensive Environmental Assessment (CEA) approach, which offers both a *framework* for systematically organizing complex information and a *process* of collective judgment to evaluate such information. This document is structured around the CEA framework (Figure 7-1) with chapters devoted to product life-cycle stages (feedstocks, production processes, uses, disposal, and other aspects of the life-cycle value chain); transport, transformation, and fate processes; exposure-dose; and ecological and human health impacts. Such an extended perspective on the “cradle-to-grave” life-cycle approach ultimately will support a more holistic understanding of nano-Ag in research planning and risk management efforts. Given the relatively immature state of the science and limited understanding of many issues surrounding nanomaterials, this document is focused on research planning rather than attempts to complete an actual assessment. It therefore does not draw conclusions about environmental, ecological, or human health risks related to nano-Ag in disinfectant spray. Instead, this case study provided a basis for identifying and prioritizing research areas to support future assessment efforts and contribute ultimately to policy and regulatory decision-making.

As summarized in Figure 7-2, the first step of the CEA process is to compile information in the CEA framework, which is represented by this document. For this nano-Ag case study, the next step of the process involved having selected reviewers and the general public evaluate the External Review Draft of this document (dated August 2010) for completeness, accuracy, clarity, and other considerations, including whether information gaps⁴⁴ identified throughout the document were fully and adequately stated. Selected reviewers who participated in a January 4–6, 2011 workshop also were asked to identify

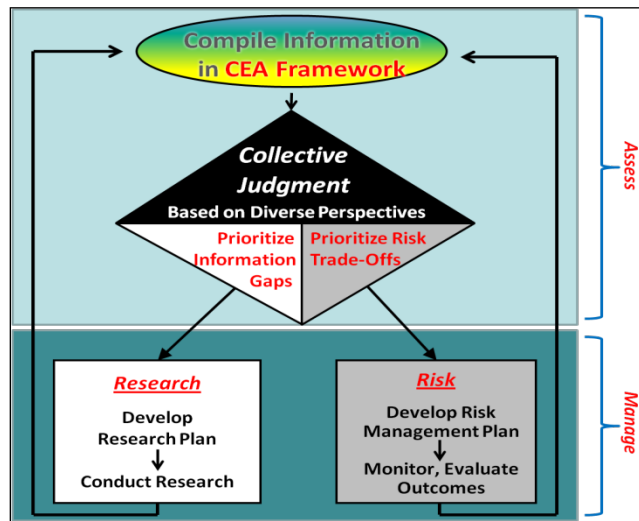
⁴⁴Information gaps are referred to throughout this document variously as data gaps or research questions or needs. Not all such “issues” would necessarily be addressed through empirical research (e.g., manufacturing data or monitoring data would not require experimental studies), but the commonly used term “research needs” is sometimes applied loosely here. Such “needs” might be more accurately termed “desired data” from a risk assessment perspective and do not signify requirements based on regulatory or policy determinations.



Source: <http://www.epa.gov/nanoscience/files/CEAPrecis.pdf>

Figure 7-1. Comprehensive environmental assessment framework.

The CEA framework is used to organize, systematically, complex information in evaluations of the environmental implications of selected chemicals, products, or technologies (i.e., materials). The framework starts with the inception of a material and encompasses the environmental fate, exposure-dose, and impacts. Notably, the sequence of events is not always linear when, for example, transfers occur between media or via the food web. In addition, a variety of factors influence each event, including differences in environmental media and the physical, chemical, biological, and social conditions in which the material event occurs. Details on these influential factors are thus included throughout the framework when possible.



Source: <http://www.epa.gov/nanoscience/files/CEAPrecis.pdf>

Figure 7-2. Steps in the CEA process.

The CEA process involves a series of steps that result in judgments about the implications of information contained in the CEA framework. Compiling information in the CEA framework is fundamental for a given material, but is only a first step in the CEA process. Next, the information in the framework is evaluated using a collective judgment technique (i.e., a structured process that allows the participants representing a variety of technical and stakeholder viewpoints to learn from one another, yet form their own independent judgments). The result of the collective judgment step is a prioritized list of risk trade-offs and information gaps that then can be used in planning research and developing adaptive risk management plans. The knowledge gained from these research and risk management activities feeds back in an iterative process of periodic CEA updates.

and prioritize information gaps or research questions on nano-Ag using a specific type of collective judgment methodology, nominal group technique. Details about the Nanoscale Silver Case Workshop are included in a summary report ([ICF, 2011](#)), and a brief description is provided in Section 7.3.1.

Section 7.3.2 discusses how the information presented in this case study document and compiled during the workshop can be used in nanomaterials research planning. Finally, Section 7.3.3 considers how the information in this document, prioritized research directions from the workshop, and emerging research can be integrated into subsequent assessment efforts guided by the CEA approach.

7.1. Case Study Highlights



This section highlights what is known about nano-Ag in disinfectant spray as it relates to each major component of the CEA framework, specifically product life-cycle stages (feedstocks, manufacturing, distribution, storage, use, and disposal/recycling); transport, transformation and fate processes; exposure-dose characterization for biota and environmental resources and for humans; and ecological and human health effects. Readers are referred to the detailed discussions and literature citations on each of these components in the preceding chapters. Some of the discussion and knowledge gaps identified below focus on nano-Ag in particular, while other parts refer to nanomaterials in general. The discussion therefore might be useful to those conducting research on nano-Ag and those involved in designing future research and assessment efforts for nanomaterials in general.

7.1.1. Terminology



Within the field of nanotechnology, several terms, including “nanomaterial” itself, are evolving. As stated in Chapter 1, this document does not attempt to use a definitive definition for nanomaterial or even for “nano-Ag.” Although nano-Ag generally refers to engineered nanoscale silver particles between 1 and 100 nanometers (nm) in size, the term encompasses a range of formulations with different physicochemical characteristics. As discussed below, physicochemical characteristics influence nanomaterial behavior and eventual impact in the environment in ways that are not entirely understood. Caution is therefore warranted when extrapolating generalizations about nano-Ag from one formulation. Forms of silver that are not intentionally engineered at the nanoscale are referred to as “conventional silver.” Various conventional silver formulations that consist of different particle sizes exist, including some with nanoscale dimensions. For other terms related to the field of nanotechnology, refer to Section 1.4.

7.1.2. Conventional Silver

In the environment, silver (Ag) rarely exists as a pure metal; instead, it is usually found as a metal alloy, associated with minerals, or a compound. Common forms of silver include gold-silver alloys, argentite (Ag_2S), cerargyrite (AgCl), silver sulfide (Ag_2S), silver nitrate (AgNO_3), and silver chloride (AgCl). These compounds form from one of the three cationic states (Ag^+ , Ag^{2+} , and Ag^{3+}) that exist in addition to the metallic state (Ag^0). Silver in various forms is released into the environment by wind and water erosion of soils and rocks containing silver. Levels of silver in the environment on the order of 0.3 part per million (ppm) in soils, 0.2 microgram per liter ($\mu\text{g/L}$) in fresh water, and 0.25 $\mu\text{g/L}$ in sea water have been observed. Silver in the microgram-per-gram ($\mu\text{g/g}$) range has been detected in biota, particularly fish and shellfish.

7.1.2.1. Historic and Current Uses of Silver and Silver Compounds

Silver has been used for centuries to sterilize liquids, treat wounds, and prevent infection, and its medicinal use continues today, such as for wound dressings and catheters. Although silver has been used heavily in photography since the late 1900s, the recent rise in digital photography has led to an approximately 20% decline in its use in this industry. With the highest thermal and electrical conductivities of any pure metal over a range of temperatures, Ag has numerous other applications, such as use in household switches and batteries, as mirror coatings, and in antibacterial disinfectants, jewelry, silverware, coins, and cloud seeding.

7.1.2.2. Historical Environmental Silver Levels

The variety of silver applications outlined above has led to environmental releases and subsequent elevations in Ag levels. Several field and oral toxicity studies indicate ecological and toxicological effects from silver concentrations reaching the nanogram-per-liter (ng/L) range in waters surrounding industrial facilities. A 1997 data analysis suggests that silver emissions to the environment were highest in North America (4,500,000 kilograms per year [kg/yr]), followed by Asia and Europe. The same analysis indicates that, within the United States, approximately 65% of emitted silver enters landfills, 18% enters the environment via tailings, and 13% derives from leachate associated with mining and production processes.

Several regulatory agencies have guidelines or restrictions for silver levels in environmental or occupational settings. The U.S. Environmental Protection Agency's (EPA's) National Secondary Drinking Water Regulations recommend that drinking water levels not exceed 0.10 milligram per liter (mg/L) or

ppm) of total silver. This guideline is not based on potential health effects, but rather a cosmetic condition known as argyria, which is characterized by silver accumulation in the skin that leads to a blue or blue-gray color. EPA has not established an ambient water quality criterion for human health due to insufficient data and thus each state may choose to enforce the 0.10 mg/L guideline. Some states have established chronic water quality criteria or maximum contaminant levels, however, to protect aquatic life. The need for more data led EPA to withdraw its proposed chronic ambient water quality criteria in the early 1990s, but EPA has established a maximum acute concentration of 3.2 µg/L in fresh water and 1.9 µg/L in salt water. State agencies are responsible for enforcing these levels/guidelines when issuing discharge permits. In addition, the Agency established an oral reference dose of 0.0005 milligram per kilogram per day (mg/kg-day) based on a chronic human exposure study. The Occupational Safety and Health Administration and the American Conference of Governmental Industrial Hygienists have established an occupational exposure limit of 0.01 milligram per cubic meter (mg/m³) for silver metal, silver compounds, and soluble silver compounds ([U.S. EPA, 2009g](#)). The National Institute for Occupational Safety and Health Administration also recommends 0.01 mg/m³ as an 8-hour, time-weighted average exposure limit for silver metal dust and soluble compounds ([U.S. EPA, 2009g](#)). For more information related to silver exposure limit recommendations and guidelines, refer to Section 2.1.2.

7.1.3. Nanoscale Silver

Although intentionally engineering silver at nanoscales is a relatively recent development, the unintentional use of nano-Ag in various applications such as colored glass and medicinal products has occurred for centuries. As mentioned above, colloidal silver suspensions contain some particles in the nanometer size range, and they likely have been available for more than a century in various products including pesticides and medications. Recent growth in the intentional use of engineered nano-Ag in consumer products has led to more than 300 products purportedly using the material according to the Woodrow Wilson Center's Project on Emerging Nanotechnologies (PEN). Notably, the reported number of products using nano-Ag grew by more than 10-fold between March 2006 and March 2011. Most of these products claim to eliminate bacteria and their related odors in a fairly extensive variety of applications, such as cooking utensils, fabrics and socks, dietary supplements, food storage containers, appliances, and personal care items such as soap, toothpaste or make-up.

As discussed in Chapter 3 and summarized below, spray disinfectants are another category of nano-Ag products that might be used in the home, garden, or commercial settings such as hospitals and schools. Federal law requires EPA to register products designed to act as an antimicrobial or disinfectant agent in any way other than direct application to humans or pets prior to sale of the product within the

United States. With a higher surface-to-volume ratio than larger, conventional silver particles, nano-Ag could confer greater antimicrobial activity to spray disinfectants using this form of silver compared to conventional silver; several manufacturers have claimed that nano-Ag disinfectant sprays kill 99% of bacteria on a variety of surfaces and prevents odor for long periods of time. Although disinfectant spray use represents only one potential way for nano-Ag to enter the environment, it is used throughout this document as an example of how increased nano-Ag use in consumer products might affect environmental levels of silver and subsequently lead to exposure and effects in humans and biota. As mentioned above, colloidal silver products can contain nano-sized particles, and thus information on conventional silver also is presented here to offer potential insight on engineered nano-silver behavior and effects. Although the comparability of conventional silver and engineered nano-Ag is not well understood, it should be considered when interpreting or using information on conventional silver in the context of nano-Ag.

7.2. Nanoscale Silver Case Study Summary

7.2.1. Physical-chemical Properties of Nanoscale Silver

As discussed above, the term nano-Ag encompasses a variety of materials having unique physical and chemical, or physicochemical, properties. Commonly discussed physicochemical properties related to nanomaterials include particle size, morphology (shape and crystal structure), surface area, chemical composition, surface chemistry and reactivity, solubility, conductivity, magnetism, and optical properties, each of which can influence the behavior and ultimate impact of nanoparticles in the environment. The relationship between these properties and the particle's interaction with the environment is complex. Indeed, the current uncertainty surrounding this relationship has led many organizations and individual researchers to recommend that data on physicochemical properties accompany any report on nanomaterial behavior or impact in the environment. No consensus on which physicochemical properties need to be reported with experimental results, however, has been reached. The complexity of the relationship between physicochemical properties of nano-Ag and its environmental behavior or effects is discussed briefly below. Section 2.3 presents additional information on the physicochemical properties of nano-Ag.

7.2.1.1. Analytical Methods

Accurate characterization of nanomaterials such as nano-Ag in disinfectant spray is critical to understanding their potential environmental and human health effects. As discussed in Chapter 2, nanomaterial physicochemical characteristics, such as size, morphology, chemical composition, and

surface chemistry, likely are instrumental in the efficacy of the products that contain them and likely play important roles in their environmental behavior, exposure, and toxicity in ecological and human populations. Importantly, physicochemical characteristics might change after the nanomaterial is produced, incorporated into a product, and released into the environment, and moves through environmental compartments and organisms. Sensitive techniques to detect and characterize nano-Ag during each stage of its existence are therefore fundamentally relevant to understanding the potential impacts of a nanomaterial throughout its life cycle.

7.2.1.2. Analytical Methods for Laboratory or Occupational Settings

Techniques to characterize nano-Ag in the laboratory during the research and development phase include spectroscopy, chromatography, electron microscopy, and spectrometry. Once the production has begun, detecting nano-Ag in the workplace can be complicated by the presence of background levels of other nano-sized particles from other ongoing processes in the manufacturing facility, such as combustion or welding. Detecting engineered nano-Ag in the workplace requires a combination of several instruments, such as a scanning mobility particle sizer, optical particle counter, and scanning electron microscope. Currently though, the standardized protocols for monitoring suspended particulate matter in the workplace do not distinguish between ultrafine and nano-sized particles, and thus the application of these measurement techniques in tandem has been rather limited.

7.2.1.3. Analytical Methods for Environmental Media

The manufacture, use, and disposal of nanomaterials can lead to their presence in the environment and thus methods are needed to measure nanomaterials in environmental media such as water and soil. Similar to measurement efforts in the workplace, measuring nano-Ag in environmental media involves combining several techniques to characterize different aspects of the nanomaterials simultaneously. For instance, using both field-flow-fractionation and inductively coupled plasma mass spectrometry can inform researchers about the size and chemical composition of a nanomaterial in soil. Such measurements are often difficult to make though, for several reasons: (1) The physical size and cost of many instruments restrict their utility in the field; (2) the relatively low concentrations of nano-Ag in the environment are often below instrument detection limits; and (3) distinguishing naturally occurring nano-Ag from engineered nano-Ag is often difficult. Chapter 2 and Appendix A present a more detailed description of efforts to overcome these challenges and to characterize nanomaterials in a variety of environmental, laboratory, and workplace settings.

7.2.1.4. Analytical Methods for Quantifying Dose and Dose Metrics

Information on physicochemical characteristics of the nanomaterial in any particular setting influences methods for evaluating the concentration, or potential dose, of the material. For nanomaterials, distinguishing between different types of the same material is necessary, such as between two distinct size ranges of nano-Ag in a disinfectant spray. The reporting of nanomaterial concentrations is thus complicated by disagreement over whether researchers should quantify the nanomaterial based on its total mass, particle number, or surface area. Although using mass as a primary metric aligns with traditional risk assessment approaches and measurement techniques, doing so can lead to misinterpretation of results. For instance, some mass-based findings show greater toxicity from nanoparticles compared to larger sized particles of the same material; the greater surface area-to-mass ratio of nanomaterials versus larger materials rather than any intrinsic toxicity of the nanoparticles, however, could explain these results. As such, particle number and surface area have been suggested as alternative metrics to use when reporting nanomaterial results at various concentrations, although these metrics also have drawbacks. Several researchers have therefore suggested using all three metrics when reporting nanomaterial results at different concentrations.

7.2.1.5. CEA Workshop Findings on Analytical Methods

The challenges in characterizing and quantifying nanomaterials in different environments have been widely recognized in several efforts to set research goals for nanomaterials. In fact, in the Nanoscale Silver Case Study Workshop ([ICF, 2011](#)), participants identified analytical methods as the top priority. Other areas related to physicochemical properties and their relationship to nanomaterial behavior or effects also were included in the top ten priority areas, for example, physical and chemical toxicity and test method development for effects on humans and the environment. Within these general themes were more specific ideas such as (1) determining a minimum set of assays in harmonized test guidelines for nano-Ag human and ecological health effects, (2) identifying standardized methods and characterization protocols to ensure results are comparable between laboratories, and (3) evaluating which physicochemical properties are essential to characterize before, during, and after toxicity experiments. Common to each of these issues is recognizing the importance of characterizing nanomaterials at multiple stages of the product life cycle and experimental protocols (e.g., before, during, and after toxicity testing), while acknowledging the practical limitations of intensive characterization procedures. By pursuing the research directions identified here, a better understanding of which kinds of measurements are consistently important could be reached over time.

7.2.2. Life Cycle Characterization

The two major sources of the world silver supply that could be used as feedstock in nano-Ag production are mining operations and recycling of scrap silver. Mining comprises 76.6%, recycling 19.9%, and net government sales 3.5% of the world silver supply. How much silver from each source is used in nano-Ag remains a question, but one estimate is that as much as 5% of total silver production is nano-Ag production. Based on 2008 estimates, therefore, approximately 500,000 kilograms (kg) of nano-Ag are produced per year worldwide. A 2011 estimate puts production of nano-Ag in the United States alone within a range of about 2–20 tons per year.

7.2.2.1. Production

The specifics of nano-Ag production procedures are largely proprietary and, as such, few details are available on possible release points or concentrations of nano-Ag emitted during the manufacturing process. Although PEN lists a growing number of companies claiming to produce nano-Ag products, and spray disinfectants in particular, releasing information on their use of nano-Ag is at each company's discretion. Furthermore, no system exists to verify the presence of nano-Ag in commercial products listed by PEN. This dearth of information on private manufacturing methods is countered by a growing body of literature on nano-Ag synthesis in laboratory settings. Several review papers detail the strengths and weakness of common synthesis methods including chemical reduction, laser ablation, radiolysis, and vacuum evaporation. Of these and other available methods, chemical reduction using a silver salt such as silver nitrate and a reducing agent like sodium borohydride is the most common production technique for large-scale volumes. Surface coatings such as surfactants, polymers, or stabilizing ligands also are used in the synthesis process to control the natural clustering of zero-valent silver and to maintain particles in the desired size range. Although the specific choices of silver salt, reducing agent, and surface coating dictate particle size and shape, most synthesis procedures yield spherical particles less than 20 nm in size. An extensive discussion on variations in nano-Ag synthesis methods and resulting particle characteristics is included in Chapter 3.

Based on information available from patents and company websites, manufacturing nano-Ag disinfectant sprays requires mixing nano-Ag with several other ingredients such as chlorine-releasing compounds. Although specific information on the manufacturing process is sparse, procedures generally might include the following: nano-Ag synthesis, either in-house or by a supplier, followed by mechanical or chemical processes to ensure uniform consistency of all ingredients in the spray mixture, filtration to remove impurities, short-term storage of bulk spray product in tanks, and, finally, automated dispensing into bottles. Individual spray bottles presumably would be sealed after quality control procedures are

completed and then packaged into cardboard cartons for distribution to retailers. Nano-Ag, other spray ingredients, and by-products could be released during any manufacturing step but few data are available to support whether such releases in fact do occur. An exception are the two studies that demonstrated nano-Ag release into the air of a manufacturing facility during particle synthesis procedures. The possibility for worker exposure during manufacturing is discussed further in Section 5.3.2. Notably, the production life stage could also lead to nano-Ag releases into the environment from manufacturing waste deposited in landfills and wastewater streams after flushing or cleaning processing equipment, improperly treated processing waste, and cleaning surfaces contaminated with nano-Ag.

7.2.2.2. Distribution

As outlined above, nano-Ag disinfectant sprays are likely distributed in sealed plastic bottles that are then transported in cardboard cartons containing several dozen spray bottles. The cartons could be stored at an intermediate storage site, but more likely they would be opened only at retail locations where individual consumers purchase them. Damage to cartons, leaking bottles, or spills resulting from accidents involving transport vehicles all offer potential release scenarios during transport. Unless damage occurs or sealing methods are improper, however, minimal release is expected during transport.

7.2.2.3. Use

After purchasing nano-Ag disinfectant sprays, consumers might use the product, per manufacturer's recommendations, on a variety of surfaces such as walls, floors, sinks, door knobs, appliances, and furniture. Consumers are likely to use the spray in both residential and occupational settings such as restaurants, hospitals, and schools. Use in these settings likely will result in nano-Ag in air, on intended surfaces, and on other areas contaminated by overspray (e.g., human skin, pets, and food). Importantly, the conditions present where the spray is used can affect nano-Ag or spray by-products. For example, using oxidizing agents like hydrogen peroxide (H_2O_2) in conjunction with the disinfectant spray could oxidize nano-Ag particles, which would release ionic silver. Other ingredients in the spray also could affect particle behavior. The duration over which nano-Ag from disinfectant sprays remains on surfaces likely will vary based on the formulation of the spray and characteristics of the surface, but at least one company states that its product is effective for up to 24 hours. These factors (length of time the nano-Ag remains on the surface and the context in which the spray is used) likely will affect the availability of the product for uptake by humans, other biota, and environmental resources.

Various nano-Ag release scenarios are possible during the product use stage, including one in which nano-Ag might enter waste streams such as landfills or wastewater. Scenarios include disposing of

cloths used to wipe down surfaces sprayed with disinfectant, washing cleaning supplies or clothing with disinfectant on them, or spraying sinks, bathtubs, and other surfaces near drains. Releases also could occur when products containing nano-Ag, such as socks or shirts, are laundered depending on the washing conditions and fabric characteristics. In addition, direct release of nano-Ag into the environment could occur in the disinfection of trash cans, furniture, and children's toys.

7.2.2.4. Disposal



After use, nano-Ag spray disinfectant bottles likely would end up in landfills or recycling centers and thus ultimately be incorporated into municipal solid waste streams. Incineration of the solid waste could release nano-Ag into the air, while waste in landfills could release nano-Ag into the surrounding soil and ground water. Alternatively, recycling the bottles could lead to their use in manufacturing new products, which could result in nano-Ag exposure to both workers and consumers coming into contact with these new products. If spray bottles are disposed of before they are empty (e.g., by retailers clearing off shelf space), more nano-Ag would end up in municipal waste streams. Finally, disposal of products sprayed with nano-Ag disinfectant is another potential source of nano-Ag in waste sites or other areas such as illegal dumping grounds.

7.2.2.5. CEA Workshop Findings on Life Cycle Characterization

Participants in the Nanoscale Silver Case Study Workshop ([ICF, 2011](#)) suggested several ways to address the information gaps in the product life cycle for nano-Ag disinfectant sprays. For instance, they proposed evaluating issues such as (1) the potential exposure vectors for nano-Ag or nano-Ag by-products during each life-cycle stage, (2) the associated feedstocks and by-products of each life-cycle stage and how these materials might be released, and (3) ways to engage consumers and workers in conversations about how nano-Ag sprays are used. Such data-gathering efforts can play a significant role in future assessments by identifying when and how nano-Ag releases occur in the environment and subsequently lead to exposure in ecological and human populations.

7.2.3. Transport, Transformation, and Fate Processes

Each stage of the product life cycle for nano-Ag disinfectant spray could result in environmental releases. The propensity for nanomaterial physicochemical properties to change as the material moves through different environmental compartments such as air, water, and soil emphasizes the importance of understanding nano-Ag transformation, transport, and fate processes. Yet, little is known about what

governs these processes for engineered nanomaterials in general, let alone for nano-Ag. Chapter 4 summarizes what is known about environmental behavior, and key points are highlighted below.

7.2.3.1. Factors Influencing Transport, Transformation, and Fate Processes in Environmental Media

Upon release into the environment, nanoparticles generally behave in one or more of the following ways: (1) stay in suspension as individual particles; (2) form clusters with other particles (and potentially deposit or undergo facilitated transport); (3) dissolve in a liquid; and (4) chemically transform by reacting with natural organic matter (NOM) or other particles. The degree to which particle behavior follows any of these patterns depends on particle characteristics, the surrounding environment, and several physical, chemical, and biological processes. Processes affecting particle behavior include particle dissolution, during which particles release silver ions; particle clustering and deposition; and particle adsorption, transport, and transformation. The extent to which each process occurs largely depends on particle characteristics, such as size, shape, and surface coating, and on environmental conditions, such as oxygen content, pH, organic matter content, ligand concentration, and temperature. Importantly, although these processes can alter nano-Ag so that it is no longer in particle form, silver will remain in the system in other physical and chemical forms, such as free silver ions, associated with other ions, or in another speciated form. Section 4.1.2 provides a more detailed description of the ways that environmental conditions can affect nano-Ag behavior.

7.2.3.2. Transport, Transformation, and Fate Processes in Air

As discussed above, nano-Ag can enter indoor and outdoor air environments at multiple life-cycle stages. Individual nano-Ag particles diffuse at a rate inversely related to their diameter, and their size thus suggests that they likely will diffuse more readily than micrometer-sized particles of similar composition. Indoors, the diffusion rate of nanoparticle aerosols can vary with changes in indoor air movement due to temperature, ventilation, or other factors. In general though, single nanoparticles have short resident times in air due to rapid diffusion, diffusive deposition on surfaces, nanoparticle clustering, and association with larger particles. Most aerosol sprays contain nanoparticles in clusters,⁴⁵ however, which behave

⁴⁵As summarized by Nichols et al. (2002) and discussed in more detail in Chapter 1, the meanings of the terms “aggregate” and “agglomerate” as they refer to the formation of particle “clusters” are sometimes interchanged in the literature; thus, the definitions of these terms are neither specific nor consistent. To simplify the discussion for this case study, the term “cluster” is used throughout this document to indicate an aggregate or agglomerate of nanoparticles, regardless of the nature or strength of particle cohesion or the mechanisms by which the particles assemble.

differently from individual particles. As clusters, the particles can diffuse over relatively larger distances (e.g., throughout a residence) and persist for a longer time indoors than smaller particles. Importantly, individual particles that deposit on walls, floors, and other surfaces could be resuspended if they form clusters with dust particles or the surface is disturbed, for example, by individuals touching it.

Outdoors (i.e., in ambient air), all particles are eventually deposited (dry deposition) or washed out (wet deposition) to aquatic or terrestrial systems. Particles between 0.1 and 10 micrometers (μm) in size, however, generally remain in the atmosphere longer and can undergo long-range transport by wind and other forces. To reach micron size for long-range transport, nanoparticles could associate with larger particles or with other nano-sized particles through London or van der Waals forces to form clusters. The behavior of engineered nano-sized particles, such as nano-Ag, in indoor and outdoor environments is influenced by unique physicochemical properties, such as surface coatings that manufacturers use to prevent cluster formation and improve their persistence after release. Other ingredients in the spray also could affect the transport and persistence of nano-Ag in indoor and outdoor air.

7.2.3.3. Transport, Transformation, and Fate Processes in Terrestrial Systems

Similar to the discussion of nano-Ag in air, information on nanoparticle transport, transformation, and fate processes in terrestrial systems is limited. No studies specifically addressing nano-Ag transport, transformation, and fate in terrestrial systems were identified. In soil, nanoparticles can be highly mobile due to their small size, but their large surface areas (relative to size) increase their propensity to sorb to soil, which could render them relatively immobile. A combination of particle and environmental characteristics coupled with physical factors, such as temperature and precipitation, thus will influence the balance between particle movement and sorption in soil. In soils with pore water rich in dissolved organic molecules, nanoparticle stability is enhanced and in turn particles are more mobile. Changes in pH due to fertilizer addition or rain events also can increase particle mobility, while salt ions in soil reduce particle mobility by augmenting the propensity to form clusters. Nano-Ag in air, water, or soil could result in exposure to leaf surfaces and roots of plants.

7.2.3.4. Transport, Transformation, and Fate Processes in Aquatic Systems

In natural aquatic systems, the sensitivity of many organisms to silver ion means that the release of the ion from nano-Ag during transport and transformation could have a large influence on exposure and toxicity. Among the key influences of nanoparticle transport, transformation, and fate processes in aquatic systems are particle surface properties, dissolution rates, and clustering, and environmental factors such as salinity, pH, and water hardness. For example, surface properties of nanoparticles dictate how mobile they

are in aquatic environments by influencing their propensity to cluster with other particles or to deposit in sediment. Thus, nanoparticles engineered to have surface coatings that improve their solubility and suspension might be more mobile than non-coated nano-sized or larger particles.

Particle dissolution, or the release of silver ions from nano-Ag particles, also impacts transport, transformation, and fate processes for a variety of reasons. First, dissolution alters particle size and other characteristics that might affect the particle's behavior in water. Second, nano-Ag toxicity in aquatic organisms could be due to nano-Ag, silver ions from the nanoparticles, or a combination of the two; thus, understanding both particle and silver ion behavior is key. Free silver ions are rarely observed in water because they have a tendency to associate with other ions. Although the predominant form of silver ultimately will depend on the characteristics of the aquatic environment, the free ion generally associates with negatively charged ions or ligands, in solution, on particle surfaces, or on dissolved organic matter. In areas with a high oxygen content, such as on sediment surfaces or in shallow waters, silver generally forms strong complexes with ligands in organic matter, whereas in less oxygen-rich areas silver forms stable complexes with sulfide. Silver also complexes with chloride anions, although the nature of the reaction depends on whether the metal is in fresh or salt water. Environmental conditions also affect the behavior of silver in nanoparticle form; increases in salinity or ionic strength lead to greater particle clustering, which in turn decreases particle mobility. Similarly, nanoparticles can form large clusters with high-molecular-weight NOM present in many aquatic systems, which also could lead to particle deposition into sediments; association with lower molecular-weight organic matter, however, can increase particle mobility. The composition of NOM therefore can be highly influential on nanoparticle behavior, reinforcing the importance of environmental conditions in understanding transport, transformation, and fate of these materials. Likewise, pH and water hardness impact nanoparticle clustering and, in general, lower pH levels and higher mineral content result in greater mobility.

As discussed, nano-Ag could end up in natural waters after flowing through wastewater streams. Characteristics that influence nano-Ag behavior in wastewater systems include surface charge, formation of particle clusters, the presence of other spray ingredients, and the treatment method used at the facility. Although most nano-Ag and associated silver ions are removed during wastewater treatment, some could remain in treated water and ultimately enter water bodies. Evidence to date shows that most of the nano-Ag removed during treatment processes ends up in sewage sludge; sewage sludge however, is used as fertilizer for agricultural soils, and the nano-Ag could end up in soil and ground water runoff that enters surrounding terrestrial systems and waterways. Alternatively, sewage sludge disposed of in landfills could lead to leaching of the nano-Ag into subsurface soils and ground water. The degree to which nano-Ag adheres to activated sludge and is removed in wastewater treatment depends on the surface properties of the nanoparticles. In turn, adding surface coatings to stabilize particles in suspension also

might impede their clearance during wastewater treatment. Additionally, the treatment process itself can alter nanoparticle characteristics and result in transformation products such as silver sulfide as the dominate form of silver coming out of the process.

7.2.3.5. Transport, Transformation, and Fate Models

The complexity of nano-Ag environmental transport, transformation, and fate processes elucidates the need for models to predict these processes for nanomaterials. Although no models currently exist to estimate nanoparticle movement in all environmental compartments, the potential exists to link current models of airborne particle dispersion and convection with models of particles in surface waters and soils; such a linkage could create an adapted, holistic model of nanomaterial transport, transportation, and fate processes. The Models Knowledge Base that EPA's Council for Regulatory Environmental Modeling⁴⁶ has compiled contains models that might serve as a starting point for development of a nanomaterial flow model. Important possible adjustments to the models to represent nanoparticles accurately include accounting for particle clustering, sorption to suspended particles, and the potential for colloidal behavior. The verification of model predictions is hindered, however, by the limited ability to detect and quantify nanoparticles reliably under different environmental conditions with current analytical techniques.

Despite this dilemma, a few models are available that predict nano-Ag or silver ion concentrations in environmental compartments. As discussed in Section 4.5, one of these models uses estimates of nano-Ag levels in Switzerland to predict levels in air, water, and soil. The model relies on several simplifying assumptions, including that no nano-Ag transformation, degradation, bioaccumulation, or flow occurs through secondary compartments. Authors estimated that most nano-Ag is discharged to wastewater via wastewater treatment plants and that risk quotients (calculated as predicted environmental concentrations [PECs] divided by predicted no-effect concentrations) were less than 1 for both “realistic” (500 tons nano-Ag used per year) and “high” (1,230 tons nano-Ag used per year) emissions scenarios. A second model predicted silver ion fate and transport in rivers and sediments based on release from biocidal plastics and textiles using nano-Ag. Again, the lack of data made several assumptions necessary but authors showed that PECs in river waters generally were consistent with empirical data (>0.01–148 ng/L). Sediment PECs on the other hand generally were higher than measured concentrations (0.2–2 milligrams per kilogram [mg/kg]), although they were below the level reported in heavily affected river beds (150 mg/kg). Recent work used the results of the first nano-Ag model described above to develop a probabilistic material flow analysis of nano-Ag and subsequently derive probability distributions of PECs.

⁴⁶<http://www.epa.gov/crem/knownbase/index.htm>

In the United States, PECs were lowest for nano-Ag in air and sewage treatment plant effluent and highest in sediments and sewage treatment plant sludge; with the numerous assumptions used in the model, however, the ranges for some results spanned two orders of magnitude for several environmental compartments and pathways.

7.2.3.6. CEA Workshop Findings on Transport, Transformation, and Fate Processes

As described above, environmental transport, transformation, and fate of nanomaterials is a complex issue, which likely will be of critical importance in future risk assessments. Participants in the Nanoscale Silver Case Study Workshop ([ICF, 2011](#)) highlighted this topic in several suggested research themes: Fate and transport, particle dissolution, and kinetics all were identified as top research themes to pursue. Within these themes, participants suggested specific research worthy of consideration:

(1) determining which nano-Ag physicochemical properties can predict fate and transport in environmental media, (2) identifying existing information on temporal changes in ionic silver release from nanoparticles, and (3) evaluating how reactions between nano-Ag and other materials like organic matter or polymers alter particle properties.

7.2.4. Exposure-Dose

Transport, transformation, and fate processes of nano-Ag eventually lead to exposure in humans and biota. Exposure occurs when a primary or secondary contaminant, such as nano-Ag or a spray by-product, comes in contact with an outer barrier of an organism. In contrast, uptake is the process by which the material crosses a biological barrier to enter the organism, which results in the dose, or amount of substance available to interact with biological receptors or metabolic processes within the organism.

7.2.4.1. Biotic Exposure and Uptake

In biota, exposure might occur when nano-Ag disinfectant spray ingredients in wastewater treatment plants and in sewage sludge are applied to agricultural land. Alternatively, disposal of sewage sludge or solid waste containing nano-Ag in landfills might result in exposure to organisms in the surrounding soil or ground water. Aquatic species, particularly those dwelling near or in sediments, might experience higher exposure levels than those in terrestrial environments. Little information exists on how much nano-Ag use will elevate environmental concentrations of nano-Ag or species of silver, but current estimates predict that levels will increase (see Section 4.5). Actual exposure levels and related bioavailable concentrations are heavily influenced by particle characteristics, environmental conditions,

characteristics of the organism, and route(s) of uptake into the organism. An extensive discussion on the influence of each factor is included in Chapter 5. For example, particle characteristics such as size can impact whether nano-Ag passes through an organism's outer layer. On the other hand, environmental conditions such as low pH can alter particle size, which in turn might result in preferential uptake during a particular life stage of an organism, or via a specific uptake route (e.g., through the gastrointestinal tract versus the skin). In addition, other ingredients in the spray could affect nano-Ag behavior or be taken up to a greater extent in the presence of nano-Ag. Although some of the factors outlined above, such as pH, affect silver regardless of whether it is in nanoparticle form, others, like changes to surface coatings, might apply exclusively to nano-Ag.

Understanding the role that particle and environmental factors play in determining the concentration of nanoparticles taken up by an organism is complicated by the difficulty in measuring such uptake with current analytical techniques. Data do show, however, that biota, including bacteria, fungi, algae, and fish readily take up, and in some instances bioaccumulate, nano-Ag. To date, several studies focused on nano-Ag in fish demonstrate that, although fairly limited, bioaccumulation occurs to a greater extent in freshwater species. In adult fish, nano-Ag appears to absorb to the gills, which can serve as a point of entry for both nano-Ag and silver ions; in developing fish, nanoparticles can cross the egg barrier (chorion) and accumulate in tissues, including the brain. Studies evaluating nano-Ag uptake and bioaccumulation in other organisms are forthcoming, but data indicate conventional silver bioaccumulates in several organisms, including bivalve mollusks and aquatic crustaceans. In general, bioaccumulation of nano-Ag and silver ions decreases with trophic level in the water column, but statements about this relationship are tempered by the current lack of evaluations of nano-Ag in higher order species, such as fish.

Several plants, including agricultural crops such as corn, take up and accumulate conventional silver in the root system, but rarely in aboveground parts such as leaves. Little evidence is available regarding whether this pattern is applicable to nano-Ag; initial work in plants is not consistent regarding whether uptake of nano-Ag is comparable to, greater than, or less than uptake of conventional silver. Soil-dwelling invertebrates such as worms also take up nano-Ag and can pass them on to the next generation, but data in this case also are limited to a few laboratory studies. No information was identified on bioaccumulation of nano-Ag in larger terrestrial organisms, although effects in invertebrates and soil microorganisms could affect terrestrial ecosystems as a whole.

7.2.4.2. Human Exposure and Uptake



In humans, the growing number of products containing nano-Ag suggests that exposure is increasingly likely; methods to measure nanoparticle exposures are generally lacking, however, and thus information from manufacturers is the main source of information on potential exposure. As discussed in Section 5.3, the extent of exposure inevitably will depend in part on: (1) nanomaterial characteristics, such as shape and form; (2) product characteristics, like how the material is incorporated; and (3) the route of exposure to the nano-Ag in the product. The types of products claiming to contain nanomaterials and the likely exposure scenarios for those products led one group of authors to suggest that, of all of the nanomaterials considered, nano-Ag has the highest potential to result in consumer exposure. To that end, experts agree that use of cleaning products such as nano-Ag disinfectant spray is likely to result in high exposure levels via inhalation and dermal pathways, particularly to consumers. Initial evidence characterizing emissions from consumer spray products containing nano-Ag indicates that inhalation exposure to nanosized particles and larger clusters might occur, although the type of spray application method and product composition likely will influence these exposures. In both consumer and occupational populations, exposure also can occur through hand-to-mouth contact from touching or handling treated surfaces, a behavior that is particularly prevalent in children. Higher metabolic rates and greater consumption of food and water per body weight also indicate that children could be a susceptible population to nano-Ag spray use. In occupational settings, current exposure limits for conventional silver span an order of magnitude, depending on which regulatory guidelines apply. Part of the difference in exposure limits reflects higher absorption potential of soluble silver compared to non-soluble silver, but little evidence exists regarding how these limits might relate to nano-Ag exposure levels. This knowledge gap could be important, given that initial studies evaluating worker exposure in a laboratory setting and traditional manufacturing facilities found the potential for both inhalation and dermal exposures. Notably, as a disinfectant spray, nano-Ag exposure could occur in worker populations, such as janitorial staff, who are not traditionally considered in occupational studies.

The degree to which exposure leads to absorption, distribution, biotransformation (metabolism), or excretion (clearance) in humans depends on particle properties, the presence of other spray ingredients, and the route of exposure. Data indicate that nano-Ag is taken up via both inhalation and oral exposure pathways and subsequently crosses biological barriers to accumulate in tissues, including the liver, stomach, brain, and blood. Whether the silver in these tissues is ionic, soluble silver, or nano-Ag, however, is unclear. Particle size is instrumental in how inhaled particles deposit or move through the body. Studies show that nano-Ag is more likely to enter the alveolar region of the lung than conventional silver, and some translocation to other tissues can occur in a size-dependent fashion that favors nanoscale particles. Following inhalation, levels of nano-Ag and other species of silver in the lung are much higher

than in other organs, suggesting relatively limited potential translocation from the respiratory tract to other tissues. Oral exposure to nano-Ag generally leads to lower absorption than from other exposure routes, but still results in silver accumulation in multiple organs. Conventional silver also is taken up across the intestinal lining after oral exposure. Although conventional silver is likely not taken up after dermal exposure, data indicate that nano-Ag can cross the upper layers of the stratum corneum under some circumstances, and silver ions released from these particles might then penetrate into deeper layers of the skin. Exposure to nano-Ag in burn wounds results in silver accumulation in tissues, and in one case led to neurological symptoms, but absorption through healthy skin depends on the exposure conditions, particle size, and other factors. Whether absorption via any of the above pathways leads to silver in any form passing the blood-brain barrier is controversial, although at least one study shows that nanoparticles as small as 1–2 nm cannot penetrate this barrier.

Data on metabolism or transformation of nano-Ag in tissues, as well as its excretion, are currently lacking. Therefore no evidence exists on whether these processes are similar for conventional silver and nano-Ag. Importantly though, the high surface area-to-volume ratio of nanoparticles results in a dynamic coating of proteins and other extracellular molecules on the particle surface, which can ultimately impact the particle's interaction with cells and, in turn, metabolism, transformation, or excretion.

7.2.4.3. Aggregate Exposure in Humans and Biota

Even a single product like nano-Ag disinfectant spray can lead to exposure via multiple routes in humans and biota. This observation, compounded by the ever-expanding number of products claiming to contain nano-Ag and the numerous sources of naturally occurring and incidental nanoscale silver particles, points to the likelihood of aggregate exposures in both human and ecological receptors. Moreover, the high surface area-to-volume ratio and enhanced chemical reactivity of nanoparticles can modify the bioreactivity of other contaminants, such as manufacturing by-products or environmental toxicants; in turn, repeated exposure to nano-Ag via multiple pathways also could lead to greater cumulative exposures to other contaminants. In this light, models estimating the potential for nano-Ag exposure, particularly from multiple routes, would be informative; due to the lack of empirical data in relevant occupational and environmental settings, however, exposure concentrations currently are estimated with fate and transport models. As mentioned in the previous section, such models require assumptions and their applicability has yet to be determined, given the unique properties of nanomaterials compared to conventional chemicals.

7.2.4.4. Exposure and Uptake Models

The lack of data on environmental or occupational levels of nano-Ag dictates that exposure estimates are based on the few fate and transport models noted in Section 7.1.3. Although no models currently exist to estimate nano-Ag absorption, distribution, metabolism, and excretion, some tools are available to model nanoparticle deposition based on size, including the Human Respiratory Tract Model for Radiological Protection developed by the International Commission on Radiological Protection. More information on this model and estimates of particle deposition in the respiratory tract is included in Section 5.7.2.1.

7.2.4.5. CEA Workshop Findings on Exposure and Uptake

Several reports from national bodies such as the Scientific Advisory Panel for the Federal Insecticide, Fungicide, and Rodenticide Act and the Netherlands National Institute for Public Health and the Environment and in the peer-reviewed literature conclude that data on nano-Ag exposure and potential toxicity are insufficient to reach meaningful conclusions about the material's risk. Participants in the Nanoscale Silver Case Study Workshop ([ICF, 2011](#)) supported this evaluation by highlighting several research themes that could improve scientific understanding of exposure and uptake to eventually facilitate risk assessments of nano-Ag. For example, general research themes for the workshop, such as analytical methods, exposure and susceptibility, surface properties, and sources and release, included specific ways to address some of the data gaps outlined above. In particular, participants suggested the following research activities: (1) determining how to detect and characterize nano-Ag exposure in different environmental media and food, (2) investigating how parameters such as behavior and life stages of humans and biota affect susceptibility to nano-Ag, (3) identifying any influence that surface properties have on processes such as uptake and bioaccumulation, and (4) evaluating the potential exposure vectors through which nano-Ag and nano-Ag products are released to the environment during each product life-cycle stage.

7.2.5. Characterization of Effects

Nanoparticle effects on ecological and human health also are influenced greatly by particle properties and environmental conditions. Readers can refer to Chapter 6 for an extensive discussion on how specific factors, such as particle size, morphology, surface charge, and test or environmental conditions, can influence nano-Ag effects. One parameter evaluated in several studies is the potential effect that particle surface coatings have on particle cluster formation, and in turn the concentration of

particles taken up into organisms and cells. Conclusive data are lacking, however, on the degree to which specific particle or environmental characteristics impact nano-Ag toxicity. Moreover, few studies have been able to differentiate between effects from nano-Ag and silver ions released from nanoparticles. Given this technical difficulty, the discussion below highlights information on both nano-Ag and conventional silver.

7.2.5.1. Ecological Effects

Studies on conventional silver and nano-Ag effects in ecological receptors largely have focused on their bactericidal effects and outcomes in a few laboratory animals. Researchers found that similar to conventional silver, nano-Ag is toxic to many types of bacteria, both gram negative and gram positive. Data further indicate that nano-Ag is more toxic than silver ions alone, potentially due to greater ion exposure as a result of silver ions released from nano-Ag particles directly at the cell surface.

A fairly extensive body of work shows that conventional silver is toxic to fungi and bacteria, aquatic invertebrates, algae, and fish, and to some terrestrial plants. Organisms most sensitive to conventional silver include freshwater and marine phytoplankton, freshwater salmonids, and early life stage marine invertebrates. Numerous studies also have found that conventional silver disrupts ion regulation in fish, particularly freshwater species. Although sensitivity in these aquatic organisms is counterbalanced by the low bioavailability of free silver ion, nano-Ag might become more bioavailable under certain conditions, and thus pose a greater concern to these organisms as a reservoir of silver ions. To date though, relatively few studies are available on nano-Ag effects in aquatic environments. Existing work does show differences in the toxic responses of freshwater invertebrates exposed to ionic silver, silver complexes, or nano-Ag, and water conditions influence the differences in these exposures. In general, model aquatic organisms such as *Ceriodaphnia reinhardtii*, *Daphnia magna*, and *Danio rerio* are sensitive to nano-Ag, but less so than bacterial populations. Most studies on aquatic organisms have focused on fish with little to no information available on nano-Ag in aquatic mammals, amphibians, and other aquatic vertebrates. Within the body of work on fish, zebrafish (*D. rerio*) are the most widely used test species. Results indicate nano-Ag uptake and subsequent developmental effects in embryonic zebrafish. Other studies in fish suggest that nano-Ag toxicity results, at least in part, from its entry into key organs and organelles followed by changes in cellular signaling pathways and gene expression. As noted above, the extent to which nano-Ag, silver ions released from nano-Ag, or a combination of the two, is responsible for nano-Ag toxicity in fish is a topic of debate. The ability to predict toxicity in aquatic environments from nano-Ag versus conventional silver would help to shed light on this debate, but no models are currently available to assess nano-Ag toxicity. The Predicted Water Column No-Effect Concentration model and the biotic ligand model, however, are available to predict the toxicity of silver

ions released from nanoparticles in aquatic environments. Readers should refer to Chapter 6 for details these models.

Information on nano-Ag effects in terrestrial organisms is even scarcer than for aquatic species. In fact, no data were identified on nano-Ag toxicity in soil. Mixed results of conventional silver effects in terrestrial plants indicate that conventional silver might affect growth and germination. Effects of nano-Ag in plants are highly dose-dependent, but survival and growth apparently can be altered. Data suggest that nano-Ag effects are not solely due to silver ion release, but could result in part from interaction with thiol groups in cellular tubulin. Limited evidence suggests that conventional and nano-Ag can affect behavior, growth, reproduction, and survival in terrestrial invertebrates, specifically worms. These effects might be driven in part by free-radical generation followed by DNA damage and subsequent cell death, but conclusive evidence for this mechanism of action is lacking. The limited data identified for nano-Ag effects in terrestrial vertebrates indicate minimal toxicity in these animals, but further study is needed to substantiate these findings.

7.2.5.2. Human Effects

As detailed in Section 6.3, studies to elucidate effects of conventional silver and nano-Ag in humans have used a variety of in vitro, in vivo, and some epidemiology approaches. In vitro data indicate that silver ions alter mitochondrial function, resulting in release of apoptogenic signals and subsequent cell death. Other work shows dose-dependent effects of silver ion on cell replication and other developmental endpoints in mammalian cells. Nano-Ag also can penetrate cells and result in cytotoxicity, possibly due to one or a combination of the following observed effects in mammalian cells: oxidative stress, inflammation response, DNA and molecular damage, growth inhibition, mitochondrial disruption, and changes in cell morphology. Although specific responses can vary by cell type, nano-Ag elicits a toxic response from a variety of cell types.

As described in Section 6.3.2, in vivo mammalian studies indicate systemic toxicity from conventional silver exposure, as demonstrated by decreased weight gain following ingestion and dermal exposure, and cell death following inhalation exposure. In a 1990 overview of conventional silver effects, the Agency for Toxic Substances and Disease Registry determined a no observed adverse effect level of 181.2 mg Ag/kg-day). The no observed adverse effect level was based on animal mortality from a study of rats ingesting AgNO₃ in drinking water over a 2-week exposure period. The lowest observed adverse effect level for this study was 362.4 mg Ag/kg-day due to decreased weight gain. Findings indicate that nano-Ag exposure via one of several routes (e.g., oral, intravenous) can lead to gene expression changes, inflammatory response in the liver and kidney, and adverse functional effects in the lungs, heart, intestine, and spleen. Of these responses, several studies suggest that the liver might be particularly susceptible to

nano-Ag exposure. Ultimately, the route of exposure and particle characteristics will influence which specific effects are observed but the multitude of studies in this area suggests that nano-Ag exposure could result in toxic responses in mammals.

In humans, chronic exposure to conventional silver can lead to argyria, or skin discoloration, and argyrosis, or discoloration of the eyes, as soluble silver is incorporated in the tissue. Importantly, exposure to different forms of silver leads to distinct outcomes. Whereas elemental silver exposure is not associated with health effects, soluble silver is associated with several effects, including lowered blood pressure, diarrhea, respiratory irritation, and fatty degeneration in the liver and kidneys. A few case studies suggest that conventional silver exposure also can lead to neurological symptoms, but conclusions cannot be drawn due to the small sample size. A single case study of nano-Ag exposure in a teenage boy revealed elevated silver concentrations in blood and urine coupled with several symptoms, such as loss of appetite and elevated liver enzyme. Blood and urine levels of silver were still elevated 7 weeks later, but returned to normal by 10 months post-exposure.

7.2.5.3. CEA Workshop Findings on Effects

The above discussion outlines some of the large data gaps related to the effects of nano-Ag on ecological and human health. The need for better understanding of nano-Ag effects and how they relate to product life-cycle stages, transport, transformation, and fate processes, and to exposure was recognized by participants in the Nanoscale Silver Case Study Workshop ([ICF, 2011](#)). Eight research themes related to nano-Ag effects were identified, including: physical and chemical toxicity, toxicity mechanisms, and test method development for humans and ecological populations. Within these broad themes were more specific research activities such as (1) evaluating which physicochemical characteristics can help predict toxicity in humans or biota, (2) distinguishing between nano-Ag and ionic silver effects after nano-Ag exposure, and (3) measuring biological responses after short- and long-term exposures to nano-Ag in occupational settings.

7.3. Role of Case Study in Research Planning and Assessment Efforts

This document is part of a larger process to support research planning that ultimately supports future assessment and risk management efforts for selected nanomaterials or nanomaterial-enabled products or both. The purpose of this case study, and others like it ([U.S. EPA, 2010d](#)), is to help identify what data are available and what information needs to be developed to complete assessments of

nanomaterials. Compiling available information using the CEA framework (see Figure 7-1), as is done in this case study, is only an initial step in the CEA process (see Figure 7-2). A key aspect of the CEA process is engaging diverse perspectives in a structured collective judgment procedure to evaluate the information in a CEA framework (e.g., this case study). Outlined below are the results of such a collective judgment process for nano-Ag in disinfectant spray and how this information informs research planning and assessment efforts.

7.3.1. Workshop Outcomes

A variety of methods exist for deriving collective judgments about setting priorities. In this instance, a specific approach known as nominal group technique was selected and carried out in a 3-day workshop ([ICF, 2011](#)). The 23 participants in the workshop represented a cross-section of technical disciplines (e.g., manufacturing, environmental fate, exposure, ecology, toxicology, risk management) and sectors (academia, government, industry, and others). During the workshop, participants used the information in this case study document in conjunction with their own experience and knowledge to identify what types of data would be useful for completing assessments of nano-Ag in disinfectant sprays. To do this, individuals participated in round-robin fashion to describe the type of research or information they felt would most inform future assessment efforts (e.g., characterization techniques for nano-Ag in wastewater streams, or determining the half-life of nano-Ag in the environment).

Following the identification of data gaps, participants combined similar issues into broader research area themes, such as “Analytical Methods” and “Mechanism of Action.” Some questions were similar or overlapped (e.g., “How does surface coating affect toxicity to humans or biota?” and “To what extent do particle properties determine biological responses to nano-Ag?” are both related to a “Physical and Chemical Toxicity” Theme). Therefore, combining similar issues was useful provided the participants in the process agreed that no significant distinction was being overlooked. After combining individual issues into broader research area themes, a voting process ensued whereby each participant allotted 10 points to the most important research theme, 9 points to the second most critical theme, and so on, down to 1 point. Combining the points from all participants for each broader theme resulted in a prioritized list of research directions that would help support assessments of nano-Ag that then could be used to identify risk-related trade-offs using the CEA approach (see Figure 7-2). More information on the workshop itself and the prioritized research themes is in a summary report ([ICF, 2011](#)), but a brief description of the top research themes is included below. Appendix D, which is an excerpt of the summary report produced by the EPA contractor that independently conducted the workshop process, contains the complete list of prioritized research questions and the themes that participants grouped them into.

The broader research themes identified as the highest priorities for nano-Ag in disinfectant sprays focused on improving characterization methods for the materials themselves; exposure scenarios; transformation, transport, and fate processes; and toxicity in humans and other biota. Specific data gaps within these themes include, for example: (1) evaluations of nano-Ag kinetics and dissolution, such as measuring its half-life in different environmental compartments; (2) determining how nano-Ag differs from conventional silver, for instance, in terms of environmental behavior and effectiveness in consumer products; and (3) obtaining manufacturing information by, for example, collaborating with other federal agencies. The workshop process resulted in participants' identifying several issues that were not considered in the first draft of this case study, such as (1) evaluating exposure scenarios for vulnerable populations, (2) investigating whether nano-Ag releases could contribute to climate change, and (3) developing effective communication techniques to convey information on nano-Ag risks and benefits to the general public. Although some of these research needs specifically relate to nano-Ag research, others apply more broadly to nanomaterials as a whole. As such, these outcomes can support a research strategy that addresses both the data needs for individual nanomaterials and those necessary to support a better understanding of nanomaterials in general.

7.3.2. Implications for Research Planning

This work on nano-Ag and other, similar efforts on different nanomaterials ([U.S. EPA, 2010c, d](#)) are not the first to identify data needs for nanomaterials ([U.S. EPA, 2009e](#); [NSTC, 2008](#); [Tsuji et al., 2006](#)). Nevertheless, the CEA approach to research planning provides a unique perspective in four important ways: (1) emphasis on prioritization, (2) attention to general and specific nanomaterial research needs, (3) breadth of perspective, and (4) transparency.

Prioritization. As noted in the description of the Nanoscale Silver Case Study Workshop above, prioritizing information gaps is a key focus of the CEA approach. As with previous case studies, the prioritized research gaps that emerge are intended to inform decision-makers in EPA and the broader scientific community in developing research agendas that support future risk assessment and risk management goals. Such information would be expected to be considered in the context of the particular focus, budgetary constraints, ongoing research, and other considerations of any organization; however, the prioritization of potential research areas could make clearer where to focus funding within an agency's or organization's purview to support future risk management goals.

Attention to General and Specific. As demonstrated by the research needs summarized above, the case study approach lends itself to developing a research plan pertinent to individual types or applications of these materials and to nanomaterials in general. Because even small changes in the properties of a

nanomaterial or its application can influence its behavior and ultimate effects, an approach that balances research needs for many types of nanomaterials with those for specific materials or applications is necessary for the field to progress.

Breadth of Perspective. The use of the CEA framework (see Figure 7-1), coupled with input from diverse perspectives during the collective judgment step, facilitates a strategy that includes research needs spanning individual technical disciplines and sectors. This approach contrasts with the more narrowed perspective on research directions that might develop from a single agency or organization.

Transparency. Finally, the CEA approach emphasizes the need for a clear record of what information was considered and how certain information gaps were identified as high priorities. This case study and the accompanying Workshop Summary Report and others like it ([ICF, 2011](#); [U.S. EPA, 2010c](#)) illustrate an effort to provide a transparent account of how judgments about research priorities were reached.

7.3.3. Implications for Future Assessment Efforts

Efforts thus far to assess nanomaterial impacts on environmental and human health demonstrate that data gaps such as those outlined above currently impede carrying out assessments and generally restrict evaluations to limited aspects of specific nanomaterials ([Aschberger et al., 2011](#); [Walser et al., 2011](#); [Christensen et al., 2010](#); [Savolainen et al., 2010](#); [O'Brien and Cummins, 2009](#); [Zuin et al., In Press](#)). This document, and the CEA approach in general, are intended to help address the lack of data by identifying and prioritizing research areas using the holistic CEA framework and process to support a broader understanding of nanomaterials. For example, one of the top priority research themes for nano-Ag is evaluating how parameters such as nanoparticle characteristics influence exposure. Methods that are developed to characterize nano-Ag particles in environmental or occupational exposure settings could be used to improve exposure models for several nanomaterials, and thus reduce uncertainty surrounding exposure estimates in nanomaterial risk assessments. Subsequent applications of the CEA approach can then incorporate this research and other results from the research priorities identified here to develop comparative risk assessments that include life-cycle considerations, a collective decision process, and possibly additional perspectives, such as sustainability considerations, stakeholders' values, and other decision-makers' considerations.

Synthesizing information from areas as diverse as ecological and human toxicity, exposure, environmental fate, and physicochemical properties is a challenge for risk assessment in general, and not a specific issue for nanomaterials. As outlined above, CEA addresses this challenge by combining a holistic framework (see Figure 1-1) to organize information on the material under consideration and a

process that supports the structured evaluation of the available information from a diverse set of perspectives. Although CEA does not offer the only solution for integrating information from numerous scientific fields, its emphasis on holistic, transparent, and structured evaluations of such information should demonstrate an improved approach to addressing complex and difficult issues in research planning and risk management.

This page intentionally left blank.

References

- [ACGIH](#) (American Conference of Governmental Industrial Hygienists). (2010). 2010 TLVs and BEIs: Based on the documentation of the threshold limit values for chemical substances and physical agents and biological exposure indices. Cincinnati, OH.
- [ACHS](#) (Advisory Committee on Hazardous Substances). (2009). Report on nanosilver. London, England: Department for Environment, Food and Rural Affairs.
<http://www.defra.gov.uk/environment/quality/chemicals/achs/documents/achs-report-nanosilver.pdf>
- [AFSSET](#) (French Agency for Environmental and Occupational Health Safety). (2006). Nanomaterials: Effects on the environment and human health (pp. 251). France.
<http://www.afsset.fr/upload/bibliotheque/138750949955923936400847724164/afsset-report-nanomaterials.pdf>
- [Ahamed, M; Karns, M; Goodson, M; Rowe, J; Hussain, SM; Schlager, JJ; Hong, Y.](#) (2008). DNA damage response to different surface chemistry of silver nanoparticles in mammalian cells. *Toxicol Appl Pharmacol* 233: 404-410. <http://dx.doi.org/10.1016/j.taap.2008.09.015>
- [Ahamed, M; Posgai, R; Gorey, T; Nielsen, M; Hussain, S; Rowe, J.](#) (2010). Silver nanoparticles induced heat shock protein 70, oxidative stress and apoptosis in *Drosophila melanogaster*. *Toxicol Appl Pharmacol* 242: 263-269. <http://dx.doi.org/10.1016/j.taap.2009.10.016>
- [Ahmad, A; Mukherjee, P; Senapati, S; Mandal, D; Khan, M; Kumar, R; Sastry, M.](#) (2003). Extracellular biosynthesis of silver nanoparticles using the fungus *Fusarium oxysporum*. *Colloids Surf B Biointerfaces* 28: 313-318. [http://dx.doi.org/10.1016/S0927-7765\(02\)00174-1](http://dx.doi.org/10.1016/S0927-7765(02)00174-1)
- [Aitken, RJ; Creely, KS; Tran, CL.](#) (2004). Nanoparticles: An occupational hygiene review. Edinburgh, UK: Institute of Occupational Medicine for the Health and Safety Executive.
- [Akaighe, N; Maccuspie, RI; Navarro, DA; Aga, DS; Banerjee, S; Sohn, M; Sharma, VK.](#) (2011). Humic acid-induced silver nanoparticle formation under environmentally relevant conditions. *Environ Sci Technol* 45: 3895-3901. <http://dx.doi.org/10.1021/es103946g>
- [Albright, LJ; Wilson, EM.](#) (1974). Sub-lethal effects of several metallic salts - organic compounds combinations upon the heterotrophic microflora of a natural water. *Water Res* 8: 101-105.
[http://dx.doi.org/10.1016/0043-1354\(74\)90133-X](http://dx.doi.org/10.1016/0043-1354(74)90133-X)
- [Allen, H; Impellitteri, C; Macke, D; Heckman, J; Poynton, H; Lazorchak, J; Govindaswamy, S; Roose, D; Nadagouda, M.](#) (2010). Effects from filtration, capping agents, and presence/absence of food on the toxicity of silver nanoparticles to *Daphnia magna*. *Environ Toxicol Chem* 29: 2742-2750.
<http://dx.doi.org/10.1002/etc.329>
- [Almofti, MR; Ichikawa, T; Yamashita, K; Terada, H; Shinohara, Y.](#) (2003). Silver ion induces a cyclosporine a-insensitive permeability transition in rat liver mitochondria and release of apoptogenic cytochrome C. *J Biochem* 134: 43-49. <http://dx.doi.org/10.1093/jb/mvg111>
- [Amendola, V; Polizzi, S; Meneghetti, M.](#) (2007). Free silver nanoparticles synthesized by laser ablation in organic solvents and their easy functionalization. *Langmuir* 12: 6766-6770.
- [Andren, AW; Bober, TW.](#) (2002). Silver in the environment: Transport, fate, and effects (Proceedings of Argentum International Conference (August 1999) in Madison, WI). In AW Andren; TW Bober (Eds.). Pensacola, FL: Society of Environmental Toxicology and Chemistry (SETAC) Press.
<http://digital.library.wisc.edu/1711.dl/EcoNatRes.Argentumv06>
- [Armitage, SA; White, MA; KerrWilson, H.](#) (1996). The determination of silver in whole blood and its application to biological monitoring of occupationally exposed groups. *Ann Occup Hyg* 40: 331-338.

- [Arora, S; Jain, J; Rajwade, JM; Paknikar, KM.](#) (2009). Interactions of silver nanoparticles with primary mouse fibroblasts and liver cells. *Toxicol Appl Pharmacol* 236: 310-318. <http://dx.doi.org/10.1016/j.taap.2009.02.020>
- [Aschberger, K; Micheletti, C; Sokull-Klüttgen, B; Christensen, FM.](#) (2011). Analysis of currently available data for characterising the risk of engineered nanomaterials to the environment and human health--lessons learned from four case studies. *Environ Int* 37: 1143-1156. <http://dx.doi.org/10.1016/j.envint.2011.02.005>
- [Asharani, PV; Low Kah Mun, G; Hande, MP; Valiyaveetil, S.](#) (2009). Cytotoxicity and genotoxicity of silver nanoparticles in human cells. *ACS Nano* 3: 279-290.
- [Asharani, PW; Gong, ZY; Valiyaveetil, S.](#) (2008). Toxicity of silver nanoparticles in zebrafish models. *Nanotechnology* 19: 1-8.
- [ATSDR](#) (Agency for Toxic Substances and Disease Registry). (1990). Toxicological profile for silver [ATSDR Tox Profile]. (7440-22-4). Atlanta, GA: U.S. Department of Health and Human Services, Public Health Service. <http://www.atsdr.cdc.gov/toxprofiles/tp146.html>
- [Auffan, M; Rose, J; Bottero, JY; Lowry, G; Jolivet, JP; Wiesner, M.](#) (2009a). Towards a definition of inorganic nanoparticles from an environmental health and safety perspective. *Nat Nanotechnol* 4: 634-641. <http://dx.doi.org/10.1038/nnano.2009.242>
- [Auffan, M; Rose, J; Wiesner, MR; Bottero, JY.](#) (2009b). Chemical stability of metallic nanoparticles: A parameter controlling their potential cellular toxicity in vitro. *Environ Pollut* 157: 1127-1133.
- [Babu, K; Deepa, MA; Shankar, SG; Rai, S.](#) (2008). Effect of nano-silver on cell division and mitotic chromosomes: A prefatory siren. *IJNT* 2: 1.
- [Bae, E; Park, HJ; Lee, J; Kim, Y; Yoon, J; Park, K; Choi, K; Yi, J.](#) (2010). Bacterial cytotoxicity of the silver nanoparticle related to physicochemical metrics and agglomeration properties. *Environ Toxicol Chem* 29: 2154-2160. <http://dx.doi.org/10.1002/etc.278>
- [Baes, CF, III; Sharp, RD; Sjoreen, AL; Shor, RW.](#) (1984). A review and analysis of parameters for assessing transport of environmentally released radionuclides through agriculture. Oak Ridge, TN: Oak Ridge National Laboratory.
- [Baker, C; Pradhan, A; Pakstis, L; Pochan, DJ; Shah, SI.](#) (2005). Synthesis and antibacterial properties of silver nanoparticles. *J Nanosci Nanotechnol* 5: 244-249. <http://dx.doi.org/10.1166/jnn.2005.034>
- [Balogh, L; Swanson, D; Tomalia, D; Hagnauer, G; McManus, A.](#) (2001). Dendrimer-silver complexes and nanocomposites as antimicrobial agents. *Nano Lett* 1: 18-21. <http://dx.doi.org/10.1021/nl005502p>
- [Bankar, A; Joshi, B; Kumar, AR; Zinjarde, S.](#) (2010). Banana peel extract mediated novel route for the synthesis of silver nanoparticles. *Colloid Surface Physicochem Eng Aspect* 368: 58-63. <http://dx.doi.org/10.1016/j.colsurfa.2010.07.024>
- [Bar-Ilan, O; Albrecht, RM; Fako, VE; Furgeson, DY.](#) (2009). Toxicity assessments of multisized gold and silver nanoparticles in zebrafish embryos. *Small* 5: 1897-1910. <http://dx.doi.org/10.1002/sml.200801716>
- [Barber, MC.](#) (2008). Bioaccumulation and Aquatic System Simulator (BASS) user's manual version 2.2. (600/R-01/035). Research Triangle Park, NC: U.S. Environmental Protection Agency. <http://nsdi.epa.gov/ceampubl/fchain/bass/BASS%20Manual.pdf>
- [Barron, A; Smith, C.](#) (2010). Physical methods in inorganic and nano chemistry. Module: crystal structure. Houston, TX: Connexions Project, Rice University. <http://cnx.org/content/m16927/latest/>
- [Baun, A; Hartmann, NB; Grieger, K; Kusk, KO.](#) (2008a). Ecotoxicity of engineered nanoparticles to aquatic invertebrates: A brief review and recommendations for future toxicity testing [Review]. *Ecotoxicology* 17: 387-395.
- [Baun, A; Sørensen, SN; Rasmussen, RF; Hartmann, NB; Koch, CB.](#) (2008b). Toxicity and bioaccumulation of xenobiotic organic compounds in the presence of aqueous suspensions of aggregates of nano-C60. *Aquat Toxicol* 86: 379-387. <http://dx.doi.org/10.1007/s10646-008-0208-y>

- [Bearer, CF.](#) (1995). How are children different from adults? *Environ Health Perspect* 103: 7-12.
- [Behra, R; Krug, H.](#) (2008). Nanoecotoxicology: Nanoparticles at large. *Nat Nanotechnol* 3: 253-254.
- [Benn, T; Cavanagh, B; Hristovski, K; Posner, J; Westerhoff, P.](#) (2010). The release of nanosilver from consumer products used in the home. *J Environ Qual* 39: 1875-1882.
<http://dx.doi.org/10.2134/jeq2009.0363>
- [Benn, TM; Westerhoff, P.](#) (2008). Nanoparticle silver released into water from commercially available sock fabrics. *Environ Sci Technol* 42: 41334139. <http://dx.doi.org/10.1021/es7032718>
- [Bennett, I.](#) (2005). Recent developments in the physical characterisation of ultra fine particles. Paper presented at Environmental Nanoparticles - Exploring the links between Vehicle Emissions and Ambient Air: A meeting of the Automation and Analytical Management Group of the Royal Society of Chemistry in collaboration with the National Physical Laboratory, 8 June 2005, Birmingham, UK.
- [Berthet, B; Amiard, J; Amiard-Triquet, C; Martoja, M; Jeantet, A.](#) (1992). Bioaccumulation, toxicity and physico-chemical speciation of silver in bivalve molluscs: Ecotoxicological and health consequences. *Sci Total Environ* 125: 97-122. [http://dx.doi.org/10.1016/0048-9697\(92\)90385-6](http://dx.doi.org/10.1016/0048-9697(92)90385-6)
- [Bhainsa, K; D'Souza, S.](#) (2006). Extracellular biosynthesis of silver nanoparticles using the fungus *Aspergillus fumigatus*. *Colloids Surf B Biointerfaces* 2: 160-164.
- [Bianchini, A; Bowles, KC; Brauner, CJ; Gorsuch, JW; Kramer, JR; Wood, CM.](#) (2002). Evaluation of the effect of reactive sulfide on the acute toxicity of silver (I) to *Daphnia magna*. Part 2: Toxicity results. *Environ Toxicol Chem* 21: 1294-1300.
- [Bianchini, A; Playle, RC; Wood, CM; Walsh, PJ.](#) (2005a). Mechanism of acute silver toxicity in marine invertebrates. *Aquat Toxicol* 72: 67-82.
- [Bianchini, A; Rouleau, C; Wood, CM.](#) (2005b). Silver accumulation in *Daphnia magna* in the presence of reactive sulfide. *Aquat Toxicol* 72: 339-349.
- [Bianchini, A; Wood, CM.](#) (2003). Mechanism of acute silver toxicity in *Daphnia magna*. *Environ Toxicol Chem* 22: 1361-1367.
- [Bianchini, A; Wood, CM.](#) (2008). Does sulfide or water hardness protect against chronic silver toxicity in *Daphnia magna*? A critical assessment of the acute-to-chronic toxicity ratio for silver. *Ecotoxicol Environ Saf* 71: 32-40.
- [Bielmyer, GK; Brix, KV; M, G.](#) (2008). Is Cl⁻ protection against silver toxicity due to chemical speciation? *Aquat Toxicol* 87: 81-87.
- [Bilberg, K; Malte, H; Wang, T; Baatrup, E.](#) (2010). Silver nanoparticles and silver nitrate cause respiratory stress in Eurasian perch (*Perca fluviatilis*). *Aquat Toxicol* In Press, Corrected Proof: 159-165.
<http://dx.doi.org/10.1016/j.aquatox.2009.10.019>
- [Biswas, P; Wu, CY.](#) (2005). 2005 critical review: Nanoparticles and the environment [Review]. *J Air Waste Manag Assoc* 55: 708-746.
- [Bitter, W; Koster, M; Latijnhouwers, M; deCock, H; Tommassen, J.](#) (1998). Formation of oligomeric rings by XcpQ and PilQ, which are involved in protein transport across the outer membrane of *Pseudomonas aeruginosa*. *Mol Microbiol* 27: 209-219. <http://dx.doi.org/10.1046/j.1365-2958.1998.00677.x>
- [Blaser, SA; Scheringer, M; MacLeod, M; Hungerbuhler, K.](#) (2008). Estimation of cumulative aquatic exposure and risk due to silver: Contribution of nano-functionalized plastics and textiles. *Sci Total Environ* 390: 396-409. <http://dx.doi.org/10.1016/j.scitotenv.2007.10.010>
- [Bonnemann, H; Richards, R.](#) (2001). Nanoscopic metal particles - synthetic methods and potential applications. *Eur J Inorg Chem* 10: 2455. [http://dx.doi.org/10.1002/1099-0682\(200109\)2001](http://dx.doi.org/10.1002/1099-0682(200109)2001)
- [Boosalis, M; McCall, J; Ahrenholz, D; Solem, L; McClain, C.](#) (1987). Serum and urinary silver levels in thermal injury patients. *Surgery* 1: 40-43.

- [Borm, P; Klaessig, FC; Landry, TD; Moudgil, B; Pauluhn, J; Thomas, K; Trottier, R; Wood, S.](#) (2006a). Research strategies for safety evaluation of nanomaterials. Part V: Role of dissolution in biological fate and effects of nanoscale particles. *Toxicol Sci* 90: 23-32.
- [Borm, PJA; Robbins, D; Haubold, S; Kuhlbusch, T; Fissan, H; Donaldson, K; Schins, R; Stone, V; Kreyling, W; Lademann, J; Krutmann, J; Warheit, DB; Oberdorster, E.](#) (2006b). The potential risks of nanomaterials: A review carried out for ECETOC [Review]. *Part Fibre Toxicol* 3: 1-35.
- [Bottomly, JT; Edmunds, CW; Hunt, R.](#) (1909). Collargal (Crede's Colloidal Silver) reports of the committee appointed to consider the claims made regarding its effects. *JAMA* 52: 862-876.
- [Bouwmeester, H; Poortman, J; Wijma, E; vanPolanen, A; Peters, R; Hendriksen, P.](#) (2010). Transcriptomic analysis following exposure of Ag NPs on an in vitro model of the human intestinal epithelium. Paper presented at 2nd NanoImpactNet Conference, March 9-12, 2010, Lausanne, Switzerland.
- [Boxall, AB; Tiede, K; Chaudhry, Q.](#) (2007). Engineered nanomaterials in soils and water: How do they behave and could they pose a risk to human health? *Nanomed* 2: 919-927.
<http://dx.doi.org/10.2217/17435889.2.6.919>
- [Boyle, RW.](#) (1968). Geochemistry of silver and its deposit notes on geochemical prospecting for the element. Geological Survey of Canada, Vol 160. Ottawa, Ontario: Department of Energy, Mines and Resources.
- [Bradford, A; Handy, RD; Readman, JW; Atfield, A; Mühling, M.](#) (2009). Impact of silver nanoparticle contamination on the genetic diversity of natural bacterial assemblages in estuarine sediments. *Environ Sci Technol* 43: 4530-4536. <http://dx.doi.org/10.1021/es9001949>
- [Brady, MJ; Lisay, CM; Yurkovetskiy, AV; Sawan, SP.](#) (2003). Persistent silver disinfectant for the environmental control of pathogenic bacteria. *Am J Infect Control* 31: 208-214.
- [Brown, DM; Hutchison, L; Donaldson, K; Stone, V.](#) (2007). The effects of PM10 particles and oxidative stress on macrophages and lung epithelial cells: modulating effects of calcium-signaling antagonists. *Am J Physiol Lung Cell Mol Physiol* 292: 1444-1451.
- [BSI](#) (British Standards Institution). (2007). Terminology for nanomaterials. (PAS 136:2007). London, UK.
- [Bury, NR.](#) (2005). The changes to apical silver membrane uptake, and basolateral membrane silver export in the gills of rainbow trout (*Oncorhynchus mykiss*) on exposure to sublethal silver concentrations. *Aquat Toxicol* 72: 135-145.
- [Bury, NR; Galvez, F; Wood, CM.](#) (1999). Effects of chloride, calcium, and dissolved organic carbon on silver toxicity: Comparison between rainbow trout and fathead minnows. *Environ Toxicol Chem* 18: 56-62.
- [Carlson, C; Hussain, SM; Schrand, AM; Braydich-Stolle, LK; Hess, KL; Jones, RL; Schlager, JJ.](#) (2008). Unique cellular interaction of silver nanoparticles: Size-dependent generation of reactive oxygen species. *J Phys Chem B* 112: 13608-13619.
- [Cedervall, T; Lynch, I; Lindman, S; Berggård, T; Thulin, E; Nilsson, H; Dawson, K; Linse, S.](#) (2007). Understanding the nanoparticle-protein corona using methods to quantify exchange rates and affinities of proteins for nanoparticles. *PNAS* 104: 2050.
- [Cha, K; Hong, H; Choi, Y; Lee, MJ; Park, JH; Chae, H; Ryu, G; Myung, H.](#) (2008). Comparison of acute responses of mice livers to short-term exposure to nano-sized or micro-sized silver particles. *Biotechnol Lett* 30: 1893-1899. <http://dx.doi.org/10.1007/s10529-008-9786-2>
- [Chae, Y; Pham, C; Lee, J; Bae, E; Yi, J; Gu, M.](#) (2009). Evaluation of the toxic impact of silver nanoparticles on Japanese medaka (*Oryzias latipes*). *Aquat Toxicol* 94: 320-327.
<http://dx.doi.org/10.1016/j.aquatox.2009.07.019>
- [Chappell, JB; Greville, GD.](#) (1954). Effect of silver ions on mitochondrial adenosine triphosphatase. *Nature* 174: 930-931.
- [Chen, KL; Elimelech, M.](#) (2007). Influence of humic acid on the aggregation kinetics of fullerene (C60) nanoparticles in monovalent and divalent electrolyte solutions. *J Colloid Interface Sci* 309: 126-134.
<http://dx.doi.org/10.1016/j.jcis.2007.01.074>

- Chen, XS; Schluesener, HJ. (2008). Nanosilver: A nanoparticle in medical application. *Toxicol Lett* 176: 1-12. <http://dx.doi.org/10.1016/j.toxlet.2007.10.004>
- Chi, Z; Liu, R; Zhao, L; Qin, P; Pan, X; Sun, F; Hao, X. (2009). A new strategy to probe the genotoxicity of silver nanoparticles combined with cetylpyridine bromide. *Spectrochim Acta A Mol Biomol Spectrosc* 72: 577-581. <http://dx.doi.org/10.1016/j.saa.2008.10.044>
- Cho, WS; Kim, KM; Kim, SY. (2008a). Occupational generalized argyria after exposure to aerosolized silver. *J Dermatol* 35: 759-760. <http://dx.doi.org/10.1111/j.1346-8138.2008.00562.x>
- Cho, Y; Lee, B; Son, J. (2008b). Growth responses of lettuce and pak-choi to silver nano-particle concentration in functional water. Asian Horticultural Congress, December 11-23, 2008, Jeju, Korea.
- Choi, J; Kim, S; Ahn, J; Youn, P; Kang, J; Park, K; Yi, J; Ryu, D. (2010). Induction of oxidative stress and apoptosis by silver nanoparticles in the liver of adult zebrafish. *Aquat Toxicol* 100: 151-159. <http://dx.doi.org/10.1016/j.aquatox.2009.12.012>
- Choi, O; Clevenger, TE; Deng, B; Surampalli, RY; Ross, L, Jr; Hu, Z. (2009). Role of sulfide and ligand strength in controlling nanosilver toxicity. *Water Res* 43: 1879-1886.
- Choi, O; Deng, KK; Kim, NJ; Ross, L, Jr; Surampalli, RY; Hu, Z. (2008). The inhibitory effects of silver nanoparticles, silver ions, and silver chloride colloids on microbial growth. *Water Res* 42: 3066-3074.
- Choi, O; Hu, Z. (2008). Size dependent and reactive oxygen species related nanosilver toxicity to nitrifying bacteria. *Environ Sci Technol* 42: 4583-4588.
- Chopra, I. (2007). The increasing use of silver-based products as antimicrobial agents: A useful development or a cause for concern? *J Antimicrob Chemother* 59: 587-590.
- Chou, M. (2010). Email to A. Turley Re: Top Nano Technology Co., Ltd. - Contact Us Form, March 8. Available online
- Christensen, FM; Johnston, HJ; Stone, V; Aitken, RJ; Hankin, S; Peters, S; Aschberger, K. (2010). Nano-silver - Feasibility and challenges for human health risk assessment based on open literature. *Nanotoxicology* 4: 1-12. <http://dx.doi.org/10.3109/17435391003690549>
- Colvin, VL. (2003). The potential environmental impact of engineered nanomaterials. *Nat Biotechnol* 21: 1166-1170.
- ConSealInternational (ConSeal International Inc.). (2010). NanoSil Solution. Available online at <http://www.nanosilproducts.com/cms/> (accessed February 11, 2010).
- Cornfield, J. (1977). Carcinogenic risk assessment. *Science* 198: 693-699. <http://dx.doi.org/10.1126/science.910152>
- Crawford, DR; Davies, KJ. (1994). Adaptive response and oxidative stress. *Environ Health Perspect* 102: 25-28.
- Cumberland, S; Lead, J. (2009). Particle size distributions of silver nanoparticles at environmentally relevant conditions. *J Chromatogr A* 1216: 9099-9105. <http://dx.doi.org/10.1016/j.chroma.2009.07.021>
- Danilczuk, M; Lund, A; Sadlo, J; Yamada, H; Michalik, J. (2006). Conduction electron spin resonance of small silver particles. *Spectrochim Acta A Mol Biomol Spectrosc* 63: 189-191. <http://dx.doi.org/10.1016/j.saa.2005.05.002>
- Dasari, T; Hwang, H. (2010). The effect of humic acids on the cytotoxicity of silver nanoparticles to a natural aquatic bacterial assemblage. *Sci Total Environ* 408: 5817-5823. <http://dx.doi.org/10.1016/j.scitotenv.2010.08.030>
- Davies, PH; Goettl, JP, Jr; Sinley, JR. (1978). Toxicity of silver to rainbow trout (*Salmo gairdneri*). *Water Res* 12: 113-117. [http://dx.doi.org/10.1016/0043-1354\(78\)90014-3](http://dx.doi.org/10.1016/0043-1354(78)90014-3)
- Davis, JM. (2007). How to assess the risks of nanotechnology: Learning from past experience. *J Nanosci Nanotechnol* 7: 402-409.

- DEFRA (Department for Environment Food and Rural Affairs (DEFRA)). (2007). Characterising the potential risks posed by engineered nanoparticles. A second UK government research report. Retrieved from: <http://www.defra.gov.uk/environment/quality/nanotech/reports.htm#risks>.
- del Olmo, A; Caramelo, C; SanJose, C. (2003). Fluorescent complex of pyoverdin with aluminum. *J Inorg Biochem* 97: 384-387. [http://dx.doi.org/10.1016/S0162-0134\(03\)00316-7](http://dx.doi.org/10.1016/S0162-0134(03)00316-7)
- Demirbilek, Z; Smith, J; Zundel, A; Jones, R; MacDonald, N; Davies, M. (2005). Particle Tracking Model (PTM) in the SMS: III. Tutorial with examples. Available online at <http://www.stormingmedia.us/70/7045/A704534.html>
- Demou, E; Peter, P; Hellweg, S. (2008). Exposure to manufactured nanostructured particles in an industrial pilot plant. *Ann Occup Hyg* 52: 695-706. <http://dx.doi.org/10.1093/annhyg/men058>
- DiToro, DM; Allen, HE; Bergman, HL; Meyer, JS; Paquin, PR; Santore, RC. (2001). Biotic ligand model of the acute toxicity of metals. 1. Technical basis. *Environ Toxicol Chem* 20: 2383-2396. <http://dx.doi.org/10.1002/etc.5620201034>
- Domingos, RF; Baalousha, MA; Ju-Nam, Y; Reid, MM; Tufenkji, N; Lead, JR; Leppard, GG; Wilkinson, KJ. (2009a). Characterizing manufactured nanoparticles in the environment: Multimethod determination of particle sizes. *Environ Sci Technol* 43: 7277-7284. <http://dx.doi.org/10.1021/es900249m>
- Domingos, RF; Tufenkji, N; Wilkinson, KJ. (2009b). Aggregation of titanium dioxide nanoparticles: Role of a fulvic acid. *Environ Sci Technol* 43: 1282-1286. <http://dx.doi.org/10.1021/es8023594>
- Drake, PL; Hazelwood, KJ. (2005). Exposure-related health effects of silver and silver compounds: A review [Review]. *Ann Occup Hyg* 49: 575-585.
- DunphyGuzman, KA; Finnegan, MP; Banfield, JF. (2006). Influence of surface potential on aggregation and transport of titania nanoparticles. *Environ Sci Technol* 40: 7688-7693.
- ECB (European Chemicals Bureau). (2003). Technical guidance document on risk assessment: Part II. (EUR 20418 EN/1). Luxembourg: Office for Official Publications of the European Communities. <http://ecb.jrc.ec.europa.eu/documentation/>
- Eckelman, MJ; Graedel, TE. (2007). Silver emissions and their environmental impacts: A multilevel assessment. *Environ Sci Technol* 41: 6283-6289. <http://dx.doi.org/10.1021/es062970d>
- Eisler, R. (1996). Silver hazards to fish, wildlife, and invertebrates: A synoptic review. Laurel, MD: U.S. National Biological Service.
- El Badawy, A; Silva, R; Morris, B; Scheckel, K; Suidan, M; Tolaymat, T. (2011). Surface charge-dependent toxicity of silver nanoparticles. *Environ Sci Technol* 45: 283-287. <http://dx.doi.org/10.1021/es1034188>
- Elder, A; Gelein, R; Silva, V; Feikert, T; Opanashuk, L; Carter, J; Potter, R; Maynard, A; Ito, Y; Finkelstein, J; Oberdorster, G. (2006). Translocation of inhaled ultrafine manganese oxide particles to the central nervous system. *Environ Health Perspect* 114: 1172-1178. <http://dx.doi.org/10.1289/ehp.9030>
- Elder, A; Lynch, I; Grieger, K; Chan-Remillard, S; Gatti, A; Gnewuch, H; Kenawy, E; Korenstein, R; Kuhlbusch, T; Linker, F; Matias, S; Monteiro-Riviere, N; Pinto, VRS; Rudnitsky, R; Savolainen, K; Shvedova, A. (2009). Human health risks of engineered nanomaterials. In *Nanoparticles: Risks and Benefits*. The Netherlands: Springer Netherlands.
- Elechiguerra, J; Burt, J; Morones, J; Camacho-Bragado, A; Gao, X; Lara, H; Yacaman, M. (2005). Interaction of silver nanoparticles with HIV-1. *Journal of Nanobiotechnology* 3: 1477-3155. <http://dx.doi.org/10.1186/1477-3155-3-6>
- Elzey, S; Grassian, VH. (2010). Agglomeration, isolation and dissolution of commercially manufactured silver nanoparticles in aqueous environments. *J Nanopart Res* 12: 1945-1958. <http://dx.doi.org/10.1007/s11051-009-9783-y>
- EnvironmentalDefense - DuPontNanoPartnership. (2007). Nano risk framework. Washington, DC: Environmental Defense Fund. <http://nanoriskframework.com/page.cfm?tagID=1095>

- [Erickson, RJ; Brooke, LT; Kahl, MD; Vende Venter, FV; Harting, SL; Markee, TP; Spehar, RL.](#) (1998). Effects of laboratory test conditions on the toxicity of silver to aquatic organisms. *Environ Toxicol Chem* 17: 572-578. <http://dx.doi.org/10.1002/etc.5620170407>
- [Evanoff, DD, Jr; Chumanov, G.](#) (2005). Synthesis and optical properties of silver nanoparticles and arrays. *Chemphyschem* 6: 1221-1231. <http://dx.doi.org/10.1002/cphc.200500113>
- [Ewell, WS; Gorsuch, JW; Ritter, M; Ruffing, CJ.](#) (1993). Ecotoxicological effects of silver compounds. 1st Argentum International Conference on the Transport, Fate and Effects of Silver in the Environment, 8/8/1993-8/10/1993, Madison, WI.
- [Fabrega, J; Fawcett, SR; Renshaw, JC; Lead, JR.](#) (2009). Silver nanoparticle impact on bacterial growth: Effect of pH, concentration, and organic matter. *Environ Sci Technol* 43: 7285-7290. <http://dx.doi.org/10.1021/es803259g>
- [Farkas, J; Christian, P; Gallego-Urrea, J; Roos, N; Hassellöv, M; Tollefsen, K; Thomas, K.](#) (2011). Uptake and effects of manufactured silver nanoparticles in rainbow trout (*Oncorhynchus mykiss*) gill cells. *Reprod Toxicol* 101: 117-125. <http://dx.doi.org/10.1016/j.aquatox.2010.09.010>
- [Fauss, E.](#) (2008). The silver nanotechnology commercial inventory. Washington, DC: Woodrow Wilson International Center for Scholars. http://www.nanotechproject.org/process/assets/files/7039/silver_database_fauss_sept2_final.pdf
- [Feldmann, H.](#) (2005). Yeast cell architecture and function. In *Yeast Molecular Biology: A Short Compendium on Basic Features and Novel Aspects*. Munich: Adolf-Butenandt Institute.
- [Feng, QL; Wu, J; Chen, GQ; Cui, FZ; Kim, TN; Kim, JO.](#) (2000). A mechanistic study of the antibacterial effect of silver ions on *Escherichia coli* and *Staphylococcus aureus*. *J Biomed Mater Res* 52: 662-668.
- [Fent, K; Weisbrod, C; Wirth-Heller, A; Pieles, U.](#) (2010). Assessment of uptake and toxicity of fluorescent silica nanoparticles in zebrafish (*Danio rerio*) early life stages. *Aquat Toxicol* 100: 218-228. <http://dx.doi.org/10.1016/j.aquatox.2010.02.019>
- [Filloux, A.](#) (2004). The underlying mechanisms of type II protein secretion. *Biochim Biophys Acta* 1694: 163-179. <http://dx.doi.org/10.1016/j.bbamcr.2004.05.003>
- [Flegal, AR; Brown, CL; Squire, S; Ross, JR; Scelfo, GM; Hibdon, S.](#) (2007). Spatial and temporal variations in silver contamination and toxicity in San Francisco Bay. *Environ Res* 105: 34-52.
- [Ford, L.](#) (2001). Development of chronic aquatic water quality criteria and standards for silver. *Water Environ Res* 73: 248-253.
- [Fraser, JF; Cuttle, L; Kempf, M; Kimble, RM.](#) (2004). Cytotoxicity of topical antimicrobial agents used in burn wounds in Australasia. *ANZ J Surg* 74: 139-142.
- [Fujitani, Y; Kobayashi, T; Arashidani, K; Kunugita, N; Suemura, K.](#) (2008). Measurement of the physical properties of aerosols in a fullerene factory for inhalation exposure assessment. *J Occup Environ Hyg* 5: 380-389.
- [Galloway, T; Sanger, R; Smith, K; Fillmann, G; Readman, J; Ford, T; Depledge, M.](#) (2002). Rapid assessment of marine pollution using multiple biomarkers and chemical immunoassays. *Environ Sci Technol* 10: 2219-2226.
- [Gammons, CH; Yu, Y.](#) (1997). The stability of aqueous silver bromide and iodide complexes at 25300C: Experiments, theory and geologic applications. *Chem Geol* 137: 155-173. [http://dx.doi.org/10.1016/S0009-2541\(96\)00160-X](http://dx.doi.org/10.1016/S0009-2541(96)00160-X)
- [Gan, X; Liu, T; Zhong, J; Liu, X; Li, G.](#) (2004). Effect of silver nanoparticles on the electron transfer reactivity and the catalytic activity of myoglobin. *Chembiochem* 5: 1686-1691.
- [Gao, J; Wang, Y; Hovsepyan, A; Bonzongo, J.](#) (2011). Effects of engineered nanomaterials on microbial catalyzed biogeochemical processes in sediments. *J Hazard Mater* 186: 940-945. <http://dx.doi.org/10.1016/j.jhazmat.2010.11.084>

- [Gao, J; Youn, S; Hovsepyan, A; Llana, VL; Wang, Y; Bitton, G; Bonzongo, JC.](#) (2009). Dispersion and toxicity of selected manufactured nanomaterials in natural river water samples: Effects of water chemical composition. *Environ Sci Technol* 43: 3322-3328.
- [Garnier-Laplace, J; Baudin, JP; Foulquier, L.](#) (1992). Experimental study of 110mAg transfer from sediment to biota in a simplified freshwater ecosystem. *Hydrobiologia* 235-236: 393-406.
<http://dx.doi.org/10.1007/BF00026229>
- [Garza-Ocañas, L; Ferrer, D; Burt, J; Diaz-Torres, L; Ramírez Cabrera, M; Rodríguez, V; Luján Rangel, R; Romanovicz, D; Jose-Yacaman, M.](#) (2010). Biodistribution and long-term fate of silver nanoparticles functionalized with bovine serum albumin in rats. *Metallomics* 2: 204-210.
<http://dx.doi.org/10.1039/b916107d>
- [Gaul, LE; Staud, AH.](#) (1935). Clinical spectroscopy. Seventy cases of generalized argyrosis following organic and colloidal silver medication. *JAMA* 104: 1387-1390.
<http://dx.doi.org/10.1001/jama.1935.02760160011004>
- [Geiser, M; Casaulta, M; Kupferschmid, B; Schulz, H; Semmler-Behnke, M; Kreyling, W.](#) (2008). The role of macrophages in the clearance of inhaled ultrafine titanium dioxide particles. *Am J Respir Cell Mol Biol* 38: 371-376. <http://dx.doi.org/10.1165/rcmb.2007-0138OC>
- [Geranio, L; Heuberger, M; Nowack, B.](#) (2009). The behavior of silver nanotextiles during washing. *Environ Sci Technol* 43: 8113-8118. <http://dx.doi.org/10.1021/es9018332>
- [GFMS Limited.](#) (2009). World silver survey 2009: A summary (pp. 1-11). Washington, DC: The Silver Institute.
- [Gilmore, D.](#) (2010). Email to Audrey Turley: Info about NanoSil products to include in case study report. Available online
- [Goia, D; Matijevi, E.](#) (1998). Preparation of monodispersed metal particles. *New J Chem* 22: 1203-1215.
- [Gottschalk, F; Scholz, RW; Nowack, B.](#) (2010). Probabilistic material flow modeling for assessing the environmental exposure to compounds: Methodology and an application to engineered nano-TiO₂ particles. *Environ Modell Softw* 25: 320-332. <http://dx.doi.org/10.1016/j.envsoft.2009.08.011>
- [Gottschalk, F; Sonderer, T; Scholz, RW; Nowack, B.](#) (2009). Modeled environmental concentrations of engineered nanomaterials (TiO₂, ZnO, Ag, CNT, Fullerenes) for different regions. *Environ Sci Technol* 43: 9216-9222. <http://dx.doi.org/10.1021/es9015553>
- [Grady, CPL, Jr; Daigger, GT; Lim, HC.](#) (1999). *Biological wastewater treatment* (2 ed.). New York, NY: Marcel Dekker, Inc.
- [Grassian, VH.](#) (2009). New directions: Nanodust A source of metals in the atmospheric environment? *Atmos Environ* 43: 4666-4667. <http://dx.doi.org/10.1016/j.atmosenv.2009.06.032>
- [Greulich, C; Kittler, S; Epple, M; Muhr, G; Köller, M.](#) (2009). Studies on the biocompatibility and the interaction of silver nanoparticles with human mesenchymal stem cells (hMSCs). *Langenbecks Arch Surg* 394: 495-502. <http://dx.doi.org/10.1007/s00423-009-0472-1>
- [Griffitt, R; Hyndman, K; Denslow, N; Barber, D.](#) (2009). Comparison of molecular and histological changes in zebrafish gills exposed to metallic nanoparticles. *Toxicol Sci* 107: 404.
<http://dx.doi.org/10.1093/toxsci/kfn256>
- [Griffitt, RJ; Luo, J; Gao, J; Bonzongo, JC; Barber, DS.](#) (2008). Effects of particle composition and species on toxicity of metallic nanomaterials in aquatic organisms. *Environ Toxicol Chem* 27: 1972-1978.
- [Griscom, SB; Fisher, NS; Aller, RC; Lee, BG.](#) (2002). Effects of gut chemistry in marine bivalves on the assimilation of metals from ingested sediment particles. *J Mar Res* 60: 101-120.
- [Grodzik, M; Sawosz, E.](#) (2006). The influence of silver nanoparticles on chicken embryo development and bursa of Fabricius morphology. *J Anim Feed Sci* 15: 111-114.

- [Grosell, M; Brauner, CJ; Kelly, SP; Mcgeer, JC; Bianchini, A; Wood, CM.](#) (2002). Physiological responses to acute silver exposure in the freshwater crayfish (*Cambarus diogenes diogenes*): A model invertebrate? *Environ Toxicol Chem* 21: 369-374.
- [Grosell, M; Wood, C.](#) (2001). Branchial versus intestinal silver toxicity and uptake in the marine teleost *Parophrys vetulus*. *J Comp Physiol [B]* 171: 585-594. <http://dx.doi.org/10.1007/s003600100209>
- [Gulson, B; McCall, M; Korsch, M; Gomez, L; Casey, P; Oytam, Y; Taylor, A; McCulloch, M; Trotter, J; Kinsley, L; Greenoak, G.](#) (2010). Small amounts of zinc from zinc oxide particles in sunscreens applied outdoors are absorbed through human skin. *Toxicol Sci* 118: 140-149. <http://dx.doi.org/10.1093/toxsci/kfq243>
- [Györi, J; Kiss, T; Shcherbatko, AD; Belan, PV; Tepikin, AV; Osipenko, ON; Salánki, J.](#) (1991). Effect of Ag⁺ on membrane permeability of perfused *Helix pomatia* neurons. *J Physiol* 442: 1.
- [Hackenberg, S; Scherzed, A; Kessler, M; Hummel, S; Technau, A; Froelich, K; Ginzkey, C; Koehler, C; Hagen, R; Kleinsasser, N.](#) (2011). Silver nanoparticles: Evaluation of DNA damage, toxicity and functional impairment in human mesenchymal stem cells. *Toxicol Lett* 201: 27-33. <http://dx.doi.org/10.1016/j.toxlet.2010.12.001>
- [Hagendorfer, H; Lorenz, C; Kaegi, R; Sinnet, B; Gehrig, R; Natalie, VG; Scheringer, M; Christian, L; Ulrich, A.](#) (2009). Size-fractionated characterization and quantification of nanoparticle release rates from a consumer spray product containing engineered nanoparticles. *J Nanopart Res TBD: TBD*. <http://dx.doi.org/10.1007/s11051-009-9816-6>
- [Hagens, WI; Oomen, AG; de Jong, WH; Cassee, FR; Sips, AJ.](#) (2007). What do we (need to) know about the kinetic properties of nanoparticles in the body? *Regul Toxicol Pharmacol* 49: 217-229. <http://dx.doi.org/10.1016/j.yrtph.2007.07.006>
- [Hahn, A; Stöver, T; Paasche, G; Löbler, M; Sternberg, K; Rohm, H; Barcikowski, S.](#) (2010). Therapeutic window for bioactive nanocomposites fabricated by laser ablation in polymer-doped organic liquids. *Adv Eng Mater* 12: B156-B162. <http://dx.doi.org/10.1002/adem.200980071>
- [Handy, R; Henry, T; Scown, T; Johnston, B; Tyler, C.](#) (2008a). Manufactured nanoparticles: Their uptake and effects on fish. A mechanistic analysis. *Ecotoxicology* 17: 396-409.
- [Handy, RD; Eddy, FB.](#) (2004). Transport of solutes across biological membranes in eukaryotes: An environmental perspective. In *Physicochemical Kinetics and Transport at Biointerfaces*. New York: John Wiley. <http://dx.doi.org/10.1002/0470094044.ch7>
- [Handy, RD; Owen, R; Valsami-Jones, E.](#) (2008b). The ecotoxicology of nanoparticles and nanomaterials: Current status, knowledge gaps, challenges, and future needs. *Ecotoxicology* 17: 315-325.
- [Handy, RD; Shaw, BJ.](#) (2007). Ecotoxicity of nanomaterials to fish: Challenges for ecotoxicity testing. *Integr Environ Assess Manag* 3: 458-460.
- [Hansen, SF; Larsen, BH; Olsen, SI; Baun, A.](#) (2007). Categorization framework to aid hazard identification of nanomaterials. *Nanotoxicology* 1: 243-250. <http://dx.doi.org/10.1080/17435390701727509>
- [Hansen, SF; Michelson, ES; Kamper, A; Borling, P; Stuer-Lauridsen, F; Baun, A.](#) (2008). Categorization framework to aid exposure assessment of nanomaterials in consumer products. *Ecotoxicology* 17: 438-447.
- [Harris, AT; Bali, BR.](#) (2008). On the formation and extent of uptake of silver nanoparticles by live plants. *J Nanopart Res* 10: 691-695. <http://dx.doi.org/10.1007/s11051-007-9288-5>
- [Hatchett, DW; White, HS.](#) (1996). Electrochemistry of sulfur adlayers on the low-index faces of silver. *J Phys Chem A* 100: 9854-9859. <http://dx.doi.org/10.1021/jp953757z>
- [Hawthorne, J; Musante, C; Sinha, SK; White, JC.](#) (2012). Accumulation and phytotoxicity of engineered nanoparticles to cucurbita pepo. *Int J Phytoremediation* 14: 429-442. <http://dx.doi.org/10.1080/15226514.2011.620903>

- [Heckmann, L; Hovgaard, M; Sutherland, D; Autrup, H; Besenbacher, F; Scott-Fordsmand, J.](#) (2011). Limit-test toxicity screening of selected inorganic nanoparticles to the earthworm *Eisenia fetida*. *Ecotoxicology* 20: 226-233. <http://dx.doi.org/10.1007/s10646-010-0574-0>
- [Hendren, CO; Mesnard, X; Dröge, J; Wiesner, MR.](#) (2011). Estimating production data for five engineered nanomaterials as a basis for exposure assessment. *Environ Sci Technol* 45: 2562-2569. <http://dx.doi.org/10.1021/es103300g>
- [Henglein, A.](#) (1998). Colloidal silver nanoparticles: photochemical preparation and interaction with O₂, CCl₄, and some metal ions. *Chem Mater* 10: 444-450. <http://dx.doi.org/10.1021/cm970613j>
- [Herodotus.](#) (1920). *The Histories*. In AD Godley (Ed.). Cambridge: Harvard University Press. <http://www.perseus.tufts.edu/hopper/text?doc=Perseus:text:1999.01.0126>
- [Hinthner, A; Vawda, S; Skirrow, R; Veldhoen, N; Collins, P; Cullen, J; van Aggelen, G; Helbing, C.](#) (2010). Nanometals induce stress and alter thyroid hormone action in amphibia at or below North American water quality guidelines. *Environ Sci Technol* 44: 8314-8321. <http://dx.doi.org/10.1021/es101902n>
- [Hirsch, M.](#) (1998a). Availability of sludge-borne silver to agricultural crops. *Environ Toxicol Chem* 17: 610-616. <http://dx.doi.org/10.1002/etc.5620170413>
- [Hirsch, MP.](#) (1998b). Toxicity of silver sulfide-spiked sediments to the freshwater amphipod (*Hyalella azteca*). *Environ Toxicol Chem* 17: 601-604. <http://dx.doi.org/10.1002/etc.5620170411>
- [Ho, C; Yau, S; Lok, C; So, M; Che, C.](#) (2010). Oxidative dissolution of silver nanoparticles by biologically relevant oxidants: a kinetic and mechanistic study. *Chem Asian J* 5: 285-293. <http://dx.doi.org/10.1002/asia.200900387>
- [Hogstrand, C; Galvez, F; Wood, CM.](#) (1996). Toxicity, silver accumulation and metallothionein induction in freshwater rainbow trout during exposure to different silver salts. *Environ Toxicol Chem* 15: 1102-1108. <http://dx.doi.org/10.1002/etc.5620150713>
- [Hogstrand, C; Wood, CM.](#) (1996). *The toxicity of silver to marine fish*. In *Transport, fate and effects of silver in the environment*. Madison, WI: Sea Grant Institute.
- [Holladay, RJ; Christensen, H; Moeller, WD.](#) (2004). Apparatus and method for producing antimicrobial silver solution. (U.S. Patent No. 6,743,348). Washington, DC: U.S. Patent and Trademark Office.
- [Hornberger, M; Luoma, S; Cain, D; Parchaso, F; Brown, C; Bouse, R; Wellise, C; Thompson, J.](#) (2000). Linkage of bioaccumulation and biological effects to changes in pollutant loads in South San Francisco Bay. *Environ Sci Technol* 34: 2401-2409. <http://dx.doi.org/10.1021/es991185g>
- [Hostynek, JJ.](#) (2003). Factors determining percutaneous metal absorption. *Food Chem Toxicol* 41: 327-345. [http://dx.doi.org/10.1016/S0278-6915\(02\)00257-0](http://dx.doi.org/10.1016/S0278-6915(02)00257-0)
- [Hu, Y; Ge, J; Lim, D; Zhang, T; Yin, Y.](#) (2008). Size-controlled synthesis of highly water-soluble silver nanocrystals. *J Solid State Chem* 7: 1524-1529.
- [Huang, CP; Cha, DK; Ismat, SS.](#) (2005). 2005 Progress report: Short-term chronic toxicity of photocatalytic nanoparticles to bacteria, algae, and zooplankton. Available online at http://cfpub.epa.gov/ncer_abstracts/INDEX.cfm/fuseaction/display.abstractDetail/abstract/7384 (accessed May 15, 2009).
- [Hussain, SM; Hess, KL; Gearhart, JM; Geiss, KT; Schlager, JJ.](#) (2005). In vitro toxicity of nanoparticles in BRL 3A rat liver cells. *Toxicol In Vitro* 19: 975-983. <http://dx.doi.org/10.1016/j.tiv.2005.06.034>
- [Hussain, SM; Schlager, JJ.](#) (2009). Safety evaluation of silver nanoparticles: Inhalation model for chronic exposure. *Toxicol Sci* 108: 223-224. <http://dx.doi.org/10.1093/toxsci/kfp032>
- [Hutchinson, TC; Stokes, PM.](#) (1975). *Heavy metal toxicity and algal bioassays*. (ASTM STP 573). Philadelphia, PA: American Society for Testing and Materials.
- [Hwang, ET; Lee, JH; Chae, YJ; Kim, YS; Kim, BC; Sang, BI; Gu, MB.](#) (2008). Analysis of the toxic mode of action of silver nanoparticles using stress-specific bioluminescent bacteria. *Small* 4: 746-750.

- [Hyun, J; Lee, B; Ryu, H; Sung, J; Chung, K; Yu, J.](#) (2008). Effects of repeated silver nanoparticles exposure on the histological structure and mucins of nasal respiratory mucosa in rats. *Toxicol Lett* 182: 24-28. <http://dx.doi.org/10.1016/j.toxlet.2008.08.003>
- [Hyung, H; Fortner, JD; Hughes, JB; Kim, JH.](#) (2007). Natural organic matter stabilizes carbon nanotubes in the aqueous phase. *Environ Sci Technol* 41: 179-184. <http://dx.doi.org/10.1021/es061817g>
- [ICF](#) (ICF International). (2011). Nanomaterial case study workshop: Developing a comprehensive environmental assessment research strategy for nanoscale silver - Workshop report. Research Triangle Park, NC: U.S. Environmental Protection Agency.
- [ICRP](#) (International Commission on Radiological Protection). (1994). Human respiratory tract model for radiological protection: A report of a task group of the International Commission on Radiological Protection. ICRP Publication 66. *Ann ICRP* 24: 1-482.
- [Illum, L.](#) (2000). Transport of drugs from the nasal cavity to the central nervous system. *Eur J Pharm Sci* 11: 1-18. [http://dx.doi.org/10.1016/S0928-0987\(00\)00087-7](http://dx.doi.org/10.1016/S0928-0987(00)00087-7)
- [Inoue, Y; Hoshino, M; Takahashi, H; Noguchi, T; Murata, T; Kanzaki, Y; Hamashima, H; Sasatsu, M.](#) (2002). Bactericidal activity of Ag-zeolite mediated by reactive oxygen species under aerated conditions. *J Inorg Biochem* 92: 37-42. [http://dx.doi.org/10.1016/S0162-0134\(02\)00489-0](http://dx.doi.org/10.1016/S0162-0134(02)00489-0)
- [Ivask, A; Bondarenko, O; Jephthina, N; Kahru, A.](#) (2010). Profiling of the reactive oxygen species-related ecotoxicity of CuO, ZnO, TiO₂, silver and fullerene nanoparticles using a set of recombinant luminescent *Escherichia coli* strains: differentiating the impact of particles and solubilised metals. *Anal Bioanal Chem* 398: 701-716. <http://dx.doi.org/10.1007/s00216-010-3962-7>
- [Iwasaki, S; Yoshimura, A; Ideura, T; Koshikawa, S; Sudo, M.](#) (1997). Elimination study of silver in a hemodialyzed burn patient treated with silver sulfadiazine cream. *Am J Kidney Dis* 30: 287-290. [http://dx.doi.org/10.1016/S0272-6386\(97\)90067-6](http://dx.doi.org/10.1016/S0272-6386(97)90067-6)
- [Jaisi, DP; Elimelech, M.](#) (2009). Single-walled carbon nanotubes exhibit limited transport in soil columns. *Environ Sci Technol* 43: 9161-9166. <http://dx.doi.org/10.1021/es901927y>
- [Jeffery, P; Li, D.](#) (1997). Airway mucosa: secretory cells, mucus and mucin genes. *Eur Respir J* 10: 1655-1662.
- [Jeong, G; Jo, G; Jo, U; Yu, I.](#) (2006). Effects of repeated welding fumes exposure on the histological structure and mucins of nasal respiratory mucosa in rats. *Toxicol Lett* 167: 19-26. <http://dx.doi.org/10.1016/j.toxlet.2006.08.007>
- [Ji, JH; Jung, JH; Kim, SS; Yoon, JU; Park, JD; Choi, BS; Chung, YH; Kwon, IH; Jeong, J; Han, BS; Shin, JH; Sung, JH; Song, KS; JI, Y.](#) (2007). Twenty-eight-day inhalation toxicity study of silver nanoparticles in Sprague-Dawley rats. *Inhal Toxicol* 19: 857-871.
- [Jiang, JK; Oberdorster, G; Biswas, P.](#) (2009). Characterization of size, surface charge, and agglomeration state of nanoparticle dispersions for toxicological studies. *J Nanopart Res* 11: 77-89.
- [Jin, R; Cao, Y; Mirkin, C; Kelly, K; Schatz, G; Zheng, J.](#) (2001). Photoinduced conversion of silver nanospheres to nanoprisms. *Science* 294: 1901-1903. <http://dx.doi.org/10.1126/science.1066541>
- [Jin, X; Li, M; Wang, J; Marambio-Jones, C; Peng, F; Huang, X; Damoiseaux, R; Hoek, E.](#) (2010). High-throughput screening of silver nanoparticle stability and bacterial inactivation in aquatic media: Influence of specific ions. *Environ Sci Technol* 44: 7321-7328. <http://dx.doi.org/10.1021/es100854g>
- [Johnson, J; Jirikowic, J; Bertram, M; Van Beers, D; Gordon, RB; Henderson, K; Klee, RJ; Lanzano, T; Lifset, R; Oetjen, L; Graedel, TE.](#) (2005). Contemporary anthropogenic silver cycle: A multilevel analysis. *Environ Sci Technol* 39: 4655-4665. <http://dx.doi.org/10.1021/es048319x>
- [Johnston, CJ; Finkelstein, JN; Mercer, P; Corson, N; Gelein, R; Oberdorster, G.](#) (2000). Pulmonary effects induced by ultrafine PTFE particles. *Toxicol Appl Pharmacol* 168: 208-215.
- [Johnston, HJ; Hutchison, GR; Christensen, FM; Peters, S; Hankin, S; Stone, V.](#) (2009). Identification of the mechanisms that drive the toxicity of TiO₂ particulates: the contribution of physicochemical characteristics. *Part Fibre Toxicol* 6: 33. <http://dx.doi.org/10.1186/1743-8977-6-33>

- Judy, JD; Unrine, JM; Bertsch, PM. (2011). Evidence for biomagnification of gold nanoparticles within a terrestrial food chain. *Environ Sci Technol* 45: 776-781. <http://dx.doi.org/10.1021/es103031a>
- Jung, WK; Koo, HC; Kim, KW; Shin, S; Kim, SH; Park, YH. (2008). Antibacterial activity and mechanism of action of the silver ion in *Staphylococcus aureus* and *Escherichia coli*. *Appl Environ Microbiol* 74: 2171-2178. <http://dx.doi.org/10.1128/AEM.02001-07>
- Kaegi, R; Sinnet, B; Zuleeg, S; Hagendorfer, H; Mueller, E; Vonbank, R; Bollner, M; Burkhardt, M. (2010). Release of silver nanoparticles from outdoor facades. *Environ Pollut* 158: 2900-2905. <http://dx.doi.org/10.1016/j.envpol.2010.06.009>
- Kaegi, R; Voegelin, A; Sinnet, B; Zuleeg, S; Hagendorfer, H; Burkhardt, M; Siegrist, H. (In Press) Behavior of metallic silver nanoparticles in a pilot wastewater treatment plant. *Environ Sci Technol* 45: 3902-3908. <http://dx.doi.org/10.1021/es1041892>
- Kahru, A; Dubourguier, H. (2010). From ecotoxicology to nanoecotoxicology. *Toxicology* 269: 105-119. <http://dx.doi.org/10.1016/j.tox.2009.08.016>
- Kakurai, M; Demitsu, T; Umemoto, N; Ohtsuki, M; Nakagawa, H. (2003). Activation of mast cells by silver particles in a patient with localized argyria due to implantation of acupuncture needles. *Br J Dermatol* 148: 822. <http://dx.doi.org/10.1046/j.1365-2133.2003.05188.x>
- Kaluza, S; Balderhaar, J; Orthen, B; Honnert, B; Jankowska, E; Pietrowski, P; Rosell, MG; Tanarro, C; Tejedor, J; Zugasti, A. (2009). Literature review - workplace exposure to nanoparticles. Bilboa, Spain: European Agency for Safety and Health at Work.
- Kamat, P. (2002). Photophysical, photochemical and photocatalytic aspects of metal nanoparticles. *J Phys Chem B* 32: 7729-7744.
- Kandlikar, M; Ramachandran, G; Maynard, A; Murdock, B; Toscano, WA. (2007). Health risk assessment for nanoparticles: A case for using expert judgment. *J Nanopart Res* 9: 137-156.
- Kennedy, A; Hull, M; Bednar, A; Goss, J; Gunter, J; Bouldin, J; Vikesland, P; Steevens, J. (2010). Fractionating nanosilver: importance for determining toxicity to aquatic test organisms. *Environ Sci Technol* 44: 9571-9577. <http://dx.doi.org/10.1021/es1025382>
- Khan, S; Mukherjee, A; Chandrasekaran, N. (2011). Silver nanoparticles tolerant bacteria from sewage environment. *J Environ Sci* 23: 346-352. [http://dx.doi.org/10.1016/S1001-0742\(10\)60412-3](http://dx.doi.org/10.1016/S1001-0742(10)60412-3)
- Khaydarov, RR; Khaydarov, RA; Estrin, Y; Evgrafova, S; Scheper, T; Endres, C; Cho, SY. (2009). Silver nanoparticles: Environmental and human health impacts. In I Linkov; J Steevens (Eds.), *Nanomaterials: Risks and Benefits* (pp. 287-297). Netherlands: Springer. http://dx.doi.org/10.1007/978-1-4020-9491-0_22
- Kim, B; Park, C; Murayama, M; Hochella, M. (2010a). Discovery and characterization of silver sulfide nanoparticles in final sewage sludge products. *Environ Sci Technol* 44: 7509-7514. <http://dx.doi.org/10.1021/es101565j>
- Kim, JS; Kuk, E; Yu, KN; Kim, JH; Park, SJ; Lee, HJ; Kim, SH; Park, YK; Park, YH; Hwang, CY. (2007). Antimicrobial effect of silver nanoparticles. *Nanomed* 3: 95-101. <http://dx.doi.org/10.1016/j.nano.2006.12.001>
- Kim, KJ; Sung, WS; Suh, BK; Moon, SK; Choi, JS; JG, K; Lee, DG. (2009). Antifungal activity and mode of action of silver nano-particles on *Candida albicans*. *Biometals* 22: 235-242.
- Kim, YJ; Yang, SI; Ryu, JC. (2010b). Cytotoxicity and genotoxicity of nano-silver in mammalian cell lines. *Mol Cell Toxicol* 6: 119-125. <http://dx.doi.org/10.1007/s13273-010-0018-1>
- Kim, YS; Kim, JS; Cho, HS; Rha, DS; Kim, JM; Park, JD; Choi, BS; Lim, R; Chang, HK; Chung, YH; Kwon, IH; Jeong, J; Han, BS; Yu, JJ. (2008). Twenty-eight-day oral toxicity, genotoxicity, and gender-related tissue distribution of silver nanoparticles in Sprague-Dawley rats. *Inhal Toxicol* 20: 575-583.
- Kiser, MA; Ryu, H; Jang, H; Hristovski, K; Westerhoff, P. (2010). Biosorption of nanoparticles to heterotrophic wastewater biomass. *Water Res* 44: 4105-4114. <http://dx.doi.org/10.1016/j.watres.2010.05.036>

- [Klaine, SJ; Alvarez, PJ; Batley, GE; Fernandes, TF; Handy, RD; Lyon, DY; Mahendra, S; McLaughlin, MJ; Lead, JR.](#) (2008). Nanomaterials in the environment: Behavior, fate, bioavailability, and effects. *Environ Toxicol Chem* 27: 1825-1851.
- [Klasen, HJ.](#) (2000). Historical review of the use of silver in the treatment of burns. I. Early uses [Review]. *Burns* 26: 117-130. [http://dx.doi.org/10.1016/S0305-4179\(99\)00116-3](http://dx.doi.org/10.1016/S0305-4179(99)00116-3)
- [Klein, DA.](#) (1978). Environmental impacts of artificial ice nucleating agents. In DA Klein (Ed.). Stroudsburg, PA: Dowden, Hutchinson & Ross.
- [Kramer, J; Bell, R; Smith, S; Gorsuch, J.](#) (2009). Silver nanoparticle toxicity and biocides: Need for chemical speciation. *Integr Environ Assess Manag* 5: 720-722.
- [Kramer, JR; Bell, RA; Collins, PV; Malcolmson, S; Rogers, C.](#) (1994). Nature and fate of silver, part I. In *Proceedings of the Second International Conference on Transport, Fate and Effects of Silver in the Environment*. Madison, WI: University of Wisconsin System, Sea Grant Institute.
- [Kreyling, WG; Semmler-Behnke, M; Moller, W.](#) (2006). Health implications of nanoparticles. *J Nanopart Res* 8: 543-562.
- [Kreyling, WG; Semmler, M; Erbe, F; Mayer, P; Takenaka, S; Schulz, H; Oberdorster, G; Ziesenis, A.](#) (2002). Translocation of ultrafine insoluble iridium particles from lung epithelium to extrapulmonary organs is size dependent but very low. *J Toxicol Environ Health A* 65: 1513-1530.
- [Krut'akov, YA; Kudrinskiy, AA; Olenin, AY; Lisichkin, GV.](#) (2008). Synthesis and properties of silver nanoparticles: Advances and prospects. *Russian Chemical Reviews* 77: 233-257. <http://dx.doi.org/10.1070/RC2008v077n03ABEH003751>
- [Kulthong, K; Srisung, S; Boonpavanitchakul, K; Kangwansupamonkon, W; Maniratanachote, R.](#) (2010). Determination of silver nanoparticle release from antibacterial fabrics into artificial sweat. Part *Fibre Toxicol* 7: 8. <http://dx.doi.org/10.1186/1743-8977-7-8>
- [Kumar, C; Mamidyalu, S; Das, B; Sridhar, B; Devi, G; Karuna, M.](#) (2010). Synthesis of biosurfactant-based silver nanoparticles with purified rhamnolipids isolated from *Pseudomonas aeruginosa* BS-161R. *J Microbiol Biotechnol* 20: 1061-1068.
- [Kumari, M; Mukherjee, A; Chandrasekaran, N.](#) (2009). Genotoxicity of silver nanoparticles in *Allium cepa*. *Sci Total Environ* 407: 5243-5246. <http://dx.doi.org/10.1016/j.scitotenv.2009.06.024>
- [Kvítek, L; Panáček, A; Soukupová, J; Kolář, M; Večeřová, R; Pucek, R; Holecová, M; R, Z.](#) (2008). Effect of surfactants and polymers on stability and antibacterial activity of silver nanoparticles (NPs). *J Phys Chem C* 112: 5825-5834. <http://dx.doi.org/10.1021/jp711616v>
- [Kvítek, L; Pucek, R; Panacek, A; Novotny, R; Hrbac, J; Zboril, R.](#) (2005). The influence of complexing agent concentration on particle size in the process of SERS active silver colloid synthesis. *J Mater Chem* 15: 1099-1105. <http://dx.doi.org/10.1039/b417007e>
- [Kvítek, L; Vanickova, M; Panacek, A; Soukupova, J; Dittrich, M; Valentova, E; Pucek, R; Bancirova, M; Milde, D; Zboril, R.](#) (2009). Initial study on the toxicity of silver nanoparticles (NPs) against *Paramecium caudatum*. *J Phys Chem B* 113: 4296-4300.
- [Kyriacou, S; Brownlow, W; Xu, X.](#) (2004). Using nanoparticle optics assay for direct observation of the function of antimicrobial agents in single live bacterial cells. *Biochemistry* 43: 140-147. <http://dx.doi.org/10.1021/bi0351110>
- [Laban, G; Nies, L; Turco, R; Bickham, J; Sepúlveda, M.](#) (2009). The effects of silver nanoparticles on fathead minnow (*Pimephales promelas*) embryos. *Ecotoxicology* 19: 185-195. <http://dx.doi.org/10.1007/s10646-009-0404-4>
- [Lam, PK; Chan, ES; Ho, WS; Liew, CT.](#) (2004). In vitro cytotoxicity testing of a nanocrystalline silver dressing (Acticoat) on cultured keratinocytes. *Br J Biomed Sci* 61: 125-127.

- [Lankveld, DP; Oomen, AG; Krystek, P; Neigh, A; Troost-de Jong, A; Noorlander, CW; Van Eijkeren, JC; Geertsma, RE; De Jong, WH.](#) (2010). The kinetics of the tissue distribution of silver nanoparticles of different sizes. *Biomaterials* 31: 8350-8361. <http://dx.doi.org/10.1016/j.biomaterials.2010.07.045>
- [Lansdown, AB.](#) (2007). Critical observations on the neurotoxicity of silver [Review]. *Crit Rev Toxicol* 37: 237-250. <http://dx.doi.org/10.1080/10408440601177665>
- [Lapied, E; Moudilou, E; Exbrayat, J; Oughton, D; Joner, E.](#) (2010). Silver nanoparticle exposure causes apoptotic response in the earthworm *Lumbricus terrestris* (Oligochaeta). *Nanomed* 5: 975-984. <http://dx.doi.org/10.2217/nnm.10.58>
- [Larese, FF; D'Agostin, F; Crosera, M; Adami, G; Renzi, N; Bovenzi, M; Maina, G.](#) (2009). Human skin penetration of silver nanoparticles through intact and damaged skin. *Toxicology* 255: 33-37.
- [Le, AT; Huy, PT; Tam, PD; Huy, TQ; Cam, PD; Kudrinskiy, AA; Krutyakov, YA.](#) (2010). Green synthesis of finely-dispersed highly bactericidal silver nanoparticles via modified Tollens technique. *Curr Appl Phys* 10: 910-916. <http://dx.doi.org/10.1016/j.cap.2009.10.021>
- [Lea, MC.](#) (1889). On allotropic forms of silver. *Am J Sci* 37: 476-491.
- [Lee, D; Fortin, C; Campbell, P.](#) (2005). Contrasting effects of chloride on the toxicity of silver to two green algae, *Pseudokirchneriella subcapitata* and *Chlamydomonas reinhardtii*. *Aquat Toxicol* 2: 127-135.
- [Lee, HY; Choi, YJ; Jung, EJ; Yin, HQ; Kwon, JT; Kim, JE; Im, HT; Cho, MH; Kim, JH; Kim, HY; Lee, BH.](#) (2010). Genomics-based screening of differentially expressed genes in the brains of mice exposed to silver nanoparticles via inhalation. *J Nanopart Res* 12: 1567-1578. <http://dx.doi.org/10.1007/s11051-009-9666-2>
- [Lee, JH; Kwon, M; Ji, JH; Kang, CS; Ahn, KH; Han, JH; Yu, IJ.](#) (2011). Exposure assessment of workplaces manufacturing nanosized TiO₂ and silver. *Inhal Toxicol* 23: 226-236. <http://dx.doi.org/10.3109/08958378.2011.562567>
- [Lee, KJ; Nallathamby, PD; Browning, LM; Osgood, CJ; Z-HN, X.](#) (2007). In vivo imaging of transport and biocompatibility of single silver nanoparticles in early development of zebrafish embryos. *ACS Nano* 1: 133-143.
- [Lee, P; Meisel, D.](#) (1982). Adsorption and surface-enhanced Raman of dyes on silver and gold sols. *J Phys Chem B* 86: 3391-3395.
- [Lehman-McKeeman, L., D.](#) (2008). Absorption, distribution, and excretion of toxicants. In CD Klaassen (Ed.), *Casarett and Doull's toxicology: The basic science of poisons* (7 ed., pp. 131-159). New York: McGraw-Hill Medical.
- [Leopold, N; Lendl, B.](#) (2003). A new method for fast preparation of highly surface-enhanced Raman scattering (SERS) active silver colloids at room temperature by reduction of silver nitrate with hydroxylamine hydrochloride. *J Phys Chem B* 107: 5723-5727. <http://dx.doi.org/10.1021/jp027460u>
- [Li, P; Kuo, T; Chang, J; Yeh, J; Chan, W.](#) (2010a). Induction of cytotoxicity and apoptosis in mouse blastocysts by silver nanoparticles. *Toxicol Lett* 197: 82-87. <http://dx.doi.org/10.1016/j.toxlet.2010.05.003>
- [Li, T; Albee, B; Alemayehu, M; Diaz, R; Ingham, L; Kamal, S; Rodriguez, M; Bishnoi, S.](#) (2010b). Comparative toxicity study of Ag, Au, and Ag-Au bimetallic nanoparticles on *Daphnia magna*. *Anal Bioanal Chem* 398: 689-700. <http://dx.doi.org/10.1007/s00216-010-3915-1>
- [Li, X; Lenhart, J; Walker, H.](#) (2010c). Dissolution-accompanied aggregation kinetics of silver nanoparticles. *Langmuir* 26: 16690-16698. <http://dx.doi.org/10.1021/la101768n>
- [Liang, Z; Das, A; Hu, Z.](#) (2010). Bacterial response to a shock load of nanosilver in an activated sludge treatment system. *Water Res* 44: 5432-5438. <http://dx.doi.org/10.1016/j.watres.2010.06.060>
- [Lide, DR.](#) (2000). *CRC Handbook of Chemistry and Physics*. In DR Lide (Ed.), *CRC Handbook of Chemistry and Physics* (81st ed.). Boca Raton, FL: CRC Press LLC.

- [Limbach, LK; Li, Y; Grass, RN; Brunner, TJ; Hintermann, MA; Muller, M; Gunther, D; Stark, WJ.](#) (2005). Oxide nanoparticle uptake in human lung fibroblasts: Effects of particle size, agglomeration, and diffusion at low concentrations. *Environ Sci Technol* 39: 9370-9376.
- [Liu, J; Aruguete, DM; Murayama, M; Hochella, MF.](#) (2009). Influence of Size and Aggregation on the Reactivity of an Environmentally and Industrially Relevant Nanomaterial (PbS). *Environ Sci Technol* 43: 8178-8183. <http://dx.doi.org/10.1021/es902121r>
- [Liu, J; Hurt, RH.](#) (2010). Ion release kinetics and particle persistence in aqueous nano-silver colloids. *Environ Sci Technol* 44: 2169-2175. <http://dx.doi.org/10.1021/es9035557>
- [Liu, J; Sonshine, D; Shervani, S; Hurt, R.](#) (2010a). Controlled release of biologically active silver from nanosilver surfaces. *ACS Nano* 4: 6903-6913. <http://dx.doi.org/10.1021/nn102272n>
- [Liu, W; Wu, Y; Wang, C; Li, H; Wang, T; Liao, C; Cui, L; Zhou, Q; Yan, B; Jiang, G.](#) (2010b). Impact of silver nanoparticles on human cells: Effect of particle size. *Nanotoxicology* 4: 319-330. <http://dx.doi.org/10.3109/17435390.2010.483745>
- [Livingstone, D.](#) (2001). Contaminant-stimulated reactive oxygen species production and oxidative damage in aquatic organisms. *Mar Pollut Bull* 42: 656-666. [http://dx.doi.org/10.1016/S0025-326X\(01\)00060-1](http://dx.doi.org/10.1016/S0025-326X(01)00060-1)
- [Lok, CN; Ho, CM; Chen, R; He, QY; Yu, WY; Sun, H; Tam, PK; Chiu, JF; Che, CM.](#) (2007). Silver nanoparticles: Partial oxidation and antibacterial activities. *J Biol Inorg Chem* 12: 527-534. <http://dx.doi.org/10.1007/s00775-007-0208-z>
- [Lok, CN; Ho, CM; Chen, R; He, QY; Yu, WY; Sun, HZ; Tam, PKH; Chiu, JF.](#) (2006). Proteomic analysis of the mode of antibacterial action of silver nanoparticles. *J Proteome Res* 5: 916-924. <http://dx.doi.org/10.1021/pr0504079>
- [Lovern, SB; Strickler, JR; Klaper, R.](#) (2007). Behavioral and physiological changes in *Daphnia magna* when exposed to nanoparticle suspensions (titanium dioxide, nano-C60, and C60HxC7OHx). *Environ Sci Technol* 41: 4465-4470.
- [Lowry, GV; Casman, EA.](#) (2009). Nanomaterial transport, transformation, and fate in the environment: A risk-based perspective on research needs. In *Nanomaterials: Risks and Benefits*. The Netherlands: Springer Netherlands.
- [Lu, W; Senapati, D; Wang, S; Tovmachenko, O; Singh, AK; Yu, H; Ray, PC.](#) (2010). Effect of surface coating on the toxicity of silver nanomaterials on human skin keratinocytes. *Chem Phys Lett* 487: 92-96. <http://dx.doi.org/10.1016/j.cplett.2010.01.027>
- [Lubick, N.](#) (2008). Nanosilver toxicity: Ions, nanoparticles or both? *Environ Sci Technol* 42: 8617.
- [Luoma, SN.](#) (2008). Silver nanotechnologies and the environment: Old problems or new challenges. Washington, DC: Project on Emerging Nanotechnologies.
- [Luoma, SN; Ho, YB; Bryan, GW.](#) (1995). Fate, bioavailability and toxicity of silver in estuarine environments. *Mar Pollut Bull* 31: 44-54. [http://dx.doi.org/10.1016/0025-326X\(95\)00081-W](http://dx.doi.org/10.1016/0025-326X(95)00081-W)
- [Lynch, I; Elder, A.](#) (2009). Disposition of nanoparticles as a function of their interactions with biomolecules. In *Nanoparticles: Risks and Benefits*. The Netherlands: Springer Netherlands.
- [Ma-Hock, L; Gamer, AO; Landsiedel, R; Leibold, E; Frechen, T; Sens, B; Linsenbuehler, M; Van Ravenzwaay, B.](#) (2007). Generation and characterization of test atmospheres with nanomaterials. *Inhal Toxicol* 19: 833-848.
- [Ma, X; Geiser-Lee, J; Deng, Y; Kolmakov, A.](#) (2010). Interactions between engineered nanoparticles (ENPs) and plants: phytotoxicity, uptake and accumulation. *Sci Total Environ* 408: 3053-3061. <http://dx.doi.org/10.1016/j.scitotenv.2010.03.031>
- [Maccuspie, RI.](#) (2011). Colloidal stability of silver nanoparticles in biologically relevant conditions. *J Nanopart Res* 13: 2893-2908. <http://dx.doi.org/10.1007/s11051-010-0178-x>

- [MacCuspie, RI; Rogers, K; Patra, M; Suo, Z; Allen, AJ; Martin, MN; Hackley, VA.](#) (2011). Challenges for physical characterization of silver nanoparticles under pristine and environmentally relevant conditions. *J Environ Monit* 13: 1212-1226. <http://dx.doi.org/10.1039/c1em10024f>
- [Mafune, F; Kohno, J; Takeda, Y; Kondow, T; Sawabe, H.](#) (2000). Structure and stability of silver nanoparticles in aqueous solution produced by laser ablation. *J Phys Chem B* 104: 8333-8337. <http://dx.doi.org/10.1021/jp001803b>
- [Mann, RM; Ernste, MJ; Bell, RA; Kramer, JR; Wood, CM.](#) (2004). Evaluation of the protective effects of reactive sulfide on the acute toxicity of silver to rainbow trout (*Oncorhynchus mykiss*). *Environ Toxicol Chem* 23: 1201-1210.
- [Mark, D.](#) (2007). Occupational exposure to nanoparticles and nanotubes. In RE Hester; RM Harrison (Eds.), *Nanotechnology: Consequences for human health and the environment* (pp. 50-80). Cambridge, UK: The Royal Society of Chemistry.
- [Martinez-Gutierrez, F; Olive, P; Banuelos, A; Orrantia, E; Nino, N; Sanchez, E; Ruiz, F; Bach, H; Av-Gay, Y.](#) (2010). Synthesis, characterization, and evaluation of antimicrobial and cytotoxic effect of silver and titanium nanoparticles. *Nanomed* 6: 681-688. <http://dx.doi.org/10.1016/j.nano.2010.02.001>
- [Matson, C.](#) (2010). Silver toxicity in *Fundulus heteroclitus* along a salinity gradient. Personal communication with A. Marenberg. Available online
- [Matuk, Y; Ghosh, M; McCulloch, C.](#) (1981). Distribution of silver in the eyes and plasma proteins of the albino rat. *Can J Ophthalmol* 16: 145-150.
- [Maynard, AD.](#) (2006). Nanotechnology: Assessing the risks. *Nano Today* 1: 22-33.
- [Maynard, AD; Aitken, RJ.](#) (2007). Assessing exposure to airborne nanomaterials: Current abilities and future requirements. *Nanotoxicology* 1: 26-41.
- [Maynard, AD; Kuempel, ED.](#) (2005). Airborne nanostructured particles and occupational health. *J Nanopart Res* 7: 587-614.
- [McMurry, PH.](#) (2000). A review of atmospheric aerosol measurements [Review]. *Atmos Environ* 34: 1959-1999. [http://dx.doi.org/10.1016/S1352-2310\(99\)00455-0](http://dx.doi.org/10.1016/S1352-2310(99)00455-0)
- [McNeil, SE.](#) (2009). Nanoparticle therapeutics: A personal perspective. *Wiley Interdiscip Rev Nanomed Nanobiotechnol* 1: 264-271. <http://dx.doi.org/10.1002/wnan.6>
- [Melchizedek, D.](#) (2010). Crystal clear nano silver. Available online at http://spiritofmaat.com/maatshop/n2_silver.htm (accessed March 19, 2010).
- [Methner, M; Hodson, L; Dames, A; Geraci, C.](#) (2010). Nanoparticle emission assessment technique (NEAT) for the identification and measurement of potential inhalation exposure to engineered nanomaterials - Part B: Results from 12 field studies. *J Occup Environ Hyg* 7: 163-176. <http://dx.doi.org/10.1080/15459620903508066>
- [Metropolitan Museum of Art Department of Photography.](#) (2004). Heilbrunn timeline of art history. New York: The Metropolitan Museum of Art. http://www.metmuseum.org/toah/hd/dagu/hd_dagu.htm
- [Meyer, J; Lord, C; Yang, X; Turner, E; Badireddy, A; Marinakos, S; Chilkoti, A; Wiesner, M; Auffan, M.](#) (2010). Intracellular uptake and associated toxicity of silver nanoparticles in *Caenorhabditis elegans*. *Aquat Toxicol* 100: 140-150. <http://dx.doi.org/10.1016/j.aquatox.2010.07.016>
- [Miao, AJ; Schwehr, K; Xu, C; Zhang, AJ; Luo, Z; Quigg, A.](#) (2009). The algal toxicity of silver engineered nanoparticles and detoxification by copolymeric substances. *Environ Pollut* 157: 3034-3041. <http://dx.doi.org/10.1016/j.envpol.2009.05.047>
- [Miller, AL; Hoover, MD; Mitchell, DM; Stapleton, BP.](#) (2007). The nanoparticle information library (NIL): A prototype for linking and sharing emerging data. *J Occup Environ Hyg* 4: D131-134. <http://dx.doi.org/10.1080/15459620701683947>

- [Mills, HJ; Hunter, E; Humphrys, M; Kerkhof, L; McGuinness, L; Huettel, M; Kostka, JE.](#) (2008). Characterization of nitrifying, denitrifying, and overall bacterial communities in permeable marine sediments of the northeastern Gulf of Mexico. *Appl Environ Microbiol* 74: 4440-4453. <http://dx.doi.org/10.1128/aem.02692-07>
- [MINCharInitiative](#) (Minimum Information on Nanoparticle Characterization). (2008). Recommended minimum physical and chemical parameters for characterizing nanomaterials on toxicology studies. Washington, DC: The Minimum Information for Nanomaterial Characterization Initiative. <http://characterizationmatters.org/parameters/>
- [Mirsattari, SM; Hammond, RR; Sharpe, MD; Leung, FY; Young, GB.](#) (2004). Myoclonic status epilepticus following repeated oral ingestion of colloidal silver. *Neurology* 62: 1408-1410.
- [Miura, N; Shinohara, Y.](#) (2009). Cytotoxic effect and apoptosis induction by silver nanoparticles in HeLa cells. *Biochem Biophys Res Commun* 390: 733-737. <http://dx.doi.org/10.1016/j.bbrc.2009.10.039>
- [Monteiro-Riviere, N; Inman, A; Riviere, J.](#) (2001). Effects of short-term high-dose and low-dose dermal exposure to Jet A, JP-8 and JP-8 + 100 jet fuels. *J Appl Toxicol* 21: 485-494. <http://dx.doi.org/10.1002/jat.785>
- [Monteiro-Riviere, NA; Riviere, J.](#) (1996). The pig as a model for cutaneous pharmacology and toxicology research. In *Advances in swine in biomedical research*. New York, NY: Plenum Press.
- [Monteiro-Riviere, NA; Riviere, JE.](#) (2009). Interaction of nanomaterials with skin: Aspects of absorption and biodistribution. *Nanotoxicology* 3: 188-193. <http://dx.doi.org/10.1080/17435390902906803>
- [Moore, M; Lowe, D; Soverchia, C; Haigh, S; Hales, S.](#) (1997). Uptake of a non-calorific, edible sucrose polyester oil and olive oil by marine mussels and their influence on uptake and effects of anthracene. *Aquat Toxicol* 39: 307-320. [http://dx.doi.org/10.1016/S0166-445X\(97\)00028-3](http://dx.doi.org/10.1016/S0166-445X(97)00028-3)
- [Moore, MN.](#) (2006). Do nanoparticles present ecotoxicological risks for the health of the aquatic environment? *Environ Int* 32: 967-976.
- [Morgan, IJ; Henry, RP; Wood, CM.](#) (1997). The mechanism of acute silver nitrate toxicity in freshwater rainbow trout (*Oncorhynchus mykiss*) is inhibition of gill Na⁺ and Cl⁻ transport. *Aquat Toxicol* 38: 145-163. [http://dx.doi.org/10.1016/S0166-445X\(96\)00835-1](http://dx.doi.org/10.1016/S0166-445X(96)00835-1)
- [Morgan, K.](#) (2005). Development of a preliminary framework for informing the risk analysis and risk management of nanoparticles. *Risk Anal* 25: 1621-1635.
- [Morones, JR; Elechiguerra, JL; Camacho, A; Holt, K; Kouri, JB; Ramirez, JT; Yacaman, MJ.](#) (2005). The bactericidal effect of silver nanoparticles. *Nanotechnology* 16: 2346-2353. <http://dx.doi.org/10.1088/0957-4484/16/10/059>
- [Moulton, M; Braydich-Stolle, L; Nadagouda, M; Kunzelman, S; Hussain, S; Varma, R.](#) (2010). Synthesis, characterization and biocompatibility of. *Nanoscale Res Lett* 2: 763-770. <http://dx.doi.org/10.1039/c0nr00046a>
- [Mueller, NC; Nowack, B.](#) (2008). Exposure modeling of engineered nanoparticles in the environment. *Environ Sci Technol* 42: 4447-4453. <http://dx.doi.org/10.1021/es7029637>
- [Muhling, M; Woolven-Allen, J; Murrell, JC; Joint, I.](#) (2008). Improved group-specific PCR primers for denaturing gradient gel electrophoresis analysis of the genetic diversity of complex microbial communities. *ISME J* 2: 379-392. <http://dx.doi.org/10.1038/ismej.2007.97>
- [Mukherjee, B; Weaver, JW.](#) (2010). Aggregation and charge behavior of metallic and nonmetallic nanoparticles in the presence of competing similarly-charged inorganic ions. *Environ Sci Technol* 44: 3332-3338. <http://dx.doi.org/10.1021/es903456e>
- [Mukherjee, P; Ahmad, A; Mandal, D; Senapati, S; Sainkar, S; Khan, M; Parishcha, R; Ajaykumar, P; Alam, M; Kumar, R.](#) (2001). Fungus-mediated synthesis of silver nanoparticles and their immobilization in the mycelial matrix: A novel biological approach to nanoparticle synthesis. *Nano Lett* 1: 515-519. <http://dx.doi.org/10.1021/nl0155274>

- Muller, GL. (1926). Experimental bone marrow reactions: I. Anemia produced by collargol. *J Exp Med* 43: 533-553. <http://dx.doi.org/10.1084/jem.43.4.533>
- Murdock, RC; Braydich-Stolle, L; Schrand, AM; Schlager, JJ; Hussain, SM. (2008). Characterization of nanomaterial dispersion in solution prior to in vitro exposure using dynamic light scattering technique. *Toxicol Sci* 101: 239-253. <http://dx.doi.org/10.1093/toxsci/kfm240>
- Murphy, C; Jana, N. (2002). Controlling the aspect ratio of inorganic nanorods and nanowires. *Adv Mater Deerfield* 1: 80.
- Murray, KS; Rogers, DT; Kaufman, MM. (2004). Heavy metals in an urban watershed in southeastern Michigan. *J Environ Qual* 33: 163-172.
- Musee, N. (2011). Simulated environmental risk estimation of engineered nanomaterials: a case of cosmetics in Johannesburg City. *Hum Exp Toxicol* 30: 1181-1195. <http://dx.doi.org/10.1177/0960327110391387>
- Naddya, RB; Gorsuch, JW; Rehner, AB; Mc Nerney, GR; Bell, RA; Kramer, JR. (2007). Chronic toxicity of silver nitrate to *Ceriodaphnia dubia* and *Daphnia magna*, and potential mitigating factors. *Aquat Toxicol* 84: 1-10. <http://dx.doi.org/10.1016/j.aquatox.2007.03.022>
- Nadworny, PL; Wang, JF; Tredget, EE; Burrell, RE. (2008). Anti-inflammatory activity of nanocrystalline silver in a porcine contact dermatitis model. *Nanomed* 4: 241-251. <http://dx.doi.org/10.1016/j.nano.2008.04.006>
- Nahmani, J; Hodson, ME; Black, S. (2007). Effects of metals on life cycle parameters of the earthworm *Eisenia fetida* exposed to field-contaminated, metal-polluted soils. *Environ Pollut* 149: 44-58. <http://dx.doi.org/10.1016/j.envpol.2006.12.018>
- Nahmani, J; Hodson, ME; Devin, S; Vijver, MG. (2009). Uptake kinetics of metals by the earthworm *Eisenia fetida* exposed to field-contaminated soils. *Environ Pollut* 157: 2622-2628. <http://dx.doi.org/10.1016/j.envpol.2009.05.002>
- Nair, P; Park, S; Lee, S; Choi, J. (2011). Differential expression of ribosomal protein gene, gonadotrophin releasing hormone gene and Balbiani ring protein gene in silver nanoparticles exposed *Chironomus riparius*. *Aquat Toxicol* 101: 31-37. <http://dx.doi.org/10.1016/j.aquatox.2010.08.013>
- Nallathamby, P; Lee, K; Xu, X. (2008). Design of stable and uniform single nanoparticle photonics for in vivo dynamics imaging of nanoenvironments of zebrafish embryonic fluids. *ACS Nano* 2: 1371-1380.
- Nanosafe. (2008). Dissemination report: Are conventional protective devices such as fibrous filter media, respirator cartridges, protective clothing and gloves also efficient for nanoaerosols? (DR-325/326-200801-1). France: Sixth Framework Programme. <http://www.nanosafe.org/scripts/home/publigen/content/templates/show.asp?P=63&L=EN&ITEMID=13>
- Navarro, E; Baun, A; Behra, R; Hartmann, NB; Filser, J; Miao, AJ; Quigg, A; Santschi, PH; Sigg, L. (2008a). Environmental behavior and ecotoxicity of engineered nanoparticles to algae, plants, and fungi. *Ecotoxicology* 17: 372-386.
- Navarro, E; Piccapietra, F; Wagner, B; Marconi, F; Kaegi, R; Odzak, N; Sigg, L; Behra, R. (2008b). Toxicity of silver nanoparticles to *Chlamydomonas reinhardtii*. *Environ Sci Technol* 42: 8959-8964. <http://dx.doi.org/10.1021/es801785m>
- Nazarenko, Y; Han, TW; Liroy, PJ; Mainelis, G. (2011). Potential for exposure to engineered nanoparticles from nanotechnology-based consumer spray products. *J Expo Sci Environ Epidemiol* 21: 515-528. <http://dx.doi.org/10.1038/jes.2011.10>
- NC DEHNR (North Carolina Department of Environment Health and Natural Resources). (2007). Surface water and wetland standards (pp. A1-A5).
- Neal, AL. (2008). What can be inferred from bacterium-nanoparticle interactions about the potential consequences of environmental exposure to nanoparticles? *Ecotoxicology* 17: 362-371. <http://dx.doi.org/10.1007/s10646-008-0217-x>

- [Nichols, G; Byard, S; Bloxham, MJ; Botterill, J; Dawson, NJ; Dennis, A; Diart, V; North, NC; Sherwood, JD.](#) (2002). A review of the terms agglomerate and aggregate with a recommendation for nomenclature used in powder and particle characterization [Review]. *J Pharm Sci* 91: 2103-2109. <http://dx.doi.org/10.1002/jps.10191>
- [Nichols, JB; Wirgin, I; Chambers, R; Gordon, T.](#) (2009). Abstract no. 251: Toxicities of nanoparticles in an environmentally relevant fish model [Abstract]. *Toxicologist* 108: 52.
- [Nichols, JW; Brown, S; Wood, CM; Walsh, PJ; Playle, RC.](#) (2006). Influence of salinity and organic matter on silver accumulation in Gulf toadfish (*Opsanus beta*). *Aquat Toxicol* 78: 253-261.
- [Nielsen, HD; Berry, LS; Stone, V; Burrige, TR; Fernandes, TF.](#) (2008). Interactions between carbon black nanoparticles and the brown algae *Fucus serratus*: Inhibition of fertilization and zygotic development. *Nanotoxicology* 2: 88-97. <http://dx.doi.org/10.1080/17435390802109185>
- [NIOSH](#) (National Institute for Occupational Safety and Health). (2009). Approaches to safe nanotechnology: Managing the health and safety concerns associated with engineered nanomaterials. (2009-125). Cincinnati, OH. <http://cdc.gov/niosh/docs/2009-125/>
- [NIOSH](#) (National Institute for Occupational Safety and Health). (2010). NIOSH pocket guide to chemical hazards: Silver (metal dust and soluble compounds, as Ag). <http://www.cdc.gov/niosh/npg/npgd0557.html>
- [Niskanen, J; Shan, J; Tenhu, H; Jiang, H; Kauppinen, E; Barranco, V; Picó, F; Yliniemi, K; Kontturi, K.](#) (2010). Synthesis of copolymer-stabilized silver nanoparticles for coating materials. *Colloid and Polymer Science* 288: 543-553. <http://dx.doi.org/10.1007/s00396-009-2178-x>
- [NOSH Consortium](#) (Nanoparticle Occupational Safety and Health Consortium). (2008). Nanoparticle occupational safety and health consortium presentations. Paper presented at Nanoparticle occupational safety and health consortium, November 14, 2006, Unknown.
- [Nowack, B; Bucheli, TD.](#) (2007). Occurrence, behavior and effects of nanoparticles in the environment. *Environ Pollut* 150: 5-22. <http://dx.doi.org/10.1016/j.envpol.2007.06.006>
- [Nowack, B; Krug, H; Height, M.](#) (2011). 120 years of nanosilver history: Implications for policy makers. *Environ Sci Technol* 45: 3189. <http://dx.doi.org/10.1021/es103316q>
- [NSTC](#) (NationalScienceandTechnologyCouncil). (2008). The National Nanotechnology Initiative (NNI) - Strategy for nanotechnology-related environmental, health, and safety (EHS) research. Washington, DC: The National Nanotechnology Initiative (NNI); Nanotechnology Environmental and Health Implications (NEHI) Working Group; Subcommittee on Nanoscale Science, Engineering, and Technology (NSET); Committee on Technology (CT); National Science and Technology Council (NSTC). http://www.nano.gov/NNI_EHS_Research_Strategy.pdf
- [NSTC](#) (NationalScienceandTechnologyCouncil). (2011). National nanotechnology initiative: Strategic plan. National Science and Technology Council. http://www.nano.gov/sites/default/files/pub_resource/2011_strategic_plan.pdf
- [O'Brien, N; Cummins, E.](#) (2009). Development of a three-level risk assessment strategy for nanomaterials. In *Nanomaterials: Risks and Benefits*. The Netherlands: Springer Netherlands. <http://dx.doi.org/10.1007/978-1-4020-9491-0>
- [O'Hara, AM; Shanahan, F.](#) (2006). The gut flora as a forgotten organ. *EMBO Rep* 7: 688-693. <http://dx.doi.org/10.1038/sj.embor.7400731>
- [Oberdörster, G.](#) (1988). Lung clearance of inhaled insoluble and soluble particles. *J Aerosol Med* 1: 289-330.
- [Oberdorster, G; Gelein, RM; Ferin, J; Weiss, B.](#) (1995). Association of particulate air pollution and acute mortality: involvement of ultrafine particles? *Inhal Toxicol* 7: 111-124.
- [Oberdörster, G; Maynard, A; Donaldson, K; Castranova, V; Fitzpatrick, J; Ausman, K; Carter, J; Karn, B; Kreyling, W; Lai, D; Olin, S; Monteiro-Riviere, N; Warheit, D; Yang, H.](#) (2005a). Principles for characterizing the potential human health effects from exposure to nanomaterials: Elements of a screening strategy. *Part Fibre Toxicol* 2: 1-35. <http://dx.doi.org/10.1186/1743-8977-2-8>

- [Oberdorster, G; Oberdorster, E; Oberdorster, J.](#) (2007). Concepts of nanoparticle dose metric and response metric [letter] [Letter]. *Environ Health Perspect* 115: A290-A294.
- [Oberdörster, G; Oberdörster, E; Oberdörster, J.](#) (2005b). Nanotoxicology: An emerging discipline evolving from studies of ultrafine particles. *Environ Health Perspect* 113: 823-839.
- [Oberdörster, G; Sharp, Z; Atudorei, V; Elder, A; Gelein, R; Kreyling, W; Cox, C.](#) (2004). Translocation of inhaled ultrafine particles to the brain. *Inhal Toxicol* 16: 437-445. <http://dx.doi.org/10.1080/08958370490439597>
- [OECD](#) (Organisation for Economic Co-operation and Development). (2008). Series on the safety of manufactured nanomaterials, Number 6: List of manufactured nanomaterials and list of endpoints for phase one of the OECD testing programme. (ENV/JM/MONO(2008)13/REV). Paris, France. [http://www.olis.oecd.org/olis/2008doc.nsf/LinkTo/NT000034C6/\\$FILE/JT03248749.PDF](http://www.olis.oecd.org/olis/2008doc.nsf/LinkTo/NT000034C6/$FILE/JT03248749.PDF)
- [Oh, SG; Yi, SC; Shin, SI; Kim, DW; Jeong, SH.](#) (2003). Preparation of silver and silver alloyed nanoparticles in surfactant solutions. (U.S. Patent No. 6,660,058). Washington, DC: U.S. Patent and Trademark Office.
- [Ohbo, Y; Fukuzako, H; Takeuchi, K; Takigawa, M.](#) (1996). Argyria and convulsive seizures caused by ingestion of silver in a patient with schizophrenia. *Psychiatr Clin Neurosci* 50: 89-90.
- [Ono-Ogasawara, M; Serita, F; Takaya, M.](#) (2009). Distinguishing nanomaterial particles from background airborne particulate matter for quantitative exposure assessment. *J Nanopart Res* 11: 1651-1659.
- [Oregon Department of Environmental Quality.](#) (2004). Water quality standards: Beneficial uses, policies, and criteria for Oregon: Toxic substances.
- [OSHA](#) (Occupational Safety & Health Administration). (2010). OSHA Standard 1915.1000 for Air Contaminants. Part Z, Toxic and Hazardous Substances. Available online at http://www.osha.gov/pls/oshaweb/owadisp.show_document?p_table=STANDARDS&p_id=10286 (accessed May 24, 2010).
- [Ostraat, ML.](#) (2009). Industry-led initiative for occupational health and safety. In M Hull; S Friedrichs (Eds.), *Risk governance of nanotechnology: Environmental, health and safety concerns* (pp. 181-246). Norwich, NY: William Andrew Publishing.
- [Ostrowski, A; Martin, T; Conti, J; Hurt, I; Harthorn, B.](#) (2009). Nanotoxicology: Characterizing the scientific literature, 2000-2007. *J Nanopart Res* 11: 251-257. <http://dx.doi.org/10.1007/s11051-008-9579-5>
- [Owen, G.](#) (1970). The fine structure of the digestive tubules of the marine bivalve *Cardium edule*. *Philos Trans R Soc Lond B Biol Sci* 258: 245-260. <http://dx.doi.org/10.1098/rstb.1970.0035>
- [Paddle-Ledinek, JE; Nasa, Z; Cleland, HJ.](#) (2006). Effect of different wound dressings on cell viability and proliferation. *Plast Reconstr Surg* 117: 110S-118S; discussion 119S-120S. <http://dx.doi.org/10.1097/01.prs.0000225439.39352.ce>
- [Pal, S; Tak, YK; Song, JM.](#) (2007). Does the antibacterial activity of silver nanoparticles depend on the shape of the nanoparticle? A study of the gram-negative bacterium *Escherichia coli*. *Appl Environ Microbiol* 73: 1712-1720. <http://dx.doi.org/10.1128/aem.02218-06>
- [Panáček, A; Kvítek, L; Pucek, R; Kolář, M; Večeřová, R; Pizúrová, N; Sharma, VK; Tj, N; Zbořil, R.](#) (2006). Silver colloid nanoparticles: Synthesis, characterization, and their antibacterial activity. *J Phys Chem B* 110: 16248-16253. <http://dx.doi.org/10.1021/jp063826h>
- [Pandis, SN; Davidson, C.](#) (1999). Aerosols and water droplets. In SS Olin (Ed.), *Exposure to contaminants in drinking water: estimating uptake through the skin and by inhalation*. Boca Raton, FL: CRC Press.
- [Panyala, N; Pena-Mendze, E; Havel, J.](#) (2008). Silver or silver nanoparticles: A hazardous threat to the environment and human health? *J Appl Biomed* 6: 117-129.
- [Park, EJ; Bae, E; Yi, J; Kim, Y; Choi, K; Lee, SH; Yoon, J; Lee, BC; Park, K.](#) (2010a). Repeated-dose toxicity and inflammatory responses in mice by oral administration of silver nanoparticles. *Environ Toxicol Pharmacol* 30: 162-168. <http://dx.doi.org/10.1016/j.etap.2010.05.004>

- [Park, J; Kwak, B; Bae, E; Lee, J; Kim, Y; Choi, K; Yi, J.](#) (2009). Characterization of exposure to silver nanoparticles in a manufacturing facility. *J Nanopart Res* 11: 1705-1712.
- [Park, M; Kim, K; Lee, H; Kim, J; Hwang, S.](#) (2010b). Selective inhibitory potential of silver nanoparticles on the harmful cyanobacterium *Microcystis aeruginosa*. *Biotechnol Lett* 32: 423-428. <http://dx.doi.org/10.1007/s10529-009-0161-8>
- [Pascal, LE; Tessier, DM.](#) (2004). Cytotoxicity of chromium and manganese to lung epithelial cells in vitro. *Toxicol Lett* 147: 143-151.
- [Pedroso, MS; Pinho, GLL; Rodrigues, SC; Bianchini, A.](#) (2007). Mechanism of acute silver toxicity in the euryhaline copepod *Acartia tonsa*. *Aquat Toxicol* 82: 173-180.
- [Pietropaoli, AP; Frampton, MW; Hyde, RW; Morrow, PE; Oberdorster, G; Cox, C; Speers, DM; Frasier, LM; Chalupa, DC; Huang, LS; Utell, MJ.](#) (2004). Pulmonary function, diffusing capacity, and inflammation in healthy and asthmatic subjects exposed to ultrafine particles. *Inhal Toxicol* 16: 59-72.
- [Pifer, JW; Friedlander, BR; Kintz, RT; Stockdale, DK.](#) (1989). Absence of toxic effects in silver reclamation workers. *Scand J Work Environ Health* 15: 210-221.
- [Postlethwait, JH; Woods, IG; Ngo-Hazelett, P; Yan, YL; Kelly, PD; Chu, F; Huang, H; Hill-Force, A; Talbot, WS.](#) (2000). Zebrafish comparative genomics and the origins of vertebrate chromosomes. *Genome Res* 10: 1890-1902.
- [Powers, C; Yen, J; Linney, E; Seidler, F; Slotkin, T.](#) (2010a). Silver exposure in developing zebrafish (*Danio rerio*): persistent effects on larval behavior and survival. *Neurotoxicol Teratol* 32: 391-397. <http://dx.doi.org/10.1016/j.ntt.2010.01.009>
- [Powers, CM; Wrench, N; Ryde, IT; Smith, AM; Seidler, FJ; TA, S.](#) (2010b). Silver impairs neurodevelopment: Studies in PC12 cells. *Environ Health Perspect* 118: 73-79. <http://dx.doi.org/10.1289/ehp.0901149>
- [Powers, KW; Brown, SC; Krishna, VB; Wasdo, SC; Moudgil, BM; Roberts, SM.](#) (2006). Research strategies for safety evaluation of nanomaterials. Part VI. Characterization of nanoscale particles for toxicological evaluation. *Toxicol Sci* 90: 296-303.
- [Powers, KW; Palazuelos, M; Moudgil, BM; Roberts, SM.](#) (2007). Characterization of the size, shape, and state of dispersion of nanoparticles for toxicological studies. *Nanotoxicology* 1: 42-51. <http://dx.doi.org/10.1080/17435390701314902>
- [Price, OT; Asgharian, B; Miller, FJ; Cassee, FR; deWinter-Sorkina, R.](#) (2002). Multiple path particle dosimetry model (MPPD v 1.0): A model for human and rat airway particle dosimetry (Version v 1.0) [Computer Program]. Bilthoven, The Netherlands: National Institute for Public Health and the Environment (RIVM). Retrieved from <http://www.rivm.nl/bibliotheek/rapporten/650010030.html>
- [Project on Emerging Nanotechnologies.](#) (2009). Inventory of nanotechnology-based consumer products. Available online at <http://www.nanotechproject.org/inventories/consumer/> (accessed March 1, 2009).
- [Pronk, MEJ; Wijnhoven, SWP; Bleeker, EAJ; Heugens, EHW; Peijnenburg, WJG, M; Luttik, R; Hakkert, BC.](#) (2009). Nanomaterials under REACH: Nanosilver as a case study. Bilthoven, the Netherlands: National Institute for Public Health and the Environment. <http://www.rivm.nl/bibliotheek/rapporten/601780003.pdf>
- [Purcell, TW; Peters, JJ.](#) (1998). Sources of silver in the environment. *Environ Toxicol Chem* 17: 539-546.
- [Quadros, ME; Marr, LC.](#) (2010). Environmental and human health risks of aerosolized silver nanoparticles. *J Air Waste Manag Assoc* 60: 770-781. <http://dx.doi.org/10.3155/1047-3289.60.7.770>
- [Quadros, ME; Marr, LC.](#) (2011). Silver nanoparticles and total aerosols emitted by nanotechnology-related consumer spray products. *Environ Sci Technol* 45: 10713-10719. <http://dx.doi.org/10.1021/es202770m>
- [Rahman, M; Wang, J; Patterson, T; Saini, U; Robinson, B; Newport, G; Murdock, R; Schlager, J; Hussain, S; Ali, S.](#) (2009). Expression of genes related to oxidative stress in the mouse brain after exposure to silver-25 nanoparticles. *Toxicol Lett* 187: 15-21. <http://dx.doi.org/10.1016/j.toxlet.2009.01.020>

- Ratte, HT. (1999). Bioaccumulation and toxicity of silver compounds: A review [Review]. *Environ Toxicol Chem* 18: 89-108.
- Raymond, KN. (2003). Bioinorganic Chemistry Special Feature: Enterobactin: An archetype for microbial iron transport. *PNAS* 100: 3584-3588. <http://dx.doi.org/10.1073/pnas.0630018100>
- Reinfelder, JR; Fisher, NS; Luoma, SN; Nichols, JW; Wang, WX. (1998). Trace element trophic transfer in aquatic organisms: A critique of the kinetic model approach. *Sci Total Environ* 219: 117-135. [http://dx.doi.org/10.1016/S0048-9697\(98\)00225-3](http://dx.doi.org/10.1016/S0048-9697(98)00225-3)
- Reinhart, DR; Berge, ND; Santra, S; Bolyard, SC. (2010). Emerging contaminants: Nanomaterial fate in landfills. *Waste Manag* 30: 2020-2021. <http://dx.doi.org/10.1016/j.wasman.2010.08.004>
- Ringwood, A; McCarthy, M; Bates, T; Carroll, D. (2010). The effects of silver nanoparticles on oyster embryos. *Neurotoxicol Teratol* 69: S49-S51. <http://dx.doi.org/10.1016/j.marenvres.2009.10.011>
- Rogers, D. (2003). The airway goblet cell. *Int J Biochem Cell Biol* 35: 1-6.
- Roh, JY; Sim, SJ; Yi, J; Park, K; Chung, KH; Ryu, DY; Choi, J. (2009). Ecotoxicity of silver nanoparticles on the soil nematode *Caenorhabditis elegans* using functional ecotoxicogenomics. *Environ Sci Technol* 43: 3933-3940.
- Rojó, I; Uriarte, M; Obieta, I; Bustero, I; Egizabal, A; Pardo, MA; De Martinez Ilarduya, O. (2007). Toxicogenomics study of nanomaterials on the model organism zebrafish. In *NSTI Nanotech Technical Proceedings, Vol 2*. Boston, MA: Nano Science and Technology Institute.
- Rosas-Hernández, H; Jiménez-Badillo, S; Martínez-Cuevas, PP; Gracia-Espino, E; Terrones, H; Terrones, M; Hussain, SM; Ali, SF; González, C. (2009). Effects of 45-nm silver nanoparticles on coronary endothelial cells and isolated rat aortic rings. *Toxicol Lett* 191: 305-313. <http://dx.doi.org/10.1016/j.toxlet.2009.09.014>
- Rosenman, K; Seixas, N; Jacobs, I. (1987). Potential nephrotoxic effects of exposure to silver. *Br J Ind Med* 44: 267-272.
- Rostami, AA; Shahsavar, A. (2009). Nano-silver particles eliminate the in vitro contaminations of olive 'mission' explants. *Asian J Plant Sci* 8: 1-5.
- Rozan, T; Hunter, K; Benoit, G. (1995). Silver in fresh water: Sources, transport and fate in Connecticut rivers. In *AW Andren; TW Bober (Eds.), The 3rd international conference proceedings: Transport, fate and effects of silver in environment* (pp. 181184). Madison, WI: University of Wisconsin System, Sea Grant Institute. <http://digital.library.wisc.edu/1711.dl/EcoNatRes.Argentumv03>
- Rozan, TF; Hunter, KS. (2001). Effects of discharge on silver loading and transport in the Quinnipiac River, Connecticut. *Sci Total Environ* 279: 195-205. [http://dx.doi.org/10.1016/S0048-9697\(01\)00781-1](http://dx.doi.org/10.1016/S0048-9697(01)00781-1)
- Rungby, J; Danscher, G. (1983). Neuronal accumulation of silver in brains of progeny from argyric rats. *Acta Neuropathol* 61: 258-262.
- Rungby, J; Slomianka, L; Danscher, G; Holst Andersen, A; West, M. (1987). A quantitative evaluation of the neurotoxic effect of silver on the volumes of the components of the developing rat hippocampus. *Toxicology* 43: 261-268. [http://dx.doi.org/10.1016/0300-483X\(87\)90085-0](http://dx.doi.org/10.1016/0300-483X(87)90085-0)
- Sadauskas, E; Wallin, H; Stoltenberg, M; Vogel, U; Doering, P; Larsen, A; Danscher, G. (2007). Kupffer cells are central in the removal of nanoparticles from the organism. *Part Fibre Toxicol* 4: 10. <http://dx.doi.org/10.1186/1743-8977-4-10>
- Saleh, N; Pfefferle, L; Elimelech, M. (2008). Aggregation kinetics of multiwalled carbon nanotubes in aquatic systems: Measurements and environmental implications. *Environ Sci Technol* 42: 7963-7969. <http://dx.doi.org/10.1021/es801251c>
- Salnikov, DS; Pogorelova, AS; Makarov, SV; Vashurina, IY. (2009). Silver ion reduction with peat fulvic acids. *Russian Journal of Applied Chemistry* 82: 545-548. <http://dx.doi.org/10.1134/S107042720904003X>

- [Samberg, ME; Oldenburg, SJ; Monteiro-Riviere, NA.](#) (2010). Evaluation of silver nanoparticle toxicity in skin in vivo and keratinocytes in vitro. *Environ Health Perspect* 118: 407-413. <http://dx.doi.org/10.1289/ehp.0901398>
- [Sap-Iam, N; Homklincha, C; Larpudomle, R; Warisnoich, W; Sreemaspu, A; Dubas, ST.](#) (2010). UV irradiation-induced silver nanoparticles as mosquito larvicides. *Journal of Applied Sciences* 10: 3132-3136. <http://dx.doi.org/10.3923/jas.2010.3132.3136>
- [Saulou, C; Jamme, F; Maranges, C; Fourquaux, I; Despax, B; Raynaud, P; Dumas, P; Mercier-Bonin, M.](#) (2010). Synchrotron FTIR microspectroscopy of the yeast *Saccharomyces cerevisiae* after exposure to plasma-deposited nanosilver-containing coating. *Anal Bioanal Chem* 396: 1441-1450. <http://dx.doi.org/10.1007/s00216-009-3316-5>
- [Savolainen, K; Alenius, H; Norppa, H; Pylkkänen, L; Tuomi, T; Kasper, G.](#) (2010). Risk assessment of engineered nanomaterials and nanotechnologies--A review. *Toxicology* 269: 92-104. <http://dx.doi.org/10.1016/j.tox.2010.01.013>
- [Sawafta, R; Haik, Y; Hitchcock, W; Kuturu, V; Ciubotaru, I; Lee, YS.](#) (2008). Nanocomposites with residual biocidal and biostatic properties. (U.S. Patent Application No. 11/671,675). Washington, DC: U.S. Patent and Trademark Office.
- [Sawosz, E; Binek, M; Grodzik, M; Zielinska, M; Sysa, P; Szmidt, M; Niemiec, T; Chwalibog, A.](#) (2007). Influence of hydrocolloidal silver nanoparticles on gastrointestinal microflora and morphology of enterocytes of quails. *Arch Anim Nutr* 61: 444-451.
- [Sayes, CM; Wahi, R; Kurian, PA; Liu, Y; West, JL; Ausman, KD; Warheit, DB; Colvin, VL.](#) (2006). Correlating nanoscale titania structure with toxicity: A cytotoxicity and inflammatory response study with human dermal fibroblasts and human lung epithelial cells. *Toxicol Sci* 92: 174-185. <http://dx.doi.org/10.1093/toxsci/kfj197>
- [Sayes, CM; Warheit, DB.](#) (2009). Characterization of nanomaterials for toxicity assessment. *Wiley Interdiscip Rev Nanomed Nanobiotechnol* 1: 660-670. <http://dx.doi.org/10.1002/wnan.58>
- [SCHER](#) (European Commission, Health & Consumer Protection Directorate-General, Scientific Committee on Health and Environmental Risks). (2009). Risk assessment of products of nanotechnologies (pp. 1-71). Brussels, Belgium: Scientific Committee on Emerging and Newly Identified Health Risks, Directorate-General for Health & Consumers. http://ec.europa.eu/health/ph_risk/committees/04_scenihr/docs/scenihr_o_023.pdf
- [Schmittschmitt, JP; Shaw, JR; Birge, WJ.](#) (1996). Effects of silver on green algae and prospects for trophic transfer. In *The 4th international Conference Proceedings: Transport, Fate and Effects of Silver in the Environment*. Madison, WI: University of Wisconsin System, Sea Grant Institute. <http://digital.library.wisc.edu/1711.dl/EcoNatRes.Argentumv04>
- [Schuster, A; Franz, UF; Daschner, D.](#) (2004). Persistent silver disinfectant for the environment: Myth and reality. *Am J Infect Control* 32: 309.
- [Scown, T; Santos, E; Johnston, B; Gaiser, B; Baalousha, M; Mitov, S; Lead, J; Stone, V; Fernandes, T; Jepson, M; van Aerle, R; Tyler, C.](#) (2010). Effects of aqueous exposure to silver nanoparticles of different sizes in rainbow trout. *Toxicol Sci* 115: 521-534. <http://dx.doi.org/10.1093/toxsci/kfq076>
- [Seipenbusch, M; Binder, A; Kasper, G.](#) (2008). Temporal evolution of nanoparticle aerosols in workplace exposure. *Ann Occup Hyg* 52: 707-716. <http://dx.doi.org/10.1093/annhyg/men067>
- [Senjen, R.](#) (2007). *Nanosilver: A threat to soil, water and human health?* Australia: Friends of the Earth Australia.
- [Shahbazzadeh, D; Ahari, H; Rahimi, NM; Dastmalchi, F; Soltani, M; Fotovat, M; Rahmannya, J; Khorasani, N.](#) (2009). The effects of nanosilver (Nanocid(R)) on survival percentage of rainbow trout (*Oncorhynchus mykiss*). *Pakistan J Nutr* 8: 1178-1179.

- [Shanghai Huzheng Nanotechnology Co.](#) (Shanghai Huzheng Nanotechnology Co. Ltd). (2009). Shanghai Huzheng Nanotechnology Company. Available online at <http://www.hznano.com/en/productsall.asp> (accessed February 11, 2010).
- [Shatkin, JA.](#) (2008). Informing environmental decision making by combining life cycle assessment and risk analysis. *J Ind Ecol* 12: 278-281. <http://dx.doi.org/10.1111/j.1530-9290.2008.00031.x>
- [Shin, YM; Kim, HS; Kang, HS.](#) (2007). The effects of nano-silver on the proliferation and cytokine expression by peripheral blood mononuclear cell. *Int Immunopharmacol* 7: 1813-1818.
- [Shoultz-Wilson, WA; Reinsch, BC; Tsyusko, OV; Bertsch, PM; Lowry, GV; Unrine, JM.](#) (2011a). Effect of silver nanoparticle surface coating on bioaccumulation and reproductive toxicity in earthworms (*Eisenia fetida*). *Nanotoxicology* 5: 432-444. <http://dx.doi.org/10.3109/17435390.2010.537382>
- [Shoultz-Wilson, WA; Zhurbich, OI; Mcnear, DH; Tsyusko, OV; Bertsch, PM; Unrine, JM.](#) (2011b). Evidence for avoidance of Ag nanoparticles by earthworms (*Eisenia fetida*). *Ecotoxicology* 20: 385-396. <http://dx.doi.org/10.1007/s10646-010-0590-0>
- [Shrivastava, S; Bera, T; Roy, A; Singh, G; Ramachandrarao, P; Dash, D.](#) (2007). Characterization of enhanced antibacterial effects of novel silver nanoparticles. *Nanotechnology* 18: 1-9. <http://dx.doi.org/10.1088/0957-4484/18/22/225103>
- [Shrivastava, S; Bera, T; Singh, SK; Singh, G; Ramachandrarao, P; Dash, D.](#) (2009). Characterization of antiplatelet properties of silver nanoparticles. *ACS Nano* 3: 1357-1364. <http://dx.doi.org/10.1021/nn900277t>
- [Siekkinen, A; McLellan, J; Chen, J; Xia, Y.](#) (2006). Rapid synthesis of small silver nanocubes by mediating polyol reduction with a trace amount of sodium sulfide or sodium hydrosulfide. *Chem Phys Lett* 432: 491-496.
- [Silver Nanotechnology Working Group](#) (Silver Institute, Silver Nanotechnology Working Group). (2009). Comments of the silver nanotechnology working group for review by the FIFRA scientific advisory panel. Washington, DC. <http://www.silverinstitute.org/snwg.php>
- [Simonet, BM; Valcarcel, M.](#) (2009). Monitoring nanoparticles in the environment. *Anal Bioanal Chem* 393: 17-21. <http://dx.doi.org/10.1007/s00216-008-2484-z>
- [Sinha, R; Karan, R; Sinha, A; Khare, SK.](#) (2011). Interaction and nanotoxic effect of ZnO and Ag nanoparticles on mesophilic and halophilic bacterial cells. *Bioresour Technol* 102: 1516-1520. <http://dx.doi.org/10.1016/j.biortech.2010.07.117>
- [Smith, GJ; Flegal, AR.](#) (1993). Silver in San Francisco Bay estuarine waters. *Estuaries Coasts* 16: 547-558. <http://dx.doi.org/10.2307/1352602>
- [Smith, IC; Carson, BL.](#) (1977). Trace metals in the environment: Volume 2 - Silver. Ann Arbor, MI: Ann Arbor Science Publishers.
- [Sondi, I; Salopek-Sondi, B.](#) (2004). Silver nanoparticles as antimicrobial agent: A case study on *E. coli* as a model for gram-negative bacteria. *J Colloid Interface Sci* 275: 177-182. <http://dx.doi.org/10.1016/j.jcis.2004.02.012>
- [Sotiriou, GA; Pratsinis, SE.](#) (2010). Antibacterial activity of nanosilver ions and particles. *Environ Sci Technol* 44: 5649-5654. <http://dx.doi.org/10.1021/es101072s>
- [Speshock, J; Murdock, R; Braydich-Stolle, L; Schrand, A; Hussain, S.](#) (2010). Interaction of silver nanoparticles with Tacaribe virus. *Journal of Nanobiotechnology* 8: 19. <http://dx.doi.org/10.1186/1477-3155-8-19>
- [Stampoulis, D; Sinha, S; White, J.](#) (2009). Assay-dependent phytotoxicity of nanoparticles to plants. *Environ Sci Technol* 43: 9473-9479. <http://dx.doi.org/10.1021/es901695c>
- [Stolpe, B; Hasselov, M.](#) (2007). Changes in size distribution of fresh water nanoscale colloidal matter and associated elements on mixing with seawater. *Geochim Cosmo Acta* 71: 3292-3301. <http://dx.doi.org/10.1016/j.gca.2007.04.025>

- StroyprojectLTD. (2009). Cloud seeding info. Available online at <http://www.cloud-seeding.com/?&show=item&usbid=10053> (accessed January 29, 2010).
- Stumm, W; Morgan, JJ. (1995). Aquatic chemistry: chemical equilibria and rates in natural waters.
- Sun, H; Zhang, X; Niu, Q; Chen, Y; Crittenden, JC. (2007). Enhanced accumulation of arsenate in carp in the presence of titanium dioxide nanoparticles. *Water Air Soil Pollut* 178: 245-254.
- Sun, RWY; Chen, R; Chung, NPY; Ho, CM; Lin, CLS; Che, CM. (2005). Silver nanoparticles fabricated in Hepes buffer exhibit cytoprotective activities toward HIV-1 infected cells. *Chem Commun (Camb)* 2005: 5059-5061. <http://dx.doi.org/10.1039/b510984a>
- Sun, Y; Mayers, BT; Xia, Y. (2002). Template-engaged replacement reaction: A one-step approach to the large-scale synthesis of metal nanostructures with hollow interiors. *Nano Lett* 5: 481-485. <http://dx.doi.org/10.1021/nl025531v>
- Sun, Y; Xia, Y. (1991). Large-scale synthesis of uniform silver nanowires through a soft, self-seeding, polyol process. *Adv Mater Deerfield* 14: 833-837. [http://dx.doi.org/10.1002/1521-4095\(20020605\)14:11<833::AID-ADMA833>3.0.CO;2-K](http://dx.doi.org/10.1002/1521-4095(20020605)14:11<833::AID-ADMA833>3.0.CO;2-K)
- Sun, Y; Xia, Y. (2002). Shape-controlled synthesis of gold and silver nanoparticles. *Science* 5601: 2176.
- Sung, JH; Ji, JH; Park, JD; Yoon, JU; Kim, DS; Jeon, KS; Song, MY; Jeong, J; Han, BS; Han, JH; Chung, YH; Chang, HK; Lee, JH; Cho, MH; Kelman, BJ; Yu, IJ. (2009). Subchronic inhalation toxicity of silver nanoparticles. *Toxicol Sci* 108: 452-461. <http://dx.doi.org/10.1093/toxsci/kfn246>
- Sung, JH; Ji, JH; Yoon, JU; Kim, DS; Song, MY; Jeong, J; Han, BS; Han, JH; Chung, YH; Kim, J; Kim, TS; Chang, HK; Lee, EJ; Lee, JH; Yu, IJ. (2008). Lung function changes in Sprague-Dawley rats after prolonged inhalation exposure to silver nanoparticles. *Inhal Toxicol* 20: 567-574.
- Suresh, A; Pelletier, D; Wang, W; Moon, J; Gu, B; Mortensen, N; Allison, D; Joy, D; Phelps, T; Doktycz, M. (2010). Silver nanocrystallites: Biofabrication using *Shewanella oneidensis*, and an evaluation of their comparative toxicity on gram-negative and gram-positive bacteria. *Environ Sci Technol* 44: 5210-5215. <http://dx.doi.org/10.1021/es903684r>
- Sutter, TR. (1995). Molecular and cellular approaches to extrapolation for risk assessment. *Environ Health Perspect* 103: 386-389.
- Sweet, S; Singh, G. (1995). Accumulation of Human Promyelocytic Leukemia (HL-60) Cells at Two Energetic Cell Cycle Checkpoints. *Cancer Res* 55: 5164-5167.
- Takenaka, S; Karg, E; Möller, W; Roth, C; Ziesenis, A; Heinzmann, U; Schramel, P; Heyder, J. (2000). A morphologic study on the fate of ultrafine silver particles: Distribution pattern of phagocytized metallic silver in vitro and in vivo. *Inhal Toxicol* 12: 291-299. <http://dx.doi.org/10.1080/08958370050165166>
- Takenaka, S; Karg, E; Roth, C; Schulz, H; Ziesenis, A; Heinzmann, U; Schramel, P; Heyder, J. (2001). Pulmonary and systemic distribution of inhaled ultrafine silver particles in rats. *Environ Health Perspect* 4: 547-551.
- Tang, J; Xiong, L; Wang, S; Wang, J; Liu, L; Li, J; Wan, Z; Xi, T. (2008). Influence of silver nanoparticles on neurons and blood-brain barrier via subcutaneous injection in rats. *Appl Surf Sci* 255: 502-504. <http://dx.doi.org/10.1016/j.apsusc.2008.06.058>
- Taurozzi, JS; Hackley, VA; Wiesner, MR. (2011). Ultrasonic dispersion of nanoparticles for environmental, health and safety assessment--issues and recommendations. *Nanotoxicology* 5: 711-729. <http://dx.doi.org/10.3109/17435390.2010.528846>
- Taylor, MR. (2008). Assuring the Safety of Nanomaterials in Food Packaging. The Regulatory Process and Key Issues. Washington, DC: Woodrow Wilson International Center for Scholars. http://www.nanotechproject.org/process/assets/files/6704/taylor_gma_pen_packaging1.pdf
- Temgire, M; Joshi, S. (2004). Optical and structural studies of silver nanoparticles. *Radiat Phys Chem Oxf Engl* 1993 5: 1039-1044.

- Terhaar, C; Ewell, W; Dziuba, S; White, W; Murphy, P. (1977). A laboratory model for evaluating the behaviour of heavy metals in an aquatic environment. *Water Res* 11: 101-110.
- The Silver Institute. (2009a). Silver facts. Available online at http://www.silverinstitute.org/silver_facts.php (accessed January 14, 2010).
- The Silver Institute. (2009b). Silver history. Available online at http://www.silverinstitute.org/silver_history.php (accessed October 11, 2009).
- Thomas, K; Sayre, P. (2005). Research strategies for safety evaluation of nanomaterials, Part I: Evaluating the human health implications of exposure to nanoscale materials. *Toxicol Sci* 87: 316-321.
- Tiede, K; Boxall, ABA; Tear, SP; Lewis, J; David, H; Hassellöv, M. (2008). Detection and characterization of engineered nanoparticles in food and the environment. *Food Addit Contam Part A Chem Anal Control Expo Risk Assess* 25: 795-821. <http://dx.doi.org/10.1080/02652030802007553>
- Tiede, K; Boxall, ABA; Wang, X; Gore, D; Tiede, D; Baxter, M; David, H; Tear, SP; Lewis, J. (2010). Application of hydrodynamic chromatography-ICP-MS to investigate the fate of silver nanoparticles in activated sludge. *J Anal At Spectrom* 25: 1149-1154. <http://dx.doi.org/10.1039/B926029C>
- Tiede, K; Hasselov, M; Breitbarth, E; Chaudhry, Q; AB, B. (2009). Considerations for environmental fate and ecotoxicity testing to support environmental risk assessments for engineered nanoparticles. *J Chromatogr A* 1216: 503-509.
- Tiwari, DK; Jin, T; Behari, J. (2011). Dose-dependent in-vivo toxicity assessment of silver nanoparticle in Wistar rats. *Toxicol Mech Meth* 21: 13-24. <http://dx.doi.org/10.3109/15376516.2010.529184>
- Tolaymat, TM; El Badawy, AM; Genaidy, A; Scheckel, KG; Luxton, TP; Suidan, M. (2010). An evidence-based environmental perspective of manufactured silver nanoparticle in syntheses and applications: A systematic review and critical appraisal of peer-reviewed scientific papers. *Sci Total Environ* 408: 999-1006. <http://dx.doi.org/10.1016/j.scitotenv.2009.11.003>
- Torkzaban, S; Kim, Y; Mulvihill, M; Wan, J; Tokunaga, T. (2010). Transport and deposition of functionalized CdTe nanoparticles in saturated porous media. *J Contam Hydrol* 118: 208-217. <http://dx.doi.org/10.1016/j.jconhyd.2010.10.002>
- Trickler, W; Lantz, S; Murdock, R; Schrand, A; Robinson, B; Newport, G; Schlager, J; Oldenburg, S; Paule, M; Slikker, W; Hussain, S; Ali, S. (2010). Silver nanoparticle induced blood-brain barrier inflammation and increased permeability in primary rat brain microvessel endothelial cells. *Toxicol Sci* 118: 160-170. <http://dx.doi.org/10.1093/toxsci/kfq244>
- Trop, M; Novak, M; Rodl, S; Hellbom, B; Kroell, W; Goessler, W. (2006). Silver-coated dressing Acticoat caused raised liver enzymes and argyria-like symptoms in burn patient. *J Trauma* 60: 648-652. <http://dx.doi.org/10.1097/01.ta.0000208126.22089.b6>
- TRS Environmental. (2009). TSI-AeroTrak model 9000 nanoparticle aerosol monitor. Available online at http://www.trs-environmental.com/Model/TSI_AEROTRAK_9000.aspx (accessed June 2, 2009).
- Tsai, SJ; Ada, E; Isaacs, JA; MJ, E. (2009). Airborne nanoparticle exposures associated with the manual handling of nanoalumina and nanosilver in fume hoods. *J Nanopart Res* 11: 147-161. <http://dx.doi.org/10.1007/s11051-008-9459-z>
- Tsai, SJ; Huang, RF; Ellenbecker, MJ. (2010). Airborne nanoparticle exposures while using constant-flow, constant-velocity, and air-curtain-isolated fume hoods. *Ann Occup Hyg* 54: 78-87. <http://dx.doi.org/10.1093/annhyg/mep074>
- Tsuji, JS; Maynard, AD; Howard, PC; James, JT; Lam, CW; Warheit, DB; Santamaria, AB. (2006). Research strategies for safety evaluation of nanomaterials, part IV: risk assessment of nanoparticles. *Toxicol Sci* 89: 42-50.
- Turkevich, J; Stevenson, P; Hillier, J. (1951). A study of the nucleation and growth processes in the synthesis of colloidal gold. *Faraday Discuss* 11: 55-75.

- [U.N. Statistics Division](#). (2008). Composition of macro geographical (continental) regions, geographical sub-regions, and selected economic and other groupings. Available online at <http://millenniumindicators.un.org/unsd/methods/m49/m49regin.htm> (accessed March 11, 2010).
- [U.S. EPA](#) (U.S. Environmental Protection Agency). (1987). Ambient aquatic life water quality criteria for silver [EPA Report]. (EPA-440/5-87-011). Duluth, MN.
- [U.S. EPA](#) (U.S. Environmental Protection Agency). (1992). Guidelines for exposure assessment [EPA Report]. (EPA/600/Z-92/001). Washington, DC. <http://cfpub.epa.gov/ncea/cfm/recordisplay.cfm?deid=15263>
- [U.S. EPA](#) (U.S. Environmental Protection Agency). (1993). Silver Reregistration Eligibility Decision (R.E.D.) fact sheet [EPA Report]. (EPA-738-F-93-005). Washington, DC. <http://www.epa.gov/oppsrrd1/REDs/factsheets/4082fact.pdf>
- [U.S. EPA](#) (U.S. Environmental Protection Agency). (2003a). Health Effects Assessment Summary Tables (HEAST). Available online at <http://epa-heast.ornl.gov/>
- [U.S. EPA](#) (U.S. Environmental Protection Agency). (2003b). Methodology for deriving ambient water quality criteria for the protection of human health (2000), technical support document Volume 2: Development of national bioaccumulation factors [EPA Report]. (EPA-822-R-03-030). Washington, DC. <http://www.epa.gov/waterscience/criteria/humanhealth/method/tsdvol2.pdf>
- [U.S. EPA](#) (U.S. Environmental Protection Agency). (2005). Guidelines for carcinogen risk assessment [EPA Report]. (EPA/630/P-03/001F). Washington, DC. <http://www.epa.gov/cancerguidelines/>
- [U.S. EPA](#) (U.S. Environmental Protection Agency). (2007a). Exposure and Fate Assessment Screening Tool Version 2.0 (E-FAST V2.0). Available online at <http://www.epa.gov/opptintr/exposure/pubs/efast.htm> (accessed June 2, 2009).
- [U.S. EPA](#) (U.S. Environmental Protection Agency). (2007b). Nanotechnology white paper [EPA Report]. (EPA 100/B-07/001). Washington, DC. <http://www.epa.gov/osa/pdfs/nanotech/epa-nanotechnology-whitepaper-0207.pdf>
- [U.S. EPA](#) (U.S. Environmental Protection Agency). (2009a). Exposure assessment models. Available online at <http://www.epa.gov/ceampubl/> (accessed June 2, 2009).
- [U.S. EPA](#) (U.S. Environmental Protection Agency). (2009b). Integrated science assessment for particulate matter [EPA Report]. (EPA/600/R-08/139F). Research Triangle Park, NC. <http://cfpub.epa.gov/ncea/cfm/recordisplay.cfm?deid=216546>
- [U.S. EPA](#) (U.S. Environmental Protection Agency). (2009c). Models knowledge base. Available online at http://cfpub.epa.gov/crem/knowledge_base/knowledge.cfm (accessed June 2, 2009).
- [U.S. EPA](#) (U.S. Environmental Protection Agency). (2009d). Nanomaterial case studies: Nanoscale titanium dioxide in water treatment and topical sunscreen (external review draft) [EPA Report]. (EPA/600/R-09/057). Research Triangle Park, NC. <http://cfpub.epa.gov/ncea/cfm/recordisplay.cfm?deid=210206>
- [U.S. EPA](#) (U.S. Environmental Protection Agency). (2009e). Nanomaterial research strategy (final report) [EPA Report]. (EPA/620/K-09/011). Washington, DC. http://www.epa.gov/nanoscience/files/nanotech_research_strategy_final.pdf
- [U.S. EPA](#) (U.S. Environmental Protection Agency). (2009f). National recommended water quality criteria [EPA Report]. Washington, DC. <http://www.epa.gov/waterscience/criteria/wqctable/nrwqc-2009.pdf>
- [U.S. EPA](#) (U.S. Environmental Protection Agency). (2009g). National secondary drinking water regulation [EPA Report]. (EPA/816/F-09/004). Washington, DC. <http://www.epa.gov/safewater/consumer/pdf/mcl.pdf>
- [U.S. EPA](#) (U.S. Environmental Protection Agency). (2010a). List of lists: Consolidated list of chemicals subject to the emergency planning and community right-to-know act (epcra), comprehensive environmental response, compensation and liability act (cercla) and section 112(r) of the clean air act [EPA Report]. (EPA 550-B-10-001). Washington, DC.

- [U.S. EPA](#) (U.S. Environmental Protection Agency). (2010b). Meeting minutes of the FIFRA Scientific Advisory Panel meeting held November 3-5, 2009 on the evaluation of hazard and exposure associated with nanosilver and other nanometal pesticide products [EPA Report]. Washington, DC. <http://www.epa.gov/scipoly/sap/meetings/2009/november/110309ameetingminutes.pdf>
- [U.S. EPA](#) (U.S. Environmental Protection Agency). (2010c). Nanomaterial case studies workshop: Developing a comprehensive environmental assessment research strategy for nanoscale titanium dioxide [EPA Report]. (EPA/600/R-10/042). Research Triangle Park, NC.
- [U.S. EPA](#) (U.S. Environmental Protection Agency). (2010d). Nanomaterial case studies: Nanoscale titanium dioxide in water treatment and in topical sunscreen (final) [EPA Report]. (EPA/600/R-09/057F). Research Triangle Park, NC. <http://cfpub.epa.gov/ncea/cfm/recordisplay.cfm?deid=230972>
- [U.S. EPA](#) (U.S. Environmental Protection Agency). (2012). Integrated risk information system (IRIS). Available online at <http://www.epa.gov/iris/index.html>
- [U.S. NCAR](#) (U.S. National Center for Atmospheric Research). (2006). Silver Clouds. *Weatherwise* 3: 15.
- [Van de Voorde, K; Nijsten, T; Schelfhout, K; Moorkens, G; Lambert, J.](#) (2005). Long-term use of silver containing nose-drops resulting in systemic argyria. *Acta Clin Belg* 60: 33-35.
- [vandenBrink, W.](#) (2008). Monitoring of airborne nano particles at industrial workplaces by means of a portable device will enable strategies to reduce exposure levels and improve the health and safety of workers. Paper presented at Nanosafe 2008, November 3-7, 2008, Grenoble, France.
- [Venugopal, B; Luckey, T.](#) (1978). Metal toxicity in mammals. In *Chemical toxicity of metals and metalloids*. New York: Plenum Press.
- [Verdugo, P; Alldredge, A; Azam, F; Kirchman, D; Passow, U; Santschi, P.](#) (2004). The oceanic gel phase: A bridge in the DOM-POM continuum. *Mar Chem* 92: 67-85. <http://dx.doi.org/10.1016/j.marchem.2004.06.017>
- [Wahlberg, JE.](#) (1965). Percutaneous toxicity of metal compounds: a comparative investigation in guinea pigs. *Arch Environ Occup Health* 11: 201-204.
- [Walker, F.](#) (1971). Experimental argyria: a model for basement membrane studies. *Br J Exp Pathol* 52: 589-593.
- [Wallace, WE; Keane, MJ; Murray, DK; Chisholm, WP; Maynard, AD; Ong, TM.](#) (2007). Phospholipid lung surfactant and nanoparticle surface toxicity: lessons from diesel soots and silicate dusts. *J Nanopart Res* 9: 23-38.
- [Walser, T; Demou, E; Lang, DJ; Hellweg, S.](#) (2011). Prospective environmental life cycle assessment of nanosilver T-shirts. *Environ Sci Technol* 45: 4570-4578. <http://dx.doi.org/10.1021/es2001248>
- [Wardak, A; Gorman, ME; Swami, N; Deshpande, S.](#) (2008). Identification of risks in the life cycle of nanotechnology-based products. *J Ind Ecol* 12: 435-448. <http://dx.doi.org/10.1111/j.1530-9290.2008.00029.x>
- [Warheit, DB; Borm, PJA; Hennes, C; Lademann, J.](#) (2007a). Testing strategies to establish the safety of nanomaterials: Conclusions of an European Centre for Ecotoxicology and Toxicology of Chemicals workshop. *Inhal Toxicol* 19: 631-643.
- [Warheit, DB; Hoke, RA; Finlay, C; Donner, EM; Reed, KL; Sayes, CM.](#) (2007b). Development of a base set of toxicity tests using ultrafine TiO₂ particles as a component of nanoparticle risk management. *Toxicol Lett* 171: 99-110.
- [WHO](#) (World Health Organization). (2002). Silver and silver compounds: Environmental aspects (pp. 53). (CICAD 44). Geneva, Switzerland. <http://www.inchem.org/documents/cicads/cicads/cicad44.htm>
- [Wiberg, E; Wiberg, N; Holleman, AF.](#) (2001). Holleman-Wiberg's Inorganic Chemistry. In N Wiberg (Ed.). San Diego, CA: Academic Press.

- [Wiesner, MR; Lowry, GV; Alvarez, P; Dionysiou, D; Biswas, P.](#) (2006). Assessing the risks of manufactured nanomaterials. *Environ Sci Technol* 14: 4336-4345.
- [Wiesner, MR; Lowry, GV; Jones, KL; Hochella, MF; DiGiulio, RT; Casman, E; Bernhardt, ES.](#) (2009). Decreasing uncertainties in assessing environmental exposure, risk, and ecological implications of nanomaterials. *Environ Sci Technol* 43: 6458-6462. <http://dx.doi.org/10.1021/es803621k>
- [Wijnhoven, SWP; Dekkers, S; Hagens, WI; WH, dJ.](#) (2009a). Exposure to nanomaterials in consumer products. The Netherlands: National Institute for Public Health and the Environment. <http://www.rivm.nl/bibliotheek/rapporten/340370001.pdf>
- [Wijnhoven, SWP; Peijnenburg, WJG, M; Herberts, CA; Hagens, WI; Oomen, AG; Heugens, EHW; Roszek, B; Bisschops, J; Gosens, I; van de Meent, D; Dekkers, S; deJong, WH; van Zijverden, M; Sips, AJA, M; Geertsma, RE.](#) (2009b). Nano-silver: A review of available data and knowledge gaps in human and environmental risk assessment [Review]. *Nanotoxicology* 3: 109-138. <http://dx.doi.org/10.1080/17435390902725914>
- [Wilkinson, KJ; Reinhardt, A.](#) (2005). Contrasting roles of natural organic matter on colloidal stabilization and flocculation in freshwaters. In SN Liss; IG Droppo; GG Leppard; TG Milligan (Eds.), *Flocculation in natural and engineered environmental systems* (pp. 143-170). Boca Raton, FL: CRC Press. <http://www.informaworld.com/smpp/content~content=a744757236~db=all~jumpype=rss>
- [Williams, N.](#) (1999). Longitudinal medical surveillance showing lack of progression of argyrosis in a silver refiner. *Occup Med (Lond)* 49: 397-399. <http://dx.doi.org/10.1093/occmed/49.6.397>
- [Williams, N; Garner, I.](#) (1995). Absence of symptoms in silver refiners with raised blood silver levels. *Occup Med (Lond)* 45: 205-208.
- [Wise, JP; Kraus, S; Payne, R; Wise, SS; Kerr, I; LaCerte, C; Wise, J; Gianios, C; Shaffiey, F; Chen, TL; Perkins, C; Thomson, W; Zhang, T; Zhang, Y; Zhu, C; O'Hara, T.](#) (2009). Comparative toxicity of silver nanoparticles in human, marine mammal, and fish cells [Abstract]. *Toxicologist* 108: 255.
- [Wittmaack, K.](#) (2007). In search of the most relevant parameter for quantifying lung inflammatory response to nanoparticle exposure: particle number, surface area, or what? *Environ Health Perspect* 115: 187-194.
- [Wood, CM; Grosell, M; Hogstrand, C; Hansen, H.](#) (2002). Kinetics of radiolabelled silver uptake and depuration in the gills of rainbow trout (*Oncorhynchus mykiss*) and European eel (*Anguilla anguilla*): The influence of silver speciation. *Aquat Toxicol* 56: 197-213. [http://dx.doi.org/10.1016/S0166-445X\(01\)00182-5](http://dx.doi.org/10.1016/S0166-445X(01)00182-5)
- [Wood, CM; McDonald, MD; Walker, P; Grosell, M; Barimo, JF; Playle, RC; Walsh, PJ.](#) (2004). Bioavailability of silver and its relationship to ionoregulation and silver speciation across a range of salinities in the gulf toadfish (*Opsanus beta*). *Aquat Toxicol* 70: 137-157.
- [Wright, JB; Lam, K; Hansen, D; Burrell, RE.](#) (1999). Efficacy of topical silver against fungal burn wound pathogens. *Am J Infect Control* 27: 344-350. [http://dx.doi.org/10.1016/S0196-6553\(99\)70055-6](http://dx.doi.org/10.1016/S0196-6553(99)70055-6)
- [Wu, Y; Zhou, Q; Li, H; Liu, W; Wang, T; Jiang, G.](#) (2010). Effects of silver nanoparticles on the development and histopathology biomarkers of Japanese medaka (*Oryzias latipes*) using the partial-life test. *Aquat Toxicol* 100: 160-167. <http://dx.doi.org/10.1016/j.aquatox.2009.11.014>
- [Xia, T; Kovochich, M; Brant, J; Hotze, M; Sempf, J; Oberley, T; Sioutas, C; Yeh, JI; Wiesner, MR; Nel, AE.](#) (2006). Comparison of the abilities of ambient and manufactured nanoparticles to induce cellular toxicity according to an oxidative stress paradigm. *Nano Lett* 6: 1794-1807.
- [Xu, XH; Brownlow, WJ; Kyriacou, SV; Wan, Q; Viola, JJ.](#) (2004). Real-time probing of membrane transport in living microbial cells using single nanoparticle optics and living cell imaging. *Biochemistry* 43: 10400-10413. <http://dx.doi.org/10.1021/bi036231a>
- [Yang, W; Shen, C; Ji, Q; An, H; Wang, J; Liu, Q; Zhang, Z.](#) (2009). Food storage material silver nanoparticles interfere with DNA replication fidelity and bind with DNA. *Nanotechnology* 20: 1-7. <http://dx.doi.org/10.1088/0957-4484/20/8/085102>

- [Yeo, M; Kang, M.](#) (2008). Effects of nanometer sized silver materials on biological toxicity during zebrafish embryogenesis. *Bull Kor Chem Soc* 29: 1179-1184.
- [Yeo, MK; Pak, SW.](#) (2008). Exposing zebrafish to silver nanoparticles during caudal fin regeneration disrupts caudal fin growth and p53 signaling. *Mol Cell Toxicol* 4: 311-317.
- [Yin, L; Cheng, Y; Espinasse, B; Colman, BP; Auffan, M; Wiesner, M; Rose, J; Liu, J; Bernhardt, ES.](#) (2011). More than the ions: the effects of silver nanoparticles on *Lolium multiflorum*. *Environ Sci Technol* 45: 2360-2367. <http://dx.doi.org/10.1021/es103995x>
- [Yin, Y; Li, Z; Zhong, Z; Gates, B; Xia, Y; Venkateswaran, S.](#) (2002). Synthesis and characterization of stable aqueous dispersions of silver nanoparticles through the Tollens process. *J Mater Chem* 3: 522-527.
- [Yoon, KY; Byeon, J; Park, JH; Hwang, J.](#) (2007). Susceptibility constants of *Escherichia coli* and *Bacillus subtilis* to silver and copper nanoparticles. *Sci Total Environ* 373: 572-575. <http://dx.doi.org/10.1016/j.scitotenv.2006.11.007>
- [Yu, D; Yam, V.](#) (2004). Controlled synthesis of monodisperse silver nanocubes in water. *J Am Chem Soc* 126: 13200-13201. <http://dx.doi.org/10.1021/ja046037r>
- [Zhang, W; Qiao, X; Chen, J.](#) (2007a). Synthesis of silver nanoparticles: Effects of concerned parameters in water/oil microemulsion. *Mater Sci Eng B* 1: 1-15.
- [Zhang, X; Sun, H; Zhang, Z; Niu, Q; Chen, Y; Crittenden, JC.](#) (2007b). Enhanced bioaccumulation of cadmium in carp in the presence of titanium nanoparticles. *Chemosphere* 67: 160-166.
- [Zhao, CM; Wang, WX.](#) (2010). Biokinetic uptake and efflux of silver nanoparticles in *Daphnia magna*. *Environ Sci Technol* 44: 7699-7704. <http://dx.doi.org/10.1021/es101484s>
- [Zook, JM; Maccuspie, RI; Locascio, LE; Halter, MD; Elliott, JT.](#) (2011). Stable nanoparticle aggregates/agglomerates of different sizes and the effect of their size on hemolytic cytotoxicity. *Nanotoxicology* 5: 517-530. <http://dx.doi.org/10.3109/17435390.2010.536615>
- [Zuin, S; Micheletti, C; Critto, A; Pojana, G; Johnston, H; Stone, V; Tran, L; Marcomini, A.](#) (In Press) Weight of Evidence approach for the relative hazard ranking of nanomaterials. *Nanotoxicology*. <http://dx.doi.org/10.3109/17435390.2010.512986>

Appendix A. Common Analytical Methods for Characterization of Nanomaterials

This page intentionally left blank.

Appendix A. Common Analytical Methods for Characterization of Nanomaterials

A.1.	Introduction	A-4
A.2.	Aggregation	A-5
A.3.	Chemical Composition	A-6
A.4.	Crystal Structure	A-7
A.5.	Dissolution	A-7
A.6.	Heterogeneity	A-8
A.7.	Mass Concentration	A-8
A.8.	Melting Point	A-9
A.9.	Particle Number Concentration	A-9
A.10.	Porosity	A-9
A.11.	Shape	A-10
A.12.	Size	A-11
A.13.	Size Distribution	A-12
A.14.	Speciation	A-13
A.15.	Structure	A-14
A.16.	Surface Area	A-14
A.17.	Surface Charge	A-15
A.18.	Surface Chemistry	A-15
A.19.	Surface Contamination	A-16
	Appendix A References	A-17

This page intentionally left blank.

A.1. Introduction

Presented in this appendix is a compilation of analytical methods that have been used to characterize nanoparticles, including nano-Ag. This information is not intended to be exhaustive in reporting every applicable method, or to be comprehensive in describing available methods; rather, it is a summary of relatively common or known methods for characterizing nanoparticles based on the U.S. Environmental Protection Agency's (EPA) experience and knowledge at the time this case study was developed. Because of the rapid pace at which the field of nanotechnology continues to evolve and grow, undoubtedly there are additional methods that are not included here, and some information presented about specific methods might not fully reflect the current state of the science. Furthermore, the most appropriate methods for characterizing certain nanomaterials or the best methods for specific contexts could vary, and having such a general compilation cover each of these nuances is not possible. Nevertheless, this appendix is expected to be useful in that it lists some of the more commonly used methods and provides general information relevant to evaluating the research needs regarding nano-Ag.

The methods summarized here are grouped into 19 tables, presented alphabetically according to the properties and characteristics being analyzed. Within each table, information is presented regarding the approximate detection range and advantages and disadvantages for each technique. Although the techniques included in each table have not been prioritized according to accuracy, cost, or other characteristics (methods are listed alphabetically within each table), the most commonly employed techniques are listed in bold font.

Staff in EPA's Office of Pesticide Programs compiled most of this information. Although citations are not provided for individual techniques, several important sources used to develop these tables, such as some websites of manufacturers that produce equipment used to characterize nanomaterials, are cited here: ([AZoNano, 2010](#); [Buchan Lawton, 2010](#); [General Electric Company, 2010](#); [Imaging Technology Group, 2010](#); [NCEM, 2010](#); [PerkinElmer, 2010](#); [Quantachrome Instruments, 2010](#); [Shimadzu Scientific Instruments, 2010](#); [TSI Inc., 2010](#); [Varian, 2010](#); [Becker, 2008](#); [Tiede et al., 2008](#); [Zuin et al., 2007](#); [Oberdörster et al., 2005](#); [Coulson et al., 2002](#); [Tsuda and Tanaka, 1996](#)). Full citations are listed at the end of this appendix.

A.2. Aggregation

Technique	Detection Range	Advantages	Disadvantages
Analytical Ultracentrifugation (ANUC)	>nm range		
Atomic Force Microscopy (AFM)	>0.1 nm	Can be used to analyze dry, moist, and liquid samples	Artifacts can result from tip smearing Prone to overestimations
Chemical Force Microscopy (CFM)	>0.1 nm	Used in biology Many modifications to AFM tip	
Confocal Laser Scanning Microscopy (CLSM)			
Differential Interference Contrast Microscopy (DIC)		Can be used to analyze unstained biological samples High resolution with no artifacts	Calls for transparent specimen with refractive index similar to its surroundings Expensive
Differential Mobility Analyzer (DMA) ¹	3 nm– μm range	Can be used in combination with many techniques	Possible sample degradation
Dynamic Light Scattering (DLS)	3 nm– μm range	Allows in situ measurement Fast and simple Convenient for analyzing aggregation	Dust particles can ruin measurement High particle interactions
Field Emission Scanning Electron Microscopy (FE-SEM) ²		Ultra high resolution Images secondary electrons with backscatter detector	Requires high vacuum for sample preparation
Flow Field-Flow Fractionation (FIFFF)	1 nm–1 μm		
Fluorescence Microscopy (FLM)	>10 nm		
Nuclear Magnetic Resonance (NMR)	mM range	Used to analyze solid or liquid samples Convenient temperature range	Solid-state experiments are more difficult
Scanning Electron Microscopy (SEM) ²	1 nm–1 μm	High resolution	Requires high vacuum for sample preparation
Scanning Transmission Electron Microscopy (STEM) ³	resolution: <0.1 nm	Used to analyze low concentrations (ppm)	
Scanning Tunneling Electron Microscopy (STM)	nm in x, y, and z directions	Allows three-dimensional characterization	
Size Exclusion Chromatography (SEC)	5 nm–100 μm	Good separation efficiency	Interactions of solute and solid phase
Small Angle Neutron Scattering (SANS)	1 nm–1 μm	Used to analyze liquids Used to characterize structural details of pores of all types (open, blind, and closed)	Careful data analysis needed
Transmission Electron Microscopy (TEM) ⁴	>0.1 nm	High resolution	Requires high vacuum for sample preparation
Ultracentrifugation (UC)	nm range	Currently used in carbon nanotubes	More qualitative than quantitative Requires homogeneous sample preparation
X-ray Diffraction (XRD)	1–3 wt%		
Zeta Potential	5 nm–10 μm		

Bold font indicates most commonly employed techniques.

¹Can be used in combination with Electron Spectroscopy (ES), Condensation Particle Counter (CPC), Inductively Coupled Plasma Optical Emission Spectrometry (ICP-OES), Inductively Coupled Plasma Mass Spectrometry (ICP-MS), and Aerosol Time-of-Flight Mass Spectrometry (ATOF-MS).

²Can be used in combination with Auger Electron Microscopy (AES) and Energy-Dispersive X-ray Spectroscopy (EDS).

³Can be used in combination with X-ray Diffraction (XRD), High Angle Annular Dark-Field Imaging (HAADF), Coherent Electron Nanodiffraction (CEND), Annular Dark Field Imaging (ADF), Thermophilic Aerobic Digestion (TAD), Analytical Electron Microscopy (AEM), and Convergent Beam Electron Diffraction (CBED).

⁴Can be used in combination with Electron Energy Loss Spectroscopy (EELS) and Energy-Dispersive X-ray Spectroscopy (EDS).

A.3. Chemical Composition

Technique	Detection Range	Advantages	Disadvantages
Aerosol Time-of-Flight Mass Spectroscopy (ATOF-MS)	0.32–1.8 μm		
Analytical Electron Microscopy (AEM)¹	>0.5 nm	Electron Energy Loss Spectroscopy (EELS) can be used (< Zn)	
Atomic Absorption Spectroscopy (AAS)	ppm range		
Auger Electron Microscopy (AES) ²	1–2 nm		
Chemical Force Microscopy (CFM)	>0.1 nm	Used in biology Many modifications to Atomic Force Microscopy (AFM) tip	
Electron Backscattered Diffraction (EBSD)	20–100 nm		
Electron Paramagnetic Resonance (EPR)	mM range	Can be used to analyze paramagnetic samples	Data interpretation can be difficult
Field Emission Scanning Electron Microscopy (FE-SEM) ³		Ultra high resolution Images secondary electrons with backscatter detector	Requires high vacuum for sample preparation
Flow Field-Flow Fractionation (FIFFF)	1 nm–1 μm		
Fourier Transform Infrared Spectroscopy (FT-IR)	ppm range	Can be used to analyze solid or liquid samples	
Gel Permeation Chromatography (GPC)	5 nm–100 μm	Used to determine molecular weight and distribution of polymers	
High Performance Liquid Chromatography (HPLC)	$\mu\text{g/mL}$ range		
Inductively Coupled Plasma Mass Spectroscopy (ICP-MS)	1 ppt–0.1 ppb		Sample must be soluble in suitable solvent
Mossbauer Spectroscopy (MS)	mM range		
Nuclear Magnetic Resonance (NMR)	mM range	Can be used to analyze solid or liquid samples Good temperature range	Solid-state experiments are more difficult
Raman Spectroscopy	ppm range	Can be used to analyze solid or liquid samples	
Scanning Electron Microscopy (SEM)³	1 nm–1 μm	High resolution	Requires high vacuum for sample preparation
Secondary Ion Mass Spectrometry (SIMS)	1,012–1,016 atom/ cm^3	Small sample size	Requires high vacuum for sample preparation Possible sample degradation
Surface Enhanced Raman Spectroscopy (SERS)	Can detect single molecules		Sensitive to the surface on which the experiment is conducted
Transmission Electron Microscopy (TEM)⁴	>0.1 nm	High resolution	Requires high vacuum for sample preparation
Ultraviolet/Visible Spectroscopy (UV/Vis)	mM range	Fast	
X-ray Diffraction (XRD)	1–3 wt%		
X-ray Photoelectron Spectroscopy (XPS)	>1 μm	Reveals atomic composition of layers (1–10 μm)	

Bold font indicates most commonly employed techniques.

¹Can be used in combination with Transmission Electron Microscopy (TEM), Scanning Electron Microscopy (SEM), and Scanning Transmission Electron Microscopy (STEM).

²Can be used in combination with Scanning Electron Microscopy (SEM).

³Can be used in combination with Auger Electron Microscopy (AES) and Energy-Dispersive X-ray Spectroscopy (EDS).

⁴Can be used in combination with Electron Energy Loss Spectroscopy (EELS) and Energy-Dispersive X-ray Spectroscopy (EDS).

A.4. Crystal Structure

Technique	Detection Range	Advantages	Disadvantages
Differential Scanning Calorimetry (DSC)	mg range	Allows the study of phase transitions	
Electron Paramagnetic Resonance (EPR)	mM range	Can be used to analyze paramagnetic samples	Data interpretation can be difficult
Field Emission Scanning Electron Microscopy (FE-SEM) ¹		Ultra high resolution Images secondary electrons with backscatter detector	Requires high vacuum for sample preparation
Fourier Transform Infrared Spectroscopy (FTIR)	ppm range	Can be used to analyze solid or liquid samples	
Nuclear Magnetic Resonance (NMR)	mM range	Can be used to analyze solid or liquid samples Good temperature range	Solid-state experiments more difficult
Raman Spectroscopy	ppm range	Can be used to analyze solid or liquid samples	
Scanning Electron Microscopy (SEM) ¹	1 nm–1 μm	High resolution	Requires high vacuum for sample preparation
Thermo-Gravimetric Analysis (TGA)	mg range	Allows the study of weight loss in samples	
Transmission Electron Microscopy (TEM) ²	>0.1 nm	High resolution	Requires high vacuum for sample preparation
X-ray Diffraction (XRD)	1–3 wt%		

Bold font indicates most commonly employed techniques.

¹Can be used in combination with Auger Electron Microscopy (AES) and Energy-Dispersive X-ray Spectroscopy (EDS).

²Can be used in combination with Electron Energy Loss Spectroscopy (EELS) and Energy-Dispersive X-ray Spectroscopy (EDS).

A.5. Dissolution

Technique	Detection Range	Advantages	Disadvantages
Cross Flow Ultrafiltration (CFUF)	1 nm–1 μm	High speed High volume Low concentration	Not good for high concentrations Not well defined size fractionation Not fully quantitative Separation is based only on size Titration limits: micromolar to millimolar lower limits
Dialysis	<5 nm		
Diffusive gradients in thin films	nM–μM range	Simple Concentrating effect helps lower detection limits	
Voltammetry	mM–ppm range		

Bold font indicates most commonly employed techniques.

A.6. Heterogeneity

Technique	Detection Range	Advantages	Disadvantages
Atomic Force Microscopy (AFM)	>0.1 nm	Can be used to analyze dry, moist, and liquid samples	Artifacts can result from tip smearing
Differential Mobility Analyzer (DMA) ¹	3 nm– μm range	Can be used in combination with many techniques	Possible sample degradation
Field Emission Scanning Electron Microscopy (FE-SEM) ²		Ultra high resolution Images secondary electrons with backscatter detector	Requires high vacuum for sample preparation
Infrared Spectroscopy (IR)	ppm range	Can be used to analyze solid or liquid samples	
Nuclear Magnetic Resonance (NMR)	mM range	Can be used to analyze solid or liquid samples Good temperature range	Solid-state experiments more difficult
Raman Spectroscopy	ppm range	Can be used to analyze solid or liquid samples	
Scanning Electron Microscopy (SEM) ²	1 nm–1 μm	High resolution	Requires high vacuum for sample preparation
Scanning Tunneling Electron Microscopy (STM)	nm in x, y, and z directions	Allows three-dimensional characterization	
Transmission Electron Microscopy (TEM) ³	>0.1 nm	High resolution	Requires high vacuum for sample preparation
Ultraviolet/Visible Spectroscopy (UV/Vis)	mM range	Fast	

Bold font indicates most commonly employed techniques.

¹Can be used in combination with Electron Spectroscopy (ES), Condensation Particle Counter (CPC), Inductively Coupled Plasma Optical Emission Spectrometry (ICP-OES), Inductively Coupled Plasma Mass Spectroscopy (ICP-MS), and Aerosol Time-of-Flight Mass Spectroscopy (ATOF-MS).

²Can be used in combination with Auger Electron Microscopy (AES) and Energy-Dispersive X-ray Spectroscopy (EDS).

³Can be used in combination with Electron Energy Loss Spectroscopy (EELS) and Energy-Dispersive X-ray Spectroscopy (EDS).

A.7. Mass Concentration

Technique	Detection Range	Advantages	Disadvantages
Analytical Electron Microscopy (AEM) ¹	>0.5 nm	Electron Energy Loss Spectroscopy (EELS) can be used (< Zn)	
Chemical Force Microscopy (CFM)	>0.1 nm	Used in biology Many modifications to Atomic Force Microscopy (AFM) tip	
Gravimetrics	ppb range	Precise measurements Stable Inexpensive	Gravity difference measurements are site dependent and require calibration Less efficient than spectrophotometry
Thermal Analysis	mg range		

Bold font indicates most commonly employed techniques.

¹Can be used in combination with Transmission Electron Microscopy (TEM), Scanning Electron Microscopy (SEM), and Scanning Transmission Electron Microscopy (STEM).

A.8. Melting Point

Technique	Detection Range	Advantages	Disadvantages
Differential Scanning Calorimetry (DSC)	mg range		

A.9. Particle Number Concentration

Technique	Detection Range	Advantages	Disadvantages
Condensation Particle Counter (CPC) ¹	5–1,100 nm		
Particle Counter	>1 μm		Meets clean room standards

Bold font indicates most commonly employed technique.

¹Can be used in combination with a Differential Mobility Analyzer (DMA).

A.10. Porosity

Technique	Detection Range	Advantages	Disadvantages
Brunauer Emmett Teller (BET)	>1,000 m ² /g		
Differential Mobility Analyzer (DMA) ¹	3 nm– μm range	Can be used in combination with many techniques	Possible sample degradation
Transmission Electron Microscopy (TEM) ²	>0.1 nm	High resolution	Requires high vacuum for sample preparation

Bold font indicates most commonly employed techniques (all three techniques are common).

¹Can be used in combination with Electron Spectroscopy (ES), Condensation Particle Counter (CPC), Inductively Coupled Plasma Optical Emission Spectrometry (ICP-OES), Inductively Coupled Plasma Mass Spectrometry (ICP-MS), and Aerosol Time-of-Flight Mass Spectrometry (ATOF-MS).

²Can be used in combination with Electron Energy Loss Spectroscopy (EELS) and Energy-Dispersive X-ray Spectroscopy (EDS).

A.11. Shape

Technique	Detection Range	Advantages	Disadvantages
Atomic Force Microscopy (AFM)	>0.1 nm	Can be used to analyze dry, moist, and liquid samples	Artifacts can result from tip smearing
Confocal Laser Scanning Microscopy (CLSM)			
Differential Interference Contrast Microscopy (DIC)		Can be used to analyze unstained biological samples High resolution with no artifacts	Calls for transparent specimen with refractive index similar to its surroundings Expensive
Differential Mobility Analyzer (DMA) ¹	3 nm–μm range	Can be used in combination with many techniques	Possible sample degradation
Dynamic Light Scattering (DLS)	3 nm–μm range	Allows in situ measurement Fast and simple Convenient for analyzing aggregation	Dust particles can ruin measurement Higher particle interactions
Field Emission Scanning Electron Microscopy (FE-SEM) ²		Ultra high resolution Images secondary electrons with backscatter detector	Requires high vacuum for sample preparation
Flow Field-Flow Fractionation Static Light Scattering (FIFFF-SLS)	1 nm–1 μm		
Fluorescence Microscopy (FLM)	>10 nm		
Scanning Electron Microscopy (SEM) ²	1 nm–1 μm	High resolution	Requires high vacuum for sample preparation
Scanning Transmission Electron Microscopy (STEM) ³	resolution: <0.1 nm	Can be used to analyze low concentrations (ppm)	
Scanning Tunneling Electron Microscopy (STM)	nm in x, y, and z directions	Allows three-dimensional characterization	
Sedimentation Field-Flow Fractionation Dynamic Light Scattering (SedFFF-DLS)	1 nm–1 μm		
Transmission Electron Microscopy (TEM) ⁴	>0.1 nm	High resolution	Requires high vacuum for sample preparation
Ultracentrifugation (UC)	nm range	Currently used in carbon nanotubes	More qualitative than quantitative Requires homogeneous sample preparation

Bold font indicates most commonly employed techniques.

¹Can be used in combination with Electron Spectroscopy (ES), Condensation Particle Counter (CPC), Inductively Coupled Plasma Optical Emission Spectrometry (ICP-OES), Inductively Coupled Plasma Mass Spectrometry (ICP-MS), and Aerosol Time-of-Flight Mass Spectrometry (ATOF-MS).

²Can be used in combination with Auger Electron Microscopy (AES) and Energy-Dispersive X-ray Spectrometry (EDS).

³Can be used in combination with X-ray Diffraction (XRD), High Angle Annular Dark-Field Imaging (HAADF), Coherent Electron Nanodiffraction (CEND), Annular Dark Field Imaging (ADF), Thermophilic Aerobic Digestion (TAD), Analytical Electron Microscopy (AEM), and Convergent Beam Electron Diffraction (CBED).

⁴Can be used in combination with Electron Energy Loss Spectrometry (EELS) and Energy-Dispersive X-ray Spectrometry (EDS).

A.12. Size

Technique	Detection Range	Advantages	Disadvantages
Atomic Force Microscopy (AFM)	>0.1 nm	Can be used to analyze dry, moist, and liquid samples	Artifacts can result from tip smearing
Confocal Laser Scanning Microscopy (CLSM)			
Differential Interference Contrast Microscopy (DIC)		Can be used to analyze unstained biological samples High resolution with no artifacts	Calls for transparent specimen with refractive index similar to its surroundings Expensive
Differential Mobility Analyzer (DMA) ¹	3 nm– μm range	Can be used in combination with many techniques	Possible sample degradation
Dynamic Light Scattering (DLS)	3 nm– μm range	Allows in situ measurement Fast and simple Convenient for analyzing aggregation	Dust particles can ruin measurement Higher particle interactions
Field Emission Scanning Electron Microscopy (FE-SEM) ²		Ultra high resolution Images secondary electrons with backscatter detector	Requires high vacuum for sample preparation
Fluorescence Microscopy (FLM)	>10 nm		
Scanning Electron Microscopy (SEM) ²	1 nm–1 μm	High resolution	Requires high vacuum for sample preparation
Scanning Transmission Electron Microscopy (STEM) ³	resolution: <0.1 nm	Can be used to analyze samples of low concentrations (ppm)	
Scanning Tunneling Electron Microscopy (STM)	nm in x, y, and z directions	Allows three-dimensional characterization	
Size Exclusion Chromatography (SEC)	5 nm–100 μm	Can be used to determine molecular weight and distribution of polymers	
Transmission Electron Microscopy (TEM) ⁴	>0.1 nm	High resolution	Requires high vacuum for sample preparation

Bold font indicates most commonly employed techniques.

¹Can be used in combination with Electron Spectroscopy (ES), Condensation Particle Counter (CPC), Inductively Coupled Plasma Optical Emission Spectrometry (ICP-OES), Inductively Coupled Plasma Mass Spectroscopy (ICP-MS), and Aerosol Time-of-Flight Mass Spectroscopy (ATOF-MS).

²Can be used in combination with Auger Electron Microscopy (AES) and Energy-Dispersive X-ray Spectroscopy (EDS).

³Can be used in combination with X-ray Diffraction (XRD), High Angle Annular Dark-Field Imaging (HAADF), Coherent Electron Nanodiffraction (CEND), Annular Dark Field Imaging (ADF), Thermophilic Aerobic Digestion (TAD), Analytical Electron Microscopy (AEM), and Convergent Beam Electron Diffraction (CBED).

⁴Can be used in combination with Electron Energy Loss Spectroscopy (EELS) and Energy-Dispersive X-ray Spectroscopy (EDS).

A.13. Size Distribution

Technique	Detection Range	Advantages	Disadvantages
Atomic Force Microscopy (AFM)	>0.1 nm	Can be used to analyze dry, moist, and liquid samples	Artifacts can result from tip smearing
Cross Flow Ultrafiltration (CFUF)	1 nm–1 μ m	High speed Higher volume Less clogging than piston filtration or stirred cells	Potential alterations due to increased particle concentration Turbulent flow Large surface exposure Size fractionation is not well defined
Cross-Flow Filtration (CFF)	7 nm–2 μ m	Can be used to separate several compounds based on size	
Differential Mobility Analyzer (DMA) ¹	3 nm– μ m range	Can be used in combination with many techniques	Possible sample degradation
Dynamic Light Scattering (DLS)	3 nm– μ m range	Allows in situ measurement Fast and simple Convenient for analyzing aggregation	Dust particles can ruin measurement Higher particle interactions
Field Emission Scanning Electron Microscopy (FE-SEM) ²		Ultra high resolution Images secondary electrons with backscatter detector	Requires high vacuum for sample preparation
Field Flow Fractionation (FFF) ³	Flow FFF: 1 nm–1 μ m Sedimentation FFF: 50 nm–1 μ m	Good size range Direct relation between retention time and size	Experienced operator needed
Flow Field-Flow Fractionation (FIFFF)	1 nm–1 μ m		
High Performance Liquid Chromatography (HPLC)	μ g/mL range	Can be used to separate and analyze several compounds	
Hydrodynamic Chromatography (HDC) ⁴	5–1,200 nm		Mobile phase interactions
Scanning Electron Microscopy (SEM) ²	1 nm–1 μ m	High resolution	Requires high vacuum for sample preparation
Scanning Mobility Particle Sizer (SMPS) ⁵	3–1,000 nm	Particle Concentration Range 20–10,000,000 particles/cc Higher resolution than DMPS ¹⁰	
Scanning Transmission Electron Microscopy (STEM) ⁶	resolution: <0.1 nm	Can be used to analyze low concentrations (ppm)	
Scanning Tunneling Electron Microscopy (STM)	nm in x, y, and z directions	Allows three dimensional characterization	
Single Particle Mass Spectrometry (SPMS) ⁵	3–1,000 nm	Particle Concentration Range 20–10,000,000 particles/cc Higher resolution than DMPS ¹⁰	
Size Exclusion Chromatography (SEC) ⁷	5 nm–100 μ m	Simple; good separation efficiency Can be used to determine molecular weight and distribution of polymers	Limited size separation range
Small-Angle X-ray Scattering (SAXS) ⁸	5–25 nm	Averaged particle sizes Shapes, distribution, and surface-to-volume ratio can be determined. Can be used to analyze liquids or solids	
Transmission Electron Microscopy (TEM) ⁹	>0.1 nm	High resolution	Requires high vacuum for sample preparation
Ultracentrifugation (UC)	nm range	Currently used in carbon nanotubes	More qualitative than quantitative Requires homogeneous sample preparation

A.13. Size Distribution (continued)

Technique	Detection Range	Advantages	Disadvantages
Ultrafine Condensation Particle Counter (UCPC)	2.7–10 nm		
X-ray Diffraction (XRD)	1–3 wt%		

Bold font indicates most commonly employed techniques.

¹Can be used in combination with Electron Spectroscopy (ES), Condensation Particle Counter (CPC), Inductively Coupled Plasma Optical Emission Spectrometry (ICP-OES), Inductively Coupled Plasma Mass Spectrometry (ICP-MS), and Aerosol Time-of-Flight Mass Spectrometry (ATOF-MS).

²Can be used in combination with Auger Electron Microscopy (AES) and Energy-Dispersive X-ray Spectroscopy (EDS).

³Can be used in combination with Ultraviolet/Visible Spectroscopy (UV/Vis) and Inductively Coupled Plasma Mass Spectrometry (ICP-MS) on line; and Atomic Force Microscopy (AFM) off line.

⁴Can be used in combination with Ultraviolet/Visible Spectroscopy (UV/Vis) and Inductively Coupled Plasma Mass Spectrometry (ICP-MS).

⁵A Differential Mobility Analyzer (DMA) can be used in combination.

⁶Can be used in combination with Electron Energy Loss Spectroscopy (EELS) and Energy-Dispersive X-ray Spectroscopy (EDS).

⁷Can be used in combination with Ultraviolet/Visible Spectroscopy (UV/Vis) and Inductively Coupled Plasma Mass Spectrometry (ICP-MS).

⁸Ultra-Small Angle X-ray Scattering (USAXS) can be used in combination.

⁹Can be used in combination with X-ray Diffraction (XRD), High Angle Annular Dark-Field Imaging (HAADF), Coherent Electron Nanodiffraction (CEND), Annular Dark Field Imaging (ADF), Thermophilic Aerobic Digestion (TAD), Analytical Electron Microscopy (AEM), and Convergent Beam Electron Diffraction (CBED).

¹⁰Differential particle mass spectrometry (DMPS).

A.14. Speciation

Technique	Detection Range	Advantages	Disadvantages
Size Exclusion Chromatography with Inductively Coupled Plasma Mass Spectroscopy (SEC-ICP-MS)		Element-specific separation	
Titration	μM–mM range	Simple	Prevalent human errors Sample must be soluble
X-ray Absorption Fine Structure (XAFS)	ppm to ppb range	Nearly all elements have binding energies in range of X-rays	Inadequate for lighter elements
X-ray Diffraction (XRD)	1–3 wt%		
X-ray Photoelectron Spectroscopy (XPS)	>1 μm	Reveals atomic composition of layers (1–10 μm)	

Bold font indicates most commonly employed techniques.

A.15. Structure

Technique	Detection Range	Advantages	Disadvantages
Atomic Force Microscopy (AFM)	>0.1 nm	Can be used to analyze dry, moist, and liquid samples	Artifacts can result from tip smearing
Field Emission Scanning Electron Microscopy (FE-SEM) ¹		Ultra high resolution Images secondary electrons with backscatter detector	Requires high vacuum for sample preparation
Scanning Electron Microscopy (SEM)¹	1 nm–1 μm	High resolution	Requires high vacuum for sample preparation
Scanning Transmission Electron Microscopy (STEM)²	resolution: <0.1 nm	Can be used to analyze low concentrations (ppm)	
Scanning Tunneling Electron Microscopy (STM)	nm in x, y, and z directions	Allows three-dimensional characterization	
Secondary Ion Mass Spectrometry (SIMS)	10 ¹² –10 ¹⁶ atom/cm ³	Small sample size	Requires high vacuum, which can degrade sample
Small Angle Neutron Scattering (SANS)	nm–μm range	Can be used to analyze liquids	
Transmission Electron Microscopy (TEM)³	>0.1 nm	High resolution	Requires high vacuum for sample preparation
X-ray Diffraction (XRD)	1–3 wt%		

Bold font indicates most commonly employed techniques.

¹Can be used in combination with Auger Electron Microscopy (AES) and Energy-Dispersive X-ray Spectroscopy (EDS).

²Can be used in combination with X-ray Diffraction (XRD), High Angle Annular Dark-Field Imaging (HAADF), Coherent Electron Nanodiffraction (CEND), Annular Dark Field Imaging (ADF), Thermophilic Aerobic Digestion (TAD), Analytical Electron Microscopy (AEM), and Convergent Beam Electron Diffraction (CBED).

³Can be used in combination with Electron Energy Loss Spectroscopy (EELS) and Energy-Dispersive X-ray Spectroscopy (EDS).

A.16. Surface Area

Technique	Detection Range	Advantages	Disadvantages
Atomic Force Microscopy (AFM)	>0.1 nm	Can be used to analyze dry, moist, and liquid samples	Artifacts can result from tip smearing
Brunauer Emmett Teller (BET)	>1,000 m ² /g		
Differential Mobility Analyzer (DMA) ¹	3 nm–μm range	Can be used in combination with many techniques	Possible sample degradation
Dynamic Light Scattering (DLS)	3 nm–μm range		
Field Emission Scanning Electron Microscopy (FE-SEM) ²		Ultra high resolution Images secondary electrons with backscatter detector	Requires high vacuum for sample preparation
Scanning Electron Microscopy (SEM)²	1 nm–1 μm	High resolution	Requires high vacuum for sample preparation
Scanning Tunneling Electron Microscopy (STM)	nm in x, y, and z directions	Allows three-dimensional characterization	
Transmission Electron Microscopy (TEM)³	>0.1 nm	High resolution	Requires high vacuum for sample preparation
Ultracentrifugation (UC)	nm range	Currently used in carbon nanotubes	More qualitative than quantitative Requires homogeneous sample preparation

Bold font indicates most commonly employed techniques.

¹Can be used in combination with Electron Spectroscopy (ES), Condensation Particle Counter (CPC), Inductively Coupled Plasma Optical Emission Spectrometry (ICP-OES), Inductively Coupled Plasma Mass Spectrometry (ICP-MS), and Aerosol Time-of-Flight Mass Spectrometry (ATOF-MS).

²Can be used in combination with Auger Electron Microscopy (AES) and Energy-Dispersive X-ray Spectroscopy (EDS).

³Can be used in combination with Electron Energy Loss Spectroscopy (EELS) and Energy-Dispersive X-ray Spectroscopy (EDS).

A.17. Surface Charge

Technique	Detection Range	Advantages	Disadvantages
Capillary Electrophoresis (CE)	25–100 μm diameter	Run time is short	
Zeta Potential	5 nm–10 μm		

Bold font indicates most commonly employed technique.

A.18. Surface Chemistry

Technique	Detection Range	Advantages	Disadvantages
Analytical Electron Microscopy (AEM) ¹	>0.5 nm		
Atomic Force Microscopy (AFM)	>0.1 nm	Can be used to analyze dry, moist, and liquid samples	Artifacts can result from tip smearing
Auger Electron Microscopy (AES) ²	1–2 nm		
Chemical Force Microscopy (CFM)	>0.1 nm	Used in biology Many modifications to AFM tip	
Differential Scanning Calorimetry (DSC)	mg range	Allows the study of phase transitions	
Electron Paramagnetic Resonance (EPR)	mM range	Can be used to analyze paramagnetic samples	Data interpretation can be difficult
Field Emission Scanning Electron Microscopy (FE-SEM) ³		Ultra high resolution Images secondary electrons with backscatter detector	Requires high vacuum for sample preparation
Flow Field-Flow Fractionation (FIFFF)			
Fourier Transform Infrared Spectroscopy (FT-IR)	ppm range	Can be used to analyze solid or liquid samples	
High Performance Liquid Chromatography (HPLC)	$\mu\text{g/mL}$ range	Can separate and analyze several compounds	
Nuclear Magnetic Resonance (NMR)	mM range	Can be used to analyze solid or liquid samples Good temperature range	Solid-state experiments more difficult
Raman Spectroscopy	ppm range	Can be used to analyze solid or liquid samples	
Scanning Electron Microscopy (SEM)³	1 nm–1 μm	High resolution	Requires high vacuum for sample preparation
Scanning Tunneling Electron Microscopy (STM)	nm in x, y, and z directions	Allows three-dimensional characterization	
Secondary Ion Mass Spectrometry (SIMS)	10^{12} – 10^{16} atom/cm ³	Small amount of sample necessary for analysis	Requires high vacuum for sample preparation Possible sample degradation
Size Exclusion Chromatography (SEC) ⁴	5 nm–100 μm	Good separation efficiency Simple Can be used to determine molecular weight and distribution of polymers	Limited size separation range
Surface Enhanced Raman Spectroscopy (SERS)	Can detect single molecules		Sensitive to the surface on which the experiment is conducted
Thermo-Gravimetric Analysis (TGA)	mg range	Allows the study of weight loss in samples	

A.18. Surface Chemistry (continued)

Technique	Detection Range	Advantages	Disadvantages
Transmission Electron Microscopy (TEM) ⁵	>0.1 nm	High resolution	Requires high vacuum for sample preparation
Ultraviolet/Visible Spectroscopy (UV/Vis)	mM range	Fast	
X-ray Photoelectron Spectroscopy (XPS)	>1 μm	Can be used to determine atomic composition of layers (1–10 μm)	
Zeta Potential	5 nm–10 μm		

Bold font indicates most commonly employed techniques.

¹Can be used in combination with Transmission Electron Energy Loss Spectroscopy (EELS) (<Zn), Electron Microscopy (TEM), Scanning Electron Microscopy (SEM), and Scanning Transmission Electron Microscopy (STEM).

²Can be used in combination with Scanning Electron Microscopy (SEM).

³Can be used in combination with Auger Electron Microscopy (AES) and Energy-Dispersive X-ray Spectroscopy (EDS).

⁴Can be used in combination with Ultraviolet/Visible Spectroscopy (UV/Vis) and Inductively Coupled Plasma Mass Spectrometry (ICP-MS).

⁵Can be used in combination with Electron Energy Loss Spectroscopy (EELS) and Energy-Dispersive X-ray Spectroscopy (EDS).

A.19. Surface Contamination

Technique	Detection Range	Advantages	Disadvantages
Aerosol Time-of-Flight Mass Spectroscopy (ATOF-MS)	0.32–1.8 μm		Efficiencies decrease as particle gets smaller
Atomic Force Microscopy (AFM)	>0.1 nm	Can be used to analyze dry, moist, and liquid samples	Artifacts can result from tip smearing
Auger Electron Microscopy (AES) ¹	1–2 nm		
Differential Scanning Calorimetry (DSC)	mg range	Allows the study of phase transitions	
Infrared Spectroscopy (IR)	ppm range	Can be used to analyze solid or liquid samples	
Nuclear Magnetic Resonance (NMR)	mM range	Can be used to analyze solid or liquid samples Good temperature range	Solid-state experiments more difficult
Raman Spectroscopy	ppm range	Can be used to analyze solid or liquid samples	
Scanning Tunneling Electron Microscopy (STM)	nm in x, y, and z directions	Allows three-dimensional characterization	
Thermo-Gravimetric Analysis (TGA)	mg range	Allows the study of weight loss in samples	
Transmission Electron Microscopy (TEM) ²	>0.1 nm	High resolution	Requires high vacuum for sample preparation
Ultraviolet/Visible Spectroscopy (UV/Vis)	mM range	Fast	
X-ray Photoelectron Spectroscopy (XPS)	>1 μm	Can be used to determine the atomic composition of layers (1–10 μm)	

Bold font indicates most commonly employed techniques.

¹Can be used in combination with Scanning Electron Microscopy (SEM).

²Can be used in combination with Electron Energy Loss Spectroscopy (EELS) and Energy-Dispersive X-ray Spectroscopy (EDS).

Appendix A References

- [AZoNano](http://www.azonano.com/nanotechnology-equipment.asp?cat=9). (2010). Atomic force microscopes. Available online at <http://www.azonano.com/nanotechnology-equipment.asp?cat=9> (accessed May 17, 2010).
- [Becker, JS.](#) (2008). Inorganic mass spectrometry: Principles and applications. West Sussex, England: Wiley-Interscience.
- [Buchan Lawton](#) (Buchan Lawton Parent Ltd). (2010). Bruker technologies: Our product lines. Available online at <http://www.bruker.com/product.html> (accessed May 17, 2010).
- [Coulson, JM; Richardson, JF; Harker, JH; Backhurst, JR.](#) (2002). Coulson and Richardson's chemical engineering: Particle technology and separation processes (5th ed.). Woburn, MA: Butterworth-Heinemann.
- [General Electric Company.](#) (2010). Cross flow filtration systems. Available online at http://www5.gelifsciences.com/aptrix/upp01077.nsf/Content/bioprocess~filtration1~systems_complete (accessed May 17, 2010).
- [Imaging Technology Group.](#) (2010). Environmental scanning electron microscope (ESEM). Available online at http://itg.beckman.illinois.edu/microscopy_suite/equipment/ESEM/ (accessed May 17, 2010).
- [NCEM](#) (National Center for Electron Microscopy). (2010). Analytical electron microscopy. Available online at <http://ncem.lbl.gov/frames/aem.htm> (accessed May 17, 2010).
- [Oberdörster, G; Maynard, A; Donaldson, K; Castranova, V; Fitzpatrick, J; Ausman, K; Carter, J; Karn, B; Kreyling, W; Lai, D; Olin, S; Monteiro-Riviere, N; Warheit, D; Yang, H.](#) (2005). Principles for characterizing the potential human health effects from exposure to nanomaterials: Elements of a screening strategy. Part Fibre Toxicol 2: 1-35. <http://dx.doi.org/10.1186/1743-8977-2-8>
- [PerkinElmer.](#) (2010). Technologies. Available online at http://www.perkinelmer.com/Technologies/default/cat1/NAV_04_TCH_Technologies_001/Country/USA/Ecommerce/Yes/Dealer/No (accessed May 17, 2010).
- [Quantachrome Instruments.](#) (2010). Surface area and pore size by gas sorption. Available online at http://www.quantachrome.com/product_listing/surface_area_analyzers.html?gclid=CPbd9quyJzWCFR2dnAadj34CZQ (accessed May 17, 2010).
- [Shimadzu Scientific Instruments.](#) (2010). Laboratory instruments. Available online at http://www.ssi.shimadzu.com/products/products_main.cfm?maincategory=Laboratory%20Instruments (accessed May 17, 2010).
- [Tiede, K; Boxall, ABA; Tear, SP; Lewis, J; David, H; Hassellöv, M.](#) (2008). Detection and characterization of engineered nanoparticles in food and the environment. Food Addit Contam Part A Chem Anal Control Expo Risk Assess 25: 795-821. <http://dx.doi.org/10.1080/02652030802007553>
- [TSI Inc.](#) (Trust Science Innovation Incorporated). (2010). Aerosol time-of-flight mass spectrometers. Available online at http://www.tsi.com/en-1033/segments/chemical_analysis/2194/aerosol_time-of-flight_mass_spectrometers.aspx (accessed May 17, 2010).
- [Tsuda, K; Tanaka, M.](#) (1996). Interferometry by coherent convergent-beam electron diffraction. J Electron Microsc (Tokyo) 45: 59-63.
- [Varian](#) (Varian Inc.). (2010). Products. Available online at <http://www.varianinc.com/cgi-bin/nav?products/index&cid=LLPLMOLIFQ> (accessed May 17, 2010).
- [Zuin, S; Pojana, G; Marcomini, A.](#) (2007). Effect-oriented physicochemical characterization of nanomaterials. In NA Monteiro-Riviere; CL Tran (Eds.), Nanotoxicology: Characterization, dosing, and health effects (pp. 19-57). New York, NY: Informa Healthcare.

Appendix B. Summary of Ecological Effects Studies of Nano-Ag

This page intentionally left blank.

Appendix B. Summary of Ecological Effects Studies of Nano-Ag

B.1. Study Selection Criteria	B-4
B.2. Summary of Nano-Ag Effects in Microorganisms (Excluding Algae)	B-5
Bae et al. (2010) Bacterial cytotoxicity of the silver nanoparticle related to physicochemical metrics and agglomeration properties.	B-5
Bradford et al. (2009) Impact of silver nanoparticle contamination on the genetic diversity of natural bacterial assemblages in estuarine sediments.	B-6
Choi and Hu (2008) Size dependent and reactive oxygen species related nanosilver toxicity to nitrifying bacteria.	B-7
Choi et al. (2008) The inhibitory effects of silver nanoparticles, silver ions, and silver chloride colloids on microbial growth.	B-8
Choi et al. (2009) Role of sulfide and ligand strength in controlling nanosilver toxicity.	B-9
Dasari and Hwang (2010) The effect of humic acids on the cytotoxicity of silver nanoparticles to a natural aquatic bacterial assemblage.	B-10
El Badawy et al. (2011) Surface charge-dependent toxicity of silver nanoparticles.	B-11
Gao et al. (2011) Effects of engineered nanomaterials on microbial catalyzed biogeochemical processes in sediments.	B-12
Hwang et al. (2008) Analysis of the toxic mode of action of silver nanoparticles using stress-specific bioluminescent bacteria.	B-13
Ivask et al. (2010) Profiling of the reactive oxygen species-related ecotoxicity of CuO, ZnO, TiO ₂ , silver and fullerene nanoparticles using a set of recombinant luminescent <i>Escherichia coli</i> strains: differentiating the impact of particles and solubilised metals.	B-14
Jin et al. (2010) High throughput screening of silver nanoparticle stability and bacterial inactivation in aquatic media: influence of specific ions.	B-15
Khan et al. (2011) Silver nanoparticles tolerant bacteria from sewage environment.	B-16
Kim et al. (2009) Antifungal activity and mode of action of silver nano-particles on <i>Candida albicans</i> .	B-17
Kvitek et al. (2008) Effect of surfactants and polymers on stability and antibacterial activity of silver nanoparticles (NPs).	B-18
Lok et al. (2006) Proteomic analysis of the mode of antibacterial action of silver nanoparticles.	B-19
Martinez-Gutierrez et al. (2010) Synthesis, characterization, and evaluation of antimicrobial and cytotoxic effect silver and titanium nanoparticles.	B-20
Morones et al. (2005) Bactericidal effect of silver nanoparticles.	B-21
Pal et al. (2007) Does the antibacterial activity of silver nanoparticles depend on the shape of the nanoparticle? A study of the Gram-negative bacterium <i>Escherichia coli</i> .	B-22
Saulou et al. (2010) Synchrotron FTIR microspectroscopy of the yeast <i>Saccharomyces cerevisiae</i> after exposure to plasma-deposited nanosilver-containing coating.	B-23
Shrivastava et al. (2007) Characterization of enhanced antibacterial effects of novel silver nanoparticles.	B-24
Sinha et al. (2011) Interaction and nanotoxic effect of ZnO and Ag nanoparticles on mesophilic and halophilic bacterial cells.	B-25
Sondi and Salopek-Sondi (2004) Silver nanoparticles as antimicrobial agent: a case study on <i>E. coli</i> as a model for Gram-negative bacteria.	B-26
Sotiriou and Pratsinis (2010) Antibacterial activity of nanosilver ions and particles.	B-27
B.3. Summary of Nano-Ag Effects in Algae	B-28
Griffitt et al. (2008) Effects of particle composition and species on toxicity of metallic nanomaterials in aquatic organisms.	B-28
Park et al. (2010b) Selective inhibitory potential of silver nanoparticles on the harmful cyanobacterium <i>Microcystis aeruginosa</i> .	B-29
Miao et al. (2009) The algal toxicity of silver engineered nanoparticles and detoxification by exopolymeric substances.	B-30
Navarro et al. (2008) Toxicity of silver nanoparticle to <i>Chlamydomonas reinhardtii</i> .	B-31
B.4. Summary of Nano-Ag Effects in Aquatic Invertebrates	B-32
Allen et al. (2010) Effects from filtration, capping agents, and presence/ absence of food on the toxicity of silver nanoparticles to <i>Daphnia magna</i> .	B-32

Gao et al. (2009) Dispersion and toxicity of selected manufactured nanomaterials in natural river-water samples: effects of water chemical composition. _____	B-33
Griffitt et al. (2008) Effects of particle composition and species on toxicity of metallic nanomaterials in aquatic organisms. _____	B-34
Li et al. (2010b) Comparative toxicity study of Ag, Au, and Ag-Au bimetallic nanoparticles on <i>Daphnia magna</i> . _____	B-35
Kvitek et al. (2009) Initial study on the toxicity of silver nanoparticles (NPs) against <i>Paramecium caudatum</i> . _____	B-36
Nair et al. (2011) Differential expression of ribosomal protein gene, gonadotrophin releasing hormone gene and Balbiani ring protein gene in silver nanoparticles exposed <i>Chironomus riparius</i> . _____	B-37
Ringwood et al. (2010) The effects of silver nanoparticles on oyster embryos. _____	B-38
B.5. Summary of Nano-Ag Effects in Aquatic Vertebrates _____	B-39
Asharani et al. (2008) Toxicity of silver nanoparticles in zebrafish models. _____	B-39
Bar-Ilan et al. (2009) Toxicity assessments of multisized gold and silver nanoparticles in zebrafish embryos. _____	B-40
Bilberg et al. (2010) Silver nanoparticles and silver nitrate cause respiratory stress in Eurasian perch (<i>Perca fluviatilis</i>). _____	B-41
Chae et al. (2009) Evaluation of the toxic impact of silver nanoparticles on Japanese medaka (<i>Oryzias latipes</i>). _____	B-42
Choi et al. (2010) Induction of oxidative stress and apoptosis by silver nanoparticles in the liver of adult zebrafish. _____	B-43
Farkas et al. (2011) Uptake and effects of manufactured silver nanoparticles in rainbow trout (<i>Oncorhynchus mykiss</i>) gill cells. _____	B-44
Griffitt et al. (2009) Comparison of molecular and histological changes in zebrafish gills exposed to metallic nanoparticles. _____	B-45
Hinther et al. (2010) Nanometals induce stress and alter thyroid hormone action in amphibia at or below North American water quality guidelines. _____	B-46
Kennedy et al. (2010) Fractionating nanosilver: importance for determining toxicity to aquatic test organisms. _____	B-47
Laban et al. (2009) The effects of silver nanoparticles on fathead minnow (<i>Pimephales promelas</i>) embryos. _____	B-48
Lee et al. (2007) In vivo imaging of transport and biocompatibility of single silver nanoparticles in early development of zebrafish embryos. _____	B-49
Scown et al. (2010) Effects of aqueous exposure to silver nanoparticles of different sizes in rainbow trout. _____	B-50
Shahbazzadeh et al. (2009) The effects of nanosilver (Nanocid®) on survival percentage of rainbow trout (<i>Oncorhynchus mykiss</i>). _____	B-51
Wu et al. (2010) Effects of silver nanoparticles on the development and histopathology biomarkers of Japanese medaka (<i>Oryzias latipes</i>) using the partial-life test. _____	B-52
Yeo and Kang (2008) Effects of nanometer-sized silver materials on biological toxicity during zebrafish embryogenesis. _____	B-53
Yeo and Pak (2008) Exposing zebrafish to silver nanoparticles during caudal fin regeneration disrupts caudal fin growth and p53 signaling. _____	B-54
B.6. Summary of Nano-Ag Effects on Terrestrial Plants _____	B-55
Babu et al. (2008) Effect of nano-silver on cell division and mitotic chromosomes: a prefatory siren. _____	B-55
Kumari et al. (2009) Genotoxicity of silver nanoparticles in <i>Allium cepa</i> . _____	B-56
Rostami and Shahstavar (2009) Nano-silver particles eliminate the in vitro contamination of olive 'Mission' explants. _____	B-57
Stampoulis et al. (2009) Assay-dependent phytotoxicity of nanoparticles to plants. _____	B-58
B.7. Summary of Nano-Ag Effects on Terrestrial Invertebrates _____	B-59
Ahamed et al. (2010) Silver nanoparticles induced heat shock protein 70, oxidative stress and apoptosis in <i>Drosophila melanogaster</i> . _____	B-59
DNA Damage. Levels of p53 and p38 were significantly increased in treated larvae from those of the control in a time- and dose-related manner, indicating significant DNA damage caused by exposure to nano-Ag. _____	B-59
Apoptosis. Activities of caspase-3 and caspase-9 were significantly increased in treated larvae from the control levels, suggesting that nano-Ag exposure is involved in the apoptotic pathway. _____	B-59
Heckmann et al. (2011) Limit-test toxicity screening of selected inorganic nanoparticles to the earthworm <i>Eisenia fetida</i> . _____	B-60
Lapied et al. (2010) Silver nanoparticle exposure causes apoptotic response in the earthworm <i>Lumbricus terrestris</i> (Oligochaeta). _____	B-61
Meyer et al. (2010) Intracellular uptake and associated toxicity of silver nanoparticles in <i>Caenorhabditis elegans</i> . _____	B-62
Roh et al. (2009) Ecotoxicity of silver nanoparticles on the soil nematode <i>Caenorhabditis elegans</i> using functional ecotoxicogenomics. _____	B-63
Sap-lam et al. (2010) UV irradiation-induced silver nanoparticles as mosquito larvicides. _____	B-64
Shoultz-Wilson et al. (2011) Evidence for avoidance of Ag nanoparticles by earthworms (<i>Eisenia fetida</i>). _____	B-65

B.8. Summary of Nano-Ag Effects on Non-mammalian Terrestrial Vertebrates	B-66
Grodzik and Sawosz (2006) The influence of silver nanoparticles on chicken embryo development and bursa of Fabricius morphology.	B-66
Sawosz et al. (2007) Influence of hydrocolloidal silver nanoparticles on gastrointestinal microflora and morphology of enterocytes of quail.	B-67
Appendix B References	B-68

B.1. Study Selection Criteria

The process used to select studies for inclusion in the ecological effects tables differed for each category of organism based on the quantity and quality of available ecotoxicological data. In general, literature searches were conducted for each category of organism (e.g., bacteria and fungi, aquatic plants, terrestrial vertebrates). To reflect the most current state of the science, the tables in this appendix include only studies published in or after 2000. The information presented here is up to date as of March 1, 2011, when the last broad literature search to identify new information was conducted. For those categories for which a substantial amount of ecotoxicity data was available (e.g., bacteria, fish), studies examining relevant endpoints were selected based on the data quality and the relative contribution of the results to the state of the science (determined largely by examining the number of articles in which the study was later cited). Also, studies were included if the investigators examined an endpoint for which there was otherwise little information, used a novel technique to assess toxicity, or compared the relative toxicities of nano-Ag possessing different sets of characteristics (e.g., nano-Ag of different sizes, surface areas, shapes). For categories with very little available ecotoxicological information (e.g., terrestrial organisms), all identified studies were included unless they were judged to be of poor quality.

Information in the tables is organized to take into account the minimum requirements for physicochemical characterization proposed by the Minimum Information for Nanomaterial Characterization (MINChar) Initiative ([MINCharInitiative, 2008](#)). The limited understanding of nano-Ag toxicity and its mechanisms, and the equivocal nature of some studies that give conflicting results, preclude the direct comparison of results for many studies. To emphasize that caution is warranted in interpreting the results of the available nano-Ag toxicological studies, these tables are organized in a way that emphasizes each study's relevant attributes in the context of this case study – especially characterization of the nano-Ag used in the study – rather than to facilitate direct comparison of results among studies.

B.2. Summary of Nano-Ag Effects in Microorganisms (Excluding Algae)

Bae et al. (2010) Bacterial cytotoxicity of the silver nanoparticle related to physicochemical metrics and agglomeration properties.

Test Species

Escherichia coli (strain ATCC 8739)

Material

Nano-Ag powder (Sigma-Aldrich) prepared as a suspension in an aqueous phase via ultrasonication with deionized water and tetrahydrofuran.

Shape: Polyhedral (determined using TEM)

Composition: Not reported

Crystal Structure: Ag (111), (200), and (220) (determined using TEM)

Average Size: 38 ± 1.4 nm (Determined using HR-TEM); 43 ± 3.2 nm (Determined using DLS)

Size Distribution: <150 nm (reported by manufacturer)

Solubility: Not reported

Surface Area: ca 1,255 nm² (determined using image analysis)

Surface Treatment: Not reported

Surface Charge: Not reported

Protocol

Exposure Duration: 30 minutes

Endpoints: Activity and morphological abnormalities

Exposure Concentrations: 0.2, 0.4, 0.6, 0.8, and 1.0 mg/L.

Exposure Medium: Phosphate-buffered saline

Bacterial Density: 5×10^5 CFU/mL

Methods: Toxicity was evaluated for three controlled parameters at several ionic ratios, average hydrodynamic particle diameters, and total Ag and AgNO₃ and was measured by the extent of inactivation of *E. coli* by viable cell count. Sensitivity for toxicity and agglomeration was determined using the principle of the tornado diagram whereby positive and negative changes relative to the baseline were represented by a bar graph.

Study Outcome

The rate of agglomeration was dependent on particle size rather than total Ag concentration or Ag⁺ ratio. Agglomeration rate increased rapidly with particle sizes <50 nm. Total Ag concentration was the most important determinant of toxicity, rather than size distribution or ionic ratio. Sensitivity to agglomeration was inversely correlated with toxicity.

Microbial Activity. The inactivation of *E. coli* was found to be dependent on the concentration of nano-Ag and Ag⁺. 1.0 mg/L nano-Ag caused 3.9 log inactivation, whereas Ag⁺ caused 3.6 log inactivation at the same total Ag concentration. Inactivation was also a function of the Ag⁺ ion ratio. The log inactivation of *E. coli* increased for an ionic ratio in the range of 5–24% (ionic ratio), while ionic ratios beyond 24% were associated with depressed toxicity. In terms of particle size, at 0.8 mg/L, log inactivation increased in the range of 21–323 nm diameter and decreased in the range of 4–21 nm. At this concentration inactivation was depressed more strongly in relation to ionic ratio than size. At 0.4 mg/L, microbial activity was independent of nano-Ag size. Depression in inactivation effect was correlated with changes in the agglomeration rate for each of the properties for nano-Ag (depressed significantly in the case of a high agglomeration rate: a high ionic ratio and small sized particles induced higher agglomeration rates). In the inactivation test, factors in order of importance were: dosage, ionic ratio, and size.

Morphological Abnormalities. Structural abnormalities included partial loss of the outer membrane, localized or complete separation of the cytoplasm from the cell wall, and cellular degradation.

Bradford et al. (2009) Impact of silver nanoparticle contamination on the genetic diversity of natural bacterial assemblages in estuarine sediments.

Test Species

Natural bacterial assemblages

Material

Commercial nano-Ag (form not reported) supplied by Sigma-Aldrich (location not reported).

Shape: Assumed to be spherical (not verified experimentally)	Solubility: Not reported
Composition: Not reported	Surface Area: Not reported
Crystal Structure: Not reported	Surface Treatment: Not reported
Average Size: 58.6 ± 18.6 nm (determined using TEM)	Surface Charge: Not reported

Protocol

Exposure Duration: 30 days	Exposure Media: Estuarine sediment and water from Tamar Estuary in Plymouth Sound ("St John's Lake" mud flats OSGB grid ref SX412539)
Endpoints: Prokaryotic abundance and genetic diversity	
Exposure Concentrations: 0, 25, and 1,000 µg/L	
	Bacterial Density: Not reported (natural assemblage)

Methods: To achieve final concentrations of 25 and 1,000 µg/L in the experimental tanks, daily doses 1/20th of the final concentration were added for 20 days to estuarine water overlying estuarine sediment, followed by 10 days in which no dose was administered. Prokaryotic abundance in the water column of each of the experimental tanks was determined using a Becton Dickinson flow cytometer for 10-mL subsamples from experimental tanks. Clades were defined on cytogram plots of side scatter vs. green fluorescence to define high and low nucleic acid cells. Environmental DNA was extracted from sediment samples and a two-step nested PCR-denaturing gradient gel electrophoresis (DGGE) approach, using PCR primers specific to the "phylum Bacteria," was adopted to assess bacterial diversity. Fragments of the 16S rRNA gene were amplified from the environmental DNA. DGGE profiles of PCR-amplified 16S rRNA gene fragments were converted to binary (presence/absence) data and analyzed using analysis of similarities.

Study Outcome

Abundance. Flow cytometric analysis of samples from the overlying water revealed that mean prokaryotic cell counts did not change significantly between treatments over time but were highly correlated ($p = 0.725$), indicating that bacterial and archaeal abundance in the water was not affected by the presence of nano-Ag.

Diversity. Independent of the nano-Ag-dosing, there were no changes in bacterial diversity in the surface of the sediment over the 30-day exposure. DGGE-PCR results for sediment samples taken at the start and finish of the dosing period (Day 1–20) for the control tank and the 1,000 µg/L tank differed slightly but significantly ($p = 0.04$). However, similarity profile permutation analysis revealed that most of the clustering of the bacterial diversity in these samples could have arisen by chance.

Choi and Hu (2008) Size dependent and reactive oxygen species related nanosilver toxicity to nitrifying bacteria.

Test Species

Nitrifying bacteria (species not reported)

Material

Nano-Ag synthesized using AgNO_3 by varying the molar ratios (R) of BH_4^- to Ag^+ due to changes in NaBH_4 concentration.

Shape: Not reported

Size Distribution: 5–70 nm

Composition: Not reported

Solubility: Not reported

Crystal Structure: Not reported

Surface Area: Not reported

Average Size: 9 ± 5 nm (R = 0.1), 15 ± 9 nm (R = 0.2), 14 ± 6 nm (R = 0.36), 12 ± 4 nm (R = 0.6), or 21 ± 14 nm (R = 1.2) (determined using TEM)

Surface Treatment: Capped with polyvinyl alcohol (PVA)

Surface Charge: Not reported

Protocol

Exposure Duration: 30 minutes

Exposure Concentrations: 0.05–1 mg Ag/L

Endpoints: Growth and reactive oxygen species (ROS) generation

Exposure Medium: Nitrifying biomass from tank reactor

Bacterial Density: Not reported

Methods: Growth inhibition of nitrifying bacteria was inferred from oxygen uptake rates due to ammonia oxidation and measured using batch extant respirometric assay. EC_{50} s were determined using a saturation-type biological toxicity model. Intracellular ROS concentrations were determined using fluorescence assays following exposure to nano-Ag with an average size of 15 nm. Photocatalytic ROS concentrations were determined using the same method but in the absence of nitrifying cultures to determine exogenous influence of ROS generation.

Study Outcome

Growth Inhibition.

EC_{50} (nano-Ag): 0.14 mg/L

EC_{50} (silver chloride [AgCl] colloid): 0.25 mg/L

EC_{50} (Ag^+): 0.27 mg/L

ROS Generation. Exposure to nano-Ag resulted in an increase of intracellular ROS concentrations, which correlated strongly with the degree of growth inhibition ($R^2 = 0.86$). Photocatalytic ROS concentrations did not correlate strongly with observed inhibition and were therefore not deemed a good predictor of growth inhibition by nano-Ag.

Choi et al. (2008) The inhibitory effects of silver nanoparticles, silver ions, and silver chloride colloids on microbial growth.

Test Species

Autotrophic bacteria (nitrifying; species not reported) and heterotrophic bacteria (*Escherichia coli* PHL628-gfp)

Material

Nano-Ag synthesized through reduction of AgNO₃ with NaBH₄.

Shape: Polydisperse (spherical and ellipsoidal)

Composition: Not reported

Crystal Structure: Not reported

Average Size: 14 ± 6 nm (determined using STEM)

Size Distribution: 10–40 nm (determined using STEM)

Solubility: Not reported

Surface Area: Not reported

Surface Treatment: Capped with polyvinyl alcohol (PVA)

Surface Charge: Not reported

Protocol

Exposure Duration: 24 hours

Endpoint: Growth

Exposure Concentrations: 0.1–1 mg Ag/L

Exposure Media: Mixed liquor from sludge tank reactor (autotrophic) or BBL™ medium containing Gelysate peptone and beef extract (heterotrophic)

Bacterial Density: Not reported

Methods: Antibacterial activity of nano-Ag was assessed using LIVE/DEAD BacLight™ bacterial viability kit. The degree of growth inhibition in autotrophic bacteria was inferred from oxygen uptake rates due to ammonia oxidation and measured using a batch extant respirometric assay. The degree of growth inhibition in heterotrophic bacteria was determined using an automated microtiter assay using hourly fluorescence intensity measurements to derive a microbial growth rate.

Study Outcome

Autotrophic Bacterial Growth. At 1 mg Ag/L in the nitrifying suspension, nano-Ag inhibited growth by 86%, while Ag⁺ and AgCl colloids inhibited growth by 42% and 46%, respectively.

Heterotrophic Bacterial Growth. IC₅₀ = 4.0 μM. No inhibitory effect was observed at concentrations below 1 μM. The inhibitory effect of nano-Ag increased to 55% at 4.2 μM (~0.5 mg/L Ag), while Ag⁺ and AgCl colloids inhibited growth by 100% and 66%, respectively. At 100 mg Ag/L, nano-Ag inhibited growth completely.

Choi et al. (2009) Role of sulfide and ligand strength in controlling nanosilver toxicity.

Test Species

Nitrifying bacteria (species not reported)

Material

Nano-Ag suspension synthesized through reduction of AgNO₃ with NaBH and capped with polyvinyl alcohol (PVA); in suspension with Ag⁺.

Shape: Not reported

Composition: Not reported

Crystal Structure: Not reported

Average Size: 15 ± 9 nm (method not reported)

Size Distribution: Not reported

Solubility: Not reported

Surface Area: Not reported

Surface Treatment: PVA-capped

Surface Charge: Not reported

Protocol

Exposure Duration: 300 seconds (inhibition test) or 8 or 18 hours (Ag₂S stability test)

Endpoints: Enzyme inhibition and uptake

Exposure Concentrations: 1 mg Ag/L

Exposure Media: Nitrifying enriched culture to which MOPS was added

Bacterial Density: Nitrifying biomass concentrations of 540 mg/L chemical oxygen demand (COD) or 210 mg/L COD

Methods: Following nano-Ag exposure, inhibition of ammonia monooxygenase (AMO), hydroxylamine oxidoreductase (HAO), and nitrite oxidoreductase (NOR), three critical enzymes involved in nitrification, was calculated by relative oxygen uptake rate after the addition of aliquots of ammonium, hydroxylamine, and nitrate to the respirometric bottles. Effects of ligands on nano-Ag toxicity were determined through a one-time addition of Ag-ligand complexes as well as sequential addition of a specific ligand followed by nano-Ag to the nitrifying cultures. The ligands tested were chloride, sulfate, phosphate, EDTA⁴⁻, and sulfide. Toxicity was determined using a respirometric assay which also determined stability of Ag₂S complexes made from nano-Ag and sulfide. Nano-Ag attachment to cells was determined using a back-scattered electron detector coupled with a secondary electron detector, and elemental composition of specimens was determined using energy dispersive X-ray spectroscopy.

Study Outcome

Inhibition of Enzyme Activity. AMO was the most sensitive of the three enzymes tested when exposed to both nano-Ag and Ag⁺ at nitrifying biomass concentrations of 540 mg/L COD.

Influence of Ligand Complexation. At 1 mg Ag/L and nitrifying biomass concentrations of 210 mg/L COD, nano-Ag inhibited nitrification by 100%. A 10 µM concentration of sulfide reduced nano-Ag toxicity by 80%, while the other ligands also reduced toxicity, but to a lesser degree. Additional phosphate concentrations up to 0.3 mM had little effect on toxicity, while chloride concentrations of 2.8 mM reduced nano-Ag toxicity up to 20%, and a sulfide concentration of 15 µM reduced nano-Ag toxicity from 86% to 15%.

Adsorption to Cell Floccs. Nano-Ag embeds in cell floccs. When sulfide was added prior to nano-Ag exposure, embedding largely decreased.

Dasari and Hwang (2010) The effect of humic acids on the cytotoxicity of silver nanoparticles to a natural aquatic bacterial assemblage.

Test Species

Natural aquatic bacterial assemblages (Species not determined)

Material

Nano-Ag synthesized using citrate reduction method

Shape: Spherical (determined using TEM)

Composition: Not reported

Crystal Structure: Not reported

Average Size: 15 – 25 nm (determined using TEM)

Size Distribution: Not reported

Solubility: Not reported

Surface Area: Not reported

Surface Treatment: Not reported

Surface Charge: Not reported

Protocol

Exposure Duration: 2 hours

Endpoints: Bacterial viability cytotoxicity

Exposure Concentrations: 0, 2.5, and 5.0 μM

Exposure Medium: Standard terrestrial humic acid (HA) from the Sigma Aldrich (St. Louis, MO); standard Suwannee river humic acid from International Humic Substances Society (St. Paul, MN); both in 1 mM sodium phosphate buffer

Bacterial Density: 0, 10, 20, and 40 ppm HA

Methods: HA solutions were prepared in 1 mM sodium phosphate buffer. Nano-Ag was synthesized and centrifuged for spherical geometry. In a 4-way factorial design experiment the independent variables identified were: HA concentration, nano-Ag concentration, HA source, and light effect. The HA solutions were prepared and incubated for a total of 12 treatments. TEM measurements were performed on 10 μL samples that were dried overnight. A cell permanent ROS indicator was used to detect ROS production in bacterial cells. After ROS results were obtained, silver ion concentration was measured in select groups by ICP-OES.

Study Outcome

Exposure to concentrations of 2.5 and 5.0 μM nano-Ag alone decreased viability of bacteria by 48–89% and 65–84%, respectively, when compared to the control group and exposed under darkened conditions. ROS production caused in the dark was negligible (with the exception of 5.0 μM nano-Ag); therefore, the observed nano-Ag toxicity in the dark was attributed to mechanisms other than the production of ROS. Bacterial viability was inhibited more in the light exposure groups than in the darkness exposure groups; shrinkage in the size of cells occurred after they were exposed to sunlight irradiation. Larger reductions in bacterial viability count were observed in the combined treatment of HA and nano-Ag under light exposures; the light exposure inhibited viability more than the darkness exposure. There was a statistically significant difference in the influence on bacterial viability imposed by the type of HA used. When exposed to the terrestrial HA, viability was statistically significantly affected by each variable (i.e., light/darkness, HA concentration, and nano-Ag concentration) independently, and by some of the two-way or three-way interactions among variables. When exposed to the Suwannee River HA, viability was also statistically significantly affected by the independent variable and some two-way interactions, but no three-way interactions were statistically significant.

El Badawy et al. (2011) Surface charge-dependent toxicity of silver nanoparticles.

Test Species

Bacillus spp. (Gram-positive bacteria) obtained from Interlab Supply

Material

Synthesis of uncoated (H₂-AgNP), citrate-coated (citrate-AgNP), and branched polyethyleneimine (BPEI)-coated nano-Ag (BPEI-AgNP) suspensions described in a previous study (El Badawy et al., 2010). Polyvinylpyrrolidone (PVP)-coated nano-Ag (PVP-AgNP) synthesized by modified Lee and Meisel procedure. All characteristics of synthesized nano-Ag are reported in author's previous research.

Shape: Spherical (determined using TEM)

Composition: Not reported

Crystal Structure: Not reported

Average Size: 18 nm as prepared/immediately after purification, 17 nm after 3 weeks (H₂-AgNP); 10 nm as prepared/immediately after purification, 11 nm after 3 weeks (citrate-AgNP); 12 nm as prepared/immediately after purification/after 3 weeks (PVP-AgNP); 10 nm as prepared/immediately after purification/after 3 weeks (BPEI-AgNP)

Size Distribution: Not reported

Solubility: Not reported

Surface Area: Not reported

Surface Treatment: uncoated, citrate-coated, PVP-coated, or BPEI-coated

Surface Charge: ~ -22.5 mV (uncoated); ~ -39 mV (citrate-coated); ~ -11 mV (PVP-coated); ~ 40 mV (BPEI-coated) (determined using a Zetasizer Nanoseries; average measurements for post-purification and 3 weeks post-purification)

Protocol

Exposure Duration: 120 ± 2 hours (O₂ consumption)

Endpoints: Oxygen consumption and mortality

Exposure Concentrations: Not reported

Exposure Medium: BOD₅ test media

Bacterial Density: Not reported – three replications per test concentration

Methods: A 5-day oxygen consumption test was carried out on *Bacillus spp.*, and the live/dead technique was used as a rapid screening method to evaluate toxicity. Oxygen consumption was determined by method 2510 B (Eaton et al., 2005) Dissolved oxygen was measured by Thermo Scientific Orion DO probe. Microbial live/dead measurements were obtained using *BacLight* live/dead kit with two-color fluorescence assay and fluorescence spectroscopy.

Study Outcome

Oxygen Consumption and Live/Dead Test. A direct correlation between toxicity and surface charge was observed. The more negatively charged citrate-capped nano-Ag particles were the least toxic, whereas the positively charged BPEI-capped nano-Ag particles were the most toxic (both in terms of oxygen consumption and in the live/dead test). The surface charge of the citrate-capped nanoparticles was assumed to be less toxic due to the fact that the *Bacillus spp.* has been shown to have a similar charge under test conditions (caused by the carboxyl, phosphate, and amino groups on the cellular membrane) leading to repulsion between the two negative charges. As the negative zeta potential gradually decreased (with different capping agents), the repulsion, or electrostatic barrier, is reduced causing a higher degree of toxicity. No statistical significance was reported for this study.

Gao et al. (2011) Effects of engineered nanomaterials on microbial catalyzed biogeochemical processes in sediments.

Test Species

Unspecified sediment microorganisms (nitrate-reducing bacteria)

Material

Nano-Ag from Quantum Spheres, Inc. (Santa Ana, CA) produced by gas-phase condensation. A suspension (initial concentration 200 mg/L) was prepared by shaking in Nanopure water at room temperature for 28 hours followed by filtration.

Shape: Not reported

Composition: Purity >99.9%

Crystal Structure: Not reported

Average Size: Primary particles: 26.6 ± 8.8 nm (determined by Coulter LS 13320) (Griffitt et al., 2008); suspended particles: 66 ± 27 nm (determined by Coulter LS 13320)

Size Distribution: Not reported

Solubility: 0.07% of mass dissolved after 48 hours (Griffitt et al., 2008)

Surface Area: 14.53 m²/g (Griffitt et al., 2008)

Surface Treatment: Not reported

Surface Charge: -27 mV (Griffitt et al., 2008)

Protocol

Exposure Duration: 17 days

Endpoints: Changes in acetate oxidation

Exposure Concentrations: 0.5 mg/L (determined using inductively coupled plasma atomic emission spectrometry [ICP-AES])

Exposure Medium: Freshwater sediment from an urban lake

Bacterial Density: Not reported

Methods: Sediment slurries were prepared and purged with N₂ for 2 hours. The terminal electron acceptors (TEAs) naturally present, primarily oxygen and nitrate, were allowed to be consumed over time. Sediment slurries were incubated under anaerobic conditions, and changes in concentrations in sulfate, nitrate, and nitrite were tracked (determined by ion chromatography) to assess effect on microbial-catalyzed oxidation and nitrate reduction of organic matter as evidenced by determination of the impacts on the terminal electron accepting process. Aliquots of well-homogenized sediment slurries were spiked with de-aerated solution of sodium acetate with or without the addition of nano-Ag. Another set of slurries was spiked with both acetate and nitrate with or without the addition of nano-Ag. The microbial degradation of acetate was monitored.

Study Outcome

Changes in Acetate Oxidation. Decreases in acetate concentrations in control slurries and in those with the addition of nano-Ag (without the addition of nitrate) were similar. In the second set of studies where both acetate and nitrate were added to the slurries, acetate degradation occurred at a faster rate, however the addition of nano-Ag did not produce any statistically significant results compared to control. Parallel and slightly decreasing nitrite concentration trends were observed in both nano-Ag treated slurries and in the control. The acetate oxidation rate of reaction (k_{app}) was comparatively smaller in nano-Ag spiked slurries ($k_{app} = -0.24 \text{ day}^{-1}$) than in the control ($k_{app} = 0.44 \text{ day}^{-1}$), without a statistically significant inhibitory effect.

Hwang et al. (2008) Analysis of the toxic mode of action of silver nanoparticles using stress-specific bioluminescent bacteria.

Test Species

Wild-type bacteria (*Escherichia coli* RFM443) and recombinant bioluminescent bacteria (All *E. coli* strains: DS1 [*yoda::luxCDABE*], DK1 [*katG::luxCDABE*], DC1 [*clpB::luxCDABE*], DPD2794 [*recA::luxCDABE*])

Material

Commercial nano-Ag purchased from Nanopoly Company (Republic of Korea), and synthesized by the company through reduction of AgNO₃ with hydrazine hydrate, formaldehyde, and sodium formaldehydesulfoxylate.

Shape: Not reported

Composition: Pure silver (provided by the manufacturer based on X-ray diffraction pattern and thermogravimetric/differential thermal analyzer [TG/DTA] curves)

Crystal Structure: Not reported

Average Size: 10 nm (provided by the manufacturer and supported by TEM)

Size Distribution: Not reported

Solubility: Not reported

Surface Area: Not reported

Surface Treatment: Not reported

Surface Charge: Not reported

Protocol

Exposure Duration: 2 hours or 60 minutes (RT-PCR analysis)

Endpoints: Growth, oxidative stress, protein/membrane and DNA damage

Exposure Concentrations: 0.1–1 mg/L

Exposure Media: Luria-Bertani culture media

Bacterial Density: 0.08 O.D.₆₀₀

Methods: Growth inhibition was determined in the wild-type *E. coli* based on O.D.₆₀₀. DS1 and DK1 were exposed to incremental concentrations of nano-Ag and 15 units/mL catalase and superoxide dismutase to measure response to superoxide radicals and hydroxyl radicals, respectively, based on maximum relative bioluminescence (RBL). DC1 was exposed to incremental concentrations of nano-Ag to measure response to protein/membrane damage based on RBL. DPD2794 was exposed to incremental concentrations of nano-Ag to measure response to DNA damage based on RBL and real-time quantitative RT-PCR.

Study Outcome

Growth Inhibition. Growth rates declined significantly after exposure to concentrations above 0.5 mg/L.

Oxidative Stress Damage. Nano-Ag led to production of superoxide radicals but little or no production of hydroxyl radicals.

Protein/Membrane Damage. Nano-Ag induced a bioluminescent response indicative of protein/membrane damage seen most strongly at the 0.4 mg/L nano-Ag. Greater concentrations led to a reduction in bioluminescence due to toxic conditions (as seen in growth inhibition test). DC1 did not discriminate between toxicity caused by nano-Ag or Ag⁺.

DNA Damage. Nano-Ag did not induce a response; therefore, no DNA damage was inferred.

Ivask et al. (2010) Profiling of the reactive oxygen species-related ecotoxicity of CuO, ZnO, TiO₂, silver and fullerene nanoparticles using a set of recombinant luminescent *Escherichia coli* strains: differentiating the impact of particles and solubilised metals.

Test Species

Escherichia coli. Eight constitutively luminescent recombinant strains (*E. coli* AB1157 [pSLlux], *E. coli* J1130 [pSLlux], *E. coli* J1131c [SLlux], *E. coli* AS393 [pSLlux], *E. coli* J1132 [pSLlux], *E. coli* AS391 [pSLlux], *E. coli* K12::lux, and *E. coli* MC1061 [pDNLux]), one superoxide-inducible recombinant luminescent strain (*E. coli* K12::soxRSSodAlux), and two metal-inducible recombinant luminescent strains (*E. coli* MC1061 [pSLzntR/pDNPzntAlux] and *E. coli* MC1061 [pSLcueR/pDNPcopAlux]).

Material

Nano-Ag purchased from Sigma-Aldrich. Stock solution of nano-Ag (40 g/L) prepared in MilliQ water, sonicated in ultrasonication bath, and stored in the dark.

Shape: Not reported

Composition: Not reported

Crystal Structure: Not reported

Average Size: <100 nm (reported by the manufacturer; stock contained aggregates, SEM showed suspensions contained non-nanosized particles).

Size Distribution: Not reported

Solubility: AgNO₃ reported as reference chemical for solubility effects (100%); 3.3% of nano-Ag reported to be soluble and released to the test environment as bioavailable metal ions.

Surface Area: Not reported

Surface Treatment: Not reported

Surface Charge: Not reported

Protocol

Exposure Duration: 30 minutes or, 2, 5, or 12 hours

Endpoints: ROS-generating potential (toxicity) and superoxide anion production

Exposure Concentrations: 40 g/L nano-Ag prepared in MilliQ (specific concentration not reported)

Exposure Medium: Microplate

Bacterial Density: 5×10⁷ cells/mL (toxicity test), 10⁷ cells/mL (induction assay), OD₆₀₀~0.1 (bioluminescence induction assay)

Methods: Maximum specific growth rate and ATP content were determined. Superoxide dismutase activity (SOD) was analyzed using a commercial SOD determination kit. ROS-generated toxicity was evaluated by *sod*-deficient *E. coli* strains that were transformed with *luxCDABE* genes to build luminescent ROS-sensitive strains, and by the use of a recombinant *E. coli* strain specifically induced by superoxide anions. Toxicity was measured by the inhibition of luminescence of *E. coli*. Luminescence was continuously recorded during the first 5 seconds of exposure, then once after 30 minutes and 2 hours of incubation using Orion II plate luminometer. Bioluminescence inhibition was calculated as the percentage of the negative control. Measurements were repeated in three independent assays. The presence of superoxide anions in bacterial cells after exposure was analyzed with superoxide anion-inducible *E. coli* K12::soxRSSodAlux biosensor. The presence of silver ions from nano-Ag was determined using Ag sensor bacteria *E. coli* MC1061(pSLcueR/pDNPcopAlux). Nano-Ag (100 µL) was mixed with 100 µL of bacterial suspension on 96-well microplate, and bacterial bioluminescence was measured after 30 minutes, 2 hours, 5 hours, 7 hours, and 24 hours of exposure.

Study Outcome

ROS Generating Potential. The toxicity of nano-Ag to ROS-sensitive strains was shown to increase with time: EC_{50s}= 571, 331, 485, 329, 17.9, and 5.8 mg nano-Ag/L at 30 min for *sod wt*, *sodA*⁻, *sodB*⁻, *sodC*⁻, *sodAB*⁻, *sodABC*⁻, respectively, and 45.9, 30.9, 18.8, 19.7, 3.79, and 3.11 mg nano-Ag/L at 2 h for *sod wt*, *sodA*⁻, *sodB*⁻, *sodC*⁻, *sodAB*⁻, *sodABC*⁻, respectively. Similar results were observed for AgNO₃ (EC_{50s} ranging from 0.1–1,374 mg/L at 30 min exposure and 0.34–1.11 mg/L at 2 h exposure). In general *sodAB*⁻ and *sodABC*⁻ were more susceptible to ROS generation than other strains.

Superoxide Anion Production. Nano-Ag induced bioluminescence of the sensor strain, indicating the presence of intracellular superoxide anions after 5 hours of exposure. When corrected for solubility, EC_{50s} were 1.52 mg/L in wild-type *E. coli* with intact *sod* genes and 0.1 mg/L in *E. coli* with *sodABC*-defective genes. Maximum induction of superoxide dismutase sensor corrected for solubility seemed to be specific to a nanoparticle effect and not to silver ions alone (EC_{50s} = 0.054 mg/L [AgNO₃] and 0.0035 mg/L [nano-Ag]).

Jin et al. (2010) High throughput screening of silver nanoparticle stability and bacterial inactivation in aquatic media: influence of specific ions.

Test Species

Bacillus subtilis and *Pseudomonas putida*

Material

Nano-Ag powder (QuantumSphere Inc., Santa Ana, CA); silver nitrate (99% pure) (Sigma-Aldrich, St. Louis, MO). Nano-Ag suspensions were prepared in ultrapure sterile water by ultrasonication.

Shape: Not reported

Composition: Not reported

Crystal Structure: Not reported

Average Size: 25 nm (reported by manufacturer), 26 ± 8 nm (determined using TEM)

Size Distribution: Not reported

Solubility: Not reported

Surface Area: Not reported

Surface Treatment: Used as received

Surface Charge: Approximately -10 to -60 mV (determined using Zeta-PALS)

Protocol

Exposure Duration: 24 hours

Endpoints: Bacterial viability

Exposure Concentrations: 19 concentrations from 0.2 $\mu\text{g/L}$ to 50 mg/L

Exposure Medium: Model freshwater electrolyte with ionic strength maintained at 5.6 mM by replacing specific cation or anion with Na^+ or Cl^- (pH varied)

Bacterial Density: 10^8 cells/mL

Methods: Silver concentrations were measured using ICP-OES; samples were centrifuged and filtered to determine the concentration of dissolved nano-Ag. USGS software PHREEQC was used to calculate the theoretical maximum free Ag^+ concentration. The high-throughput bacterial viability assay was based on a Live/Dead BacLight bacterial viability kit; 25 μL of nano-Ag suspension and 25- μL of bacterial suspensions were dispensed into wells and incubated and stains were added to the wells. A fluorescence microreader provided the percentage of live bacteria in each well. Data were fitted by a dose-response model using a nonlinear regression with four-parameter logistic equation.

Study Outcome

The measured particle size increased significantly, indicating that Ca^{2+} and Mg^{2+} ions enhanced aggregation of nano-Ag in the matrix containing divalent cations. There was no correlation between aggregate size and zeta potential.

Bacterial Viability. IC_{50} values for the addition of nano-Ag were statistically significantly higher (by several orders of magnitude) than those values for the addition of AgNO_3 in the high-throughput assays. In general, Gram positive *B. subtilis* was less resistant to the antibacterial activity of nano-Ag than Gram negative *P. putida* (statistical significance not reported). Both bacteria were more resistant to nanotoxicity when bicarbonate was in the media.

Khan et al. (2011) Silver nanoparticles tolerant bacteria from sewage environment.

Test Species

Bacillus pumilus, *Escherichia coli*, *Staphylococcus aureus*, and *Micrococcus luteus*.

Material

Nano-Ag obtained from Sigma Aldrich (USA).

Shape: Spherical (determined using TEM and SEM)

Composition: Not reported

Crystal Structure: Not reported

Average Size: Not reported

Size Distribution: 10–40 nm (determined using TEM and SEM)

Solubility: Not reported

Surface Area: 0.26 m²/g (determined using Smart Sorb 93 Single point BET surface area analyzer)

Surface Treatment: Exopolysaccharide capping

Surface Charge: Not reported

Protocol

Exposure Duration: 30 minutes

Endpoints: Growth rate and viability

Exposure Concentrations: 25, 50, and 100 µg/disc (disc diffusion method); 10, 25, 50, 100, and 200 µg/well (agar-well diffusion method); 10, 25, 50, 100, and 200 µg/plate (dilution plate count method); 10–200 mg/L (growth kinetics study).

Exposure Medium: Nutrient agar, Muller Hinton agar, and LB agar (disc diffusion); Unspecified agar (agar-well diffusion); LB agar (dilution plate count); or LB broth (growth kinetics study)

Bacterial Density: 10³–10⁴ CFU/mL (disc diffusion) 10²–10³ CFU/mL (growth kinetics study); densities for other methods not reported.

Methods: A nano-Ag tolerant *B. pumilus* strain was isolated and identified by 16S rRNA analysis and lack of diameter of inhibition zone (DIZ) using disc diffusion and agar well diffusion test. Exopolysaccharides were extracted from *B. pumilus*, quantified, purified, and reacted with nano-Ag; lyophilized nanoparticles were analyzed by XRD. Toxicity of exopolysaccharides-coated nano-Ag tested on *E. Coli*, *S. aureus*, and *M. luteus* by culturing organisms on LB broth supplemented with coated and uncoated nano-Ag particles (100 mg/L) was measured by disc diffusion, dilution plate count method, and agar well diffusion test. Growth kinetics were measured as increases in absorbance at 600 nm using a colorimeter after sonication of nano-Ag (10–200 mg/L) to prevent aggregation after inoculation with bacterial culture.

Study Outcome

Lyophilized nano-Ag did not give the characteristic peak of silver with XRD analysis due to persistence of exopolysaccharide capping. Similarly, SPR analysis showed a peak shift for nano-Ag before and after capping possibly due to the repelling action of the exopolysaccharides-capped nano-Ag.

Growth Rate and Viability. Growth kinetics of bacteria exposed to exopolysaccharides-coated nano-Ag were similar to controls indicating reduction of toxicity compared to documented growth inhibition zones when bacteria were exposed to uncoated nano-Ag. The observed bacterial count (mean ± standard error) in the agar plates were 95.0 ± 0.966, 95.2 ± 0.833, 96.0 ± 0.931, 94.7 ± 1.145, 94.8 ± 1.138, and 94.8 ± 0.792 for control, 10, 25, 50, 100, and 200 µg of nano-Ag, respectively. When SNPs are present on the surface of the nutrient agar plates, they could completely inhibit the bacterial growth compared to liquid broth; however, the growth inhibition was not observed in any of the plates in dilution plate count method. Bacterial tolerance was suggested to be due to the secretion of exopolysaccharides which inhibit interaction of nano-Ag with the bacterial cell wall.

Kim et al. (2009) Antifungal activity and mode of action of silver nano-particles on *Candida albicans*.

Test Species

Diploid fungus (*Candida albicans* ATCC 90028)

Material

Nano-Ag synthesized by dissolving solid silver in nitric acid and adding sodium chloride.

Shape: Spherical

Composition: Not reported

Crystal Structure: Not reported

Average Size: 3 nm (determined using TEM)

Size Distribution: Not reported

Solubility: Not reported

Surface Area: Not reported

Surface Treatment: Not reported

Surface Charge: Not reported

Protocol

Exposure Durations: 2 hours (membrane dynamics and released glucose and trehalose), 3 hours (membrane integrity), 8 hours (cell cycle), 24 hours (envelope structure), 48 hours (growth inhibition)

Endpoints: Growth, membrane damage/disruption, and cell-cycle arrest

Exposure Concentrations: 20, 40, 60, and 80 µg/mL (membrane dynamics); 20 µg/mL (released glucose and trehalose), 30 µg/mL (membrane integrity); 40 µg/mL (cell cycle); and not reported for envelope structure or growth inhibition tests.

Exposure Media: Yeast extract, peptone, and dextrose broth for all tests but released glucose and trehalose, which used phosphate-buffered saline

Bacterial Density: 2×10^4 cells/mL (growth inhibition) or 1×10^8 cells/mL

Methods: Growth was assayed with a microtiter enzyme-linked immunosorbent assay (ELISA) reader by monitoring absorption at the 580-nm wavelength. Minimum inhibitory concentrations (MICs) were defined as the lowest concentrations that inhibited 90% of fungal growth when compared to the control. MICs were determined by a series of 2-fold dilutions. Membrane integrity was assessed using flow cytometric analysis, and membrane dynamics were determined by steady-state fluorescence anisotropy using spectrofluorometry. Released glucose and trehalose were measured by weighing dry fungal pellets and measuring color formations in supernatants. Fungal envelope structure was examined using TEM, and cell cycle arrest was assessed using flow cytometric analysis.

Study Outcome

Growth Inhibition. MIC: 2 µg/mL

Membrane Damage/Disruption. Membrane depolarization occurred. Plasma membrane 1,6-diphenyl-1,3,5-hexatriene (DPH) significantly decreased with increasing concentrations of nano-Ag. Nano-Ag-treated cells both accumulated more intracellular and more extracellular glucose and trehalose than untreated cells. Extracellular glucose and trehalose amounts were 30.3 µg/mg fungal dry wt. Treated fungal cells showed significant damage characterized by pits in the cell walls and pores in the plasma membranes.

Arrest of Cell Cycle. The percentage of cells in the gap 2/mitosis (G_2/M) phase increased by 15%, while cells in gap 1 (G_1) phase significantly decreased by about 20%. This indicates that the budding process was inhibited.

Kvitek et al. (2008) Effect of surfactants and polymers on stability and antibacterial activity of silver nanoparticles (NPs).

Test Species

Gram-positive bacteria (*Enterococcus faecalis* CCM 4224, *Staphylococcus aureus* CCM 3953, *Staphylococcus aureus* MRSA, *Staphylococcus epidermidis* [methicillin-susceptible], *Staphylococcus epidermidis* [methicillin-resistant], *Enterococcus faecium* VRE) and Gram-negative bacteria (*Escherichia coli* CCM 3954, *Pseudomonas aeruginosa* CCM 3955, *Pseudomonas aeruginosa*; *Klebsiella pneumoniae* ESBL).

Material

Nano-Ag synthesized by modified Tollens process, prepared by reduction of the $\text{Ag}(\text{NH}_3)_2^+$ with D(+)-maltose monohydrate.

Shape: Spherical

Composition: Not reported

Crystal Structure: Not reported

Average Size: 26 nm with 2.3% polydispersity (determined using DLS and a Zeta plus analyzer)

Size Distribution: Not reported

Solubility: Not reported

Surface Area: Not reported

Surface Treatment: Unmodified or modified with anionic sodium dodecyl sulfate (SDS), nonionic polyoxyethylene-sorbitan monooleat (Tween 80), or polyvinylpyrrolidone (PVP 360)

Surface Charge: -25 mV (ζ potential in aqueous dispersion)

Protocol

Exposure Duration: 24 hours

Endpoint: Growth

Exposure Concentrations: 0.84 to 54 $\mu\text{g}/\text{mL}$

Exposure Medium: Mueller-Hinton broth

Bacterial Density: 10^5 – 10^6 CFU/mL

Methods: Modifiers were added to dispersions of nano-Ag prior to titration in the final amount of 1% (w/w). Stability of unmodified and modified nano-Ag was tested using serial additions of a destabilizer, cationic polyelectrolyte poly(diallyldimethylammonium) chloride (PDDA, 20% [w/w] aqueous solution), and was confirmed using DLS and UV/vis absorption spectra.

Study Outcome

Minimum inhibitory concentrations (MICs) in $\mu\text{g}/\text{mL}$ listed below for unmodified nano-Ag, and nano-Ag modified with SDS, Tween 80, and PVP 360, respectively.

E. faecalis CCM 4224: 6.75, 3.38, 6.75, 6.75

S. aureus CCM 3953: 3.38, 1.69, 3.38, 3.38

S. aureus MRSA: 3.38, 1.69, 3.38, 1.69

S. epidermidis (methicillin-susceptible): 1.69, 0.84, 1.69, 1.69

S. epidermidis (methicillin-resistant): 1.69, 1.69, 1.69, 1.69

E. faecium VRE: 6.75, 3.38, 3.38, 3.38

E. coli CCM 3954: 1.69, 1.69, 1.69, 3.38

P. aeruginosa CCM 3955: 3.38, 1.69, 3.38, 1.69

P. aeruginosa: 3.38, 3.38, 1.69, 1.69

K. pneumoniae ESBL: 6.75, 6.75, 3.38, 6.75

Lok et al. (2006) Proteomic analysis of the mode of antibacterial action of silver nanoparticles.

Test Species

Wild-type gram-negative bacteria (*Escherichia coli* K12, MG1655)

Material

Nano-Ag synthesized by borohydride reduction of AgNO₃ in the presence of citrate as a stabilizing agent.

Shape: Spherical

Composition: Not reported

Crystal Structure: Not reported

Average Size: 9.3 ± 2.8 nm (determined using TEM)

Size Distribution: Not reported

Solubility: Not reported

Surface Area: Not reported

Surface Treatment: Stabilized with bovine serum albumin (BSA) when in M9 medium, but uncoated when in HEPES buffer

Surface Charge: Not reported

Protocol

Exposure Duration: ≥600 minutes (growth) or 30 minutes

Endpoints: Growth, protein expression, membrane damage/disruption

Exposure Concentrations: 0.4 and 0.8 nM

Exposure Medium: M9 defined medium for growth inhibition and proteomic analyses and sodium or potassium HEPES buffers containing glucose for membrane analyses.

Bacterial Density: 0.15 O.D.₆₅₀ for growth inhibition and proteomic analyses and 0.1 O.D.₆₅₀ for membrane analyses.

Methods: Growth inhibition was assessed by monitoring the O.D.₆₅₀. Proteomes were analyzed using two-dimensional electrophoresis (2-DE) followed by silver staining. Proteins stimulated by nano-Ag were identified using matrix-assisted laser desorption/ionization–time-of-flight mass spectrometry (MALDI-TOF MS) and tandem mass spectrometry (MS/MS) on the tryptic digests of protein spots of interest. Expression of cell envelope protein OmpA was examined using immunoblots. Membrane damage was determined by pretreating *E. coli* with 1 nM nano-Ag and followed by exposure to 0.1% sodium dodecyl sulfate (SDS). Effects of nano-Ag at the minimum inhibitory concentration (MIC: 1 nM) on the cytoplasmic membrane potential were examined using fluorescence.

Study Outcome

Growth Inhibition. Inhibition became apparent at concentrations of 0.4 nM and 6 μM, for nano-Ag and AgNO₃, respectively. Statistical significance of the results was not reported.

Protein Expression. No global changes in proteomes due to nano-Ag exposure were found. Expressions of “at least” 8 proteins were stimulated by nano-Ag and by AgNO₃. Expressions of a number of cell envelope proteins (OmpA, OmpC, OmpF, and MetQ) were stimulated by nano-Ag. The 37 kDa band was enhanced by nano-Ag. Nano-Ag resulted in accumulation of precursor forms of OmpA.

Membrane Damage. Rapid cell lysis occurred in cells pretreated with nano-Ag and subsequently exposed to SDS, where no cell lysis occurred with only exposure to SDS or nano-Ag alone. DiSC₃(5) fluorescence decreased upon addition to *E. coli* cells and stabilized. After nano-Ag was added, fluorescence rapidly recovered, indicating a dissipation of membrane potential. Also, an almost complete loss of potassium from the cell and depletion of ATP was observed after 5 minutes.

Martinez-Gutierrez et al. (2010) Synthesis, characterization, and evaluation of antimicrobial and cytotoxic effect silver and titanium nanoparticles.

Test Species

Escherichia coli, *Acinetobacter baumannii*, and *Pseudomonas aeruginosa* (gram-negative); *Bacillus subtilis*, *Mycobacterium smegmatis*, *Mycobacterium bovis*, and *Staphylococcus aureus* (gram-positive); *Candida albicans*, *Cryptococcus neoformans*, and *Aspergillus niger* (fungi); and human-derived monocyte cell lines.

Material

Nano-Ag synthesized from AgNO₃ (purchased from Sigma-Aldrich, USA) with gallic acid and sodium hydroxide (20–25 nm particles) or AgNO₃ with a UV light reactor, and gallic acid (80–90 nm particles). TiO₂-Ag nanoparticles were synthesized from TiO₂ particles (purchased from Ti-Pure R-902 [Dupont Wilmington, DE] and Degussa P25 [Degussa, Parsippany, NJ], Ti¹ and Ti², respectively), dispersed by ultrasound in deionized water and the addition of different quantities of AgNO₃ with NaBH₄ and NH₄OH using UV light as a reacting agent to produce particles with TiO₂-Ag molar ratios of 10:1, 25:1, and 50:1.

Shape: Not reported

Composition: Ag only, TiO₂ only, Ti¹ or 2-Ag NaBH₄, Ti¹ or 2-Ag UV

Crystal Structure: Not reported

Average Size: Not reported

Size Distribution: 20–25 nm and 80–90 nm (nano-Ag only); 250–300 nm (TiO₂-Ag bimetallic) (determined by TEM)

Solubility: Not reported

Surface Area: Not reported

Surface Treatment: Not reported

Surface Charge: Not reported

Protocol

Exposure Duration: 24 hours

Endpoints: Viability and cytotoxicity

Bacterial Density: Not reported

Exposure Concentrations: 107.8 µg/mL (nano-Ag only); 10 µg/mL (Ti¹ or 2-Ag NaBH₄ or UV 10:1); 0.5 µg/mL (Ti¹ or 2-Ag NaBH₄ or UV 25:1); 0.35 (Ti¹ or 2-Ag NaBH₄ or UV 50:1)

Exposure Medium: Not reported

Methods: Organisms were exposed to serial dilutions of nanoparticles and viability assessed to calculate MICs. A cytotoxicity assay, including DNA damage and cell viability, was carried out on monocyte cells. Toxicity was measured by staining with propidium iodide. The viability of cells was assayed by Trypan blue staining. The effectiveness of the nanoparticles was expressed as the therapeutic index (TI), which represents the amount of a therapeutic agent that causes a therapeutic effect of 50% in the population and estimates the extent to which the administration of the agent is safe (TI = LD₅₀/MIC). DNA single-strand breaks and alkali-labile lesions were detected using the alkaline comet assay and were tested using only nano-Ag (20–25 nm) and Ti²-Ag NaBH₄. The cytotoxicity studies were carried out using 10 different concentrations (dilutions not specified) of nano-Ag, Ti²-Ag NaBH₄ nanoparticles, and Ti²-Ag UV particles.

Study Outcome

Viability. The highest antimicrobial activity was observed with the smallest nano-Ag particles (20-25 nm) with MIC averages between 0.4 – 1.7 µg/mL (bacteria) and 3-25 µg/mL (fungi), which is comparable to results obtained using commercial antibiotics. TiO₂-Ag nanoparticles showed fungal-specific activity but resulted in low MIC levels for bacteria (5 - >100 µg/mL for bacteria, and 3-25 µg/mL for fungi). Nano-Ag (only) was found to possess the highest TI calculated for bacterial strains (13.86 ± 1.31 for gram-positive, 23.25 ± 0.63 for gram-negative), but the lowest TI value for fungal strains (0.9 ± 0.35) when compared to Ti²-Ag UV 50:1 (1.57, 5.03, and 10.7 for gram-positive, gram-negative, and fungi, respectively), and Ti²-Ag NaBH₄ (2.6, 2.56, and 22.1 for gram-positive, gram-negative, and fungi, respectively).

Cytotoxicity. The smallest nano-Ag particles (20–25 nm) resulted in a dose-dependent increase in death rate of the monocytes. Concentrations <2 µg/mL resulted in no significant cytotoxicity (<20% death rate), while concentrations >5 µg/mL resulted in statistically significant increases in toxicity reaching >50%. The Ti-Ag nanoparticles showed only slight toxicity, with cell death rates ranging from 15 to 25%, even at the highest concentrations (25 µg/mL). LD₅₀s were calculated as 10 ± 3.4 µg/mL for nano-Ag and only 55.9 µg/mL and 367.3 µg/mL for the Ti-Ag bimetallic nanoparticles (Ti²-Ag UV 50:1 and Ti²-Ag NaBH₄ 10:1, respectively). Results of DNA damage assay showed no evidence of the production of DNA single-strand breaks above the background level.

Morones et al. (2005) Bactericidal effect of silver nanoparticles.

Test Species

Gram-negative bacteria (*Escherichia coli*, *Vibrio cholerae*, *Pseudomonas aeruginosa*, and *Salmonella typhi*)

Material

Commercial nano-Ag powder inside a carbon matrix, supplied by Nanotechnologies, Inc. (location not reported).

Shape: Cuboctahedral and multiple-twinned icosahedral and decahedral

Composition: Not reported

Crystal Structure: {111} lattice plane

Average Size: 16 ± 8 nm (determined using TEM)

Size Distribution: Not reported

Solubility: Not reported

Surface Area: Not reported

Surface Treatment: Not reported

Surface Charge: Not reported

Protocol

Exposure Duration: 30 minutes

Endpoints: Growth and membrane damage

Exposure Concentrations: 0, 25, 50, 75, and 100 $\mu\text{g/mL}$

Exposure Media: Agar plates with Luria-Bertani medium broth

Bacterial Density: 0.5 O.D.₅₉₅ which corresponds to $\sim 5 \times 10^7$ CFU/mL solution

Methods: Growth inhibition was assessed by monitoring the O.D.₅₉₅. Effects on the bacterial membrane were examined using high angle annular dark field scanning transmission electron microscopy (HAADF-STEM).

Study Outcome

Growth Inhibition. At nano-Ag concentrations above 75 $\mu\text{g/mL}$, there was no bacterial growth for any species. *E. coli* and *S. typhi* were more sensitive to nano-Ag exposure than *P. aeruginosa* and *V. cholerae*.

Membrane Damage. Individual silver nanoparticles were attached to the cell membrane and distributed throughout the cell. Only particles of the sizes attached to the membrane were observed inside the cell. The mean size of the nano-Ag interacting with bacteria was 5 nm, even though the mean nano-Ag size in solution was 16 nm.

Pal et al. (2007) Does the antibacterial activity of silver nanoparticles depend on the shape of the nanoparticle? A study of the Gram-negative bacterium *Escherichia coli*.

Test Species

Gram-negative bacteria (*Escherichia coli* ATCC 10536).

Material

Nano-Ag powder reduced from aqueous AgNO₃ with sodium citrate or produced via large-scale preparation in particle growth solution containing AgNO₃, ascorbic acid, CTAB, silver seeds, and NaOH.

Shape: Rod, truncated triangular plate, or spherical
Composition: Pure silver (triangular), composition of other shapes was not reported
Crystal Structure: {111} basal lattice plane (triangular)
Average Size: 133–192 nm (rod edge), 16 nm (rod diameter), 40 nm (triangle edge), 39 nm (spherical) (determined using EFTEM)

Size Distribution: Not reported
Solubility: Not reported
Surface Area: Not reported
Surface Treatment: CTAB, a cationic quaternary ammonium surfactant, was used in synthesis of truncated triangular and rod-shaped nano-Ag
Surface Charge: Not reported

Protocol

Exposure Duration: Not reported (nutrient broth) or 24 hours (agar plate)
Endpoint: Growth and membrane damage
Exposure Concentrations: 1–100 µg (delivered to either 100 mL nutrient broth or onto agar plates; concentrations not reported)

Exposure Media: Difco nutrient broth or Difco nutrient agar
Bacterial Density: 10⁸ CFU/mL (in broth) or 10⁷ and 10⁵ CFU/mL (on agar plate)

Methods: Colonies were exposed to concentrations of nano-Ag of different shapes and counted at the end of the exposure period. Membranes were examined using EFTEM.

Study Outcome

Growth. A dose of 10 µg of triangular particles added to 100 mL of the nutrient broth inhibited growth after 24 hours, and 100 µg of AgNO₃ and spherical nano-Ag delayed growth up to 10 hours. At cell concentrations of 10⁷ CFU/mL, almost complete growth inhibition was observed at a triangular nano-Ag content of 1 µg on the agar plate. An amount of 12.5 µg spherical nano-Ag reduced bacterial colonies significantly on the agar plate, and 100% inhibition was seen at contents of 50–100 µg. Even at 100 µg, rod-shaped nano-Ag and AgNO₃ did not inhibit growth completely on the agar plate. Nano-Ag inhibition of bacterial growth was also dependent on the initial number of bacterial cells. At cell concentrations of 10⁵ CFU/mL, spherical nano-Ag almost completely prevented growth at 6 µg, and 12 µg of AgNO₃ inhibited growth completely on the agar plate.

Membrane Damage. Nano-Ag-treated bacterial cells were significantly changed, and major damage was observed on the outer membrane, characterized by pitting. Nanoparticles also accumulated in both the membrane and within the cells.

Saulou et al. (2010) Synchrotron FTIR microspectroscopy of the yeast *Saccharomyces cerevisiae* after exposure to plasma-deposited nanosilver-containing coating.

Test Species

Sessile *Saccharomyces cerevisiae* BY4741 yeast cells

Material

Nano-Ag in plasma-mediated thin films surrounded by organosilicon matrix (Determined using XPS)

Shape: Granular-type structure with spherical metal clusters (determined using SEM)

Composition: Ag: 20.5%, Si: 15.1%, C: 43.5%, O:20.9%

Crystal Structure: Not reported

Average Size: Not reported

Size Distribution: 5–10 nm (TEM)

Solubility: 2-mM AgNO₃

Surface Area: Not reported

Surface Treatment: Coating mainly composed of C, O, and Si

Surface Charge: Not reported

Protocol

Exposure Duration: 24 hours

Endpoints: Cell composition and antifungal properties

Exposure Concentrations: Not reported

Exposure Medium: Plasma-coated AISI 316L stainless steel coupons

Bacterial Density: 2.10⁷ CFU/mL

Methods: Stainless steel square (10 mm × 10 mm) coupons were chemically cleaned, coated in an organosilicon matrix, and used as a substrate. A silver disc RF powered electrode was used in conjunction with an RF generator. The steel coupons were placed over the bottom of the sample holder electrode in front of the silver target, and silver atoms from the electrode formed nanoclusters embedded in the organosilicon matrix. A batch preculture of *S. cerevisiae* BY4741 was prepared, stationary growth phase was reached, and yeast cells were harvested by centrifugation. A suspension that corresponded to 2.10⁷ CFU/mL was used for adhesion tests to the organosilicon matrix and the nano-Ag-containing coating. The plasma-coated samples were immersed in the yeast suspension for a 24-h contact time; sessile cells were removed by sonication. Synchrotron FTIR analysis was performed on yeast suspensions. TEM observations were performed parallel to the synchrotron FTIR analysis.

Study Outcome

Antifungal Properties. A significant loss of cell viability was observed for the nano-Ag-containing coating; the CFU/total cell number ratio was decreased by a 1.4 log reduction. This was indicative of the antifungal properties of the nano-composite coating.

Composition. Significant downshifts of amide I and II bands were observed in the protein absorption region. Following exposure to silver nitrate, the IR spectrum of the yeast suspension revealed a downshift (30 cm⁻¹) of the peak at 1,655 cm⁻¹, corresponding to a loss in α -helix structures. The nano-Ag-containing coating displayed a slightly weaker downshift (20 cm⁻¹). This was indicative of the inhibitory action of silver against *S. cerevisiae* targeted against mannoproteins and intracellular proteins. Disordered secondary structures of proteins were observed, marking striking differences in cell composition.

Shrivastava et al. (2007) Characterization of enhanced antibacterial effects of novel silver nanoparticles.

Test Species

Gram-negative bacteria (*Escherichia coli* ATCC 25922, ampicillin-resistant *E. coli*, multi- drug-resistant strain of *Salmonella typhus*) and Gram-positive bacteria (*Staphylococcus aureus* ATCC 25923).

Material

Nano-Ag synthesized through reduction of AgNO₃ with a blend of reducing agents including D-glucose and hydrazine.

Shape: Spherical or polyhedral	Size Distribution: Approximately 5–47 nm
Composition: Not reported	Solubility: Not reported
Crystal Structure: Face centered cubic	Surface Area: Not reported
Average Size: Approximately 10–15 nm (determined using TEM)	Surface Treatment: Not reported
	Surface Charge: Not reported

Protocol

Exposure Duration: 24 hours (agar plates)	Exposure Media: Luria-Bertani agar plates or liquid broth
Endpoints: Growth and membrane damage	Bacterial Density: 10 ⁶ CFU per agar plate or 10 ⁸ CFU per mL liquid broth
Exposure Concentrations: 10, 25, 35, 50 (only <i>S. aureus</i>), and 100 (only <i>S. aureus</i>) µg/mL	

Methods: Growth inhibition on the agar plates was assessed by counting the colonies following exposure, and growth rate in the liquid broth was determined by measuring the optical density of bacterial cultures at 600 nm (O.D.₆₀₀). Bacterial cells were also cultured for 60 minutes in the presence of nano-Ag, after which they were re-cultured in a fresh medium without nano-Ag. Growth was then measured in these cells and compared to controls that were not exposed initially to nano-Ag. The effect on bacterial signal transduction was explored by measuring phosphotyrosine content of proteins. Membrane damage was examined using transmission electron microphotographs.

Study Outcome

Growth Inhibition. For non-resistant *E. coli*, 60% growth inhibition was observed at the 5-µg/mL level, which increased to 90% inhibition at 10 µg/mL and complete inhibition at 25 µg/mL. For ampicillin-resistant *E. coli* and *S. typhi*, 70–75% inhibition was observed at 10 µg/mL and complete inhibition at 25 µg/mL. Similar effects were observed in the liquid medium, where lag time before growth was 8 hours at 25 µg/mL. No reduction in *S. aureus* growth was observed at 25 µg/mL on the agar plate. Cells that were re-cultured in fresh medium following exposure to nano-Ag (concentration not reported) exhibited significant retardation in growth relative to controls. There was very little change in the tyrosine phosphotyrosine profile in *S. aureus*, but noticeable dephosphorylation of two peptides (unidentified) occurred in *E. coli*.

Membrane Damage. Clusters of nano-Ag were observed anchored to bacterial cell wall, which perforated the cell membrane, and accumulated inside the cell.

Sinha et al. (2011) Interaction and nanotoxic effect of ZnO and Ag nanoparticles on mesophilic and halophilic bacterial cells.

Test Species

Mesophilic and halophilic bacteria. Mesophiles: *Enterobacter* spp. (Gram negative) and *Bacillus subtilis* (Gram positive). Halophiles: *Marinobacter* spp. (Gram negative) and EMB4 (Gram positive)

Material

Ag nanopowder (Cat. No 576832) from Sigma Aldrich, St. Louis mixed in Milli-Q water and ultrasonicated for 30 minutes; ZnO nanopowder (Cat. No 544906) from Sigma Aldrich, St Louis; bulk ZnO from Qualigens Fine Chemicals, Mumbai, India; bulk Ag from Central Drug House Pvt. Ltd New Delhi, India

Shape: Not reported

Composition: Not reported

Crystal Structure: Not reported

Average Size: Not reported

Size Distribution: less than 100 nm (reported by manufacturer)

Solubility: Not reported

Surface Area: Not reported

Surface Treatment: Not reported

Surface Charge: Not reported

Protocol

Exposure Duration: Not reported

Endpoints: Growth, viability, and membrane structure

Exposure Concentrations: 2 mM, except in *B. subtilis* tests at 10 mM

Exposure Medium: Analytical grade (% w/v) yeast extract 0.5, peptone 0.5, dextrose 1.0, NaCl 0.25 and 10.0 (for mesophiles and halophiles, respectively), MgSO₄ 0.05.

Adjusted to pH 7.0 for mesophiles and pH 8.0 for halophiles.

Bacterial Density: Not reported

Methods: 12-hr culture was prepared and used as inoculum. The inoculated medium was incubated and nanoparticle suspensions were aseptically added to the nutrient medium. The bacterial growth was monitored by UV-Visible spectrophotometry. Viable cells were counted and CFUs were calculated. Cultures were centrifuged, fixed with Karnovsky's fluid, dehydrated, and the SEM micrographs of the dehydrated samples were recorded by SEM. The processed cells were micrographed in TEM. The samples were analyzed for energy dispersive X-ray analysis.

Study Outcome

Nano-Ag accumulated in the cytoplasm of both *Enterobacter* and *Marinobacter* species, but Nano-Ag was more toxic to halophilic gram negative cells than mesophilic gram negative cells.

Growth and Viability. Nano-Ag caused a substantial decrease in growth rate and viable cell count of *Enterobacter*. Exposure to nano-Ag also resulted in changes in morphology and reduction in size of *Enterobacter*. The growth of the *B. subtilis* was not affected by exposure to nano-Ag (acknowledging a marginal reduction at 10mM exposure). There was an 80% reduction in the growth rate of *Marinobacter* cells after exposure to nano-Ag. Exposure to nano-Ag particles did not affect EMB4 bacterial growth.

Membrane Structure. The cell membranes of *Enterobacter* and *Marinobacter* were disrupted after exposure to nano-Ag, while the cell membranes of *B. subtilis* and EMB4 remained intact.

Sondi and Salopek-Sondi (2004) Silver nanoparticles as antimicrobial agent: a case study on *E. coli* as a model for Gram-negative bacteria.

Test Species

Gram-negative bacteria (*Escherichia coli* Strain B)

Material

Nano-Ag powder synthesized by reduction of AgNO₃ with ascorbic acid and Daxad 19, a dispersing and thinning agent.

Shape: Not reported

Composition: Not reported

Crystal Structure: Not reported

Average Size: 12.3 ± 4.2 nm (determined using TEM)

Size Distribution: 4–29 nm

Solubility: Not reported

Surface Area: 158 m²/g (dried powder)

Surface Treatment: Daxad 19 reportedly removed prior to bacterial exposure

Surface Charge: Not reported

Protocol

Exposure Duration: 24 hours (agar plates)

Endpoints: Growth and membrane damage

Exposure Concentrations: 10–100 µg/cm³

Exposure Media: Luria-Bertani agar plates or liquid broth

Bacterial Density: 10⁵ CFU per agar plate or 10⁷ CFU per mL liquid broth

Methods: Growth inhibition was assessed by counting colonies on agar plates following exposure. Growth rate was determined by measuring O.D.₆₀₀ in the liquid broth. SEM and TEM were used to evaluate the surface morphology of the cells. The qualitative chemical composition of the membranes was assayed by energy dispersive X-ray analysis (EDX).

Study Outcome

Growth Inhibition. Nano-Ag at a concentration of 10 µg/cm³ inhibited growth on the agar plates by 70%. The number of colonies was reduced when compared to controls and most were located on edges of agar plates at exposure concentrations of 20 µg/cm³ nano-Ag, and concentrations of 50–60 µg/cm³ nano-Ag inhibited growth completely. The number of cells applied to the plate was related to the degree of antibacterial activity (i.e., less cells resulted in more antibacterial activity). All concentrations of nano-Ag applied to the liquid medium resulted in delayed growth, with the higher concentrations resulting in longer delays.

Membrane Damage. Nano-Ag-treated cells were significantly changed, showing major damage, characterized by formation of pits in the cell walls. EDX showed that nano-Ag was incorporated into the bacterial membrane, which was confirmed by TEM. TEM also revealed penetration of nano-Ag into cells and intracellular substances, in addition to coagulated nano-Ag on the bacterial surface.

Sotiriou and Pratsinis (2010) Antibacterial activity of nanosilver ions and particles.

Test Species

E. coli

Material

Nano-Ag on nanostructured silica was synthesized using flame spray pyrolysis using silver acetate, 2-ethylhexanoic acid, and acetonitrile.

Shape: Spherical (TEM)

Composition: Ag, Si, O

Crystal Structure: Monocrystalline (XRD)

Average Size: 4–16 nm (HRTEM)

Size Distribution: 4–16 nm (HRTEM)

Solubility: Not reported

Surface Area: <40 AgSSA_E m²/g of Ag (O₂ pulse chemisorptions)

Surface Treatment: Not reported

Surface Charge: Not reported

Protocol

Exposure Duration: 330 minutes

Endpoints: Bacterial growth (fluorescence)

Exposure Concentrations: Ag content x in Ag/SiO₂ wt % = 0-100

Exposure Medium: DI water

Bacterial Density: 10⁷ CFU/mL

Methods: Bacterial growth was monitored by fluorescence intensity in the assessment of relative impacts of particle size, surface area, and Ag⁺ content (wt %).

Study Outcome

When exposed to the smaller nano-Ag particles with lower Ag content, a much stronger antibacterial activity was observed compared to higher Ag-content particles that were larger in size (reduced surface area). By controlling the Ag content in the treatment (Ag/SiO₂ particles), the antibacterial was also controlled: $x = 1 - 10$ wt % Ag resulting in little or no bacterial growth, compared to maximum bacterial growth reached for $x = 50$ (at $C = a$ mg/L of Ag). When the Ag content within particles was equal, smaller particles disassociated more rapidly into Ag⁺ ions, indicating that the antibacterial activity is largely dictated by the ions themselves rather than the nanoparticles. However, when larger particles associated with low ionic release were tested, the nano-Ag particles themselves also played an important role in toxicity (when Ag/SiO₂ particles were removed, bacterial growth was restored for both Ag mass concentrations of 20 and 30 mg/L at $x > 90$ wt %). When only Ag⁺ ions were present, the antibacterial activity was comparable to that in the presence of the larger nanoparticles). Authors conclude that antibacterial activity depends on size, which increases the amount of ions released into the environment, but that larger particles play a significant role in toxicity themselves when the ionic release is reduced.

B.3. Summary of Nano-Ag Effects in Algae

Griffitt et al. (2008) Effects of particle composition and species on toxicity of metallic nanomaterials in aquatic organisms.

Test Species

Freshwater green algae (*Pseudokirchneriella subcapitata*)

Material

Commercial nano-Ag powder produced by gas-phase condensation and coated with a thin layer (2–3 nm) of metal oxide; supplied by Quantum Sphere (Santa Ana, CA, USA).

Shape: Not reported

Composition: Not reported

Crystal Structure: Not reported

Average Size: 26.6 ± 8.8 nm (determined using a laser diffraction particle size analyzer)

Size Distribution: Approximately 20–1,000 nm

Solubility: Dissolution 48 hours after resuspension was 0.07% of total mass

Surface Area: 14.53 m²/g (determined using the Brunauer, Emmett, and Teller method)

Surface Treatment: Sodium citrate stabilizer

Surface Charge: -27.0 mV (ζ potential in moderately hard freshwater with pH 8.2, determined using a Zeta Reader Mk 21-II)

Protocol

Exposure Duration: 96 hours

Endpoint: Growth

Exposure Concentrations: EC₅₀ from the ranging-finding test, and concentrations 0.6-, 0.36-, 1.67-, and 2.78-times the estimated EC₅₀ from the range-finding test

Exposure Medium: Moderately hard freshwater (dissolved oxygen 8.5–8.9 mg/L; pH 8.2 ± 1 , hardness 142 ± 2 mg/L CaCO₃; conductivity 395 μ S; un-ionized ammonia <0.5 mg/L)

Cell Density: Not reported

Methods: Algal growth media were prepared to produce a concentration gradient before being inoculated with a similar volume of algal culture. Algal growth was assessed by measurement of chlorophyll *a*. These results from exposure to nanometals of copper, aluminum, and nickel were compared to controls.

Study Outcome

EC₅₀: 0.19 mg/L

P. subcapitata was more susceptible to nano-Ag than to any of the other nanometals tested. The reported test concentrations are nominal; therefore actual concentrations to which the organisms were exposed may be lower or higher than reported.

Park et al. (2010b) Selective inhibitory potential of silver nanoparticles on the harmful cyanobacterium *Microcystis aeruginosa*.

Test Species

Cyanobacteria *Microcystis aeruginosa*, and green algae *A. convolutus*, and *S. quadricauda*

Material

Nano-Ag prepared in two solutions. Solution 1 was prepared by reducing silver nitrate with tannic acid. Solution 2 was prepared by adding silver nitrate, sodium persulfate, and NaOH with the application of heat and Tween 20 as a dispersing agent (producing silver oxide nanoparticles).

Shape: Not reported

Composition: Not reported

Crystal Structure: Not reported

Average Size: Not reported

Size Distribution: 20–50 nm at 200 mg/L for both solutions (determined by TEM)

Solubility: Not reported

Surface Area: Not reported

Surface Treatment: Not reported

Surface Charge: Not reported

Protocol

Exposure Duration: 10 days

Endpoint: Colony growth inhibition; chlorophyll α concentration, community composition, and growth inhibition; community composition, and cell count

Exposure Concentrations: 0.001, 0.01, 0.1, or 1 mg/L (solution 1, experiment 1); 1 mg/L (solution 1 and 2, experiments 2 and 3)

Exposure Medium: Pre-filtered eutrophic lake water

Cell Density: 10 mL in 90 mL lake water

Methods: 10 mL *M. aeruginosa* culture was added to 90 mL lake water. The inhibition of algal growth was calculated as: algal inhibition efficiency (%) = [(control – treatment)/control] X 100. Cell count was taken by removing 1 mL from the flask and fixing with Lugol's solution. In a separate experiment, plastic containers filled with 2 L lake water, 100 mL of algal mixture (*M. aeruginosa*, *A. convolutus*, and *S. quadricauda* at 2:1:1 by vol), plus solutions 1 and 2 nano-Ag (1 mg/L). 10 mL aliquots taken at various times to determine chlorophyll α concentration spectrometrically. In a third experiment, the enclosure experiment was carried out in a eutrophic lake with six enclosures receiving 150 L lake water and exposed to precipitation and sunlight penetration. Solutions 1 and 2 of nano-Ag were added to 1 mg/L, and chlorophyll α concentration and cell numbers were measured as above.

Study Outcome

Colony Growth: In the first experiment, bacterial growth was inhibited by 87% at 1 mg/L nano-Ag compared to control, and lower concentrations 0.001, 0.01, 0.1 mg/L inhibited bacterial growth at 2.5, 14, and 39%, respectively.

Growth, Community Composition, and Chlorophyll Concentration: In experiment 2, both solutions decreased chlorophyll α in the algal mixture (84% with solution 1, 73% with solution 2). *M. aeruginosa* was more sensitive than *A. convolutus*, and *S. quadricauda* to both nano-Ag solutions (decrease from 95.5% of algal composition in control to 49% (solution 1) and 21% (solution 2)). *M. aeruginosa* growth was also inhibited 93% by solution 1 and 95% by solution 2, whereas there was little/no inhibition for *A. convolutus* (31% and 0%, respectively) or *S. quadricauda* (0% for both solutions) on day 10.

Community Composition and Cell Count: In experiment 3, both solutions inhibited algal growth (55% and 64%, respectively). Solution 1 reduced cyanobacteria percent composition from 69% (control) to 41% (treatment), and solution 2 reduced bacterial composition to 37% on day 10. Cell count for green algae was not significantly impacted, while *M. aeruginosa* cell numbers were reduced by 85 and 87% (addition of solutions 1 and 2, respectively).

Miao et al. (2009) The algal toxicity of silver engineered nanoparticles and detoxification by copolymeric substances.

Test Species

Coastal marine diatom (*Thalassiosira weissflogii* CCMP 1336)

Material

Commercial nano-Ag powder supplied by Nanostructured & Amorphous Materials Inc. (Houston, TX, USA).

Shape: Not reported

Composition: Not reported

Crystal Structure: Not reported

Average Size: 60–70 nm (determined using TEM)

Size Distribution: Not reported

Solubility: Not reported

Surface Area: 9–11 m²/g (provided by manufacturer)

Surface Treatment: polyvinylpyrrolidone (PVP) surfactant and suspended with Suwannee River Fulvic Acid

Surface Charge: Not reported

Protocol

Exposure Duration: 48 hours

Endpoints: Growth, quantum yield, and chlorophyll *a* production

Exposure Concentrations: Dispersed in the 0.22 μM fraction as (1) Total Ag: 2.12 × 10⁻¹⁰, 1.06 × 10⁻⁹, 5.30 × 10⁻⁹, 2.65 × 10⁻⁹, and 1.03 × 10⁻⁷ M; (2) Total dissolved Ag: 2.28 × 10⁻⁹, 4.56 × 10⁻⁸, 2.28 × 10⁻⁷, 1.14 × 10⁻⁶, 5.70 × 10⁻⁶, and 2.21 × 10⁻⁵ M; or (3) Free Ag⁺: 1.23 × 10⁻¹⁴, 2.46 × 10⁻¹³, 1.23 × 10⁻¹², 6.14 × 10⁻¹², 3.07 × 10⁻¹¹, and 1.19 × 10⁻¹⁰ M.

Exposure Media: f/2 Medium with a basis of artificial seawater containing different nutrient conditions (nutrient-enriched [+NE], nitrogen-limited [-N], and phosphorous-limited [-P])

Cell Density: 15,000 to 65,000 cells/mL, with higher cell density used in nutrient-limited and higher nano-Ag concentration treatments.

Methods: In +NE experiment, diatoms were harvested after acclimating in f/2 medium and arriving at mid-exponential growth phase. Cells were then suspended in toxicity media to which a range of nano-Ag concentrations had been added. In -N and -P test, +NE cells further incubated in f/2 medium without any addition of N or P for 2 and 4 days, respectively, before resuspension in the -N (or -P) toxicity media. Quantum yield was determined by fluorescence induction and relaxation system, and chlorophyll *a* content was quantified using a fluorometer. To separate effects of Ag⁺ from Ag nanoparticles, 4 additional tests were conducted with +NE culture in f/2 medium. (1) nano-Ag was removed by ultrafiltration through 1 kiloDalton (kDa) membrane to examine indirect effects on nano-Ag (<1 kDa). (2) Diafiltration was performed to compare photosynthesis, chlorophyll *a*, and growth in treatments and control. (3) Glutathione (GSH) and cysteine were added to the nano-Ag stock to assess direct effects from nano-Ag. (4) Nano-Ag aggregate toxicity was assessed by mixing 4.5 × 10⁻⁴ M GSH with 4.63 × 10⁻⁴ M nano-Ag and adding to nutrient enriched cells.

Study Outcome

Because the concentration of Ag was so much higher in the <1 kDa fraction than in the <1 kDa–0.22 μm fraction (2.21 × 10⁻⁵ versus 1.03 × 10⁻⁷ M), and because the cellular concentration of Ag⁺ was 10-fold higher than maximum possible nano-Ag concentrations, it was deemed that the direct effects from the nanoparticles were negligible compared to the indirect effects from the released Ag⁺. Results are therefore presented in terms of indirect effects from free and cellularly accumulated Ag⁺.

IC ₅₀ for Free Ag ⁺ (M)				IC ₅₀ for Ag ⁺ Accumulated in the Cell (M)			
+NE	-N	-P	<1kDa	+NE	-N	-P	<1 kDa
Growth Inhibition				Growth Inhibition			
2.16 × 10 ⁻¹²	1.02 × 10 ⁻¹¹	2.14 × 10 ⁻¹¹	1.03 × 10 ⁻¹²	3.11 × 10 ³	1.61 × 10 ⁴	2.08 × 10 ⁴	1.37 × 10 ³
Quantum Yield Inhibition				Quantum Yield Inhibition			
8.83 × 10 ⁻¹¹	Not inhibited more than 50%		6.36 × 10 ⁻¹¹	1.84 × 10 ⁵	Not inhibited more than 50%		1.72 × 10 ⁵
Chlorophyll <i>a</i> Inhibition				Chlorophyll <i>a</i> Inhibition			
5.82 × 10 ⁻¹²	Not inhibited more than 50%		4.13 × 10 ⁻¹²	7.39 × 10 ³	Not inhibited more than 50%		6.29 × 10 ³

Navarro et al. (2008) Toxicity of silver nanoparticle to *Chlamydomonas reinhardtii*.

Test SpeciesFreshwater green algae (*Chlamydomonas reinhardtii*)**Material**

Commercial nano-Ag suspension supplied by Nanosys GmbH (Wolfhaldon, Switzerland).

Shape: Not reported**Composition:** Not reported**Crystal Structure:** Not reported**Average Size:** 44 nm (determined using DLS and TEM)**Size Distribution:** <10–200 nm**Solubility:** Not reported**Surface Area:** Not reported**Surface Treatment:** Carbonate-coated**Surface Charge:** -36.6 ± 3.2 mV (ζ potential at pH 7.52 determined using DLS with Zeta Sizer)**Protocol****Exposure Duration:** 1–5 hours**Endpoint:** Photosynthetic yield**Exposure Concentrations:** 10–100,000 nM**Exposure Media:** MOPS media**Cell Density:** 2×10^5 cells/mL

Methods: Toxicity of nano-Ag and AgNO₃ to algal photosynthesis was assessed by dose-response experiments, and photosynthetic yield was measured periodically. To examine effects of Ag⁺, cysteine, an amino acid, was added in varying concentrations to 100 nM AgNO₃ solution to which algae were exposed for 1 hour, and photosynthetic yield was recorded. The role of Ag⁺ in toxicity of nano-Ag was examined by exposing algae for 1 hour to 5 or 10 μM nano-Ag and cysteine concentrations ranging from 10 to 500 nM, and results were plotted as a function of calculated Ag⁺. Photosynthetic values were reported as percent of the controls, and values were plotted as a function of measured values of total Ag and Ag⁺ to obtain EC_{50s}.

Study Outcome

EC_{50s} for nano-Ag are presented as a function of total Ag content and free Ag⁺ concentrations, respectively, at the beginning of the experiment. The EC_{50s} for nano-Ag complexed with cysteine are also presented. Based on total Ag concentration, AgNO₃ appeared to be more toxic than nano-Ag, but based on Ag⁺, nano-Ag appeared to be more toxic than AgNO₃.

Total Ag	Free Ag⁺	Nano-Ag + cysteine (expressed as free Ag⁺)
1-hour: 3,300 nM	1-hour: 33 nM	1-hour (5 μM nano-Ag + cysteine): 57 nM
2-hour: 1,049 nM	2-hour: 10 nM	1-hour (10 μM nano-Ag + cysteine): 61 nM
3-hour: 879 nM	3-hour: 9 nM	
4-hour: 801 nM	4-hour: 8 nM	
5-hour: 829 nM	5-hour: 8 nM	

B.4. Summary of Nano-Ag Effects in Aquatic Invertebrates

Allen et al. (2010) Effects from filtration, capping agents, and presence/ absence of food on the toxicity of silver nanoparticles to *Daphnia magna*.

Test Species

Daphnia magna

Material

Commercial nano-Ag from Sigma Aldrich (organically coated or uncoated); laboratory synthesized nano-Ag from AgNO₃ in combination with citrate or coffee solutions.

Shape: Not reported

Composition: Not reported

Crystal Structure: Not reported

Average Size: 681.4 and 5,412 nm (commercial uncoated nano-Ag in moderately hard reconstituted water [MHRW]); 39.39 and 249.8 nm (commercial coated nano-Ag in MHRW); 101.5 and 773.6 nm (coffee-capped nano-Ag in MHRW); and 5.94 and 39.75 nm (citrate-capped nano-Ag in Nanopure)

Solubility: Not reported

Surface Area: Not reported

Surface Treatment: Proprietary (commercial capping agent); coffee or citrate (synthesized nanoparticle capping agents)

Surface Charge: -20.4 mV (commercial, uncoated in MHRW); -18.3 mV (commercial coated in MHRW); -9.3 mV (coffee-capped in MHRW); and -39.7 mV (citrate-capped in Nanopure)

Protocol

Exposure Duration: 48 hours

Endpoints: Mortality

Exposure Concentrations: Approximately >100,000 ppb (commercial uncoated); >100,000 ppb commercial coated; 215, 800 ppb (coffee capped, 1:10 dilution); 21,580 ppb (coffee capped, 1:100 dilution); 70,000 ppb (citrate capped)

Exposure Media: MHRW, PH 7.8–8.0, polished to ASTM type II specifications by a Barnstead Nanopure Ultrapure (Barnstead Thermolyne) system. Additional characteristics provided in the supplemental information.

Organisms per Replicate: Not reported

Methods: Toxicity assays exposed *D. magna* to commercially available nano-Ag (either organically capped or uncapped) and laboratory synthesized nano-Ag (capped with coffee or citrate). These assays were also carried out for fed and unfed replicates, as well as replicates using filtered or unfiltered nano-Ag suspensions. X-ray diffraction was used to identify crystalline phases of nano-Ag. STEM was used to characterize particles and *D. magna* specimens. Particle size and hydrodynamic diameter were measured with DLS. Zeta potentials were calculated from micro electrophoresis measurements.

Study Outcome

TEM imaging of *D. magna* exposed to the LC₅₀ concentrations showed a few silver particles along the membrane of the mid-gut following exposure to commercial coated nano-Ag, accumulation of silver particles around the gill and gut following exposure to coffee-capped nano-Ag, accumulation of relatively more particles attaching to the gills and gut following exposure to citrate-capped nano-Ag. At approximately three times the LC₅₀ exposure, silver particles were observed in about the same areas as with the LC₅₀ exposure, but an increased incidence of particles was identified in tissues.

Mortality. Dose-response results spanned an order of magnitude for the various nano-Ag formulations tested. The laboratory synthesized nano-Ag coated with coffee or citrate resulted in dose-response relationships that were similar to, but slightly higher than the AgNO₃ solution (LC₅₀S = 1.0 µg/L [coffee]; 1.1 µg/L [citrate]; 0.7 µg/L [AgNO₃]). Commercial nano-Ag was less toxic when coated than when uncoated (LC₅₀S = 31.5 µg/L [coated]; 16.7 µg/L [uncoated]). Filtered suspensions for both coated and uncoated commercial nano-Ag were more toxic than when suspensions were unfiltered (LC₅₀S = 4.4 µg/L [coated, filtered]; 31.5 µg/L [coated, unfiltered]; 1.4 µg/L [uncoated, filtered] and 16.7 µg/L [uncoated, unfiltered]). Addition of food resulted in increased total organic carbon content, and decreased toxicity of unfiltered coated commercial nano-Ag (LC₅₀S = 176.4 µg/L [fed, coated, unfiltered]; 31.5 µg/L [unfed, coated, unfiltered]).

Gao et al. (2009) Dispersion and toxicity of selected manufactured nanomaterials in natural river-water samples: effects of water chemical composition.

Test Species

Water flea neonates (*Ceriodaphnia dubia*)

Material

Commercial nano-Ag powder produced by gas-phase condensation and coated with a thin layer (2–3 nm) of metal oxide; supplied by Quantum Sphere (Santa Ana, CA, USA).

Shape: Not reported

Composition: Not reported

Crystal Structure: Not reported

Average Size: ~80 nm (DI water and SR-1 sample), ~300 nm (SR-2 sample), >1,000 nm (SR-3 sample), all determined using DLS

Size Distribution: 20–30 nm (nominal; provided by manufacturer), but larger in solution

Solubility: The highest analyzed total dissolved and particulate Ag concentration in the original suspensions was in DI water, with concentrations in SR-1 and SR-3 an order of magnitude lower. The concentrations in SR-2 were an order of magnitude lower than SR-1 and SR-3.

Surface Area: 14.53 m²/g [reported by Griffith et al. (2008)]

Surface Treatment: Not reported

Surface Charge: -27.0 mV [ζ potential in moderately hard freshwater with pH 8.2, determined using a Zeta Reader Mk 21-II by Griffith et al. (2008)]

Protocol

Exposure Duration: 48 hours

Endpoint: Mortality/immobility

Exposure Concentrations: Not reported

Exposure Media: DI water, Suwannee River headwater sample (SR-1), midsection water sample (SR-2), or delta water sample (SR-3) diluted with moderately hard water used as culture medium.

Organisms per Replicate: 5 neonates × 3 replicates

Methods: Neonates were exposed to 5 incremental concentrations of nano-Ag (not reported) and survival was assessed visually after 48 hours.

Study Outcome

LC₅₀ (DI-water): 0.46 µg/L

LC₅₀ (SR-1): 6.18 µg/L

LC₅₀ (SR-2): 0.771 µg/L

LC₅₀ (SR-3): 0.696 µg/L

Griffitt et al. (2008) Effects of particle composition and species on toxicity of metallic nanomaterials in aquatic organisms.

Test Species

Adult water fleas (*Daphnia pulex*) and water flea neonate (*Ceriodaphnia dubia*)

Material

Commercial nano-Ag powder produced by gas-phase condensation and coated with a thin layer (2–3 nm) of metal oxide; supplied by Quantum Sphere (Santa Ana, CA, USA).

Shape: Not reported

Composition: Not reported

Crystal Structure: Not reported

Average Size: 26.6 ± 8.8 nm (determined using laser diffraction particle size analyzer)

Size Distribution: Approximately 20–1,000 nm

Solubility: Dissolution 48 hours after resuspension was 0.07% of total mass

Surface Area: 14.53 m²/g (determined using the Brunauer, Emmett, and Teller method)

Surface Treatment: Sodium citrate stabilizer

Surface Charge: -27.0 mV (ζ potential in moderately hard freshwater with pH 8.2, determined using a Zeta Reader Mk 21-II)

Protocol

Exposure Duration: 48 hours

Endpoint: Mortality/Immobility

Exposure Concentrations: The estimated LC₅₀ from the range-finding test and concentrations 0.6-, 0.36-, 1.67-, and 2.78-times the estimated LC₅₀ (approximately 0.01, 0.02, 0.04, 0.07, and 0.1 mg/L for *D. pulex* and 0.02, 0.04, 0.07, 0.1, and 0.2 mg/L for *C. dubia*)

Exposure Medium: Moderately hard freshwater (dissolved oxygen 8.5 to 8.9 mg/L; pH 8.2 ± 1 ; hardness 142 ± 2 mg/L as CaCO₃; conductivity 395 μ S; un-ionized ammonia <0.5 mg/L)

Organisms per Replicate: 5 adult *D. pulex* or 10 *C. dubia* neonates \times 4 replicates

Methods: Death was assessed by lack of movement or response to gentle prodding. Significance of these results were determined by comparing nanometal-induced (copper, aluminum, and nickel) effects relative to control.

Study Outcome

LC₅₀ (*D. pulex* adults): 0.04 mg/L

LC₅₀ (*C. dubia* neonates): 0.067 mg/L

Daphnia were more susceptible to nano-Ag than to any of the other nanometals tested. The concentration data in this test are nominal, and the actual concentrations to which the organisms were exposed may be lower than reported, with the nanometals being correspondingly more toxic.

Li et al. (2010b) Comparative toxicity study of Ag, Au, and Ag-Au bimetallic nanoparticles on *Daphnia magna*.

Test Species

Daphnia magna

Material

Ag nanoparticles synthesized reduction of AgNO₃ in the presence of different additions of sodium citrate, producing nanoparticles with different molar ratios of silver ion to citrate. Gold nanoparticles were synthesized in a similar manner. Ag-Au bimetallic nanoparticles were produced through co-reduction of metal precursor salts and sodium citrate as a reducing and capping agent.

Shape: Spherical, prismatic, and rod-shaped (determined using STEM)

Composition: Nano-Ag with small amounts of sulfur and oxygen present (determined using XEDS)

Crystal Structure: Not reported

Average Size: 36–66 nm (nano-Ag:citrate ratios 1:1.6–1:4.2, as prepared); 58–71 nm (nano-Ag:citrate ratios 1:1.6–1:4.2, in standard synthetic freshwater [SSF] after 0.5 hour); 378–553 nm (nano-Ag:citrate ratios 1:1.6–1:4.2, in SSF after 24 hours); 41–72 nm (nano-Ag:Ag ratios 1:4–4:1, as prepared); 14–73 nm (nano-Ag:Ag ratios 1:4–4:1, in SSF after 0.5 hour); and 17–77 nm (nano-Ag:Ag ratios 1:4–4:1, in SSF after 24 hours) (determined using DLS).

Size Distribution: Not reported

Solubility: Not reported

Surface Area: Not reported

Surface Treatment: Sodium citrate-capped

Surface Charge: Not reported

Protocol

Exposure Duration: 48 hours

Endpoints: Mortality

Exposure Concentrations: 7.8–32 mg/L (determined by AAS)

Exposure Medium: Standard synthetic freshwater (SSF)

Organisms per Replicate: 4 organisms per replicate, 4 replicates per concentration

Methods: Nanoparticles were characterized by absorbance measurements, atomic force or electron microscopy, flame atomic absorption spectrometry, and dynamic light scattering (most morphological details not reported). Acute toxicity tests were conducted using multi-concentration test including control and ionic silver. Four *Daphnia* neonates were placed in a centrifuge tube which was diluted with SSF to obtain the desired concentration of nano-Ag particles. Mortality was assessed at 24 and 48 hours.

Study Outcome

Mortality. The toxicity of all nanoparticles tested was dose- and composition-dependent. Nano-Ag toxicity was found to decrease with increasing amounts of citrate added in the synthesis process (expressed as ratios of Ag:citrate), which corresponded to an increase in particle size. Toxicity was not, however, found to be a function of particle size when total silver concentration was adjusted according to AAS (lethal concentrations ranged from 3 to 4 µg/L for all three particle sizes tested). Authors suggest that this was due to the large degree of aggregation (analyzed by DLS). Ionic silver was more toxic than nano-Ag in this study. The LC₅₀ for Au nanoparticles was 65–75 mg/L. LC₅₀ values for Au-Ag nanoparticles were between those for Au and Ag, but closer to that of Ag. A 4:1 Ag to Au ratio was less toxic (LC₅₀= 15 µg/L) than pure nano-Ag. A 1:4 Ag to Au ratio was more toxic than anticipated (LC₅₀= 12 µg/L) given the low silver content, but in general, the introduction of gold into silver nanoparticles reduced the toxicity of the nano-Ag.

Kvitek et al. (2009) Initial study on the toxicity of silver nanoparticles (NPs) against *Paramecium caudatum*.

Test Species

Unicellular eukaryote (*Paramecium caudatum*)

Material

Nano-Ag synthesized through a modified Tollens process using AgNO₃, NH₃, NaOH, and D(+)-maltose monohydrate.

Shape: Spherical

Composition: Not reported

Crystal Structure: Not reported

Average Size: 27 nm (determined using TEM and UV/vis absorption spectra)

Size Distribution: Not reported

Solubility: Not reported

Surface Area: Not reported

Surface Treatment: Unmodified and modified with nonionic surfactant polyethylene (2) sorbitan mono oleate (Tween 80), polyethylene glycol with molecular weight 35,000 (PEG 35000), and polyvinylpyrrolidone with a molecular weight of 360,000 (PVP 360)

Surface Charge: -37 mV (ζ potential determined using dynamic light scattering in diluted solution with pH 11.5), 1.23 mS/cm (conductivity)

Protocol

Exposure Duration: 1 hour

Endpoint: Mortality

Exposure Concentrations: Approximately 0.1–100 mg/L

Exposure Media: Culture medium (type not reported)

Organisms per Replicate: 1–5 mL containing 200–300 organisms/mL \times 3 replicates

Methods: A set of about 50 organisms was monitored over an area of 1 cm². LT₅₀ was measured from the moment of the addition of the nano-Ag into the culture up to the point when 50% of the organisms died. LC₅₀s were then determined from the dependence of the LT₅₀ on nano-Ag concentration.

Study Outcome

LC₅₀ (unmodified nano-Ag): 39 mg/L

LC₅₀ (modified with Tween 80): 16 mg/L

LC₅₀ (modified with PEG 35000): ~39 mg/L

LC₅₀ (modified with PVP 360): ~39 mg/L

Nair et al. (2011) Differential expression of ribosomal protein gene, gonadotrophin releasing hormone gene and Balbiani ring protein gene in silver nanoparticles exposed *Chironomus riparius*.

Test Species

Fourth instar larvae of aquatic midge *Chironomus riparius* (Korea Institute of Toxicology, Daejeon, Korea).

Material

Nano-Ag particles (Sigma-Aldrich, St. Louis, MO).

Shape: Not reported

Composition: Not reported

Crystal Structure: Not reported

Average Size: Not reported

Size Distribution: 40–70 nm (determined using DLS)

Solubility: Not reported

Surface Area: Not reported

Surface Treatment: Not reported

Surface Charge: Not reported

Protocol

Exposure Duration: 24 hours (acute), 25 days (chronic)

Endpoint: Mortality (acute), pupation, emergence failure, reproduction (chronic), and differential gene expression

Exposure Concentrations: 0.5, 1, 2, and 4 mg/L (acute); 0, 0.2, 0.5, 1 mg/L (chronic)

Exposure Media: Dechlorinated water

Organisms per Replicate: 10 larvae per concentration (acute), 50 larvae per concentration (chronic)

Methods: Acute ecotoxicity was assessed in a 24-hour exposure assay using mortality as the endpoint. Chronic ecotoxicity was determined after a 25-day exposure assay by numbers of successfully emerged adults, pupae, and sex ratio. A Comet assay was used to determine genotoxicity.

Study Outcome

Mortality. Mortality was observed at acute exposure concentrations of 4 mg/L. LC₅₀ was unable to be determined due to absence of mortality at lower dose levels.

Reproduction. Pupation and adult emergence were statistically significantly inhibited at concentrations ≥ 0.2 mg/L. Sex ratio was also affected by exposure, producing a greater proportion of female midges in all treated groups.

Genotoxicity. DNA damage increased in a dose-related manner; statistically significant results were observed at 1 mg/L.

Gene Expression. CrGnRH1 and CrBR2.2 were observed to be significantly upregulated, while CrL15 was observed to be significantly downregulated.

Ringwood et al. (2010) The effects of silver nanoparticles on oyster embryos.

Test Species

Crassostrea virginica

Material

Commercial nano-Ag supplied and characterized by the Wake Forest University Center for Nanotechnology.

Shape: Not reported

Composition: Not reported

Crystal Structure: Not reported

Average Size: 15 ± 6 nm

Solubility: Not reported

Surface Area: Not reported

Surface Treatment: Not reported

Surface Charge: Not reported

Protocol

Exposure Duration: 48 hours

Endpoints: Development, lysosomal destabilization, and metallothionein (MT) gene expression

Exposure Concentrations: 0.0016–1.6 µg/L (embryo);
0.0016–16 µg/L (adult)

Exposure Media: Natural seawater adjusted to 25 psu

Organisms per Replicate: Embryo: 200 per replicate for developmental assay, and 4L with 50 embryos/mL for MT assay. Adult replicates not reported.

Methods: Embryos were studied in 48-hour developmental assays (range of concentrations) and in tests for sublethal effect on MT (0.16 µg/L). Adults were tested for effects of lysosomal destabilization of hepatopancreas cells by neutral red assay. Effect of nano-Ag (0.16 µg/L) on MT gene expression was analyzed in embryos and adults by quantitative real-time PCR.

Study Outcome

Development. Nano-Ag impaired normal embryonic development in a threshold response manner characterized by limited change compared to control at low doses, and highly significant impairment (approximately 10% normal development rate) at the highest dose.

Lysosomal Destabilization. In adult oysters, significant adverse effects were noted in a dose-response manner with increasing dose corresponding with increased percentage of destabilized cells (ranging from approximately 30% to 55% destabilized cells).

MT Gene Expression. Increases in MT mRNA levels were observed in both adults and embryos exposed to 0.16 µg/L. Adults showed 2.4-fold increase compared to controls, and embryos showed 80-fold increase compared to controls.

B.5. Summary of Nano-Ag Effects in Aquatic Vertebrates

Asharani et al. (2008) Toxicity of silver nanoparticles in zebrafish models.

Test Species

Zebrafish embryos (*Danio rerio*)

Material

Nano-Ag synthesized through reduction of AgNO₃ with NaBH₄.

Shape: Not reported

Composition: Not reported

Crystal Structure: Not reported

Average Size: Not reported

Size Distribution: 5–20 nm (for both types of surface-treated nano-Ag, determined using TEM)

Solubility: Not reported

Surface Area: Not reported

Surface Treatment: Capped with soluble potato starch or bovine serum albumin (BSA)

Surface Charge: Not reported

Protocol

Exposure Duration: 72 hours

Endpoints: Mortality, hatching rate, heart rate, phenotypic changes, and apoptosis

Exposure Concentrations: 5, 10, 25, 50, and 100 µg/mL

Exposure Medium: Embryo water (60 mg sea salt per L ultrapure water)

Organisms per Replicate: 10 embryos × 6 replicates

Methods: To differentiate between dead and malformed embryos, opaque embryos were transferred to well plates with 4 mL medium and incubated for 24 hours. Mortality was determined by counting the number dead after 72 hours. Hatching rate was determined by the number of embryos hatched by 72 hours, and heart rate was recorded using a stopwatch at various stages post-fertilization. Other phenotypic deformities were also recorded. Embryos were examined using a photographic method. To assess the level of apoptic cells, acridine orange was added to all embryos exposed to nano-Ag above 50 µg/mL and samples were examined under a microscope. Embryos at various stages were collected and the chorion poked to aspirate fluid containing unidentified brown flakes. Flakes were examined using DAPI staining.

Study Outcome

Nano-Ag was uniformly distributed throughout the embryos, on the skin, and in brain and heart cells, showing affinity for the cell nucleus. Nano-Ag in the brain was well-dispersed, but clumping was observed elsewhere.

Mortality. LC_{50s} varied from 25 to 50 µg/mL, and were dependent on the growth stage (64–128 cell stage) of the embryo, with the later embryonic stages exhibiting more resistance to nano-Ag.

Hatching Rate and Heart Rate. Delay was observed with increasing nano-Ag concentrations, with 15% of embryos exposed to BSA-capped nano-Ag and 33% of embryos exposed to starch-capped nano-Ag hatching at the 100 µg/mL level. Heart rate decreased with increasing nano-Ag concentration, reached an average of 39 beats/minute above a concentration of 50 µg/mL (versus 150 beats/minute in the controls).

Phenotypic Changes and Apoptosis. Above 50 µg/mL concentrations of BSA-capped nano-Ag and starch-capped nano-Ag, 60–90% of embryos exhibited severe phenotypic changes characterized by bent and twisted notochord, accumulation of blood in blood vessels near the tail, low heart rate, pericardial edema, degeneration of body parts, and distorted yolk sacs. About 40–50% of embryos displayed apoptosis spots all over the body. Decay was observed primarily near the head and tail.

Bar-Ilan et al. (2009) Toxicity assessments of multisized gold and silver nanoparticles in zebrafish embryos.

Test Species

Zebrafish embryos (*Danio rerio*)

Material

Nano-Ag of various sizes synthesized using commonly used methods utilizing various strengths and types of reducing agents (no specific details provided).

Shape: Not reported

Composition: Not reported

Crystal Structure: Not reported

Average Sizes: 5.9 nm (nominally 3 nm), 15.3 nm (nominally 10 nm), 51.2 nm (nominally 50 nm), and 108.9 nm (nominally 100 nm) (determined using TEM)

Size Distribution: <4.5 to >7.5 nm (3 nm group), <12 to >20.1 nm (10 nm group), <31 to >71 nm (50 nm group), and <85 to >120 nm (100 nm group)

Solubility: Not reported

Surface Area: Not reported

Surface Treatment: Not reported

Surface Charge: Not reported

Protocol

Exposure Duration: 120 hours (5 days)

Endpoints: Mortality and morphology

Exposure Concentrations: 0.25, 2.5, 25, 100, and 250 μM

Exposure Medium: Egg water

Organisms per Replicate: 12 embryos \times 3 replicates

Methods: Dosing solutions were prepared by transferring nano-Ag in reverse osmosis water to egg water, which was changed daily to prevent destabilization of nano-Ag in solution. Using a scoring system, embryos were evaluated for severity of morphological defects, survival, and toxic adverse effects. The 100 μM treatment group was used to analyze sublethal toxic effects. At 120-h post fertilization, embryos exposed to 75 μM nano-Ag were examined by instrumental neutron activation analysis (INAA) to determine whether nano-Ag were taken up or adsorbed.

Study Outcome

Mortality. Almost 100% mortality occurred in all size groups at 250 μM nano-Ag 120-h post-fertilization.

LC₅₀ (3 nm nano-Ag): 93.31 μM

LC₅₀ (10 nm nano-Ag): 125.66 μM

LC₅₀ (50 nm nano-Ag): 126.96 μM

LC₅₀ (100 nm nano-Ag): 137.26 μM

Phenotypic Effects. Sublethal endpoints that were statistically significant from controls were opaque and nondepleted yolk; small head; jaw and snout malformations; stunted growth; circulatory malformations, such as hemorrhages and blood clots; tail malformations; body degradation, such as bubble-like formations on yolk sac and decaying tail tissue; pericardial edema; bent spine; and not hatching. Preliminary findings suggest that there was embryonic uptake and/or adsorption of nano-Ag.

Bilberg et al. (2010) Silver nanoparticles and silver nitrate cause respiratory stress in Eurasian perch (*Perca fluviatilis*).

Test Species

Eurasian perch (*Perca fluviatilis*), unspecified age

Material

Commercial nano-Ag powder purchased from NanoAmor (Houston, USA). A water dispersion was prepared by suspending 0.5 g nano-Ag powder in 100 mL Milli-Q water followed by ultrasonication and filtration. AgNO₃ pellets were purchased from SigmaAldrich.

Shape: Spherical (reported by manufacturer); elliptical, multifaceted, and triangular shapes (determined using TEM)

Composition: 99.5% purity (reported by manufacturer)

Crystal Structure: basic cubic orientation, crystallite size of ~78.1 nm (determined using PXRD)

Average Size: 81 ± 2 nm with aspect ratio of 1.2 ± 0.2 nm (determined using TEM)

Size Distribution: 30–40 nm (reported by manufacturer)

Solubility: Not reported

Surface Area: Not reported

Surface Treatment: 0.2% PVP coated

Surface Charge: -28.5 ± 0.8 mV (determined using DLS)

Protocol

Exposure Duration: 24 hours

Endpoints: Changes in oxygen consumption (Mo₂) as expressed by the basal metabolic rate (BMR) and the critical oxygen tension (P_{crit}) (below which the fish cannot maintain aerobic metabolism)

Exposure Concentrations: 0, 63, 129, and 300 µg/L (measured by ICP-OES)

Exposure Medium: Aarhus city tap water

Organisms per Replicate: 6 animals per test group (no replicates)

Methods: Five test groups of six perch (male and female) were exposed to nano-Ag in water. Oxygen consumption (Mo₂) was measured by automated intermittent closed respirometry. Each fish was tested for one day pre-exposure for background BMR and P_{crit} before the 24-hour exposure.

Study Outcome

BMR. Pre-exposure BMR was similar for all groups. The three concentrations of nano-Ag did not have any effect on exposure BMR. Only the high dose of AgNO₃ (386 µg/L) resulted in statistically significant elevation in exposure BMR.

P_{crit}. Pre-exposure P_{crit} was similar for all groups. No significant differences were observed for the two lowest nano-Ag concentration test groups (63 and 129 µg/L). However, P_{crit} statistically significantly increased from 4.8 to 9.2 kPa after exposure to 300 µg/L nano-Ag, P_{crit} also significantly increased for both exposure doses of AgNO₃ (increased 31% for low dose and 48% for high dose).

Chae et al. (2009) Evaluation of the toxic impact of silver nanoparticles on Japanese medaka (*Oryzias latipes*).

Test Species

Japanese medaka d-rR (*Oryzias latipes*), 4 to 5 months old

Material

Commercial nano-Ag powder purchased from Sigma Aldrich (Korea).

Shape: Cuboctahedral and decahedral

Composition: Not reported

Crystal Structure: Not reported

Average Size: 49.6 nm (determined using TEM)

Size Distribution: Approximately 10–120 nm

Solubility: Not reported

Surface Area: 50,710 nm² (determined using X-ray diffraction)

Surface Treatment: Not reported

Surface Charge: 29.9 ± 3.55 mV at pH 7.5 (ζ potential determined using electrophoretic light scattering [ELS] spectrophotometry)

Protocol

Exposure Duration: 24–96 hours and 10 days

Endpoints: Acute toxicity (mortality), gene expression

Exposure Concentrations: 0–50 µg/L total Ag (determined using inductively coupled plasma-optical emission spectroscopy [ICP-OES])

Exposure Medium: Water (pH 7.0–8.0)

Organisms per Replicate: 7–8 fish × 3 replicates

Methods: Fish were exposed to a flow-through system (1 L/24 hours to renew 50% of aquaria each day), and lethality was assessed after 96 hours. After 24, 48, and 96 hours, 2 fish exposed to concentrations of 1 µg/L and 25 µg/L from each replicate were killed and livers examined. The remaining 2 fish were exposed only to 1 µg/L and livers extracted after 10 days. RNA was isolated from livers and gene expression analyzed using real-time RT-PCR method. Genes analyzed were metallothionein (MT), heat shock protein 70 (HSP70), glutathione S transferase (GST), p53, cytochrome p450 1A (CYP1A), and transferrin (TF). The 18S rRNA gene was the endogenous control.

Study Outcome

LOEC: 25 µg/L

LC₅₀: 34.6 µg/L

Gene Expression. Nano-Ag exposure led to significant induction (6-fold increase) of MT after 24 hours in the 25 µg/L group and increased levels of mRNA (2.2-fold) after 48 hours, but after 4 days, mRNA returned to the basal level. Statistically significant induction of HSP70 also occurred at 25 µg/L nano-Ag and mRNA increased 2.5-fold after 24 hours, then decreased by 3.5-fold after 96 hours. 10-day exposure did not result in statistically significant induction of HSP70. At 1 µg/L, GST was significantly induced initially, with the highest mRNA levels seen at 24 hours (3-fold increase) and 48 hours (2.5-fold increase), but were not significantly different for 10-day exposure. At 25 µg/L, GST was statistically significantly induced at both 24 hours and 96 hours. CYP1A was significantly induced after 24 hours in both the 1 and 25 µg/L groups (4- and 3.2-fold increase, respectively), but no statistically significant induction occurred after 10-day exposure. Significant induction of P53 occurred after 24 hours in both the 1 and 25 µg/L groups (3.5- and 3.4-fold increase, respectively), but no significant induction occurred after 10-day exposure. TF was significantly down-regulated in the 25 µg/L group after 48 hours (73.3-fold lower) and 96 hours (35.7-fold lower), and significantly down-regulated in the 1 µg/L group after 48 hours (8-fold lower) and after 10-day exposure.

Choi et al. (2010) Induction of oxidative stress and apoptosis by silver nanoparticles in the liver of adult zebrafish.

Test Species

Adult zebrafish (*Danio rerio*)

Material

Water-based solution of 1.0 g/L nano-Ag (Nanopoly, Seoul, Korea).

Shape: Spherical

Composition: Not reported

Crystal Structure: Not reported

Average Size: Not reported

Size Distribution: 5–20 nm (determined using TEM)

Solubility: Not reported

Surface Area: Not reported

Surface Treatment: Not reported

Surface Charge: Not reported

Protocol

Exposure Duration: 24 hours

Endpoints: Acute toxicity (mortality) and hepatocellular toxicity

Exposure Concentrations: 30, 60, and 120 mg/L

Exposure Medium: Deionized water

Organisms per Replicate: 5 organisms per treatment (no replicates)

Methods: Fish were exposed to various concentrations of nano-Ag deionized by treatment with C ion exchange resin. Histopathology was performed on liver tissues to identify any cellular alterations.

Study Outcome

Mortality. 24 hour LC₅₀ of approximately 250 mg/L.

Hepatocellular Toxicity. Disruption of hepatic cell cords, chromatin condensation, and pyknosis were observed in the livers of all treated fish. A TUNEL assay confirmed that these changes were due to apoptosis. MT2 mRNA expression significantly increased in a dose-dependent manner (3.9-, 5.4-, and 7.1-fold at 30, 60, and 120 mg/L, respectively). MDA levels increased at 60 and 120 mg/L concentrations (1.5- and 1.7-fold, respectively), and GSH levels increased at the highest concentration (120 mg/L). DNA damage was detected in tissues of fish exposed to 120 mg/L nano-Ag. Authors did not find evidence of altered mRNA levels of the p53 protein.

Farkas et al. (2011) Uptake and effects of manufactured silver nanoparticles in rainbow trout (*Oncorhynchus mykiss*) gill cells.

Test Species

Rainbow trout (*Oncorhynchus mykiss*) gill cells isolated from juvenile fish with body weights of 150–200 g.

Material

Nano-Ag synthesized by sodium borohydride reduction of AgNO₃ dissolved in Milli-Q water with citrate as a capping agent. PVP-coated nano-Ag was obtained from the University of Manchester, UK.

Shape: Not reported

Composition: Not reported

Crystal Structure: Not reported

Average Size: 12 nm (citrate-capped); 7 nm (PVP-coated) (determined using TEM)

Size Distribution: 3–40 nm (citrate-capped); 1–60 nm (PVP-coated) (determined using TEM)

Solubility: Not reported

Surface Area: Not reported

Surface Treatment: Citrate-capped or PVP-coated

Surface Charge: –8 mV (citrate-capped) and –4 mV (PVP-coated)

Protocol

Exposure Duration: 48 hours (monolayer, cytotoxicity, and oxidative stress tests); 48 hours or 24 hours (multilayer)

Endpoints: Cytotoxicity and oxidative stress

Exposure Concentrations: 20 mg/L citrate-capped or 10 mg/L PVP-capped (monolayer); 10 mg/L citrate- or PVP-capped (multilayer); 0.1, 1, 5, or 10 mg/L (cytotoxicity and oxidative stress tests)

Exposure Medium: L15 cell culture media (monolayer, cytotoxicity, and oxidative stress tests); L15 or artificial freshwater (multilayer)

Organisms per Replicate: Isolated cell density = 5×10^5 to 1×10^6 cells/cm (monolayer); $1.4\text{--}2.5 \times 10^6$ cells/mL (multilayer); 4 individuals (cytotoxicity test)

Methods: Gill cells were isolated by a modified procedure described by Kelly et al. (2000) and seeded onto culture dishes to produce monolayers or multilayers. Cultures of cell multilayers were evaluated for transepithelial resistance (TER) by Epithelial Voltohmmeter. The uptake of nano-Ag into monolayered cells was evaluated by exposing cells to citrate-capped or PVP-capped nano-Ag and observing the possible clearance of nanoparticles using light microscopy imaging. Monolayer cells were also examined using TEM and EDX for nano-Ag accumulation from exposure media. The uptake and transport of nano-Ag into multilayered cells was evaluated in a similar manner. Multilayer cells were sampled by detachment with Trypsin and analyzed for total silver content using ICP-MS. Multilayer cells were also analyzed for the number of nanoparticles associated with the cell surface. Cytotoxicity was measured as the reduction of membrane integrity (Schreer et al., 2005) as indicated by fluorescence measurements. Oxidative stress was measured by the depletion of reduced glutathione (GSH) as indicated by fluorescent probe (monochlorobimane, or mBCI).

Study Outcome

In monolayered cells, accumulated nanoparticles were observed within the gill cells around the nuclei of citrate-capped nano-Ag-exposed cells, whereas no accumulated particles were observed in the control cells. No effective clearance of accumulated particles was observed. No nanoparticle accumulations were observed in PVP-coated treatment groups. TEM and EDX verified citrate-nano-Ag accumulation within lamellar bodies and single particles present in the cytosol and PVP-coated nano-Ag in vesicle-like structures. In multilayered cells, nano-sized particles were observed in epithelia for both nano-Ag exposures but were too small for EDX analysis. Silver transported through the epithelium was approximately 19 ng/cm² for citrate-capped nano-Ag, and 47 ng/cm² for PVP-capped nano-Ag (combined results for both exposure media – when separated, FW showed reduced uptake compared to L15). Silver transport through epithelia was dependent on TER in all cases.

Cytotoxicity and Oxidative Stress. Cells exposed to citrate-capped nano-Ag or PVP-coated nano-Ag showed statistically significant dose-dependent reduction in viability as evidenced by reduced membrane integrity at exposures levels ≥ 5 mg/L. Cells exposed to silver ions significantly reduced viability at levels ≥ 1 mg/L. Significantly higher levels of GSH were found at exposure levels ≥ 5 mg/L for citrate-capped nano-Ag and for silver ions, while PVP-coated nano-Ag exposure significantly increased GSH at exposure levels ≥ 1 mg/L.

Griffitt et al. (2009) Comparison of molecular and histological changes in zebrafish gills exposed to metallic nanoparticles.

Test Species

Adult female zebrafish (*Danio rerio*)

Material

Commercial nano-Ag powder produced by gas-phase condensation and coated with a thin layer (2–3 nm) of metal oxide; supplied by Quantum Sphere (Santa Ana, CA, USA).

Shape: Not reported

Composition: Not reported

Crystal Structure: Not reported

Average Size: 26.6 ± 8.8 nm (determined using laser diffraction particle size analyzer)

Size Distribution: Approximately 20–1,000 nm

Solubility: After 24 and 48 hours, only 5.1% of initial nano-Ag dose remained, with the rest aggregating and settling out. Soluble Ag decreased over time, reaching a peak concentration of 4.9 µg/L at 2 hours, and decreasing to 0.2 µg/L at 48 hours.

Surface Area: 14.53 m²/g (determined using the Brunauer, Emmett, and Teller method)

Surface Treatment: Not reported

Surface Charge: -27.0 mV (ζ potential in moderately hard freshwater with pH 8.2, determined using a Zeta Reader Mk 21-II)

Protocol

Exposure Duration: 48 hours

Endpoints: Mortality, gill histopathology, and gene expression

Exposure Concentration: 1,000 µg/L nano-Ag (corresponding to 0.014 m²/L if monodispersed)

Exposure Medium: 0.22 µm filtered moderately hard water

Organisms per Replicate: 4 fish × 3 replicates

Methods: Static renewal assays were conducted using the no observed effect concentration (NOEC) of nano-Ag. Gills and whole carcasses were analyzed for metal concentration at 24 and 48 hours, and lethality was assessed. After 48 hours, gills were examined for structural changes in filament and lamellae, characterized by increased cellularity in intramellar space. RNA from gill tissue samples was also analyzed by microarray to determine gene response.

Study Outcome

Lethality. NOEC concentrations were used, and no mortality occurred. There were no changes in appearance or behavior.

Gill Histopathology. No significant change in gill filament width resulted from exposure to nano-Ag.

Gene Expression. At 24 hours, nano-Ag-exposed fish exhibited 66 significantly upregulated genes and 82 downregulated. At 48 hours, there were 126 significantly upregulated and 336 downregulated genes.

Hinther et al. (2010) Nanometals induce stress and alter thyroid hormone action in amphibia at or below North American water quality guidelines.

Test Species

Rana catesbeiana tissue.

Material

Commercial nano-Ag supplied by Northern Nanotechnologies (ViveNano, Toronto, Canada).

Shape: Not reported

Composition: Not reported

Crystal Structure: Not reported

Average Size: Not reported

Size Distribution: Approximately 2–10 nm (determined using TEM and DLS)

Solubility: Soluble in water

Surface Area: Not reported

Surface Treatment: Carboxyl-functionalized coating

Surface Charge: 41.14 mV

Protocol

Exposure Duration: 48 hours

Endpoints: Acute toxicity (cell viability), thyroid hormone receptor (TR β) transcript levels, and Rana larval keratin I (RLKI) transcript levels

Exposure Concentration: 0.06 μ g/L–5.5 mg/L

Exposure Medium: Not reported

Organisms per Replicate: 8–16 animals per replicate; 8–10 biopsies per animal

Methods: Stress and thyroid hormone signaling were assessed in frog tissue after exposure to nano-Ag using a cultured tail fin biopsy (C-fin) assay. Nano-Ag effects were assessed in the presence and absence of T₃ using a quantitative real-time polymerase chain reaction technique.

Study Outcome

Cell viability. LC₅₀ = 0.95 mg/L

TR β and RLK1. Thyroid-hormone-response gene transcript levels were observed to significantly decrease after exposure to 10nM nano-Ag and stress-response gene transcript levels to significantly increase after exposure to 5 and 10nM nano-Ag. Catalase transcript levels were significantly decreased after exposure to 10 nM nano-Ag.

Kennedy et al. (2010) Fractionating nanosilver: importance for determining toxicity to aquatic test organisms.

Test Species

Fathead minnow (*Pimephales promelas*) larvae (24 hours old).

Material

Nano-Ag dispersions obtained from NanoComposix (Biopure, San Diego, CA), PVP-coated nano-Ag synthesized at Luna Innovations (Blacksburg, VA), and citrate and EDTA stabilized nano-Ag synthesized at VA Tech (Blacksburg, VA).

Shape: Mostly spherical with some rods (determined using TEM)	Size Distribution: 10–50 nm (determined using TEM)
Composition: Not reported	Solubility: Not reported
Crystal Structure: Not reported	Surface Area: Not reported
Average Size: Not reported	Surface Treatment: Citrate-, PVP-, or EDTA-coated
	Surface Charge: -15 to -34 mV

Protocol

Exposure Duration: 48 hours

Endpoints: Mortality

Exposure Concentrations: ~6–126 µg/L

Exposure Medium: Moderately hard reconstituted water

Organisms per Replicate: Not reported, 4 replicates

Methods: Mortality was measured as an indicator of acute toxicity after 48 hours of exposure to nano-Ag of various sizes and coatings.

Study Outcome:

LC₅₀ (AgNO₃): 6.5 µg/L

LC₅₀ (citrate-coated): 19.2 µg/L

LC₅₀ (10 nm): 41.0 µg/L

LC₅₀ (20 nm): 64.1 µg/L

LC₅₀ (50 nm): 60.7 µg/L

LC₅₀ (PVP-coated): >69.9 µg/L

LC₅₀ (EDTA-coated): 55.2 µg/L

Laban et al. (2009) The effects of silver nanoparticles on fathead minnow (*Pimephales promelas*) embryos.

Test Species

Fathead minnow embryos (*Pimephales promelas*)

Material

Commercial nano-Ag supplied by either NanoAmor (Houston, TX, USA) or Sigma-Aldrich (St. Louis, MO, USA)

Shape: Not reported

Composition: Not reported

Crystal Structure: Not reported

Average Size: approximately 31–50 nm (NanoAmor) and 21–60 nm (Sigma-Aldrich) (determined using TEM)

Size Distribution 29–100 nm (NanoAmor) and 21 to >300 nm (Sigma-Aldrich)

Solubility: Increasing concentrations of nano-Ag (Sigma-Aldrich) resulted in a decreased percentage of dissolved silver

Surface Area: Not reported

Surface Treatment: Not reported

Surface Charge: Not reported

Protocol

Exposure Duration: 96 hours

Endpoints: Mortality and morphology

Exposure Concentrations: 0.625, 1.25, 2.5, 5, 7.5, 10, 15, 20, and 25 mg/L

Exposure Medium: Test water with dissolved oxygen content of 7.5 mg/L, pH 8.3–8.5, and water hardness 215–240 mg/L as CaCO₃

Organisms per Replicate: 10 embryos × 3 replicates

Methods: Static nonrenewal tests were conducted using both commercial nano-Ag products and AgNO₃. To assess mortality and developmental changes, dead and abnormal embryos were counted, and uptake was analyzed by TEM. Toxicity was assessed using both stirred and sonicated samples.

Study Outcome

LC₅₀ (sonicated NanoAmor): 1.25 mg/L LC₅₀ (sonicated Sigma-Aldrich): 1.36 mg/L LC₅₀ (AgNO₃): 15 µg/L

LC₅₀ (stirred NanoAmor): 9.4 mg/L LC₅₀ (stirred Sigma-Aldrich): 10.6 mg/L

Significant abnormalities included absence of air sac, pericardial and yolk sac edema, hemorrhages to head and pericardial area, and lordosis (upward bending of vertebral column).

Lee et al. (2007) In vivo imaging of transport and biocompatibility of single silver nanoparticles in early development of zebrafish embryos.

Test Species

Zebrafish embryos (*Danio rerio*), at the 8–64-cell stages and 0.75–2.25 hours post fertilization

Material

Nano-Ag synthesized by sAgClO₄ reduction with sodium citrate and NaBH₄.

Shape: Spherical

Composition: Not reported

Crystal Structure: Not reported

Average Size: 11.6 ± 3.5 nm (determined using high-resolution TEM)

Size Distribution: Approximately 5–46 nm

Solubility: Stable in egg water

Surface Area: Not reported

Surface Treatment: Not reported

Surface Charge: Not reported

Protocol

Exposure Duration: 120 hours (5 days)

Endpoints: Mortality and morphology

Exposure Concentrations: 0.04, 0.06, 0.07, 0.08, 0.29, 0.38, 0.57, 0.66, and 0.71 nM

Exposure Medium: Egg water

Organisms per Replicate: 35–40 embryos × 3 replicates

Methods: Nano-Ag effects on embryonic development and survival were determined through direct observation. Single nanoparticle transport was analyzed in vivo in embryos exposed to nano-Ag in real-time using dark-field single-nanoparticle optical microscopy and spectroscopy (SNOMS).

Study Outcome

Ag nanoparticles were observed embedded in retina, brain, heart, gill arches, and tail. The number of dead and deformed zebrafish increased with increasing dose, with no normal development occurring after the 0.19 nM concentration level (i.e., all zebrafish were either dead or deformed at concentrations higher than 0.19 nM). Finfold abnormality and tail/spinal cord flexure and truncation were observed at all concentrations. Cardiac malformation and yolk sac edema were observed in the 0.07 to 0.71 nM concentration range. Head edema and eye deformity were observed only at the higher concentrations ranging from 0.44–0.71 and 0.66–0.71, respectively. Multiple deformities in a single embryo were observed concentrations higher than 0.38 nM.

Scown et al. (2010) Effects of aqueous exposure to silver nanoparticles of different sizes in rainbow trout.

Test Species

Juvenile female rainbow trout (*Oncorhynchus mykiss*), mean weight 19.52 g (Hatchlands Trout Farm, Devon, UK)

Material

Commercial nano-Ag provided by Nanostructured and Amorphous Materials Inc. (Houston, TX).

Shape: Not reported

Composition: Not reported

Crystal Structure: Cubic (determined using XRD)

Average Size: 49 nm (small particles N₁₀) and 114 nm (medium particles N₃₅) (determined using TEM)

Size Distribution: Not reported

Solubility: Not reported

Surface Area: 2.0 m²/g (small particles), 2.9 m²/g (medium particles) (determined using BET)

Surface Treatment: Not reported

Surface Charge: -12.52 mV (small particles), -6.5 mV (medium particles)

Protocol

Exposure Duration: 10 days

Endpoint: Lipid peroxidation and gene expression

Exposure Concentrations: 10 and 100 µg/L

Exposure Medium: Dechlorinated tap water (pH 7.79, conductivity 189.58 µs, temperature 9–11°C)

Organisms per Replicate: 8 fish per treatment × 2 replicates

Methods: A 10-day exposure assay using AgNO₃ and two sizes of nano-Ag was conducted. Particle uptake into various tissues was examined by inductively coupled plasma-optical emission spectrometry. Levels of thiobarbituric-acid-reactive substances (TBARS) were monitored as indicators of lipid peroxidation. Differential expression of *cyp1a2*, *cyp3a45*, *hsp70a*, *gpx*, and *g6pd* were analyzed in the gills and liver using real-time PCR.

Study Outcome

Silver amounts were statistically significantly increased in and on the gills and livers of fish treated with 10 µg/L N₁₀ and N₃₅ nano-Ag and 100 µg/L N₃₅ nano-Ag compared to control.

Lipid Peroxidation. No evidence of lipid peroxidation was observed after analysis of TBARS except in the group treated with 100 µg/L N₁₀ nano-Ag.

Gene Expression. Expression of gene *cyp1a2* was increased threefold compared to control in the gills of fish exposed to 100 µg/L N₁₀ nano-Ag.

Shahbazzadeh et al. (2009) The effects of nanosilver (Nanocid®) on survival percentage of rainbow trout (*Oncorhynchus mykiss*).

Test Species

Rainbow trout (*Oncorhynchus mykiss*), median weight 1.049 g

Material

Commercial colloidal Ag suspension (Nanocid L-series colloidal product) provided by Nasb Pars Co. (Iran).

Shape: Not reported

Composition: Not reported

Crystal Structure: Not reported

Average Size: Not reported

Size Distribution: Not reported

Solubility: Not reported

Surface Area: Not reported

Surface Treatment: Not reported

Surface Charge: Not reported

Protocol

Exposure Duration: 96 hours

Endpoint: Mortality

Exposure Concentrations: 1.25, 2.5, 5, 10, 20, 30-50, and 60–70 ppm

Exposure Medium: Tap water maintained at $16 \pm 1^\circ\text{C}$, dissolved oxygen >8 mg/L, carbon dioxide <6 mg/L, ammonia <0.01 mg/L, nitrite <0.1 mg/L, water hardness <200 mg/L as CaCO_3 , conductivity 780 μS , pH 7.5–8.4

Organisms per Replicate: 30 fish \times 3 replicates

Methods: Partial mortality data at 24 and 96 hours were used to determine LC_{50} values, and all calculations were based on mean measured concentrations in the aquarium, rather than nominal concentrations.

Study Outcome

LC_{50} (48-hour): 3.5 mg/L

LC_{50} (72-hour): 3 mg/L

LC_{50} (96-hour): 2.3 mg/L

Wu et al. (2010) Effects of silver nanoparticles on the development and histopathology biomarkers of Japanese medaka (*Oryzias latipes*) using the partial-life test.

Test Species

Japanese medaka (*Oryzias latipes*) aged 7 days postfertilization to 60 days posthatch.

Material

Nano-Ag synthesized through reduction of 16.9% AgNO₃ with sodium hexametaphosphate, sodium hypophosphite, and PVP.

Shape: Spherical (determined using TEM)

Composition: Not reported

Crystal Structure: Face-centered cubic phase (determined using XRD)

Average Size: 25 nm (determined using TEM)

Size Distribution: 20–37 nm (determined using TEM)

Solubility: Not reported

Surface Area: Not reported

Surface Treatment: Not reported

Surface Charge: Not reported

Protocol

Exposure Duration: 48 hours (adult acute toxicity); 168 hours (embryo acute toxicity); ~ 70 days (developmental toxicity)

Endpoints: Mortality (adult/embryo acute toxicity); developmental retardation, morphological defects, hatching rate, and histopathology (developmental toxicity)

Exposure Concentrations: 0, 0.5, 1.0, 2.0, 4.0, and 8.0 mg/L (adult acute toxicity); 0, 0.5, 1.0, 2.0, and 4.0 mg/L (embryo acute toxicity); 0, 100, 200, 400, 600, 800, and 1,000 µg/L (developmental toxicity)

Exposure Medium: Not reported

Organisms per Replicate: 16 adult × 2 replicates (adult acute toxicity); 30 embryos × 2 replicates (embryo acute toxicity); 95 embryo × 3 replicates (developmental toxicity)

Methods: Mortality was recorded for calculating the LC₅₀ based on the Karber method. In the developmental toxicity study, embryos were exposed to 0–1,000 µg/L until 60 days post-hatch. On Days 5 and 7 postfertilization (dpf), morphological abnormalities were noted with a stereo dissecting microscope, and the maximum width of the optic tectum (correlating to brain development) was measured. Embryos were also observed under an inverted fluorescence microscope to evaluate the autofluorescence of leucophores. Histopathological assessment of optic development was carried out on six 2-day-old larvae (pooled) from each group using light microscopy. Remaining fish were collected on 60 dph and examined for body weight and length.

Study Outcome

Mortality. In adults, 100% mortality was observed in the 2.0 mg/L group (mortality in groups exposed to higher concentrations is unclear), while 0% was observed in the 0.5 mg/L group. The adult LC₅₀ was determined to be 1.03 mg/L (Karber analysis). In the embryonic study, 100% mortality was also observed in the 2.0 mg/L group. An LC₅₀ for embryos was not reported.

Developmental Retardation. While control embryos developed to stages 34, 35, or 36 on 5 dpf and stages 36, 37, or 38 on 7 dpf, treated embryos exhibited delayed development. For 5 dpf this trend represented a U-shaped dose-response pattern where more delayed embryos were observed in groups exposed to 200, 400, and 1,000 µg/L when compared to other treatments. A significant dose-related increase in heart rate was also observed on 5 dpf for exposure groups 400–1,000 µg/L compared to control. Pigmentation in exposed groups was inhibited by exposure on 5 dpf. The width of the optic tectum decreased significantly with increasing exposure concentration, indicating that neural development might be affected by nano-Ag exposure.

Morphological Defects. Observed impairments included sluggish circulation; hemorrhage and hemostasis; circulatory abnormalities (pericardial edema/tube heart); eye abnormalities (e.g., microphthalmia, anisophthalmia, cyclopia, exophthalmia, anophthalmia); finfold abnormalities; vertebral abnormalities (e.g., scoliosis, lordosis, upward curvature); edema of the yolk sac, head, heart, and gallbladder; and, most commonly, skeletal flexure and truncation. Individual abnormalities did not display a concentration-dependent relationship; however, a significant increase in the occurrence of total abnormalities was observed in low-dose exposed groups (100–400 µg/L) and in the high-dose group (1,000 µg/L). The total abnormality rate increased to 32.3% at 400 µg/L, decreased to 18.9–23.3% at 600–800 µg/L, and finally increased again to 56.8% at 1,000 µg/L.

Hatching Rate. A dose-dependent reduction in hatching rate was observed. The hatching rate was reduced by 37.62% at 1,000 µg/L compared to control. Embryos exposed to 100–800 µg/L resulted in precocious hatching (hatching time reduced by 1.2–1.7 days). Larval survival rates decreased to 0% at 800 and 1,000 µg/L.

Histopathology. Microscopic changes in the shape and structure of the eyes were observed in exposed medaka. Ganglion cells were deficient, and the thickness of the inner nuclear cell layer was decreased, while retinal pigment epithelium thickness increased.

Yeo and Kang (2008) Effects of nanometer-sized silver materials on biological toxicity during zebrafish embryogenesis.

Test Species

Zebrafish embryos, 64- to 265-cell stages and 2.5 hours post fertilization (*Danio rerio*)

Material

Commercial nano-Ag supported by titanium oxide purchased from N Corporation (Korea)

Shape: Not reported

Composition: Ag₃O, Ag₄H, and TiO

Crystal Structure: Not reported

Average Size: Not reported

Size Distribution: Approximately 10–20 nm (determined using TEM)

Solubility: Not reported

Surface Area: Not reported

Surface Treatment: Supported by TiO

Surface Charge: Not reported

Protocol

Exposure Duration: 72 hours

Endpoints: Hatching rate, morphology, and gene expression

Exposure Concentrations: 10 and 20 ppt

Exposure Medium: Carbon-filtered city water

Organisms per Replicate: 300 embryos × 3 replicates

Methods: Hatching rates were determined based on the number of hatched embryos 72 hours post-fertilization. RNA was isolated from nano-Ag exposed zebrafish 72 hours post-fertilization and expression of SEL N1 and N2 genes were analyzed by RT PCR.

Study Outcome

Hatching Rate. Hatching rates were significantly decreased in both 10 and 20 ppt treatment groups, and catalase activity increased significantly in the 20-ppt groups.

Phenotypic Changes. Almost all individuals in the 10- and 20-ppt nano-Ag groups exhibited abnormal properties, with more observed in the 20-ppt compared to the 10-ppt groups (significance was not reported). Observed phenotypic changes included abnormal notochord development, undeveloped eyes, weak heartbeats, and edema.

SEL N Gene Expression. SEL N1 and N2 gene expression reduced in a concentration-dependent manner (significance not reported). SEL N2 gene expression was 38% that of control group.

Yeo and Pak (2008) Exposing zebrafish to silver nanoparticles during caudal fin regeneration disrupts caudal fin growth and p53 signaling.

Test Species

Zebrafish (*Danio rerio*), age not specified

Material

Commercial nano-Ag supported by titanium oxide purchased from N Corporation (Korea).

Shape: Not reported

Composition: Ag₃O, Ag₄H, and TiO

Crystal Structure: Not reported

Average Size: Not reported

Size Distribution: Approximately 10–20 nm (determined using TEM)

Solubility: Not reported

Surface Area: Not reported

Surface Treatment: Supported by TiO

Surface Charge: Not reported

Protocol

Exposure Duration: 36 days

Endpoints: Caudal fin regeneration, histology, and gene expression

Exposure Concentrations: 0.4 and 4 ppm

Exposure Medium: Distilled water, supplemented with 0.3 g/L Instant Ocean Sea Salt, filtered through 0.45 µm mesh, denitrified by bacterial filtration, and disinfected by ultraviolet light exposure

Organisms per Replicate: 1 fish × 5 replicates

Methods: Regeneration experiments were performed on caudal fins amputated at approximately 50% proximal-distal level. Phenotypic comparisons were made between fish challenged to regenerate in the presence of nano-Ag when compared to the controls. Photographs of the regeneration area were taken intermittently. To examine histological effects from exposure to nano-Ag, tissues were fixed, post-fixed, dehydrated, and then embedded in Embed 812-Araldite 502 resin. Ultra-thin sections were then mounted, stained, and examined using a field emission TEM. RNA was isolated in nano-Ag-exposed zebrafish 52 hours post-fertilization, and gene expression profiles were analyzed by microarray analysis.

Study Outcome

Caudal Fin Regeneration. Caudal fin regeneration was significantly inhibited at 4 ppm of nano-Ag while only a delay in regeneration was observed at 0.4 ppm.

Histological Effects. Nano-Ag penetrated all organelles, including the nucleus, and accumulated in blood vessels in both treatment groups. Destroyed or swollen mitochondria with empty matrices were observed in fin, gill, and muscle tissue.

Gene Expression. Genes coding for tumor protein p53; bc12-associated X protein; phosphatidylinositol glycan, class C; phosphatidylinositol glycan, class P; and insulin-like growth factor binding protein 3 were upregulated (range: 2.05- to 3.08-fold). Gene coding for insulin-like growth factor 1 was significantly downregulated (0.38-fold).

B.6. Summary of Nano-Ag Effects on Terrestrial Plants

Babu et al. (2008) Effect of nano-silver on cell division and mitotic chromosomes: a prefatory siren.

Test Species

Onion (*Allium cepa*)

Material

Commercial nano-Ag (source not reported).

Shape: Not reported

Composition: Pure Ag (method not reported)

Crystal Structure: Not reported

Average Size: 2 nm (method not reported)

Size Distribution: Not reported

Solubility: Approximately 80% nano-Ag and 20% ionic Ag in solution (method not reported)

Surface Area: Not reported

Surface Treatment: Not reported

Surface Charge: Not reported

Protocol

Exposure Duration: 0.5, 1, 2, or 4 hours

Endpoints: Cell proliferation and chromosomal damage

Exposure Concentrations: 10, 20, 40, and 50 ppm

Exposure Medium: Distilled water

Plants per Replicate: 8 meristems

Methods: Root tips (meristems) from *A. cepa* bulbs were treated with nano-Ag concentrations of 10, 20, 40, or 50 ppm. Chromosomal preparations were made and approximately 10,000 cells from 10 root tips and 5 bulbs were analyzed to score the frequency of mitotic index and chromosomal aberrations.

Study Outcome

Significantly reduced frequency in mitotic index was observed at all concentrations and exposure durations except 10 ppm concentration for 0.5- and 1-hour exposure periods and 40 and 50 ppm for the shortest exposure period (0.5 hour).

Chromosomal aberrations increased in a dose-and duration-dependent manner, and were significantly different from the controls for all concentrations and exposure durations. Structural aberrations included C-metaphase, disturbed metaphase, fragments, sticky metaphase, laggards, anaphasic bridge, disturbed anaphase, and micronuclei.

Kumari et al. (2009) Genotoxicity of silver nanoparticles in *Allium cepa*.

Test Species

Onion (*Allium cepa*)

Material

Commercial nano-Ag purchased from Sigma-Aldrich (USA).

Shape: Not reported

Composition: Not reported

Crystal Structure: Not reported

Average Size: <100 nm (provided by the manufacturer)

Size Distribution: Not reported

Solubility: Not reported

Surface Area: 5.0 m²/g (provided by the manufacturer)

Surface Treatment: Not reported

Surface Charge: Not reported

Protocol

Exposure Duration: 4 hours

Endpoints: Cell proliferation and chromosomal damage

Exposure Concentrations: 25, 50, 75, or 100 ppm

Exposure Medium: Deionized water

Plants per Replicate: 4 bulbs and 8 root tips × 3 replicates

Methods: Roots 2–3 cm in length were treated with nano-Ag, and mitotic index and aberrant cells were quantified after microscopic observation.

Study Outcome

There was a concentration-dependent decrease in mitotic index (MI), with the lowest MI (27%) occurring in the 100 ppm group. MI was significantly different from the controls at the 50-, 75-, and 100-ppm levels. Different chromosomal aberrations occurred at the different nano-Ag concentrations. At 50 ppm, chromatin bridge, stickiness, and disturbed metaphase were observed; at 75 ppm, chromosomal breaks were observed; complete disintegration of the cell walls was observed at 100 ppm.

Rostami and Shahstavar (2009) Nano-silver particles eliminate the in vitro contamination of olive 'Mission' explants.

Test Species

Olive (*Olea europea L.*)

Material

Commercial nano-Ag (L2000 Series) purchased from NanoCid (Iran).

Shape: Not reported

Composition: Not reported

Crystal Structure: Not reported

Average Size: Not reported

Size Distribution: Not reported

Solubility: Not reported

Surface Area: Not reported

Surface Treatment: Not reported

Surface Charge: Not reported

Protocol

Exposure Duration: 1 hour (submerged in nano-Ag solution) or 30 days (amended media)

Endpoints: Decontamination and mortality

Exposure Concentrations: 100, 200, 300, and 400 mg/L (submerged) or 0, 4, 8, and 16 mg/L (amended media)

Exposure Medium: Sterile distilled water or Murashige and Skoog half strength media

Organisms per Replicate: 20 explants × 4 replicates

Methods: Explants with nodes and shoot apices were submerged in 100 mg/L ascorbic acid and 100 mg/L citric acid to control phenolic compounds. Explants were then submerged in 70% ethylic ethanol for 0, 0.5, or 1 min, rinsed, then submerged in 0.1% Clorox solution for 0, 5, or 10 min, then washed. Explants were then submerged in nano-Ag solution for 1 hour, after which they were placed in uncontaminated media and monitored for 30 days. In a separate experiment, some explants were placed in Murashige and Skoog half strength media amended with concentrations of 2, 4, or 6 mg/L nano-Ag and grew for 30 days in the amended media. After 30 days, infected and developed plants were recorded, but the method by which these endpoints were quantified was not reported.

Study Outcome

Nano-Ag at all concentrations appeared to effectively reduce or eliminate internal bacterial contamination in both submerged explants and those in contaminated media, though significance was not reported and the method by which contamination was assessed was not reported. Nano-Ag resulted in increased mortality in explants submerged in nano-Ag solutions in a dose-dependent manner, with no explants surviving in the 300 and 400 mg/L treatment groups (significance not reported). Mortality decreased with increasing nano-Ag concentrations in media up to 4 mg/L, after which mortality increased (significance not reported).

Stampoulis et al. (2009) Assay-dependent phytotoxicity of nanoparticles to plants.

Test Species

Zucchini (*Cucurbita pepo* cv Costata Romanesco)

Material

Commercial nano-Ag purchased from Sigma-Aldrich (St. Louis, MO, USA).

Shape: Not reported

Composition: Not reported

Crystal Structure: Not reported

Average Size: <100 nm (provided by the manufacturer)

Size Distribution: Not reported

Solubility: Not reported

Surface Area: Not reported

Surface Treatment: Sodium dodecyl sulfate (SDS) surfactant

Surface Charge: Not reported

Protocol

Exposure Duration: 5 days (elongation), 12 days (germination), 15 days (biomass), 17 days (transpiration)

Endpoints: Changes in time to germination, root elongation, biomass, and transpiration volume

Exposure Concentrations: 1,000 mg/L (elongation and germination) or 1.0, 10, 50, 100, 500, and 1,000 mg/L (biomass and transpiration)

Exposure Medium: Reverse osmosis water (elongation and germination) or Hoagland solution (biomass and transpiration)

Organisms per Replicate: 3 seeds × 5 replicates (germination and elongation) or 1 plant × 6 replicates (biomass and transpiration)

Methods: Pre-germinated seeds with radicals of 0.5 mm were selected for the root elongation assay. Root elongation was measured after a 5-day exposure to nano-Ag. To assess time to germination, seeds were placed on Petri dishes and amended with 1,000 mg/L nano-Ag with or without 0.2% SDS. A batch hydroponic experiment was conducted to determine the effect of nano-Ag on biomass of seedlings. 18-day-old seedlings were exposed to 1,000 mg/L nano-Ag in Hoagland solution after which biomass was monitored for 15 days. In addition, 4-day-old seedlings were exposed to concentrations of nano-Ag ranging from 0 to 1,000 mg/L nano-Ag in Hoagland solution and biomass and transpiration volume (determined by mass change of solution) were measured over a 17-day exposure period.

Study Outcome

Seed Germination. There was no significant impact on seed germination in the nano-Ag or nano-Ag plus SDS treatment groups when compared to controls. Nor did conventional Ag affect seed germination.

Root Elongation. There was no significant impact on root growth in the nano-Ag or nano-Ag plus SDS treatment groups when compared to controls. Nor did conventional Ag affect root growth.

Biomass. Nano-Ag exposure resulted in 69% reduction in plant biomass compared to the control and 1,000 mg/L conventional Ag groups.

Transpiration. Exposure to 500 and 1,000 mg/L nano-Ag resulted in 51 and 70% reduction in biomass when compared to controls and conventional Ag, respectively. Transpiration volume decreased significantly at and above 100 mg/L nano-Ag.

B.7. Summary of Nano-Ag Effects on Terrestrial Invertebrates

Ahamed et al. (2010) Silver nanoparticles induced heat shock protein 70, oxidative stress and apoptosis in *Drosophila melanogaster*.

Test Species

Third instar larvae of wild-type *Drosophila melanogaster* (Oregon RS, Bloomington Stock Centre, Bloomington, IN).

Material

Nano-Ag particles (Clarkson University, Potsdam, NY) synthesized by reduction of silver ions in a polysaccharide solution (acacia gum).

Shape: Spherical (determined using TEM)

Composition: Not reported

Crystal Structure: Not reported

Average Size: 11 nm (determined using TEM), 48 nm (determined using DLS)

Size Distribution: Not reported

Solubility: Not reported

Surface Area: Not reported

Surface Treatment: Coated with polysaccharide

Surface Charge: -38.6 (determined using LDV)

Protocol

Exposure Duration: 24, 48 hours

Endpoints: Oxidative stress, DNA damage, and apoptosis

Exposure Concentrations: 50, 100 µg/mL

Exposure Medium: Standard cornmeal

Organisms per Replicate: 25 organisms × 3 replicates

Methods: Larvae were administered nano-Ag for 2 durations of exposure. Oxidative stress and apoptosis were assessed by levels of malondialdehyde (MDA), glutathione (GSH), superoxide dismutase (SOD), catalase (CAT), and caspase enzymes. Levels of DNA-damage markers p53 and p38 were also assessed.

Study Outcome

Oxidative Stress. Levels of hsp70, MDA, and SOD and CAT activity were statistically significantly increased in treated larvae when compared to controls, while GSH levels were statistically significantly lower in treated larvae, indicating high levels of biological stress.

DNA Damage. Levels of p53 and p38 were significantly increased in treated larvae from those of the control in a time- and dose-related manner, indicating significant DNA damage caused by exposure to nano-Ag.

Apoptosis. Activities of caspase-3 and caspase-9 were significantly increased in treated larvae from the control levels, suggesting that nano-Ag exposure is involved in the apoptotic pathway.

Heckmann et al. (2011) Limit-test toxicity screening of selected inorganic nanoparticles to the earthworm *Eisenia fetida*.

Test Species

Adult earthworm (*Eisenia fetida*) purchased from Skandinavisk Miljøgodning (Grindsted, Denmark).

Material

Nano-Ag (NanoAmor).

Shape: Spherical, multi-faceted, or slightly elongated (determined using TEM)

Composition: Not reported

Crystal Structure: Cubic (determined using PXRD)

Average Size: 81.8 nm (determined using TEM)

Size Distribution: Not reported

Solubility: Not reported

Surface Area: 5–10 m²/g

Surface Treatment: Coated with 0.2% w/w PVP

Surface Charge: -28.6 mV (determined using DLS)

Protocol

Exposure Duration: 28 days

Endpoints: Adult survival and reproductive toxicity

Exposure Concentrations: 1,000 mg/kg-dry soil

Exposure Medium: Sandy loam soil (pH 5.8; TOC 1.36%, clay 11.6%, silt 21.4%, and sand 64.7%)

Organisms per Replicate: 10 organisms × 4 replicates

Methods: Using a limit-test design, ecotoxicological life history trait data including survival and reproduction success were evaluated in earthworms following exposure to 1,000 mg/kg-soil to nano-Ag. Particles were characterized thoroughly in order to relate any observed toxicity to particle characteristics.

Study Outcome

Survival. Survival was not statistically significantly affected by nano-Ag exposure.

Reproductive Toxicity. Exposure to nano-Ag caused 100% reproductive failure. Cocoon production in the exposed group (0%) was significantly different ($p < 0.05$) from that of the control group (100%). Hatchability and juvenile production were not able to be assessed due to the lack of cocoon production.

Lapied et al. (2010) Silver nanoparticle exposure causes apoptotic response in the earthworm *Lumbricus terrestris* (Oligochaeta).

Test Species

Depurated adult earthworm (*Lumbricus terrestris*).

Material

Commercial QSI nano-Ag purchased from Quantum Sphere (Santa Ana, CA).

Shape: Not reported

Composition: Not reported

Crystal Structure: Not reported

Average Size: 20.2 nm (determined using TEM)

Size Distribution: Not reported

Solubility: Not reported

Surface Area: Not reported

Surface Treatment: None

Surface Charge: Not reported

Protocol

Exposure Duration: 24 hours (water), 8 weeks (diet), 4 weeks (soil)

Endpoints: Mortality and apoptosis

Exposure Concentrations: 1, 10, 100 mg/L (water); 0, 1, 10, 100 mg/kg-food (diet); 1, 10, 100 mg/kg-soil (soil)

Exposure Medium: Water, nonmedicated horse manure, and agricultural soil

Organisms per Replicate: 5 organisms × 3 replicates (water), 10 organisms per treatment (no replicates, diet and soil)

Methods: Earthworms were exposed to nano-Ag via water, food, and soil, and were examined for apoptosis in cuticle, circular musculature, longitudinal musculature, intestinal epithelium, and chloragogenous matrix tissues using TUNEL and Apostain methods.

Study Outcome

Mortality. 40% mortality after 24 hours was observed in earthworms exposed to 100 mg nano-Ag per L water, though no mortality was observed in either the dietary exposure experiment or the soil-exposure experiment.

Apoptosis. Highly statistically significant levels of apoptosis were observed in all tissues at exposures of 100 mg nano-Ag per L water. The number of apoptotic cells per mm² was lower in both of the exposures in soil, but followed the same dose-related pattern as exposure in water. Cuticle, intestinal epithelium, and chloragog cells showed significantly higher apoptotic responses than that of muscular tissue at the highest exposure of each experiment.

Meyer et al. (2010) Intracellular uptake and associated toxicity of silver nanoparticles in *Caenorhabditis elegans*.

Test Species

Wild-type (N2) strains RB877 (*nth-1*), RB1072 (*sod-2*), RB864 (*xpa-1*), JF23 (*mtl-2*), and TK22 (*mev-1*) larvae of nematode *Caenorhabditis elegans*.

Material

Commercial PVP-coated nano-Ag purchased from NanoAmor (Los Alamos, NM) or citrate-coated nano-Ag synthesized by combining solutions of silver nitrate and sodium citrate.

Shape: Spherical (determined using TEM)

Composition: Not reported

Crystal Structure: Not reported

Average Size: 3, 13, and 76 nm (citrate-coated, small PVP-coated, large PVP-coated particles, respectively)

Size Distribution: Not reported

Solubility: Not reported

Surface Area: Not reported

Surface Treatment: Coated with PVP and citrate

Surface Charge: -33.0, -22.5, and -23.4 mV (citrate-coated, small PVP-coated, and large PVP-coated particles, respectively)

Protocol

Exposure Duration: 3 days

Endpoints: Growth

Exposure Concentrations: 0.5, 5, and 50 mg/L

Exposure Medium: Complete K⁺ medium

Organisms per Replicate: ~200 organisms × 24 replicates

Methods: Accounting for confounding due to toxic effects to the bacterial food supply and exposure to the particle coatings, the growth of *C. elegans* was measured after exposure to various sizes of nano-Ag particles by 50x magnification imaging.

Study Outcome

Internal retention of developing eggs, also known as "bagging" was observed in nematodes exposed to citrate-coated nano-Ag, indicating the uptake of significant amounts of nano-Ag particles as the cause of a stress response.

Growth. Growth was inhibited in wild-type nematodes exposed to citrate-coated nano-Ag at concentrations of 5 and 50 mg/L and to PVP-coated nano-Ag at a concentration of 50 mg/L. Authors ruled out mediation of toxicity due to toxic effects on the food source of the nematodes or toxic effects of the coatings of the particles.

Roh et al. (2009) Ecotoxicity of silver nanoparticles on the soil nematode *Caenorhabditis elegans* using functional ecotoxicogenomics.

Test Species

Soil nematode (3 days old), wild type and 3 mutants (*Caenorhabditis elegans* N2 var. Bristol, *mtl-2* [gk125], *sod-3* [gk235], and *daf-12* [rh286])

Material

Commercial nano-Ag purchased from Sigma-Aldrich (St. Louis, MO, USA).

Shape: Not reported

Composition: Not reported

Crystal Structure: Not reported

Average Size: Approximately 14–20 nm (determined using DLS)

Size Distribution: Not reported

Solubility: Not reported

Surface Area: Not reported

Surface Treatment: Not reported

Surface Charge: Not reported

Protocol

Exposure Duration: 24 (gene expression, survival, and growth) or 72 hours (reproduction)

Endpoints: Gene expression, survival, growth, and reproduction

Exposure Concentrations: 0.05, 0.1, and 0.5 mg/L

Exposure Medium: K-media

Organisms per Replicate: 800–1,000 × 3 replicates (gene expression), 10 × 5 replicates (survival), 150 × 5 replicates (growth), and 1 × 5 replicates (reproduction)

Methods: To determine effects on gene expression following exposure to nano-Ag, RNA was prepared and analyzed by microarray analysis and 26 genes were analyzed by real-time RT-PCR. At the end of the exposure period, survival was assessed by counting live and dead individuals, and growth was assessed in heat-killed samples by measuring body length. Reproduction was assessed by counting the number of offspring at all developmental stages beyond the egg following exposure of young adults to nano-Ag.

Study Outcome

Gene Expression. Microarray analysis revealed upregulation of 415 gene probes and downregulation of 1,217 by more than 2-fold compared to the controls. Thirteen gene ontology categories were significantly represented within upregulated genes and 149 in downregulated genes. Four genes analyzed by PCR were significantly upregulated (*M162.5*, nonannotated; *mtl-2*, stress-response metallothionein; *sod-3*, stress-response superoxide dismutase; and *daf-12*, stress-response abnormal dauer formation protein).

Survival and Growth. Survival and growth were not significantly affected in either the wild type or mutant *C. elegans*.

Reproduction. Reproduction decreased significantly in both wild type and mutant strains at all treatment levels except in *sod-3*(gk235) mutant exposed to 0.05 mg/L nano-Ag. Wild type and *daf-12*(rh286) were the most sensitive of the four types tested.

Sap-lam et al. (2010) UV irradiation-induced silver nanoparticles as mosquito larvicides.

Test Species

Fourth-stage larvae of mosquito (*Aedes aegypti*) from Chulalongkorn University, Bangkok, Thailand.

Material

Silver nanoparticles synthesized by adding PMA to AgNO₃ and exposed to low intensity UV lamp for 90 minutes.

Shape: Not reported

Composition: Not reported

Crystal Structure: Not reported

Average Size: 5–10 nm (determined by TEM)

Size Distribution: Not reported

Solubility: Not reported

Surface Area: Not reported

Surface Treatment: Polymethacrylic acid (PMA)-coated

Surface Charge: -27.7 mV (determined by zetasizer apparatus)

Protocol

Exposure Duration: 24 hours

Endpoints: Survival and hatchability

Exposure Concentrations: 0.01, 0.1, 1, and 5 ppm nano-Ag

Exposure Medium: Not reported

Organisms per Replicate: 20 organisms × 8 replicates

Methods: Survival of mosquito larvae was monitored after exposure to various concentrations of nano-Ag over 24 hours. Morphology of larvae was evaluated microscopically. Hatchability was also assessed.

Study Outcome

Survival. No significant increase in mortality was observed at concentrations of 0.01 and 0.1 ppm. Survival of larvae exposed to 1 ppm decreased to 88% after 24 hours of exposure, and at 5 ppm 90% mortality was observed after 3 hours of exposure.

Morphology. Authors noted dark spots in the abdomens of treated larvae.

Hatchability. A number of eggs hatched in the 5-ppm solution of nano-Ag; however, the mortality of the larvae upon hatching was immediate.

Shoultz-Wilson et al. (2011) Evidence for avoidance of Ag nanoparticles by earthworms (*Eisenia fetida*).

Test Species

Adult earthworm (*Eisenia fetida*).

Material

Nano-Ag powders purchased from NanoAmor (Houston, TX)

Shape: Not reported

Composition: Not reported

Crystal Structure: Not reported

Average Size: 10 nm (small PVP-coated particles) (determined by TEM)

Size Distribution: 15–25 nm (small citrate-coated particles); 30–50 nm (large PVP-coated particles and large oleic acid-coated particles) (determined by TEM)

Solubility: Not reported

Surface Area: Not reported

Surface Treatment: PVP, oleic acid, and citrate

Surface Charge: Not reported

Protocol

Exposure Duration: 48 hours

Endpoints: Contaminated soil avoidance

Exposure Concentrations: 9.0, 18, 27, 36, and 54 mg/kg-soil (small PVP-coated particles); 0.3, 1.0, 3.0, 9.0, and 27 mg/kg-soil (large PVP-coated particles); 9.0 mg/kg-soil (large oleic acid-coated and small citrate-coated particles)

Exposure Medium: Yeager Sandy Loam natural soil (Estill County, KY) or artificial soils with high and low pH

Organisms per Replicate: 10 organisms × 5 replicates

Methods: Earthworm soil preference of untreated soils and soils treated with nano-Ag was monitored in an avoidance assay performed according to standard protocol (ISO 2008). Soil type, soil characteristics, nano-Ag coating, and nano-Ag size were all tested as potential mediating variables of toxicity.

Study Outcome

Earthworms displayed avoidance of soils treated with nano-Ag after 48 hours, while displaying avoidance to soil treated with AgNO₃ immediately. Assays performed in natural soil revealed a significantly higher tendency of earthworms to avoid nano-Ag treated soil than in artificial soils. Earthworms avoided soils treated with small citrate-coated particles in natural soil significantly more than soil treated with large PVP-coated particles.

B.8. Summary of Nano-Ag Effects on Non-mammalian Terrestrial Vertebrates

Grodzik and Sawosz (2006) The influence of silver nanoparticles on chicken embryo development and bursa of Fabricius morphology.

Test Species

Ross hen embryos

Material

Commercial hydrocolloidal Ag suspension purchased from NanoTech (Poland) and diluted with NaCl.

Shape: Not reported

Solubility: Not reported

Composition: Not reported

Surface Area: Not reported

Crystal Structure: Not reported

Surface Treatment: Not reported

Average Size: Not reported

Surface Charge: Not reported

Size Distribution: Not reported

Protocol

Exposure Duration: 13 days

Exposure Medium: Egg interior

Endpoint: Development

Organisms per Replicate: 30 eggs × 1 replicate

Dose: 10 ppm administered on incubation days 5, 11, and 17

Methods: Eggs were injected with 10 ppm nano-Ag on incubation days 5, 11, and 17. Eggs were weighed on day 18, opened and sacrificed. Embryos' livers, hearts, and eyes were weighed and examined according to Hamburger and Hamilton standard (1951). Bursae of Fabricius (BF) were collected and treated for examination by microscope.

Study Outcome

Exposure to nano-Ag did not affect embryo weight or weights of liver, heart, or eyes. There was no significant difference in apoptotic signs between control and nano-Ag groups, and no necrosis was observed. The number and luminal intensity of cell nuclei in BFs of nano-Ag group were decreased and a slight increase was observed in the population of cells with peripherally deep staining nuclei (significance not reported).

Sawosz et al. (2007) Influence of hydrocolloidal silver nanoparticles on gastrointestinal microflora and morphology of enterocytes of quail.

Test Species

Quail (*Coturnix coturnix japonica*), approximately 10 days old, and quail gut microflora (*Escherichia coli*, *Enterobacter*, *Streptococcus bovis*, *Enterococcus faecium*, *Bacteroides* spp., *Actinomyces naeslundii*, *Lactobacillus salivarius*, *Lactobacillus fermentum*, and *Leuconostoc lactis*)

Material

Commercial hydrocolloidal Ag suspension purchased from NanoTech (Poland) and produced by solid-liquid phase discharge method.

Shape: Not reported

Solubility: Not reported

Composition: Not reported

Surface Area: Not reported

Crystal Structure: Not reported

Surface Treatment: Not reported

Average Size: 52% of Ag nanoparticles were 3–4 nm in size.

Surface Charge: Not reported

Size Distribution: 2 to >7nm (determined using TEM)

Protocol

Exposure Duration: 12 days

Exposure Medium: Drinking water

Endpoints: Bacterial content and tissue damage

Organisms per Replicate: 15 birds × 1 replicate

Exposure Concentrations: 0, 5, 15, and 25 mg/kg

Methods: Quail were allowed to drink freely from water containing nano-Ag. Following exposure for 12 days, quail were killed and caeca were opened. The mucosa was scraped and the number of total culturable anaerobic bacteria was enumerated along with other enterobacteria. Tissues samples of the duodenum were also analyzed.

Study Outcome

No pathological changes or behavioral changes were observed in quail exposed to nano-Ag. Composition of the gut microflora was significantly altered in the 25 mg/kg nano-Ag group, with significant increases in the *Lactobacillus* spp., *L. lactis*, and *A. naeslundii*. No significant changes were observed in the other bacteria tested. There were no changes in the structure of enterocytes, glands, or connective tissue of intestinal villi. There was also no change in number of leucocytes.

Appendix B References

- [Ahamed, M; Posgai, R; Gorey, T; Nielsen, M; Hussain, S; Rowe, J.](#) (2010). Silver nanoparticles induced heat shock protein 70, oxidative stress and apoptosis in *Drosophila melanogaster*. *Toxicol Appl Pharmacol* 242: 263-269. <http://dx.doi.org/10.1016/j.taap.2009.10.016>
- [Allen, H; Impellitteri, C; Macke, D; Heckman, J; Poynton, H; Lazorchak, J; Govindaswamy, S; Roose, D; Nadagouda, M.](#) (2010). Effects from filtration, capping agents, and presence/absence of food on the toxicity of silver nanoparticles to *Daphnia magna*. *Environ Toxicol Chem* 29: 2742-2750. <http://dx.doi.org/10.1002/etc.329>
- [Asharani, PW; Gong, ZY; Valiyaveetil, S.](#) (2008). Toxicity of silver nanoparticles in zebrafish models. *Nanotechnology* 19: 1-8.
- [Babu, K; Deepa, MA; Shankar, SG; Rai, S.](#) (2008). Effect of nano-silver on cell division and mitotic chromosomes: A prefatory siren. *IJNT* 2: 1.
- [Bae, E; Park, HJ; Lee, J; Kim, Y; Yoon, J; Park, K; Choi, K; Yi, J.](#) (2010). Bacterial cytotoxicity of the silver nanoparticle related to physicochemical metrics and agglomeration properties. *Environ Toxicol Chem* 29: 2154-2160. <http://dx.doi.org/10.1002/etc.278>
- [Bar-Ilan, O; Albrecht, RM; Fako, VE; Furgeson, DY.](#) (2009). Toxicity assessments of multisized gold and silver nanoparticles in zebrafish embryos. *Small* 5: 1897-1910. <http://dx.doi.org/10.1002/smll.200801716>
- [Bilberg, K; Malte, H; Wang, T; Baatrup, E.](#) (2010). Silver nanoparticles and silver nitrate cause respiratory stress in Eurasian perch (*Perca fluviatilis*). *Aquat Toxicol* In Press, Corrected Proof: 159-165. <http://dx.doi.org/10.1016/j.aquatox.2009.10.019>
- [Bradford, A; Handy, RD; Readman, JW; Atfield, A; Mühling, M.](#) (2009). Impact of silver nanoparticle contamination on the genetic diversity of natural bacterial assemblages in estuarine sediments. *Environ Sci Technol* 43: 4530-4536. <http://dx.doi.org/10.1021/es9001949>
- [Chae, Y; Pham, C; Lee, J; Bae, E; Yi, J; Gu, M.](#) (2009). Evaluation of the toxic impact of silver nanoparticles on Japanese medaka (*Oryzias latipes*). *Aquat Toxicol* 94: 320-327. <http://dx.doi.org/10.1016/j.aquatox.2009.07.019>
- [Choi, J; Kim, S; Ahn, J; Youn, P; Kang, J; Park, K; Yi, J; Ryu, D.](#) (2010). Induction of oxidative stress and apoptosis by silver nanoparticles in the liver of adult zebrafish. *Aquat Toxicol* 100: 151-159. <http://dx.doi.org/10.1016/j.aquatox.2009.12.012>
- [Choi, O; Clevenger, TE; Deng, B; Surampalli, RY; Ross, L, Jr; Hu, Z.](#) (2009). Role of sulfide and ligand strength in controlling nanosilver toxicity. *Water Res* 43: 1879-1886.
- [Choi, O; Deng, KK; Kim, NJ; Ross, L, Jr; Surampalli, RY; Hu, Z.](#) (2008). The inhibitory effects of silver nanoparticles, silver ions, and silver chloride colloids on microbial growth. *Water Res* 42: 3066-3074.
- [Choi, O; Hu, Z.](#) (2008). Size dependent and reactive oxygen species related nanosilver toxicity to nitrifying bacteria. *Environ Sci Technol* 42: 4583-4588.
- [Dasari, T; Hwang, H.](#) (2010). The effect of humic acids on the cytotoxicity of silver nanoparticles to a natural aquatic bacterial assemblage. *Sci Total Environ* 408: 5817-5823. <http://dx.doi.org/10.1016/j.scitotenv.2010.08.030>
- [Eaton, AD; Clesceri, LS; Rice, EW; Greenberg, AE; Franson, MAH.](#) (2005). *Standard Methods for the Examination of Water and Wastewater*. In AD Eaton; LS Clesceri; EW Rice; AE Greenberg; MAH Franson (Eds.), (21 ed.). Denver, CO: American Water Works Association.
- [El Badawy, A; Silva, R; Morris, B; Scheckel, K; Suidan, M; Tolaymat, T.](#) (2011). Surface charge-dependent toxicity of silver nanoparticles. *Environ Sci Technol* 45: 283-287. <http://dx.doi.org/10.1021/es1034188>

- El Badawy, AME; Luxton, TP; Silva, RG; Scheckel, KG; Suidan, MT; Tolaymat, TM. (2010). Impact of environmental conditions (pH, ionic strength, and electrolyte type) on the surface charge and aggregation of silver nanoparticles suspensions. *Environ Sci Technol* 44: 1260-1266. <http://dx.doi.org/10.1021/es902240k>
- Farkas, J; Christian, P; Gallego-Urrea, J; Roos, N; Hassellöv, M; Tollefsen, K; Thomas, K. (2011). Uptake and effects of manufactured silver nanoparticles in rainbow trout (*Oncorhynchus mykiss*) gill cells. *Reprod Toxicol* 101: 117-125. <http://dx.doi.org/10.1016/j.aquatox.2010.09.010>
- Gao, J; Wang, Y; Hovsepyan, A; Bonzongo, J. (2011). Effects of engineered nanomaterials on microbial catalyzed biogeochemical processes in sediments. *J Hazard Mater* 186: 940-945. <http://dx.doi.org/10.1016/j.jhazmat.2010.11.084>
- Gao, J; Youn, S; Hovsepyan, A; Llana, VL; Wang, Y; Bitton, G; Bonzongo, JC. (2009). Dispersion and toxicity of selected manufactured nanomaterials in natural river water samples: Effects of water chemical composition. *Environ Sci Technol* 43: 3322-3328.
- Griffitt, R; Hyndman, K; Denslow, N; Barber, D. (2009). Comparison of molecular and histological changes in zebrafish gills exposed to metallic nanoparticles. *Toxicol Sci* 107: 404. <http://dx.doi.org/10.1093/toxsci/kfn256>
- Griffitt, RJ; Luo, J; Gao, J; Bonzongo, JC; Barber, DS. (2008). Effects of particle composition and species on toxicity of metallic nanomaterials in aquatic organisms. *Environ Toxicol Chem* 27: 1972-1978.
- Grodzik, M; Sawosz, E. (2006). The influence of silver nanoparticles on chicken embryo development and bursa of Fabricius morphology. *J Anim Feed Sci* 15: 111-114.
- Heckmann, L; Hovgaard, M; Sutherland, D; Autrup, H; Besenbacher, F; Scott-Fordsmand, J. (2011). Limit-test toxicity screening of selected inorganic nanoparticles to the earthworm *Eisenia fetida*. *Ecotoxicology* 20: 226-233. <http://dx.doi.org/10.1007/s10646-010-0574-0>
- Hinther, A; Vawda, S; Skirrow, R; Veldhoen, N; Collins, P; Cullen, J; van Aggelen, G; Helbing, C. (2010). Nanometals induce stress and alter thyroid hormone action in amphibia at or below North American water quality guidelines. *Environ Sci Technol* 44: 8314-8321. <http://dx.doi.org/10.1021/es101902n>
- Hwang, ET; Lee, JH; Chae, YJ; Kim, YS; Kim, BC; Sang, BI; Gu, MB. (2008). Analysis of the toxic mode of action of silver nanoparticles using stress-specific bioluminescent bacteria. *Small* 4: 746-750.
- Ivask, A; Bondarenko, O; Jephthina, N; Kahru, A. (2010). Profiling of the reactive oxygen species-related ecotoxicity of CuO, ZnO, TiO₂, silver and fullerene nanoparticles using a set of recombinant luminescent *Escherichia coli* strains: differentiating the impact of particles and solubilised metals. *Anal Bioanal Chem* 398: 701-716. <http://dx.doi.org/10.1007/s00216-010-3962-7>
- Jin, X; Li, M; Wang, J; Marambio-Jones, C; Peng, F; Huang, X; Damoiseaux, R; Hoek, E. (2010). High-throughput screening of silver nanoparticle stability and bacterial inactivation in aquatic media: Influence of specific ions. *Environ Sci Technol* 44: 7321-7328. <http://dx.doi.org/10.1021/es100854g>
- Kelly, SP; Fletcher, M; Pärt, P; Wood, CM. (2000). Procedures for the preparation and culture of 'reconstructed' rainbow trout branchial epithelia. *Meth Cell Sci* 22: 153-163.
- Kennedy, A; Hull, M; Bednar, A; Goss, J; Gunter, J; Bouldin, J; Vikesland, P; Steevens, J. (2010). Fractionating nanosilver: importance for determining toxicity to aquatic test organisms. *Environ Sci Technol* 44: 9571-9577. <http://dx.doi.org/10.1021/es1025382>
- Khan, S; Mukherjee, A; Chandrasekaran, N. (2011). Silver nanoparticles tolerant bacteria from sewage environment. *J Environ Sci* 23: 346-352. [http://dx.doi.org/10.1016/S1001-0742\(10\)60412-3](http://dx.doi.org/10.1016/S1001-0742(10)60412-3)
- Kim, KJ; Sung, WS; Suh, BK; Moon, SK; Choi, JS; JG, K; Lee, DG. (2009). Antifungal activity and mode of action of silver nano-particles on *Candida albicans*. *Biometals* 22: 235-242.
- Kumari, M; Mukherjee, A; Chandrasekaran, N. (2009). Genotoxicity of silver nanoparticles in *Allium cepa*. *Sci Total Environ* 407: 5243-5246. <http://dx.doi.org/10.1016/j.scitotenv.2009.06.024>

- [Kvítek, L; Panáček, A; Soukupová, J; Kolář, M; Večeřová, R; Pruček, R; Holecová, M; R, Z.](#) (2008). Effect of surfactants and polymers on stability and antibacterial activity of silver nanoparticles (NPs). *J Phys Chem C* 112: 5825-5834. <http://dx.doi.org/10.1021/jp711616v>
- [Kvítek, L; Vanickova, M; Panacek, A; Soukupova, J; Dittrich, M; Valentova, E; Pruček, R; Bancirova, M; Milde, D; Zboril, R.](#) (2009). Initial study on the toxicity of silver nanoparticles (NPs) against *Paramecium caudatum*. *J Phys Chem B* 113: 4296-4300.
- [Laban, G; Nies, L; Turco, R; Bickham, J; Sepúlveda, M.](#) (2009). The effects of silver nanoparticles on fathead minnow (*Pimephales promelas*) embryos. *Ecotoxicology* 19: 185-195. <http://dx.doi.org/10.1007/s10646-009-0404-4>
- [Lapied, E; Moudilou, E; Exbrayat, J; Oughton, D; Joner, E.](#) (2010). Silver nanoparticle exposure causes apoptotic response in the earthworm *Lumbricus terrestris* (Oligochaeta). *Nanomed* 5: 975-984. <http://dx.doi.org/10.2217/nnm.10.58>
- [Lee, KJ; Nallathamby, PD; Browning, LM; Osgood, CJ; Z-HN, X.](#) (2007). In vivo imaging of transport and biocompatibility of single silver nanoparticles in early development of zebrafish embryos. *ACS Nano* 1: 133-143.
- [Li, T; Albee, B; Alemayehu, M; Diaz, R; Ingham, L; Kamal, S; Rodriguez, M; Bishnoi, S.](#) (2010b). Comparative toxicity study of Ag, Au, and Ag-Au bimetallic nanoparticles on *Daphnia magna*. *Anal Bioanal Chem* 398: 689-700. <http://dx.doi.org/10.1007/s00216-010-3915-1>
- [Lok, CN; Ho, CM; Chen, R; He, QY; Yu, WY; Sun, HZ; Tam, PKH; Chiu, JF.](#) (2006). Proteomic analysis of the mode of antibacterial action of silver nanoparticles. *J Proteome Res* 5: 916-924. <http://dx.doi.org/10.1021/pr0504079>
- [Martinez-Gutierrez, F; Olive, P; Banuelos, A; Orrantia, E; Nino, N; Sanchez, E; Ruiz, F; Bach, H; Av-Gay, Y.](#) (2010). Synthesis, characterization, and evaluation of antimicrobial and cytotoxic effect of silver and titanium nanoparticles. *Nanomed* 6: 681-688. <http://dx.doi.org/10.1016/j.nano.2010.02.001>
- [Meyer, J; Lord, C; Yang, X; Turner, E; Badireddy, A; Marinakos, S; Chilkoti, A; Wiesner, M; Auffan, M.](#) (2010). Intracellular uptake and associated toxicity of silver nanoparticles in *Caenorhabditis elegans*. *Aquat Toxicol* 100: 140-150. <http://dx.doi.org/10.1016/j.aquatox.2010.07.016>
- [Miao, AJ; Schwehr, K; Xu, C; Zhang, AJ; Luo, Z; Quigg, A.](#) (2009). The algal toxicity of silver engineered nanoparticles and detoxification by copolymeric substances. *Environ Pollut* 157: 3034-3041. <http://dx.doi.org/10.1016/j.envpol.2009.05.047>
- [MINCharInitiative](#) (Minimum Information on Nanoparticle Characterization). (2008). Recommended minimum physical and chemical parameters for characterizing nanomaterials on toxicology studies. Washington, DC: The Minimum Information for Nanomaterial Characterization Initiative. <http://characterizationmatters.org/parameters/>
- [Morones, JR; Elechiguerra, JL; Camacho, A; Holt, K; Kouri, JB; Ramirez, JT; Yacaman, MJ.](#) (2005). The bactericidal effect of silver nanoparticles. *Nanotechnology* 16: 2346-2353. <http://dx.doi.org/10.1088/0957-4484/16/10/059>
- [Nair, P; Park, S; Lee, S; Choi, J.](#) (2011). Differential expression of ribosomal protein gene, gonadotrophin releasing hormone gene and Balbiani ring protein gene in silver nanoparticles exposed *Chironomus riparius*. *Aquat Toxicol* 101: 31-37. <http://dx.doi.org/10.1016/j.aquatox.2010.08.013>
- [Navarro, E; Piccapietra, F; Wagner, B; Marconi, F; Kaegi, R; Odzak, N; Sigg, L; Behra, R.](#) (2008). Toxicity of silver nanoparticles to *Chlamydomonas reinhardtii*. *Environ Sci Technol* 42: 8959-8964. <http://dx.doi.org/10.1021/es801785m>
- [Pal, S; Tak, YK; Song, JM.](#) (2007). Does the antibacterial activity of silver nanoparticles depend on the shape of the nanoparticle? A study of the gram-negative bacterium *Escherichia coli*. *Appl Environ Microbiol* 73: 1712-1720. <http://dx.doi.org/10.1128/aem.02218-06>

- [Park, M; Kim, K; Lee, H; Kim, J; Hwang, S.](#) (2010b). Selective inhibitory potential of silver nanoparticles on the harmful cyanobacterium *Microcystis aeruginosa*. *Biotechnol Lett* 32: 423-428. <http://dx.doi.org/10.1007/s10529-009-0161-8>
- [Ringwood, A; McCarthy, M; Bates, T; Carroll, D.](#) (2010). The effects of silver nanoparticles on oyster embryos. *Neurotoxicol Teratol* 69: S49-S51. <http://dx.doi.org/10.1016/j.marenvres.2009.10.011>
- [Roh, JY; Sim, SJ; Yi, J; Park, K; Chung, KH; Ryu, DY; Choi, J.](#) (2009). Ecotoxicity of silver nanoparticles on the soil nematode *Caenorhabditis elegans* using functional ecotoxicogenomics. *Environ Sci Technol* 43: 3933-3940.
- [Rostami, AA; Shahsavar, A.](#) (2009). Nano-silver particles eliminate the in vitro contaminations of olive 'mission' explants. *Asian J Plant Sci* 8: 1-5.
- [Sap-Iam, N; Homklincha, C; Larpudomle, R; Warisnoich, W; Sereemaspu, A; Dubas, ST.](#) (2010). UV irradiation-induced silver nanoparticles as mosquito larvicides. *Journal of Applied Sciences* 10: 3132-3136. <http://dx.doi.org/10.3923/jas.2010.3132.3136>
- [Saulou, C; Jamme, F; Maranges, C; Fourquaux, J; Despax, B; Raynaud, P; Dumas, P; Mercier-Bonin, M.](#) (2010). Synchrotron FTIR microspectroscopy of the yeast *Saccharomyces cerevisiae* after exposure to plasma-deposited nanosilver-containing coating. *Anal Bioanal Chem* 396: 1441-1450. <http://dx.doi.org/10.1007/s00216-009-3316-5>
- [Sawosz, E; Binek, M; Grodzik, M; Zielinska, M; Sysa, P; Szmidt, M; Niemiec, T; Chwalibog, A.](#) (2007). Influence of hydrocolloidal silver nanoparticles on gastrointestinal microflora and morphology of enterocytes of quails. *Arch Anim Nutr* 61: 444-451.
- [Schreer, A; Tinson, C; Sherry, JP; Schirmer, K.](#) (2005). Application of Alamar blue/5-carboxyfluorescein diacetate acetoxymethyl ester as a noninvasive cell viability assay in primary hepatocytes from rainbow trout. *Anal Biochem* 344: 76-85. <http://dx.doi.org/10.1016/j.ab.2005.06.009>
- [Scown, T; Santos, E; Johnston, B; Gaiser, B; Baalousha, M; Mitov, S; Lead, J; Stone, V; Fernandes, T; Jepson, M; van Aerle, R; Tyler, C.](#) (2010). Effects of aqueous exposure to silver nanoparticles of different sizes in rainbow trout. *Toxicol Sci* 115: 521-534. <http://dx.doi.org/10.1093/toxsci/kfq076>
- [Shahbazzadeh, D; Ahari, H; Rahimi, NM; Dastmalchi, F; Soltani, M; Fotovat, M; Rahmannya, J; Khorasani, N.](#) (2009). The effects of nanosilver (Nanocid(R)) on survival percentage of rainbow trout (*Oncorhynchus mykiss*). *Pakistan J Nutr* 8: 1178-1179.
- [Shoultz-Wilson, WA; Zhurbich, OI; Mcnear, DH; Tsyusko, OV; Bertsch, PM; Unrine, JM.](#) (2011). Evidence for avoidance of Ag nanoparticles by earthworms (*Eisenia fetida*). *Ecotoxicology* 20: 385-396. <http://dx.doi.org/10.1007/s10646-010-0590-0>
- [Shrivastava, S; Bera, T; Roy, A; Singh, G; Ramachandrarao, P; Dash, D.](#) (2007). Characterization of enhanced antibacterial effects of novel silver nanoparticles. *Nanotechnology* 18: 1-9. <http://dx.doi.org/10.1088/0957-4484/18/22/225103>
- [Sinha, R; Karan, R; Sinha, A; Khare, SK.](#) (2011). Interaction and nanotoxic effect of ZnO and Ag nanoparticles on mesophilic and halophilic bacterial cells. *Bioresour Technol* 102: 1516-1520. <http://dx.doi.org/10.1016/j.biortech.2010.07.117>
- [Sondi, I; Salopek-Sondi, B.](#) (2004). Silver nanoparticles as antimicrobial agent: A case study on *E. coli* as a model for gram-negative bacteria. *J Colloid Interface Sci* 275: 177-182. <http://dx.doi.org/10.1016/j.jcis.2004.02.012>
- [Sotiriou, GA; Pratsinis, SE.](#) (2010). Antibacterial activity of nanosilver ions and particles. *Environ Sci Technol* 44: 5649-5654. <http://dx.doi.org/10.1021/es101072s>
- [Stampoulis, D; Sinha, S; White, J.](#) (2009). Assay-dependent phytotoxicity of nanoparticles to plants. *Environ Sci Technol* 43: 9473-9479. <http://dx.doi.org/10.1021/es901695c>
- [Wu, Y; Zhou, Q; Li, H; Liu, W; Wang, T; Jiang, G.](#) (2010). Effects of silver nanoparticles on the development and histopathology biomarkers of Japanese medaka (*Oryzias latipes*) using the partial-life test. *Aquat Toxicol* 100: 160-167. <http://dx.doi.org/10.1016/j.aquatox.2009.11.014>

[Yeo, M; Kang, M.](#) (2008). Effects of nanometer sized silver materials on biological toxicity during zebrafish embryogenesis. *Bull Kor Chem Soc* 29: 1179-1184.

[Yeo, MK; Pak, SW.](#) (2008). Exposing zebrafish to silver nanoparticles during caudal fin regeneration disrupts caudal fin growth and p53 signaling. *Mol Cell Toxicol* 4: 311-317.

Appendix C. Summary of Human Health Effects Studies of Nano-Ag

This page intentionally left blank.

Appendix C. Summary of Human Health Effects Studies of Nano-Ag

C.1. Study Selection Criteria	C-3
C.2. Summary of Key In Vitro Studies	C-4
Ahamed et al. (2008) DNA damage response to different surface chemistry of silver nanoparticles in mammalian cells.	C-4
Arora et al. (2009) Interactions of silver nanoparticles with primary mouse fibroblasts and liver cells.	C-5
Asharani et al. (2009) Cytotoxicity and genotoxicity of silver nanoparticles in human cells.	C-6
Carlson et al. (2008) Unique cellular interaction of silver nanoparticles: size-dependent generation of reactive oxygen species.	C-7
Greulich et al. (2009) Studies on the biocompatibility and the interaction of silver nanoparticles with human mesenchymal stem cells (hMSCs).	C-8
Hussain et al. (2005) In vitro toxicity of nanoparticles in BRL 3A rat liver cells.	C-9
Kim et al. (2010) Cytotoxicity and genotoxicity of nano-silver in mammalian cell lines.	C-10
Li et al. (2010a) Induction of cytotoxicity and apoptosis in mouse blastocysts by silver nanoparticles.	C-11
Liu et al. (2010) Impact of silver nanoparticles on human cells: effect of particle size.	C-12
Lu et al. (2010) Effect of surface coating on the toxicity of silver nanomaterials on human skin keratinocytes.	C-13
Paddle-Ledinek et al. (2006) Effect of different wound dressings on cell viability and proliferation.	C-14
Rosas-Hernández et al. (2009) Effects of 45-nm silver nanoparticles on coronary endothelial cells and isolated rat aortic rings.	C-15
Samberg et al. (2010) Evaluation of silver nanoparticle toxicity in vivo and keratinocytes in vitro.	C-16
Shin et al. (2007) The effects of nano-silver on the proliferation and cytokine expression by peripheral blood mononuclear cells.	C-17
Shrivastava et al. (2009) Characterization of antiplatelet properties of silver nanoparticles.	C-18
Trickler et al. (2010) Silver nanoparticle-induced blood-brain barrier inflammation and increased permeability in primary rat brain microvessel endothelial cells.	C-19
C.3. Summary of Key In Vivo Studies	C-20
Cha et al. (2008) Comparison of acute responses of mice livers to short-term exposure to nano-sized or micro-sized silver particles.	C-20
Ji et al. (2007) Twenty-eight-day inhalation toxicity study of silver nanoparticles in Sprague-Dawley rats.	C-21
Kim et al. (2008) Twenty-eight-day oral toxicity, genotoxicity, and gender-related tissue distribution of silver nanoparticles in Sprague-Dawley rats.	C-22
Lee et al. (2010) Genomics-based screening of differentially expressed genes in the brains of mice exposed to silver nanoparticles via inhalation.	C-23
Li et al. (2010a) Induction of cytotoxicity and apoptosis in mouse blastocysts by silver nanoparticles.	C-24
Park et al. (2010a) Repeated-dose toxicity and inflammatory responses in mice by oral administration of silver nanoparticles.	C-25
Samberg et al. (2010) Evaluation of silver nanoparticle toxicity in vivo and keratinocytes in vitro.	C-26
Shrivastava et al. (2009) Characterization of antiplatelet properties of silver nanoparticles.	C-27
Sung et al. (2008) Lung function changes in Sprague-Dawley rats after prolonged inhalation exposure to silver nanoparticles.	C-28
Sung et al. (2009) Subchronic inhalation toxicity of silver nanoparticles.	C-29
Takenaka et al. (2001) Pulmonary and systemic distribution of inhaled ultrafine silver particles in rats.	C-30
Tang et al. (2008) Influence of silver nanoparticles on neurons and blood-brain barrier via subcutaneous injection in rats.	C-31
Tiwari et al. (2011) Dose-dependent in-vivo toxicity assessment of silver nanoparticles in Wistar rats.	C-32
Appendix C References	C-33

This page intentionally left blank.

C.1. Study Selection Criteria

The process by which studies were selected for inclusion in the human health effects tables differed for each category of study (i.e., in vitro, in vivo) based on the quantity and quality of available toxicological data. In general, literature searches were conducted for specific human and rodent cell types, and later for specific toxicological endpoints, to identify relevant in vitro studies. Literature searches were also conducted for exposure pathways (e.g., inhalation, oral, dermal) to identify relevant rodent in vivo studies. To reflect the most current state of the science, the tables in this appendix include only studies published in or after 2000. The information presented here is up to date as of March 1, 2011, when the last broad literature search to identify new information was conducted. For those toxicological endpoints for which a substantial amount of information was available (e.g., mitochondrial function, reactive oxidative stress), studies examining relevant endpoints were selected based on the data quality and the relative contribution of the results to the state of the science (determined largely by examining the number of articles in which the study was later cited). Studies were also included if the investigators examined an endpoint for which there was otherwise little information, used a novel technique to assess toxicity, or compared the relative toxicities of nano-Ag with different sets of characteristics (e.g., nano-Ag of different sizes, surface areas, shapes). For study categories with very little available toxicological information, all identified studies were included unless they were judged to be of poor quality. In this case study, no studies were included for toxicity due to occupational exposure because no occupational effects studies specific to nano-Ag were identified.

Information in the tables is organized to take into account the minimum requirements for physicochemical characterization proposed by the Minimum Information for Nanomaterial Characterization (MINChar) Initiative and others ([MINCharInitiative, 2008](#)). The limited understanding of nano-Ag toxicity and its mechanisms, and the equivocal nature of some studies that give conflicting results, preclude the direct comparison of study results. To emphasize that caution is warranted in interpreting the results of the available toxicological studies of nano-Ag, these tables are organized in a way that emphasizes each study's relevant attributes in the context of this case study – especially characterization of the nano-Ag used in the study – rather than to facilitate direct comparison of results among studies.

C.2. Summary of Key In Vitro Studies

Ahamed et al. (2008) DNA damage response to different surface chemistry of silver nanoparticles in mammalian cells.

Test Species

Mouse embryonic stem cells (mES) and mouse embryonic fibroblasts (MEF)

Material

Commercial uncoated nano-Ag, supplied by Novacentrix, Austin, Texas, and polysaccharide-coated nano-Ag, supplied by Clark University, Potsdam, NY. Nano-Ag dispersions were vortexed.

Shape: Not reported

Solubility: Not reported

Composition: Not reported

Surface Area: Not reported

Crystal Structure: Not reported

Surface Treatment: Uncoated and polysaccharide-coated

Average Size: 25 nm (reported by manufacturer)

Surface Charge: Not reported

Size Distribution: Not reported

Protocol

Exposure Duration: 4, 24, 48, and 72 hours

Exposure Medium: Ham's F12 Dulbecco's modified eagle medium (DMEM)

Endpoint: Uptake, morphology, viability, and apoptosis

Exposure Concentrations: 50 µg/mL

Cell Density: Not reported

Methods: Uptake and morphology were measured by fluorescence and confocal microscopy. Morphology was also analyzed with sodium dodecyl sulfate polyacrylamide gel electrophoresis (SDS-Page) immunoblotting. Cell viability was assessed by 3-MTT-based cell viability test and by measuring annexin V protein.

Study Outcome

Uptake. The uncoated particles tended to agglomerate, suggesting they may not be found in some organelles (e.g., nucleus and mitochondria), while the coated particles appeared dispersed.

Membrane Integrity. Exposure to 50 µg/mL of uncoated or coated nano-Ag up-regulated cell cycle checkpoint protein p53 in mES and MEF cells. After 4 hours, p53 was phosphorylated only by coated nano-Ag, and only in mES cells. After 4 and 24 hours, both types of nano-Ag resulted in increased levels of the DNA damage repair proteins Rad51 and phosphorylated-H2AX expression in mES cells. Though significance was not reported, they report that cellular response to coated nano-Ag appears greater than uncoated nano-Ag.

Mitochondrial Function. Exposure to 50 µg/mL of uncoated and coated nano-Ag induced mES and MEF cell death (annexin V protein expression and MTT assay). The annexin V expression was higher in MEF cells treated with coated nano-Ag.

Arora et al. (2009) Interactions of silver nanoparticles with primary mouse fibroblasts and liver cells.

Test Species

Primary mouse fibroblasts and liver cells

Material

Nano-Ag synthesized by photo-assisted reduction of Ag⁺ to metallic nanoparticles.

Shape: Spherical

Composition: Not reported

Crystal Structure: Not reported

Average Size: 16.6 nm (determined using DLS)

Size Distribution: 6.5–43.8 nm (determined using DLS)

Solubility: Not reported

Surface Area: Not reported

Surface Treatment: Not reported

Surface Charge: Not reported

Protocol

Exposure Duration: 24 hours

Endpoint: Morphology, viability, antioxidant defense, and apoptosis

Exposure Concentrations: 0, 0.78, 1.56, 3.12, 6.25, 12.5, 25, 50, 100, 150, 200, 250, 300, 350, 400, and 500 µg/mL

Exposure Medium: Colloidal aqueous solution

Cell Density: 2 × 10⁴ cells/2 mL growth medium/plate (morphology and apoptosis); 1 × 10⁴ cells/200 µL growth medium/well (cytotoxicity)

Methods: Cell morphology was examined by phase contrast microscopy and cell viability was assessed by XTT-based cell viability test. Glutathione (GSH) reduction and antioxidant defense were used in the estimation of enzyme activity. Apoptosis was measured by using a colorimetric assay and fluorescence microscopy.

Study Outcome

Morphology. Cells less polyhedral, more fusiform, and shrunken with treatment concentration from 50 µg/mL to 100 µg/mL. Primary liver cells displayed no changes relative to control cells at concentrations of 100 µg/mL and below. At 200 µg/mL and above, primary liver cells displayed damaged irregular cell membranes.

Membrane Integrity. IC₅₀: 61 µg/mL primary fibroblasts; 449 µg/mL primary liver cells; spherical assemblages were found inside the mitochondria of both treated fibroblasts and liver cells, also in the vacuoles of liver cells.

Superoxide Dismutase (SOD). In primary fibroblasts, changes in SOD levels were statistically insignificant. In primary liver cells, SOD levels increased from 9.2 micromoles per milligram (µM/mg) protein in untreated cells to 13 µM/mg protein in treated cells, a factor of 1.4.

Lipid Peroxidation. In primary fibroblasts, lipid peroxidation decreased from 0.31 µM/mg protein in untreated cells to 0.22 µM/mg protein in treated cells, a factor of 1.4. In primary liver cells, changes in lipid peroxidation were statistically insignificant.

GSH Reduction. In primary fibroblasts, GSH levels increased from 0.82 µM/mg protein in untreated cells to 0.95 µM/mg protein in treated cells, a factor of 1.2. In primary liver cells, GSH levels increased from 72.3 µM/mg protein in untreated cells to 79 µM/mg protein in treated cells, a factor of 1.1.

Apoptosis. Nano-Ag induced apoptosis at concentrations in the ranges 3.12–50 µg/mL and 12.5–400 µg/mL for primary fibroblasts and primary liver cells, respectively. For primary fibroblasts, 69% live cells, 24% apoptotic cells, and 7% necrotic cells were observed at nano-Ag concentration 30 µg/mL (~ ½ IC₅₀) whereas, at 4-fold higher nano-Ag concentration (~2 × IC₅₀), 37% live cells, 17% apoptotic cells, and 46% necrotic cells were observed. In the case of primary liver cells, 71% live cells, 24% apoptotic cells, and 5% necrotic cells and 32% live cells, 14% apoptotic cells, and 54% necrotic cells for ~1/2 IC₅₀ and ~2 × IC₅₀, respectively.

Asharani et al. (2009) Cytotoxicity and genotoxicity of silver nanoparticles in human cells.

Test Species

Normal human lung fibroblast cells (IMR-90) and human glioblastoma cells (U251)

Material

Nano-Ag synthesized by reducing AgNO₃ solution using NaBH₄

Shape: Not reported

Composition: Not reported

Crystal Structure: Not reported

Average Size: 6 to 20 nm (determined using TEM and UV absorption)

Size Distribution: Not reported

Size Distribution: Not reported

Solubility: Not reported

Surface Area: Not reported

Surface Treatment: Coated with starch

Surface Charge: Not reported

Protocol

Exposure Duration: 24, 48, and 72 hours

Endpoint: Morphology, viability, reactive oxygen species (ROS) generation, cell cycle, apoptosis, genotoxicity, and uptake

Exposure Concentrations: 0, 25, 50, 100, 200, and 400 µg/mL

Exposure Media: Dulbecco's modified eagle medium (DMEM) with 10% fetal bovine serum (FBS) and 1% penicillin streptomycin (U251); glutamine with 15% FBS, 1% each of penicillin streptomycin, nonessential amino acids, vitamins, and 2% essential amino acids

Cell Density: 1 × 10⁴ cells

Methods: Morphology was assessed by TEM and STEM; ATP concentration was measured using Cell-Titer glow luminescent cell viability assay; mitochondrial function was analyzed using a CellTiter blue cell viability assay; ROS generation was assessed using DCF-DA and DHE staining methods; apoptosis was measured using Annexin-V staining; genotoxicity was analyzed using comet assay and cytokinesis-blocked micronucleus assay; and uptake was studied using TEM.

Study Outcome

Cell Morphology. Treated cells were clustered with few cellular extensions and displayed restricted spreading patterns.

ATP Concentration. ATP assays demonstrated a concentration- and time-dependent decrease in luminescence intensity in both IMR-90 and U251 cells, with ATP content declining statistically after 48 hours.

Mitochondrial Function. CellTiter blue cell viability assays demonstrated a concentration-dependent decrease in mitochondrial activity in both IMR-90 and U251 cells.

ROS Generation. Statistically significant increase in hydrogen peroxide and superoxide production in cells treated with 25 and 50 µg/mL; however no significant increase was observed beyond 100 µg/mL.

Cell Cycle. Possible mechanism of toxicity is proposed which involves disruption of the mitochondrial respiratory chain by Ag-NP leading to production of ROS and interruption of ATP synthesis, which in turn cause DNA damage. It is anticipated that DNA damage is augmented by deposition, followed by interactions of nano-Ag to the DNA leading to cell cycle arrest in the gap-2/mitosis (G2/M) phase.

Apoptosis. Apoptotic cells populations increased from 25 to 100 µg/mL in IMR-90 cells. Late apoptosis and necrosis caused 16% (±5) of cell death.

Chromosomal Aberrations. Chromosomal breaks were observed in cells treated with nano-Ag.

DNA Damage. A concentration-dependent increase was observed in tail momentum. A concentration-dependent increase in DNA damage was observed in U251 cells, while DNA damage did not increase beyond 100 µg/mL in IMR-90 cells.

Uptake. Treated cells displayed endosomes containing many nanoparticles near the cell and nuclear membrane, suggesting nanoparticles more likely entered through endocytosis than diffusion. Nanoparticles were found throughout the cytoplasm, as well as inside lysosomes, mitochondria, nucleolus, and nucleus.

Carlson et al. (2008) Unique cellular interaction of silver nanoparticles: size-dependent generation of reactive oxygen species.

Test Species

Rat alveolar macrophages (NR8383 CRL-2192)

Material

Commercially-available hydrocarbon-coated silver (NovaCentrix, formerly Nanotechnologies, Inc.).

Shape: Spherical (confirmed by SEM)

Composition: Not reported

Crystal Structure: Not reported

Average Size: 15, 20, and 50 nm (reported by manufacturer); 15, 30, and 55 nm (determined using microscopy)

Size Distribution: Not reported

Solubility: Insoluble

Solubility: Insoluble

Surface Area: Not reported

Surface Treatment: Hydrocarbon coated (~2 nm thick) to prevent sintering during plasma synthesis and maintain constant coating in aqueous solutions

Surface Charge: Not reported

Protocol

Exposure Duration: 24 hours

Endpoint: Uptake, morphology, viability, inflammatory response, reactive oxygen species (ROS) generation

Exposure Concentrations: 0, 5, 10, 25, 50, and 75 µg/mL

Exposure Medium: Ham's Nutrient Mixture F12K

Cell Density: 80% confluency

Methods: Following 24-hour incubation of treated samples, uptake, and morphology examined by light microscopy and TEM (uptake only). Cell viability assessed by MTT-based cell viability test, membrane integrity assessed using fluorescence to measure lactate dehydrogenase (LDH) released, and mitochondrial membrane potential assay measured by fluorescence. Glutathione (GSH) levels and inflammatory responses measured by GSH assay and enzyme-linked immunosorbent assay (ELISA), respectively. ROS generation determined using dichlorofluorescein diacetate (DCFH-DA).

Study Outcome

Uptake. Nanoparticles of all sizes taken up into cells.

Cell Morphology. Cells dosed with 15-nm particles (only 0, 25, and 75 µg/mL tested) appeared shrunken and lacked defined plasma membrane. Agglomerated nano-Ag observed inside and outside cells dosed with 30-nm particles, and macrophages appeared larger. 55-nm particles agglomerated and were not observed inside the cells.

Mitochondrial Function. EC₅₀: 27.87 ± 12.23 µg/mL 15-nm particles; EC₅₀: 33.38 ± 11.48 µg/mL 30-nm particles; EC₅₀ greater than 75 µg/mL 55-nm particles; tests with silver nitrate (AgNO₃) produced results similar to 15-nm nano-Ag.

Mitochondrial Membrane Potential (MMP). Statistically significant loss of MMP observed with increasing dose for 15- and 30-nm nano-Ag. Loss of MMP may be size dependent and warrants further study to determine if cell death is result of mitochondrial-instigated apoptosis.

Membrane Integrity. Statistically significant, dose-dependent decrease in cell viability for 15-nm and 30-nm nano-Ag at concentrations between 10 and 75 µg/mL. Decrease in cell viability as compared to control not statistically significant until 75 µg/mL dose for samples treated with 55-nm nano-Ag.

GSH Reduction. GSH levels decreased with increasing dose for both 15-nm and 30-nm, and the GSH level was undetectable at 50 µg/mL. However, the same responses were not seen for the 55-nm doses.

ROS Generation. For 15-nm particles, statistically significant increases in ROS with increasing dose from 10 µg/mL to 50 µg/mL. Results for 30- and 55-nm particles not statistically different from control.

Inflammatory Response. Statistically significant increases in the cytokines, TNF-α, MIP-2, and IL-1β at all doses (5, 10, and 25 µg/mL tested), but responses showed no trend with size or concentration. No increases occurred in IL-6 cytokine, but this was unexplained in the study.

Greulich et al. (2009) Studies on the biocompatibility and the interaction of silver nanoparticles with human mesenchymal stem cells (hMSCs).

Test Species

Human mesenchymal stem cells (hMSC)

Material

Nano-Ag particles prepared by polyol process using AgNO_3 in $\text{C}_2\text{H}_6\text{O}_2$ and polyvinylpyrrolidone (PVP).

Shape: Spherical

Composition: Pure silver

Crystal Structure: Not reported

Average Size: 100 nm (determined using DLS)

Size Distribution: 35 nm to 350 nm with median of 100 nm (determined using DLS)

Solubility: Not reported

Surface Area: Not reported

Surface Treatment: PVP

Surface Charge: Not reported

Protocol

Exposure Duration: 7 days

Endpoint: Morphology, viability, inflammatory response, and chemotaxis

Exposure Concentrations: 0, 0.05, 0.5, 1, 2.5, 3, 3.5, 4, 5, and 50 $\mu\text{g}/\text{mL}$

Exposure Medium: Cell culture medium RPMI1640 with 10% fetal calf serum

Cell Density: Not reported

Methods: hMSCs treated with nano-Ag/ultrapure water solution or silver acetate/ultrapure water solution. Cell viability assessed by fluorescence staining and microscopy after 7 days of incubation. Morphology of cells in same samples observed by phase-contrast microscopy. Chemotaxis analyzed by transwell assay using peripheral blood mononuclear cells as chemoattractants. Inflammatory response assessed via enzyme-linked immunosorbent assay (ELISA).

Study Outcome

Preliminary experiment with nano-Ag in different fluids and cell media showed no agglomeration of nano-Ag particles in cell culture media with fetal calf serum but agglomeration when cells were incubated in phosphate-buffered saline or culture medium alone.

Viability. No viable cells detected in samples treated at concentrations between 3.5 and 50 $\mu\text{g}/\text{mL}$ nano-Ag particles and between 2.5 and 50 $\mu\text{g}/\text{mL}$ silver acetate.

Chemotaxis. Observed decreasing chemotactic response with increasing silver concentration for both nano-Ag particles and silver acetate solution. Response statistically significant compared to control for nano-Ag doses of 3.5, 4, and 5 $\mu\text{g}/\text{mL}$ and for silver acetate doses of 2.5, 3, 3.5, 4, and 5 $\mu\text{g}/\text{mL}$.

Inflammatory Response. Observed decrease in the release of interleukin-6 (IL-6), interleukin-8 (IL-8), and vascular endothelial growth factor (VEGF) from cells for Ag particle and Ag ion doses of 0.05–50 $\mu\text{g}/\text{mL}$. Release of interleukin-11 (IL-11) in adherent cells was not affected following silver treatment; however IL-11 release resembled that of IL-6 or VEGF when silver was added during cell seeding.

Hussain et al. (2005) In vitro toxicity of nanoparticles in BRL 3A rat liver cells.

Test Species

BRL 3A (ATCC, CRL-1442) immortalized rat liver

Material

Commercial nano-Ag, supplied by Air Force Research Laboratory, Brooks AFB, Texas.

Shape: Not reported

Composition: Not reported

Crystal Structure: Not reported

Average Size: 15 and 100 nm (reported by manufacturer)

Size Distribution: Not reported

Solubility: Ag-100 nm was not homogeneously suspended in solution

Surface Area: Not reported

Surface Treatment: Not reported

Surface Charge: Not reported

Protocol

Exposure Duration: 24 hours

Endpoint: Morphology, viability, and reactive oxygen species (ROS) generation

Exposure Concentrations: 0, 2.5, 5, 10, 25, 50 and 150 $\mu\text{g/mL}$

Exposure Medium: Culture media with 5% fetal bovine serum

Cell Density: Confluent

Methods: After exposure, morphology was observed by microscopy. Membrane integrity was measured by measuring lactate dehydrogenase (LDH) leakage, cell viability was assessed spectrophotometrically by MTT-based cell viability test, ROS generation was determined using dichlorodihydrofluorescein diacetate (H_2 DCFDA), mitochondrial membrane potential was determined by the uptake of rhodamine 123, reduced glutathione (GSH) measured by GSH assay.

Study Outcome

Cell Morphology. Cells began to shrink and became irregular in shape with increasing doses of nano-Ag.

Membrane Integrity. LDH EC_{50} : $24 \pm 9.25 \mu\text{g/mL}$ 100-nm particles; LDH EC_{50} : $50 \pm 10.25 \mu\text{g/mL}$ 15-nm particles; statistically significant concentration-dependent decrease in cell viability for 100-nm and 15-nm particles at concentrations between 10 and 50 $\mu\text{g/mL}$, with 100-nm particles demonstrating higher toxicity at 25 and 50 $\mu\text{g/mL}$.

Mitochondrial Function. MTT EC_{50} : $19 \pm 5.2 \mu\text{g/mL}$ 100-nm particles; MTT EC_{50} : $24 \pm 7.25 \mu\text{g/mL}$ 15-nm particles; Ag exposure demonstrated a significant cytotoxicity from 5 to 50 $\mu\text{g/mL}$.

GSH Reduction. Statistically significant decrease of GSH (70%) at 25 $\mu\text{g/mL}$, relative to controls.

ROS Generation. Statistically significant concentration-dependent increase in ROS generation from 10 $\mu\text{g/mL}$, with an approximately 10-fold increase in ROS generation at 25 and 50 $\mu\text{g/mL}$ over control levels.

Mitochondrial Membrane Potential (MMP). Statistically significant decrease (80%) of MMP at 25 and 50 $\mu\text{g/mL}$

Kim et al. (2010) Cytotoxicity and genotoxicity of nano-silver in mammalian cell lines.

Test Species

Mouse lymphoma L5178Y cells and human bronchial epithelial BEAS-2B cells

Material

Silver nanopowder purchased from Aldrich, USA.

Shape: Not reported

Composition: Not reported

Crystal Structure: Not reported

Average Size: Not reported

Size Distribution: <100 nm (reported by the manufacturer)

Solubility: Not reported

Surface Area: Not reported

Surface Treatment: Not reported

Surface Charge: Not reported

Protocol

Exposure Duration: 3 hours

Endpoint: DNA damage, cytotoxicity, mutation frequency

Exposure Concentrations: 0, 942.38, 1,884.77, 3,769.53 µg/mL (mouse lymphoma cells, with S-9), 449.22, 898.44, 1,796.88 µg/mL (mouse lymphoma cells, without S-9), 292.97, 585.94, 1,171.88 µg/mL (human bronchial epithelial cells, with S-9), 190.43, 380.86, 761.72 µg/mL (human bronchial epithelial cells, without S-9) (comet assay); 0, 313, 625, 1,250, 2,500, 3,750 (mouse lymphoma assay).

Exposure Medium: Cell culture medium RPMI-1640 with 1 mM sodium pyruvate, 0.1% pluronic, 10% heat-inactivated horse serum, and S-9 mixture (comet assay); THMG medium and S-9 mixture (mouse lymphoma assay)

Cell Density: Not reported

Methods: DNA damage and cytotoxicity were determined by a comet assay involving both mouse lymphoma cells and human bronchial epithelial cells with and without metabolic activation. Genotoxicity was assessed in a mouse lymphoma assay performed with and without metabolic activation.

Study Outcome

DNA Damage. Nano-Ag significantly induced a higher incidence of DNA damage at all exposure levels with and without the addition of S-9 mixture in the comet assay.

Cytotoxicity. Exposure to nano-Ag increased cytotoxicity in a dose-dependent manner without metabolic activation in the mouse lymphoma assay, with pronounced but not significant drops in RS and RTG.

Mutation Frequency. Mutation frequencies were comparable to historical controls. Exposure to nano-Ag did not significantly affect the level of mutation frequencies at any dose level with or without metabolic activation by S-9 fraction.

Li et al. (2010a) Induction of cytotoxicity and apoptosis in mouse blastocysts by silver nanoparticles.

Test Species

ICR mouse blastocytes

Material

Nano-Ag prepared by the polyol process (reduction of AgNO₃ with C₂H₆O₂ in the presence of polyvinylpyrrolidone [PVP]).

Shape: Not reported

Solubility: Not reported

Composition: Not reported

Surface Area: Not reported

Crystal Structure: Not reported

Surface Treatment: Coated with a shell of polymer to reduce cluster formation

Average Size: 13 nm (determined using TEM)

Size Distribution: 6–24 nm (determined using TEM)

Surface Charge: Not reported

Protocol

Exposure Duration: 24 hours

Exposure Concentrations: 0, 25, and 50 μM

Endpoint: Cytotoxicity, embryonic developmental potential, and cell proliferation

Exposure Medium: BSA-free M₂ medium with 0.1% PVP

Cell Density: Not reported

Methods: DNA fragmentation, a characteristic of cell apoptosis, was assessed using a Terminal deoxynucleotidyl transferase dUTP nick end labeling (TUNEL) assay. Cell proliferation and assessment of whether inner cell mass (ICM) or thymic epithelial (TE) cells were most affected by exposure was performed following differential staining and cell counting. Embryonic developmental potential was tested by comparing the ratio of morulas to blastocysts in treated and untreated cells.

Study Outcome

Cytotoxicity. A nine-fold increase in incidence of apoptosis was observed in cells treated with 50 μM nano-Ag.

Embryonic Developmental Potential. The ratio of morulas to blastocysts was significantly lower in cells treated with 50 μM nano-Ag than that of the control cells. The rate of embryo attachment to culture dishes was higher, and the number of post-implantation developmental milestones lower, in blastocysts treated with 50 μM nano-Ag.

Cell Proliferation. Significantly fewer ICM and TE cells were observed in cells treated with 50 μM nano-Ag than in control cells. These cells also contained a higher incidence of apoptotic cells.

Liu et al. (2010) Impact of silver nanoparticles on human cells: effect of particle size.

Test Species

Human lung adenocarcinoma epithelial (A549) cells, human stomach cancer (SGC-7901) cells, human hepatocellular carcinoma (HepG2) cells, and human breast adenocarcinoma (MCF-7) cells

Material

5- and 20-nm nano-Ag particles purchased from Huzheng Nano Technology Limited Company, Shanghai, China; 50-nm particles synthesized by reduction of AgNO₃.

Shape: Not reported

Solubility: Not reported

Composition: Not reported

Surface Area: Not reported

Crystal Structure: Not reported

Surface Treatment: 5- and 20-nm particles coated with PVP

Average Size: 5.9, 23.8, and 47.5 nm (determined using TEM)

Surface Charge: Not reported

Size Distribution: 2.6–9.2 nm, 17.1–30.5 nm, 25.4–69.6 nm (determined using TEM)

Protocol

Exposure Duration: 24 hours

Exposure Medium: Unspecified medium containing 10% fetal bovine serum

Endpoint: Cytotoxicity, cell morphology, cellular uptake, oxidative stress, cell cycle progression

Cell Density: 1×10^5 cells per dish

Exposure Concentrations: 0, 0.01, 0.1, 0.5, 1, 2.5, 5, 10, 25, 50, and 100 µg/mL

Methods: Cytotoxicity was evaluated in an MTT assay and morphological changes evaluated visually. Cellular uptake of particles, cellular oxidative stress, and cell cycle progression were also assessed.

Study Outcome

Cytotoxicity. Dose-dependent toxicity was observed in all cell types. Toxicity was size-dependent, with the smaller particles producing the most and the larger particles producing the least toxic reaction. An increased fraction of apoptotic cells was observed in cells exposed to nano-Ag.

Cell Morphology. Dose-related morphological alterations were observed in HepG2 cells.

Cellular Uptake. 0.004–0.031% of silver entered the cells in a potentially size-dependent manner.

Oxidative Stress. Strongly fluorescent cells were observed in treated groups, indicating that reactive oxygen species were evoked by silver nanoparticles.

Cell Cycle Progression. Changes in proportion of cells in G1 and S phases from treated cells to controls suggest that the cell cycle was disturbed by exposure to nano-Ag.

Lu et al. (2010) Effect of surface coating on the toxicity of silver nanomaterials on human skin keratinocytes.

Test Species

Human skin HaCaT keratinocytes

Material

Silver nanoparticles synthesized according to the conventional citrate reduction method.

Shape: Spheres and prisms (characterized by TEM)

Solubility: Not reported

Composition: Not reported

Surface Area: Not reported

Crystal Structure: Not reported

Surface Treatment: Coated with citrate ions and PVP

Average Size: 30 nm (determined using TEM)

Surface Charge: Not reported

Size Distribution: Not reported

Protocol

Exposure Duration: 3 weeks

Exposure Medium: Modified Eagle's Medium with 10% FBS

Endpoint: Cell viability, cytotoxicity, genotoxicity

Exposure Concentrations: 10 to 100 µg/mL

Cell Density: Not reported

Methods: HaCaT cell viability was assessed after exposure to spherical and prism-shaped silver nanoparticles in the comet assay. A separate assay compared the toxicity of particles coated with citrate ions or PVP after exposure to sunlight.

Study Outcome

Viability and Cytotoxicity. No difference in cell viability was observed between treated and untreated cells with colloidal nanoparticles in the presence or absence of sunlight. Cell viability was significantly decreased when exposed to powder form of the citrate-coated particles that had been dried under direct sunlight. This decrease in viability was not observed in cells treated with the powder form of PVP-coated particles.

Genotoxicity. Citrate-coated colloidal nanoparticles at 100 µg/mL were not genotoxic.

Paddle-Ledinek et al. (2006) Effect of different wound dressings on cell viability and proliferation.

Test Species

Human keratinocytes

Material

Acticoat (nanocrystalline Ag/Polyethylene mesh), manufactured by Smith & Nephew; Aquacel-Ag (Ag ions/cm cellulose), manufactured by ConvaTec; Avance (Ag/Polyurethane foam), manufactured by SSL; and Constreet-H (Ag/Hydrocolloid/alginate), manufactured by Coloplast.

Shape: Not reported**Composition:** Not reported**Crystal Structure:** Not reported**Average Size:** Not reported**Size Distribution:** Not reported**Solubility:** Not reported**Surface Area:** Not reported**Surface Treatment:** Not reported**Surface Charge:** Not reported**Protocol****Exposure Duration:** 40 hours**Endpoint:** Viability, proliferation, morphology**Exposure Concentrations:** Acticoat (109 mg/100 cm²);Aquacel-Ag (19.7 mg/100 cm²); Avance (1.6 mg/100 cm²);Constreet-H (31–32 mg/100 cm²)**Exposure Medium:** Basal keratinocyte serum-free medium supplemented with L-glutamine, bovine pituitary extract, and recombinant epidermal growth factor**Cell Density:** 6,000 cells/well

Methods: Cell viability was assessed by estimation of mitochondrial ability to reduce MTT and cell proliferation was estimated by measuring the incorporation of bromodeoxyuridine (Br-dU) into nuclear DNA, both using a microplate reader. Phase contrast microscopy was used to assess cell morphology.

Study Outcome

Viability and Proliferation. Percent MTT reduction and percent Br-dU incorporation listed below.

Sample	Percent MTT Reduction		Percent Br-dU Incorporation	
	% Control (mean ± SE)	% Control (range)	% Control (mean ± SE)	% Control (range)
Acticoat	1.3 ± 0.3	0.5–2.5	8.5 ± 0.8	5.2–11.4
Aquacel-Ag	0.6 ± 0.1	0.3–1.4	5.6 ± 1.6	0.0–8.7
Avance	15.2 ± 6.3	1.9–46.0	12.5 ± 1.8	4.7–18.4
Contreet-H	1.0 ± 0.2	0.2–1.9	9.8 ± 3.0	0–34.2

Cell Morphology. In no extracts was there any evidence of a monolayer, and cell apposition did not follow the normal pattern. All treated cells lacked conspicuous nuclei, had missing nucleoli, and cultures displayed particulate and irregularly shaped cell debris. Cells treated with Contreet-H and Avance extracts were three times larger than control cells and displayed abundant polygonal cytoplasm with many cells showing cytoplasmic projections. Cells treated with Aquacel-Ag and Acticoat extracts had a round to ovoid cytoplasm.

Rosas-Hernández et al. (2009) Effects of 45-nm silver nanoparticles on coronary endothelial cells and isolated rat aortic rings.

Test Species

Rat coronary endothelial cells (CECs)

Material

Commercial nano-Ag, supplied by Novacentrix Inc., Austin, Texas.

Shape: Irregular spheres

Composition: Not reported

Crystal Structure: Not reported

Average Size: 45 nm (reported by manufacturer);

35.75 ± 13.1 nm (determined using TEM)

Size Distribution: 10–90 nm (determined using TEM)

Solubility: Not reported

Surface Area: Not reported

Surface Treatment: Not reported

Surface Charge: Not reported

Protocol

Exposure Duration: 24 hours

Endpoint: Proliferation, nitric oxide production, cytotoxicity, aortic ring vascular tone

Exposure Concentrations: 0, 0.1, 0.5, 1, 5, 10, 50, and 100 µg/mL

Exposure Medium: Dulbecco's modified eagle medium (DMEM) for cultured cells; Krebs-Henseleit (K-H) for rat aortic ring

Cell Density: Not reported

Methods: Proliferation was measured by MTT assay, and nitric oxide production was measured using the Griess reaction to determine the ratio of total nitrites to total nitrates. Cytotoxicity was assessed using a cytotoxicity assay kit to detect the level of lactate dehydrogenase (LDH). Aortic ring vascular tone was analyzed by pre-contracting rat aortic vessels with 5 and 100 µg/mL nano-Ag.

Study Outcome

Proliferation. Mitochondrial function was significantly decreased at concentrations of 1, 5, and 10 µg/mL and significantly increased at concentrations of 50 and 100 µg/mL.

Nitric Oxide Production. Concentrations of 10, 50, and 100 µg/mL were associated with significantly increased production of nitric oxide.

Cytotoxicity. LDH activity was significantly increased at concentrations of 1, 5, and 10 µg/mL.

Aortic Ring Vascular Tone. Rat aortic rings were constricted at 5 µg/mL and relaxed at 100 µg/mL.

Samberg et al. (2010) Evaluation of silver nanoparticle toxicity in vivo and keratinocytes in vitro.

Test Species

Primary neonatal human epidermal keratinocytes (HEKs)

Material

Three sizes (reported by manufacturer as 20, 50, and 80 nm in diameter) of commercial unwashed/uncoated and washed/uncoated nano-Ag in deionized water and two sizes (reported by manufacturer as 25 and 35 nm in diameter) of dried/carbon-coated nano-Ag powder, all supplied by nanoComposix, San Diego, CA. Unwashed and washed nano-Ag synthesized by manufacturer using ammonium hydroxide-catalyzed growth onto 5-nm gold seed particles. Carbon-coated nano-Ag synthesized by manufacturer using pulsed plasma reactor and coated with polyaromatic graphitic carbon.

Shape: Not reported

Composition: Not reported

Crystal Structure: Not reported

Average Size: Unwashed: 30.8 ± 0.6 , 47.7 ± 0.5 , and 75.5 ± 1.0 nm (determined using DLS) or 22.4 ± 2.6 , 49.4 ± 6.2 , and 79.2 ± 8.0 nm (determined using TEM). Washed: 25.5 ± 0.4 , 43.7 ± 1.1 , and 79.9 ± 28.0 nm (determined using DLS) or 21.4 ± 3.1 , 50.0 ± 5.9 , and 77.0 ± 6.0 nm (determined using TEM). Carbon-coated: 149.0 ± 89 and 167.0 ± 110 nm (determined using DLS) or 27.2 ± 10.3 and 37.0 ± 11.6 nm (determined using TEM).

Size Distribution: Not reported

Solubility: Not reported

Surface Area: Not reported

Surface Treatment: None (unwashed and washed), polyaromatic graphite carbon (carbon-coated)

Surface Charge: Unwashed: -29.7 mV (~ 20 -nm size), -27.8 mV (~ 50 -nm size), and -33.2 mV (~ 80 -nm size). Washed: -46.0 mV (~ 20 -nm size), -44.3 mV (~ 50 -nm size), and -43.7 mV (~ 80 -nm size). Carbon-coated: -24.0 mV (~ 25 -nm size) and -29.0 mV (~ 35 -nm size) (expressed as ζ potential in deionized water)

Protocol

Exposure Duration: 24 hours

Endpoint: Viability and cytokine release

Exposure Concentrations: 0.000544 to 1.7 $\mu\text{g}/\text{mL}$ for all nano-Ag types, and up to 45 $\mu\text{g}/\text{mL}$ for washed and carbon-coated nano-Ag

Exposure Medium: Keratinocyte Growth Medium-2 (KGM-2)

Cell Density: Initial density of 12,500 cells/well grown over 18–24 hours to 80% confluency

Methods: HEKs were exposed to either KGM-2 (control) or to serial dilution of each of the eight types of nano-Ag. To assess viability, HEKs were exposed to nano-Ag diluted in KGM-2 at concentrations ranging from 0.000544 to 1.7 $\mu\text{g}/\text{mL}$ for 24 hours using MTT, alamarBlue (aB), and Celltiter 96 Aqueous One (96AQ) assays. Concentrations up to 42.5 $\mu\text{g}/\text{mL}$ of the washed and carbon-coated nano-Ag particles were also tested. To determine if the supernatants or washing permeates resulting from the synthesis and washing of the unwashed/uncoated and washed/uncoated particles, respectively, were contributing to observed cytotoxicity, HEKs were treated with either the supernatant or permeates for 24 hours at concentrations ranging from 0.068 to 1.7 $\mu\text{g}/\text{mL}$. For those nano-Ag concentrations resulting in cytotoxicity, cytokine analysis was conducted by assessing release of interleukin (IL)-8, IL-6, tumor necrosis factor- α (TNF- α), IL-10, and IL-1 β . Results were presented with those from an in vivo porcine skin test conducted as part of the same study. These results are presented in presented in Section C.3 of this appendix.

Study Outcome

Viability. Exposure of HEKs to unwashed/uncoated nano-Ag resulted in a dose-dependent decrease in cell viability in all three assays, with significant ($p < 0.05$) decreases occurring at the 0.34- $\mu\text{g}/\text{mL}$ level in the ~ 20 - and ~ 50 -nm groups using the aB and 96AQ assays and at the 1.7- $\mu\text{g}/\text{mL}$ level for these size groups using the MTT assay. The ~ 80 -nm group resulting in a significant decrease in viability at the 0.34- $\mu\text{g}/\text{mL}$ level using all three assays. No significant decrease in viability was observed in any assay for the washed/uncoated or carbon-coated nano-Ag samples. The unwashed nano-Ag supernatant contained 5.55 mg/mL formaldehyde solvent and methanol by-product from synthesis. Exposure to this supernatant resulted in significantly decreased viability at the 0.34- $\mu\text{g}/\text{mL}$ level using the aB and MTT assays and at the 1.7- $\mu\text{g}/\text{mL}$ level using the 96AQ assay. Exposure to the washing permeates from the washed and uncoated samples did not result in any loss in viability.

Cytokine Release. Following exposure to 0.34 $\mu\text{g}/\text{mL}$ unwashed nano-Ag of all sizes, significant ($p < 0.05$) increases were observed in IL-1 β , IL-6, IL-8, and TNF- α .

Shin et al. (2007) The effects of nano-silver on the proliferation and cytokine expression by peripheral blood mononuclear cells.

Test Species

Human peripheral blood mononuclear cells (PMBCs)

Material

Nano-Ag colloidal solution synthesized from AgNO₃.

Shape: Not Reported

Composition: Not Reported

Crystal Structure: Not Reported

Average Size: 1.3 nm

Size Distribution: 1–2.5 nm

Solubility: Not Reported

Surface Area: Not Reported

Surface Treatment: Not Reported

Surface Charge: Not Reported

Protocol

Exposure Duration: 72 hours

Endpoint: Cytotoxic effects on PMBCs

Exposure Concentrations: 0, 1, 3, 5, 10, 20, 30 ppm
nano-Ag

Exposure Medium: Not reported

Cell Density: 2 × 10⁶ cells/mL

Methods: PMBCs from healthy human volunteers were stimulated with 5 µg/ml phytohaemagglutinin (PHA) in the presence of varying concentrations of nano-Ag. PMBC proliferations were measured using an aqueous cell proliferation assay kit and supernatants were analyzed using enzyme-linked immunosorbent assays.

Study Outcome

Inflammatory Response. Proliferation of PMBCs showed cytotoxicity levels of nano-Ag over 15 ppm. At low levels nano-Ag decreased cytokine production (PHA-induced IL-5: at 10 ppm, interferon (INF)-gamma and tumor necrosis factor (TNF)-alpha at 3 ppm).

Shrivastava et al. (2009) Characterization of antiplatelet properties of silver nanoparticles.

Test Species

Human primary platelets

Material

Nano-Ag synthesized from AgNO₃ using deionized water, NaOH, and NH₃.

Shape: Spherical

Solubility: Not reported

Composition: Not reported

Surface Area: Not reported

Crystal Structure: Face centered cubic

Surface Treatment: Not reported

Average Size: 10–15 nm (determined using diffraction)

Surface Charge: Not reported

Size Distribution: Monodispersed

Protocol

Exposure Duration: 10 minutes

Exposure Medium: Aqueous

Endpoint: Morphology and membrane integrity

Cell Density: Not reported

Exposure Concentrations: 0, 25, 50, 100, 150, 200, 250, and 500 µM

Methods: Morphology was assessed by labeling cells with ANS and recording fluorescence emission spectra. Membrane integrity was measured by assaying lactate dehydrogenase (LDH) activity from the decrease in reduced NADH absorbance.

Study Outcome

Morphology. Fluorescence intensity declined in a dose-dependence manner, suggesting nano-Ag contributes significantly to platelet membrane disorder.

Viability. Nano-Ag did not cause significant release of LDH from platelet cytosol. Platelet membrane integrity was not compromised nor did cell lysis occur.

Trickler et al. (2010) Silver nanoparticle-induced blood-brain barrier inflammation and increased permeability in primary rat brain microvessel endothelial cells.

Test Species

Sprague-Dawley rat brain microvessel endothelial (rBMEC) cells

Material

Nano-Ag, gift from Nanocomposix, San Diego, CA.

Shape: Spherical

Composition: Not reported

Crystal Structure: Not reported

Average Size: 28.3, 47.5, and 102.2 nm (determined using TEM)

Size Distribution: 20–40, 40–55, and 60–140 nm (determined using TEM)

Solubility: Not reported

Surface Area: Not reported

Surface Treatment: PVP coating

Surface Charge: -44.2, -46.0, and -29.5 mV (determined using LDV)

Protocol

Exposure Duration: 24 hours

Endpoint: Cytotoxicity and proinflammatory mediators

Exposure Concentrations: 6.25–50 $\mu\text{g}/\text{cm}^3$

Exposure Medium: rBMEC complete media

Cell Density: Not reported

Methods: Cytotoxicity was assessed by the mitochondrial dependent conversion of XTT reagent. Release of proinflammatory mediators TNF, IL-1B and PGE₂ were also monitored.

Study Outcome

Cytotoxicity. Significantly decreased cell viability was observed in cells treated with 25 and 40 nm particles at 25 and 50 $\mu\text{g}/\text{cm}^3$, and in cells treated with 80 nm particles at only 50 $\mu\text{g}/\text{cm}^3$. Significant morphological changes were observed to be size- and dose-dependent.

Proinflammatory Mediators. Association with nano-Ag particles was observed to increase the release of proinflammatory mediators, suggesting that morphological changes in rBMEC cells are associated with increased permeability.

C.3. Summary of Key In Vivo Studies

Cha et al. (2008) Comparison of acute responses of mice livers to short-term exposure to nano-sized or micro-sized silver particles.

Test Species

Balb/c mouse (male), 7 weeks old

Material

Nano-Ag, synthesized by the reduction of AgNO₃ with NaBH₄

Shape: Not reported

Composition: Not reported

Crystal Structure: Not reported

Average Size: 13 nm, or 2–3.5 μm (determined using TEM)

Size Distribution: Not reported

Solubility: Not reported

Surface Area: Not reported

Surface Treatment: Not reported

Surface Charge: Not reported

Protocol

Exposure Duration: 24 hours

Endpoint: Acute liver effects

Exposure Concentrations: 2.5 g

Exposure Media/Route: Gastric intubation

Methods: Livers, hearts, intestines, and spleens from test species were obtained 3 days after treatment, fixed in 10% formalin, and subjected to histopathological analysis. A total RNA isolation kit was used to isolate the RNA from the livers and results were confirmed by a semi-quantitative RT-PCR.

Study Outcome

Nanoparticle and microparticle-treated livers showed lymphocyte infiltration, which indicated inflammation. Nonspecific focal hemorrhages in the heart, focal lymphocyte infiltration in the intestine, and nonspecific medullary congestion in the spleen were also observed in mice treated with nano-Ag. RNA microarray analysis of livers showed altered apoptosis and inflammatory responses in the livers of nanoparticle-exposed mice, as indicated by the up-regulation of seven genes in the apoptotic pathway and five in the inflammatory pathway gene expression.

Ji et al. (2007) Twenty-eight-day inhalation toxicity study of silver nanoparticles in Sprague-Dawley rats.

Test Species

Sprague-Dawley rat, 40 males and females (10 rats per dosing group), 10 weeks old at start of experiment (~283-g males, ~169-g females)

Material

Nano-Ag; particles generated by evaporation/condensation using a small ceramic heater within a quartz tube case

Shape: Spherical

Composition: Not Reported

Crystal Structure: Not Reported

Average Size: 16 nm (determined using differential mobility analyzer and a condensation particle counter)

Size Distribution: 1.98–64.9 nm; geometric mean diameter and geometric standard deviation of 15.38 nm and 1.58, 12.60 nm and 1.53, and 12.61 nm and 1.52 in the high-, middle-, and low-concentration chambers, respectively

Solubility: Not Reported

Surface Area: 1.41×10^9 , 9.68×10^7 , and 1.32×10^7 nm²/cm³ in the high-, middle-, and low-concentration chambers, respectively

Surface Treatment: Not Reported

Surface Charge: Not Reported

Protocol

Exposure Duration: Subchronic 28-day inhalation

Endpoint: Inflammatory response

Exposure Concentrations: 1.32×10^6 particles/cm³ (high dose), 1.27×10^5 particles/cm³ (middle dose), and 1.73×10^4 particles/cm³ (low dose) for 6 hours/day, 5 days/week

Exposure Media/Route: Whole-body inhalation chamber

Methods: Exposure-related effects including respiratory, dermal, behavioral, nasal, and genitourinary changes suggestive of irritancy were studied daily on weekdays. Body weights were measured after purchase, grouping, weekly during exposure, and at study termination. Hematological analysis was conducted 24 hours after study termination. Organ weights were then measured, followed by a complete histopathological analysis and determination of tissue silver using an atomic absorption spectrophotometer.

Study Outcome

Despite deposition of nano-Ag particles in the liver, olfactory bulb, and brain, no significant exposure-related adverse health effects were observed.

Kim et al. (2008) Twenty-eight-day oral toxicity, genotoxicity, and gender-related tissue distribution of silver nanoparticles in Sprague-Dawley rats.

Test Species

Sprague-Dawley rat, 40 males and females (10 rats per dosing group), 6 weeks old at start of experiment (~283-g males, ~192-g females)

Material

Commercial nano-Ag, micro-sized Ag; purchased from NAMATECH Co., Ltd.

Shape: Not reported

Composition: Not reported

Crystal Structure: Not reported

Average Size: 60 nm

Size Distribution: 52.7–70.9 nm

Solubility: Not reported

Surface Area: Not reported

Surface Treatment: Not reported

Surface Charge: Not reported

Protocol

Exposure Duration: 28 days

Endpoint: Effects on hematology and blood biochemistry; genotoxic effect on rat bone marrow; and Ag distribution in tissue.

Exposure Concentrations: Vehicle control (0.5% carboxymethylcellulose), low-dose group (30 mg/kg), middle-dose group, (300 mg/kg), and high-dose group (1,000 mg/kg).

Exposure Media/Route: Daily oral gavage

Methods: After exposure, the blood biochemistry and hematology were investigated using a blood cell counter, along with a histopathological examination and Ag distribution study using spectrophotometry.

Study Outcome

Hematology and Blood Biochemistry. Dose-dependent changes in serum alkaline phosphatase, with a significant increase in high- and middle-dose male rats and high-dose female rats. Similarly, high-dose male rats and high- and middle-dose female rats displayed significant increases in cholesterol. Total protein significantly decreased in high-dose male rats. Mean corpuscular volume significantly increased in high-dose male rats, while the red blood cell count, hemoglobin content, and hematocrit significantly increased in high- and middle-dose female rats.

Inflammation. Dose-dependent bile duct hyperplasia with increase in inflammatory cells.

Genotoxic Effect on Rat Bone Marrow. Nano-Ag did not induce genetic toxicity in bone marrow.

Ag Accumulation in Tissues. All tissues revealed significant dose-dependent accumulation of Ag in tissues. Two-fold increase in the female kidneys compared with the male kidneys.

Lee et al. (2010) Genomics-based screening of differentially expressed genes in the brains of mice exposed to silver nanoparticles via inhalation.

Test Species

28 Male C57BL/6 mice (20–25 g), 7 per group

Material

Nano-Ag produced using a nanoparticle generator.

Shape: Not reported

Composition: Not reported

Crystal Structure: Not reported

Average Size: 22.18 nm (determined using SEM)

Size Distribution: 20.46–23.9 nm (determined using SEM)

Solubility: Not reported

Surface Area: 1.46×10^{10} nm²/cm³

Surface Treatment: Not reported

Surface Charge: Not reported

Protocol

Exposure Duration: 6 hours/day, 5 days/week for 2 weeks

Endpoint: Gene expression and morphology

Exposure Concentrations: 1.91×10^7 particles/cm³

Exposure Media/Route: Inhalation, nose-only exposure system

Methods: Total RNA isolated from brain tissues of exposed mice was assessed by subjection to hybridization. Real-time polymerase chain reaction (PCR) procedures were used to analyze whole blood samples. Brain tissues were also examined histopathologically for structural and functional changes.

Study Outcome

Gene Expression. 468 genes in the cerebrum and 952 genes in the cerebellum of treated rats were observed to have been affected by nano-Ag exposure in a significant manner. Those genes associated with signal transduction were the most affected, along with genes involved in protein metabolism, developmental processes, and nucleic acid metabolism. Five genes in the whole blood analysis were downregulated in response to nano-Ag exposure.

Morphology. No structural changes were observed in tissues after hematoxylin and eosin staining.

Li et al. (2010a) Induction of cytotoxicity and apoptosis in mouse blastocysts by silver nanoparticles.

Test Species

ICR mouse blastocytes

Material

Nano-Ag prepared by the polyol process (reduction of AgNO₃ with C₂H₆O₂ in the presence of polyvinylpyrrolidone [PVP]).

Shape: Not reported

Composition: Not reported

Crystal Structure: Not reported

Average Size: 13 nm (determined using TEM)

Size Distribution: 6–24 nm (determined using TEM)

Solubility: Not reported

Surface Area: Not reported

Surface Treatment: Coated with a shell of polymer to reduce cluster formation

Surface Charge: Not reported

Protocol

Exposure Duration: 24 hours

Endpoint: Blastocyst development

Exposure Concentrations: 0, 25, and 50 µM

Exposure Media/Route: Implantation of pre-treated blastocysts

Methods: Blastocysts pretreated with 0, 25, or 50 µM nano-Ag were transferred to female recipient ICR mice and uterine content was examined 13 days after transfer.

Study Outcome

Developmental Potential. The implantation ratio of blastocysts pretreated with 50 µM nano-Ag was significantly lower than that of the control cells. The proportion of successfully implanted embryos that failed to develop normally was significantly higher in the group pretreated with 50 µM nano-Ag. Overall fetal weight was lower in the group pretreated with 50 µM nano-Ag.

Park et al. (2010a) Repeated-dose toxicity and inflammatory responses in mice by oral administration of silver nanoparticles.

Test Species

Male and female ICR mice, 6 weeks old, 5 mice per group in 14-day study, 6 mice per group in 28-day study

Material

Nano-Ag particles (Sigma-Aldrich, USA) suspended with sonication in tetrahydrofuran (THF) and evaporated.

Shape: Not reported

Composition: Not reported

Crystal Structure: Not reported

Average Size: 22, 42, 71, 323 nm (14-day study); 42 nm (28-day study) (determined using DLS)

Size Distribution: Not reported

Solubility: Not reported

Surface Area: Not reported

Surface Treatment: Not reported

Surface Charge: Not reported

Protocol

Exposure Duration: 14, 28 days

Endpoint: Tissue distribution, cell function, cell phenotype, body weight (14-day study), serum biochemistry, lymphocyte phenotype, histopathological changes (28-day study)

Exposure Concentrations: 0, 1 mg/kg (14-day study), 0, 0.25, 0.5, 1 mg/kg (28-day study)

Exposure Media/Route: Daily oral gavage in deionized water

Methods: Mice were administered equal doses of varying sizes of nano-Ag particles in a size-differentiated toxicity test, and the same size particle in different doses in a repeated-dose toxicity test. Toxicity was examined by determination of blood biochemistry, nanoparticle distribution in the body, concentration of cytokines, blood serum levels, and histopathology.

Study Outcome

Tissue Distribution. In the 14-day study, nano-Ag was observed to significantly accumulate in dose groups administered 22, 42, or 71 nm particles, but not in the group administered 323 nm particles.

Cell Function. Small particles (22, 42, and 71 nm) significantly increased the level of TGF- β in the 14-day study.

Cell Phenotype. The 14-day study revealed increased distribution of NK and B cells in the groups treated with 22, 42, or 71 nm particles. The ratio of T-cell subtype was also noticeably decreased in these dose groups.

Body Weight. Body weight and organ-to-body-weight ratios were not affected by administration of various sizes of nano-Ag particles administered for 14 days.

Serum Biochemistry. In the 28-day study, significantly increased levels of AST and ALP were observed in males and females at the 1 mg/kg dose level. ALT was also increased in female mice at the 1 mg/kg dose level.

Cytokine Levels. Pro-inflammatory cytokine levels increased in a dose-dependent manner in the 28-day study. Levels were not detectable in control mice, and increased to 8.8 ± 0.70 pg/mL at 1 mg/kg.

Histopathology. No significant histopathological findings were observed in the 28-day study.

Samberg et al. (2010) Evaluation of silver nanoparticle toxicity in vivo and keratinocytes in vitro.

Test Species

Pig, two weanling females (20–30 kg)

Material

Two sizes (reported by manufacturer as 20 and 50 nm in diameter) of commercial unwashed/uncoated and washed/uncoated nano-Ag in deionized water, both supplied by nanoComposix, San Diego, CA. Unwashed and washed nano-Ag synthesized by manufacturer using ammonium hydroxide-catalyzed growth onto 5-nm gold seed particles.

Shape: Not reported

Composition: Not reported

Crystal Structure: Not reported

Average Size: Unwashed: 30.8 ± 0.6 , 47.7 ± 0.5 , and 75.5 ± 1.0 nm (determined using DLS) or 22.4 ± 2.6 , 49.4 ± 6.2 , and 79.2 ± 8.0 nm (determined using TEM). Washed: 25.5 ± 0.4 , 43.7 ± 1.1 , and 79.9 ± 28.0 nm (determined using DLS) or 21.4 ± 3.1 , 50.0 ± 5.9 , and 77.0 ± 6.0 (determined using TEM).

Size Distribution: Not reported

Solubility: Not reported

Surface Area: Not reported

Surface Treatment: None

Surface Charge: Unwashed: -29.7 mV (~20-nm size), -27.8 mV (~50-nm size), and -33.2 mV (~80-nm size).

Washed: -46.0 mV (~20-nm size), -44.3 mV (~50-nm size), and -43.7 mV (~80-nm size).

Protocol

Exposure Duration: 14 days

Endpoint: Morphological alterations

Exposure Concentrations: 0.34 to 34 $\mu\text{g/mL}$

Exposure Media/Route: Daily dermal application

Methods: Pigs were topically dosed once per day for 14 days at 14 sites on back skin with nano-Ag concentrations ranging from 0.34 to 34 $\mu\text{g/mL}$. The Draize system was then used to evaluate the skin for erythema and edema. Microscopic observations were taken on harvested skin samples after pigs were euthanized on Day 14. Samples were analyzed for intercellular and intracellular edema, dermal edema, and inflammation. Results were presented with those from an in vitro test using human epidermal keratinocytes conducted as part of the same study. These results are presented in Appendix C.2.

Study Outcome

Macroscopic observations of porcine skin exposed topically with nano-Ag of all types and sizes revealed no gross erythema or edema. Microscopic observations of the exposed skin samples revealed a concentration-dependent response that was not related to particle size or washing. Effects observed following exposure to the washed ~20-nm nano-Ag solutions were intracellular and intercellular epidermal edema (all doses), focal epidermal and dermal inflammation (mid dose), epidermal hyperplasia (high dose), parakeratosis (high dose), and extension of rete pegs into the superficial papillary layer of the dermis (high dose). Effects observed following exposure to the unwashed ~20-nm nano-Ag solutions were intracellular epidermal edema (all doses), intercellular edema (mid and high dose), and focal areas of intraepidermal infiltrates and superficial papillary dermal inflammation (high dose).

Shrivastava et al. (2009) Characterization of antiplatelet properties of silver nanoparticles.

Test Species

AKR and PARKES mouse, 50 males (25 from each strain), 7–8 weeks

Material

Nano-Ag synthesized from AgNO₃ using deionized water, NaOH, and NH₃.

Shape: Spherical

Composition: Not reported

Crystal Structure: Face centered cubic

Average Size: 10–15 nm (determined using TEM)

Size Distribution: Monodispersed

Solubility: Not reported

Surface Area: Not reported

Surface Treatment: Not reported

Surface Charge: Not reported

Protocol

Exposure Duration: 10 minutes

Endpoint: Hematology and mortality

Exposure Concentrations: 2, 4, 6, and 8 mg/kg body weight

Exposure Media/Route: Intravenous injection into tail veins

Methods: Mice were divided into 10 groups of 5 animals each. Aggregation was measured in whole blood by electronic impedance. Tail bleeding was monitored at 15-minute increments until no blood was observed on the filter paper.

Study Outcome

Hematology. Intravenous nano-Ag (2–8 mg/kg) inhibited platelet aggregation in whole blood. No adverse effect on bleeding time was observed.

Mortality. Survival was unaffected.

Sung et al. (2008) Lung function changes in Sprague-Dawley rats after prolonged inhalation exposure to silver nanoparticles.

Test Species

Sprague-Dawley rat, 40 males and females (10 rats per dosing group), 8 weeks old at start of experiment (~253-g males, ~162-g females)

Material

Nano-Ag; particle generation described in Ji et al. (2007)

Shape: Spherical; non-aggregated/agglomerated forms with diameters under 55 nm (determined using TEM)

Composition: Not Reported

Crystal Structure: Not Reported

Average Size: 18–19 nm (determined using differential mobility analyzer and a condensation particle counter)

Size Distribution: 1.98–64.9 nm

Solubility: Not Reported

Surface Area: 1.08×10^9 , 2.37×10^9 , and 6.61×10^9 nm²/cm³ in the low-, middle-, and high-concentration chambers, respectively

Surface Treatment: Not Reported

Surface Charge: Not Reported

Protocol

Exposure Duration: Subchronic 90-day inhalation

Endpoint: Inflammatory response; pulmonary function changes

Exposure Concentrations: 0.7×10^6 particles/cm³ (low dose), 1.4×10^6 particles /cm³ (middle dose), and 2.9×10^6 particles /cm³ (high dose) for 6 hours/day

Exposure Media/Route: Whole-body inhalation chamber

Methods: The lung function was measured every week after the daily exposure, and the animals were sacrificed after the 90-day exposure period. Cellular differential counts and inflammatory measurements, such as albumin, lactate dehydrogenase (LDH), and total protein, were also monitored in the acellular bronchoalveolar lavage (BAL) fluid of the rats.

Study Outcome

Lung Function. Tidal volume and minute volume showed a statistically significant decrease during the 90 days of nano-Ag exposure.

Inflammatory Response. Although BAL fluid cellular differential counts were not found to be statistically significant, increased inflammation measurements were observed in the high-dose female rats. Dose-dependent increases in lesions related to nano-Ag exposure, such as infiltrate mixed cell and chronic alveolar inflammation, including thickened alveolar walls and small granulomatous lesions.

Sung et al. (2009) Subchronic inhalation toxicity of silver nanoparticles.

Test Species

Sprague-Dawley rat, 40 males and females (10 rats per dosing group), 8 weeks old at start of experiment (~253-g males, ~162-g females)

Material

Nano-Ag; particle generation described in Ji et al. (2007)

Shape: Spherical; non-aggregated/agglomerated forms with diameters under 55 nm (determined using TEM)

Composition: Not Reported

Crystal Structure: Not Reported

Average Size: 18–19 nm (determined using differential mobility analyzer and a condensation particle counter)

Size Distribution: 1.98–64.9 nm

Solubility: Not Reported

Surface Area: 1.08×10^9 , 2.37×10^9 , and 6.61×10^9 nm²/cm³ in the low-, middle-, and high-concentration chambers, respectively

Surface Treatment: Not Reported

Surface Charge: Not Reported

Protocol

Exposure Duration: Subchronic 13-week inhalation

Endpoint: Inflammatory response; pulmonary function changes; liver toxicity; and Ag distribution in tissue

Exposure Concentrations: 0.6×10^6 particles/cm³; 49 µg/m³ (low dose), 1.4×10^6 particles/cm³; 133 µg/m³ (middle dose), and 2.9×10^6 particles/cm³; 515 µg/m³ (high dose) for 6 h/day, 5 days/week

Exposure Media/Route: Whole-body inhalation chamber

Methods: At the end of the study, the rats were subjected to a full necropsy, blood samples were collected for hematology and clinical chemistry tests, and the organ weights were measured.

Study Outcome

NOAEL: 100 µg/m³.

Inhalation Toxicity. Dose-dependent increases in lesions related to nano-Ag exposure, including mixed inflammatory cell infiltrate, chronic alveolar inflammation, and small granulomatous lesions.

Liver Toxicity. Dose-dependent bile duct hyperplasia in liver.

Ag Distribution in Tissue. Statistically significant dose-dependent increases in Ag concentration in lung tissue. Dose-dependent increase in the Ag concentration in the blood. Dose-dependent increase in the liver Ag concentration. Ag concentration in the olfactory bulb was higher than in brain, and increased in a dose dependent manner in both genders ($p < 0.01$). Ag concentrations in the kidneys showed a gender difference, with female kidneys containing 2–3 times more Ag accumulation than in male kidneys.

Takenaka et al. (2001) Pulmonary and systemic distribution of inhaled ultrafine silver particles in rats.

Test Species

Female Fischer 344 rat, (150–200 g)

Material

Nano-Ag; particles generated by spark discharging through an argon atmosphere.

Shape: Spherical

Composition: Not Reported

Crystal Structure: Not Reported

Average Size: 14.6 nm (determined using differential mobility analyzer)

Size Distribution: Not Reported

Solubility: Not Reported

Surface Area: Not Reported

Surface Treatment: Not Reported

Surface Charge: Not Reported

Protocol

Exposure Duration: Acute 6-hour inhalation; intratracheal instillation

Endpoint: Accumulation in the lungs and brain

Exposure Concentrations: Inhalation mass concentration of 133 $\mu\text{g Ag}/\text{m}^3$ and a particle number concentration of $3 \times 10^6 \text{ cm}^{-3}$ for 6 hours; injected with 150 μL aqueous solution of 7 $\mu\text{g AgNO}_3$ (4.4 $\mu\text{g Ag}$) or 150 μL aqueous suspension of 50 μg elemental Ag.

Exposure Media/Route: Whole-body inhalation chamber; intratracheal instillation

Methods: Rats were sacrificed 0, 1, 4, and 7 days after exposure or intratracheal instillation for morphology and elemental analysis. The ultrastructure of nano-Ag particles was examined using a transmission electron microscope.

Study Outcome

After inhalation exposure, silver accumulation was largest in the lungs, followed by the nasal cavities, in particular the posterior portion, and the lung-associated lymph nodes. Only 4% of the initial body burden in the lungs remained on day 7. Low concentrations of silver were observed in the brain at day 0 and day 1, but no data were collected for the brain on days 4 and 7. Following intratracheal instillation, particles were observed within the alveolar walls, and the rate of clearance was seen to be much slower than following inhalation.

Tang et al. (2008) Influence of silver nanoparticles on neurons and blood-brain barrier via subcutaneous injection in rats.

Test Species

Wistar rat, 90 females (110–130 g), divided into 3 groups (control, nano-Ag, micro-sized Ag)

Material

Commercial nano-Ag, micro-sized Ag; obtained from Sigma-Aldrich (USA).

Shape: Globular (nano-Ag; determine by TEM); irregular cubes (micro-sized Ag; determined by SEM)

Composition: Not Reported

Crystal Structure: Not Reported

Average Size: Not Reported

Size Distribution: 50–100 nm (nano-Ag; determined by TEM); 2–20 μm (micro-sized Ag; determined by SEM)

Solubility: Not Reported

Surface Area: Not Reported

Surface Treatment: Not Reported

Surface Charge: Not Reported

Protocol

Exposure Duration: Single injection

Endpoint: Accumulation in the brain and blood-brain barrier effects

Exposure Concentrations: 1 mL suspension, 62.8 mg/kg

Exposure Media/Route: Subcutaneous injection

Methods: Rat brains were obtained for ultra-structural observation and Ag level detection. Five rats from each group were sacrificed at weeks 2, 4, 8, 12, 18, and 24 to obtain brain tissue. The remaining brain tissue was digested to measure Ag levels.

Study Outcome

Ag levels were significantly higher in the nano-Ag group than in the micro-Ag and control groups. Results show that micro-sized Ag did not traverse into the brain, whereas nano-Ag did and accumulated in the brain at least 24 weeks. Nano-Ag can induce neuronal degeneration and necrosis by accumulating in the brain over a long period of time.

Tiwari et al. (2011) Dose-dependent in-vivo toxicity assessment of silver nanoparticles in Wistar rats.

Test Species

Male and female Wistar rats (8–10 weeks old, 200–225 g), divided into groups of six animals

Material

Silver nanoparticles dispersed in ethylene glycol obtained from Sigma-Aldrich (USA).

Shape: Rounded (characterized by TEM)

Solubility: Not Reported

Composition: Not Reported

Surface Area: Not Reported

Crystal Structure: Not Reported

Surface Treatment: Not Reported

Average Size: Not Reported

Surface Charge: Not Reported

Size Distribution: 15–40 nm

Protocol

Exposure Duration: 32 days

Exposure Concentrations: 0, 4, 10, 20, 40 mg/kg

Endpoint: Analysis of enzymes related to liver and kidney function

Exposure Media/Route: Intravenous injection administered in phosphate buffer

Methods: Rats were exposed intravenously to silver nanoparticles over 32 days. Blood samples were collected each week and analyzed for levels of AST, ALT, GGTP, ALP, total protein, and bilirubin.

Study Outcome

Levels of AST, ALT, and ALP significantly increased after exposure to nano-Ag particles at doses of 20 and 40 mg/kg. No significant changes were observed in the 4 and 10 mg/kg groups with respect to control. GGTP also showed a significant increase in the 40 mg/kg group. Increased levels of bilirubin along with correlated decreases in hemoglobin indicated changes in liver function.

Appendix C References

- [Ahamed, M; Karns, M; Goodson, M; Rowe, J; Hussain, SM; Schlager, JJ; Hong, Y.](#) (2008). DNA damage response to different surface chemistry of silver nanoparticles in mammalian cells. *Toxicol Appl Pharmacol* 233: 404-410. <http://dx.doi.org/10.1016/j.taap.2008.09.015>
- [Arora, S; Jain, J; Rajwade, JM; Paknikar, KM.](#) (2009). Interactions of silver nanoparticles with primary mouse fibroblasts and liver cells. *Toxicol Appl Pharmacol* 236: 310-318. <http://dx.doi.org/10.1016/j.taap.2009.02.020>
- [Asharani, PV; Low Kah Mun, G; Hande, MP; Valiyaveetil, S.](#) (2009). Cytotoxicity and genotoxicity of silver nanoparticles in human cells. *ACS Nano* 3: 279-290.
- [Carlson, C; Hussain, SM; Schrand, AM; Braydich-Stolle, LK; Hess, KL; Jones, RL; Schlager, JJ.](#) (2008). Unique cellular interaction of silver nanoparticles: Size-dependent generation of reactive oxygen species. *J Phys Chem B* 112: 13608-13619.
- [Cha, K; Hong, H; Choi, Y; Lee, MJ; Park, JH; Chae, H; Ryu, G; Myung, H.](#) (2008). Comparison of acute responses of mice livers to short-term exposure to nano-sized or micro-sized silver particles. *Biotechnol Lett* 30: 1893-1899. <http://dx.doi.org/10.1007/s10529-008-9786-2>
- [Greulich, C; Kittler, S; Epple, M; Muhr, G; Köller, M.](#) (2009). Studies on the biocompatibility and the interaction of silver nanoparticles with human mesenchymal stem cells (hMSCs). *Langenbecks Arch Surg* 394: 495-502. <http://dx.doi.org/10.1007/s00423-009-0472-1>
- [Hussain, SM; Hess, KL; Gearhart, JM; Geiss, KT; Schlager, JJ.](#) (2005). In vitro toxicity of nanoparticles in BRL 3A rat liver cells. *Toxicol In Vitro* 19: 975-983. <http://dx.doi.org/10.1016/j.tiv.2005.06.034>
- [Ji, JH; Jung, JH; Kim, SS; Yoon, JU; Park, JD; Choi, BS; Chung, YH; Kwon, IH; Jeong, J; Han, BS; Shin, JH; Sung, JH; Song, KS; JI, Y.](#) (2007). Twenty-eight-day inhalation toxicity study of silver nanoparticles in Sprague-Dawley rats. *Inhal Toxicol* 19: 857-871.
- [Kim, YJ; Yang, SI; Ryu, JC.](#) (2010). Cytotoxicity and genotoxicity of nano-silver in mammalian cell lines. *Mol Cell Toxicol* 6: 119-125. <http://dx.doi.org/10.1007/s13273-010-0018-1>
- [Kim, YS; Kim, JS; Cho, HS; Rha, DS; Kim, JM; Park, JD; Choi, BS; Lim, R; Chang, HK; Chung, YH; Kwon, IH; Jeong, J; Han, BS; Yu, IJ.](#) (2008). Twenty-eight-day oral toxicity, genotoxicity, and gender-related tissue distribution of silver nanoparticles in Sprague-Dawley rats. *Inhal Toxicol* 20: 575-583.
- [Lee, HY; Choi, YJ; Jung, EJ; Yin, HQ; Kwon, JT; Kim, JE; Im, HT; Cho, MH; Kim, JH; Kim, HY; Lee, BH.](#) (2010). Genomics-based screening of differentially expressed genes in the brains of mice exposed to silver nanoparticles via inhalation. *J Nanopart Res* 12: 1567-1578. <http://dx.doi.org/10.1007/s11051-009-9666-2>
- [Li, P; Kuo, T; Chang, J; Yeh, J; Chan, W.](#) (2010a). Induction of cytotoxicity and apoptosis in mouse blastocysts by silver nanoparticles. *Toxicol Lett* 197: 82-87. <http://dx.doi.org/10.1016/j.toxlet.2010.05.003>
- [Liu, W; Wu, Y; Wang, C; Li, H; Wang, T; Liao, C; Cui, L; Zhou, Q; Yan, B; Jiang, G.](#) (2010). Impact of silver nanoparticles on human cells: Effect of particle size. *Nanotoxicology* 4: 319-330. <http://dx.doi.org/10.3109/17435390.2010.483745>
- [Lu, W; Senapati, D; Wang, S; Tovmachenko, O; Singh, AK; Yu, H; Ray, PC.](#) (2010). Effect of surface coating on the toxicity of silver nanomaterials on human skin keratinocytes. *Chem Phys Lett* 487: 92-96. <http://dx.doi.org/10.1016/j.cplett.2010.01.027>
- [MINCharInitiative](#) (Minimum Information on Nanoparticle Characterization). (2008). Recommended minimum physical and chemical parameters for characterizing nanomaterials on toxicology studies. Washington, DC: The Minimum Information for Nanomaterial Characterization Initiative. <http://characterizationmatters.org/parameters/>

- Paddle-Ledinek, JE; Nasa, Z; Cleland, HJ. (2006). Effect of different wound dressings on cell viability and proliferation. *Plast Reconstr Surg* 117: 110S-118S; discussion 119S-120S. <http://dx.doi.org/10.1097/01.prs.0000225439.39352.ce>
- Park, EJ; Bae, E; Yi, J; Kim, Y; Choi, K; Lee, SH; Yoon, J; Lee, BC; Park, K. (2010a). Repeated-dose toxicity and inflammatory responses in mice by oral administration of silver nanoparticles. *Environ Toxicol Pharmacol* 30: 162-168. <http://dx.doi.org/10.1016/j.etap.2010.05.004>
- Rosas-Hernández, H; Jiménez-Badillo, S; Martínez-Cuevas, PP; Gracia-Espino, E; Terrones, H; Terrones, M; Hussain, SM; Ali, SF; González, C. (2009). Effects of 45-nm silver nanoparticles on coronary endothelial cells and isolated rat aortic rings. *Toxicol Lett* 191: 305-313. <http://dx.doi.org/10.1016/j.toxlet.2009.09.014>
- Samberg, ME; Oldenburg, SJ; Monteiro-Riviere, NA. (2010). Evaluation of silver nanoparticle toxicity in skin in vivo and keratinocytes in vitro. *Environ Health Perspect* 118: 407-413. <http://dx.doi.org/10.1289/ehp.0901398>
- Shin, YM; Kim, HS; Kang, HS. (2007). The effects of nano-silver on the proliferation and cytokine expression by peripheral blood mononuclear cell. *Int Immunopharmacol* 7: 1813-1818.
- Shrivastava, S; Bera, T; Singh, SK; Singh, G; Ramachandrarao, P; Dash, D. (2009). Characterization of antiplatelet properties of silver nanoparticles. *ACS Nano* 3: 1357-1364. <http://dx.doi.org/10.1021/nn900277t>
- Sung, JH; Ji, JH; Park, JD; Yoon, JU; Kim, DS; Jeon, KS; Song, MY; Jeong, J; Han, BS; Han, JH; Chung, YH; Chang, HK; Lee, JH; Cho, MH; Kelman, BJ; Yu, IJ. (2009). Subchronic inhalation toxicity of silver nanoparticles. *Toxicol Sci* 108: 452-461. <http://dx.doi.org/10.1093/toxsci/kfn246>
- Sung, JH; Ji, JH; Yoon, JU; Kim, DS; Song, MY; Jeong, J; Han, BS; Han, JH; Chung, YH; Kim, J; Kim, TS; Chang, HK; Lee, EJ; Lee, JH; Yu, IJ. (2008). Lung function changes in Sprague-Dawley rats after prolonged inhalation exposure to silver nanoparticles. *Inhal Toxicol* 20: 567-574.
- Takenaka, S; Karg, E; Roth, C; Schulz, H; Ziesenis, A; Heinzmann, U; Schramel, P; Heyder, J. (2001). Pulmonary and systemic distribution of inhaled ultrafine silver particles in rats. *Environ Health Perspect* 4: 547-551.
- Tang, J; Xiong, L; Wang, S; Wang, J; Liu, L; Li, J; Wan, Z; Xi, T. (2008). Influence of silver nanoparticles on neurons and blood-brain barrier via subcutaneous injection in rats. *Appl Surf Sci* 255: 502-504. <http://dx.doi.org/10.1016/j.apsusc.2008.06.058>
- Tiwari, DK; Jin, T; Behari, J. (2011). Dose-dependent in-vivo toxicity assessment of silver nanoparticle in Wistar rats. *Toxicol Mech Meth* 21: 13-24. <http://dx.doi.org/10.3109/15376516.2010.529184>
- Trickler, W; Lantz, S; Murdock, R; Schrand, A; Robinson, B; Newport, G; Schlager, J; Oldenburg, S; Paule, M; Slikker, W; Hussain, S; Ali, S. (2010). Silver nanoparticle induced blood-brain barrier inflammation and increased permeability in primary rat brain microvessel endothelial cells. *Toxicol Sci* 118: 160-170. <http://dx.doi.org/10.1093/toxsci/kfq244>

Appendix D. Identified Research Priorities (January 2011 Workshop)

This page intentionally left blank.

Appendix D. Identified Research Priorities (January 2011 Workshop)

D.1. Introduction	D-4
D.2. Prioritized Research Themes and Specific Questions from Collective Judgment Workshop	D-5
Appendix D References	D-8

This page intentionally left blank.

D.1. Introduction

As discussed in Chapters 1 and 7, the external review draft of this case study served as the starting point for identifying and prioritizing research gaps that, if pursued, could inform future assessments of nano-Ag in disinfectant spray. The workshop process, which was funded by EPA and independently conducted by an EPA contractor, and outcomes are summarized in Section 7.3.1 and explained in more detail in a summary report produced by the EPA contractor ([ICF, 2011](#)). After identifying priority research questions participants grouped similar questions into themes. A voting process then ensued whereby each participant allotted 10 points to the most important research theme, 9 points to the second most critical theme, and so on, down to 1 point. Combining the points from all participants for each broader theme resulted in a prioritized list of research directions. This list, which is an excerpt of the summary report produced by the EPA contractor conducting the workshop process ([ICF, 2011](#)), is included in Section D.2 below.

D.2. Prioritized Research Themes and Specific Questions from Collective Judgment Workshop

Research Theme	Specific Question	Points (Votes)
1. Analytical Methods	<p>Do adequate analytical methods exist to detect and characterize exposure to nano-Ag via soil, water, and air?</p> <p>Do adequate analytical methods exist to detect and characterize nano-Ag in environmental compartments and in biota?</p> <p>Are there standard nano-Ag reference materials that can be used in exposure and effects testing to aid in comparison of results among investigators?</p> <p>Are available methods adequate to characterize nano-Ag concentrations and associated exposure via relevant matrices such as:</p> <ol style="list-style-type: none"> air? water? food? <p>At a minimum, what assays could be considered in a harmonized test guideline for determination of the human health effects of nano-Ag?</p>	120 (19)
2. Exposure and Susceptibility	<p>How should dose and exposure be characterized and how do the following parameters affect it: (1) physiological characteristics, (2) behavior, (3) lifestages, and (4) susceptibility factors?</p> <p>What are the relevant susceptibility factors in terms of exposure?</p> <p>What kinds of exposure do these populations have, including physicochemical characteristics?</p> <p>Do particular species of biota and particular human populations have greater potential for exposure to nano-Ag through the life cycle?</p> <p>Which source, pathways, and routes offer the greatest exposure potential to nano-Ag for humans?</p> <p>What is the distribution of exposure intensities and frequencies of such exposures among homemakers, children, and maintenance personnel, and are these of concern for acute and or chronic health effects?</p>	120 (17)
3. Physical and Chemical Toxicity	<p>What physicochemical properties of nano-Ag can be used to predict toxicity to humans or biota?</p> <p>How does surface coating affect toxicity to humans or biota?</p> <p>To what extent do particle properties (e.g., size, shape, chemical composition, surface treatments) determine biological responses to nano-Ag?</p> <p>Which physicochemical properties of nano-Ag are most essential to characterize before, during, and after toxicity experiments?</p>	115 (16)
4. Kinetics and Dissolution	<p>What is the half life of nano-Ag in the environment?</p>	98 (15)

Research Theme	Specific Question	Points (Votes)
5. Surface Characteristics	<p>How does surface coating affect the physicochemical properties of nano-Ag?</p> <p>Do explosion risks exist for dried nano-Ag powders or nano-Ag powders modified with certain types of surface coatings?</p> <p>What effect, if any, do surface treatments of nano-Ag particles have on:</p> <p>a. uptake?</p> <p>b. biopersistence?</p> <p>c. bioaccumulation?</p> <p>d. biomagnification?</p> <p>What effect, if any, do surface treatments of nano-Ag particles have on human exposures and uptake?</p>	81 (14)
6. Sources and Releases	<p>How effectively is nano-Ag removed from sewage and industrial process water by wastewater treatment technology, and can information on the removal of conventional silver be applied to nano-Ag removal?</p> <p>What are the potential exposure vectors by which nano-Ag or nano-Ag by-products could be released to the environment at the various life-cycle stages?</p> <p>What are the associated feedstocks and by-products (and, of these feedstocks and by-products), which might be released, in what quantities, and via which pathways?</p> <p>What are the release rates of all sources of nano-Ag into the environment?</p>	76 (15)
7. Mechanisms of Nanoscale Silver Toxicity	<p>What are the fundamental biological responses to and associated mechanisms of nano-Ag exposure at the cell, organ, and whole-animal levels?</p> <p>Are the effects observed for exposure to nano-Ag due to silver ion release or the presence of nanoparticles? Can this be distinguished?</p>	72 (11)
8. Test Methods—Mammals/ Humans	<p>At a minimum, what assays could be considered in a harmonized test guideline for determination of the human health effects of nano-Ag?</p> <p>What standardized test methods or characterization protocols are necessary to ensure that research results generated in multiple laboratories are consistent, reproducible, and reliable?</p> <p>Are the current tests for regulatory acceptance relevant to nano-Ag?</p> <p>Can nano-Ag have impacts on the F-1 (next) generation via changes in gene expression patterns?</p>	67 (11)
9. Ecotoxicity Test Methods	<p>At a minimum, what assays could be considered in a harmonized test guideline for determination of the ecological effects of nano-Ag?</p> <p>What standardized test methods or characterization protocols are necessary to ensure that research results generated in multiple laboratories are consistent, reproducible, and reliable?</p> <p>Are the current tests for regulatory acceptance relevant to nano-Ag?</p> <p>Can nano-Ag have impacts on the F-1 (next) generation via changes in gene expression patterns?</p>	59 (10)

Research Theme	Specific Question	Points (Votes)
10. Is New Nano Unique?	<p>Does nano-Ag form the same strong complexes with anions as conventional silver, and if so, is it also effectively mobilized in aquatic environments?</p> <p>What are the phys-chem properties of currently available and historic silver products?</p> <p>Do nano-Ag products actually offer more efficacy than products currently on the market?</p> <p>Do the properties of nano-Ag that differ from those of well-characterized colloidal silver, if any, cause them to behave differently in aquatic, terrestrial, and atmospheric environmental compartments?</p> <p>a. If they do differ, how do they differ?</p> <p>b. Can information about how colloidal silver behaves in these environments be used to understand how nano-Ag behaves?</p>	59 (10)
11. Biological Effects	<p>What are the most sensitive ecological endpoints to nano-Ag exposure?</p> <p>What are relevant susceptibility factors (for biological response)?</p> <p>What are the short-term and long-term biological responses observed at current nano-Ag occupational exposure levels as well as consumer exposure levels?</p> <p>Many effects of emerging substances are not known until many years after their introduction and use in commerce. What are the chronic and subchronic effects of nano-Ag, and how can we accelerate our understanding of them? Can nano-Ag have impact on F-1 (next) generation via changes in gene expression patterns?</p>	56 (10)
12. Ecological Effects Required for Risk Assessment	<p>What are the most sensitive ecological endpoints to nano-Ag exposure? Are there sufficient data/analytical techniques to determine how sensitive specific endpoints and organisms are to nano-Ag exposure, including:</p> <p>a. Benthic invertebrates;</p> <p>b. Marine invertebrates; and</p> <p>c. Freshwater invertebrates?</p> <p>Is the available ecological effects evidence adequate to support ecological risk assessment for nano-Ag? If no, what research is needed to make an assessment possible?</p>	43 (9)
12. Communication, Engagement, and Education	<p>How do we effectively communicate risk/benefit information for nano-Ag to the general public?</p> <p>How do we engage citizens and workers in discussions about how nano-Ag sprays are being used?</p> <p>How do we educate people about the risks, benefits, and safety related to nano products?</p> <p>We need an integrated holistic approach to nano risk assessment. How can we do this?</p>	43 (9)
14. Fate and Transport of Nano-Ag	<p>What physicochemical properties of nano-Ag can be used to predict fate and transport in environmental media?</p> <p>How could existing models applicable to conventional silver be used to adequately predict the transport and fate of nano-Ag through environmental compartments, or how could they be modified to do so?</p>	39 (12)
14. Adequacy of Current Data	<p>Do current publications describing the health effects of nano-Ag particles and laboratory-generated nano-Ag particles accurately depict the toxicity of commercially available nano-Ag materials?</p> <p>Are there any parallels between health effects of conventional silver and those in emerging studies on nanosilver?</p>	39 (6)

Research Theme	Specific Question	Points (Votes)
16. Dissolution	<p>What information exists on the temporal changes in the release of ionic silver by nanoparticles physicochemical and environmental characteristics?</p> <p>What are the rates of dissolution of nano-Ag into the environment?</p> <p>Does particle size of nano-Ag affect the rate of release of silver ions in environmental compartments?</p>	36 (9)
17. Information from Manufacturers	<p>Has the database and risk assessment methodology used by FDA during approval of nano-Ag medical devices been integrated with EPA's database and risk assessment processes?</p> <p>What are realistic strategies for collecting data on production quantities and product characteristics given that much of this information is proprietary?</p>	35 (10)
17. Adaptive Tolerance / Resistance	<p>The majority of toxicity studies with conventional silver were conducted over a decade ago. Are more studies needed that utilize state-of-the-art technology for comparing its mode of toxicity to that of nano-Ag? In other words, can we accurately say that nano-Ag and conventional silver have different modes of toxicity if most of the studies available for conventional silver were not conducted using current methods?</p> <p>Is the nano-Ag harmful to the beneficial organisms in wastewater treatment?</p>	35 (8)
19. Metrics	<p>How should dose and exposure be characterized for human exposures?</p> <p>For the purpose of assessing potential risk, what metrics are most informative for quantifying exposure and dose of nano-Ag?</p>	33 (7)
20. Kinetics II	<p>Does nano-Ag react with materials (i.e., organic matter, other metals, polymers) and alter properties such as REDOX potential or leached metal ion rates?</p> <p>What changes occur to the physicochemical properties of nano-Ag throughout the life-cycle stages, either as a function of process and product engineering or as a function of incidental encounters with other substances and the environment?</p> <p>Does the release of nano-Ag contribute to climate change?</p>	22 (5)
21. Benefits	<p>Do nano-Ag products actually offer more efficacy than products on the market?</p>	9 (5)
22. Incentivize Research for CEA	<p>How can we incentivize researchers to focus in on the most critical questions and best methods for CEA?</p> <p>How urgent is the need for the benefits offered by the candidate application/material?</p>	8 (1)
23. CEA Framework	<p>How can CEA framework be improved to ensure passive or active consumer/occupational exposure research is completed for nano-Ag and for other nanomaterials?</p>	1 (1)

Appendix D References

[ICF](#) (ICF International). (2011). Nanomaterial case study workshop: Developing a comprehensive environmental assessment research strategy for nanoscale silver - Workshop report. Research Triangle Park, NC: U.S. Environmental Protection Agency.